

VOL. 537 NOS. 1 + 2 JANUARY 11, 1991

COMPLETE IN ONE ISSUE

JOURNAL OF

# CHROMATOGRAPHY

INCLUDING ELECTROPHORESIS AND OTHER SEPARATION METHODS

## EDITORS

R. W. Giese (Boston, MA)  
J. K. Haken (Kensington, N.S.W.)  
K. Macek (Prague)  
L. R. Snyder (Orinda, CA)

## EDITORS, SYMPOSIUM VOLUMES,

E. Heftmann (Orinda, CA), Z. Deyl (Prague)

## EDITORIAL BOARD

D. W. Armstrong (Rolla, MO)  
W. A. Aue (Halifax)  
P. Boček (Brno)  
A. A. Boulton (Saskatoon)  
P. W. Carr (Minneapolis, MN)  
N. H. C. Cooke (San Ramon, CA)  
V. A. Davankov (Moscow)  
Z. Deyl (Prague)  
S. Dilli (Kensington, N.S.W.)  
H. Engelhardt (Saarbrücken)  
F. Erni (Basle)  
M. B. Evans (Hatfield)  
J. L. Glajch (N. Billerica, MA)  
G. A. Guiochon (Knoxville, TN)  
P. R. Haddad (Kensington, N.S.W.)  
I. M. Hais (Hradec Králové)  
W. S. Hancock (San Francisco, CA)  
S. Hjertén (Uppsala)  
Cs. Horváth (New Haven, CT)  
J. F. K. Huber (Vienna)  
K.-P. Hupe (Waldbrunn)  
T. W. Hutchens (Houston, TX)  
J. Janák (Brno)  
P. Jandera (Pardubice)  
B. L. Karger (Boston, MA)  
E. sz. Kováts (Lausanne)  
A. J. P. Martin (Cambridge)  
L. W. McLaughlin (Chestnut Hill, MA)  
E. D. Morgan (Keele)  
J. D. Pearson (Kalamazoo, MI)  
H. Poppe (Amsterdam)  
F. E. Regnier (West Lafayette, IN)  
P. G. Righetti (Milan)  
P. Schenckmakers (Eindhoven)  
G. Schuster (Münheim/Ruhr)  
R. Th. A. M. Went (Dübenndorf)  
R. E. Shoup (West Lafayette, IN)  
A. M. Siouffi (Marseille)  
D. J. Strydom (Boston, MA)  
K. K. Unger (Mainz)  
R. Verpoorte (Leiden)  
G. Vigh (College Station, TX)  
J. T. Watson (East Lansing, MI)  
B. D. Westerlund (Uppsala)

## EDITORS, BIBLIOGRAPHY SECTION

Z. Deyl (Prague), J. Janák (Brno), V. Schwarz (Prague), K. Macek (Prague)

ELSEVIER

**Scope.** The *Journal of Chromatography* publishes papers on all aspects of chromatography, electrophoresis and related methods. Contributions consist mainly of research papers dealing with chromatographic theory, instrumental development and their applications. The section *Biomedical Applications*, which is under separate editorship, deals with the following aspects: developments in and applications of chromatographic and electrophoretic techniques related to clinical diagnosis or alterations during medical treatment; screening and profiling of body fluids or tissues with special reference to metabolic disorders; results from basic medical research with direct consequences in clinical practice; drug level monitoring and pharmacokinetic studies; clinical toxicology; analytical studies in occupational medicine.

**Submission of Papers.** Manuscripts (in English; four copies are required) should be submitted to: Editorial Office of *Journal of Chromatography*, P.O. Box 681, 1000 AR Amsterdam, The Netherlands, Telefax (+31-20) 5862 304, or to: The Editor of *Journal of Chromatography, Biomedical Applications*, P.O. Box 681, 1000 AR Amsterdam, The Netherlands. Review articles are invited or proposed by letter to the Editors. An outline of the proposed review should first be forwarded to the Editors for preliminary discussion prior to preparation. Submission of an article is understood to imply that the article is original and unpublished and is not being considered for publication elsewhere. For copyright regulations, see below.

**Subscription Orders.** Subscription orders should be sent to: Elsevier Science Publishers B.V., P.O. Box 211, 1000 AE Amsterdam, The Netherlands, Tel. (+31-20) 5803 911, Telex 18582 ESPA NL, Telefax (+31-20) 5803 598. The *Journal of Chromatography* and the *Biomedical Applications* section can be subscribed to separately.

**Publication.** The *Journal of Chromatography* (incl. *Biomedical Applications*) has 38 volumes in 1991. The subscription prices for 1991 are:

*J. Chromatogr.* (incl. *Cum. Indexes, Vols. 501-550*) + *Biomed. Appl.* (Vols. 535-572):

Dfl. 7220.00 plus Dfl. 1140.00 (p.p.h.) (total ca. US\$ 4696.50)

*J. Chromatogr.* (incl. *Cum. Indexes, Vols. 501-550*) only (Vols. 535-561):

Dfl. 5859.00 plus Dfl. 810.00 (p.p.h.) (total ca. US\$ 3746.50)

*Biomed. Appl.* only (Vols. 562-572):

Dfl. 2387.00 plus Dfl. 330.00 (p.p.h.) (total ca. US\$ 1526.50).

Our p.p.h. (postage, package and handling) charge includes surface delivery of all issues, except to subscribers in Argentina, Australia, Brazil, Canada, China, Hong Kong, India, Israel, Malaysia, Mexico, New Zealand, Pakistan, Singapore, South Africa, South Korea, Taiwan, Thailand and the U.S.A. who receive all issues by air delivery (S.A.L. — Surface Air Lifted) at no extra cost. For Japan, air delivery requires 50% additional charge; for all other countries airmail and S.A.L. charges are available upon request. Back volumes of the *Journal of Chromatography* (Vols. 1-534) are available at Dfl. 208.00 (plus postage). Claims for missing issues will be honoured, free of charge, within three months after publication of the issue. Customers in the U.S.A. and Canada wishing information on this and other Elsevier journals, please contact Journal Information Center, Elsevier Science Publishing Co. Inc., 655 Avenue of the Americas, New York, NY 10010, U.S.A., Tel. (+1-212) 633 3750, Telefax (+1-212) 633 3990.

**Abstracts/Contents Lists** published in Analytical Abstracts, Biochemical Abstracts, Biological Abstracts, Chemical Abstracts, Chemical Titles, Chromatography Abstracts, Clinical Chemistry Lookout, Current Contents/Life Sciences, Current Contents/Physical, Chemical & Earth Sciences, Deep-Sea Research/Part B: Oceanographic Literature Review, Excerpta Medica, Index Medicus, Mass Spectrometry Bulletin, PASCAL-CNRS, Pharmaceutical Abstracts, Referativnyi Zhurnal, Research Alert, Science Citation Index and Trends in Biotechnology.

**See inside back cover** for Publication Schedule, Information for Authors and information on Advertisements.

All rights reserved. No part of this publication may be reproduced, stored in a retrieval system or transmitted in any form or by any means, electronic, mechanical, photocopying, recording or otherwise, without the prior written permission of the publisher, Elsevier Science Publishers B.V., P.O. Box 330, 1000 AH Amsterdam, The Netherlands.

Upon acceptance of an article by the journal, the author(s) will be asked to transfer copyright of the article to the publisher. The transfer will ensure the widest possible dissemination of information.

Submission of an article for publication entails the authors' irrevocable and exclusive authorization of the publisher to collect any sums or considerations for copying or reproduction payable by third parties (as mentioned in article 17 paragraph 2 of the Dutch Copyright Act of 1912 and the Royal Decree of June 20, 1974 (S. 351) pursuant to article 16 b of the Dutch Copyright Act of 1912) and/or to act in or out of Court in connection therewith.

**Special regulations for readers in the U.S.A.** This journal has been registered with the Copyright Clearance Center, Inc. Consent is given for copying of articles for personal or internal use, or for the personal use of specific clients. This consent is given on the condition that the copier pays through the Center the per-copy fee stated in the code on the first page of each article for copying beyond that permitted by Sections 107 or 108 of the U.S. Copyright Law. The appropriate fee should be forwarded with a copy of the first page of the article to the Copyright Clearance Center, Inc., 27 Congress Street, Salem, MA 01970, U.S.A. If no code appears in an article, the author has not given broad consent to copy and permission to copy must be obtained directly from the author. All articles published prior to 1980 may be copied for a per-copy fee of US\$ 2.25, also payable through the Center. This consent does not extend to other kinds of copying, such as for general distribution, resale, advertising and promotion purposes, or for creating new collective works. Special written permission must be obtained from the publisher for such copying.

No responsibility is assumed by the Publisher for any injury and/or damage to persons or property as a matter of products liability, negligence or otherwise, or from any use or operation of any methods, products, instructions or ideas contained in the materials herein. Because of rapid advances in the medical sciences, the Publisher recommends that independent verification of diagnoses and drug dosages should be made.

Although all advertising material is expected to conform to ethical (medical) standards, inclusion in this publication does not constitute a guarantee or endorsement of the quality or value of such product or of the claims made of it by its manufacturer.

This issue is printed on acid-free paper.

## CONTENTS

(Abstracts/Contents Lists published in Analytical Abstracts, Biochemical Abstracts, Biological Abstracts, Chemical Abstracts, Chemical Titles, Chromatography Abstracts, Current Contents/Life Sciences, Current Contents/Physical, Chemical & Earth Sciences, Deep-Sea Research/Part B: Oceanographic Literature Review, Excerpta Medica, Index Medicus, Mass Spectrometry Bulletin, PASCAL-CNRS, Referativnyi Zhurnal, Research Alert and Science Citation Index)

## REGULAR PAPERS

*Column Liquid Chromatography*

- Method for the characterization of stationary phases for the separation of proteins by high-performance liquid chromatography  
by R. E. Huisden, J. C. Kraak and H. Poppe (Amsterdam, The Netherlands) (Received August 6th, 1990) . . . . . 1
- Chemical, physical and chromatographic properties of Superdex 75 prep grade and Superdex 200 prep grade gel filtration media  
by L. Kågedal, B. Engström, H. Ellegren, A.-K. Lieber, H. Lundström, A. Sköld and M. Schenning (Uppsala, Sweden) (Received August 20th, 1990) . . . . . 17
- Molecular interactions in liquid chromatography  
by S. N. Lanin and Yu. S. Nikitin (Moscow, U.S.S.R.) (Received June 9th, 1990) . . . . . 33
- Comparison of retention index scales based on alkyl aryl ketones, alkan-2-ones and 1-nitroalkanes for polar drugs on reversed-phase high-performance liquid chromatography  
by R. M. Smith and N. Finn (Loughborough, U.K.) (Received July 31st, 1990) . . . . . 51
- Changes in the enthalpy and entropy of hydroxyl aromatics in reversed-phase liquid chromatography with  $\beta$ -cyclodextrin in the mobile phase  
by R. M. Mohseni and R. J. Hurtubise (Laramie, WY, U.S.A.) (Received August 30th, 1990) . . . . . 61
- Comparison of the liquid chromatographic behaviour of selected steroid isomers using different reversed-phase materials and mobile phase compositions  
by M. Olsson (Stockholm, Sweden) and L. C. Sander and S. A. Wise (Gaithersburg, MD, U.S.A.) (Received August 27th, 1990) . . . . . 73
- Fatty acid conjugates of chlorinated phenols and their high-performance liquid chromatographic analysis  
by B. S. Kaphalia (Galveston, TX, U.S.A.) (Received August 28th, 1990) . . . . . 85
- Separation and identification of free phenolic acids in wines by high-performance liquid chromatography  
by G. P. Cartoni, F. Coccioli, L. Pontelli and E. Quattrucci (Rome, Italy) (Received July 13th, 1990) . . . . . 93
- High-performance liquid chromatography of red fruit anthocyanins  
by J.-P. Goiffon, M. Brun and M.-J. Bourrier (Montpellier, France) (Received August 31st, 1990) . . . . . 101
- Solid-phase reagent containing the 3,5-dinitrophenyl tag for the improved derivatization of chiral and achiral amines, amino alcohols and amino acids in high-performance liquid chromatography with ultraviolet detection  
by A. J. Bourque and I. S. Krull (Boston, MA, U.S.A.) (Received August 1st, 1990) . . . . . 123
- Automated phenylthiocarbonyl amino acid analysis of carboxypeptidase/aminopeptidase digests and acid hydrolysates  
by R. S. Thoma and D. L. Crimmins (St. Louis, MO, U.S.A.) (Received July 24th, 1990) . . . . . 153

(Continued overleaf)

ห้องสมุดเคมี มหาวิทยาลัยศรีนครินทรวิโรฒ

191111.2534

Contents (continued)

Breakthrough curves of insulin, [D-Phe <sup>6</sup> ]-Gonadotropin-releasing hormone and phenylalanine methyl ester on copolymers of alkylacrylate and divinylbenzene by P. Slonina and A. Scidel (Berlin, G.D.R.) (Received August 7th, 1990) . . . . .	167
Alternative mobile phases for reversed-phase high-performance liquid chromatography of peptides and proteins by B. S. Welinder and H. H. Sørensen (Gentofte, Denmark) (Received July 20th, 1990) . . . . .	181
Reversed-phase high-performance liquid chromatographic characterization of acetic acid extracts of the normal and the diabetic human pancreas by B. S. Welinder and S. Linde (Gentofte, Denmark) (Received July 20th, 1990) . . . . .	201
Protein-ligand interactions studied on bovine serum albumin with free and polymer-bound Cibacron Blue F3G-A as ligand with reference to affinity partitioning by G. Johansson and M. Joëlsson (Lund, Sweden) (Received August 28th, 1990) . . . . .	219
High-performance liquid chromatographic analysis of the (cyanoaquo) stereoisomers of several putative vitamin B <sub>12</sub> precursors by S. H. Ford, J. Gallery, A. Nichols and M. Shambee (Chicago, IL, U.S.A.) (Received August 30th, 1990) . . . . .	235
Elimination of peak splitting in the liquid chromatography of the proline-containing drug enalapril maleate by J. Šalamoun and K. Šlais (Brno, Czechoslovakia) (Received July 30th, 1990) . . . . .	249
Analysis of <sup>55</sup> Fe-labeled hydroxamate siderophores by high-performance liquid chromatography by R. J. Speirs and G. L. Boyer (Syracuse, NY, U.S.A.) (Received October 2nd, 1990) . . . . .	259
Simultaneous determination of arsenite, arsenate, selenite and selenate in waters using suppressed ion chromatography with ultraviolet absorbance detection by S. S. Goyal, A. Hafez and D. W. Rains (Davis, CA, U.S.A.) (Received May 30th, 1990) . . . . .	269
Separation of lanthanides and yttrium as anionic complexes by isocratic ion-interaction chromatography by E. A. Jones and H. S. Bezuidenhout (Randburg, South Africa) and J. F. van Staden (Pretoria, South Africa) (Received July 24th, 1990) . . . . .	277
Preparation of uranium by reversed-phase partition chromatography. Application to the determination of trace elements in nuclear-grade uranium compounds by inductively coupled plasma atomic emission spectrometry by A. S. Al-Ammar, H. A. Hamid, B. H. Rashid and H. M. Basheer (Baghdad, Iraq) (Received May 15th, 1990) . . . . .	287
<i>Gas Chromatography</i>	
Determination of contributions of different types of solute-sorbent interactions in gas-adsorption chromatography by linear regression of adsorption energies by O. G. Larionov, V. V. Petrenko and N. P. Platonova (Moscow, U.S.S.R.) (Received July 24th, 1990) . . . . .	295
Gas chromatographic identification of complex mixtures of halomethanes and haloethanes by using the correlation between their retention and vapour pressure by T. G. Gerbino and G. Castello (Genova, Italy) (Received July 31st, 1990) . . . . .	305
Adsorption/thermal desorption for the determination of volatile organic compounds in water by M. E. Rosen and J. F. Pankow (Beaverton, OR, U.S.A.) (Received May 16th, 1990) . . . . .	321
Isomer identification and gas chromatographic retention studies of monomeric cyclic fatty acid methyl esters by J. A. Rojo and E. G. Perkins (Urbana, IL, U.S.A.) (Received September 7th, 1990) . . . . .	329
Capillary gas chromatographic behavior of stereoisomeric bile acids with a <i>vicinal</i> glycol structure by their "mixed" alkylboronate derivatives by T. Iida and I. Komatsubara (Koriyama, Japan), F. C. Chang (Claremont, CA, U.S.A.) and J. Goto and T. Nambara (Sendai, Japan) (Received August 14th, 1990) . . . . .	345

Indirect determination of isocyanates by gas chromatography by C. B. Fanska, T. J. Byerley and J. D. Eick (Kansas City, MO, U.S.A.) (Received July 10th, 1990) . . . . .	357
Correlation between structure and gas chromatographic behaviour of nitrogen-containing heterocyclic compounds. I. Methyl substitution of pyridopyrimidine derivatives by O. Papp, Gy. Szász, J. Kőkösi and I. Hermecz (Budapest, Hungary) (Received August 21st, 1990) . . . . .	365
Correlation between structure and gas chromatographic behaviour of nitrogen-containing heterocyclic compounds. II. Alkyl substitution of quinazolone derivatives by O. Papp, Gy. Szász, L. Órfi and I. Hermecz (Budapest, Hungary) (Received August 21st, 1990) . . . . .	371
Correlation between structure and gas chromatographic behaviour of nitrogen-containing heterocyclic compounds. III. Variation of ring size by O. Papp, Gy. Szász, J. Kőkösi and I. Hermecz (Budapest, Hungary) (Received August 21st, 1990) . . . . .	377
Determination of nine acidic herbicides in water and soil by gas chromatography using an electron-capture detector by F. Ngan and T. Ikesaki (Sacramento, CA, U.S.A.) (Received August 14th, 1990) . . . . .	385

*Planar Chromatography*

Determination of selenium in organic compounds on a silica gel sintered thin-layer chromatographic plate with 2,3-diaminonaphthalene after direct digestion by R. Hasunuma and T. Ogawa (Kanagawa, Japan), J. Ishii (Tokyo, Japan) and Y. Kawanishi (Kanagawa, Japan) (Received August 7th, 1990) . . . . .	397
--	-----

*Electrophoresis*

Determination of absolute mobilities, pK values and separation numbers by capillary zone electrophoresis. Effective mobility as a parameter for screening by J. L. Beckers, F. M. Everaerts and M. T. Ackermans (Eindhoven, The Netherlands) (Received August 7th, 1990) . . . . .	407
Isotachopheresis with electroosmotic flow: open <i>versus</i> closed systems by J. L. Beckers, F. M. Everaerts and M. T. Ackermans (Eindhoven, The Netherlands) (Received August 8th, 1990) . . . . .	429

NOTES

*Column Liquid Chromatography*

Post-column oligosaccharide dehydrogenase reactor for coulometric detection of malto-oligosaccharides in a liquid chromatographic system by N. Kiba, K. Shitara and M. Furusawa (Kofu, Japan) and Y. Takata (Katsuta, Japan) (Received August 2nd, 1990) . . . . .	443
High-performance liquid chromatographic determination of flavonoid glucosides from <i>Helichrysum italicum</i> by P. Pietta, P. Mauri, C. Gardana, R. M. Facino and M. Carini (Milan, Italy) (Received September 3rd, 1990) . . . . .	449
Isocratic column liquid chromatographic separation of a complex mixture of epicuticular flavonoid aglycones and intracellular flavonol glycosides from <i>Cistus laurifolius</i> L. by T. Vogt and P.-G. Gülz (Köln, F.R.G.) (Received August 7th, 1990) . . . . .	453
Behaviour of concanavalin A on DEAE-Sephadex and CM-Sephadex by C. Elias and A. M. Diwan (Pune, India) (Received April 20th, 1990) . . . . .	460

(Continued overleaf)

Contents (continued)

Large-scale isolation and purification of human apolipoproteins A-I and A-II  
by A. Sigalov, O. Alexandrovich and E. Strizevskaya (Moscow, U.S.S.R.) (Received June 24th, 1990) . . . . . 464

Preparative high-performance liquid chromatography on chemically modified porous glass. Isolation of acidic saponins from ginseng  
by H. Kanazawa, Y. Nagata, Y. Matsushima, M. Tomoda and N. Takai (Tokyo, Japan) (Received August 14th, 1990) . . . . . 469

High-performance liquid chromatography of substituted trinuclear osmium carbonyl clusters,  $Os_3(CO)_{12-n}[P(C_6F_5)_3]_n$  ( $n=0, 1, 2$ )  
by H. G. Ang, W. L. Kwik and W. K. Leong (Singapore, Singapore) (Received August 20th, 1990) . . . . . 475

*Gas Chromatography*

Liquid chrystals for the gas chromatographic determination of the stereochemistry of insect sex pheromones  
by I. Nesterova, B. Rekhter and G. Roshka (Kishinev, U.S.S.R.) and Z. Witkiewicz (Warsaw, Poland) (Received June 19th, 1990) . . . . . 482

Simultaneous determination of tributyl phosphate and dibutyl phosphate in spent fuel reprocessing streams by gas chromatography  
by Y. Kuno, T. Hina, T. Akiyama and M. Matsui (Ibaraki, Japan) (Received September 11th, 1990) . . . . . 489

*Planar Chromatography*

Localization of amino acids on thin-layer chromatograms with acetylacetone-formaldehyde reagent  
by M. B. Devani, C. J. Shishoo, S. A. Shah, K. P. Soni and R. S. Shah (Ahmedabad, India) (Received August 31st, 1990) . . . . . 494

LETTERS TO THE EDITOR

Pitfalls in the choice of isotherms for the calculation of band profiles in preparative chromatography  
by M. Czok and G. Guiochon (Knoxville and Oak Ridge, TN, U.S.A.) (Received October 17th, 1990) . . . . . 497

Pitfalls in the choice of isotherms for the calculation of band profiles in preparative chromatography. A reply  
by L. R. Snyder (Lafayette, CA, U.S.A.) and G. B. Cox (Indianapolis, IN, U.S.A.) (Received September 25th, 1990) . . . . . 507

Detection of choline and acetylcholine by high-performance liquid chromatography. Limitations, pitfalls, sample preparation  
by E. Haen (Munich, F.R.G.), H. Hagenmaier (Tübingen, F.R.G.) and J. Remien (Munich, F.R.G.) (Received August 27th, 1990) . . . . . 514

*Author Index* . . . . . 520

\*\*\*\*\*  
\* In articles with more than one author, the name of the author to whom correspondence should be addressed is indicated in the  
\* article heading by a 6-pointed asterisk (\*)  
\*  
\*\*\*\*\*

# Computer-Assisted Method Development for High-Performance Liquid Chromatography

edited by J.L. Glajch and L.R. Snyder

(Spin-off from the *Journal of Chromatography* Vol. 485 plus an additional chapter, index and glossary)

This book deals with the use of the computer as an aid in selecting adequate or optimum conditions for a given analytical separation. Originally published as Volume 485 of the *Journal of Chromatography*, it has now been reprinted in book form, since the information is so useful that many chromatographers want a copy readily available in the lab.

An extensive Introduction is added to the book edition. This surveys the field and refers to the pages where particular items are discussed in the book. The addition of a Glossary of Terms, an Author Index and a Subject Index make this book an invaluable source of easily consulted information for the practising chromatographer.

For the purpose of this book, computer-assisted method development will be limited to specific procedures which are intended to be used with a computer - rather than their manually applied precursors. In that sense, the subject can be considered to have begun around 1980.

The ongoing, intense research activity into various forms of computer assisted HPLC method development provides the assurance that this approach can really assist the practical chromatographer working in an industrial laboratory.

Contents. Introduction Chapter: Computer-assisted method development for HPLC (J.L. Glajch & L.R. Snyder). Foreword (G.L. Glajch & L.R. Snyder). Simplex optimization of HPLC separations (J.C. Berridge). Computer-assisted optimization in HPLC method development (S.N. Deming *et al.*). Selection of mobile phase parameters and their optimization in reversed-phase LC (H.A.H. Billiet & L. de Galan). Method development in HPLC using retention mapping and experimental design techniques (J.L. Glajch & J.J. Kirkland). Isocratic elution (L.R. Snyder *et al.*). Drylab computer simulation for HPLC method development. I. Isocratic elution (L.R. Snyder *et al.*). II. Gradient elution (J.W. Dolan *et al.*). Predictive calculation methods for optimization of gradient elution using binary and ternary solvent gradients (P. Jandera). Computer-assisted retention prediction for HPLC in the ion-exchange mode (Y. Baba). Multivariate calibration strategy for reversed-phase chromatographic systems based on the characterization of stationary-mobile phase combinations with markers (A.K. Smilde *et al.*). Computer-aided optimization of HPLC in the pharmaceutical industry (E.P. Lankmayr *et al.*). Comparison of optimization methods in reversed-phase HPLC using mixture designs and multi-criteria decision making (P.M.J. Coenegracht *et al.*). Explanations and advice provided by an expert system for system optimization in HPLC (P.J. Schoenmakers & N. Dunand). Expert system for the selection of HPLC methods for the analysis of drugs (M. De Smet *et al.*). Expert system for the selection of initial HPLC conditions for the analysis of pharmaceuticals (R. Hindriks *et al.*). Expert system program for assistance in HPLC method development (S.S. Williams *et al.*). Expert system for method validation in chromatography (M. Mulholand *et al.*). Knowledge-based expert system for

troubleshooting HPLC assay methods (K. Tsuji & K.M. Jenkins). Uniform shell designs for optimization in reversed-phase LC (Y. Hu & D.L. Massart). Retention prediction of analytes in reversed-phase HPLC based on molecular structure (R.M. Smith & C.M. Burr). Cathie: expert interpretation of chromatographic data (R. Milne). Prediction of retention of metabolites in HPLC by an expert system approach (K. Valkó *et al.*). Reversed-phase chromatographic method development for peptide separations using the computer simulation program ProDigest-LC (C.T. Mant *et al.*). Rule-based approach for the determination of solute types in unknown sample mixtures as a first step of optimization parameter selection in reversed-phase ion-pair chromatography (A. Bartha & G. Vigh). Rationalization of the selection of the type of the organic modifier(s) for selectivity optimization in reversed-phase ion-pair chromatography (A. Bartha *et al.*). Predicting reversed-phase gradient elution separations by computer simulation (J. Schmidt). Computer-assisted optimization with NEMROD software (G. Mazerolles *et al.*). Multi-dimensional interpolation by the moving least squares approach for modelling of chromatographic retention data (M. Otto *et al.*). Microcomputer-assisted LC separation system (MCASYSY) for method development and data handling (K. Jinno *et al.*). Objective functions in experimental and simulated chromatographic optimization (R. Cela *et al.*). Optimization strategies for solutes exhibiting peak tailing (S. Sekulic & P.R. Haddad). Computer-assisted selection of the optimum gradient programme in TLC (W. Markowski). Prediction of retention times in ion-exchange chromatography (T. Sasagawa *et al.*). Solvent modulation in LC: optimization strategies (J.H. Wahl & V.L. McGuffin). Recent advances in fuzzy peak tracking in HPLC (E.P. Lankmayr *et al.*). Peak tracking in HPLC based on normalized band areas. A ribosomal protein sample as an example (I. Molnar *et al.*). Development of a HPLC method for fluroxypyr herbicide and metabolites using computer simulation with Drylab G software (R.G. Lehmann & J.R. Miller). Computer-assisted optimization of a HPLC separation for chlorpromazine and thirteen metabolites (J.S. Kiel *et al.*). Practical approach for HPLC method development: assaying synthetic intermediates of a leukotriene inhibitor (J. Fulper). Computer-assisted development of a HPLC method for fractionating selected nitro derivatives of polyaromatic hydrocarbons (D.J. Thompson & W.D. Ellenson). Reversed-phase LC retention and selectivity surfaces. II. Deoxyribonucleosides (E. Grushka *et al.*). Effects of different organic modifiers in optimization of reversed-phase HPLC gradient elution of a mixture of natural secoiridoid compounds (F. Donati *et al.*). Optimization of gradients in anion-exchange separations of oligonucleotides using computer-assisted retention prediction and a HPLC simulation system (Y. Baba & M.K. Ito). Separation of mixtures of *o*-phthalaldehyde-derivatized amino acids by reversed-phase gradient elution (J.D. Stuart *et al.*). Glossary of terms. Author index. Subject index.

1990 xxx + 676 pages  
Price: US\$ 79.75 / Dfl. 175.00  
ISBN 0-444-88748-2



**Elsevier Science Publishers**

P.O. Box 330, 1000 AH Amsterdam, The Netherlands

In the USA/Canada: P.O. Box 882, Madison Square Station, New York, NY 10159, USA

---

# Ion Chromatography

## Principles and Applications

---

by **P.R. Haddad**, *University of New South Wales, Kensington, N.S.W., Australia* and  
**P.E. Jackson**, *Waters Chromatography Division, Milford, MA, USA*

(Journal of Chromatography Library, 46)

Ion chromatography (IC) was first introduced in 1975 for the determination of inorganic anions and cations and water soluble organic acids and bases. Since then, the technique has grown in usage at a phenomenal rate. The growth of IC has been accompanied by a blurring of the original definition of the technique, so that it now embraces a very wide range of separation and detection methods, many of which bear little resemblance to the initial concept of ion-exchange separation coupled with conductivity detection.

*Ion Chromatography* is the first book to provide a comprehensive treatise on all aspects of ion chromatography. Ion-exchange, ion-interaction, ion-exclusion and other pertinent separation modes are included, whilst the detection methods discussed include conductivity, amperometry, potentiometry, spectroscopic methods (both molecular and atomic) and post-column reactions. The theoretical background and operating principles of each separation and detection mode are discussed in detail. A unique extensive compilation of practical applications of IC (1250 literature citations) is presented in tabular form. All relevant details of each application are given to accommodate reproduction of the method in the laboratory without access to the original publication.

This truly comprehensive text on ion chromatography should prove to be the standard reference work for researchers and those involved in the use of the subject in practical situations.

**Contents:** Chapter 1. Introduction. **PART I. Ion-Exchange Separation Methods.** Chapter 2. An introduction to ion-exchange methods. Chapter 3. Ion-exchange stationary phases for ion chromatography. Chapter 4. Eluents for ion-exchange separations. Chapter 5. Retention models for ion-exchange. **PART II. Ion-Interaction, Ion-Exclusion and Miscellaneous Separation Methods.** Chapter 6. Ion-interaction chromatography. Chapter 7. Ion-exclusion chromatography. Chapter 8. Miscellaneous separation methods. **PART III. Detection Methods.** Chapter 9. Conductivity detection. Chapter 10. Electrochemical detection (amperometry, voltammetry and coulometry). Chapter 11. Potentiometric detection. Chapter 12. Spectroscopic detection methods. Chapter 13. Detection by post-column reaction. **PART IV. Practical Aspects.** Chapter 14. Sample handling in ion chromatography. Chapter 15. Methods development. **PART V. Applications of Ion Chromatography.** Overview of the applications section. Chapter 16. Environmental applications. Chapter 17. Industrial applications. Chapter 18. Analysis of foods and plants. Chapter 19. Clinical and pharmaceutical applications. Chapter 20. Analysis of metals and metallurgical solutions. Chapter 21. Analysis of treated waters. Chapter 22. Miscellaneous applications. Appendix A. Statistical information on ion chromatography publications. Appendix B. Abbreviations and symbols. Index.

1990 798 pages  
Price: US\$ 191.50 / Dfl. 335.00  
ISBN 0-444-88232-4



**Elsevier Science Publishers**

P.O. Box 211, 1000 AE Amsterdam, The Netherlands  
P.O. Box 882, Madison Square Station, New York, NY 10159, USA



JOURNAL OF CHROMATOGRAPHY

VOL. 537 (1991)

ห้องสมุดกรมวิทยาศาสตร์บริการ



# JOURNAL of CHROMATOGRAPHY

INCLUDING ELECTROPHORESIS AND OTHER SEPARATION METHODS

## EDITORS

R. W. GIESE (Boston, MA), J. K. HAKEN (Kensington, N.S.W.), K. MACEK (Prague),  
L. R. SNYDER (Orinda, CA)

## EDITORS, SYMPOSIUM VOLUMES

E. HEFTMANN (Orinda, CA), Z. DEYL (Prague)

## EDITORIAL BOARD

D. W. Armstrong (Rolla, MO), W. A. Aue (Halifax), P. Boček (Brno), A. A. Boulton (Saskatoon), P. W. Carr (Minneapolis, MN), N. H. C. Cooke (San Ramon, CA), V. A. Davankov (Moscow), Z. Deyl (Prague), S. Dilli (Kensington, N.S.W.), H. Engelhardt (Saarbrücken), F. Erni (Basle), M. B. Evans (Hatfield), J. L. Glajch (N. Billerica, MA), G. A. Guiochon (Knoxville, TN), P. R. Haddad (Kensington, N.S.W.), I. M. Hais (Hradec Králové), W. S. Hancock (San Francisco, CA), S. Hjertén (Uppsala), Cs. Horváth (New Haven, CT), J. F. K. Huber (Vienna), K.-P. Hupe (Waldbronn), T. W. Hutchens (Houston, TX), J. Janák (Brno), P. Jandera (Pardubice), B. L. Karger (Boston, MA), E. sz. Kováts (Lausanne), A. J. P. Martin (Cambridge), L. W. McLaughlin (Chestnut Hill, MA), E. D. Morgan (Keele), J. D. Pearson (Kalamazoo, MI), H. Poppe (Amsterdam), F. E. Regnier (West Lafayette, IN), P. G. Righetti (Milan), P. Schoenmakers (Eindhoven), G. Schomburg (Mülheim/Ruhr), R. Schwarzenbach (Dübendorf), R. E. Shoup (West Lafayette, IN), A. M. Siouffi (Marseille), D. J. Strydom (Boston, MA), K. K. Unger (Mainz), R. Verpoorte (Leiden), Gy. Vigh (College Station, TX), J. T. Watson (East Lansing, MI), B. D. Westerlund (Uppsala)

## EDITORS, BIBLIOGRAPHY SECTION

Z. Deyl (Prague), J. Janák (Brno), V. Schwarz (Prague), K. Macek (Prague)



ELSEVIER

AMSTERDAM — OXFORD — NEW YORK — TOKYO

---

*J. Chromatogr.*, Vol. 537 (1991)

All rights reserved. No part of this publication may be reproduced, stored in a retrieval system or transmitted in any form or by any means, electronic, mechanical, photocopying, recording or otherwise, without the prior written permission of the publisher, Elsevier Science Publishers B.V., P.O. Box 330, 1000 AH Amsterdam, The Netherlands.

Upon acceptance of an article by the journal, the author(s) will be asked to transfer copyright of the article to the publisher. The transfer will ensure the widest possible dissemination of information.

Submission of an article for publication entails the authors' irrevocable and exclusive authorization of the publisher to collect any sums or considerations for copying or reproduction payable by third parties (as mentioned in article 17 paragraph 2 of the Dutch Copyright Act of 1912 and the Royal Decree of June 20, 1974 (S. 351) pursuant to article 16 b of the Dutch Copyright Act of 1912) and/or to act in or out of Court in connection therewith.

**Special regulations for readers in the U.S.A.** This journal has been registered with the Copyright Clearance Center, Inc. Consent is given for copying of articles for personal or internal use, or for the personal use of specific clients. This consent is given on the condition that the copier pays through the Center the per-copy fee stated in the code on the first page of each article for copying beyond that permitted by Sections 107 or 108 of the U.S. Copyright Law. The appropriate fee should be forwarded with a copy of the first page of the article to the Copyright Clearance Center, Inc., 27 Congress Street, Salem, MA 01970, U.S.A. If no code appears in an article, the author has not given broad consent to copy and permission to copy must be obtained directly from the author. All articles published prior to 1980 may be copied for a per-copy fee of US\$ 2.25, also payable through the Center. This consent does not extend to other kinds of copying, such as for general distribution, resale, advertising and promotion purposes, or for creating new collective works. Special written permission must be obtained from the publisher for such copying.

No responsibility is assumed by the Publisher for any injury and/or damage to persons or property as a matter of products liability, negligence or otherwise, or from any use or operation of any methods, products, instructions or ideas contained in the materials herein. Because of rapid advances in the medical sciences, the Publisher recommends that independent verification of diagnoses and drug dosages should be made. Although all advertising material is expected to conform to ethical (medical) standards, inclusion in this publication does not constitute a guarantee or endorsement of the quality or value of such product or of the claims made of it by its manufacturer.

This issue is printed on acid-free paper.

## Method for the characterization of stationary phases for the separation of proteins by high-performance liquid chromatography

R. E. HUISDEN\*, J. C. KRAAK and H. POPPE

*Laboratory for Analytical Chemistry, University of Amsterdam, Nieuwe Achtergracht 166, 1018 WV Amsterdam (The Netherlands)*

(First received April 12th, 1990; revised manuscript received August 6th, 1990)

---

### ABSTRACT

A conformational change of lysozyme and myoglobin can be visualized with transition curves in a high-performance liquid chromatographic (HPLC) system using a diode-array detector and UV difference spectrometry. Transition temperatures calculated from the curves are affected by the mobile phase composition and the column packing material. Flow-rates as used in HPLC do not have a measurable influence.

---

### INTRODUCTION

New and improved stationary phases for protein separations by high-performance liquid chromatography (HPLC) are constantly being announced. Accompanying such product improvements are analytical techniques developed to characterize these materials, such as solid-state NMR, diffuse reflectance infrared Fourier transform spectrometry (DRIFT) and thermogravimetric analysis (TGA).

In certain instances, protein separation by HPLC requires conditions that maintain the tertiary structure of a protein, *e.g.*, in the final stage of a preparative purification. Stationary phases used for this non-denaturing chromatography are often described as “hydrophilic” and should have a very mild interaction with the particular protein. Retention time or retention volume is often taken as a measure of the amount of interaction with the stationary phase. Strongly retained proteins will probably suffer more from denaturation than unretained proteins. Inertness is then regarded as being synonymous with unretained elution.

To synthesize and compare “mild” stationary phases, however, a technique is required that measures a conformational change of a protein in a standardized and reproducible way. There have been a number of papers on the measurement of protein conformational changes in HPLC columns [1–6]. Surface intrinsic fluorescence in a spectroscopic flow cell enabled the study of the surface dynamics of a protein in contact with an adsorbent [3]. Rapid conformational interconversions on a chromatographic detection time scale could be demonstrated with diode-array and low-angle

laser light scattering detection [2]. Here a method is presented that makes use of a transition curve of an eluted protein as measured by UV difference spectrometry. Related approaches have appeared recently [7-9].

With a stepwise increase in temperature, the fraction of denatured protein will at one point increase rapidly. This fraction, when plotted against temperature, produces a transition curve from which a transition temperature or transition point can be determined at 50% denaturation. Transition temperatures are a measure of the stability of proteins and depend on the nature of the protein and the solvent composition. A worsening of the solvent composition shifts the transition curve and lowers the transition point (Fig. 1).

Transition curves can be recorded with several techniques that measure a protein conformational change, *e.g.*, enzymatic activity [10], circular dichromism [1], viscosity [11], light scattering [12] and UV difference spectrometry [13-16]. In the last method, spectra of a protein under different conditions are subtracted, *e.g.*, at two different temperatures or two concentrations of a solvent modifier.

Spectral differences or shifts are generated by chromophoric moieties, amino acid side-chains, that turn outwards and form complexes with solvent molecules [17-18]. By recording transition curves with different techniques, it can be established that this UV difference indeed represents a conformational change. With lysozyme, comparisons were made with viscosity, optical rotation and light scattering measurements [11,12].

The lysozyme transition is clearly defined with no intermediate states. It is reversible and probably not a complete denaturation to a random coil but a partial opening of the tertiary structure [14,19]. With myoglobin intermediate states are sometimes observed, illustrating that with a transition curve one can "see" a conformational change more directly than, for instance, with a single enzymatic activity assay.

The curves have been used in the past to elucidate protein structures by study-

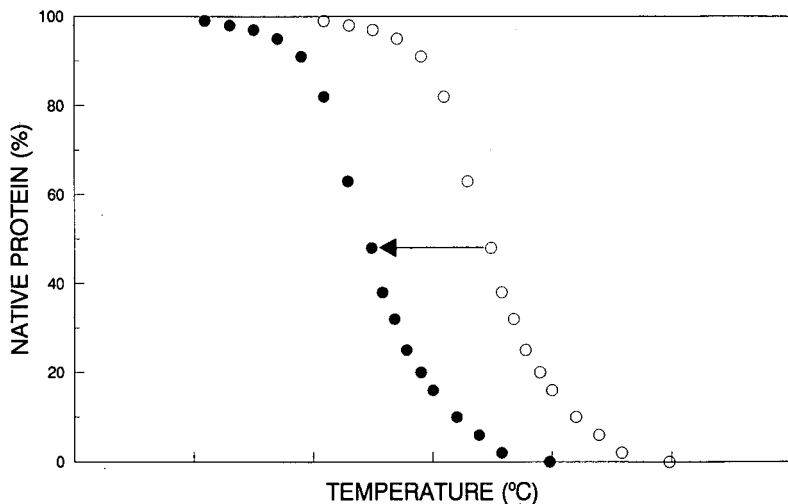


Fig. 1. Shift of transition curve with a change of solvent composition.

ing the influence of intramolecular ionic and hydrophobic bonding [15]. Here they are used to study the interaction of standard proteins with stationary phases in HPLC columns and to develop a method to determine the quality of silica coatings.

## EXPERIMENTAL

A silica support (Hypersil WP 300, 10  $\mu\text{m}$ ) was obtained from Shandon (Runcorn, U.K.). Lysozyme and myoglobin were purchased from Sigma (St. Louis, MO, U.S.A.). All other chemicals were of analytical-reagent grade.

### *Equipment*

HPLC was performed with a constant-flow pump (Spectroflow 400; Kratos, Ramsey, NJ, U.S.A.) and an injection valve (Model 7010; Rheodyne, Berkeley, CA, U.S.A.) with a 50- $\mu\text{l}$  sample loop and a stainless-steel column (150  $\times$  2 mm I.D.). The column was thermostated with a Haake thermostat (Berlin, F.R.G.) (Type F4391), plus a water-jacket. Temperatures were measured with a electronic thermometer (Amadigit ad 15th; Amarell Electronic, Kreuzwertheim, F.R.G.) with a probe in the water-jacket. The detector was a Hewlett-Packard (Waldbronn, F.R.G.) diode-array detector (Model 1040A) operated with a Hewlett-Packard (Corvallis, OR, U.S.A.) computer (Model HP-85B) and Hewlett-Packard (Guadalajara, Mexico) disk drives (Model HP-9121).

### *Procedure*

To monitor the conformational change of lysozyme by difference spectrometry a wavelength has to be selected. A value often mentioned in the literature is 292 nm [14,16]. In order to be able to check the total concentration of eluted lysozyme in the peak maximum, the absorbance at 297 nm, an isobestic point in the difference spectrum, was also recorded. Moreover, an additional measurement was done at 302 nm as a check on the internal consistency of the result. The conformational change in myoglobin is relatively easily measured at 410 nm, because a distinct maximum at that wavelength disappears on denaturation [13]. A check on total concentration was done at 280 nm, where a maximum occurs that is not affected by denaturation.

The mobile phase composition used during the procedure should not interfere with the difference spectrometry and must completely elute the native protein at room temperature.

The procedure starts with a column thermostated at 20°C. The protein sample is injected and the signals are recorded. After elution of the sample the temperature is raised in about 30 steps to 80–90°C. At each predetermined temperature a protein sample is injected and the signals are recorded.

After these measurements the data have to be retrieved and a transition plot calculated. The EVALUATE program from the DAD 1040 supplies signal values in the peak maximum. To determine the UV difference, the 20°C absorbance value, where all the protein is in its native state, has to be subtracted from the values at other temperatures, e.g.,  $A^{292}(T^\circ\text{C}) - A^{292}(20^\circ\text{C})$ . However, in this flow system the observed changes in the absorbance values are also due to small variations in the total concentration of the protein in the peak maximum. The absorbance values can be corrected for these variations by normalizing them with the absorbance of the refer-

ence wavelength. This reference wavelength is not affected by the denaturation of the protein and is thus a measure of the amount of protein. With the value of the reference wavelength at 20°C,  $A_R(20^\circ\text{C})$ , all other temperature values,  $A(T^\circ\text{C})$ , are recalculated, using

$$[A_R(20^\circ\text{C})/A_R(T^\circ\text{C})]A(T^\circ\text{C})$$

The UV difference is then determined by subtracting the 20°C value. The figures obtained in this way are equivalent to the  $\Delta e$  values used by others [14,20]. They can be plotted against the corresponding temperatures (Figs. 2 and 3). A transition is usually apparent. By identifying the observed asymptotes, with native protein ( $\Delta e_N$ ) and complete denaturation ( $\Delta e_D$ ) respectively, the vertical axis can be converted into a percentage denaturation scale. The fraction of protein in the denatured form is then calculated using

$$f_d = (\Delta e - \Delta e_N)/(\Delta e_D - \Delta e_N)$$

where  $\Delta e$  is the UV difference at a particular temperature [11].

With lysozyme, the observed asymptotes have a slope, probably due to a temperature dependence of the spectra. The percentage denaturation can be determined by performing an axis transformation. One axis is drawn parallel to the slope of the asymptotes and the other perpendicular to it. The distance between the two asymptotes in this new axis system is then used to determine the fraction of denatured protein (see Fig. 3), and related to the corresponding temperature. More often two values,  $\Delta e_N$  and  $\Delta e_D$ , are chosen visually, symmetrically around the transition (Figs. 4 and 5).

It should be noted that the procedure described so far gives information on the

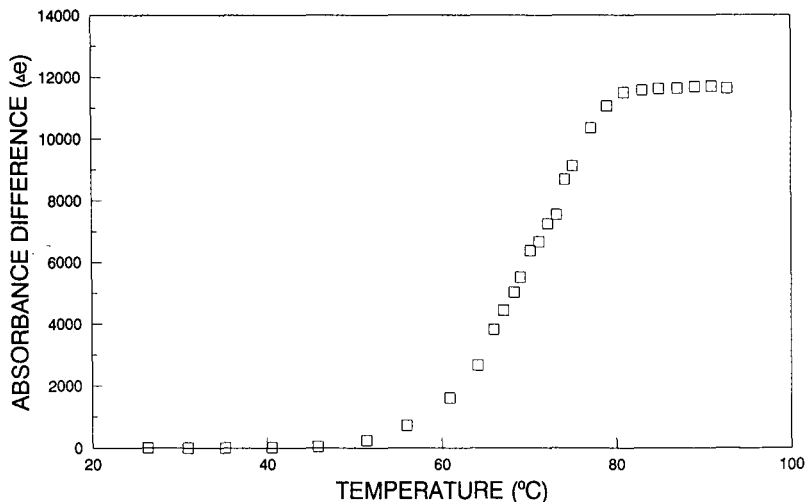


Fig. 2. UV difference of myoglobin plotted against temperature. Calculation as described in the text.



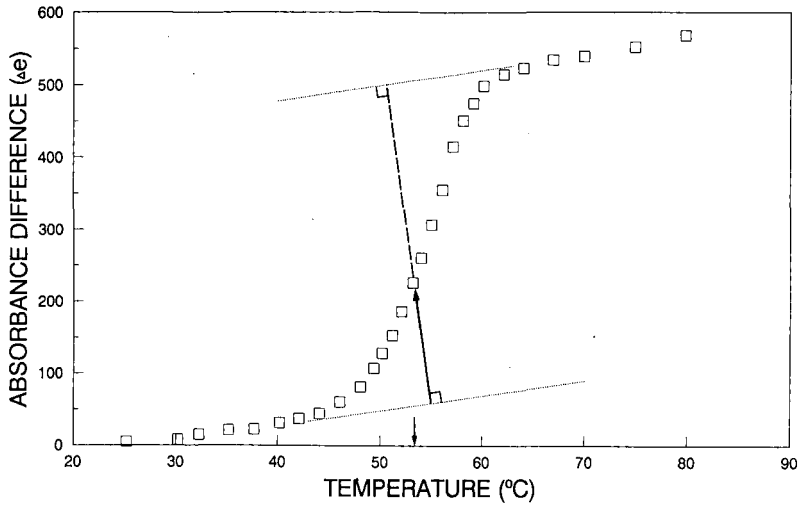


Fig. 3. UV difference of lysozyme plotted against temperature. Calculation as described in the text.

extent of denaturation of the eluted protein. In some instances, however, the protein recovery is drastically reduced at higher temperatures of the transition curve. The mobile phase allows complete elution of the native protein at room temperature. If the temperature is raised and part of the protein denatures, elution need no longer be complete as moieties from inside the protein become exposed. A particular mobile phase may still be desirable in order to study the interaction with a given hydrophilic support. Therefore, a second correction is sometimes necessary with peak-height or peak-area data. The fraction of eluted native protein as calculated from the  $\Delta e$  plot is multiplied by the fraction of protein recovery to give a more accurate figure of  $f_n$ , the

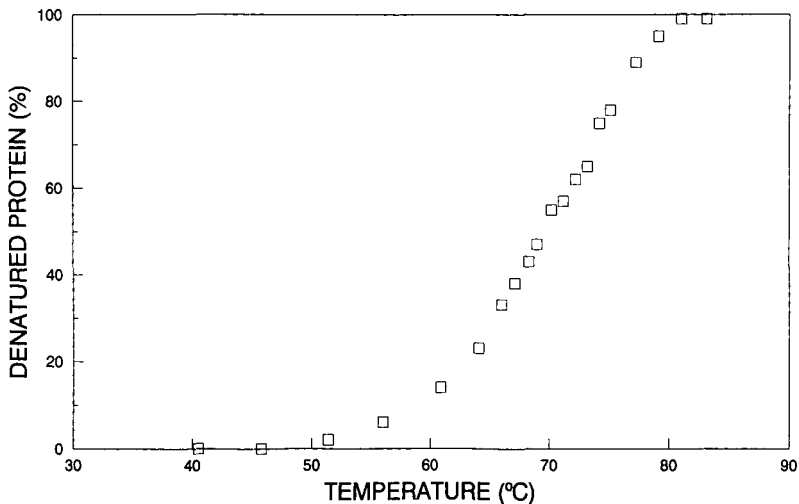


Fig. 4. Fraction denaturation of myoglobin. Calculation as described in the text.

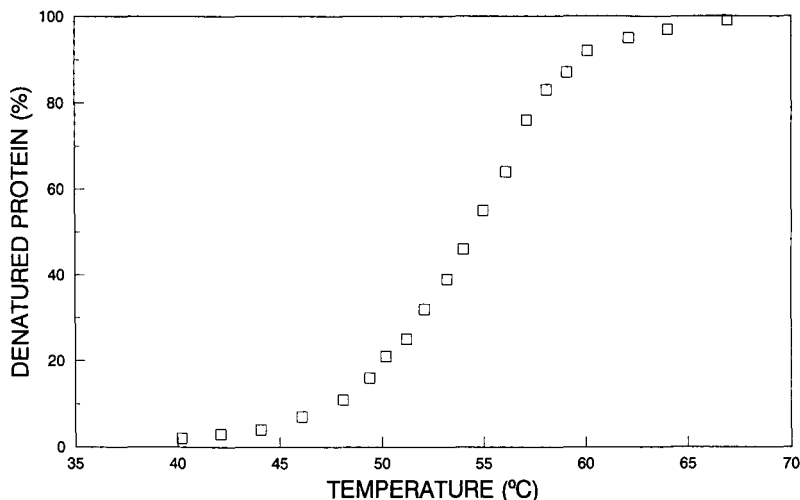


Fig. 5. Fraction denaturation of lysozyme. Calculation with an axis transformation from Fig. 2.

fraction of native protein;  $f_d$  is then  $1 - f_n$ . For most transition temperature determinations, applying this extra correction resulted in insignificant shifts that lay within the experimental error of 1–2°C. Only in the construction of Fig. 11 was a meaningful correction found to be necessary, because a drastic reduction in protein recovery occurred. With further optimization of the procedure and an experimental error below 1°C, peak-area data will have to be used as a standard procedure.

The determination of the transition point is done with a linear regression plot of  $\log K$  against  $1/T$ . Here  $K$  is the equilibrium constant, assuming an equilibrium between the native and the denatured form of the protein.  $K$  is calculated with  $f_d/(1 - f_d)$  and  $\log K = 0$  corresponds to the transition point. A transition slope or steepness is determined from the same plot using four or five values around the transition point.

## RESULTS AND DISCUSSION

### *Mobile phase*

First the influence of the mobile phase on the transition temperature of lysozyme and myoglobin is considered. Similar batchwise measurements have been done in the past; here they demonstrate the feasibility in an HPLC situation. The protein is injected in an empty stainless-steel column, using standard equipment.

Transition points for lysozyme are determined in several percentages of methanol and *n*-propanol (Fig. 6). Too high concentrations of organic modifier cause irregular transition curves, so for propanol transition points could only be measured up to 30% organic solvent. A clear relationship is apparent. The transition temperatures decrease with increasing amount of organic modifier. This decrease is greater with *n*-propanol and points at an effect caused by the apolar chain of the molecule. This apolar chain probably interferes with hydrophobic bonds within the protein molecule [10,16]. The transition points also decrease with decreasing pH (Fig. 7), which is probably due to protonation of the protein and electrostatic repulsion between parts of the macromolecule [10,11].

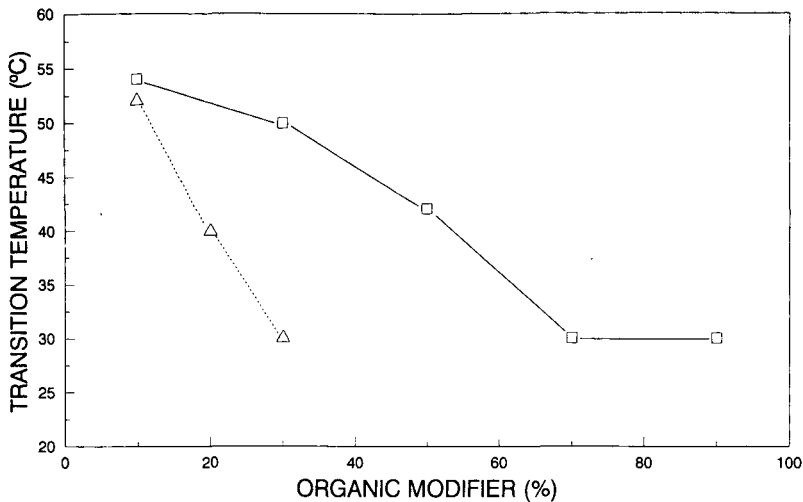


Fig. 6. Transition points of lysozyme in mobile phases containing different amounts of organic modifier, (□) methanol and (△) *n*-propanol. Mobile phase, organic modifier-0.005 *M* HCl + 0.02 *M* NaCl. Flow-rate, 1 ml/min.

It is interesting to note that the transition points of lysozyme do not decrease below 20–25°C. Attempts to decrease the transition temperature at 70% methanol by increasing the acidity were unsuccessful (Table I). An explanation must probably be sought in a stabilizing effect of the lower temperature, making the protein less vulnerable to other environmental influences. Thus it appears that lysozyme is an extremely stable protein that has to be used under very harsh conditions to create an

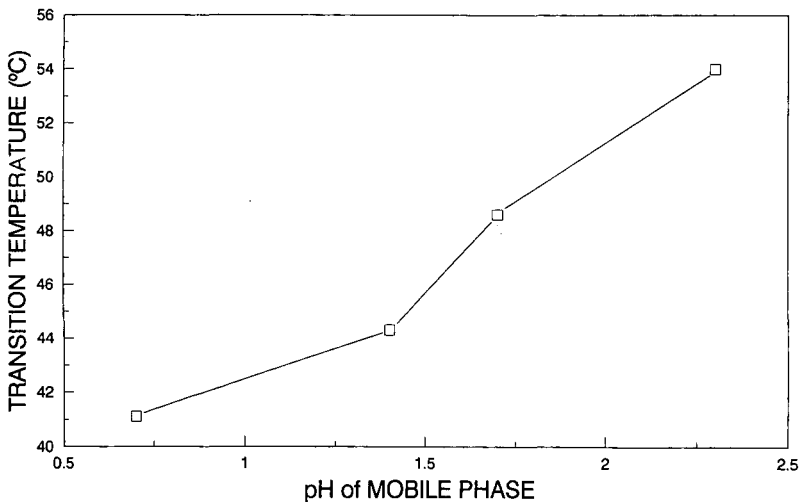


Fig. 7. Transition points of lysozyme in mobile phases with several pH values. pH as measured in the inorganic part before addition of 10% methanol. Mobile phase, methanol-HCl (10:90) + 0.02 *M* NaCl. Flow-rate, 1 ml/min.

TABLE I

EFFECT OF ACIDITY ON THE TRANSITION POINT OF LYSOZYME IN 70% METHANOL AS DETERMINED IN AN EMPTY COLUMN

Mobile phase, 70% methanol-30% HCl + 0.02 M NaCl. Flow-rate, 1 ml/min. Lysozyme concentration, 1 mg/ml.

HCl concentration (M)	Transition point (°C)
0.005	30
0.05	27
0.5	29

artificial test situation. The consequences of this phenomenon for the reliability of the transition temperature for the characterization of packing materials should be a matter of concern when developing a quantitative technique. As the transition temperatures will be part of a stationary phase classification, insight into the range of applicability is important. A method to compare stationary phases with respect to denaturing effects can probably not be achieved with a single protein as a probe.

For myoglobin similar relationships with pH and organic modifier can be found (Figs. 8-10). A considerable transition point depression is seen to occur under relatively mild mobile phase conditions, *i.e.*, a pH value not differing much from the physiological range.

The preceding measurements demonstrate the applicability of the technique in a standard HPLC flow system.

#### Residence time

Retention times in a packed column will be influenced by the mobile phase

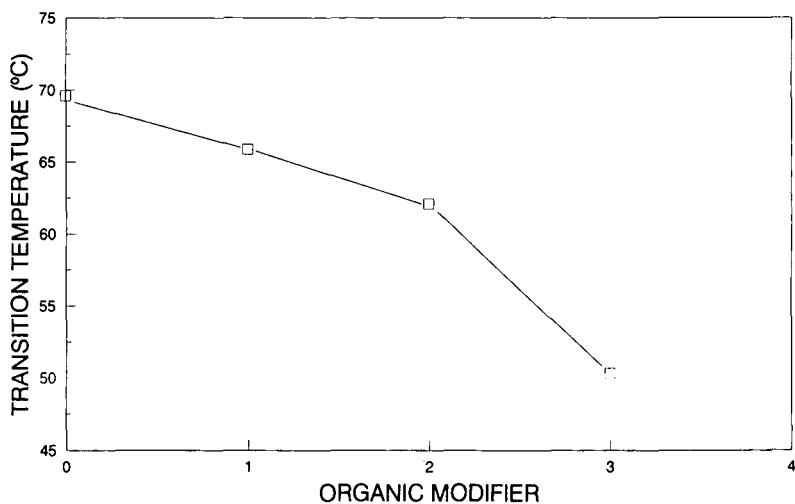


Fig. 8. Transition points of myoglobin in mobile phases containing different organic modifiers. Mobile phase, organic modifier-0.1 M phosphate-citrate buffer (pH 4.0) (10:90). 0, No organic modifier; 1 = methanol; 2 = ethanol; 3 = *n*-propanol. Flow-rate, 1 ml/min.

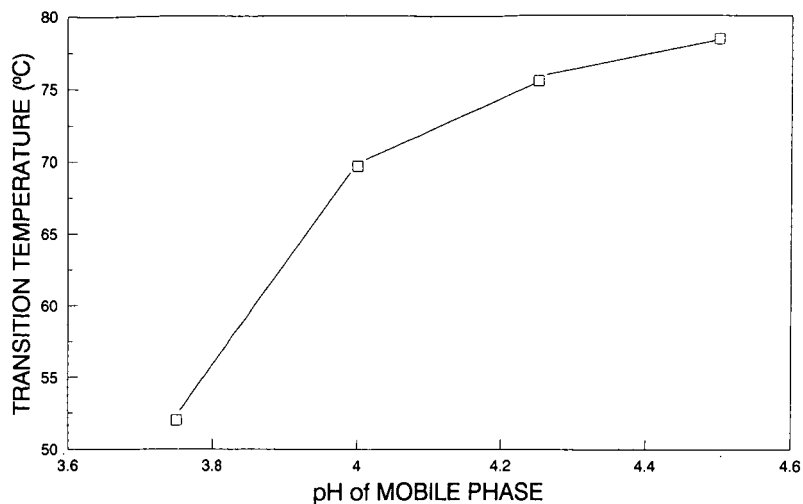


Fig. 9. Transition points of myoglobin in mobile phases with different pH values. Mobile phase, 0.01 *M* phosphate-citrate buffer. Flow-rate, 1 ml/min.

composition. It is therefore necessary to know the effect of residence in the flow system on transition points (Table II). For both lysozyme and myoglobin there appears to be an interval in which the residence time has little effect on the transition temperature, compared with the experimental error of 1–2°C. At a very short residence time in the column the transition point of lysozyme increases, probably because there is not enough time to heat the mobile phase. For myoglobin a residence from 0.5 to almost 7 min has hardly any effect on the transition point.

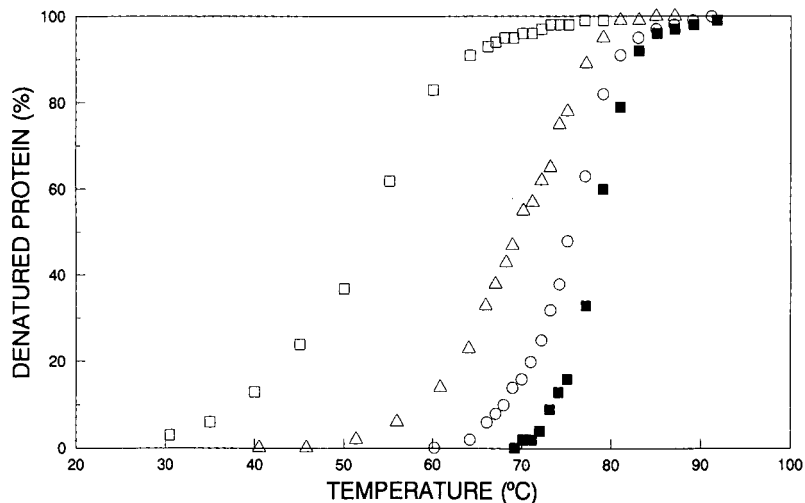


Fig. 10. Multi-transition plot of myoglobin at several pH values: □ = 3.75; △ = 4.00; ○ = 4.25; ■ = 4.50. Conditions as in Fig. 9.

TABLE II

## EFFECT OF RESIDENCE TIME IN AN EMPTY COLUMN ON TRANSITION TEMPERATURE

Residence time varied with flow-rate. Mobile phase: LYS, methanol-0.005 *M* HCl + NaCl as specified in the second column; MYO, 0.01 *M* phosphate-citrate buffer (pH 4.0). Lysozyme concentration, 1-10 mg/ml; myoglobin concentration, 2 mg/ml.

Protein	Mobile phase	$t_R$ (min)	$T_{ir}$ (°C)
LYS	10:90 + 0.25 <i>M</i> NaCl	0.2	54.8
		0.3	54.0
		0.7	53.7
		1.4	53.1
LYS	30:70 + 0.02 <i>M</i> NaCl	0.7	49.9
		0.9	49.6
		1.2	48.5
LYS	50:50 + 0.02 <i>M</i> NaCl	0.6	42.0
		0.8	42.2
		1.0	41.8
		1.2	41.1
MYO	See above	0.6	69.6
		1.2	71.4
		2.1	67.8
		3.2	66.9
		6.8	67.6

*Silica*

Next the influence of a silica packing material was considered. At several methanol concentrations there is no clear effect of the silica on the transition temperature of lysozyme (Table III). It should be noted that under the conditions employed there is hardly any retention on the silica surface. We were not able to record transition curves for lysozyme with a mobile phase that caused a retention on bare silica. To obtain retention of lysozyme on bare silica, the pH would have to be increased. This causes extensive aggregation of the denatured protein [14] and subsequently results in poor transition curves. Changes in salt concentration and flow-rate do not alter the

TABLE III

## EFFECT OF BARE SILICA ON TRANSITION TEMPERATURE OF LYSOZYME

Mobile phase, methanol-0.005 *M* HCl + NaCl as specified in the first column. Flow-rate, 1 ml/min. Lysozyme concentration, 1-10 mg/ml. Silica: Hypersil WP 300, 10  $\mu$ m.

Mobile phase	Bare silica			Empty column		
	[LYS] (mg/ml)	$T_{ir}$ (°C)	$t_R$ (min)	[LYS] (mg/ml)	$T_{ir}$ (°C)	$t_R$ (min)
10:90 + 0.25 <i>M</i> NaCl	10	53.6	0.8	10	53.7	0.7
30:70 + 0.02 <i>M</i> NaCl	5	51.0	0.7	5	50.0	0.7
50:50 + 0.02 <i>M</i> NaCl	1	40.4	0.8	5	42.0	0.6

TABLE IV

## EFFECT OF SODIUM CHLORIDE CONCENTRATION ON TRANSITION TEMPERATURE OF LYSOZYME IN A COLUMN PACKED WITH BARE SILICA

Mobile phase, methanol-0.005 *M* HCl (10:90) + NaCl. Flow-rate, 1 ml/min;  $t_{RO}$  = 0.7-0.8 min; lysozyme concentration = 1-10 mg/ml.

NaCl concentration ( <i>M</i> )	[LYS] (mg/ml)	$T_{tr}$ (°C)	$t_R$ (min)
0.02	1	53.5	0.8
0.1	1	52.6	0.8
0.25	10	53.6	0.8
0.5	10	53.0	0.8

picture (Tables IV and V). The results indicate that in the absence of retention, lysozyme can pass through a microparticulate packed bed without measurable denaturation.

A casual finding is a relationship with protein concentration (Table VI). The protein is slightly more stable when a more concentrated solution is injected. The stability of lysozyme makes this protein well suited for handling and subsequent measurement. An error of measurement of 1-2°C could not be avoided, however.

The denaturation of myoglobin by interaction with bare silica cannot be studied easily because in many instances the protein does not elute. Only at pH 10 does a clear, nearly unretained peak come off the column. Then, however, the recording of a transition curve became a problem because high temperatures combined with a high pH resulted in steep pressure rises. The transition clearly lies at lower temperatures than the situation without packing (Fig. 11). Thus, with myoglobin contact with bare

TABLE V

## EFFECT OF FLOW-RATE ON TRANSITION TEMPERATURE OF LYSOZYME IN A COLUMN PACKED WITH BARE SILICA

Mobile phase, methanol-0.005 *M* HCl + NaCl as specified in the first column. Lysozyme concentration, 1-10 mg/ml.

Mobile phase	Flow-rate (ml/min)	[LYS] (mg/ml)	$T_{tr}$ (°C)	$t_R$ (min)
50:50 + 0.02 <i>M</i> NaCl	1.0	1	40.4	0.8
	0.5	5	40.6	1.5
30:70 + 0.02 <i>M</i> NaCl	3.0	1	48.7	0.3
	1.0	1	47.8	0.8
10:90 + 0.25 <i>M</i> NaCl	2.0	10	55.7	0.4
	1.0	10	53.6	0.8
	0.5	10	55.9	1.6
10:90 + 0.10 <i>M</i> NaCl	2.0	10	54.8	0.4
	1.0	10	55.5	0.8
	0.5	10	53.5	1.5
10:90 + 0.10 <i>M</i> NaCl	3.0	1	53.8	0.3
	1.0	1	52.6	0.8

TABLE VI

## EFFECT OF LYSOZYME CONCENTRATION ON TRANSITION POINT OF LYSOZYME IN A COLUMN PACKED WITH SILICA

Flow-rate, 1 ml/min. Mobile phase, methanol-0.005 M HCl (30:70) + 0.02 M NaCl.

Protein concentration (mg/ml)	$T_{tr}$ (°C)
5	51.0
2.5	49.1
1	47.8

silica is accompanied by a significant shift in transition. The retention could not be influenced by lowering the salt concentration. It would have been interesting to see if an increase in interaction resulted in a further decrease in transition point. The protein was slightly more stable, however, in 0.01 M than in 0.1 M sodium chloride solution both in an empty column and in the column packed with silica.

*Silica coating*

After coating of the silica with epoxy glucose [21], the retention time of lysozyme is dependent on the sodium chloride concentration (Table VII; Fig. 12). With no salt added there is an unretained elution and the transition is about the same as in an empty column. At higher sodium chloride concentration the retention increases while the transition point decreases. In view of previous experiments, where the retention time and the sodium chloride concentration were varied, this decrease is consid-

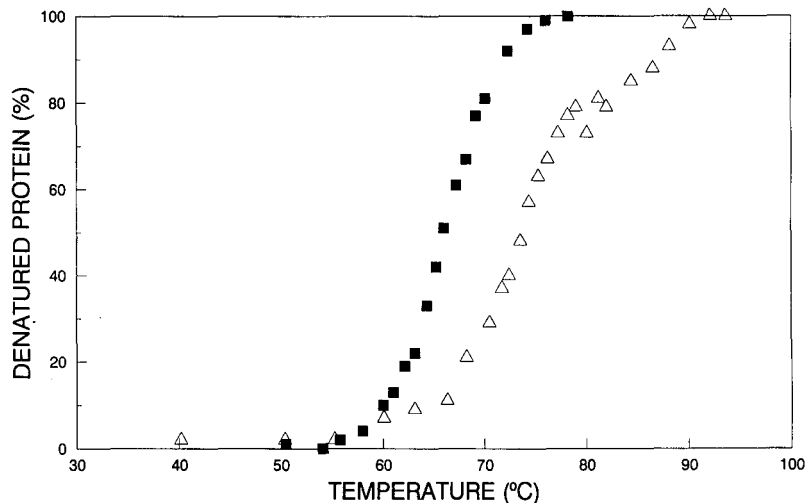


Fig. 11. Transition of myoglobin in column packed with bare silica (■, Hypersil WP) compared with transition in an empty column (△). Mobile phase, 0.01 M phosphate buffer (pH 10.0) + 0.1 M NaCl. Flow-rate, 1 ml/min. Silica column calculation with correction for protein loss using peak height as a measure of protein recovery.



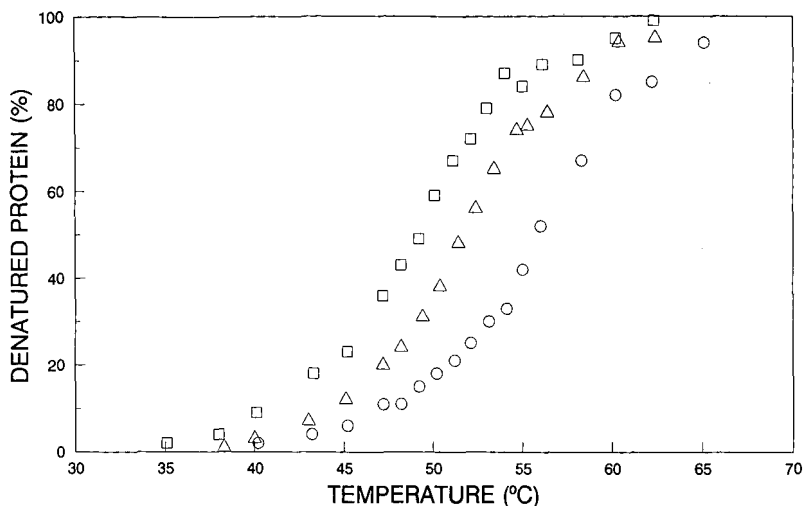


Fig. 12. Transition of lysozyme in a column packed with epoxy glucose-coated silica at three different sodium chloride concentrations: □ = 1.0; △ = 0.1; ○ = 0.01 *M*. Conditions as in Table VII.

ered to be due to the interaction with the stationary phase. This behaviour has been described in the past as hydrophobic interaction. Hence with lysozyme the generally accepted relationship between retention and denaturation is seen to apply. This detrimental interaction is not influenced by flow-rate (Table VIII). With the epoxy glucose-coated material, myoglobin transition measurements at pH 4.0 are possible. The epoxy glucose coating causes a clear depression of the transition point with unretained elution of the protein (Fig. 13) (Tables II and VIII).

#### Relative contribution

After studying a number of transition curves, the relative contribution of the stationary phase compared with the eluent contribution can be established. This should be regarded as an important advantage of transition point determinations. The effect of a packing material on the conformation change of a protein can be expressed in the same terms as the effect of a certain solvent condition. With the two

TABLE VII

EFFECT OF SURFACE INTERACTION ON TRANSITION POINT OF LYSOZYME IN A COLUMN PACKED WITH EPOXY GLUCOSE-COATED SILICA

Mobile phase, methanol-0.005 *M* HCl (10:90) + NaCl. Flow-rate, 1 ml/min. Lysozyme concentration, 2.5 ml/ml.

NaCl concentration ( <i>M</i> )	$t_R$ (min)	$T_{tr}$ (°C)
0.01	0.68	56.0
0.1	0.74	51.7
1.0	0.81	49.0

TABLE VIII

EFFECT OF FLOW-RATE ON TRANSITION TEMPERATURE IN A COLUMN PACKED WITH EPOXY GLUCOSE-COATED SILICA

Mobile phase: LYS, methanol-0.005 M HCl (10:90) + 0.5 M NaCl; MYO, 0.01 M phosphate-citrate (pH 4.0). Lysozyme concentration, 2.5 mg/ml. Myoglobin concentration, 2 mg/ml.

Protein	Flow-rate (ml/min)	$t_R$ (min)	$T_{tr}$ (°C)
LYS	1.0	0.7	48.8
	0.5	1.3	48.4
MYO	1.0	0.6	58.2
	0.5	1.1	58.1
	0.2	2.7	58.0
	0.1	5.7	57.0

proteins studied in this paper and the mobile and stationary phases that allow good elution, the effect of the stationary phase is of the same order of magnitude as the effect of a change in pH or the addition of some modifier. This can be convenient in more theoretical considerations, as the representation of denaturation as used for solvent modifiers might be applicable to the stationary phase effect.

#### Transition steepness

From the transition curves, a transition steepness or slope can be determined around the transition point. The large slope is ascribed to the phenomenon of "cooperativity" [22]. A certain small change in the conformation of the protein triggers the unwinding of the complete molecule. There seems to be a favoured route in the transition from native to denatured state and *vice versa*, with no intermediate states

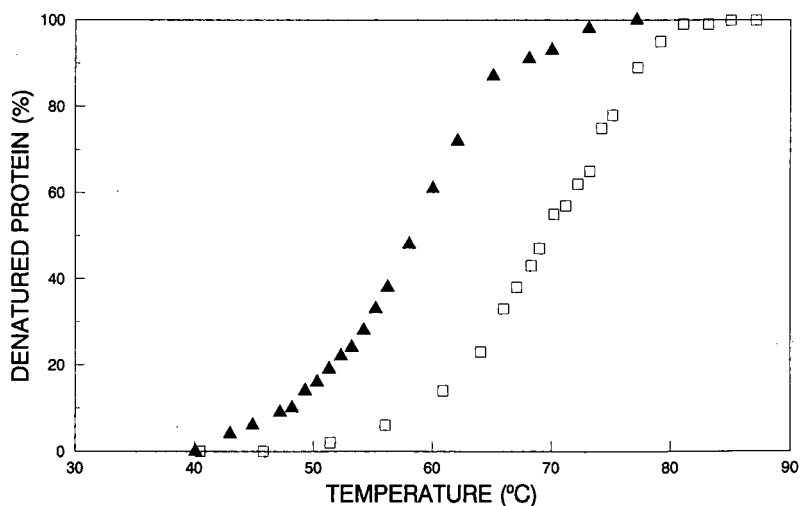


Fig. 13. Transition of myoglobin in (▲) a column packed with epoxy glucose-coated silica compared with (□) an empty column. Mobile phase, 0.01 M phosphate buffer (pH 4.0). Flow-rate, 1 ml/min.

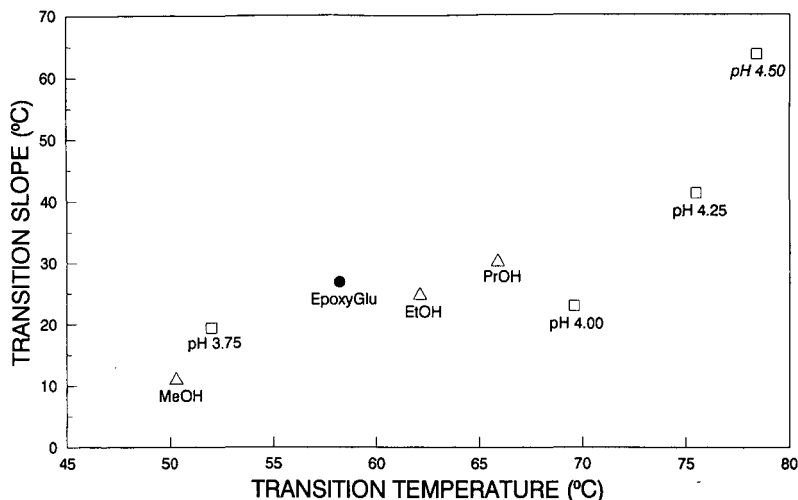


Fig. 14. Steepness of transition of myoglobin plotted against transition temperature. Calculation from  $\log K$  vs.  $1/T$  plot. Conditions as in Figs. 8, 9 and 13.  $\square$  = pH 3.75, 4.00, 4.25, 4.50;  $\triangle$  = methanol (MeOH), ethanol (EtOH), *n*-propanol (PrOH);  $\bullet$  = epoxy glucose (EpoxyGlu).

that are stable enough to be detected. A relationship with temperature seems likely (Fig. 14). Transitions in the neighbourhood of 80°C are steeper than those at 50–60°C, but the relationship is more complicated. With an increase in pH from 3.75 to 4.0 the transition temperature rises from 50 to 70°C without a significant increase in steepness. Steepness is probably also a function of factors that promote the transition such as protonation of the molecule and addition of organic modifier.

The steepness or slope of the transition has been used in the past to calculate a reaction enthalpy. The figures calculated from our results seem to correspond with values from the literature [11], given the differences in the conditions used. The precise meaning in this flow system is not completely clear, however.

Attention was concentrated on differences between packed and empty columns. An intermediate state was found repeatedly for the transition of myoglobin at pH 10, as can be seen in Fig. 11. In the transition there is a small interval where the protein has not reached in completely denatured state, but is relatively insensitive to temperature changes. On a further increase in temperature the UV difference again changes sharply to reach a final state. More information on the residual structure of denatured proteins, in particular lysozyme, can be found in the work of Aune *et al.* [19] and Kurono and Hamaguchi [14]. In a packed column, however, this transition is slightly steeper with no discernible unevenness that could suggest a stable intermediate state. This could indicate that the silica cooperates in some way in the denaturation of the protein. With the calculation of this plot as correction was made for the protein loss on the column. It is not known how intermediates elute compared with the native and the denatured molecule.

At pH 4.0 in an epoxy glucose column, where the transition of myoglobin shifts drastically, the steepness changes very little. More elaborate measurements are necessary to demonstrate a clear effect and to relate the steepness to *e.g.*, the flow-rate.

## CONCLUSION

From both lysozyme and myoglobin a transition curve can be obtained in an HPLC system using a diode-array detector and the phenomenon of UV difference spectrometry. The position of the curves can be influenced by the mobile phase composition. Shifts of the transition curves also occur in the presence of packing material. The depression of the transition point is not a function of flow-rates as used in ordinary HPLC. The procedure needs further optimization to demonstrate effects in the 0.1°C range.

The relative contribution to denaturation of the stationary phase compared with those due to mobile phase changes is easily measured with transition curves. The procedure and the findings should lead to a method for comparing stationary phases as regards denaturing effects on proteins, knowing that a conformation change is only one aspect of the broader concept of denaturation. Measurements were done with only two proteins and a limited number of mobile phase compositions. Comparisons of stationary phases will involve proteins that elute under widely different conditions. A useful study of denaturing effects should be done under normal chromatographic conditions. It is unlikely that this will be possible with a limited number of test proteins and difference spectrometry. An alternative approach would be to use another detector, *e.g.*, a flow-through light-scattering detector or a post-column enzyme reaction detector. With the latter, unpurified proteins could also be tested.

To direct synthetic approaches, however, a small number of proteins and mobile phase compositions are probably sufficient. Used in an artificial environment, these proteins become part of the product characterization. They allow the probing of surfaces and may be an important tool in the fine tuning of coating chemistry. Further efforts in this direction are being made.

## REFERENCE

- 1 T. Takakuwa, Y. Kurosu, N. Sakayanagi, F. Kaneuchi, N. Takeuchi, A. Wada and M. Senda, *J. Liq. Chromatogr.*, 10 (1987) 2759.
- 2 I. S. Krull, H. H. Stuting and S. C. Krzysko, *J. Chromatogr.*, 442 (1988) 29.
- 3 X. M. Lu, A. Figueroa and B. L. Karger, *J. Am. Chem. Soc.*, 110 (1988) 1978.
- 4 S. Y. M. Lau, A. K. Taneja and R. S. Hodges, *J. Chromatogr.*, 317 (1984) 129.
- 5 M. T. Hearn and M. I. Aguilar, *J. Chromatogr.*, 397 (1987) 47.
- 6 G. E. Katzenstein, S. A. Vrona, R. S. Wechsler, B. L. Steadman, R. V. Lewis and C. R. Middaugh, *Proc. Natl. Acad. Sci. U.S.A.*, 83 (1986) 4268.
- 7 R. J. T. Corbett and R. S. Roche, *Biochemistry*, 23 (1984) 1888.
- 8 K. Benedek, *J. Chromatogr.*, 458 (1988) 93.
- 9 M. T. Aubel and G. Guiochon, *J. Chromatogr.*, 498 (1990) 281.
- 10 R. Scopes, *Protein Purification*, Springer, New York, 1982.
- 11 A. J. Sophianopoulos and B. J. Weiss, *Biochemistry*, 3 (1964) 1920.
- 12 D.F. Nicoli and G. B. Benedek, *Biopolymers*, 15 (1976) 1421.
- 13 G. Acampora and J. Hermans, Jr., *J. Am. Chem. Soc.*, 89 (1967) 1543.
- 14 A. Kuroso and K. Hamaguchi, *J. Biochem.*, 56 (1964) 432.
- 15 C. Tanford, *Adv. Protein Chem.*, 23 (1968) 121.
- 16 J. G. Foss, *Biochem. Biophys. Acta*, 47 (1961) 569.
- 17 S. Yanari and F. A. Bovey, *J. Biol. Chem.*, 235 (1960) 2818.
- 18 S. J. Leach and H. A. Scheraga, *J. Biol. Chem.*, 235 (1960) 2827.
- 19 K. C. Aune, A. Salahuddin, M. H. Zarlengo and C. Tanford, *J. Biol. Chem.*, 242 (1967) 4486.
- 20 J. F. Brandts, *J. Am. Chem. Soc.*, 86 (1964) 4291.
- 21 R. E. Huisden, J. C. Kraak and H. Poppe, *J. Chromatogr.*, 508 (1990) 289.
- 22 A. L. Lehninger, *Biochemistry*, Worth, New York, 1970.

## Chemical, physical and chromatographic properties of Superdex 75 prep grade and Superdex 200 prep grade gel filtration media

LENNART KÅGEDAL\*, BJÖRN ENGSTRÖM<sup>a</sup>, HANS ELLEGREN<sup>b</sup>, ANNA-KARIN LIEBER, HÅKAN LUNDSTRÖM, ANNELIE SKÖLD and MIKAEL SCHENNING

*Pharmacia LKB Biotechnology, S-751 82 Uppsala (Sweden)*

(First received April 9th, 1990; revised manuscript received August 20th, 1990)

---

### ABSTRACT

Two novel gel filtration media, Superdex 75 prep grade and Superdex 200 prep grade are described. The new media have high selectivities similar to those of Sephadex G-75 and G-200, respectively, but permit the use of high flow-rates as with cross-linked agarose beads. They consist of cross-linked agarose beads modified with dextran to obtain the desired selectivity. The mean particle size is *ca.* 33  $\mu\text{m}$  (30–36  $\mu\text{m}$ ) and a reduced plate height of *ca.* 2.0 is regularly obtained in packed columns. A flow-rate of 50 cm/h can be used even in large columns. The media are chemically stable at pH 3–14 and can be used with a wide range of eluents. The performance of the media with respect to flow-rate, sample load and sample concentration for given model systems is described. Superdex 75 prep grade was used to separate monomeric forms of a recombinant fusion protein (ZZ-brain insulin-like growth factor molecular weight 22 000 dalton) from dimers and oligomers. Superdex 200 prep grade was used to obtain baseline separation of a monoclonal antibody from antibody dimer and contaminating transferrin.

---

### INTRODUCTION

In 1959, Sephadex gels were introduced as the first media for the gel filtration of water-soluble macromolecules [1,2]. Since then, a host of chromatographic supports for gel filtration have become available from a number of sources. The technique has been reviewed several times, *e.g.*, see papers by Hagel [3] and Fischer [4] and references cited therein.

Sephadex represents a class of gels termed xerogels. These are characterized by complete collapse of the gel structure on removal of solvent (water) [5–7]. In fact, such gels can, in the swollen state, be regarded as elastic solutions as opposed to ordinary viscous solutions. Cross-linked polyacrylamide gels such as those of the Bio-Gel P series belong to the same type of gels. Chromatographically they are characterized by high selectivities, *i.e.*, large differences in partition coefficients ( $K_D$ ) for proteins or other macromolecules of different molecular weight.

---

<sup>a</sup> Present address: Casco Nobel, P.O. Box 13000, S-850 13 Sundsvall, Sweden.

<sup>b</sup> Present address: Department of Animal Breeding and Genetics, Swedish University of Agricultural Sciences, Box 596, S-751 24 Uppsala, Sweden.

The main drawback with these kinds of gels is their limited rigidity, which causes the gel particle to deform when exposed to drag forces generated by liquid flow in a chromatographic column. Gels with permanent pores (aerogels), such as porous glass, are not deformed and allow much higher flow-rates to be used. Many so-called macroporous gels, used for the chromatography of biological macromolecules, are xerogel-aerogel hybrids. Gels based on agarose belong to this category, in addition to many gels based on synthetic polymers. The aerogel element in these gels confers high flow resistance but they suffer from comparatively low selectivity. It seems that the limitation with regard to selectivity is inherent in the macroporous structure of these materials.

Superdex 75 prep grade and Superdex 200 prep grade combine the high selectivity of the xerogels with the high flow resistance of the xerogel-aerogel hybrids. The Superdex gels are made by a proprietary method in which cross-linked agarose beads provide the required mechanical strength. Dextran is incorporated into the macropores of the beads by covalent binding of the polysaccharide chains to the surface of the walls of the pores and to the periphery of the beads. The immobilized chains of dextran behave in water as an immobilized polysaccharide solution and afford a gel filtration phase similar to that in beads of Sephadex.

The use of composite materials similar to the Superdex gels is not new. Ultrogel AcA supports (Reactifs IBF, France) are claimed to receive their mechanical strength from an agarose matrix encompassing an acrylamide polymer which provides high resolution in gel filtration. Sephacryl beads (Pharmacia LKB Biotechnology, Sweden) are also composite materials. They are made by cross-linking allyldextran with N,N-methylenebisacrylamide and a core structure of polymerized N,N-methylenebisacrylamide formed in this process is assumed to be the major contributor to the rigidity of the particles.

In 1987, Hjertén *et al.* [8] reported a downward shift of the exclusion limit of agarose gels when coupling dextran to residual vinyl groups after cross-linking of the gel with divinyl sulphone.

A separate paper [9] described the performance of Superdex 75 prep grade and Superdex 200 prep grade in buffers of different pH and ionic strengths and after repeated treatment with 1 M sodium hydroxide or 0.1 M hydrochloric acid. Superdex 200 prep grade and Superdex 75 prep grade have been used in the purification of a fusion protein containing a malaria antigen [10], in the large-scale purification of staphylococcal enterotoxin B [11] and in the development of a production system for recombinant human superoxide dismutase [12].

## EXPERIMENTAL

### *Nomenclature and calculations*

The following nomenclature and equations were used to characterize columns and chromatographic resolution:

$V_0$	Void volume of column
$V_c$	Geometric volume of column
$V_p$	Pore volume of column
$V_s$	Support (matrix) volume of column
$V_t$	Total liquid volume of column

$V_p/V_0$	Permeability
$V_R$	Retention (elution) volume
$V_{R,n}$	Retention volume of peak No. $n$
$K_D$	Distribution coefficient for a solute passing through a gel filtration column
$K_{av}$	Fraction of stationary gel volume accessible to a given solute
$N$	Number of theoretical plates
$R_s$	Chromatographic resolution
$W_{b,n}$	Width of peak No. $n$ at base of peak
MW	Molecular weight
$W_h$	Peak width at half-height

$$V_c = V_0 + V_s + V_p$$

$$V_{s,rel} = \frac{V_s}{V_p + V_s}$$

$$V_{p,rel} = \frac{V_p}{V_p + V_s}$$

$$K_D = \frac{V_R - V_0}{V_t - V_0}$$

$$K_{av} = \frac{V_R - V_0}{V_c - V_0}$$

$$N = 5.54(V_R/W_h)^2$$

$$R_s = \frac{2(V_{R,n+1} - V_{R,n})}{W_{b,n+1} + W_{b,n}}$$

### Chemicals

Superdex 75 prep grade, Superdex 200 prep grade, Sephadex G-75 and Sephadex G-200 were supplied by Pharmacia LKB Biotechnology. A partly purified sample of ZZ-brain IGF (recombinant brain insulin-like growth factor fused to an IgG-binding peptide) was kindly provided by KabiGen (Stockholm, Sweden) as a freeze-dried powder. Substances used in the evaluation of the chromatographic performance of the supports are listed in Table I.

### Equipment

All equipment was obtained from Pharmacia LKB Biotechnology unless specified otherwise.

(i) Determination of selectivity curves: FPLC system, HR 10/30 columns, RefractoMonitor III (Laboratory Data Control, Riviera Beach, FL, U.S.A.), Optilab 901 (Tecator, Höganäs, Sweden). (ii) Gel filtration of protein mixtures (Fig. 3): P-3500 pump, BioPilot column, Rec. 481 recorder, UV-M detector with 2-mm cell.

TABLE I  
SUBSTANCES USED FOR EVALUATION OF CHROMATOGRAPHIC PERFORMANCE

Substance	Molecular weight	Isoelectric point	Source
Blue Dextran 2000	2 000 000		Pharmacia
Thyroglobulin	669 000		Pharmacia
Ferritin	440 000		Pharmacia/Sigma
Aldolase	158 000		Pharmacia
Immunoglobulin G (IgG)	156 000		Pharmacia/Sigma
Transferrin	77 000		Kabi/Sigma
Bovine serum albumin (BSA)	67 000	ca. 5	Pharmacia/Sigma
Ovalbumin	43 000	4.7	Pharmacia
Chymotrypsinogen A (Chym A)	25 000		Pharmacia
Myoglobin	18 800		Sigma
Ribonuclease (RNase)	13 700	8.9	Pharmacia
Cytochrome <i>c</i> (Cyt <i>c</i> )	12 600	ca. 9.2	Sigma
Aprotinin	6500		Fluka/Sigma
Vitamin B <sub>12</sub>	1400		Sigma
Raffinose	594		
Cytidine	243		Fluka
Glucose	180		
Deuterium oxide	20		Merck
Dextran	<sup>a</sup>		Pharmacia

<sup>a</sup> Mean molecular weight of dextran fractions (Pharmacia): 276 500, 196 300, 123 600, 66 700, 43 500, 21 400, 9890, 4440, 1080 and 594.

(iii) Study of chemical stability (Fig. 5): P-500 pump, V-7 injector with 200- $\mu$ l loop, UV-1 detector with HR 10-mm cell, Rec. 481 recorder. (iv) Study of the influence of flow-rate, sample size and protein load: BioPilot system including a UV-M detector in work with Superdex 75 prep grade and FPLC system with a UV-1 or UV-2 detector in work with Superdex 200 prep grade. (v) Purification of ZZ-brain IGF: P-500 pump, MV-7 valve, UV-M detector, REC-482 recorder, FRAC-100 fraction collector, LCC-500 control unit, SpeedVac freeze-drier (Savant) and PhastSystem for electrophoresis. (vi) Purification of IgG<sub>2a</sub> monoclonal antibody: BioPilot system and PhastSystem. (vii) Particle size analysis: Coulter Counter ZM equipped with C-256 pulse-height analyser and calibrated with Superdex samples measured by microscope analysis [13,14].

#### *Chromatographic and electrophoretic methods*

Details regarding chromatographic conditions are given in the figure legends. Sodium dodecyl sulphate-polyacrylamide gel electrophoresis (SDS-PAGE) was performed under non-reducing conditions on PhastGel Gradient 8-25. The separations and the Commassie brilliant blue and silver staining procedures were carried out according to the PhastSystem manual. Other conditions are given in the figure legends.



## RESULTS

*Selectivity, fractionation range and other physical and chemical properties*

We used deuterium oxide as a marker for the total liquid volume of columns ( $V_t$ ). This has been shown to give an overestimate of the  $V_t$  value owing to isotope exchange with hydroxyl hydrogens of the gels [15]. No corrections were made for this effect.

In Fig. 1,  $K_D$  values of proteins and vitamin B<sub>12</sub> on Superdex 75 prep grade and Superdex 200 prep grade are presented together with corresponding data for Sephadex G-75 and Sephadex G-200. The amount of dextran incorporated in the beads of Superdex was adjusted to match the selectivities of Sephadex. It is evident that both the steepness of the selectivity curves and the exclusion limits are in good agreement when corresponding Superdex and Sephadex media are compared.

Selectivities as measured by  $K_{av}$  for dextran fractions complemented with raffinose and glucose on Superdex 75 prep grade and Superdex 200 prep grade are shown in Fig. 2.

Chromatography of mixtures of test proteins is shown in Fig. 3. Over a major part of the separation ranges, proteins with a difference in molecular weight of less than a factor of 2 could be separated. With Superdex 75 prep grade a factor of 1.5 will be sufficient in many instances.

Table II lists some properties of Superdex. In order to achieve a high performance in gel filtration, it is essential to keep the pore volume as high as possible,

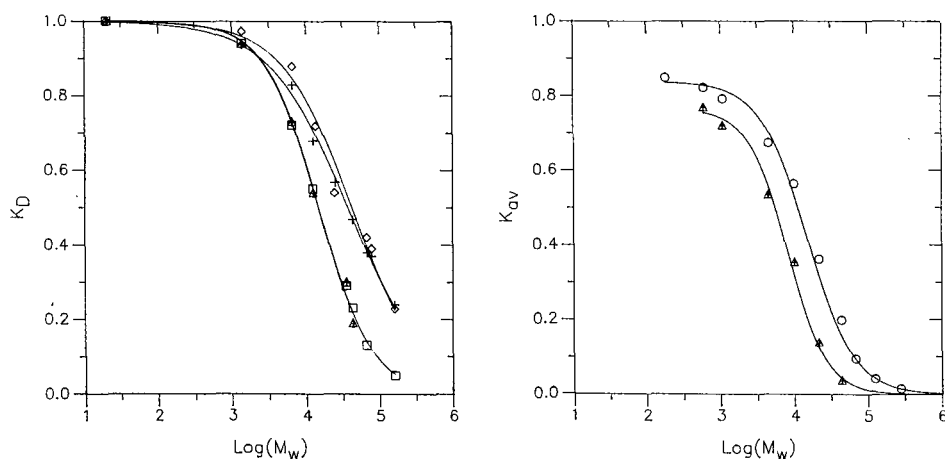


Fig. 1.  $K_D$  of globular proteins and vitamin B<sub>12</sub> versus log MW [ $\log(M_w)$ ] on ( $\square$ ) Superdex 75 prep grade, ( $+$ ) Superdex 200 prep grade, ( $\triangle$ ) Sephadex G-75 and ( $\diamond$ ) Sephadex G-200. Experiments with deuterium oxide as sample and distilled water as eluent were carried out to determine  $V_t$ . Buffer for chromatography of proteins and vitamin B<sub>12</sub>: 50 mM sodium phosphate–100 mM sodium chloride (pH 7.4). Column: HR 10/30. Flow-rates: 0.50 ml/min for Superdex gels, 0.10 or 0.25 ml/min for Sephadex gels. Detection: absorbance at 280 nm for proteins and refractive index (RefractoMonitor III) for deuterium oxide. Sample: deuterium oxide, 200  $\mu$ l; solution of proteins, vitamin B<sub>12</sub> and cytidine in elution buffer, 200  $\mu$ l.

Fig. 2.  $K_{av}$  of dextran fractions, raffinose and glucose on ( $\triangle$ ) Superdex 75 prep grade and ( $\circ$ ) Superdex 200 prep grade versus log MW. Columns: 600  $\times$  26 mm I.D. Eluent: 250 mM sodium chloride and 0.02% sodium azide in water. Flow-rate: 5 ml/min. Detection: Optilab 901.

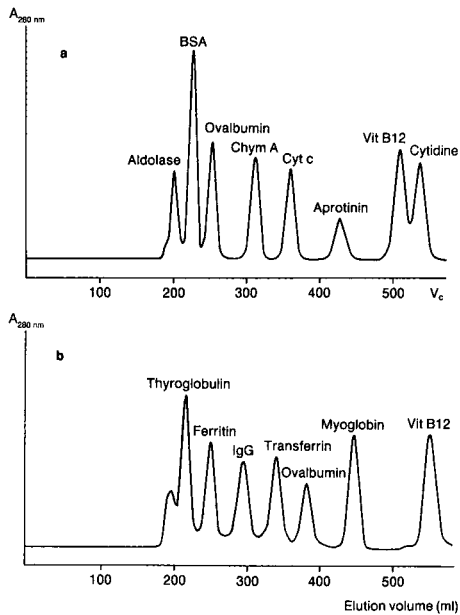


Fig. 3. Chromatography of test mixtures on (a) Superdex 75 prep grade and (b) Superdex 200 prep grade. Column: BioPilot 35/600. Flow-rate: (a) 15 cm/h (2.4 ml/min); (b) 10 cm/h (1.6 ml/min). Buffer: 50 mM sodium phosphate–150 mM sodium chloride–0.01% sodium azide (pH 7.0). Sample size: 1.0 ml. Total concentration of test substances: (a) 23.7 mg/ml; (b) 21.1 mg/ml.  $V_0$  was determined in a separate run with Blue Dextran 2000, 2 mg/ml in buffer, sample size 1.0 ml.

*i.e.*, the matrix volume should be kept to a minimum. It has been possible to reach the exclusion limits with much lower support volumes than would be possible by making conventional macroporous gels.

Particle size distributions are given in Fig. 4. A reduced plate height of *ca.* 2.0 in packed columns has been routinely achieved.

For wide-bore columns (wider than 30 mm), prepacked columns are guaranteed for use at flow-rates up to 50 cm/h. In narrower columns, flow-rates of up to 300 cm/h

TABLE II  
SOME PROPERTIES OF SUPERDEX; TYPICAL VALUES

Property	Superdex 75 prep grade	Superdex 200 prep grade
Particle size $d_{50,v}$	33 $\mu\text{m}$	33 $\mu\text{m}$
Relative matrix volume ( $V_{s,rel}$ )	11%	6%
Void volume fraction ( $V_0/V_c$ ) <sup>a</sup>	~30%	~30%
Permeability ( $V_p/V_0$ ) <sup>a</sup>	2.1	2.2
$N$ (plates/m)	15 000–20 000	15 000–20 000
Approximate separation range, proteins (dalton)	3000–70 000	3000–600 000

<sup>a</sup> In BioPilot 35/600 and 60/600 columns.

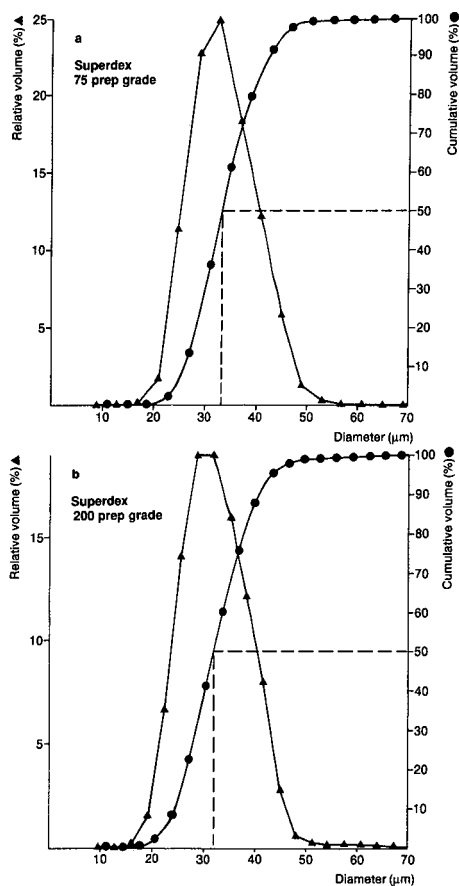


Fig. 4. Particle size distribution of typical lots of Superdex 75 prep grade and Superdex 200 prep grade.

have been used without any marked compression of the gel beds (data not shown). The influence of flow-rate on gel filtration results is discussed below.

The stability of the gels on storage in various aqueous solutions at 40°C for 1 week was studied by measuring  $K_{av}$  before and after storage (Fig. 5). An increase in the  $K_{av}$  value would indicate that some of the dextran has been removed from the pores. In most instances no change in  $K_{av}$  was observed. In 0.5 M sodium hydroxide solution a slight increase was noted. However, as shown in a more detailed study, repeated cleaning in place and sanitization of columns with sodium hydroxide solution had no significant influence on performance [9]. Autoclaving once did not cause any noticeable change in  $K_{av}$ , but after five autoclaving cycles a minor increase was observed.

*Influence of flow-rate, sample load and sample volume on chromatographic performance*

The chromatographic performance of Superdex 75 prep grade was studied using solutions of cytochrome *c* (Cyt *c*), chymotrypsinogen A (Chym A) and bovine serum

albumin (BSA). Resolution was calculated for the Cyt *c*-Chym A pair in experiments where the proteins were run separately on the columns. The results are shown in Figs. 6 and 7.

A more elaborate study was carried out with Superdex 200 prep grade (Figs. 8–15). In this instance a mixture of IgG and transferrin was used. Peaks eluting before the IgG peak represent impurities.

The results show that under conditions normally used in preparative work, flow-rate has only a minor effect on resolution, which corroborates results published by other workers [16] (Figs. 6, 8 and 9). Only with the higher molecular weight proteins used in the experiments with Superdex 200 prep grade was a substantial increase in resolution observed on going to very low flow-rates. The results suggest that it is possible to use the specified maximum flow-rate of 50 cm/h in many preparative applications of the gels.

The influence on resolution of sample load as determined by sample concentration and sample volume has been discussed by several workers [4, 17, 18]. We found that the use of high sample concentrations to obtain high sample loads (up to *ca.* 1 g of protein per litre of gel) had only a small negative effect on resolution (Figs. 10 and 11).

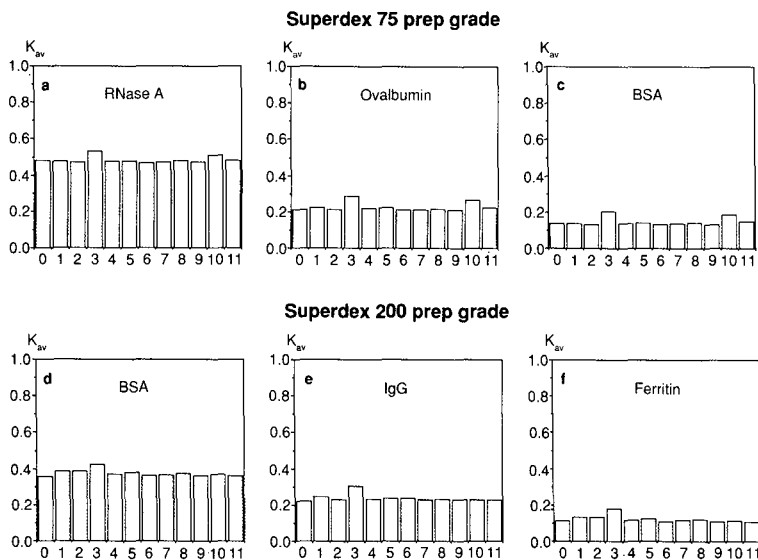


Fig. 5. Stability of Superdex 75 prep grade and Superdex 200 prep grade measured as change in  $K_{av}$  of proteins on storage in various media and after autoclaving. Storage media or autoclaving cycles: 0, control; 1, 1.0 M acetic acid; 2, 50 mM sodium phosphate, 2.0 M NaCl (pH 7.0); 3, 0.5 M NaOH; 4, 30% isopropanol; 5, 30% acetonitrile; 6, 2% SDS; 7, 6.0 M guanidinium · HCl; 8, 8.0 M urea; 9, 24% ethanol; 10, autoclaving five times; 11, autoclaving once. Storage test (1–9): the gel was washed with the storage medium on a glass filter and kept in the medium at 40°C for 7 days (experiments 1–8) and 4 weeks (experiment 9). Autoclaving: experiments 10 and 11, 121°C for 20 min. After storage or autoclaving the gels were washed with distilled water and packed in HR 16/50 columns for chromatographic testing. Chromatographic conditions: 200  $\mu$ l of a mixture of three proteins were applied and eluted at a flow-rate of 15 cm/h (Superdex 75 prep grade) or 10 cm/h (Superdex 200 prep grade). Buffers as in Fig. 2.  $V_0$  was determined in a separate run with Blue Dextran 2000, 2 mg/ml in buffer, sample size 1.0 ml.

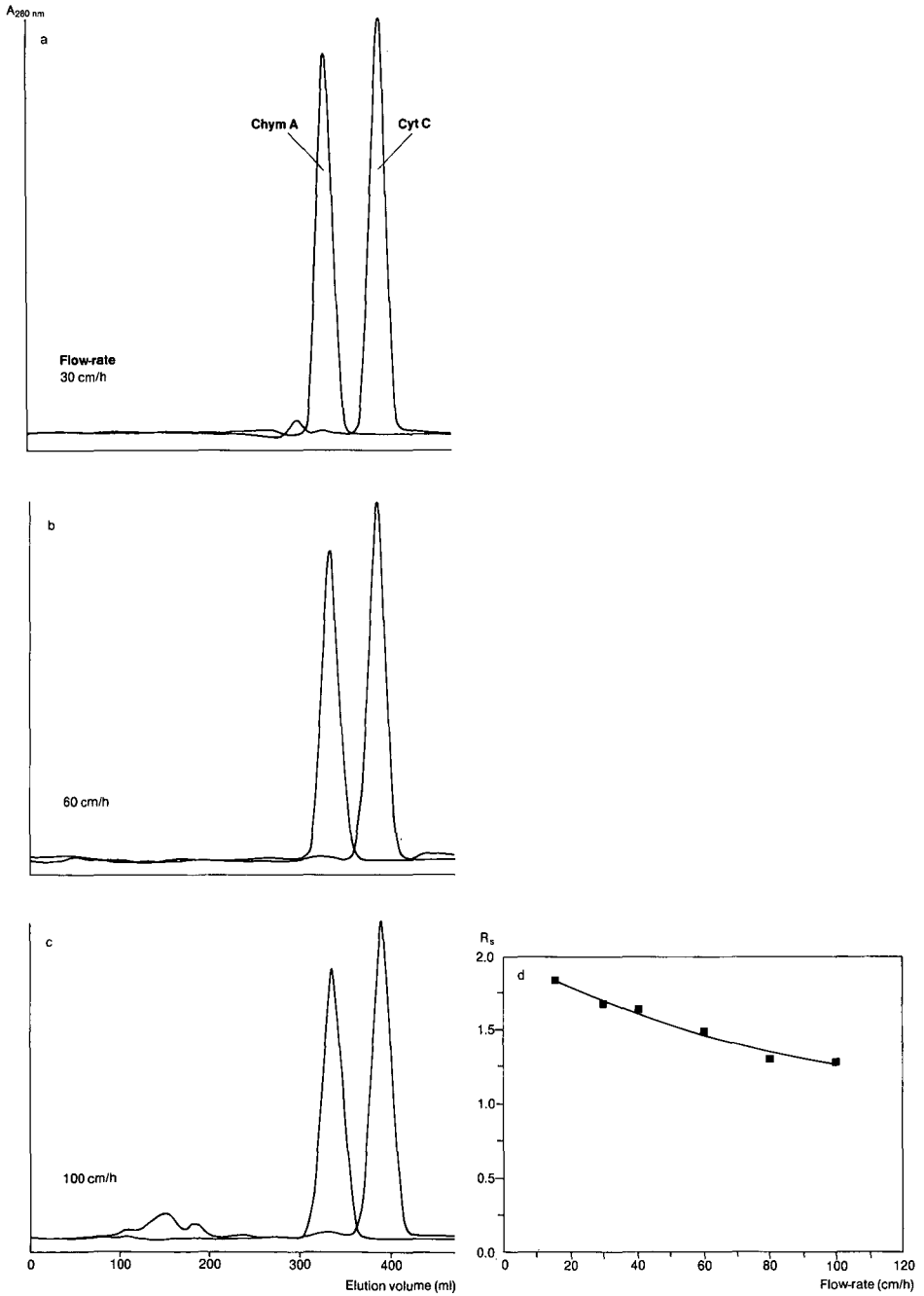


Fig. 6. Influence of flow-rate on appearance of chromatograms (a-c) and on  $R_s$  values for the Cyt c-Chym A pair (d) at constant sample load and sample volume with Superdex 75 prep grade. Column: 600 × 35 mm I.D.,  $N = 15\ 700$  plates/m (acetone). Buffer: 50 mM sodium phosphate-100 mM NaCl (pH 7.2). Sample concentration: Cyt c 2 mg/ml, Chym A 2 mg/ml. Sample volume: 16.5 ml (3% of  $V_c$ ). Each protein was run separately.

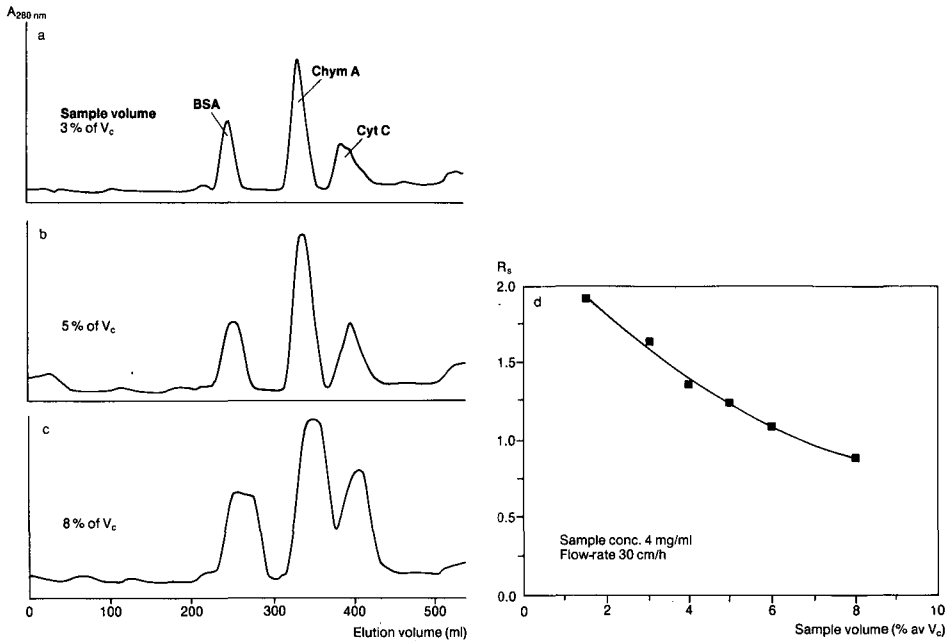


Fig. 7. Influence of sample volume on appearance of chromatograms (a-c) and on  $R_s$  values for the Cyt *c*-Chym A pair (d) at constant sample concentration and constant flow-rate with Superdex 75 prep grade. Flow-rate: 4.8 ml/min (30 cm/h). In a-c, a mixture of Cyt *c* (2 mg/ml), Chym A (2 mg/ml) and BSA (6 mg/ml) was used as a sample. In d, Cyt *c* and Chym A (both 2 mg/ml) were chromatographed separately. Other conditions as in Fig. 6.

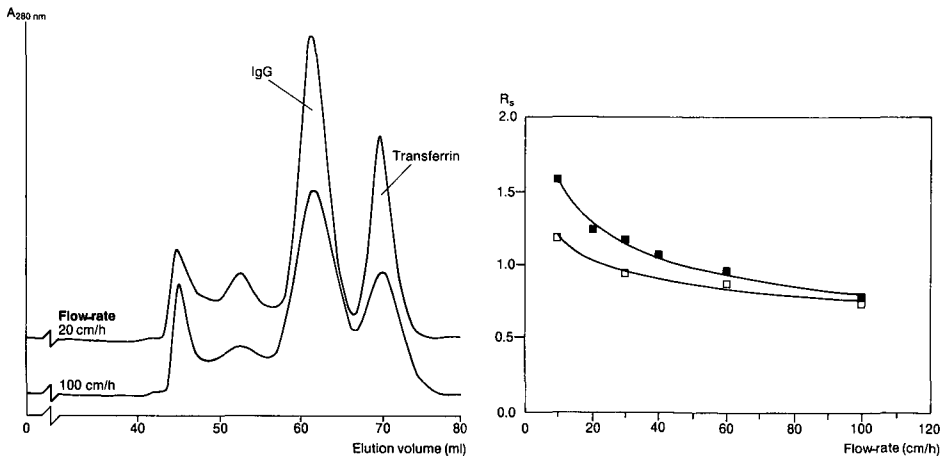


Fig. 8. Chromatography on Superdex 200 prep grade at high and low flow-rates with constant volume (0.8% of  $V_c$ ) and constant concentration of sample (8 mg protein/ml). Column: 600 × 16 mm I.D.,  $N = 18\ 500$  plates/m. Buffer: 50 mM sodium phosphate-100 mM NaCl (pH 7.2). Sample: equal amounts of transferrin and IgG.

Fig. 9. Influence of flow-rate on resolution on Superdex 200 prep grade with constant sample volume (0.8% of  $V_c$ ) and at two levels of sample load (■ = 70; □ = 530 mg/l gel). Concentration of sample: 8 and 64 mg protein/ml. Other conditions as in Fig. 8.

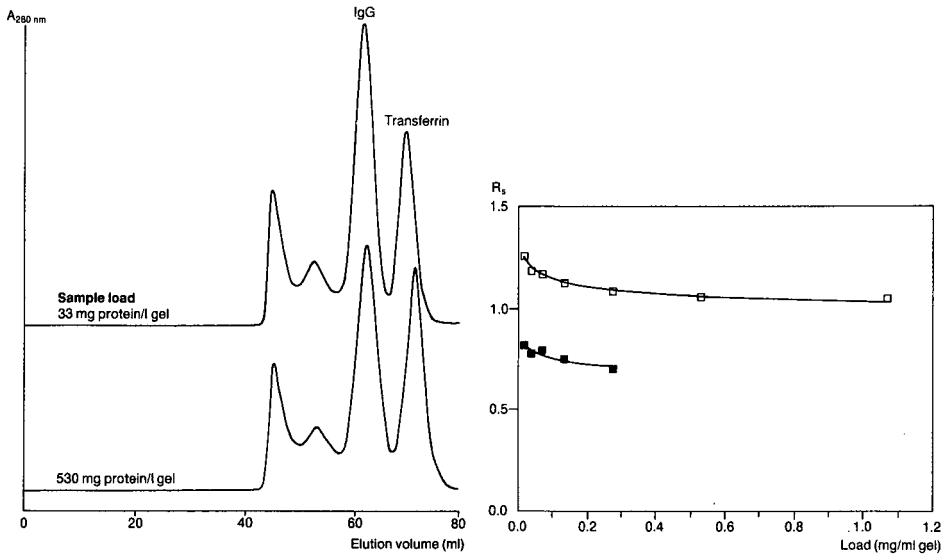


Fig. 10. Chromatography on Superdex 200 prep grade at high and low sample concentrations. Sample volume: 0.8% of  $V_c$ . Flow-rate: 30 cm/h. Other conditions as in Fig. 8.

Fig. 11. Influence of sample load on resolution on Superdex 200 prep grade at two levels of sample volume ( $\square = 0.8\%$ ;  $\blacksquare = 3.3\%$  of  $V_c$ ). Flow-rate: 30 cm/h. Other conditions as in Fig. 8.

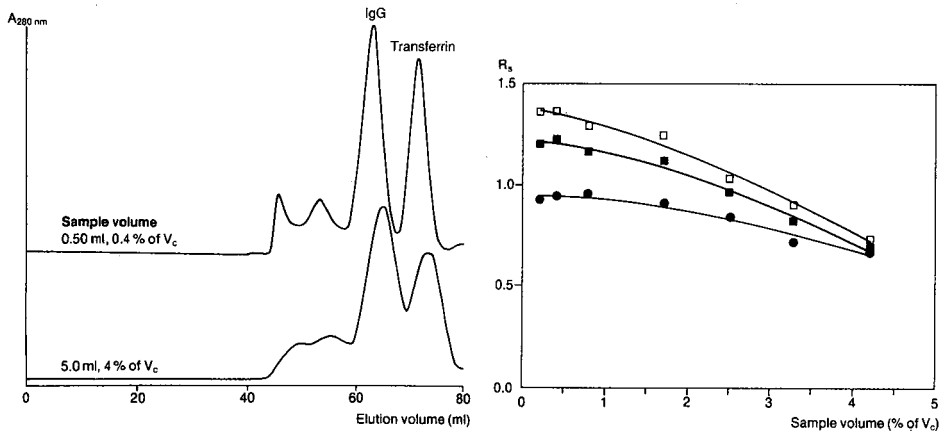


Fig. 12. Chromatography on Superdex 200 prep grade at high and low sample volumes. Sample load: 70 mg/l gel. Flow-rate: 30 cm/h. Other conditions as in Fig. 8.

Fig. 13. Influence of sample volume on resolution on Superdex 200 prep grade at three different flow-rates ( $\square = 15$ ;  $\blacksquare = 30$ ;  $\bullet = 60$  cm/h) and at constant sample (protein) load (70 mg/l gel). Other conditions as in Fig. 8.

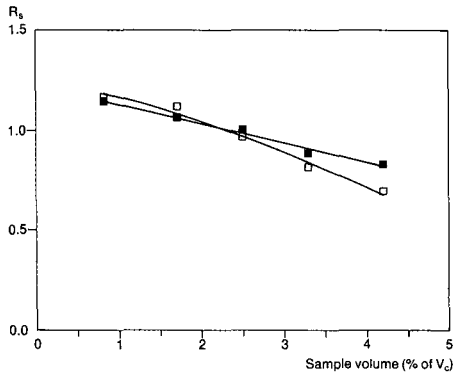


Fig. 14. Influence of sample volume on resolution on Superdex 200 prep grade at two levels of constant protein load ( $\square$  = 70;  $\blacksquare$  = 530 mg/l gel) and at constant flow-rate. Other conditions as in Fig. 8.

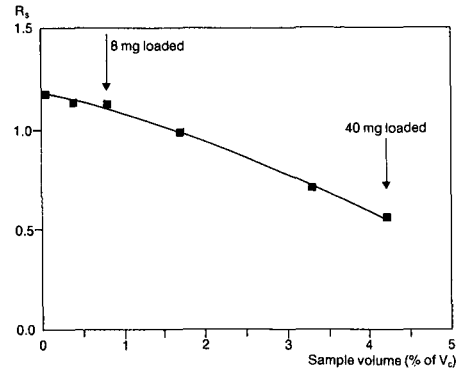


Fig. 15. Influence of sample volume on resolution on Superdex 200 prep grade at constant flow-rate and constant sample concentration. Flow-rate: 30 cm/h. Sample concentration: 8 mg protein/ml. Other conditions as in Fig. 8.

Of the parameters studied, sample volume had the greatest effect on resolution (Figs. 7 and 12–15). The effect was more pronounced when low flow-rates were used (Fig. 13). Fig. 14 shows that  $R_s$  was approximately the same at two levels of protein loads, 70 and 530 mg/l gel, when the sample volume was varied. Indications are that at high sample volumes the higher protein load gives higher  $R_s$  values. Fig. 15 shows the results of experiments in which the amount of protein increased in proportion to the sample volume. The progression of the resolution *versus* sample volume curve is similar to that obtained at constant protein load and at the same flow-rate in Fig. 13.

#### *Purification of ZZ-brain IGF on Superdex 75 prep grade*

Brain insulin-like growth factor (brain IGF) is a truncated form of IGF-1, lacking the N-terminal tripeptide, and is considered to be important for the growth and metabolism of the central nervous system. It has been expressed as a recombinant extracellular fusion protein at KabiGen. The fusion partner [19], designated ZZ, is a synthetic IgG-binding protein derived from staphylococcal protein A. The complete recombinant fusion protein is called ZZ-brain IGF. The initial purification steps, not shown here, were affinity chromatography on IgG Sepharose Fast Flow and ion-exchange chromatography.

The purpose of the gel filtration step was to remove dimers and oligomers from the monomeric ZZ-brain IGF, MW 22 000 dalton. As seen in Fig. 16, dimers and larger aggregates could be efficiently eliminated by gel filtration on Superdex 75 prep grade and a significant degree of separation of dimers and trimers was also obtained.

#### *Purification of monoclonal antibodies on Superdex 200 prep grade*

Fig. 17 shows the final purification of a monoclonal antibody from hybridoma cell culture supernatants after concentration by ultrafiltration and initial purification by cation-exchange chromatography. The principal contaminants were antibody dimer (peak 1) and transferrin (peak 3). The purity of the monoclonal antibody was >98% after the gel filtration step as determined by electrophoresis.



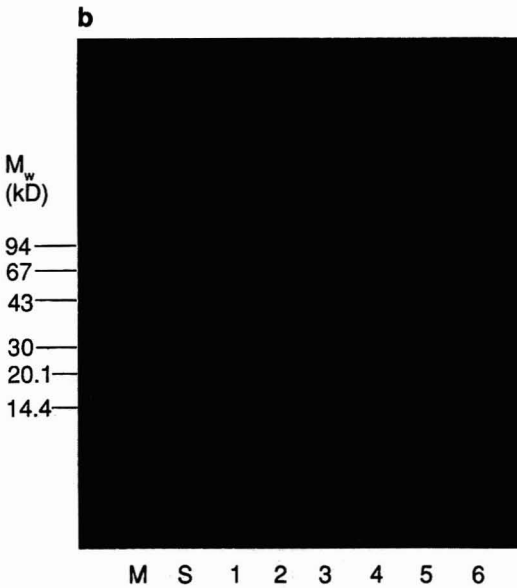
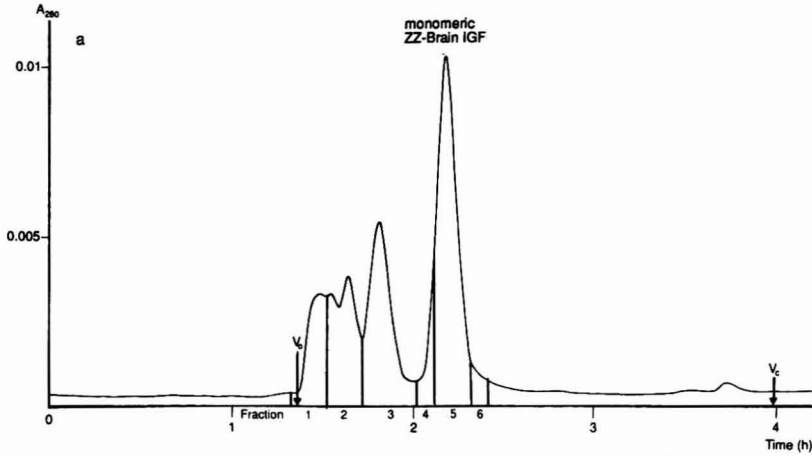


Fig. 16. Gel filtration of partly purified ZZ-brain IGF on Superdex 75 prep grade to separate the monomeric form, MW 22 000 dalton, from dimers and oligomers. (a) Chromatography. Column: 600 × 16 mm I.D. Buffer: 0.3 M ammonium acetate (pH 6.0). Flow-rate: 15 cm/h (0.5 ml/min). Sample size: 1.0 ml. Fractions were pooled as indicated. (b) SDS-PAGE of pooled fractions, non-reducing conditions, silver staining. Aliquots of the pooled ZZ-brain IGF fractions were freeze-dried. The pellets obtained were dissolved in a constant volume of sample buffer [2.5% SDS–10 mM Tris–HCl–1 mM EDTA (pH 8.0)] and heated at 95°C for 5 min. Gel: PhastGel Gradient 8–25. Lanes: M, marker proteins (LMW-kit; Pharmacia); S, start material for gel filtration; 1–6, pools 1–6 from (a). kD = Kilodalton.

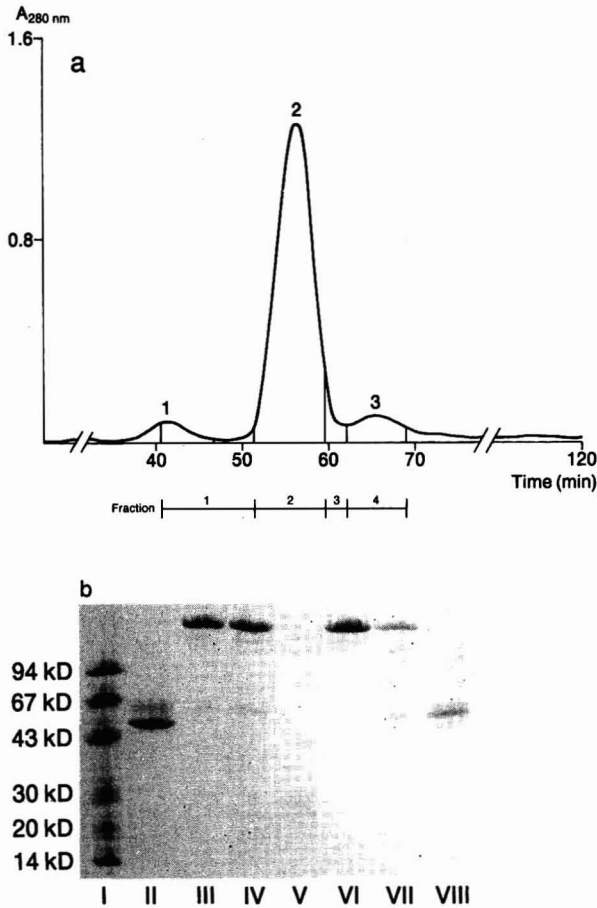


Fig. 17. Final purification of a  $\text{IgG}_{2a}$  mouse monoclonal antibody on Superdex 200 prep grade. (a) Chromatography. Column:  $600 \times 60$  mm I.D. Feed material: hybridoma cell culture supernatant concentrated by ultrafiltration, clarified by centrifugation and  $0.22\text{-}\mu\text{m}$  filtration. Desalted on Sephadex G-25 Coarse. Initial purification by cation exchange using BioPilot Column S Sepharose High Performance. Feed concentration:  $11.37$  mg total protein/ml. Feed volume:  $50$  ml ( $3\%$  of  $V_0$ ). Buffer:  $50$  mM PBS- $0.05\%$  sodium azide (pH 7.5). Flow-rate:  $30$  cm/h ( $14$  ml/min). Fractions were collected and pooled as indicated. (b) SDS-PAGE of pooled fractions, non-reducing conditions, Commassie brilliant blue staining. Gel: PhastGel Gradient 8-25. Lanes: I, LMW calibration kit; II, flow-through fraction in the preceding ion-exchange step; III and IV, monoclonal antibody from ion-exchange step; V-VIII, fractions 1-4 from Superdex 200 prep grade. kD = Kilodalton.

## DISCUSSION

High selectivity in gel filtration is, under ideal conditions, reflected in a steep  $K_D$  versus log MW curve. The selectivity depends entirely on the properties of the chromatographic support and cannot be modified by adjustment of the eluent composition as in many other chromatographic techniques [3]. The selectivity of macroreticular gels such as agarose gels can be increased by the introduction of

increasing amounts of solid material (agarose), which also leads to a lower exclusion limit. It also inevitably causes the so-called permeability,  $V_p/V_0$ , of the column to decrease, which has a clear negative effect on resolution [3,20]. Thus, to reach the exclusion limit of, for example, Sephadex G-200 by increasing the amount of solid material in any macroreticular gel will give a gel with high selectivity as measured by the  $K_D$  versus log MW relationship but the permeability will decrease dramatically and therefore the resolution will be low.

NMR studies have shown that the polymer chains in a microreticular gel such as Sephadex G-200 retain their mobility to a large extent [21,22]. The  $^{13}\text{C}$  NMR spectrum of Superdex 75 prep grade is similar to that of a dextran solution with respect to peak width and resonance frequency (results not shown). Theoretically, the apparent relative support volume,  $V_{s,rel}$ , as determined with deuterium oxide, would be zero (*i.e.*,  $V_{p,rel} = 100\%$ ) in a gel with complete freedom of movement of the polymer chains constituting the gel, as a small molecule such as deuterium oxide will be able to diffuse to any position in the gel particle. Sephadex G-75 was found in our experiments to have a  $V_{s,rel}$  value in the range 1–2%, which is much lower than would be expected for a macroreticular gel with the same content of dry material (the “water regain” of Sephadex G-75 is *ca.* 7.5 ml/g dry material).

By “immobilizing” a dextran solution in the pores of the macroreticular cross-linked agarose gel, we have been able to lower the exclusion limit substantially (from *ca.*  $10^7$  in the cross-linked agarose gel) without substantially decreasing the permeability. We have thus been able to make rigid, low-exclusion-limit gels with retained high resolution in gel filtration.

#### ACKNOWLEDGEMENTS

We thank Torvald Andersson, Hasse Hansson, Helena Hedlund, Hans Johansson, Per-Erik Sjöholm and Robert Svensson for the skilful performance of several of the experiments, and Lars Hagel and Mark Adams for valuable discussions. The original ideas for the construction of Superdex were generated by Lennart Söderberg (Uppsala), who also conducted initial experiments.

#### REFERENCES

- 1 J. Porath and P. Flodin, *Nature (London)*, 183 (1959) 1657.
- 2 J.-C. Janson, *Chromatographia*, 23 (1987) 361.
- 3 L. Hagel, in L. Rydén and J.-C. Janson (Editors), *Protein Purification. Principles, High Resolution Methods and Applications*, Verlag Chemie, Deerfield Beach, FL, 1989, Ch. 3, p. 63.
- 4 L. Fischer, in J. Å. Jönsson (Editor), *Chromatographic Theory and Basic Principles (Chromatographic Science Series, Vol. 38)*, Marcel Dekker, New York, 1987, Ch. 8, p. 347.
- 5 H. Determann, *Gel Chromatography*, Springer, Berlin, 1968, p. 4.
- 6 R. P. Bywater and N. V. B. Marsden, in E. Heftmann (Editor), *Chromatography—Fundamentals and Applications of Chromatographic and Electrophoretic Methods, Part A (Journal of Chromatography Library, Vol. 22A)*, Elsevier, Amsterdam, 1983, Ch. 8, p. A260.
- 7 R. Epton, in R. Epton (Editor), *Chromatography of Synthetic and Biological Polymers, Vol. 1, Column Packings, GPC, GF and Gradient Elution*, Ellis Horwood, Chichester, 1972, p. 3.
- 8 S. Hjertén, B.-L. Wu and J.-L. Liao, *J. Chromatogr.*, 390 (1987) 101.
- 9 I. Drevin, L. Larsson, I. Eriksson and B.-L. Johansson, *J. Chromatogr.*, 514 (1990) 137.
- 10 Å. Danielsson, presented at the *1st Conference on Advances in Purification of Recombinant Proteins, Interlaken, March 14–17, 1989*.

- 11 H. J. Johansson, T. N. Pettersson and J. H. Berglöf, *J. Chem. Tech. Biotechnol.*, 49 (1990) 233.
- 12 A. I. Daniels, N. T. Pettersson and C. J. Scandella, presented at the *1st Conference on Advances in Purification of Recombinant Proteins, Interlaken, March 14-17, 1989*.
- 13 R. A. Andersson, in M. J. Groves (Editor), *Particle Size Analysis*, Heyden, London, 1978, p. 411.
- 14 B. Göransson and E. Dagerus, in P. J. Lloyd (Editor), *Particle Size Analysis 1988*, Wiley, New York, 1988, p. 159.
- 15 N. V. B. Marsden, *J. Chromatogr.*, 58 (1971) 304.
- 16 G. L. Hagnauer, in B. A. Bidlingmeyer (Editor), *Preparative Liquid Chromatography (Journal of Chromatography Library, Vol. 38)*, Elsevier, Amsterdam, 1987, Ch. 8, p. 312.
- 17 J. J. Kirkland and P. E. Antle, *J. Chromatogr. Sci.*, 15 (1977) 137.
- 18 J. Leseq, *J. Liq. Chromatogr.*, 8 (1985) 875.
- 19 T. Moks, L. Abrahamsén, B. Österlöf, S. Josephsson, M. Östling, S.-O. Enfors, I. Persson, B. Nilsson and M. Uhlén, *BioTechnology*, 5 (1987) 379.
- 20 W. W. Yau, J. J. Kirkland and D. D. Bly, *Modern Size-Exclusion Liquid Chromatography*, Wiley, New York, 1979, p. 85.
- 21 A. Benesi and J. T. Gerig, *Carbohydr. Res.*, 53 (1977) 278.
- 22 R. Scherrer, R. Lundin, M. Benson and S. C. Witt, *Carbohydr. Res.*, 124 (1983) 151.

CHROMSYMP. 1994

## Molecular interactions in liquid chromatography<sup>a</sup>

S. N. LANIN and Yu. S. NIKITIN\*

*Department of Chemistry, M. V. Lomonosov State University of Moscow, 119899 Moscow (U.S.S.R.)*

(First received February 5th, 1990; revised manuscript received June 9th, 1990)

---

### ABSTRACT

An approach to the description of molecular interactions in normal- and reversed-phase high-performance liquid chromatography as quasi-chemical equilibria on the sorbent and in solution (of solute-sorbent, modifier-sorbent, solute-modifier and modifier-modifier types) is presented. Such an approach is of help in understanding better the role of various parameters of chromatographic systems that determine the retention of substances in HPLC. The mathematical mechanism used is the same to describe the equilibrium distribution of the sorbate between the liquid and solid phases (adsorption mechanism) or between the liquid and bonded phases (absorption mechanism) and the final equations do not take into account the type of mechanism. A general expression correlating the retention of solute molecules with the concentration of the modifying additive of the mobile phase (over a wide range of concentrations) was obtained. Numerous examples have shown that, depending on the prevalence of certain types of interactions, this relationship makes it possible to describe quantitatively and to explain various deviations of the retention dependence from linearity.

---

The study of molecular interactions in gas and liquid chromatography is of great importance for understanding the mechanisms of chromatographic separations of substances and for developing selectivity theory in chromatography. Chromatographic parameters of retention in gas adsorption chromatography at small (zero) surface coverage are determined by adsorbate-adsorbent interactions which depend on the nature of the adsorbent and the adsorbed molecules. Pioneering studies by Kiselev and co-workers [1–3] resulted in the development of the fundamentals of the molecular statistical theory of adsorption on homogeneous surfaces. This theory enables one to calculate the thermodynamic characteristics of adsorption of various organic compounds for homogeneous adsorbents [graphitized thermal carbon black (GTCB), zeolites] (the direct approach), while the chromatographic data on the adsorption on GTCB made it possible to identify, in a number of cases, the structure of the adsorbed molecules (the reverse approach, *i.e.*, chromatographic structure analysis or “chromatoscopy” [4]).

The retention mechanisms in liquid-solid chromatography (LSC) are much more complicated. In addition to sorbate-sorbent molecular interactions, also of great

---

<sup>a</sup> Dedicated to Professor J. C. Giddings on the occasion of his 60th birthday.

importance are the sorbate–mobile phase and sorbent–mobile phase interactions, in particular the interactions between the components of binary, ternary, etc., mobile phases. At present, it is impossible to calculate quantitatively the thermodynamic characteristics of retention in such a complicated system. Further development of the theory of liquid chromatography is largely due to the determination of correlation dependences between the retention parameters and various properties of sorbates [5–12], mobile phases (MP) [10–16] and stationary phases (SP) [17–21].

Kiselev and co-workers suggested that the theory of chromatographic retention and separation in liquid–solid chromatography should be based on the theory of sorption from multi-component solutions. Such an approach provides a common basis for studying the normal-phase (NP) and reversed-phase (RP) variants of high-performance liquid chromatography (HPLC). The main difference between NP- and RP-HPLC consists in the different characters of molecular interactions between the solute molecules on the one hand, and the mobile and stationary phases on the other. In NP-HPLC, the main contribution to retention is made by specific interactions of the solute molecules with the SP surface. In RP-HPLC the non-specific interactions of the solute molecules with the hydrophobic sorbent predominate over specific and non-specific interactions of the solute with components of the mobile liquid phase.

Two problems are usually considered in the theory of HPLC: (1) the effect of the mobile phase and its composition on the retention and (2) the dependence of the retention parameters on the nature and structure of the molecules of adsorbed substances. Much less study has been devoted to the effect of the adsorbent surface chemistry on retention in liquid–solid chromatography than in gas–solid chromatography, since in HPLC the regulation of retention and separation of analyte substances are often performed by changing the type and composition of the mobile phase rather than those of the adsorbent in the column.

Now let us consider the most frequently applied system in HPLC: an adsorbent (A), a substance being adsorbed, *i.e.*, the solute (S), and a two-component mobile phase consisting of the basic component, *i.e.*, the solvent (L), and a modifying additive (M). As a rule, RP-HPLC involves L = water and M = organic solvent (*e.g.*, methanol, acetonitrile, tetrahydrofuran) and NP-HPLC involves L = alkane and M = weakly polar or polar organic solvent (chloroform, alcohol). In this instance, we are dealing with sorption from a three-component solution (S, M, L), the concentration of the solute S being 3–4 orders of magnitude smaller than that of the modifier M and solvent L.

We take into account the following assumptions: the sorbent surface is chemically and geometrically homogeneous and therefore the sorption energy of the components in the mobile phase is constant on any part of the surface; sorption is of an exchange (competitive) character; the absence of molecular associations in the adsorption layer; and the surface solution and bulk solution are ideal. Considering the sorption as a quasi-chemical reversible reaction of exchange, in the simplest case, where the areas occupied by molecules S, M and L in the surface layer are equal, we have equilibria for the adsorbate:



$$K_S = S_s L_m / S_m L_s \quad (2)$$

and for the modifier:

$$M_m + L_s \rightleftharpoons M_s + L_m \quad (3)$$

$$K_M = M_s L_m / M_m L_s \quad (4)$$

where  $K_S$  and  $K_M$  are equilibrium constants and  $S_s$  and  $S_m$ ,  $M_s$  and  $M_m$  and  $L_s$  and  $L_m$  are mole fractions of the solute, modifier and solvent in the stationary phase (s) and mobile phase (m). It should be noted that eqns. 1–4, which are of general character, can describe the equilibria distribution of the adsorbate or modifier between the mobile and stationary phases for both the adsorption and partition mechanisms of retention. For the partition mechanism the assumption is made of a constant binding capacity of the sorption layer; the composition of the surface solution and that of the bulk solution are, of course, different. A similar approach was used also by Murakami [16] to describe the retention of aromatic compounds by reversed phases and by Arvidsson *et al.* [22] to describe the ion-pair chromatography.

Assuming that the bulk and surface solutions are ideal and the processes of molecular association are absent, we can easily obtain the sorption equations for the solute and modifier.

From eqns. 2 and 4, we obtain

$$M_s/S_s = K_M M_m / K_S S_m \quad (5)$$

Also,

$$L_s + M_s + S_s = 1 \quad (6)$$

where  $L_s$ ,  $M_s$ ,  $S_s$  are mole fractions of non-associated molecules of the solvent, modifier and sorbate, respectively, in the stationary phase.

$$M_s + M_s K_S S_m / K_M M_m + M_s L_m / K_M M_m = 1 \quad (7)$$

As  $S_m \ll M_m$  and  $S_m \ll L_m$ , then

$$L_m \leq 1 - M_m \quad (8)$$

and

$$M_s [1 + K_S S_m / K_M M_m + (1 - M_m) / K_M M_m] = 1 \quad (9)$$

$$M_s = K_M M_m / [1 + (K_M - 1) M_m + K_S S_m] \quad (10)$$

Dividing eqn. 2 by eqn. 4, we obtain

$$K_S / K_M = S_s M_m / S_m M_s \quad (11)$$

It is known [23] that

$$k' = \Phi K = \Phi S_s/S_m \quad (12)$$

where  $k'$  is the capacity factor,  $\Phi$  is the phase ratio (the ratio of stationary to mobile phase volumes) and  $K$  is the constant of the adsorption equilibrium of the solute (the ratio of the total mole fraction of the solute in the stationary and mobile phases).

Then, from eqns. 11 and 12, we obtain

$$K_S/K_M = k' M_m/(\Phi M_s) \quad (13)$$

and

$$1/k' = K_M M_m/(\Phi K_S M_s) \quad (14)$$

Substituting eqn. 10 in eqn. 14, we obtain

$$1/k' = [1 + (K_M - 1)M_m + K_S S_m]/(\Phi K_S) \quad (15)$$

Usually  $K_S$  is not drastically different from  $K_M$  and  $S_m \ll M_m$ . Consequently, the term  $K_S S_m$  in eqn. 15 may be neglected. Then we have

$$1/k' = [1 + (K_M - 1)M_m]/(\Phi K_S) \quad (16)$$

It follows from eqns. 12 and 15 that the equations of adsorption for the solute, modifier and solvent acquire the forms

$$S_s = K_S S_m/[1 + K_S S_m + (K_M - 1)M_m] \quad (17)$$

$$M_s = K_M M_m/[1 + K_S S_m + (K_M - 1)M_m] \quad (18)$$

$$L_s = (1 - M_m)/[1 + K_S S_m + (K_M - 1)M_m] \quad (18)$$

A rectilinear dependence of the reciprocal of the capacity factor on the content of the modifier in the eluent was initially applied by Scott [24]. In many instances this dependence can be successfully used to describe the decreasing retention of the solute with increasing content of the modifier in the solution and also reflects the gradual blocking of the active sites on the homogeneous surface of the sorbent by the modifier molecules (Figs. 1 and 2). It is applied more often and much better in NP-HPLC than in RP-HPLC [25].

Under favourable conditions (homogeneous surface, absence of adsorption on the surface covered with the modifier molecules, absence of associate formation in the solution and on the surface), the dependence in eqn. 16 should be observed until the surface is completely covered with a monolayer of the modifier and hence full deactivation is attained. However, in real circumstances the surface covered with the modifier retains its ability to have molecular interactions with the mobile phase components. Moreover, in this instance not only the interaction force may change (a



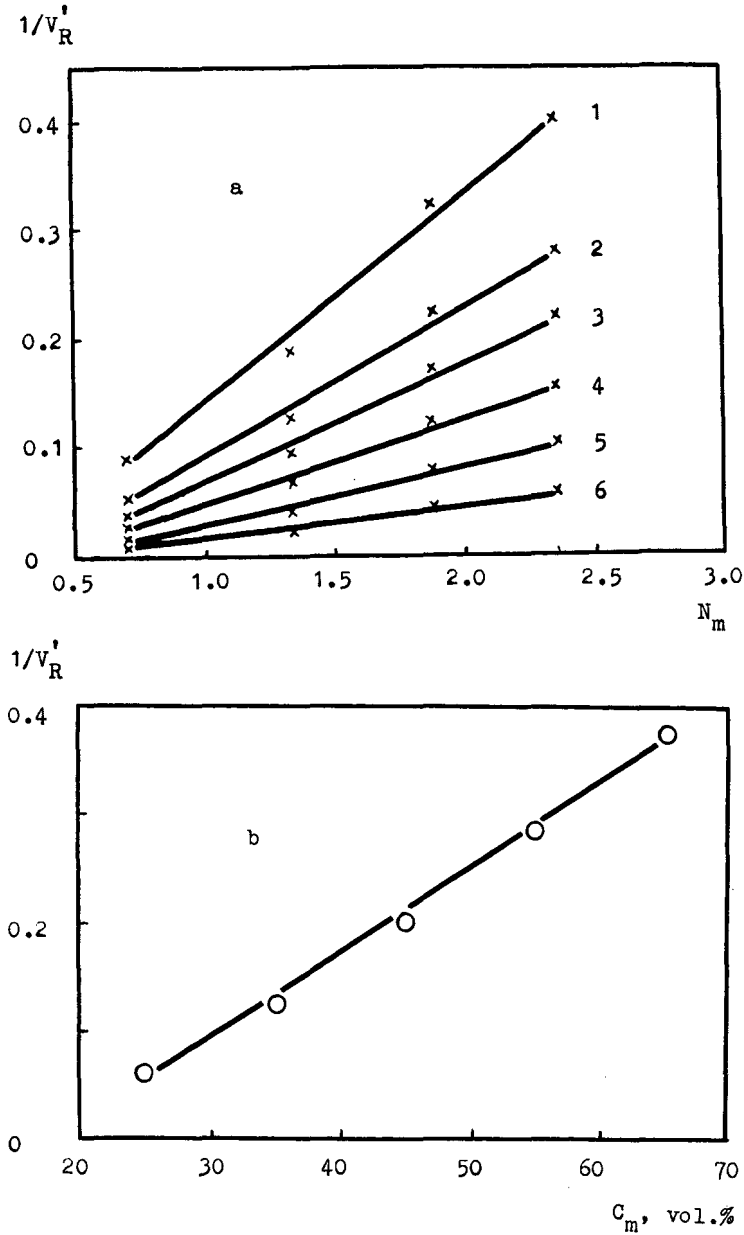


Fig. 1. Dependence of the reciprocal of the corrected retention volume ( $1/V_R'$ ) on the mobile phase composition: the mole fraction ( $N_m \times 10$ ) or volume percent ( $C_m$ , %, v/v) of the modifier. (a) Adsorbent, silica gel L; mobile phase, *n*-hexane-dioxane. 1 = *o*-Cresol; 2 = phenol; 3 = *p*-chlorophenol; 4 = *p*-methoxyphenol; 5 = *m*-nitrophenol; 6 = *p*-nitrophenol. (b) Adsorbent, Suplex pKb-100; mobile phase, water-acetonitrile; solute, *p*-toluic acid [25].

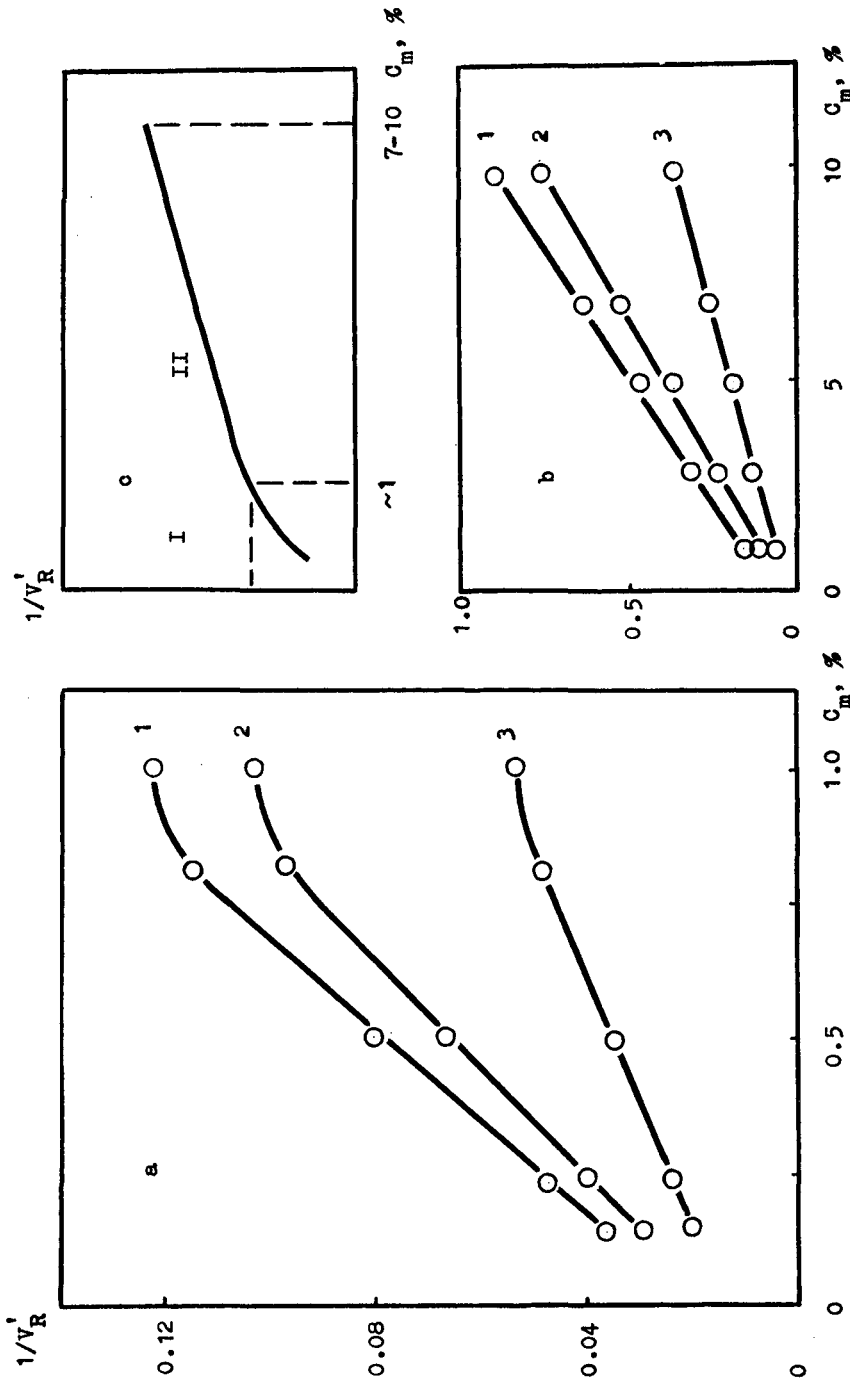


Fig. 2. Dependence of the reciprocal of the corrected retention volumes ( $1/V'_R$ ) of some substituted benzoic acids on the content of polar modifier ( $C_m$ , % v/v, of propionic acid) in the mobile phase. Adsorbent, silica gel L, 10  $\mu$ m; mobile phase, *n*-hexane-propionic acid. C: (a) 0-1; (b) 1-10; (c) 0-10% (v/v). 1 = *p*-Toluic acid; 2 = *p*-bromobenzoic acid; 3 = *p*-methoxybenzoic acid.

change in  $K_S$  and  $K_M$  on transition from the initial to the modified surface of the adsorbent) but also the very character of interactions may undergo certain changes. Hence, in studying the retention of substituted benzoic acids on silica gel with the use of an *n*-alkane and a polar additive (acetic or propionic acid) mixture as the mobile phase, it was found that the retention mechanism of benzoic acids on transition from low to higher concentrations of the polar additive in the mobile phase undergoes certain changes [26]. When the concentration of the polar additive, an aliphatic acid, is less than 1 vol.-%, the solute molecules can directly interact with silanol groups of the silica gel surface, that is, retention is mainly determined by interactions of the hydrogen bond type. In Fig. 2c this mechanism is represented by the initial, steep part (I) of the dependence of  $1/V'_R$  on the concentration  $C$  of the polar additive in the mobile phase ( $V'_R$  is the corrected retention volume of the solute). When the content of the polar additive increases from 1 to 7–9 vol.-% (II), the silica gel surface is covered more with the modifier molecules and the retention of substituted benzoic acids proceeds via adsorption on the modified surface of silica gel. In this case ( $C > 1\%$ , v/v), the slope of dependence of  $1/V'_R$  on  $C$  is smaller and the intercept on the ordinate at  $C = 0$  is greater than that for the region of low concentrations ( $C < 1\%$ , v/v), which is indicative of a weaker interaction of benzoic acids with the modified silica gel surface compared with the initial hydroxylated one.

Fig. 3 shows the adsorption isotherm of acetic acid from solution in cetane on silica gel [27], which is characterized by the presence of two horizontal sections. We believe that the first (A) corresponds to the surface coating of the adsorbent with monomeric molecules of acetic acid oriented probably parallel to the surface. The second horizontal section (B) corresponds to the coating of the surface with dimeric associates of the molecules which are either perpendicular or inclined to the surface. As is seen from Fig. 3, the surface coating with monomeric molecules of acetic acid proceeds at a concentration in solution of 150–200 mmole/l, which approximately corresponds to 1–1.3 vol.-%. Also of importance is that at modifier concentrations above 1–2 vol.-%, aliphatic acids in solution are basically in the state of dimers [28].

a, mmole/g

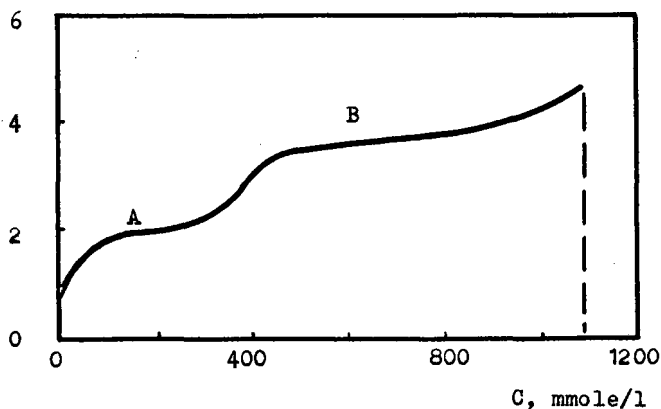


Fig. 3. Adsorption isotherm of acetic acid on silica gel KCK from solution in cetane at 20°C.

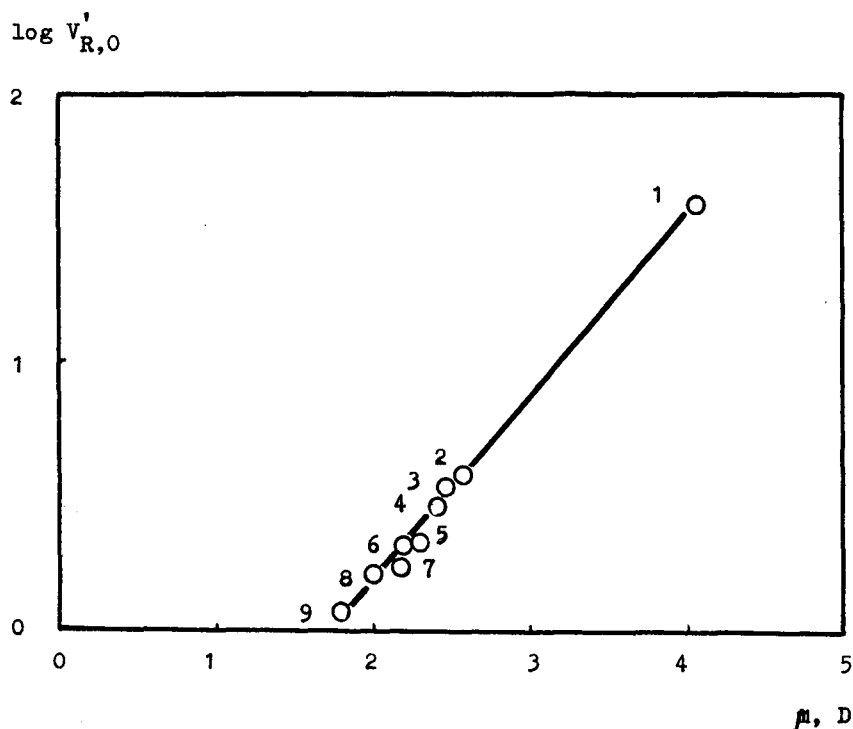


Fig. 4. Dependence of logarithm of corrected retention volume ( $\log V'_{R,0}$ ) of substituted benzoic acids on their dipole moment ( $\mu, D$ ). Adsorbent, silica gel L, 10  $\mu m$ ; mobile phase, *n*-hexane-propionic acid (20:1). 1 = *m*-nitrobenzoic acid; 2 = *o*-bromobenzoic acid; 3 = *o*-chlorobenzoic acid; 4 = *p*-methoxybenzoic acid; 5 = *m*-chlorobenzoic acid; 6 = *m*-bromobenzoic acid; 7 = *p*-bromobenzoic acid; 8 = *p*-chlorobenzoic acid; 9 = benzoic acid.

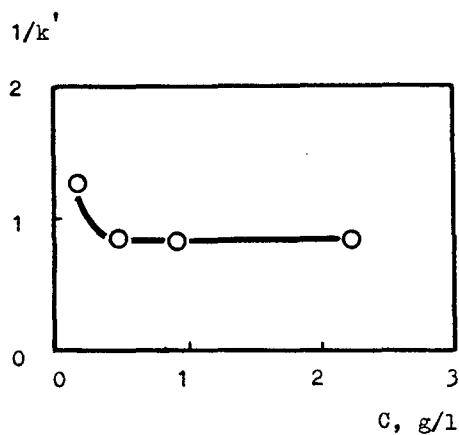


Fig. 5. Dependence of the reciprocal of the capacity factor ( $1/k'$ ) of glucose on the piperazine concentration ( $C, g/l$ ) in the mobile phase [acetone-water (7:3)]. Adsorbent, LiChrosorb Si 100 silica gel, 7  $\mu m$ .

The mechanism of retention of benzoic acids, which under these conditions yield cyclic dimers ("aromatic acid-aliphatic acid"), seems to be of pure electrostatic character. This is confirmed by a good linear correlation of the logarithm of retention with the dipole moments of substituted benzoic acids (Fig. 4). It is known [29] that substituted benzoic acids are retained on the surface of anion exchangers in conformity with the values of the Taft constants rather than with their dipole moments.

Introduction of the modifier into the mobile phase may not only result in a decrease in the activity of the adsorbent and, hence, a weaker retention of the solute molecules, but also, in certain circumstances, modification creates a more active surface. Thus, adsorption of diamines on silica gel from an acetone-water mobile phase was used for the liquid chromatography of carbohydrates [30]. Fig. 5 shows that an increase in the concentration of a cyclic diamine, piperazine, in the mobile phase first results in a considerable increase in the retention of glucose (the  $1/k'$  value decreases) and then, at concentrations above  $0.44 \text{ mg/cm}^3$  (*i.e.*, after the formation of a piperazine monolayer on the surface of silica), the retention hardly changes (or decreases slightly). Mono-, di- and trisaccharides are well separated on a silica surface modified by piperazine directly from the mobile phase (Fig. 6).

Modification of the adsorbent surface due to adsorption of the modifier from the mobile phase, often referred to as dynamic modification, has been widely applied in liquid chromatography. It enables one to change both the retention value of the separated substances and the selectivity of separation. Non-polar reversed phases (such as ODS type phases) are often used as sorbents. Compounds of various types, such as molecular, ionic and complex-forming, are employed as modifiers of two-component water-organic mobile phases. However, a quantitative description of retention depending on the mobile phase composition in RP-HPLC becomes even more complicated as the mobile phase in this instance contains at least four components: solute, modifier, organic solvent and water.

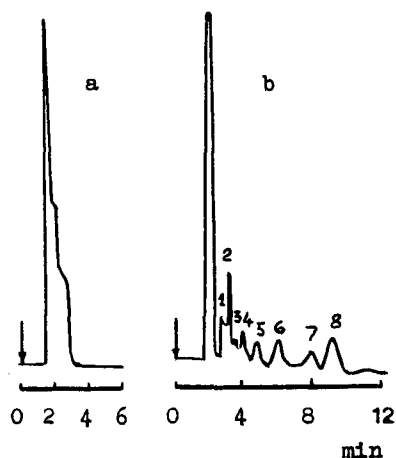


Fig. 6. Chromatogram of a carbohydrate mixture in a column ( $125 \times 4.8 \text{ mm I.D.}$ ) packed with LiChrosorb Si 100 silica gel,  $7 \mu\text{m}$ . Mobile phase, acetone-water (4:1); volume flow-rate  $F = 1 \text{ cm}^3/\text{min}$ ; temperature,  $30^\circ\text{C}$ . Adsorbent: (a) hydroxylated silica gel; (b) silica gel modified by adsorption of piperazine from the mobile phase. Piperazine concentration in the mobile phase,  $0.44 \text{ mg cm}^{-3}$ . 1 = Ribose; 2 = xylose; 3 = fructose; 4 = glucose; 5 = saccharose; 6 = cellulose; 7 = melezitose; 8 = raffinose.

In real systems the solute retention is influenced not only by molecular interactions with the stationary phase but also by molecular interactions in the mobile phase. Jaroniec and Jaroniec [31,32] proposed to take into account the association of sorbate molecules and modifier in solution ( $S_m-M_m$ ) and self-association of the modifier molecules ( $M_m-M_m$ ). In the simplest case of dimer formation the following equilibrium is attained in solution:



and



Then the dependence of the solute retention on the modifier concentration in the mobile phase, in the case of association ( $SM$ )<sub>m</sub>, is expressed by the equation

$$1/k' = [1 + (K_M - 1)M_m](1 + K_{SM}M_m)/(\Phi K_S) \quad (21)$$

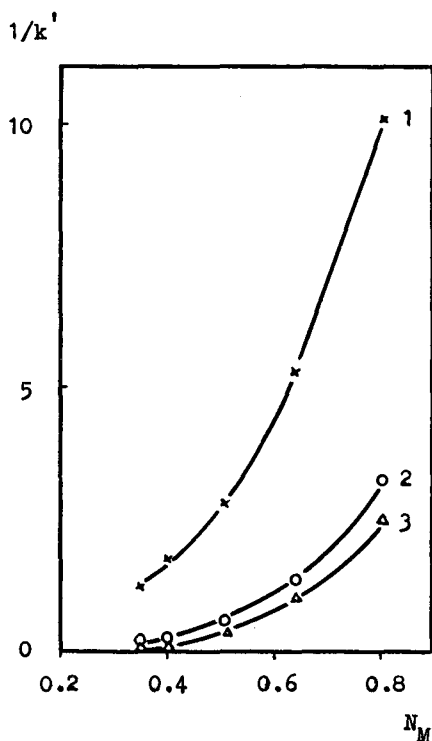


Fig. 7. Dependence of the reciprocal of the capacity factor ( $1/k'$ ) of phenols on the mole fraction ( $N_M$ ) of methanol in the binary water-organic mobile phase. Adsorbent, LiChrosorb RP-18, 5  $\mu$ m. 1 = Phenol; 2 = 3-*tert.*-butylphenol; 3 = 2-*tert.*-butylphenol.

and for association  $(MM)_m$  by the equation

$$1/k' = [1 + (K_M - 1)M_m - 2K_{MM}M_m^2]/(\Phi K_S) \quad (22)$$

The dependences of  $1/k'$  on  $M_m$  described by eqns. 21 and 22 are non-linear. Only in the region of small  $M_m$  and at small values of  $K_{MM}$  and  $K_{SM}$  are they transformed into a linear equation (eqn. 16) as previously considered. The molecular solute-modifier (S-M) interaction promotes a faster decrease of the solute retention with increasing concentration  $M$  in the mobile phase than in the absence of these interactions (Fig. 7) [33]. The formation of associates between the modifier molecules (*e.g.*, due to non-specific interactions in RP-HPLC), on the other hand, slows down the decrease in retention (Fig. 8).

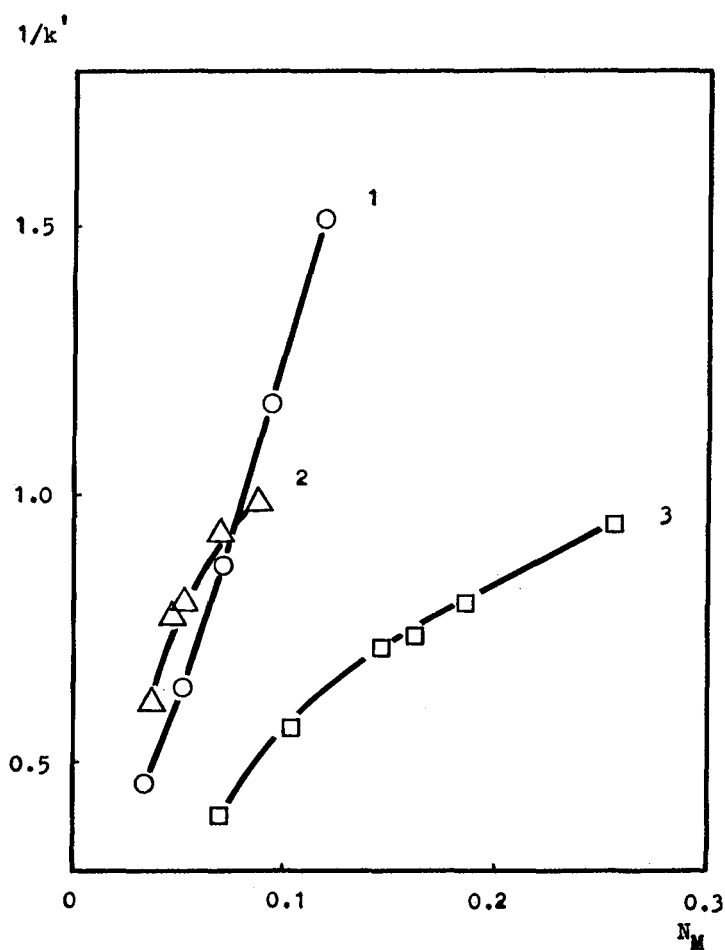


Fig. 8. Dependence of the reciprocal of the capacity factor ( $1/k'$ ) of nivalenol on the nature and mole fraction ( $N_M$ ) of the organic modifier in the binary water-organic mobile phase. Adsorbent, Nucleosil RP-18, 5  $\mu$ m. Modifier: 1 = ethanol; 2 = tetrahydrofuran; 3 = acetonitrile.

Now consider the general case when (1) the molecules of solute  $S$  and modifier  $M$  are able to form in solution polymolecular ( $C+1$ -molecular) associates and (2) the molecules of modifier  $M$  form in the mobile phase polymolecular ( $d$ -molecular) associates.

Sorption of  $S$  and  $M$  molecules occurs only on that part of the sorbent which is occupied with the solvent molecules  $L$  and is described by eqns. 1–4. Solvation of the solute molecules by the modifier molecules proceeds in the mobile phase:



for  $c = 1, 2, 3, \dots, C$  with the equilibrium constant

$$K_{SM} = (SM_c)_m / S_m M_m^c = Z_c / S_m M_m^c \quad (24)$$

where  $Z_c$  is the mole fraction of  $c+1$ -molecular associates in the mobile phase.

Simultaneously, association of the modifier molecules occurs in the mobile phase:



for  $d = 2, 3, 4, \dots, D$ , with the equilibrium constant

$$K_{MM} = (M_d)_m / M_m^d = Z_d M_m^d \quad (26)$$

where  $Z_d$  is the mole fraction of  $d$ -molecular associates in the mobile phase.

As no associates appear on the sorbent,

$$S_s = [S_s^0] \quad (27)$$

$$L_s = [L_s^0] \quad (28)$$

$$M_s = [M_s^0] \quad (29)$$

and eqn. 6 remains correct for the case in question.

In the mobile phase we have

$$[S_m^0] + [M_m^0] + L_m = 1 \quad (30)$$

where  $[S_m^0]$  and  $[M_m^0]$  are the total concentrations of the different forms of solute and modifier in the mobile phase.

Assuming that  $S_m \ll M_m$ ,  $L_m$  and  $S_s \ll M_s$ ,  $L_s$ , we have

$$L_m + [M_m^0] \approx 1 \quad (31)$$



and

$$L_s + M_s \approx 1 \quad (32)$$

On the other hand,

$$[S_m^0] = S_m + \sum_{c=1}^C Z_c = S_m \left( 1 + \sum_{c=1}^C K_{SM} M_m^c \right) \quad (33)$$

and

$$[M_m^0] = M_m + \sum_{c=1}^C c Z_c + \sum_{d=2}^D d Z_d \quad (34)$$

$$\begin{aligned} [M_m^0] &= M_m + \sum_{c=1}^C c K_{SM} S_m M_m^c + \sum_{d=2}^D d K_{MM} M_m^d \\ &= M_m \left( 1 + K_{SM} \sum_{c=1}^C c S_m M_m^{c-1} + K_{MM} \sum_{d=2}^D d M_m^{d-1} \right) \end{aligned} \quad (35)$$

As  $S_m$  is a factor of  $10^2$ – $10^3$  smaller than  $M_m$ , and  $K_{SM}$  is commensurate with  $K_{MM}$ , then

$$[M_m^0] = M_m \left( 1 + K_{MM} \sum_{d=2}^D d M_m^{d-1} \right) \quad (36)$$

It follows from eqns. 2 and 4 that

$$K_S = (S_s/S_m) \frac{K_M M_m}{M_s} \quad (37)$$

From eqns. 4, 31 and 32 we have

$$K_M = M_s(1 - [M_m^0])/M_m(1 - M_s) \quad (38)$$

Introducing eqn. 35 into eqn. 38, we obtain

$$\begin{aligned} M_s - M_s[M_m^0] &= K_M M_m - K_M M_m M_s \\ &= M_s - M_s \left[ M_m \left( 1 + K_{SM} S_m \sum_{c=1}^C c M_m^{c-1} + K_{MM} \sum_{d=2}^D d M_m^{d-1} \right) \right] \end{aligned} \quad (39)$$

and

$$M_s = K_M M_m \left[ 1 - M_m \left( 1 + K_{SM} S_m \sum_{c=1}^C c M_m^{c-1} + K_{MM} \sum_{d=2}^D d M_m^{d-1} \right) + K_M M_m \right] \quad (40)$$

$$M_s = K_M M_m \left[ 1 + M_m (K_M - 1) - K_{SM} S_m \sum_{c=1}^C c M_m^c + K_{MM} \sum_{d=2}^D d M_m^d \right] \quad (41)$$

Introducing eqn. 41 into eqn. 37, we obtain

$$K_S = (S_s/S_m) \left[ 1 + (K_M - 1)M_m - K_{SM}S_m \sum_{c=1}^C cM_m^c + K_{MM} \sum_{d=2}^D dM_m^d \right] \quad (42)$$

Since according to analogy with eqn. 12

$$k' = \Phi(S_s/[S_m^0]) = \Phi K \quad (43)$$

then, introducing eqn. 33 into eqn. 43, we obtain

$$k' = \Phi(S_s/S_m) \left( 1 + K_{SM} \sum_{c=1}^C M_m^c \right)^{-1} \quad (44)$$

Introducing the values of  $S_s/S_m$  from eqn. 42 into eqn. 44, we obtain

$$k' = \Phi K_S \left( 1 + \sum_{c=1}^C K_{SM} M_m^c \right)^{-1} \left[ 1 + M_m(K_M - 1) - K_{SM}S_m \sum_{c=1}^C cM_m^c - K_{MM} \sum_{d=2}^D dM_m^d \right]^{-1} \quad (45)$$

and

$$1/k' = (1/\Phi K_S) \left( 1 + \sum_{c=1}^C K_{SM} M_m^c \right) \left[ 1 + (K_M - 1)M_m - K_{SM}S_m \sum_{c=1}^C cM_m^c - K_{MM} \sum_{d=2}^D dM_m^d \right] \quad (46)$$

In the absence of associates in the solution, *i.e.*,  $K_{SM} = 0$  and  $K_{MM} = 0$ , we obtain eqn. 16 of the linear dependence of  $1/k'$  on  $M_m$ . When associates are formed between the molecules of the modifier and the solute,  $K_{SM} > 0$ , and in the absence of association of the modifier molecules,  $K_{MM} = 0$ , the value of  $1/k'$  increases faster (with increasing content of the modifier  $M_m$  in the mobile phase) than to the first power of  $M_m$ . In contrast, the formation of associates of modifier molecules decreases  $1/k'$  with respect to the linear dependence. Thus, in the general case, eqn. 46 represents a complex curvilinear dependence of the solute retention on the modifier concentration, its character being determined by the ratio of the constants  $K_{SM}$ ,  $K_{MM}$ ,  $K_M$  and  $K_S$  corresponding to various types of intermolecular processes occurring in a chromatographic system.

When the interaction between the molecules of the solute and modifier with the sorbent ( $K_S$  and  $K_M$ ) is stronger than the molecular interactions in the solution ( $K_{SM}$ ), which is typical for NP-HPLC, the dependence of  $1/k'$  on  $M_m$  should approach linearity. For example, phenols, which are strongly adsorbed from solution onto a silica gel surface in the *n*-hexane-dioxane system, fit eqn. 16 (see Fig. 1).

Specific and non-specific molecular interactions in the mobile phase are more strongly exhibited in RP-HPLC, which is well seen in Fig. 7, where the dependence of  $1/k'$  on  $N_m$  is non-linear. This character of the dependence shows that in RP-HPLC the contribution of specific and non-specific interactions of phenol molecules with the molecule of the mobile phase is comparable to the non-specific interactions of the solute molecules with the hydrophobic surface of the stationary phase.

In the limiting case, where adsorption of the modifier ( $K_M$ ) is much less than the interaction of the solute with the modifier ( $K_{SM}$ ), the retention of substances is approximately described by the equation

$$1/k' = (1/\Phi K_S) \left( 1 + K_{SM} \sum_{c=1}^c M_m^c \right) = (1/\Phi K_S) (1 + K_{SM} M_m^n) \quad (47)$$

where  $n$  characterizes some mean solvation number of the solute molecules in the mobile phase. Then, in the coordinates of  $1/k'$  versus  $M_m^n$ , a certain linearity is observed for phenol at  $n = 3$  (Fig. 9a) and for 3-*tert.*-butylphenol at  $n = 4$  (Fig. 9b);  $n$  is higher for the larger and more hydrophobic 3-*tert.*-butylphenol molecule than for phenol.

Considering the chromatographic retention of mycotoxins of the trichothecene series (nivalenol, deoxynivalenol and deoxynivalenol 15-acetate), which differ in the number of polar groups, we can see (Fig. 10) that the rectilinear dependence of  $1/k'$  on  $M_m$  is well realized for deoxynivalenol 15-acetate for all investigated modifiers of the mobile phase (acetonitrile, tetrahydrofuran, ethanol). The molecule of deoxynivalenol 15-acetate is the most hydrophobic among the investigated mycotoxins and is most strongly retained by the reversed phase.

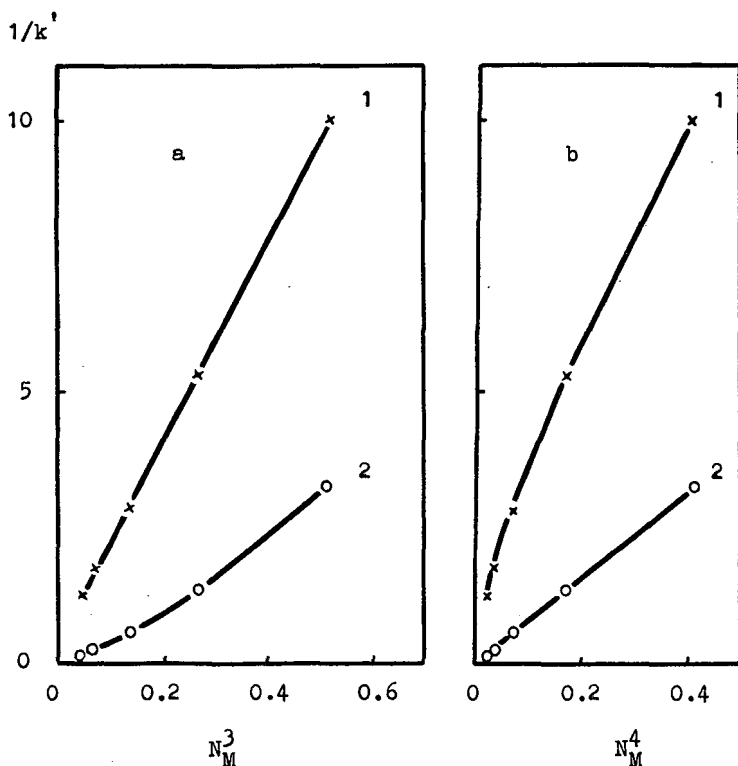


Fig. 9. Dependence of the reciprocal of the capacity factor ( $1/k'$ ) on the mole fraction ( $N_M$ ) of methanol in the mobile phase. Conditions as in Fig. 7. (a)  $N_M^3$ ; (b)  $N_M^4$ . 1 = Phenol; 2 = 3-*tert.*-butylphenol.

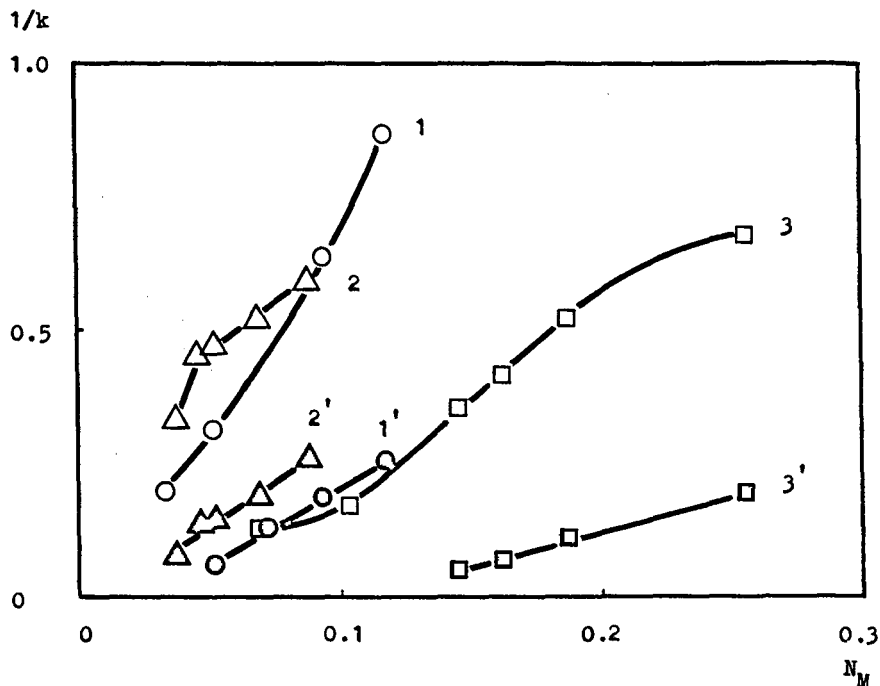


Fig. 10. Dependence of the reciprocal of the capacity factor ( $1/k'$ ) on the mole fraction ( $N_M$ ) of the organic component in binary water-organic mobile phases. Conditions as in Fig. 8. (1-3) Deoxynivalenol; (1'-3') deoxynivalenol 15-acetate.

With the more polar nivalenol, which is less strongly adsorbed on the stationary phase, a dependence close to linearity is observed only for the ethanol mobile phase (Fig. 8). The curvilinear dependence which, according to eqn. 46, indicates a considerable contribution of interactions of the modifier molecules with each other in the mobile phase, is more typical for the more hydrophobic modifiers tetrahydrofuran and acetonitrile. For deoxynivalenol, the character of the retention dependence in different mobile phases is similar to that observed for nivalenol.

As is seen in eqn. 46, at  $M_m$  approaching zero the values of  $k'$  must be equal to the value of  $\Phi K_s$ , i.e. the retention  $k'$  of the solute with water as the mobile phase. Fig. 8 shows that on extrapolation of the initial parts of the dependence of  $1/k'$  on  $M_m$  towards  $M_m = 0$  for three different modifiers, the points of intersection with the ordinate are actually close to each other and very close to zero, which is indicative of a very strong retention when water is used as the mobile phase.

The calculation of the first three points of the curves (Fig. 8) according to eqn. 48:

$$1/k' = a + bN_m \quad (48)$$

where  $a$  and  $b$  are constants resulted in values for the intersection points of  $a = 0.1 \pm 0.46$ ,  $0.13 \pm 0.58$  and  $0.15 \pm 2.2$  for ethanol, acetonitrile and tetrahydrofuran, respectively, as modifiers.

Hence eqn. 46 allows one to describe a change in the retention of substances in NP- and RP-HPLC for various cases of molecular interactions in the chromatographic system (solute–mobile phase–stationary phase).

Such an approach to the description of molecular interactions in NP- and RP-HPLC as quasi-chemical equilibria on the sorbent and in solution (of solute–sorbent, modifier–sorbent, solute–modifier and modifier–modifier types) helps in obtaining a better understanding of the retention mechanism in HPLC. It is necessary for a quantitative description of the retention dependence on the mobile phase composition to know the constants of these equilibria ( $K_S$ ,  $K_M$ ,  $K_{SM}$ ,  $K_{MM}$ ). For this purpose it is necessary to intensify studies on measuring the isotherms of adsorption from solutions of modifying additives over a wide range of concentrations and also on the determination of the association constants of substances in solutions with the use of independent techniques.

## REFERENCES

- 1 N. N. Avgul, A. V. Kiselev and D. P. Poshkus, *Adsorption of Gases and Vapours on Homogeneous Surfaces*, Khimiya, Moscow, 1975.
- 2 A. V. Kiselev, *Intermolecular Relationships in Adsorption and Chromatography*, Vysshaya Shkola, Moscow, 1986.
- 3 A. V. Kiselev, D. P. Poshkus and Ya. I. Yashin, *Molecular Principles of Adsorption Chromatography*, Khimiya, Moscow, 1986.
- 4 A. V. Kiselev, *Chromatographia*, 11 (1978) 691.
- 5 R. Kaliszan, *Quantitative Structure–Chromatographic Retention Relationships*, Wiley, New York, 1987.
- 6 R. E. Koopmans and R. F. Dekker, *J. Chromatogr.*, 285 (1984) 267.
- 7 N. Funasaki, S. Hada and S. Naya, *J. Chromatogr.*, 361 (1986) 33.
- 8 T. Hanai, K. C. Tran and J. Hubert, *J. Chromatogr.*, 239 (1982) 385.
- 9 S. N. Lanin and Yu. S. Nikitin, *Chromatographia*, 25 (1988) 272.
- 10 P. C. Sadek, P. W. Carr, R. M. Doherty, M. J. Kamlet, R. W. Taft and M. H. Abraham, *Anal. Chem.*, 57 (1985) 2971.
- 11 B. P. Johnson, M. G. Khaldi and J. G. Dorsey, *Anal. Chem.*, 58 (1986) 2354.
- 12 J. H. Park and P. W. Carr, *J. Chromatogr.*, 465 (1989) 123.
- 13 Cs. Horvath, W. Melander and J. Molnar, *J. Chromatogr.*, 125 (1976) 129.
- 14 P. Jandera and J. Churacek, *J. Chromatogr.*, 91 (1974) 207.
- 15 B. L. Karger, J. R. Gant, A. Hartkopf and P. H. Weiner, *J. Chromatogr.*, 128 (1976) 65.
- 16 F. Murakami, *J. Chromatogr.*, 178 (1979) 393.
- 17 H. Colin, A. M. Krastulovic, M. F. Connord, G. Guiochon, Z. Yun and P. Jandera, *Chromatographia*, 17 (1983) 9.
- 18 K. Karch, I. Sebastian and I. Halász, *J. Chromatogr.*, 122 (1976) 3.
- 19 R. P. W. Scott and P. Kucera, *J. Chromatogr.*, 142 (1977) 213.
- 20 N. Tanaka, Y. Tokuda, K. Iwaguchi and M. Araki, *J. Chromatogr.*, 239 (1982) 761.
- 21 S. N. Lanin, Yu. S. Nikitin, A. A. Pyatygin and S. M. Staroverov, *Chromatographia*, 27 (1989) 147.
- 22 E. Arvidsson, J. Crommen, G. Schill and D. Westerlund, *Chromatographia*, 24 (1987) 460.
- 23 L. R. Snyder, *Principles of Adsorption Chromatography*, Marcel Dekker, New York, 1968.
- 24 R. P. W. Scott, *J. Chromatogr.*, 122 (1976) 35.
- 25 *Supelco Rep.*, 8, No. 4 (1989) 1.
- 26 S. N. Sychev, N. S. Aksenova and S. S. Krivolapov, *Zh. Fiz. Khim.*, 59 (1985) 1996.
- 27 N. N. Gryazev, *Dokl. Akad. Nauk SSSR*, 118 (1958) 121.
- 28 J. Wenograd and R. A. Spurr, *J. Am. Chem. Soc.*, 79 (1957) 5844.
- 29 Yu. A. Zolotov, A. A. Ivanov and O. A. Shpigun, *Zh. Anal. Khim.*, 38 (1983) 1479.
- 30 M. Boumahraz, V. Ya. Davydov and A. V. Kiselev, *Chromatographia*, 15 (1982) 751.
- 31 M. Jaroniec and J. A. Jaroniec, *J. Chromatogr.*, 295 (1984) 377.
- 32 M. Jaroniec and J. A. Jaroniec, *J. Liq. Chromatogr.*, Suppl. 2, 7 (1984) 393.
- 33 P. Daucik, A. M. Rizzi and J. F. K. Huber, *J. Chromatogr.*, 442 (1988) 53.



CHROM. 22 791

## **Comparison of retention index scales based on alkyl aryl ketones, alkan-2-ones and 1-nitroalkanes for polar drugs on reversed-phase high-performance liquid chromatography**

ROGER M. SMITH\* and NOEL FINN

*Department of Chemistry, Loughborough University of Technology, Loughborough, Leics. LE11 3TU (U.K.)*

(First received December 12th, 1989; revised manuscript received July 31st, 1990)

---

### ABSTRACT

The potential of alkan-2-ones, alkyl aryl ketones and 1-nitroalkanes as retention index standards in reversed-phase liquid chromatography has been examined using methanol–buffer, acetonitrile–buffer and tetrahydrofuran–buffer eluents. The aliphatic standards had retention times more similar to those of rapidly eluted polar drugs than the aromatic ketones. However, the retention indices of the drugs were sensitive to eluent composition and pH and to the brand of ODS-silica column material.

---

### INTRODUCTION

Over the last ten years there have been a number of studies into the application of retention indices in high-performance liquid chromatography (HPLC) [1]. The two most widely applied homologous series of standards are the alkyl aryl ketones [2] and the alkan-2-ones [3] and both have been employed for the identification of drug compounds. They were selected because of their ready availability, reasonable stability and detectability using spectrophotometric detectors. Subsequently Bogusz and Aderjan have suggested the use of the homologous 1-nitroalkanes as retention index standards for HPLC [4] and gas–liquid chromatography [5].

All three series of standards are usable across a wide range of eluent composition but although the alkyl aryl ketones have the advantage of a strong chromophore, because of their larger size and thus longer retentions they cannot be readily applied to rapidly eluted polar drugs.

Bogusz [6] also examined the use of corrected retention indices to compensate for differences in the separations of the barbiturates on different makes of ODS-bonded stationary phases. Bogusz and co-workers subsequently reported the correction of retention indices of acidic [7], basic [8] and neutral [7,8] drugs on a range of ODS-silica stationary phases. In more recent work this approach has been extended to a comparison of the 1-nitroalkane and alkyl aryl ketone scales for corrected retention indices of basic drugs and they concluded that the former scale was superior [9].

However, the two scales were compared using different test compounds and a re-evaluation of the results has found that the differences between the scales were negligible [10].

A major role of retention indices in chromatography is to increase the robustness of analysis results because as relative retention measurements they should compensate for small differences in the experimental conditions caused by variations between laboratories, instruments, or even in the preparation of the eluent on a different day or by a different operator. They can also be used as a reference scale to monitor differences between column and separation conditions, for interlaboratory comparisons and to establish databases of retention values.

The present study examines homologous alkyl aryl ketones, alkan-2-ones and 1-nitroalkanes as potential retention index standards and compares their retentions with those of a number of typical polar drug compounds in different acetonitrile–buffer, methanol–buffer and tetrahydrofuran (THF)–buffer eluents. Limited comparisons were also carried out of the effect of pH changes and the use of a different ODS-silica column.

## EXPERIMENTAL

### *Materials and chemicals*

The retention index standard compounds, nitromethane to nitrohexane, acetone to heptan-2-one and nonan-2-one were supplied by Aldrich (Poole, U.K.). The alkyl aryl ketones, acetophenone to valerophenone, column test compounds and drug test compounds were obtained from a number of sources. Methanol, acetonitrile, THF and water were HPLC grade and disodium hydrogen orthophosphate and potassium dihydrogen phosphate were analytical grade from FSA (Loughborough, U.K.).

### *Solutions*

Standard solutions of nitroalkanes and alkyl aryl ketones (20–30  $\mu\text{l}$ /500 ml) and alkan-2-ones (100–600  $\mu\text{l}$ /5 ml) were prepared in mobile phase.

Buffer pH 7.0 was prepared from disodium hydrogenorthophosphate (0.50 g) and potassium dihydrogenphosphate (0.301 g) in water (1 l).

### *Equipment*

HPLC separations were carried out using a Philips 4010 pump and Philips 4025 variable-wavelength detector set at 220 nm. The samples (10  $\mu\text{l}$ ) were injected using a 7125 Rheodyne valve, fitted with a 20- $\mu\text{l}$  loop, onto a 100  $\times$  5 mm column packed with either ODS-Hypersil (5  $\mu\text{m}$ , batch 10/1229, Shandon Southern, Runcorn, U.K.), or ODS-Zorbax (7  $\mu\text{m}$ , DuPont, Wilmington, DE, U.S.A.). The columns were thermostated at 30°C in a circulating water jacket.

The mobile phase was pumped at 1 ml/min and the column void volumes were detected using a solution of sodium nitrate (6.25 mg/ml). Retention times were determined using a Linseis chart recorder.

### *Procedure*

The retention times were measured in triplicate and were used to calculate capacity factors. The retention indices ( $I$ ) were calculated using  $I = 100n + 100$



$(\log k'_x - \log k'_{R1}) / (\log k'_{R2} - \log k'_{R1})$  where  $k'_{R1}$  and  $k'_{R2}$  are the capacity factors of the homologous retention index standards, containing  $n$  and  $n + 1$  carbon atoms respectively, being eluted immediately before and after the analyte with retention  $k'_x$ . Some analytes were eluted outside the set of retention index standards and their indices were calculated by extrapolation from the closest available standards.

TABLE I

## CAPACITY FACTORS OF RETENTION INDEX STANDARDS AND TEST COMPOUNDS

Conditions: column, ODS-Hypersil; eluent, modifier-phosphate buffer pH 7.0; detection, 220 nm.

Compound	Capacity factors									
	Methanol (%)				Acetonitrile (%)			THF (%)		
	20	30	40	50	10	20	30	20	30	40
<i>Alkan-2-ones</i>										
Acetone	0.88	0.63	0.54	0.45	0.98	0.72	0.53	0.55	0.40	—
Butan-2-one	1.97	1.38	1.01	0.74	2.33	1.54	1.12	0.83	0.75	0.64
Pentan-2-one	5.72	3.32	2.14	1.38	6.94	3.70	2.12	1.95	1.43	1.03
Hexan-2-one	18.21	9.30	5.13	2.81	22.16	10.19	4.85	5.13	2.96	1.79
Heptan-2-one	49.08	22.87	12.35	5.66	68.56	24.94	—	13.75	6.08	2.84
Nonan-2-one	—	149.03	53.26	19.06	—	131.92	—	99.87	21.92	6.68
<i>1-Nitroalkanes</i>										
Nitromethane	0.62	0.51	0.49	0.40	0.87	0.90	0.87	0.90	0.85	0.70
Nitroethane	1.32	1.07	0.86	0.65	2.28	1.99	1.53	1.60	1.44	1.06
Nitropropane	3.84	2.59	1.82	1.22	7.01	4.88	3.18	3.70	2.72	1.70
Nitrobutane	11.95	7.07	4.20	2.41	23.32	13.20	6.80	9.63	5.50	2.84
Nitropentane	38.66	19.83	10.28	5.11	81.92	37.50	15.10	25.80	11.05	4.53
Nitrohexane	129.72	59.09	26.20	11.08	—	108.40	34.18	70.10	21.54	7.10
<i>Alkyl aryl ketones</i>										
Acetophenone	21.94	10.35	5.29	2.63	31.92	11.14	4.87	6.46	3.18	1.64
Propiophenone	62.96	26.95	11.92	5.45	98.70	30.20	11.00	16.60	6.50	2.92
Butyrophenone	182.77	69.05	27.29	10.97	—	77.24	23.31	39.73	12.20	4.56
Valerophenone	—	195.17	67.07	—	—	—	—	100.90	23.13	7.08
<i>Column test compounds</i>										
N-Methylaniline	14.61	8.11	4.70	2.60	25.53	12.00	6.09	11.75	5.94	2.97
2-Phenylethanol	15.58	8.01	4.33	2.31	19.65	6.18	2.50	4.80	2.40	1.28
<i>p</i> -Cresol	19.03	9.92	5.19	2.65	29.11	10.10	4.09	15.40	5.94	2.55
Nitrobenzene	20.51	11.55	6.49	3.47	37.90	18.40	8.20	17.20	7.05	2.98
Toluene	80.01	45.86	24.55	12.14	—	60.99	23.43	54.07	17.72	6.42
<i>Drug compounds</i>										
Aspirin	0.97	0.46	0.24	0.11	1.00	0.11	0.06	0.06	0.04	—
Paracetamol	1.58	0.84	0.57	0.41	1.92	0.81	0.51	0.94	0.67	0.48
Theophylline	2.34	1.11	0.64	0.40	1.93	0.61	0.33	0.52	0.32	0.24
Barbitone	4.62	2.20	1.18	0.69	5.61	1.66	0.78	2.45	1.70	1.13
Salicylamide	5.66	2.85	1.49	0.88	8.42	2.77	1.37	4.17	1.99	1.09
Caffeine	4.66	1.88	1.01	0.64	4.61	0.95	0.54	0.53	0.36	0.27
Phenobarbitone	13.48	5.34	2.22	1.06	24.36	4.96	1.62	8.14	3.76	1.91
Phenacetin	23.85	9.28	4.25	2.11	34.40	—	—	4.55	1.85	1.01
Diazepam	—	—	—	—	—	—	—	37.82	7.30	2.52

## RESULTS AND DISCUSSION

In order to study the relative retentions of the standards and drug compounds and to determine the influence of eluent composition on retention indices, the capacity factors of members of three homologous series, the alkan-2-ones (acetone to nonan-2-one), the nitroalkanes (nitromethane to nitrohexane) and the alkyl aryl ketones (acetophenone to valerophenone) were measured using a range of buffered pH 7.0 eluents, containing methanol, acetonitrile or THF (Table I). The retentions were also measured for a selection of polar neutral, basic and acidic drug compounds and for a set of aromatic column test compounds (nitrobenzene, toluene, *p*-cresol, 2-phenylethanol and *N*-methylaniline). These last compounds had been chosen in a previous study as characterising the different interactions between eluent and stationary phases [11]. All the compounds gave good peak shapes and reproducible results.

One reason for selecting a homologous series of standard compounds to form a retention index scale is that they are usually systematically spaced throughout the chromatogram. In an isocratic separation there is normally a linear relationship between the logarithm of the capacity factor ( $\log k'$ ) and the carbon number of each homologue. The differences in  $\log k'$  between successive homologues are the methylene increments, which in a particular eluent should be constant and independent of the functional groups present. However, differences have been found in earlier work between homologous alkyl aryl ketones and alkan-2-ones [2] and between derivatives of homologous alcohols and amines [12].

However, although the correlation coefficients were good for a linear relationship between carbon number and  $\log k'$  for the alkyl aryl ketones (0.9999–0.9995 except for 40% THF 0.9976), the correlations for the alkan-2-ones and nitroalkanes were generally much poorer (0.9995–0.9943) and the relationships were curved (Figs. 1 and 2). Nitromethane and nitroethane appeared to be more highly retained than would be anticipated. Similar deviations from linearity were also noted for nitromethane by Bogusz and Aderjan [4] in acetonitrile–water eluents. The methylene increments for

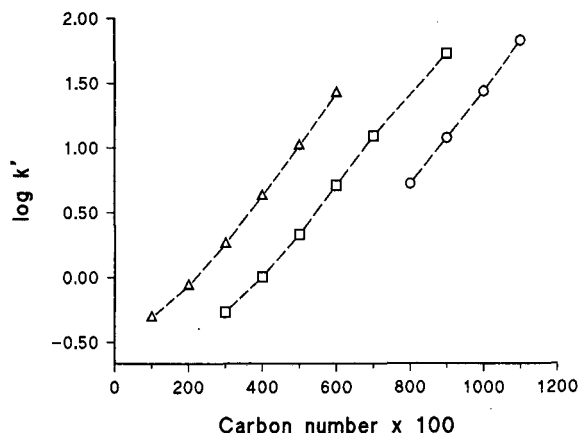


Fig. 1. Relationship of  $\log k'$  to carbon number  $\times 100$  for the three homologous series alkyl aryl ketones (O), alkan-2-ones (□) and nitroalkanes ( $\Delta$ ). Eluent, methanol–buffer pH 7.0 (40:60).

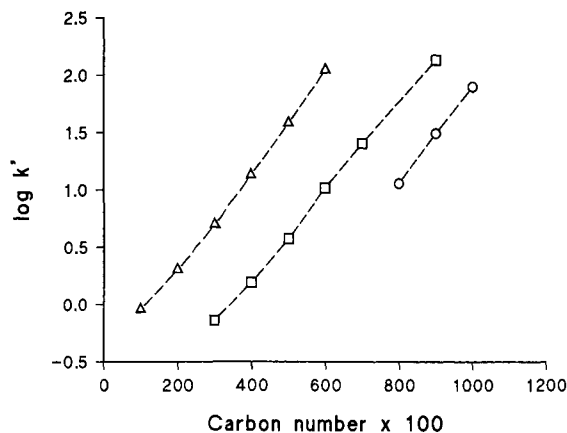


Fig. 2. As Fig. 1. Eluent, acetonitrile–buffer pH 7.0 (20:80).

each set of standards were different and generally increased with the carbon number although a drop was noted on going from heptan-2-one to nonan-2-one.

The retention indices using each of the set of homologues were therefore determined by interpolation between the logarithms of the capacity factors of adjacent pairs of standards. The indices based on the alkyl aryl ketones [ $I(\text{AAK})$ ], nitroalkanes [ $I(\text{NO}_2)$ ] and alkan-2-ones [ $I(\text{CO})$ ] were compared in a typical eluent [Table II, methanol–buffer (40:60)]. The retention index of acetophenone, the smallest alkyl aryl ketone ( $\text{C}_8$ ) [ $I(\text{CO}) = 619$ ,  $I(\text{NO}_2) = 426$ ] is close to that of hexan-2-one and a little larger than the value for nitrobutane. Acetone [ $I(\text{NO}_2) = 118$ ] and nitromethane [ $I(\text{NO}_2) = 100$ ] the smallest members of the other two series had very similar retentions. The alkyl aryl ketones were more highly retained than the drug compounds and extrapolation of the scale was therefore required to determine the  $I(\text{AAK})$  values. In contrast all the drugs, with the exception of aspirin, fell within the ranges of the two sets of aliphatic standards demonstrating the increased application of these scales for rapidly eluted compounds.

In order to compare the effects of the eluent composition on the relative retentions, the retention indices  $I(\text{CO})$  of all the analytes in the different eluents were calculated based on the alkan-2-one scale. On increasing the proportion of methanol the indices of the nitroalkanes increased only slightly but those of the alkyl aryl ketones decreased (Table III). With the exception of toluene, whose retention index increased noticeably with the proportion of methanol, the retention indices of the column test compounds also changed very little. This confirmed the robustness of the retention indices of non-ionised compounds towards small changes in eluent composition. Similar but larger effects were observed on increasing the proportion of acetonitrile or THF (Table III). The differences between the retention indices measured using the different modifiers are a measure of the changes in the elution selectivities of the eluents.

However, in all three eluent combinations the retention indices for most of the polar drugs decreased significantly, by up to 150 units, with increased proportions of

TABLE II

COMPARISON OF RETENTION INDICES CALCULATED USING DIFFERENT SCALES IN METHANOL-BUFFER (40:60)

Conditions: column, ODS-Hypersil; eluent, methanol-phosphate buffer pH 7.0 (40:60); spectroscopic detection, 220 nm. Indices in parentheses have been calculated by extrapolation.

Compound	Retention index scale		
	<i>I</i> (CO)	<i>I</i> (NO <sub>2</sub> )	<i>I</i> (AAK)
<i>Alkan-2-ones</i>			
Acetone	300 <sup>a</sup>	118	(520)
Butan-2-one	400	219	(596)
Pentan-2-one	500	319	(689)
Hexan-2-one	600	422	(796)
Heptan-2-one	700	520	904
Nonan-2-one	900	(676)	1076
<i>1-Nitroalkanes</i>			
Nitromethane	(257)	100 <sup>a</sup>	(507)
Nitroethane	342	200	(577)
Nitropropane	426	300	(669)
Nitrobutane	564	400	(772)
Nitropentane	676	500	882
Nitrohexane	798	600	992
<i>Alkyl aryl ketones</i>			
Acetophenone	619	426	800 <sup>a</sup>
Propiophenone	(723)	516	900
Butyrophenone	(833)	(607)	1000
Valerophenone	—	(700)	1100
<i>Column test compounds</i>			
N-Methylaniline	589	412	785
2-Phenylethanol	582	404	777
<i>p</i> -Cresol	603	425	799
Nitrobenzene	626	448	825
Toluene	794	593	985
<i>Drug compounds</i>			
Aspirin	(170)	(<0)	(420)
Paracetamol	308	124	(526)
Theophylline	327	147	(540)
Barbitone	421	242	(616)
Salicylamide	452	273	(644)
Caffeine	400	221	(596)
Phenobarbitone	504	324	(693)
Phenacetin	579	401	(774)

<sup>a</sup> Index standards *I* = carbon number × 100.

modifier (Table III, Fig. 3). These effects were expected from previous studies of the changes in the contributions of different functional groups to retention [13], which found that more polar groupings, such as amido, amino, hydroxyl and phenolic groups, showed larger changes with composition than did the relatively non-polar nitro and carbonyl groups. Thus the retention of compounds which are rapidly eluted

TABLE III

## RETENTION INDICES BASED ON ALKAN-2-ONES OF RETENTION INDEX STANDARDS AND TEST COMPOUNDS

Conditions as in Table I. Retention indices in parentheses are derived by extrapolation from the standards.

Compound	Retention index <i>I</i> (CO)									
	Methanol (%)				Acetonitrile (%)			THF (%)		
	20	30	40	50	10	20	30	20	30	40
<i>1-Nitroalkanes</i>										
Nitromethane	(257)	(273)	(284)	(277)	(286)	330	367	409	419	419
Nitroethane	342	367	374	374	398	429	449	477	501	504
Nitropropane	426	472	478	480	501	527	549	566	590	590
Nitrobutane	564	573	577	578	604	629	(640)	664	686	700
Nitropentane	676	684	679	685	(716)	750	(737)	764	793	809
Nitrohexane	798	801	803	811	—	876	(836)	864	897	(914)
<i>Alkyl aryl ketones</i>										
Acetophenone	619	612	604	591	631	610	600	623	610	584
Propiophenone	(723)	717	694	691	732	723	(697)	719	710	706
Butyrophenone	(833)	818	812	809	—	836	(789)	807	809	811
Valerophenone	—	(929)	931	—	—	—	—	(901)	(908)	(913)
<i>Column test compounds</i>										
N-Methylaniline	581	587	589	589	612	618	(620)	684	697	710
2-Phenylethanol	586	586	582	572	589	550	520	593	571	539
<i>p</i> -Cresol	604	608	603	592	624	599	579	712	697	676
Nitrobenzene	612	624	626	630	647	666	(663)	723	723	711
Toluene	(749)	774	794	828	—	807	(790)	838	867	890
<i>Drug compounds</i>										
Aspirin	312	(260)	(170)	(44)	302	(54)	(8)	<0	<0	—
Paracetamol	373	337	308	(282)	378	315	(295)	415	379	(340)
Theophylline	416	372	327	(277)	378	(278)	(236)	(287)	(240)	(194)
Barbitone	481	454	421	386	480	408	352	524	524	517
Salicylamide	499	483	452	428	517	467	432	579	546	510
Caffeine	485	435	400	371	463	336	303	(292)	(262)	(219)
Phenobarbitone	574	546	504	458	608	529	(602)	647	633	614
Phenacetin	627	600	579	559	639	529	—	588	535	496
Diazepam	—	—	—	—	—	—	—	802	727	674

because they contain a number of polar functions are likely to alter to a different extent on changing the composition of the eluent than smaller less polar compounds, which are rapidly eluted because of their small size. Thus it appears that the application of these retention index scales to very polar analytes may be inherently limited because the values will be susceptible to small changes in eluent composition. Because the relative retentions of the nitroalkanes and alkan-2-ones were largely unchanged with composition the effects on indices based on either scale would be similar.

Because of concern that the nitroalkanes could be ionised in high-pH eluents the capacity factors and retention indices of the standards and test compounds were measured at pH 3.2 and pH 8.2 using methanol-buffer (50:50) and acetonitrile-buffer

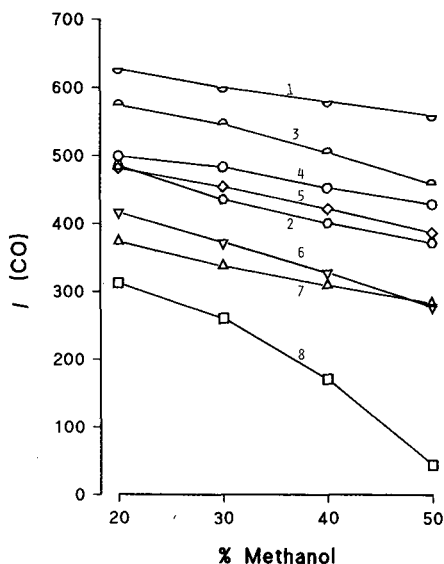


Fig. 3. Effect of proportion of methanol on the retention indices  $I(\text{CO})$  of drug compounds on ODS-Hypersil column. Compounds: 1 = phenacetin; 2 = caffeine; 3 = phenobarbitone; 4 = salicylamide; 5 = barbitone; 6 = theophylline; 7 = paracetamol; 8 = aspirin.

(30:70) eluents. However, no significant changes were observed in the relative retentions of the three homologous series or the neutral column test compounds. Because of protonation *N*-methylaniline was more rapidly eluted at pH 3.2 and its retention index dropped by 70 units in methanol and 113 units in acetonitrile compared to pH 7.0. The retention indices of the acidic drugs, salicylamide, barbitone and phenobarbitone all decreased at pH 8.2, by up to 140 units, reflecting partial ionisation.

#### *Different stationary phases*

In order to determine if the relationships between the three retention index scales were similar on different brands of ODS-silica the separations were repeated on an ODS-Zorbax column using methanol-buffer pH 7.0 (50:50), and the capacity factors and retention indices [ $I(\text{CO})$ ] were calculated (Table IV). Except for nitroethane the differences for the nitroalkanes were less than 15 units but the alkyl aryl ketones were relatively more highly retained, by up to 40 units, on the ODS-Zorbax column.

Larger differences were found for the column test compounds, with 2-phenylethanol (-68 units) and *p*-cresol (-87 units) being more rapidly eluted and nitrobenzene (+47 units) and toluene (+50 units) being more retained on the ODS-Zorbax column. These selectivity changes match those observed earlier for polar compounds on an ODS-Zorbax column, which has a generally lower retention for compounds containing hydroxylic or phenolic groups [11].

These marked differences between the selectivity of the column materials were also reflected in the retention of the acidic drugs paracetamol, barbitone, salicylamide,

TABLE IV

## COMPARISON OF CAPACITY FACTORS AND RETENTION INDICES ON DIFFERENT STATIONARY PHASES

Conditions: eluent, methanol-buffer pH 7.0 (50:50). H = Hypersil; Z = Zorbax.

Compound	$k'$		$I(\text{CO})$	
	ODS-H	ODS-Z	ODS-H	ODS-Z
<i>Alkan-2-ones</i>				
Acetone	0.45	0.51	300	300
Butan-2-one	0.74	0.80	400	400
Pentan-2-one	1.38	1.23	500	500
Hexan-2-one	2.81	2.32	600	600
Heptan-2-one	5.66	4.07	700	700
Nonan-2-one	19.06	15.73	900	900
<i>1-Nitroalkanes</i>				
Nitromethane	0.40	0.44	(277)	(267)
Nitroethane	0.65	0.63	374	347
Nitropropane	1.22	1.14	480	482
Nitrobutane	2.41	2.00	578	578
Nitropentane	5.11	3.89	685	692
Nitrohexane	11.08	7.71	811	794
<i>Alkyl aryl ketones</i>				
Acetophenone	2.63	2.81	591	634
Propiophenone	5.45	5.11	691	733
Butyrophenone	10.97	9.13	809	819
Valerophenone	—	18.07	—	920
<i>Column test compounds</i>				
N-Methylaniline	2.60	2.29	589	598
2-Phenylethanol	2.31	1.26	572	504
<i>p</i> -Cresol	2.65	1.27	592	505
Nitrobenzene	3.47	3.53	630	675
Toluene	12.14	13.60	828	878
<i>Drug compounds</i>				
Paracetamol	0.41	0.31	(282)	(189)
Theophylline	0.40	0.44	(277)	(267)
Barbitone	0.69	0.40	386	(245)
Salicylamide	0.88	0.57	428	326
Caffeine	0.64	1.50	371	533
Phenobarbitone	1.06	0.44	458	(267)
Phenacetin	2.11	1.27	559	503

phenobarbitone and phenacetin, which all had lower relative retentions on the ODS-Zorbax column. In contrast, caffeine was more highly retained.

In his work on corrected retention indices Bogusz [6] demonstrated that it was possible to compensate for differences in the retention indices of barbiturates on ODS-Hypersil and ODS-Zorbax columns. His technique corrected for systematic differences in the retentions of the analytes and the retention index scale standards by scaling the indices relative to those found on a "standard" column. However, this

approach will fail in the present study as the order of elution is different on the two different ODS-phases. These conditions are likely to occur in other cases when there are major differences in the test and standard stationary phases. Analytes which contain different interactive groups may be eluted in a different order. For these columns the correction method will only work reliably for closely related groups of compounds with a "pseudo-homologous" relationship (such as the barbiturates) in which all the analytes have the same functional groups and similar polarity but differ in the extent of alkyl substitution.

## CONCLUSION

Both the alkan-2-one and 1-nitroalkane homologues had similar retention times to a range of rapidly eluted basic drugs and thus should be more suitable as the basis of retention scales for these compounds than the more highly retained alkyl aryl ketones. However, at short retention times the relative retentions of the standards and drugs are susceptible to small changes in the proportion of modifier in the eluent. The retention indices can therefore only partially compensate for small changes in the separation conditions and this emphasises the importance of controlling the separation parameters in qualitative analysis.

Large differences in selectivity were found between two different ODS-bonded silica columns which suggests that attempts to correct retentions on "equivalent" ODS-bonded silica stationary phases may have limited applicability. For the reliable comparison of results in different laboratories it will still be necessary to closely specify the brand of stationary phase.

## REFERENCES

- 1 R. M. Smith, *Adv. Chromatogr.*, 26 (1987) 277.
- 2 R. M. Smith, *J. Chromatogr.*, 236 (1982) 313.
- 3 J. K. Baker and C.-Y. Ma, *J. Chromatogr.*, 169 (1979) 107.
- 4 M. Bogusz and R. Aderjan, *J. Chromatogr.*, 435 (1988) 43.
- 5 R. Aderjan and M. Bogusz, *J. Chromatogr.*, 454 (1988) 345.
- 6 M. Bogusz, *J. Chromatogr.*, 387 (1987) 404.
- 7 M. Bogusz and R. Aderjan, *J. Anal. Toxicol.*, 12 (1988) 67.
- 8 M. Bogusz, R. Aderjan, J. P. Franke and R. A. de Zeeuw, *Z. Rechtsmed.*, 98 (1987) 263.
- 9 M. Bogusz, G. Neidl-Fischer and R. Aderjan, *J. Anal. Toxicol.*, 12 (1988) 325.
- 10 R. M. Smith, R. Gill and M. D. Osselton, *J. Anal. Toxicol.*, 13 (1989) 375.
- 11 R. M. Smith, *Anal. Chem.*, 56 (1984) 256.
- 12 P. Jandera, *J. Chromatogr.*, 314 (1984) 13.
- 13 R. M. Smith and C. M. Burr, *J. Chromatogr.*, 475 (1989) 57.



## Changes in the enthalpy and entropy of hydroxyl aromatics in reversed-phase liquid chromatography with $\beta$ -cyclodextrin in the mobile phase

REZA M. MOHSENI<sup>a</sup> and ROBERT J. HURTUBISE\*

Chemistry Department, University of Wyoming, Laramie, WY 82071 (U.S.A.)

(First received November 7th, 1989; revised manuscript received August 30th, 1990)

---

### ABSTRACT

Standard enthalpy ( $\Delta H^\circ$ ) and entropy ( $\Delta S^\circ$ ) changes were obtained for several hydroxyl aromatics without  $\beta$ -cyclodextrin in the mobile phase, and enthalpy ( $\Delta H_f^\circ$ ) and entropy ( $\Delta S_f^\circ$ ) of complex formation were calculated for the hydroxyl aromatics with  $\beta$ -cyclodextrin in the mobile phase. Negative enthalpy and entropy values were obtained without  $\beta$ -cyclodextrin present in the mobile phase. With  $\beta$ -cyclodextrin in the mobile phase, negative values for the enthalpy of complex formation were obtained, but positive values were obtained for the entropy of complex formation. An equation was derived that relates the capacity factors with  $\beta$ -cyclodextrin in the mobile phase to  $\Delta H^\circ$ ,  $\Delta H_f^\circ$ ,  $\Delta S^\circ$ ,  $\Delta S_f^\circ$ , phase ratio, formation constant, and equilibrium concentration of  $\beta$ -cyclodextrin. Several correlations were developed for the thermodynamic properties, and it was found that the model compounds could be classified into two groups based primarily on their thermodynamic properties.

---

### INTRODUCTION

The effects of the column temperature on solute retention in reversed-phase liquid chromatography (RPLC) have been investigated by a number of researchers. For example, Melander *et al.* [1] reported the effects of temperature and solvent composition on the retention of oligo(ethylene glycol) derivatives in RPLC. Also, Melander *et al.* [2–4] considered the retention characteristics of solutes as a function of both column temperature and solvent composition. Other researchers have also considered the effects of temperature and mobile phase composition on the retention behavior of a variety of compounds [5,6].

The chromatographic results from temperature studies are also useful in exploring the thermodynamic aspects of solute retention in RPLC. Melander *et al.* [7] discussed enthalpy–entropy compensations in reversed-phase systems for several aromatic carboxylic acids and phenyl acetic acids. They showed that the reversible binding of solutes to hydrocarbonaceous bonded-phases conformed to the same

---

<sup>a</sup> Present address: Oklahoma Medical Research Foundation, 825 N.E. 13th street, Oklahoma City, OK 73104 (U.S.A.).

mechanism under the experimental conditions used. Chmielowiec and Sawatzky [8] studied the effects of temperature on the thermodynamic behavior of polynuclear aromatic hydrocarbons on a silica  $C_{18}$  column in aqueous acetonitrile mobile phases. Sander and Field [9] reported the influence of mobile phase composition on the thermodynamic properties for *N,N*-diethylaniline and isopropylbenzene with a  $\mu$ -Bondapak  $C_{18}$  column and a Zorbax CN column. Melander *et al.* [10] studied the characteristics of the stationary phase in RPLC as far as the length of the alkyl chain, column temperature, chemical nature of the hydrocarbonaceous ligands, and surface coverage. In other work, Melander and Horváth [11] analyzed a large amount of literature data from different hydrocarbonaceous bonded-phases to study the effect of stationary phase on the free energy increments for various structural elements of the solutes. Vigh and Varga-Puchony [12] reported the influence of temperature on the retention factors of  $C_6$ – $C_{16}$  *n*-alkanols,  $C_6$ – $C_{12}$  *n*-alkanal dinitrophenyl hydrazones, and  $C_6$ – $C_{11}$  2-*n*-alkanone dinitrophenyl hydrazones at various temperatures on Micropak CH-10 and Nucleosil  $C_{18}$  octadecyl packings with aqueous methanol eluents.

In related work with cyclodextrins, Harrison and Eftink [13] studied the thermodynamics of the binding of adamantanecarboxylate to cyclodextrins as a function of temperature and methanol by using flow microcalorimetry. They believed that the binding of solutes to both  $\alpha$ -cyclodextrin ( $\alpha$ -CD) and  $\beta$ -cyclodextrin ( $\beta$ -CD) was driven by strong London dispersion forces between the delocalized charge on the solute and the polar groups, namely, ether-like oxygens lining the cavity of cyclodextrin. Catena and Bright [14] reported thermodynamic parameters and stoichiometries of the binding of anilinonaphthalenesulfonates to  $\beta$ -CD by steady-state fluorescence intensity and anisotropy measurements. They obtained formation constants and enthalpy and entropy values of the inclusion complexes for different analytes. Woodburn *et al.* [15] investigated the thermodynamic properties of anilinonaphthalenesulfonates from methanol–water solvent mixtures and used enthalpy–entropy compensation concepts to interpret their data.

In this paper, the fundamental thermodynamic parameters,  $\Delta H^\circ$  and  $\Delta S^\circ$ , were obtained with and without  $\beta$ -CD present in the mobile phase for several hydroxyl aromatics using a  $C_{18}$  column and methanol–water mobile phases. The main goals of the research were to compare the  $\Delta H^\circ$  and  $\Delta S^\circ$  values with and without  $\beta$ -CD in the mobile phase in order to gain insights into the chromatographic mechanism with  $\beta$ -CD in the mobile phase and to discern the effects of some of the structural features of the model compounds on their retention characteristics.

## EXPERIMENTAL

### *Apparatus*

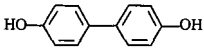
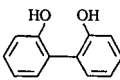
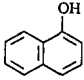
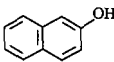
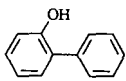
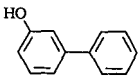
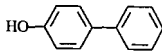
The liquid chromatograph used was a Waters unit with a Model 6000A pump (Milford, MA, U.S.A.), a U6K injector, a dual channel ultraviolet detector set at 254 nm, and an Omniscribe dual channel 10-mV strip chart recorder (Houston Instrument). A Model FIAtron (Oconomowoc, WI, U.S.A.) constant temperature control system was used to keep the temperature of the column constant. The accuracy of the column heater was  $\pm 0.1^\circ\text{C}$ . The chromatographic column employed was a 5- $\mu\text{m}$   $C_{18}$  (250 mm  $\times$  4.6 mm I.D.) obtained from Burdick and Jackson (Muskegon, MI,

U.S.A.). The carbon content and weight of the bonded packing material for the C<sub>18</sub> column were provided by Burdick and Jackson.

### Reagents

The model compounds and  $\beta$ -CD were purchased from Aldrich (Milwaukee, WI, U.S.A.). The names and structures of the model compounds are given in Table I. Methanol was HPLC grade and obtained from Burdick and Jackson.

TABLE I  
NAMES AND STRUCTURES OF THE MODEL COMPOUNDS

Compound	Structure
1 <i>p,p'</i> -Biphenol	
2 <i>o,o'</i> -Biphenol	
3 1-Naphthol	
4 2-Naphthol	
5 2-Phenylphenol	
6 3-Phenylphenol	
7 4-Phenylphenol	

### Procedure

$\beta$ -Cyclodextrin was vacuum dried under 0.78 atm pressure at 75°C for eight hours and then dissolved in prefiltered water. The appropriate amount of methanol was added to a water solution of  $\beta$ -CD. The largest analytical concentrations of  $\beta$ -CD in 50:50 and 60:40 methanol-water mixtures were 4.0 mM and 3.0 mM, respectively. The concentrations of the samples injected were 1 mg/ml in methanol. The column void volume was obtained by injection of a methanol solution of potassium nitrite.

## RESULTS AND DISCUSSION

*Theory*

The equilibrium constant ( $K$ ) of a solute binding to the stationary phase in reversed-phase systems can be related to the column temperature according to the following equations [7]:

$$\ln K = -\Delta G^\circ/RT \quad (1)$$

$$\ln K = -\Delta H^\circ/RT + \Delta S^\circ/R \quad (2)$$

where  $\Delta G^\circ$  is the Gibbs free energy for the solute-stationary phase interaction;  $R$  is the gas constant; and  $T$  is the absolute temperature.

Since  $k'_o = \phi K$ , where  $k'_o$  is the solute capacity factor in the chromatographic system, and  $\phi$  is the volume phase ratio of the stationary to the mobile phase, eqn. 2 can be written as

$$\ln k'_o = -\Delta H^\circ/RT + \Delta S^\circ/R + \ln \phi \quad (3)$$

where  $\Delta H^\circ$  and  $\Delta S^\circ$  are considered to be the standard enthalpy change and entropy change, respectively, as a solute partitions from the mobile to the stationary phase [8]. Eqn. 3 indicates that the solute retention depends upon the column temperature. An increase in the column temperature normally causes a decrease in the solute retention.

According to eqn. 3, the slope of the line that results from a plot of  $\ln k'$  vs.  $1/T$  is  $-\Delta H^\circ/R$ , and the intercept is  $\Delta S^\circ/R + \ln \phi$ . To obtain the entropy change, the phase ratio has to be known. Sentell and Dorsey [16] presented a method for calculating the volume of stationary phase with the following equation:

$$V_s = \frac{(\%C)(M)(W_\rho)}{(100)(12.011)(n_c)(\rho)} \quad (4)$$

where  $V_s$  is the stationary phase volume; %C is grams of carbon per 100 grams of bonded silica;  $n_c$  refers to the number of carbon atoms per mole of silane; the molecular weight of the silane is given by  $M$ ; the term  $W_\rho$  is the weight (g) of the bonded packing material in the column. The density of the bonded octadecylsilyl ( $\rho$ ) is assumed to be equal to 0.8607 g/cm<sup>3</sup> [17]. In this work, the mobile phase volume in the column was assumed to be the same as the retention volume of a non-retained solute, namely, potassium nitrite. The phase ratio was obtained from  $\phi = V_s/V_m$ , and the calculated value of  $\phi$  was 0.426.

With  $\beta$ -CD in the mobile phase, the solute capacity factor will be affected by the extent of complex formation of  $\beta$ -CD with the solute in the mobile phase and other parameters [18]. As discussed earlier, the solute capacity factor with  $\beta$ -CD in the mobile phase can be defined by eqn. 5 [18].

$$1/k' = 1/k'_o + [(CD)_m]/k'_o K_D \quad (5)$$

where  $k'_o$  is the capacity factor with no  $\beta$ -CD present,  $[(CD)_m]$  is the equilibrium

concentration of  $\beta$ -CD in the mobile phase, and  $K_D$  is the dissociation constant of the inclusion complex in the mobile phase. The earlier experimental data and data analysis indicated that the solute- $\beta$ -CD complexes did not interact with or interacted very little with the stationary phase [18].

By solving eqn. 5 for  $k'$  and substituting  $1/K_f$  for  $K_D$ , where  $K_f$  is the formation constant of the inclusion complex, eqn. 6 is obtained.

$$k' = k'_o \cdot 1/K_f / \{1/K_f + [(CD)_m]\} \quad (6)$$

Taking the ln of both sides of eqn. 6, eqn. 7 is obtained.

$$\ln k' = \ln k'_o - \ln K_f - \ln \{1/K_f + [(CD)_m]\} \quad (7)$$

Using eqns. 2 and 8, where  $\Delta H_f^\circ$  and

$$\ln K_f = -\Delta H_f^\circ/RT + \Delta S_f^\circ/R \quad (8)$$

$\Delta S_f^\circ$  are the standard enthalpy and entropy changes of complex formation in the mobile phase, respectively, eqn. 9 can be acquired.

$$\ln k' = (\Delta H_f^\circ - \Delta H^\circ)/RT + (\Delta S - \Delta S_f^\circ)/R + \ln \phi - \ln \{1/K_f + [(CD)_m]\} \quad (9)$$

Eqn. 9 can be used in the calculation of  $\Delta H_f^\circ$  and  $\Delta S_f^\circ$ , and this will be discussed later.

#### *Hydroxyl aromatics without $\beta$ -CD in the mobile phase*

The capacity factors for several hydroxyl aromatics (see Table I for structures) were obtained at 25, 30, 35 and 40°C with a  $C_{18}$  column. This is a limited temperature range and more work has to be performed to assess the effects of temperature on capacity factors at other temperatures. Fig. 1 shows that as the temperature is increased for the mobile phase without  $\beta$ -CD, the  $k'$  values of the compounds investigated decreased, and a linear relationship was obtained for all the hydroxyl aromatics. In the presence of  $\beta$ -CD, the same general graphs were obtained (see Fig. 2). The linear correlation coefficients with and without  $\beta$ -CD ranged from 0.956 to 0.996. At a given temperature, the presence of  $\beta$ -CD showed a decrease in the solute retention which was due to the formation of an inclusion complex between the solute and  $\beta$ -CD in the mobile phase [18]. It should be mentioned that Fujimura *et al.* [19] reported that  $\beta$ -CD and the  $\beta$ -CD complexes they studied did not show any interactions with a  $C_8$  column. This is most likely due to the hydrophilic nature of the external part of the  $\beta$ -CD molecule. Also, we recently showed that interactions of  $\beta$ -CD hydroxyl aromatic complexes were not important for compounds 1–4 in Table I [18]. For compounds 5–7 in Table I, there was an indication that there may have been slight interactions of the complexes with  $C_{18}$ , but data analysis of the graphs of  $1/k'$  vs. equilibrium concentration of  $\beta$ -CD indicated that the interactions were unimportant [18].

The thermodynamic parameters calculated from the slopes and intercepts of the  $\ln k'$  vs.  $1/T$  graphs for the hydroxyl aromatics in methanol–water (50:50) are listed in Table II. A comparison between the thermodynamic values of the structural isomers in methanol–water (50:50) is given in the following discussion. Enthalpy values can be

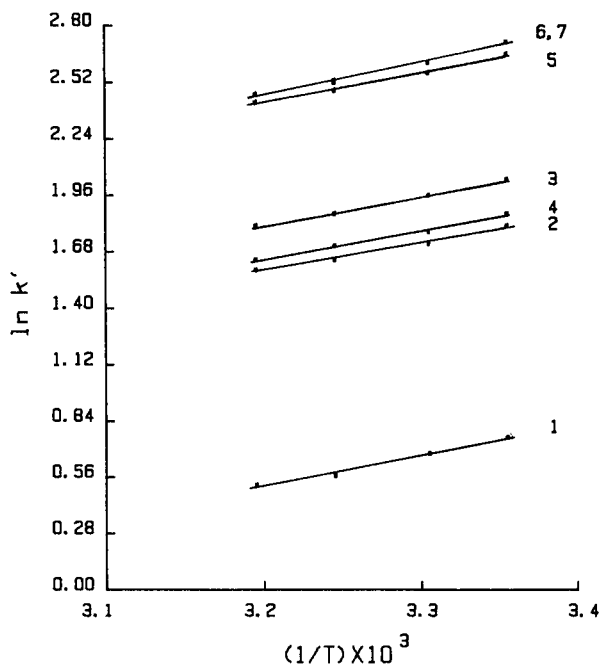


Fig. 1. Plot of  $\ln k'$  vs.  $1/T$  for several hydroxyl aromatics in methanol-water (50:50). See Table I for the names and structures of the compounds.

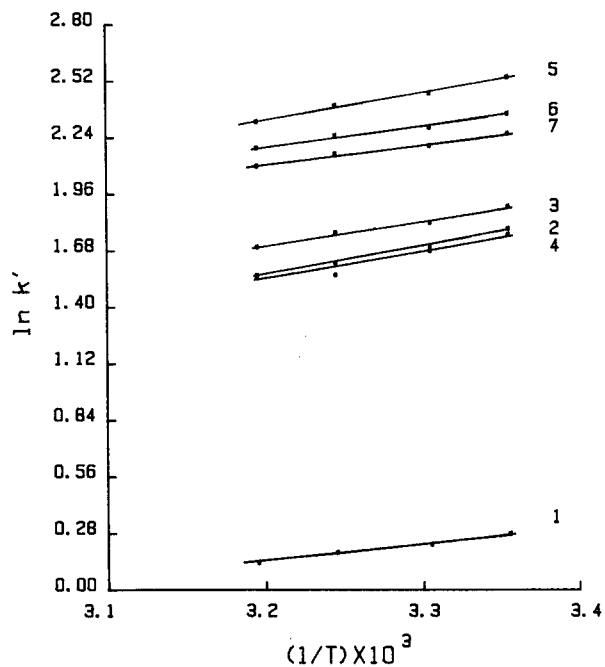


Fig. 2. Plot of  $\ln k'$  vs.  $1/T$  for several hydroxyl aromatics in methanol-water with 4.0 mM  $\beta$ -CD. See Table I for the names and structures of the compounds.

TABLE II

THE  $\Delta H^\circ$ ,  $\Delta S^\circ$ ,  $\Delta H^\circ_f$ , AND  $\Delta S^\circ_f$  VALUES OF SEVERAL HYDROXYL AROMATIC COMPOUNDS IN METHANOL-WATER (50:50) AND METHANOL-WATER (50:50) + 4.0 mM  $\beta$ -CD ON A-C<sub>18</sub> COLUMNS

The enthalpy and entropy units are kcal mol<sup>-1</sup> and cal mol<sup>-1</sup>T<sup>-1</sup>, respectively.

Solute	Methanol-water		Methanol-water + 4.0 mM $\beta$ -CD	
	$\Delta H^\circ$	$\Delta S^\circ$	$\Delta H^\circ_f$	$\Delta S^\circ_f$
1 <sup>a</sup>	-3.03	-6.92	-1.31	9.79
2	-2.72	-3.81	-	-
3	-2.87	-3.84	-0.49	10.4
4	-2.79	-3.91	-0.26	11.0
5	-2.98	-2.98	-0.34	10.7
6	-2.73	-3.73	-1.23	9.30
7	-3.20	-3.59	-1.29	9.53

<sup>a</sup> See Table I for the name and structure of the compound.

considered as a measure of the efficiency of the transfer of the solute from the mobile phase to the stationary phase. The more negative the  $\Delta H^\circ$  value, the more effectively the solute is transferred to the stationary phase. The more negative  $\Delta H^\circ$  value of *p,p'*-biphenol compared to *o,o'*-biphenol indicated that the former interacted with the stationary phase more strongly than the latter in methanol-water (50:50). The  $\Delta S^\circ$  values in Table II can be rather difficult to interpret. A  $\Delta S^\circ$  value can be considered as the change in ordering of the solute as it partitions between the mobile phase and stationary phase. Also, changes in entropy of the mobile phase and changes in the entropy of the stationary phase as a result of the solute partitioning between these two phases are important considerations. There was no attempt in this work to distinguish all of these changes. Thus, only a general interpretation of the changes in  $\Delta S^\circ$  values is given. We considered the changes in the  $\Delta S^\circ$  values as the change in ordering of the solute as it partitions between the mobile phase and stationary phase. As Table II shows, there is a substantial difference between  $\Delta S^\circ$  values for *p,p'*- and *o,o'*-biphenol. The entropy values of *p,p'*- and *o,o'*-biphenol indicate better ordering of *p,p'*-biphenol on the stationary phase relative to the mobile phase than that of the *o,o'*-biphenol with methanol-water (50:50). The somewhat more negative  $\Delta H^\circ$  value of 1-naphthol compared with  $\Delta H^\circ$  value of 2-naphthol in Table II implies that 1-naphthol interacted more strongly with C<sub>18</sub> than 2-naphthol. The difference in  $\Delta S^\circ$  values of 1- and 2-naphthol is small, namely, 0.07 cal mol<sup>-1</sup>T<sup>-1</sup>; thus the ordering of these compounds on the stationary phase relative to the mobile phase is approximately the same.

In the phenylphenol series, it is seen that the enthalpy change of 4-phenylphenol is the greatest, which indicated that 4-phenylphenol was more effectively transferred to the stationary phase than the other two isomers (Table II). 2-Phenylphenol had the smallest negative  $\Delta S^\circ$  value with methanol-water (50:50). This showed that 2-phenylphenol was less ordered on the stationary phase than in the mobile phase compared to 3- and 4-phenylphenol due to sorption [8]. The ortho position of the phenyl ring to the hydroxyl group in 2-phenylphenol resulted in intramolecular hydrogen bonding

between OH and  $\pi$  electrons of the phenyl ring [20]. This would cause the interaction of 2-phenylphenol with  $C_{18}$  to become less effective compared to the other two isomers in methanol–water (50:50).

#### *Hydroxyl aromatics with $\beta$ -CD in the mobile phase*

The addition of  $\beta$ -CD to the mobile phase in the reversed-phase systems investigated resulted in the formation of inclusion complexes, if the solutes had the correct size and shape to fit into the cavity of  $\beta$ -CD [18]. We previously showed that in methanol–water mobile phases 1:1 complexes were formed with  $\beta$ -CD for the solutes listed in Table I [18]. In addition, the earlier experimental evidence indicated that generally the  $\beta$ -CD–solute complexes did not interact with the stationary phase. However, some of the data suggested the  $\beta$ -CD complexes of the phenylphenols interacted with the stationary phase, although we concluded that these interactions were weak [18]. Fig. 2 shows that linear relationships were obtained between  $\ln k'$  and  $1/T$  for the seven model compounds when the total concentration of  $\beta$ -CD was 4.0 mM in methanol–water (50:50). Close inspection of the data in Figs. 1 and 2 for *o,o'*-biphenol shows that at a given temperature the  $k'$  values for this compound changed very little. For example, the  $k'$  value was 6.22 at 25°C without  $\beta$ -CD and with  $\beta$ -CD it was 6.10. Because the reproducibility of the  $k'$  values for this compound was about  $\pm 0.10$ , the calculation of thermodynamic values for *o,o'*-biphenol with  $\beta$ -CD present was not considered accurate enough.

For eqn. 9, it was assumed that  $\ln \varphi$  and  $\ln \{1/K_f + [(CD)_m]\}$  changed very little with temperature, and thus a plot of  $\ln k'$  vs.  $1/T$  would give a straight line with a slope of  $(\Delta H_f^\circ - \Delta H^\circ)/R$ . These aspects are supported by the linear plots in Fig. 2. Also, the  $K_f$  values were calculated for all four temperatures for solutes 1 and 3–7 using eqn. 5 with a value of  $8.04 \cdot 10^{-4} M$  for the equilibrium concentration of  $\beta$ -CD and appropriate values of  $k'$  and  $k'_o$  [18]. The equilibrium concentration of  $\beta$ -CD was not expected to change much with temperature because it was present in considerable excess compared to the solutes. With the  $K_f$  values and the equilibrium concentration of  $\beta$ -CD,  $\ln \{1/K_f + [(CD)_m]\}$  values were calculated for solutes 1 and 3–7 at the four temperatures. The percentage changes in  $\ln \{1/K_f + [(CD)_m]\}$  from 25 to 40°C for solutes 1 and 3–7 were 1.1%, 4.5%, 4.8%, 2.8%, 1.6% and 1.2%, respectively. Thus, the percentage changes in  $\ln \{1/K_f + [(CD)_m]\}$  values were considered small enough so that reasonable estimates of  $\Delta H_f^\circ$  could be made from the slopes. Additional data would have to be acquired for highly accurate values of  $\Delta H_f^\circ$ .

From the slopes of the lines in Fig. 2 and assuming  $\ln \{1/K_f + [(CD)_m]\}$  changed little with temperature, it was then possible to calculate  $\Delta H_f^\circ$  because  $\Delta H^\circ$  values were calculated earlier (Table II). Once  $\Delta H_f^\circ$  values were acquired then  $\Delta S_f^\circ$  values could be calculated from eqn. 8. The  $K_f$  values for the solutes needed for the calculation of  $\Delta S_f^\circ$  values were obtained from ref. 18. Table II lists the calculated  $\Delta H_f^\circ$  and  $\Delta S_f^\circ$  values. As shown in Table II, all the  $\Delta H_f^\circ$  values are negative indicating favorable conditions for complex formation. However, the respective  $\Delta H^\circ$  value in Table II for a given compound is more negative than the corresponding  $\Delta H_f^\circ$  value indicating that there was more of a tendency for the hydroxyl aromatics to interact with the stationary phase relative to  $\beta$ -CD molecules in the mobile phase.

In Table II, the  $\Delta S_f^\circ$  values are all positive which indicates that upon complex formation in the mobile phase a more disordered state results relative to the solute that



is uncomplexed. This is in contrast to the  $\Delta S^\circ$  values in Table II with no  $\beta$ -CD present in the mobile phase where all of the  $\Delta S^\circ$  value were negative. It should be mentioned that Lewis and Hansen [21] reported values of  $-2.6 \text{ kcal mol}^{-1}$  ( $\Delta H_f^\circ$ ) and  $7 \text{ cal mol}^{-1}\text{T}^{-1}$  ( $\Delta S_f^\circ$ ) for the binding of phenol with  $\beta$ -CD in aqueous solution using calorimetry. These values correlate, in general, with the  $\Delta H_f^\circ$  and  $\Delta S_f^\circ$  values for the hydroxyl aromatics in Table II. It is beyond the scope of this work to define all the interactions that result in positive  $\Delta S_f^\circ$  values. For example, hydrogen bonding interactions between the solute and solvent are involved in addition to interactions between water and methanol molecules in the binary mobile phase.

Of primary interest in this work were the effects of the enthalpy and entropy values on the capacity factors of the hydroxyl aromatics with  $\beta$ -CD present in the mobile phase. By subtracting eqn. 9 from eqn. 3, one obtains eqn. 10.

$$\ln k'_o - \ln k' = -\Delta H_f^\circ/RT + \Delta S_f^\circ/R + \ln\{1/K_f + [(\text{CD})_m]\} \quad (10)$$

From eqn. 10, it is seen that the change in capacity factor with the addition of  $\beta$ -CD is a function of  $T$ ,  $\Delta H_f^\circ$ ,  $\Delta S_f^\circ$ ,  $1/K_f$ , and the equilibrium concentration of  $\beta$ -CD. The three major terms in eqn. 10 ( $-\Delta H_f^\circ/RT$ ,  $\Delta S_f^\circ/R$ , and  $\ln\{1/K_f + [(\text{CD})_m]\}$ ) were calculated for solutes 1 and 3–7 at  $25^\circ\text{C}$  and are listed in Table III. The  $K_f$  values were taken from ref. 18. The data in Table III shows that solutes 1, 6, and 7 have similar numerical values for the sets of major terms and 3, 4, and 5 have similar sets of numerical values. The clustering of solutes indicates that the differences in the  $\ln$  of the capacity factors without and with  $\beta$ -CD for the solutes in a given cluster would be similar. This conclusion is supported by the  $k'$  values reported earlier for the solutes in Table III [18]. The grouping of solutes that appear in Table III implies similar interactions for these compounds in a given group. The  $\ln\{1/K_f + [(\text{CD})_m]\}$  terms have the greatest absolute values and thus determine to a large extent the magnitude of  $\ln k'_o - \ln k'$ . Because the equilibrium concentration is the same for  $\beta$ -CD for all the solutes the different values for the  $\ln\{1/K_f + [(\text{CD})_m]\}$  terms are a result of the unequal values obtained for  $K_f$  for the various solutes. For solutes 3, 4, and 5 the  $\Delta H_f^\circ/RT$  terms make relatively smaller contributions compared to the  $\Delta S_f^\circ/R$  terms. This is also indicated by comparing the appropriate  $\Delta H_f^\circ$  and  $\Delta S_f^\circ$  values in Table II. For solutes 1, 6 and 7 the same general conclusions can be made by comparing the data in Tables II and III. However, the entropy contribution is somewhat less, while the enthalpy contribution is somewhat greater.

TABLE III

COMPARISON OF THE MAJOR TERMS IN EQN. 10 AT  $25^\circ\text{C}$  FOR SIX SOLUTES

Solute <sup>a</sup>	$\Delta H_f^\circ/RT$	$\Delta S_f^\circ/R$	$\ln\{1/K_f + [(\text{CD})_m]\}$
1	-2.21	4.93	-6.44
3	-0.83	5.23	-5.79
4	-0.43	5.54	-5.69
5	-0.57	5.38	-5.71
6	-2.08	4.68	-6.23
7	-2.18	4.80	-6.36

<sup>a</sup> See Table I for names and structures of compounds.

Using data reported earlier for solutes 1 and 3–7, the percentage changes in  $k'$  values were calculated in going from 0.0 mM  $\beta$ -CD to 4.0 mM  $\beta$ -CD [18]. Percentage changes of 71.0, 39.3, 33.0, 33.9, 60.0, and 66.3 were obtained for solutes 1, 3, 4, 5, 6, and 7, respectively. By plotting  $\ln \{1/K_f + [(CD)_m]\}$  vs. percentage change of the  $k'$  values a linear relationship was obtained with a correlation coefficient of 0.999. Linear relationships were also obtained for  $-\Delta H_f^\circ/RT$  vs. percentage change of  $k'$  values and  $\Delta S_f^\circ/R$  vs. percentage change of  $k'$  values for solutes 1, 6, and 7 with both plots showing positive slopes. In addition, graphs of  $-\Delta H_f^\circ/RT$  vs. percentage change of  $k'$  values and  $\Delta S_f^\circ/R$  vs. percentage change of  $k'$  values gave linear relationships for solutes 3, 4, and 5, but the enthalpy plot had a positive slope and the entropy plot had a negative slope. These various relationships show that the major terms in eqn. 10 can be combined in a linear fashion to yield the change in capacity factors with the addition of  $\beta$ -CD. However, opposite trends were obtained for the enthalpy and entropy terms for solutes 1, 6, and 7 compared to solutes 3, 4, and 5.

## CONCLUSIONS

Without  $\beta$ -CD in the mobile phase, the negative  $\Delta H^\circ$  values for the solutes gave a measure of the effectiveness of the transfer of the solute from the mobile phase to the stationary phase. Because all of the entropy values were negative without  $\beta$ -CD in the mobile phase, this implied that the solutes were more ordered in the stationary phase relative to the solutes in the mobile phase. The less negative  $\Delta H_f^\circ$  values relative to the  $\Delta H^\circ$  values implied that the hydroxyl aromatics favored interaction in the stationary phase relative to the  $\beta$ -CD cavity. Because all the  $\Delta S_f^\circ$  values were positive a more disordered state resulted in the mobile phase as a result of complex formation.

It was shown that the change of the capacity factors with  $\beta$ -CD in the mobile phase was a function of several parameters, but these parameters could be grouped into three major terms and the quantitative contribution of each term to the change in capacity factor was evaluated. The model compounds fell into two groups with one group showing the same trend for the  $\Delta H_f^\circ$  and  $\Delta S_f^\circ$  values, while the other group of compounds showed opposite trends for the  $\Delta H_f^\circ$  and  $\Delta S_f^\circ$  values. The different trends in the  $\Delta H_f^\circ$  and  $\Delta S_f^\circ$  values for a given group of compounds showed that different interactions were operative with the two groups of hydroxyl aromatics.

## ACKNOWLEDGEMENTS

This research was partially supported by Burdick and Jackson Laboratories, Inc. and by the U.S. Department of Energy under contract No. DE-AC22-83PC60015, and the US. Department of Energy under grant No. DE-FG02-86ER13547.

## REFERENCES

- 1 W. R. Melander, A. Nahum and Cs. Horváth, *J. Chromatogr.*, 185 (1979) 129.
- 2 W. R. Melander, B. Chen and Cs. Horváth, *J. Chromatogr.*, 185 (1979) 99.
- 3 W. R. Melander and C. Horvath, *Chromatographia*, 18 (1984) 353.
- 4 W. R. Melander, B.-K. Chen and Cs. Horváth, *J. Chromatogr.*, 318 (1985) 1.
- 5 E. Grushka, H. Colin and G. Guiochon, *J. Chromatogr.*, 248 (1982) 325.

- 6 P. E. Carr, R. M. Doherty, M. J. Kamlet, R. W. Taft, W. Melander and C. Horvath, *Anal. Chem.*, 58 (1986) 2674.
- 7 W. R. Melander, D. E. Campbell and Cs. Horváth, *J. Chromatogr.*, 158 (1978) 215.
- 8 J. Chmielowiec and H. Sawatzky, *J. Chromatogr. Sci.*, 17 (1979) 245.
- 9 L. C. Sander and L. R. Field, *Anal. Chem.*, 52 (1980) 2009.
- 10 W. R. Melander, J. Stoveken and Cs. Horváth, *J. Chromatogr.*, 199 (1980) 35.
- 11 W. R. Melander and C. Horváth, *Chromatographia*, 15(2) (1982) 86.
- 12 Gy. Vigh and Z. Varga-Puchony, *J. Chromatogr.*, 196 (1980) 1.
- 13 J. C. Harrison and M. R. Eftink, *Biopolymers*, 21 (1982) 1153.
- 14 G. C. Catena and F. V. Bright, *Anal. Chem.*, 61 (1989) 905.
- 15 K. B. Woodburn, L. S. Lee, P. S. C. Rao and J. J. Delfino, *Environ. Sci. Technol.*, 23 (1989) 407.
- 16 K. B. Sentell and J. G. Dorsey, *J. Liq. Chromatogr.*, 11(9,10) (1988) 1875.
- 17 W. Cheng, *Anal. Chem.*, 57 (1985) 2409.
- 18 R. M. Mohseni and R. J. Hurtubise, *J. Chromatogr.*, 499 (1990) 395.
- 19 K. Fujimura, T. Ueda, M. Kitagawa, H. Takayanagi and T. Ando, *Anal. Chem.*, 58 (1986) 2668.
- 20 M. Oki and H. Iwamura, *J. Am. Chem. Soc.*, 89 (1967) 576.
- 21 E. A. Lewis and L. O. Hansen, *J. Chem. Soc. Perkins Trans*, 2, 2081 (1973).



CHROM. 22 778

## **Comparison of the liquid chromatographic behaviour of selected steroid isomers using different reversed-phase materials and mobile phase compositions**

MÄRIT OLSSON\*

*Kabi Pharma R&D, S-11287 Stockholm (Sweden)*

and

LANE C. SANDER and STEPHEN A. WISE

*Center for Analytical Chemistry, National Institute of Standards and Technology, Gaithersburg, MD 20899 (U.S.A.)*

(First received May 14th, 1990; revised manuscript received August 27th, 1990)

---

### ABSTRACT

The retention behaviour of steroid isomers in reversed-phase liquid chromatography was studied. Selectivity for the isomers changed as a function of both temperature and mobile-phase composition. In addition, the influence of the stationary phase on steroid retention and selectivity was studied for a number of monomeric and polymeric C<sub>18</sub> columns and  $\beta$ -cyclodextrin columns. The selectivity of a polymeric C<sub>18</sub> phase toward various androstane standards was similar to that for a liquid crystal phase used in supercritical fluid chromatography.

---

### INTRODUCTION

Different modes of liquid chromatography (LC) have long been used for the analysis of steroid hormones. The techniques used include early studies with paper, partition, ion-exchange, adsorption and gel chromatography [1,2]. Today, high-performance liquid chromatography (HPLC) is becoming a widely used technique for the separation of steroids [3], although most applications still utilize other techniques such as gas chromatography (GC) or thin-layer chromatography. The applications of HPLC for the determination of steroids are numerous and have recently been reviewed [4]. A significant limitation to the use of HPLC for steroid analysis is detection, and many steroids require derivatization for detection with available LC detectors. Low efficiency is another limitation in the LC separation of steroids. On the other hand, enhanced separation selectivity can often be achieved for various steroids by selecting from the numerous packing materials and coatings available.

Steroid analyses by HPLC can be performed in both normal- and reversed-phase modes, the latter being more widely used. Bonded octadecylsilane (C<sub>18</sub>) is the most commonly used reversed-phase material, although other supports and coatings can be utilized. It is well known that great differences exist among C<sub>18</sub> stationary phases

owing to differences in properties such as the silica matrix, pore diameter, phase synthesis and ligand density [5-7]. Reaction of octadecylsilane with the silica matrix can be carried out in different ways, yielding phases with different properties. Monomeric phases are prepared either with monofunctional silanes or with di- or trifunctional silanes in the absence of water. Polymeric phases, on the other hand, are prepared using trifunctional silanes in the presence of water [8,9]. Polymeric phases have enhanced shape selectivity towards polycyclic aromatic hydrocarbons (PAHs) compared to monomeric C<sub>18</sub> phases. It has been suggested that this shape recognition ability is a result of ordering of alkyl chains within the polymeric phase, similar to liquid crystalline phases in GC [10]. Such liquid crystalline phases have been used in supercritical fluid chromatography (SFC) for the separation of isomeric steroids (*e.g.*, androstanes and estrogens), and better separations were possible than with non-shape-selective phases [11]. Shape recognition for isomeric compounds has also been demonstrated using cyclodextrin bonded phases [12,13]. Cyclodextrin has been reported as both a mobile phase additive [14,15] and a bonded phase [16] for the separation of steroid isomers.

As steroid hormones and their numerous metabolites are structurally very similar, enhanced shape selectivity is an important consideration when selecting a suitable system for their separation. Apart from the type of stationary phase used, selectivity is dependent on parameters such as mobile phase composition and temperature [17,18]. Because mobile phase composition has a dramatic effect on column selectivity for steroids, the need for careful investigation of composition parameters in method development is crucial.

Stationary phase selectivity towards steroids can be further modified by varying the column temperature. It has been shown recently that the column selectivity toward PAHs and carotenoids changes with temperature to the extent that the elution order may be reversed [19,20]. This trend has also been observed with certain steroid isomers. The use of subambient temperature for enhanced resolution of cortisol and cortisone on a  $\mu$ Bondapak C<sub>18</sub> column has been reported [21].

In this work, the retention behaviour of some selected steroid isomers was investigated. The stationary phases used in this study differed in phase type (*e.g.*, monomeric or polymeric) and ligand type. Dramatic changes in selectivity have been observed with changes in mobile phase composition and temperature.

## EXPERIMENTAL<sup>a</sup>

### *Materials*

Steroid standards were obtained from Sigma (St. Louis, MO, U.S.A.). Methanol, acetonitrile and water (all HPLC grade) and 1,4-dioxane and tetrahydrofuran (both analytical-reagent grade) were obtained from commercial suppliers.

---

<sup>a</sup> Certain commercial equipment, instruments or materials are identified in this paper to specify adequately the experimental procedure. Such identification does not imply recommendation or endorsement by the National Institute of Standards and Technology, nor does it imply that the materials or equipment identified are necessarily the best available for the purpose.

### Columns

Standard solutions of steroid isomers were separated on the following columns: (1) polymeric  $C_{18}$  columns: Vydac 201 TP (Separations Group, Hesperia, CA, U.S.A.), Bakerbond wide-pore  $C_{18}$  (J. T. Baker, Phillipsburg, NJ, U.S.A.) and Erbasil  $C_{18}/H$  (Carlo Erba, Milan, Italy); (2) intermediate  $C_{18}$  columns: Vydac TP (custom synthesis, low load) and Bakerbond narrow-pore  $C_{18}$ ; (3) monomeric  $C_{18}$  columns: Zorbax ODS (MAC-MOD Analytical, Wilmington, DE, U.S.A.), ODS Hypersil  $C_{18}$  (Keystone Scientific, State College, PA, U.S.A.) and Supelcøsil LC-18-DB (Supelco, Bellefonte, PA, U.S.A.); and (4) cyclodextrin columns: Cyclobond I and Cyclobond I acetylated ( $\beta$ -cyclodextrin) (Astec, Whippany, NJ, U.S.A.). All the columns were  $250 \times 4.6$  mm I.D. with  $5\text{-}\mu\text{m}$  particle diameter silica.

### Chromatography

A liquid chromatograph consisting of a reciprocating piston pump, a solvent programming system, a  $20\text{-}\mu\text{l}$  loop injector and a  $254\text{-nm}$  fixed-wavelength detector was used for the separation of the estrogen standards. For the androstane standards (which have very low UV absorbance), a refractive index detector was placed in series with the UV detector.

Retention data were determined using a chromatography data system (initial studies) and, in later studies, an integrator. All samples were run isocratically with aqueous organic mobile phases, and the solutes were dissolved in methanol prior to injection. Androstane standards were eluted with aqueous methanol mobile phases at  $1.5$  ml/min. The methanol content varied between 60 and 90% depending on the polarity of the solutes. The organic content in the mobile phases for elution of the estradiol standards in the column comparison studies was varied in order to achieve comparable capacity factors ( $k'$ ) between columns.

The column temperature was controlled either by placing the column in a block heater or, for the subambient studies, in an ice-bath where the column temperature was maintained at  $0^\circ\text{C}$ .

## RESULTS AND DISCUSSION

The chromatographic selectivity of liquid crystalline phases in GC and SFC, for the separation of androstane isomers, is based on the size and shape of the steroids [11,22]. This shape discrimination ability results from the high degree of order in the liquid crystalline phase. Using similar stationary phases, selectivity is enhanced in SFC compared to GC because a lower operating temperature can be used. This produces a higher degree of order in the stationary phase and results in an increase in the strength of solute-stationary phase interactions [11].

Among LC columns, selectivity is often strongly influenced by the way in which the stationary phase is prepared. Most commercial  $C_{18}$  phases are prepared by reaction of monochlorosilanes with silica (monomeric  $C_{18}$  phases); however, a few (polymeric  $C_{18}$  phases) are prepared with polyfunctional silanes in the presence of water. These two types of bonded phases often have dissimilar properties, particularly when retention behaviour is compared for the separation of isomers or other compounds with similar overall shape. The relative monomeric and polymeric retention character of  $C_{18}$  columns can be characterized by Standard Reference

TABLE I  
RETENTION DATA FOR ANDROSTANES ( $t_R/t_R$ )

Compound	Retention relative to	Monomeric $C_{18}$ ( $\alpha_{TBN/BAP} = 1.94$ )	Polymeric $C_{18}$ ( $\alpha_{TBN/BAP} = 0.67$ )	Monomeric $C_{18}$ ( $\alpha_{TBN/BAP} = 2.01$ )
5 $\beta$ -Androstane-3 $\beta$ ,17 $\beta$ -diol	5 $\beta$ -Androstane-3 $\beta$ ,17 $\beta$ -diol	1.00	1.00	
5 $\alpha$ -Androstane-3 $\beta$ ,17 $\beta$ -diol		1.04	1.29	
5 $\beta$ -Androstane-3 $\alpha$ ,17 $\beta$ -diol		1.39	1.26	
5 $\alpha$ -Androstane-3 $\alpha$ ,17 $\beta$ -diol		1.44	1.37	
5 $\beta$ -Androstane-3 $\alpha$ ,11 $\beta$ ,17 $\beta$ -triol	5 $\beta$ -Androstane-3 $\alpha$ ,11 $\beta$ ,17 $\beta$ -triol	1.00	1.00	1.00
5 $\beta$ -Androstane-3 $\alpha$ ,11 $\alpha$ ,17 $\beta$ -triol		1.24	1.28	1.22
5 $\beta$ -Androstane-3 $\beta$ ,17 $\beta$ -diol		1.87	2.33	1.58
5 $\alpha$ -Androstane-3 $\beta$ ,17 $\beta$ -diol		1.91	3.24	1.58
5 $\beta$ -Androstane-3 $\alpha$ ,17 $\beta$ -diol		2.54	2.88	2.18
5 $\alpha$ -Androstane-3 $\alpha$ ,17 $\beta$ -diol		2.71	3.40	2.28
5 $\beta$ -Androstane-3 $\alpha$ -ol	5 $\beta$ -Androstane-3 $\alpha$ -ol	1.00	1.00	
5 $\beta$ -Androstane-3 $\beta$ -ol		1.25	1.35	
5 $\beta$ -Androstane-17 $\beta$ -ol		1.29	1.21	
5 $\alpha$ -Androstane-3 $\beta$ -ol		1.31	1.74	
5 $\alpha$ -Androstane-17 $\beta$ -ol		1.52	1.90	



Material (SRM) 869. This material contains three PAH solutes that have planar and non-planar features {benzo[*a*]pyrene (BaP), phenanthro[3,4-*c*]phenanthrene (PhPh) and 1,2:3,4:5,6:7,8-tetrabenzonaphthalene (TBN)}, and is primarily intended for characterizing LC column selectivity for solute shape. The elution order of the three components changes with  $C_{18}$  phase type. Monomeric  $C_{18}$  phases give the elution order  $BaP \leq PhPh < TBN$  whereas polymeric  $C_{18}$  phases usually give the elution order  $PhPh < TBN \leq BaP$ . A quantitative measure of phase selectivity can be calculated to enable relative comparison between different  $C_{18}$  phases. The selectivity factor  $\alpha_{TBN/BaP}$  is defined as  $k'_{TBN}/k'_{BaP}$ , where  $k' = (t_R - t_0)/t_0$  and  $t_R$  and  $t_0$  are the retention times of the analyte and void volume marker, respectively. Among commercial  $C_{18}$  columns, values for  $\alpha_{TBN/BaP}$  range from about 0.6 to 2.0, with  $\alpha_{TBN/BaP} \leq 1$  reflecting "polymeric-like" selectivity and  $\alpha_{TBN/BaP} \geq 1.7$  reflecting "monomeric-like" selectivity (selectivity values  $1 < \alpha_{TBN/BaP} < 1.7$  denote intermediate selectivity). In general, better separations of compounds with similar overall structure are possible with polymeric  $C_{18}$  phases compared to monomeric  $C_{18}$  phases. This trend is most often observed for non-polar solutes, in the absence of polar-polar (*i.e.*, silanol-solute) interactions.

Liquid crystalline phases in GC and polymeric  $C_{18}$  phases in HPLC exhibit remarkably similar selectivity towards PAHs. In both cases, this behaviour is based primarily on the shape and size of the solute [10]. Androstane isomers can exist in two structural conformations, which results from the position of the hydrogen atom at C-5: *trans* ( $\alpha$ ) or *cis* ( $\beta$ ) conformations (see Fig. 1). Chang *et al.* [11] showed that the retention of these isomers on a liquid crystalline phase is clearly affected by this conformational difference, and the bulkier *cis*-isomer ( $\beta$ ) is less retained than the more planar *trans*-isomer ( $\alpha$ ), which is more soluble in the ordered phase. This same trend was observed for LC separations performed on  $C_{18}$  bonded-phase columns. Androstane standards and relative retention data are listed in Table I. Zorbax ODS and Supelcosil LC-18-DB columns are monomeric  $C_{18}$  phases; Vydac 201 TP is a polymeric  $C_{18}$  phase. In each instance, the *cis*-isomer ( $5\beta$ -, nonplanar) elutes before the corresponding *trans*-isomer ( $5\alpha$ -, planar). This trend was observed for both monomeric and polymeric  $C_{18}$  phases; however, resolution of  $5\alpha$ - and  $5\beta$ -an-

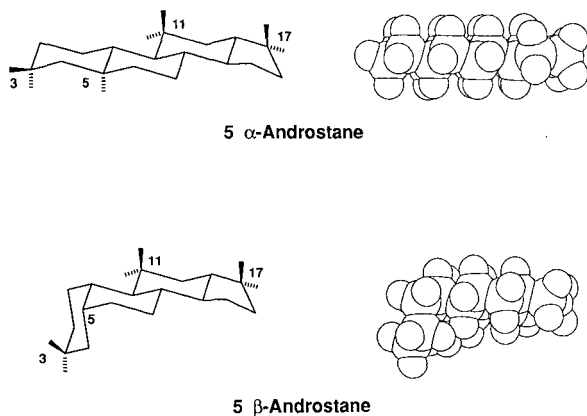


Fig. 1. Chemical structures and space-filling models for *cis* and *trans* conformational isomers of androstane. Wedge bonds denote  $\alpha$ -stereochemistry; hatched bonds denote  $\beta$ -stereochemistry.

drostanediol isomers was only possible with polymeric  $C_{18}$  phases. The fact that  $\alpha$ - and  $\beta$ -androstanediol isomers are separated on polymeric  $C_{18}$  phases, and are not separated on monomeric  $C_{18}$  phases, corresponds to similar observations reported for the separation of PAH isomers [7]. In general, polymeric  $C_{18}$  phases are more selective toward isomer shape and are more likely to resolve isomer mixtures than are monomeric  $C_{18}$  phases, at least when other effects such as silanol or other polar stationary phase interactions are insignificant.

The stereochemical position of the hydroxyl groups at positions 3 and 17 significantly affects the retention of androstanediols. The retention behaviour of four androstanediols was studied ( $3\beta,17\beta$ - and  $3\alpha,17\beta$ -diol isomer combinations of the  $5\alpha$ - and  $5\beta$ - structures shown in Fig. 1). Separations of androstanediol isomers differing only in the position of the hydroxyl at C-3 were possible for both monomeric and polymeric  $C_{18}$  phases. For example,  $5\beta$ -androstan- $3\beta,17\beta$ -diol was fully resolved from  $5\beta$ -androstan- $3\alpha,17\beta$ -diol regardless of column type. As the position of the hydroxyl group does affect polarity, but has little effect on the overall shape of the molecule, it seems reasonable to assume that the separation of these critical pairs depends more on solute polarity than on solute shape. Hydrogen bonding interactions with hydroxyl groups may also contribute to retention processes. The position of solute hydroxyl groups (*i.e.*, axial or equatorial) affects the accessibility and strength of any such interactions. This is consistent with the overall similar retention behaviour observed for these solutes on monomeric and polymeric  $C_{18}$  phases. Differences in retention behaviour would be expected between these two classes of columns, for solute pairs with dissimilar overall shape.

The effect of column temperature on the separation of various steroids was examined. Because the individual  $C_{18}$  ligands constituting the bonded phase straighten at reduced temperature, the shape recognition ability of alkyl bonded phases increases with decreasing column temperature. Stated differently, at subambient temperatures monomeric  $C_{18}$  phases gain some of the shape recognition properties exhibited by polymeric  $C_{18}$  phases at ambient temperature. At subambient temperatures, the shape recognition ability of polymeric  $C_{18}$  phases increases even more. Thus, shifts in retention behaviour for steroids are expected for the monomeric and polymeric phases. In fact, such changes in selectivity were observed when separations were carried out at  $0^\circ\text{C}$ , similar to the trends reported for PAHs [19]. The  $\alpha$ - and  $\beta$ -androstanediol isomers were separated better at subambient than at ambient temperatures. This effect was also observed by Sheikh and Touchstone for various steroid isomers [23]. The opposite trend was observed when the polymeric  $C_{18}$  phase (Vydac 201TP) was heated to  $+50^\circ\text{C}$  and the androstanediols were eluted as on the monomeric  $C_{18}$  phase. These results correspond with earlier observations concerning phase morphology [19]. At elevated temperatures the individual  $C_{18}$  ligands become more disordered than at ambient temperature, and the result is a loss in shape recognition ability. This is most dramatic for polymeric  $C_{18}$  phases, for which a high degree of shape recognition exists at ambient temperature. Correspondingly, when the polymeric  $C_{18}$  phase is cooled to  $0^\circ\text{C}$ , the distinction between  $\alpha$ - and  $\beta$ - (planar and non-planar) isomers becomes even stronger.

The results for the androstane isomers are similar to trends in retention observed for PAHs, for which solute shape and phase morphology are important aspects of the retention mechanism. Because of the difficulties in the detection of androstane

steroids, methods other than LC may prove to be simpler and more practical for routine analysis (LC may prove most useful in preparative applications).

An analytical problem more suited for HPLC is the analysis of the UV-absorbing estrogens (Fig. 2). Estrogens are produced in large amounts in the female body and are also produced as pharmaceutical products for clinical therapy. Determination of the female hormones in both biological fluids and in other media is required and, owing to the close similarity of the isomers, chromatographic separation is difficult. The selectivity and resolution of a set of estrogen standards were investigated on a number of different  $C_{18}$  columns (see Table II). These columns ranged from heavily loaded polymeric  $C_{18}$  columns ( $\alpha_{\text{TBN/BaP}} = 0.38$ , normally associated with high shape discrimination) to monomeric  $C_{18}$  columns ( $\alpha_{\text{TBN/BaP}} = 2.01$ , associated with low shape discrimination). However, little or no difference in selectivity based on solute shape and size was observed between monomeric and polymeric  $C_{18}$  columns. This similarity in retention behaviour with different phases is perhaps not unexpected, as  $17\alpha$ - and  $17\beta$ -estradiol differ only in the position of the hydroxyl group at C-17, and have very similar overall shapes (see Fig. 2). A more dramatic effect on selectivity has been observed with changes in the mobile phase composition [17,24,25].

During this investigation it was observed that  $17\alpha$ - and  $17\beta$ -estradiol were strongly affected by mobile phase changes. They were selected as probe solutes,

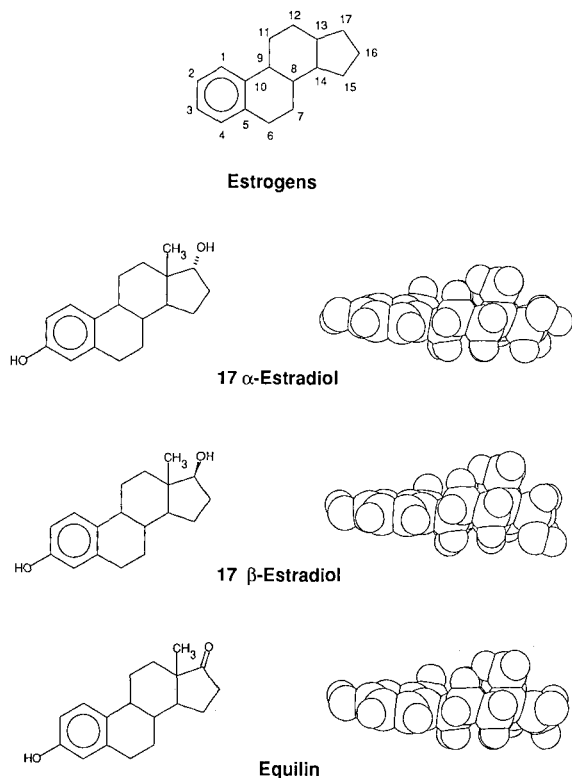


Fig. 2. Chemical structures and space-filling models for  $17\alpha$ - and  $17\beta$ -estradiol isomers and equilin. Separation of these solutes was strongly affected by the mobile phase composition.

TABLE II

## RELATIVE RETENTION DATA FOR ESTROGENS WITH DIFFERENT MOBILE PHASES

These data were determined for individual columns and do not necessarily reflect representative column performance. Intended or unintended variations in the manufacturing process may alter retention behaviour between column types.

Mobile phase	Column	$\alpha_{\text{TBN/BaP}}$	$\alpha_{17\alpha\text{-estradiol/equilin}}$	$\alpha_{17\beta\text{-estradiol/equilin}}$
Aqueous methanol	Polymeric high load	0.38	1.29	1.26
	Polymeric int. load	0.54	1.30	1.30
	Polymeric int. load	0.60	1.15	1.30
	Polymeric normal load	0.67	1.22	1.41
	Polymeric low load	1.00	1.10	1.26
	Intermediate	1.12	1.28	1.41
	Intermediate	1.32	1.18	1.26
	Monomeric	1.94	1.28	1.12
	Monomeric	1.98	1.32	1.15
	Monomeric	2.01	1.33	1.23
Aqueous acetonitrile	Polymeric high load	0.38	0.84	0.72
	Polymeric int. load	0.54	0.85	0.79
	Polymeric int. load	0.60	0.82	0.80
	Polymeric normal load	0.67	0.84	0.84
	Polymeric low load	1.00	0.85	0.81
	Intermediate	1.12	0.90	0.85
	Intermediate	1.32	0.85	0.79
	Monomeric	1.94	0.82	0.65
	Monomeric	1.98	0.84	0.67
	Monomeric	2.01	0.85	0.72

together with equilin, which has a  $k'$  close to that of estradiol in the systems investigated. Equilin was chosen as a reference for relative retention data. The  $17\alpha$ - and  $17\beta$ -estradiol isomers have identical functional groups and differ only in the stereochemical conformation at position 17. Even though the isomers are structurally very similar, the elution order was reversed when the percentage of methanol, acetonitrile and water was varied (see Table III). Changes in mobile phase composition

TABLE III

## RELATIVE RETENTION DATA FOR ESTROGENS ON VYDAC LOW LOAD

Mobile phase			$\alpha_{17\alpha\text{-estradiol/equilin}}$	$\alpha_{17\beta\text{-estradiol/equilin}}$
Methanol (%)	Acetonitrile (%)	Water (%)		
0	30	70	0.89	0.85
5	25	70	0.95	0.91
15	20	65	1.00	1.00
25	15	60	1.11	1.11
35	10	55	1.19	1.22
45	5	50	1.21	1.29
50	0	50	1.24	1.38

caused changes in the elution order of  $17\alpha$ -estradiol and equilin (also  $17\beta$ -estradiol and equilin) as well as the elution order of  $17\alpha$ - and  $17\beta$ -estradiol (e.g., the  $17\beta$ -isomer elutes first when using aqueous acetonitrile and last when using aqueous methanol), as shown in Fig. 3.

The composition and properties of the mobile phase were further changed by adding different organic modifiers (acetonitrile, methanol, 1,4-dioxane and tetrahydrofuran) to an aqueous phase. The organic modifiers were selected so that both proton donors and proton acceptors would be represented [17,24,26]. Relative retention data are presented in Table IV. Considering the very subtle differences in the estradiol isomers, it is difficult to explain how the solvent environment can effect retention in such a significant manner. It is possible that the methyl group at position 13 partially shields the hydroxyl at position 17 from interaction with solvent molecules. The extent of any such interaction would, of course, be influenced by the proton-donating and -accepting properties of the mobile phase. Although actual retention mechanisms can only be speculated on at this point, the importance of the choice of the organic modifier in the development of a separation method is clear.

The retention behaviour of estradiols was also studied for a bonded  $\beta$ -cyclodextrin ( $\beta$ -CD) stationary phase. Peak tailing was severe, probably owing to hydrogen

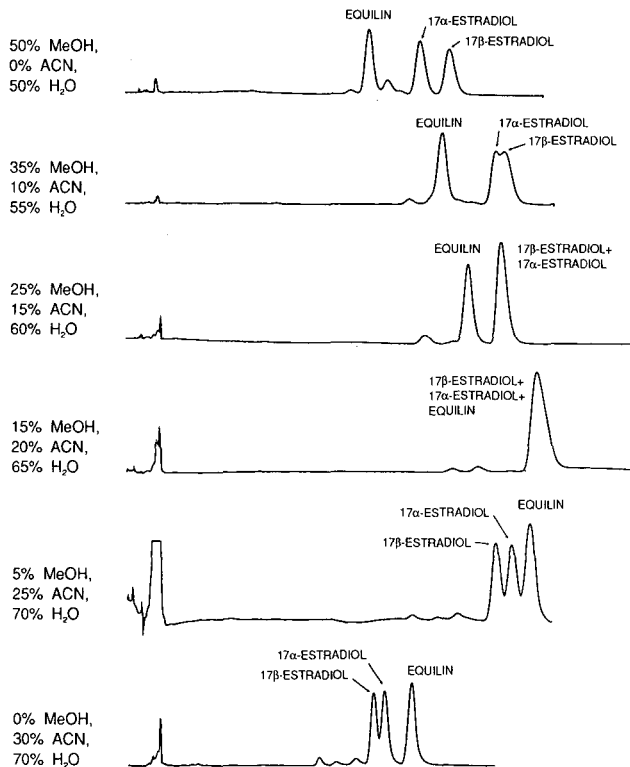


Fig. 3. Separation of  $\alpha$ - and  $\beta$ -estradiol and equilin using various mobile phase compositions with a low-load polymeric C<sub>18</sub> column. MeOH = methanol; ACN = acetonitrile.

TABLE IV  
RELATIVE RETENTION DATA FOR ESTROGENS ON BAKERBOND NARROW-PORE

Mobile phase	$\alpha_{17\alpha\text{-estradiol/equilin}}$	$\alpha_{17\beta\text{-estradiol/equilin}}$
Acetonitrile-water (35:65)	0.79	0.77
Tetrahydrofuran-water (35:65)	1.05	0.83
Methanol-water (60:40)	1.17	1.20
Dioxane-water (50:50)	1.01	0.84

bonding between hydroxyls of the estrogens and hydroxyls on the outside of the cyclodextrin cavity. Relative retention data were collected on a  $\beta$ -CD and on an acetylated  $\beta$ -CD. The peak shape was slightly improved with the acetylated  $\beta$ -CD. The selectivity on the acetylated  $\beta$ -CD resembles that on  $C_{18}$  materials, and the same reversal of elution order was observed between the ketone and hydroxyl isomers when changing the mobile phase from aqueous methanol to aqueous acetonitrile. However, the relative retention of  $17\alpha$ - and  $17\beta$ -estradiol did not change with mobile phase composition, as shown in Fig. 4. As demonstrated for  $17\alpha$ - and  $17\beta$ -estradiol, specific solute-stationary phase interactions with cyclodextrin bonded phases can give rise to enhanced selectivity for isomers and other structurally closely related solutes.

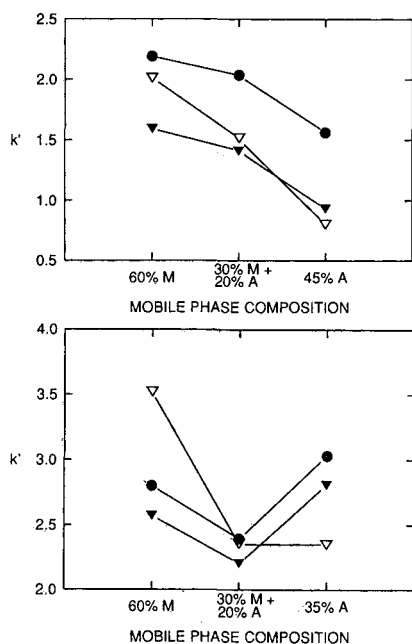


Fig. 4. Plots of retention versus mobile phase composition for aqueous methanol (M) and acetonitrile (A) mixtures, for cyclodextrin columns. Similar, but not identical, trends were observed for  $C_{18}$  phases. Top:  $\beta$ -cyclodextrin; bottom: acetylated  $\beta$ -cyclodextrin.  $\nabla$  =  $17\alpha$ -Estradiol;  $\bullet$  =  $17\beta$ -estradiol;  $\nabla$  = equilin.

## CONCLUSIONS

The retention behaviour of steroid hormones in LC is complex and is related to the overall shape and stereochemical positions of functional groups. Steroid isomers with similar functional group stereochemistry but different overall molecular shape are separated on the basis of shape, in a manner similar to that observed for polycyclic aromatic hydrocarbons (*i.e.*, planar solutes are retained longer than non-planar solutes). In such instances, phase type and column temperature are important separation parameters, and better separations of critical solute pairs may be possible with polymeric C<sub>18</sub> phases and/or low column temperatures. For similarly shaped steroid isomers, functional group position is of importance, and the separation of these critical pairs is more strongly affected by mobile phase composition than phase type.

## REFERENCES

- 1 H. L. J. Makin, in H. L. J. Makin (Editor), *Biochemistry of Steroid Hormones*, Blackwells, Oxford, 2nd ed., 1984, pp. 478–514.
- 2 E. Heftman, *Chromatography of Steroids*, Elsevier, Amsterdam, 1976.
- 3 J. W. Honour, in C. L. Kim (Editor), *HPLC of Small Molecules: A Practical Approach*, JRL Press, Washington, DC, 1986, pp. 147–156.
- 4 H. L. J. Makin and E. Heftmann, *Endocrinology*, 30 (1988) 183–234.
- 5 L. C. Sander and S. A. Wise, *CRC Crit. Rev. Anal. Chem.*, 18 (1987) 299–415.
- 6 L. C. Sander and S. A. Wise, *J. Chromatogr.*, 316 (1984) 163–181.
- 7 L. C. Sander and S. A. Wise, *J. High Resolut. Chromatogr. Chromatogr. Commun.*, 11 (1988) 383–387.
- 8 L. C. Sander and S. A. Wise, *Anal. Chem.*, 56 (1984) 504–510.
- 9 S.A. Wise and L. C. Sander, *J. High Resolut. Chromatogr. Chromatogr. Commun.*, 8 (1985) 248–255.
- 10 S. A. Wise, L. C. Sander, H.-Ch. K. Chang, K. E. Markides and L. M. Lee, *Chromatographia*, 25 (1988) 473–479.
- 11 H.-Ch. K. Chang, K. E. Markides and M. L. Lee, *J. Microcolumn Sep.*, 1 (1989) 131–135.
- 12 D. W. Armstrong, A. Alak, W. DeMond, W. L. Hinze and T. E. Riehl, *J. Liq. Chromatogr.*, 8 (1985) 261–269.
- 13 M. Olsson, L. C. Sander and S. A. Wise, *J. Chromatogr.*, 477 (1989) 277–290.
- 14 M. Gazdag, G. Szepesi and L. Huszar, *J. Chromatogr.*, 371 (1986) 227–234.
- 15 K. Shimada, T. Masue, K. Toyoda, M. Takani and T. Nambara, *J. Liq. Chromatogr.*, 11 (1988) 1475–1484.
- 16 D. W. Armstrong, W. DeMond, A. Alak, W. L. Hinze, T. E. Riehl and K. H. Bui, *Anal. Chem.*, 57 (1985) 234–237.
- 17 M. J. O'Hare and E. C. Nice, in M. P. Kautsky (Editor), *Steroid Analysis by HPLC —Recent Applications (Chromatographic Science Series, Vol. 16)*, Marcel Dekker, New York, Basle, 1981, pp. 277–322.
- 18 D. E. Anderson, D. J. O'Conner, J. F. Kirby and C. P. Sears, III, *J. Chromatogr. Sci.*, 23 (1985) 477–483.
- 19 L. C. Sander and S. A. Wise, *Anal. Chem.*, 61 (1989) 1749–1754.
- 20 L. C. Sander and N. E. Craft, *Anal. Chem.*, 62 (1990) 1545–1547.
- 21 S. Ulick, M. D. Chu and M. Land, *J. Biol. Chem.*, 258 (1983) 5498–5502.
- 22 W. L. Zielinski, Jr., K. Johnston and G. M. Muschik, *Anal. Chem.*, 48 (1976) 907–911.
- 23 S. Sheikh and J. Touchstone, *Chimicaoggi*, October (1981) 25–28.
- 24 L. R. Snyder and J. J. Kirkland, *Introduction to Modern Liquid Chromatography*, Wiley, New York, 2nd ed., 1979.
- 25 S. R. Bakalyar, R. McIlwrick and E. Roggendorf, *J. Chromatogr.*, 142 (1977) 353–365.
- 26 L. R. Snyder, in A. Weissberger and E. S. Perry (Editors), *Techniques of Chemistry*, Vol. III, Part I, Wiley-Interscience, New York, 2nd ed., 1978, Ch. 2.





## Fatty acid conjugates of chlorinated phenols and their high-performance liquid chromatographic analysis

BHUPENDRA S. KAPHALIA

*Department of Pathology, University of Texas Medical Branch, Galveston, TX 77550 (U.S.A.)*

(First received February 20th, 1990; revised manuscript received August 28th, 1990)

---

### ABSTRACT

Fatty acid ( $C_{16}$  and  $C_{18}$ ) conjugates of pentachlorophenol and four other commonly used chlorinated phenols (2,4-di-, 2,4,5- and 2,4,6-tri-, and 2,3,4,6-tetra-chlorophenols) were synthesized and their structures were established by proton nuclear magnetic resonance spectroscopy and chemical ionization mass spectrometry. The high-performance liquid chromatographic (HPLC) separation was achieved on reversed-phase (C-18) column using methanol–water (39:1, v/v) at a flow-rate of 1 ml/min. Palmitoyl- and oleoyl-2,4-dichlorophenols (19.6 min), palmitoyl- and oleoyl-2,4,5-trichlorophenols and stearoyl-2,4-dichlorophenol (28.0 min), oleoyl-2,4,6-trichlorophenol and linoleoyl-2,3,4,6-tetrachlorophenol (30.8 min), palmitoyl- and oleoyl-2,3,4,6-tetrachlorophenols and stearoyl-2,4,5-trichlorophenol (43.2 min) and palmitoyl- and oleoyl-pentachlorophenols (72.0 min) were co-eluted under the HPLC conditions described above. Therefore, reversed-phase HPLC separation of a mixture of the five chlorinated phenol conjugates of each fatty acid was achieved.

---

### INTRODUCTION

The five chlorinated phenols (CPs) namely, 2,4-dichlorophenol (DCP), 2,4,5- and 2,4,6-trichlorophenols (TCPs), 2,3,4,6-tetrachlorophenol (TeCP) and pentachlorophenol (PCP) are the common contaminants present in the environment and human body [1,2]. DCP and 2,4,5-TCP as reaction intermediates in the production of chlorophenoxy acids (herbicides) and TeCP and PCP as pesticides and wood preservatives have widely been used in the U.S.A. [3]. These CPs are also spontaneously formed when drinking or industrial waste water containing phenols is chlorinated [1,2]. Hexachlorobenzene and lindane ( $\gamma$ -hexachlorocyclohexane), widely used as fungicide and pesticide, respectively, and ubiquitous in the environment and human body, metabolize to CPs [4–7]. Among CPs, the most extensively used compound is PCP [8]. Contamination of PCP and other CPs in the environment and in humans and animals is well documented [3,9–14]. The environmental and biological transformation of PCP to DCP, TCPs and TeCP has also been demonstrated [6].

Once absorbed in the body, a significant amount of the CPs may be retained due to the formation of lipophilic conjugates of fatty acids. Surprisingly, very little is known about such conjugates and their toxicity [15,16]. A palmitic acid ester of PCP (palmitoylpentachlorophenol or PPCP) shown to be formed *in vitro* using the rat liver microsomes fortified with coenzyme A and ATP [17] has also been detected in human

fat [18]. An accumulation of such conjugates in membranes of tissues and their further metabolism may have deleterious consequences. Recently, we have found a selective toxicity of PPCP to exocrine pancreas in rats [19]. The presence and formation in the body tissues, and toxicity of other fatty acid conjugates of PCP as well as other four CPs mentioned earlier have not been studied. Therefore, the fatty acid ( $C_{16}$  and  $C_{18}$ ) conjugates of DCP, TCPs, TeCP and PCP were synthesized, characterized by proton nuclear magnetic resonance ( $^1H$  NMR) spectroscopy, chemical ionization mass spectrometry (CIMS) and reversed-phase high-performance liquid chromatography (HPLC). The conjugates synthesized in this study will be used as standards to study their formation under *in vitro* and *in vivo* conditions and toxicity.

## MATERIALS AND METHODS

### *Chemicals and reagents*

Acyl chlorides of palmitic, stearic, oleic and linoleic acids and linolenic anhydride (purity 98–99%) were obtained from Sigma (St. Louis, MO, U.S.A.). Pyridine (anhydrous), 2,4-DCP, 2,4,5- and 2,4,6-TCPs and PCP (purity 98–99%) purchased from Aldrich (Milwaukee, WI, U.S.A.) and 2,3,4,6-TeCP (purity 93.6%) from American Tokyo Kasei (Portland, OR, U.S.A.) were used. Silica gel (Bio-Sil A, 200–325 mesh) for column chromatography obtained from Bio-Rad Labs. (Richmond, CA, U.S.A.) and HPLC grade solvents from Fisher Scientific (Fairlawn, NJ, U.S.A.) were used in the present study.

### *Synthesis of fatty acid conjugates of CPs*

The fatty acid ( $C_{16}$  and  $C_{18}$ ) conjugates of the five CPs were synthesized according to the method described earlier by Ansari *et al.* [18]. Chlorinated phenol was dissolved in dry pyridine and to this fatty acid chloride or anhydride was added dropwise, in a conical flask. The contents were mixed well. The flask was screw capped and kept in a water bath at 50–60°C. The reaction was monitored periodically and after 24 h, the mixture was transferred to a separating funnel and extracted twice with diethyl ether. The extract was washed several times with 0.1 *M* hydrochloric acid and followed by 10%  $Na_2CO_3$  in order to remove the impurities of pyridine and fatty acid residues, respectively. The solvent was evaporated under nitrogen. The synthesized products were crystallized in hexane–methanol (for the CP conjugates of palmitic and stearic acids) or purified by silica gel column chromatography (for the CP conjugates of oleic, linoleic and linolenic acids) on a silica gel packed column (30 × 2 cm I.D.) to a height of 20 cm using hexane–chloroform (10:1, v/v) as eluting solvent. The elution flow-rate was 7 ml/min. A small aliquot from each fraction collected at every minute was analyzed by thin-layer chromatography (TLC) on silica gel coated glass plates (Analtech, Newark, DE, U.S.A.; 250  $\mu$ m thick) using hexane–ethyl acetate (9:1, v/v) as the solvent system. Fractions between 21 and 53 showing single spot at same  $R_F$  by TLC were pooled and the solvent was evaporated under a reduced pressure. The high-resolution  $^1H$  NMR spectra were acquired by using a WB Fourier transform NMR spectrometer (6.3 T) on JEOL GX 270. The samples were dissolved in deuterated chloroform and tetramethylsilane was used as an internal standard. Nermag, R10-10C, quadrupole mass spectrometer equipped with PDP 11/73 data system was operated under positive chemical ionization mode with ammonia

as a reagent gas (gas pressure  $10^{-1}$  Torr). The sample was dissolved in *n*-hexane (5 mg/ml) and 1–2  $\mu$ l was applied on tungsten filament probe tip. The solvent was allowed to evaporate and the probe was inserted into the ion source, set at 1.1 A. The temperature of the probe was programmed from 0 to 500 mA at 20 mA/s.

#### *HPLC analysis of fatty acid conjugates of CPs*

The fatty acid conjugates of CPs were separated on a reversed-phase (C-18) column (25  $\times$  0.46 cm I.D., 5  $\mu$ m particle size) using 334 Beckman liquid chromatograph equipped with 165 variable-wavelength UV detector. The effluent was monitored at 210 nm. A mixture of all the 25 chlorinated phenol conjugates of the five fatty acids were analyzed by reversed-phase HPLC using methanol–water (39:1, v/v) solvent system at a flow-rate of 1 ml/min. Several conjugates were co-eluted under the reversed-phase HPLC conditions described above. Therefore, a reversed-phase HPLC separation was achieved for a mixture of five chlorinated phenol conjugates of each fatty acid. The five chlorinated phenol conjugates of each palmitic, stearic and oleic acids were separated by using methanol–hexane (39:1, v/v) at a flow-rate of 1 ml/min. The five chlorinated phenol conjugates of linoleic (flow-rate 1.5 ml/min) and linolenic (flow-rate 1.0 ml/min) acids were resolved by using methanol–water (39:1, v/v) solvent system.

#### RESULTS AND DISCUSSION

The palmitic and stearic acid conjugates of all the five CPs were solids and their melting points (uncorrected) were recorded to be 49, 78, 55, 55, 77, 54, 83, 59, 62 and 85°C for the conjugates I to X (Fig. 1), respectively. Oleic, linoleic and linolenic acid conjugates of the CPs were liquids at room temperature. The  $^1\text{H}$  NMR spectra of all the conjugates synthesized in the present study gave signals at  $\delta$  0.88–2.66 for palmitoyl,  $\delta$  0.87–2.67 for stearoyl and  $\delta$  0.87–5.37 for oleoyl, linoleoyl and linolenoyl conjugates of CPs. Similarly, the signals for olefinic and allylic protons were detected from  $\delta$  5.34–5.37 and  $\delta$  2.77–2.81, respectively, for the CP conjugates of unsaturated  $\text{C}_{18}$  fatty acids depending upon the number of double bonds. The signals for the aromatic protons were observed at  $\delta$  7.04–7.46 for 2,4-dichlorophenyl,  $\delta$  7.26–7.55 for 2,4,5-trichlorophenyl,  $\delta$  7.26–7.37 for 2,4,6-trichlorophenyl and  $\delta$  7.51 for 2,3,4,6-tetrachlorophenyl conjugates of all the fatty acids (Table I). The chemical ionization mass spectral analysis of all the conjugates is summarized in Table II. The pseudomolecular ion peaks ( $\text{M} + \text{NH}_4^+$ ) of all the compounds exhibited a ratio characteristic to the number of chlorines present in dichlorophenyl, trichlorophenyls, tetrachlorophenyl, and pentachlorophenyl fatty acid conjugates, respectively. These spectral patterns of the pseudomolecular ion peaks were found similar to those reported for the di-, tri-, tetra- and penta-chlorophenols and other equivalent number of chlorine containing compounds, respectively [20]. Relatively low abundance of pseudomolecular ion peaks were observed for the fatty acid conjugates of TeCP and PCP than those of the conjugates of DCP and TCPs. Loss of one chlorine was also observed in most of the spectra of CP conjugates of unsaturated fatty acids. Other major peaks of  $\text{RCOO}^- + \text{NH}_4^+$ ,  $\text{RCOOH}$ ,  $\text{RCO}\equiv\text{O}^+$  ( $\text{R}$  = fatty acid carbon chain) were also detected in the spectra of the CP conjugates of fatty acids (Table II).

When a mixture of the 25 conjugates (I–XXV) was analyzed by reversed-phase

TABLE I  
270 MHz PROTON NMR SPECTRAL DATA FOR THE FATTY ACID CONJUGATES OF CPs  
Chemical shifts expressed in ppm,  $J$  values are given in Hz.

Compounds <sup>a</sup>	Aromatic	Olefinic	Allylic	$C_2-CH_2-$	$-CH_2-$	$C_3-CH_2-$	Other- $CH_2-$	$-CH_3$ (terminal)
I	7.04-7.45(3H)	—	—	2.60 t(2H, $J=7.51$ )	—	1.77 m(2H)	1.26 b(24H)	0.88 t(3H, $J=6.77$ )
II	7.27-7.55(2H)	—	—	2.60 t(2H, $J=7.51$ )	—	1.77 m(2H)	1.26 b(24H)	0.88 t(3H, $J=6.59$ )
III	7.37 (2H)	—	—	2.65 t(2H, $J=7.51$ )	—	1.78 m(2H)	1.26 b(24H)	0.88 t(3H, $J=6.59$ )
IV	7.51 (H)	—	—	2.66 t(2H, $J=7.51$ )	—	1.77 m(2H)	1.26 b(24H)	0.88 t(3H, $J=6.59$ )
V	—	—	—	2.66 t(2H, $J=7.51$ )	—	1.77 m(2H)	1.26 b(24H)	0.88 t(3H, $J=6.59$ )
VI	7.04-7.45(3H)	—	—	2.60 t(2H, $J=7.33$ )	—	1.77 m(2H)	1.25 b(28H)	0.87 t(3H, $J=6.59$ )
VII	7.26-7.55(2H)	—	—	2.60 t(2H, $J=7.33$ )	—	1.77 m(2H)	1.25 b(28H)	0.87 t(3H, $J=6.59$ )
VIII	7.36 (2H)	—	—	2.65 t(2H, $J=7.33$ )	—	1.77 m(2H)	1.25 b(28H)	0.87 t(3H, $J=6.59$ )
IX	7.51 (H)	—	—	2.66 t(2H, $J=7.33$ )	—	1.77 m(2H)	1.26 b(28H)	0.88 t(3H, $J=6.59$ )
X	—	—	—	2.67 t(2H, $J=7.33$ )	—	1.81 m(2H)	1.26 b(28H)	0.88 t(3H, $J=6.59$ )
XI	7.05-7.46(3H)	5.36 b(2H)	—	2.60 t(2H, $J=7.70$ )	2.03 b(4H, $C_{8,11}$ )	1.78 m(2H)	1.45 b(20H)	0.88 t(3H, $J=6.22$ )
XII	7.26-7.55(2H)	5.35 b(2H)	—	2.60 t(2H, $J=7.33$ )	2.02 b(4H, $C_{8,11}$ )	1.77 m(2H)	1.45 b(20H)	0.88 t(3H, $J=6.59$ )
XIII	7.26-7.35(2H)	5.35 b(2H)	—	2.65 t(2H, $J=7.33$ )	2.02 b(4H, $C_{8,11}$ )	1.77 m(2H)	1.45 b(20H)	0.88 t(3H, $J=6.59$ )
XIV	7.51 (H)	5.35 b(2H)	—	2.65 t(2H, $J=7.48$ )	2.02 b(4H, $C_{8,11}$ )	1.80 m(2H)	1.30 b(20H)	0.87 t(3H, $J=6.59$ )
XV	—	5.34 b(2H)	—	2.66 t(2H, $J=7.48$ )	2.02 b(4H, $C_{8,11}$ )	1.80 m(2H)	1.32 b(20H)	0.87 t(3H, $J=6.59$ )
XVI	7.04-7.45(3H)	5.35 b(4H)	2.77 t(2H, $J=7.33$ )	2.60 t(2H, $J=7.33$ )	2.03 b(4H, $C_{8,14}$ )	1.77 m(2H)	1.31 b(14H)	0.88 t(3H, $J=6.59$ )
XVII	7.26-7.54(2H)	5.36 b(4H)	2.77 t(2H, $J=5.72$ )	2.60 t(2H, $J=7.48$ )	2.03 b(4H, $C_{8,14}$ )	1.77 m(2H)	1.31 b(14H)	0.88 t(3H, $J=6.59$ )
XVIII	7.36 (2H)	5.36 b(4H)	2.77 t(2H, $J=5.72$ )	2.64 t(2H, $J=7.48$ )	2.03 b(4H, $C_{8,14}$ )	1.77 m(2H)	1.34 b(14H)	0.88 t(3H, $J=6.59$ )
XIX	7.51 (H)	5.36 b(4H)	2.77 t(2H, $J=5.72$ )	2.66 t(2H, $J=7.48$ )	2.03 b(4H, $C_{8,14}$ )	1.77 m(2H)	1.35 b(14H)	0.88 t(3H, $J=6.59$ )
XX	—	5.36 b(4H)	2.77 t(2H, $J=5.72$ )	2.67 t(2H, $J=7.48$ )	2.03 b(4H, $C_{8,14}$ )	1.77 m(2H)	1.35 b(14H)	0.88 t(3H, $J=6.80$ )
XXI	7.04-7.45(3H)	5.37 b(6H)	2.81 t(4H, $J=5.72$ )	2.60 t(2H, $J=7.48$ )	2.08 b(4H, $C_{8,17}$ )	1.76 m(2H)	1.35 b(8H)	0.97 t(3H, $J=7.48$ )
XXII	7.26-7.55(2H)	5.37 b(6H)	2.81 t(4H, $J=5.72$ )	2.60 t(2H, $J=7.48$ )	2.08 b(4H, $C_{8,17}$ )	1.76 m(2H)	1.35 b(8H)	0.97 t(3H, $J=7.48$ )
XXIII	7.26-7.37(2H)	5.37 b(6H)	2.81 t(4H, $J=5.87$ )	2.64 t(2H, $J=7.33$ )	2.08 b(4H, $C_{8,17}$ )	1.76 m(2H)	1.36 b(8H)	0.97 t(3H, $J=7.33$ )
XXIV	7.51 (H)	5.37 b(6H)	2.81 t(4H, $J=5.30$ )	2.66 t(2H, $J=7.48$ )	2.07 b(4H, $C_{8,17}$ )	1.77 m(2H)	1.35 b(8H)	0.97 t(3H, $J=7.48$ )
XXV	—	5.37 b(6H)	2.80 t(4H, $J=5.72$ )	2.66 t(2H, $J=7.48$ )	2.07 b(4H, $C_{8,17}$ )	1.77 m(2H)	1.35 b(8H)	0.97 t(3H, $J=7.68$ )

<sup>a</sup> See Fig. 1.

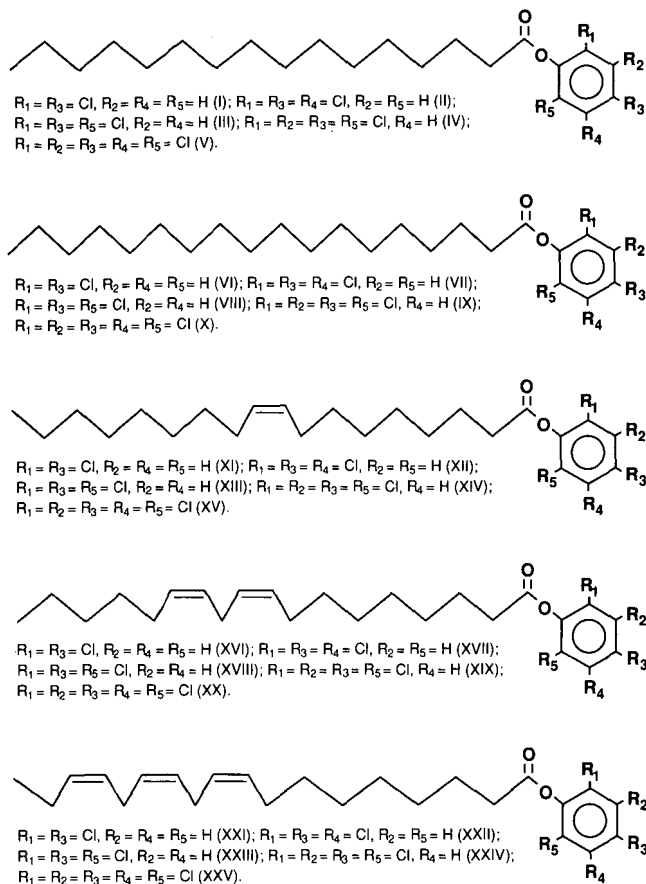


Fig. 1. Structure of palmitic (I–V), stearic (VI–X), oleic (XI–XV), linoleic (XVI–XX) and linolenic (XXI–XXV) acid conjugates of CPs.

HPLC using methanol–water (39:1, v/v) at a flow-rate of 1 ml/min, I and XI (19.6 min), II, VI and XII (28.0 min) XIII and XIX (30.8 min), IV, VII and XIV (43.2 min), and V and XV (72.0 min) co-eluted (Fig. 2). Therefore, a mixture of DCP, TCPs, TeCP and PCP conjugate of each fatty acid was separated by reversed-phase HPLC. The five chlorinated phenol conjugates of each palmitic, stearic and oleic acids could be separated by methanol–hexane (39:1, v/v) at a flow-rate of 1 ml/min. Methanol–water (39:1, v/v) was found to be a suitable solvent system to separate the five chlorinated phenol conjugates of linoleic (flow-rate 1.5 ml/min) and linolenic (flow-rate 1.0 ml/min) acids (Fig. 3). The minimum detectability of the fatty acid conjugates of CPs ranges 0.05–0.10  $\mu\text{g}$ . Among the five CP conjugates of a fatty acid, the 2,4-DCP conjugate was eluted first followed by the conjugates of 2,4,5-TCP, 2,4,6-TCP and 2,3,4,6-TeCP, and the PCP conjugate was eluted in the last. The elution time of these conjugates from the reversed-phase HPLC column depended on the number of chlorines in phenyl ring, degree of unsaturation and number of alkyl residues in the fatty

TABLE II

CHEMICAL IONIZATION MASS SPECTRAL ANALYSIS USING NH<sub>3</sub> AS A REAGENT GAS OF FATTY ACID CONJUGATES OF CPs

RCOOR'; R = fatty acid carbon chain, R' = chlorinated phenyl ring.

Compounds <sup>a</sup>	Pseudomolecular ions <sup>b</sup>	RCOO <sup>-</sup> -NH <sub>4</sub> <sup>+</sup>	RCOOH	RC≡O <sup>+</sup>	
I	(400)	418/420/422(a)	273	256	239
II	(434)	452/454/456(b)	273	256	239
III	(434)	452/454/456(b)	273	256	239
IV	(468)	486/488/490/492(c)	273	256	239
V	(502)	Reported earlier [18]			
VI	(428)	446/448/450(a)	301	284	267
VII	(462)	480/482/484(b)	301	284	267
VIII	(462)	480/482/484(b)	301	284	267
IX	(496)	514/516/518/520(c)	301	284	267
X	(530)	548/550/552/554(d)	301	284	267
XI	(426)	444/446/448(a)	—	282	265
XII	(460)	478/480/482(b)	—	282	265
XIII	(460)	478/480/482(b)	—	282	265
XIV	(494)	512/514/516/518(c)	299	282	265
XV	(528)	546/548/550/552(d)	299	282	265
XVI	(424)	442/446/446(a)	—	—	263
XVII	(458)	476/478/480(b)	—	—	263
XVIII	(458)	476/478/480(b)	—	280	263
XIX	(492)	510/512/514/516(c)	—	280	263
XX	(526)	544/546/548/550(d)	—	280	263
XXI	(422)	440/442/444(a)	—	—	261
XXII	(456)	474/476/478(b)	—	—	261
XXIII	(456)	474/476/478(b)	—	—	261
XXIV	(490)	508/510/512/514(c)	—	—	261
XXV	(524)	542/544/546/548(d)	—	—	261

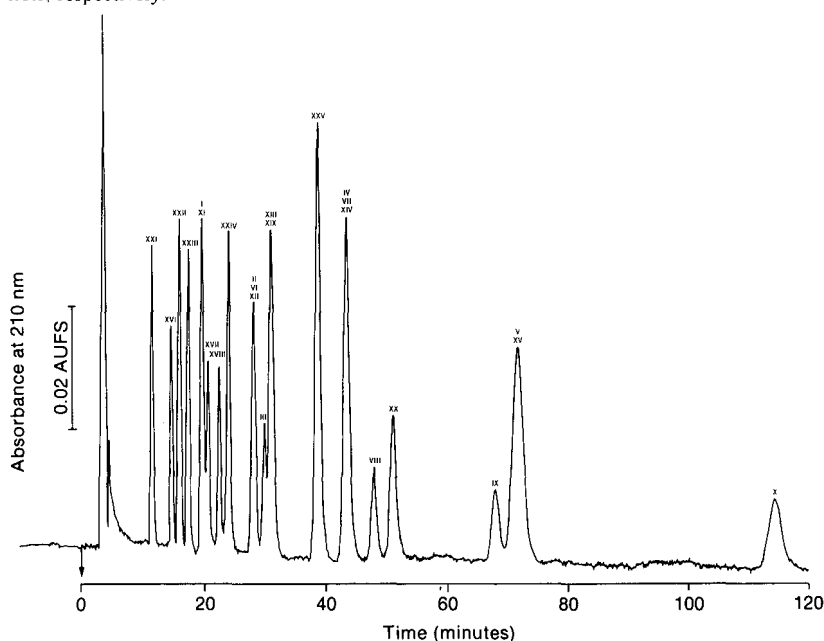
<sup>a</sup> See Fig. 1. Digits in parentheses are the molecular weights.<sup>b</sup> a, b, c and d are the *m/z* values for the fatty acid conjugates of di-, tri-, tetra- and pentachlorophenols, respectively.

Fig. 2. Reversed-phase HPLC analysis of a mixture of the 25 conjugates (I–XXV) on C-18 column (25 × 0.46 cm I.D., 5 μm particle size) using methanol–water (39:1, v/v) solvent system at a flow-rate of 1 ml/min.

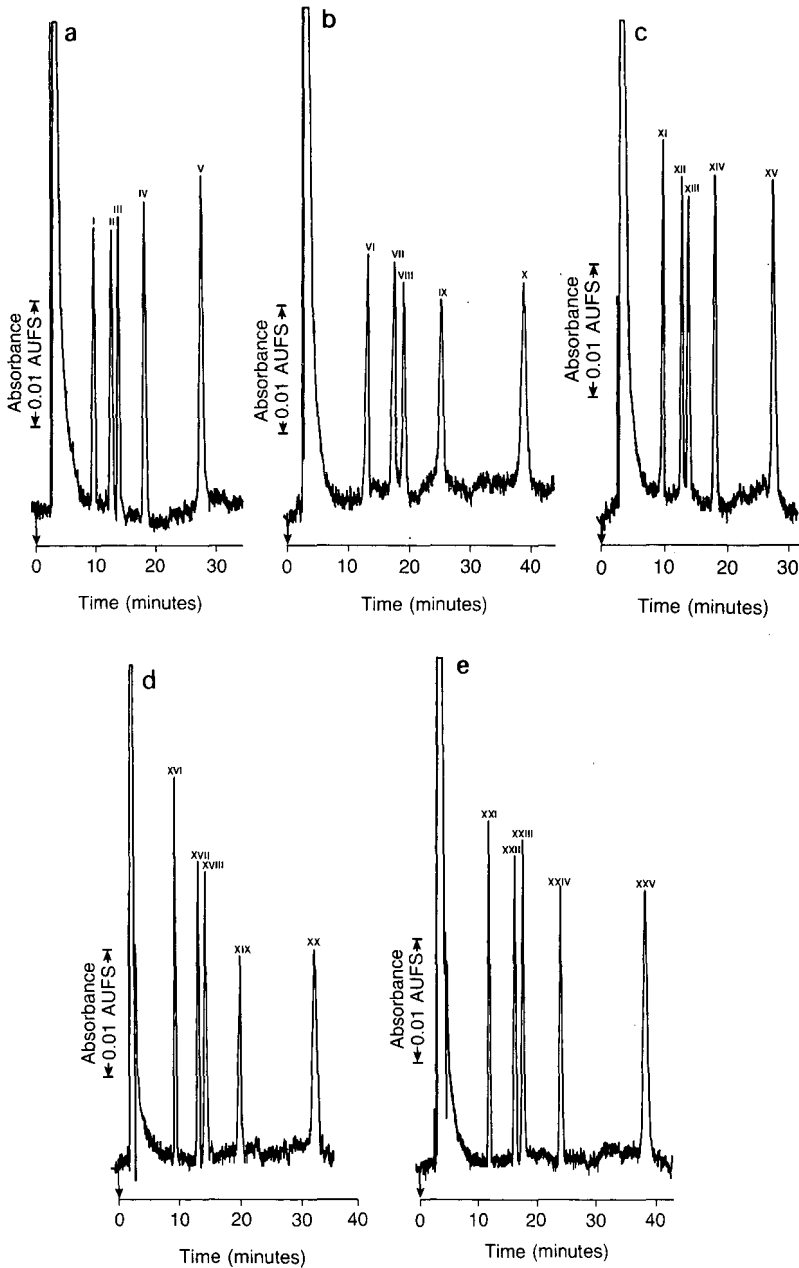


Fig. 3. Reversed-phase HPLC separation of the five CP conjugates of (a) palmitic (I-V), (b) stearic (VI-X), (c) oleic (XI-XV), (d) linoleic (XVI-XX) and (e) linolenic (XXI-XXV) acids. Conjugates I-XV were separated by methanol-hexane (39:1, v/v) at a flow-rate of 1 ml/min, XVI-XX by methanol-water (39:1, v/v) at a flow-rate of 1.5 ml/min and XXI-XXV by methanol-water (39:1, v/v) at a flow-rate of 1.0 ml/min.

acid chain. The results of  $^1\text{H}$  NMR, mass spectral and HPLC analysis of all the synthesized compounds (I-XXV) together support the synthesis of chlorinated phenol conjugates of  $\text{C}_{16}$  and  $\text{C}_{18}$  fatty acids (Fig. 1). Thus, the CP conjugates of fatty acids synthesized in the present study will be used to study their toxicity, structure activity relationship and formation under *in vitro* and *in vivo* conditions.

#### ACKNOWLEDGEMENTS

This work was supported by John Sealy Memorial Endowment Fund. NMR and mass spectrometers were purchased through the grants funded by the M. D. Anderson Foundation, Houston, TX, U.S.A.

#### REFERENCES

- 1 M. F. Deinzer, F. Schaumberg and E. Klein, *Health Perspect*, 24 (1978) 209.
- 2 NRC (National Research Council), *Drinking Water and Health: Disinfection and Disinfectant By products*, Vol. 7, National Academy Press, Washington, D.C., 1987, p. 169.
- 3 *IARC Monogr. Eval. Carcinog. Risk Chem. Humans*, 41 (1986) 319.
- 4 R. Engst, R. M. Macholz, M. Kujawa, H.-J. Lewerenz and R. Plass, *Environ. Sci. Health.*, 11 (1976) 95.
- 5 R. M. Macholz and M. Kujawa, *Residue Rev.*, 94 (1985) 119.
- 6 G. Renner and W. Muke, *Toxicol. Environ. chem.* 11 (1986) 9.
- 7 C. den-Besten, M. M. C. G. Peters and P. J. van Bladeren, *Biochem. Biophys. Res. Comm.*, 163 (1989) 1275.
- 8 D. P. Cirelli, in K. Ranga Rao (Editor), *Pentachlorophenol: Chemistry, Pharmacology, and Environmental Toxicology*, Plenum Press, New York and London, 1978, p. 13.
- 9 A. Bevenue and H. Beckman, *Residue Rev.*, 19 (1967) 84.
- 10 U. G. Ahlborg and T. M. Thunberg, *Crit. Rev. Toxicol.*, 7 (1980) 1.
- 11 H. Choudhury, J. Coleman, C. T. de Rosa and J. F. Stara, *Toxicol. Ind. Health*, 4 (1986) 483.
- 12 J. Gomez-Catalan, J. To-Figueras, J. Planas, M. Rodamilans and J. Corbella. *Human Toxicol.*, 6 (1987) 397.
- 13 K. Noren and J. Sjoval, *J. Chromatogr.*, 141 (1987) 55.
- 14 D. A. Kalman and S. W. Horstman, *J. Toxicol. Clin. Toxicol.*, 20 (1983) 343.
- 15 B. S. Kaphalia and G. A. S. Ansari, *Bull. Environ. Contam. Toxicol.* 39 (1987) 152.
- 16 B. S. Kaphalia and G. A. S. Ansari, *J. Biochem. Toxicol.*, 4 (1989) 183.
- 17 E. G. Leighty and A. F. Fentiman, *Toxicol.*, 28 (1982) 329.
- 18 G. A. S. Ansari, S. G. Britt and E. S. Reynolds, *Bull. Environ. Contam. Toxicol.*, 34 (1985) 661.
- 19 G. A. S. Ansari, B. S. Kaphalia and P. J. Boor, *Toxicol.*, 46 (1987) 57.
- 20 B. S. Middleditch, S. R. Missler and H. B. Hines, *Mass Spectrometry of Priority Pollutants*, Plenum Press, New York and London, 1981.



CHROM. 22 760

## Separation and identification of free phenolic acids in wines by high-performance liquid chromatography

G. P. CARTONI\*, F. COCCIOLI and L. PONTELLI

*Dipartimento di Chimica, Università "La Sapienza" di Roma, Piazzale Aldo Moro 5, 00185 Rome (Italy)*  
and

E. QUATTRUCCI

*Ist. Naz. Nutr., Via Ardeatina 546, 00179, Rome (Italy)*

(First received February 20th, 1990; revised manuscript received July 13th, 1990)

---

### ABSTRACT

Free phenolic acids in Italian wines and a sherry were identified by high-performance liquid chromatography. The samples were concentrated and passed through a Sep-Pak C<sub>18</sub> cartridge and the acids were recovered by elution with 2 ml of tetrahydrofuran. The separation was carried out by gradient elution on a reversed-phase column with methanol–water and phosphate buffer (pH 2.7). Detection was carried out 280 and 230 nm.

---

### INTRODUCTION

The phenolic compounds in wine are very important as they contribute to the characteristic taste (astringency, bitterness), changing with age, and also possessing vitaminic and bacteriological effects [1]. These compounds are a heterogeneous group of substances consisting of several classes [2] (catechins, leucoanthocyanidins, flavonols, flavanol glycosides, high-molecular-weight tannins, hydrocinnamic acid–tartaric esters and their glucose esters [3], proanthocyanidins and anthocyanidins [4]). They include phenolic benzoic and phenolic cinnamic acids [5–7].

In this work the free phenolic acids in Italian wines and a sherry were identified by high-performance liquid chromatography (HPLC) with UV detection.

### EXPERIMENTAL

#### *Apparatus*

An LKB two-pump gradient HPLC system was used. The LKB 2150 pump, based on the dual-piston principle, gives pulse-free flow from 5 ml/min to as low as 10  $\mu$ l/min. The system employs a high-pressure mixing system (400  $\mu$ l). A Jasco Model 100 VA variable-wavelength UV detector equipped with a 1- $\mu$ l flow cell was used. A Rheodyne model 7410 valve injector was fitted with an internal loop. A Perkin-Elmer

Series 2 liquid chromatography with a Model LC 55 B variable-wavelength detector was also used.

Column 1 (165 mm  $\times$  4.6 mm I.D.) and column 2 (250 mm  $\times$  2.1 mm I.D.) both contained ODS<sub>2</sub> (5  $\mu$ m). They were slurry-packed in the laboratory with Spherisorb obtained from Phase Separations (Norwalk, CT, U.S.A.) [8].

### Reagents

Distilled water, stored in glass, was filtered and passed through a Norganic System Cartridge supplied by Millipore (Bedford, MA, U.S.A.) to remove organic substances.

The solvents used (methanol, acetic acid and tetrahydrofuran) were of HPLC grade (Carlo Erba, Milan, Italy). Phenolic acids were purchased from Fluka (Buchs, Switzerland). The cinnamic acids were in the *trans* form.

Phosphate buffer (pH 2.7) was prepared by adding 1.425 g of disodium hydrogenphosphate dihydrate to 4.58 ml of acetic and diluting to 1 l with distilled water. It was then filtered through a 0.45- $\mu$ m Millipore filter. This stock solution was stored at 4°C.

### Samples

The samples studied were a fino sherry (Tio Pepe), Verdicchio, Pinot Grigio, Fontana Candida and wine A (our production) white wines, Chianti red wine and a white vermouth.

### Preparation of the wine sample

A 10-ml volume of wine sample was concentrated under vacuum to 3 ml at a temperature below 30°C for 20 min to remove ethanol, then transferred into a test-tube and 0.5 ml of phosphate buffer stock solution (pH 2.7) was added. This solution was passed through a Sep-Pak C<sub>18</sub> cartridge that had previously been washed with methanol and subsequently with water, then the cartridge was washed with 2 ml of phosphate buffer (pH 2.7) (1 ml of stock buffer solution diluted to 2 ml with distilled water). The phenolic acids were recovered by elution with 2 ml of tetrahydrofuran. The solvent was evaporated under nitrogen (below 30°C) and the residue was dissolved in 100  $\mu$ l of methanol.

### Preparation of standards

A 3-mg amount of each phenolic acid was dissolved in 3 ml of methanol. This solution was stored at -20°C in the dark for no longer than 2 months (gradual formation of *cis* isomers of cinnamic acids was observed on exposure to UV light) [9].

Under the elution conditions reported in Fig. 1, *trans* and *cis* isomers are well separated. The *cis* isomers are not present in nature.

Table I gives the absorption maxima for some of the phenolic acids [10]. The UV spectra were taken between 200 and 400 nm with the Perkin-Elmer LB 55 C detector by stopping the solvent flow and scanning the solute while stationary in the cell.

Each compound was injected in the isocratic mode at a mobile phase composition of methanol : water (buffer stock solution diluted 1:10) such as to obtain capacity factor,  $k' > 2$ .

TABLE I  
ABSORPTION MAXIMA NM OF SOME PHENOLIC ACIDS

	$\lambda_{\max}$ (1) (nm)	$\lambda_{\max}$ (2) (nm)
Vanillic acid	221	260
Caffeic acid	295	315
Ferulic acid	321	
Sinapic acid	235	315
<i>m</i> -Coumaric acid	280	
<i>o</i> -Coumaric acid	276	325
<i>p</i> -Coumaric acid	309	
3,4,5-Trimethoxycinnamic acid	295	
3,5-Dimethoxybenzoic acid	249	297
Syringic acid	274	

## RESULTS AND DISCUSSION

The chromatographic conditions in Table II and Fig. 1 were established through a preliminary study with a purified sample of wine.

Each phenolic acid was injected (as the single compound) at least twice. As the retention times obtained in gradient elution are not perfectly reproducible, identification of adjacent peaks was carried out by method of standard additions. The chromatogram of phenolic acids previously identified in wine was compared with each wine analysed at wavelengths of 280 and 320 nm. The recoveries of three phenolic acids added to distilled water, extracted and purified as described above were caffeic acid  $81.1 \pm 2\%$ , ferulic acids  $81.5 \pm 2\%$  and *o*-coumaric acid  $86.4 \pm 2\%$ .

TABLE II  
RETENTION TIMES OF THE PHENOLIC ACIDS INVESTIGATED

Systematic name	Trivial name	Retention time (min)
2,6-Dihydroxybenzoic acid	Resorcylic acid	6.0
2,4-Dihydroxybenzoic acid		10.0
3,4-Dihydroxybenzoic acid	Protocatechuid acid	10.1
3,4,5-Trihydroxybenzoic acid	Gallic acid	10.4
2,6-Dimethoxybenzoic acid		17.1
2-Hydroxybenzoic acid	Salicylic acid	22.0
4-Hydroxybenzoic acid		25.3
4-Hydroxy-3-methoxybenzoic acid	Vanillic acid	35.4
3,4-Dihydroxycinnamic acid	Caffeic acid	39.1
3,5-Dimethoxy-4-hydroxy acid	Syringic acid	39.1
<i>trans</i> -4-Hydroxycinnamic acid	<i>p</i> -Coumaric acid	46.4
<i>trans</i> -3-Hydroxycinnamic acid	<i>m</i> -Coumaric acid	54.7
4-Hydroxy-3-methoxycinnamic acid	Ferulic acid	54.7
3,4-Dimethoxybenzoic acid	Veratric acid	57.1
3,5-Dimethoxy-4-hydroxycinnamic acid	Sinapic acid	59.5
<i>trans</i> -2-Hydroxycinnamic acid	<i>o</i> -Coumaric acid	64.4
3,5-Dimethoxybenzoic acid		68.5
3,4,5-Trimethoxycinnamic acid		73.6

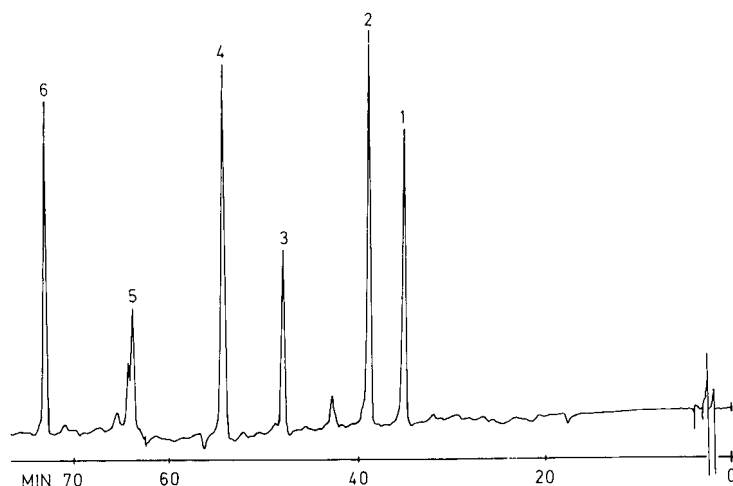


Fig. 1. Chromatogram of standard mixture detected at 280 nm. Peaks: 1 = vanillic acid; 2 = syringic acid; 3 = *p*-coumaric acid; 4 = *m*-coumaric acid; 5 = *o*-coumaric acid; 6 = 3,4,5-trimethoxycinnamic acid. Column, ODS<sub>2</sub> (250 mm × 2.1 mm I.D.); flow-rate 200 μl/min; mobile phase, (A) methanol-phosphate buffer (pH 2.7) (stock solution diluted 1:10) (95:5) and (B) phosphate buffer (pH 2.7) (stock solution diluted 1:10)-methanol (95:5) with the following gradient from B to A: 0 min, 0%; 36 min, 29%; 46 min, 29%; 72 min, 50%; and 80 min, 100% A.

Fig. 1 shows the elution of a standard mixture of phenolic acids (detected at 280 nm), prepared from the stock solution (1 μg/μl) of each phenolic acids in appropriate amounts according to the UV detector response.

Fig. 2 shows a chromatogram of a sample of Fontana Candida white wine and Fig. 3 that of a sample of white vermouth. Peaks K and F are unknown and are present in a larger amount in vermouth than in any of the other wines. The vermouth

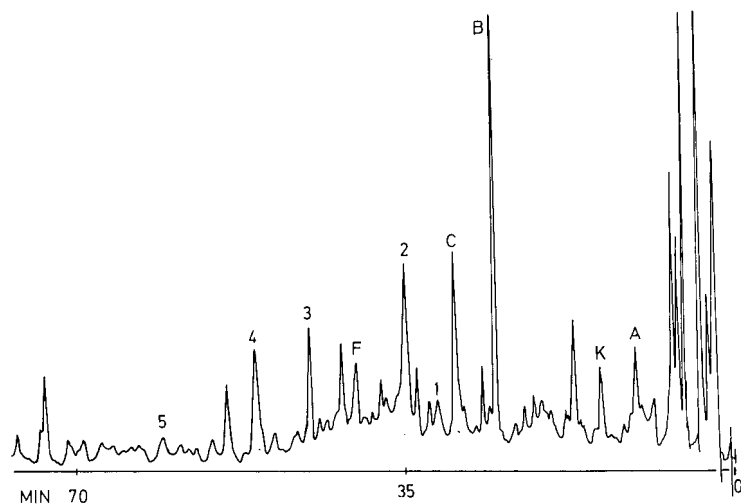


Fig. 2. Chromatogram of Fontana Candida white wine sample. Conditions as in Fig. 1 and peaks as in Table III.

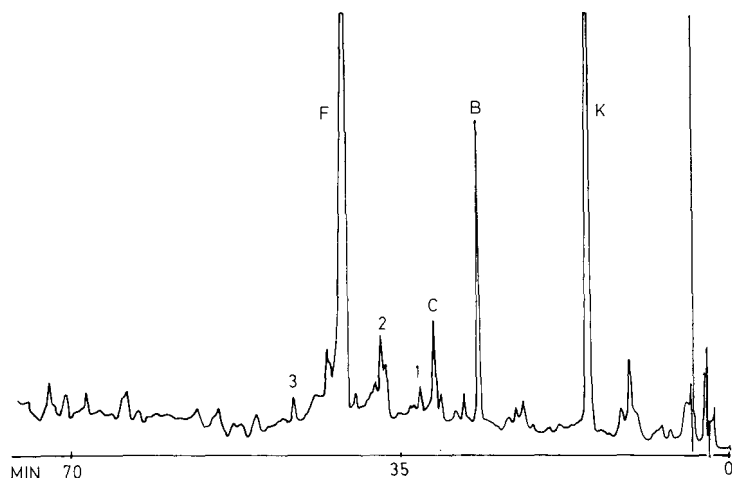


Fig. 3. Chromatogram of white vermouth sample. Conditions as in Fig. 1 and peaks as in Table III.

also contains substances from the extracts of aromatic herbs or plants, but it is not possible to establish the source of these two compounds.

Fig. 4 shows the chromatogram of the Fontana Candida white wine at 320 nm and Fig. 5 that of the Chianti red wine. The chromatogram of red wine is more complex because larger amounts of flavonoids are present.

The chromatogram for vermouth in Fig. 6 shows that compound **K** does not absorb at 320 nm. Table III reports the free phenolic acids detected in the wines and vermouth at 280 and 320 nm.

Syringic acid is not resolved from caffeic acid but the former has maxima at 295

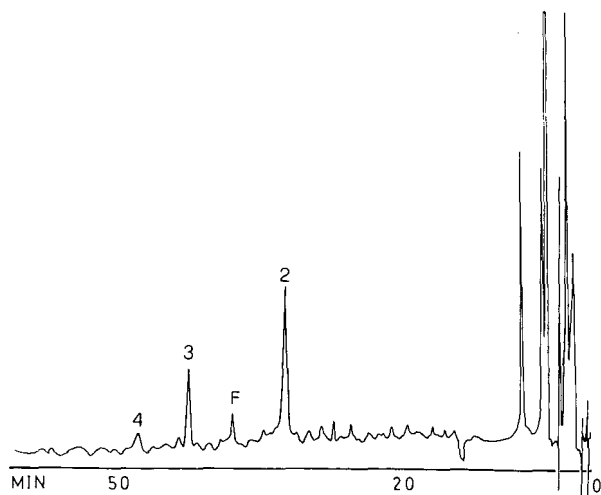


Fig. 4. Chromatogram of Fontana Candida white wine sample detected at 320 nm. Elution conditions as in Fig. 1 and peaks as in Table III.

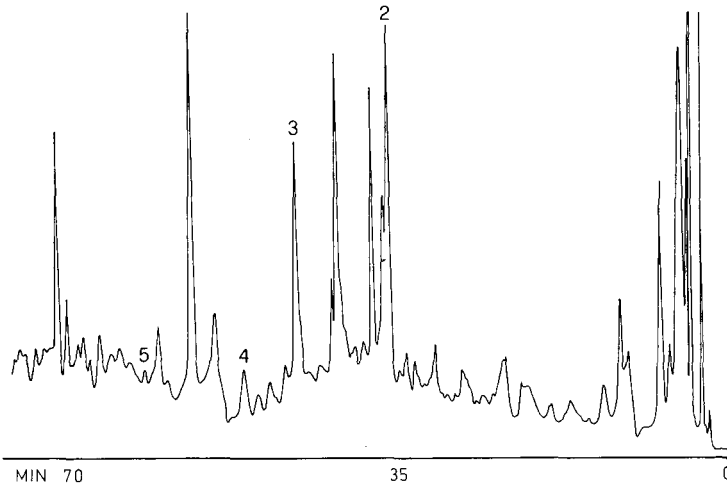


Fig. 5. Sample of Chianti detected at 320 nm. Elution conditions as in Fig. 1 and peaks as in Table III.

and 320 nm whereas former absorbs at 280 nm. Detection at 320 nm corresponds mainly to caffeic acids. Peaks C and F are characteristic of many wines but are unidentified; *M*-coumaric (absorption maximum at 280 nm) and ferulic acid (absorption maximum at 320 nm) are also not resolved.

The amounts of the acids are small and their determination is difficult, but their contribution to the conservation of wine and for the identification of hydroxycinnamic acid–tartaric acid esters are important.

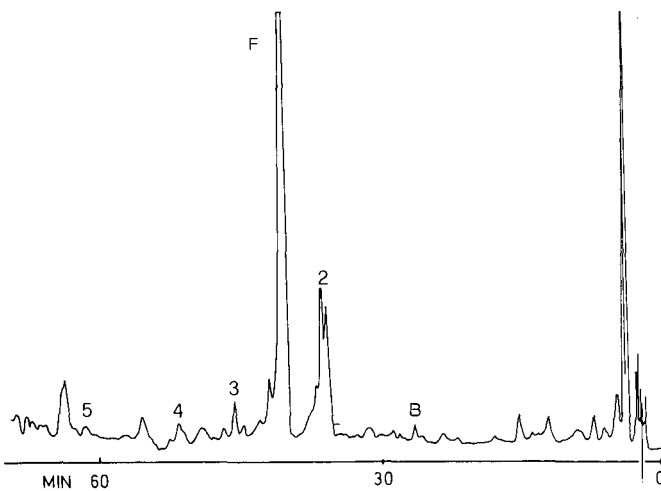


Fig. 6. Sample of vermouth detected at 320 nm. Elution conditions as in Fig. 1 and peaks as in Table III.

TABLE III  
CHARACTERISTIC PEAKS OF WINES

+ = detected; - = not detected.

Wine	Gallic acid	4-Hydroxy-benzoic acid	Unknown	Vanillic acid	Syringic acid, caffeic acid	Unknown	<i>p</i> -Coumaric acid	<i>m</i> -Coumaric acid, ferulic acid
	A <sup>a</sup>	B <sup>a</sup>	C <sup>a</sup>	1 <sup>a</sup>	2 <sup>a</sup>	F <sup>a</sup>	3 <sup>a</sup>	4 <sup>a</sup>
Tio Pepe sherry	+	+	+	+	+	-	+	+
Verdicchio	+	+	+	+	+	+	+	+
Fontana Candida	+	+	+	+	+	+	+	+
Pinot Grigio	+	+	+	+	+	+	+	+
Wine A	+	+	+	+	+	+	+	+
Unbottled wine	-	+	-	+	+	+	+	+
Chianti	+	+	+	-	+	+	+	+
Vermouth	+	+	+	+	+	+	+	+

<sup>a</sup> Peak identification on chromatograms

## REFERENCES

- 1 L. Paronetto, *Polifenoli e Tecnica Enologica*, Edagricole, Bologna, 1977.
- 2 M. L. R. Ramaraine and M. Tuchman, *J. Chromatogr. Sci.*, 24 (1985) 549-554.
- 3 B. Y. Ong and C. W. Nagel, *J. Chromatogr.*, 157 (1978) 345-355.
- 4 S. M. Lunte, *J. Chromatogr.*, 384 (1987) 371-382.
- 5 G. Garcia Barroso, R. Cela Torrijos and J. A. Perez-Bustamante, *J. Chromatographia*, 17 (1983) 249-252.
- 6 D. A. Roston and P. Miesinger, *Anal. Chem.*, 53 (1981) 1695-1697.
- 7 F. Villeneuve, G. Abravanel, M. Moutonei and G. Alberti, *J. Chromatogr.*, 224 (1982) 131-140.
- 8 M. Benincasa, G. P. Cartoni and F. Coccioli, *Ann. Chim. (Rome)*, 77 (1987) 801-811.
- 9 G. Kahnth, *Phytochemistry*, 6 (1967) 755-758.
- 10 M.-H. Salagoity-Auguste, C. Tricard and P. Sudraus, *J. Chromatogr.*, 392 (1987) 379-387.





## High-performance liquid chromatography of red fruit anthocyanins

J.-P. GOIFFON\*, M. BRUN and M.-J. BOURRIER

*Laboratoire Interrégional de la Répression des Fraudes, 2 Rue St. Pierre, B.P. 2042, 34024 Montpellier Cedex (France)*

(First received October 31st, 1989; revised manuscript received August 31st, 1990)

---

### ABSTRACT

Anthocyanins of the main red fruits (bilberry, blackcurrant, strawberry, blackberry, black cherry, morello, raspberry and elderberry) were analysed by high-performance liquid chromatography (HPLC). Some identifications could only be achieved after semi-preparative HPLC, partial hydrolysis and analysis of the fragments obtained. The various parameters affecting the retention were studied and, in particular, the respective influences of the constituent aglycone and sugars could be distinguished and quantified. The effect of the mobile phase composition was also studied and allowed the peak inversions observed to be explained and some of the coelutions to be solved.

---

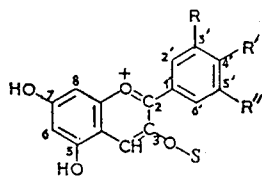
### INTRODUCTION

Anthocyanins are an important family of flavonoid compounds and have been thoroughly studied. Anthocyanin pigments of many fruits have been separated by paper chromatography [1–7], thin-layer chromatography (TLC) [8–10] and, more recently, high-performance liquid chromatography (HPLC) [11–29].

From the published data, very different chromatographic profiles are obtained when dealing with raspberries, strawberries and blackcurrants as starting material. This diversity is of interest when examining the problems of the purity of food products prepared from red fruits (fruit juices, sorbets, fruit wines, liquors, jams, etc.). An anthocyanin chromatographic profile could help to determine adulteration of these products with fruits other than those with which they are supposed to be prepared.

A serious drawback in the analysis of anthocyanins is their instability towards temperature, oxidizing agents and light [30]. Nevertheless, it is known from long experience that noticeable amounts of anthocyanins still remain in jams or heated food products. Sample pretreatment and clean-up are of major importance to keep the anthocyanins free from degradation.

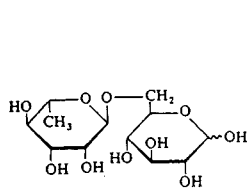
In this study, our interest was focused only on non-acetylated monomeric anthocyanins, which constitute the main part of the red pigments in most fruits (structures are shown in Fig. 1). From the literature, reversed-phase (RP) HPLC looks promising for the separation of the different anthocyanins. For this purpose, a  $C_{18}$



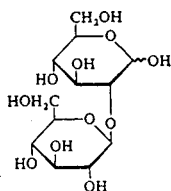
Aglycone moiety	R	R'	R''
Delphinidin	OH	OH	OH
Cyanidin	OH	OH	H
Petunidin	OH	OH	OCH <sub>3</sub>
Pelargonidin	H	OH	H
Peonidin	OCH <sub>3</sub>	OH	H
Malvidin	OCH <sub>3</sub>	OH	OCH <sub>3</sub>

Anthocyanin

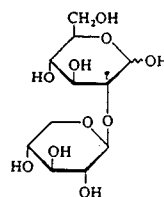
(The carbohydrate moiety S is linked to aglycone by its carbon n° 1)



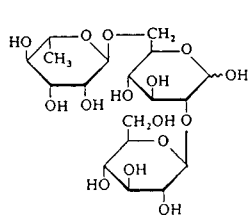
Rutinose  
( $\alpha$ -L-Rha (1 $\rightarrow$ 6) Glu)



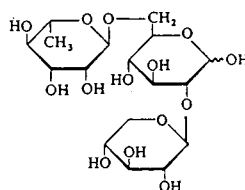
Sophorose  
( $\beta$ -D-Glu (1 $\rightarrow$ 2) Glu)



Sambubiose  
( $\beta$ -D-Xyl (1 $\rightarrow$ 2) Glu)



<sup>2</sup>G Glucosylrutinoside



<sup>2</sup>G Xylosylrutinoside

Fig. 1. Formulae of the anthocyanins and the di- and trisides present in anthocyanins.

column was selected. A large number of different mobile phases have been advocated and comparisons between published data are difficult. Some essential features are well established, as follows.

(i) As usual in RP-HPLC, the retention of the aglycone moiety is correlated with the hydrophobicity of the molecule and the observed elution order is delphinidin < cyanidin < petunidin < pelargonidin < peonidin < malvidin [11,15-17,19,20,22,26,29,31].

(ii) With an identical anthocyanin aglycone moiety, the order of elution is 3-galactoside < 3-glucoside < 3-rutinoside < 3-arabinoside [16,19,21,31]. However, Van de Castele *et al.* [15] pointed out that cyanidin 3-arabinoside is eluted between cyanidin 3-galactoside and cyanidin 3-glucoside.

(iii) Addition of a second carbohydrate moiety to a 3-glucoside anthocyanin increases its polarity, resulting in a decrease in retention. The presence of a methyl

group in the rhamnose molecule affects the chromatographic behaviour as cyanidin 3-rutinoside is eluted after cyanidin 3-glucoside [24,29].

The prediction of an absolute order of retention for all the anthocyanins is impossible as some polyglycosylated molecules elute among monoglycosylated compounds. For each of these two groups (mono- or polyglycosylated) the retention order is always the same, but the relative positions of these groups can change. For example, peak cross-over occurs between delphinidin 3-glycoside and peonidin 3,5-diglucoside [11,22,26]. Moreover, it is well known that the elution order may be dramatically affected by the origin of the alkyl-bonded phase or the treatment of silica prior to the alkyl-bonding reaction [32].

Peak identification is not a major problem when dealing with fruits containing monoglycosylated anthocyanins, such as bilberries or strawberries. Conversely, the situation is more difficult with redcurrants, raspberries or elderberries, which contain many polyglycosylated anthocyanins. Sometimes the recommended procedure is to perform hydrolysis and to analyse the fragments obtained.

The purpose of this work was to investigate the different parameters that affect retention in order to predict the elution order of a set of anthocyanins with no overlapping. This will facilitate unambiguous identification and permit the analysis time to be optimized.

## EXPERIMENTAL

### *Selection of chromatographic conditions*

We used a  $C_{18}$ -bonded silica stationary phase. Mobile phases advocated in the literature are usually water-methanol, water-acetonitrile or water-tetrahydrofuran mixtures together with formic, acetic acid or phosphoric acid to maintain acidity. Detection is usually carried out at 546 nm in the visible range and it is well established that the response factor is enhanced with an acidic mobile phase. Ribereau-Gayon [33] demonstrated that a change from pH 2.9 to 1 yields a sixfold increase in colour intensity. Unfortunately, pH 1 is not suitable with a  $C_{18}$ -bonded silica column and we selected pH 1.9, which corresponds to 10% formic acid in the mobile phase.

Owing to the wide polarity scale of anthocyanins, gradient elution has usually been performed in most studies. For the sake of unambiguous retention characteristics, the isocratic mode was selected. From the data, gradient elution was carried out to enhance the separation and to accelerate the elution of the strongly retained solutes.

### *Sample preparation*

Only fruit juices were considered. Prior to injection, centrifugation for 10 min at 3500 g and filtration through a 0.5- $\mu$ m filter were performed. The selected detection wavelength (546 nm) is specific to anthocyanins and no compounds from other fruits can interfere. Therefore, there is no need for further sample treatment.

### *Chromatography*

HPLC was performed on a Model SP 8000 instrument (Spectra-Physics, San Jose, CA, U.S.A.) equipped with a Valco (Houston, TX, U.S.A.) UHP valve with a 10- $\mu$ l sample loop for analytical injections and a 250- $\mu$ l loop for semi-preparative purposes. The analytical column was RP-18 LiChrospher (Merck, Darmstadt,

F.R.G.) (250 × 10 mm I.D.) packed with 7- $\mu$ m particles. A Model SP 8310 fixed-wavelength detector (546 nm) from Spectra-Physics was used.

The solvents were of HPLC grade, filtered through a 0.45- $\mu$ m filter and sparged with helium. In the analytical chromatography of anthocyanins two mobile phases were generally used: (a) water–acetonitrile–formic acid (84:6:10, v/v/v) (I) and (b) water–acetonitrile–formic acid (81:9:10, v/v/v) (II). Where specified, a less polar mobile phase (80:10:10, v/v/v) (III) or a more polar (3–6% acetonitrile gradient in 20 min) were used. Solvent I was used for preparative chromatography. In the chromatography of anthocyanidins water–acetonitrile–formic acid (75:15:10, v/v/v) was selected as the eluent.

The flow-rate was 1 ml/min in analytical chromatography and 6 ml/min in semi-preparative chromatography. Chromatography was performed at ambient temperature.

*Fragmentation by acid hydrolysis.* The anthocyanins isolated by semi-preparative chromatography were collected in distilling flasks and evaporated to dryness under low pressure. To prevent any degradation of the anthocyanins, the temperature must be kept below 30°C. Hydrolysis was performed either in a water-bath in test-tubes or in a drying oven directly on silica plates according to the method selected for the fractionation (HPLC or TLC).

In the water-bath hydrolysis, 1–2 ml of 2 M hydrochloric acid were added to the dry residue and heating at 100°C was performed for 45 min for complete hydrolysis or for 1, 2, 5, 10 or 20 min for partial hydrolysis. Products of the reaction were evaporated to dryness and the residue was dissolved in the minimum volume of slightly acidic water (0.1% hydrochloric acid) prior to injection.

Prior to TLC, hydrolysis was performed directly on the plate with subsequent fractionation according to the procedure of Andary *et al.* [34]. The dry residue of the collected anthocyanin was dissolved in methanol and spotted on the TLC plate under a cold air stream. A 2- $\mu$ l volume of 3 M hydrochloric acid was added to the spot, which was then covered with a glass plate. Heating at 100°C for 5–30 min was then performed.

*Thin-layer chromatography.* Precoated silica gel TLC plates (20 × 20 cm) (Merck) were used for the identification of the sugars of polyglycosylated anthocyanins following hydrolysis. The mobile phase was acetone–butanol–phosphate buffer [0.05 M Na<sub>2</sub>HPO<sub>4</sub>–0.05 M H<sub>3</sub>PO<sub>4</sub> (pH 5)] (50:40:10 v/v/v).

Detection was performed by staining with 2,3,5-triphenyltetrazolium chloride [a 4% solution in methanol–1 M sodium hydroxide solution (50:50, v/v)].

*Standards.* Glucose, galactose, arabinose, xylose and L-rhamnose were purchased from Merck. Cyanidin 3-glucoside, cyanidin 3-rhamnoside, cyanidin 3-rutinoside, cyanidin 3,5-diglucoside, pelargonidin 3,5-diglucoside, paeonidin 3,5-diglucoside, cyanidin, pelargonidin, paeonidin, petunidin, malvidin were purchased from Extra-synthèse (Gemay, France).

## RESULTS AND DISCUSSION

*Identification of anthocyanins**Bilberry, blackcurrant, strawberry, blackberry, black cherry and morello cherry*

These red fruits mainly contain monoglycosylated anthocyanins, with the exception of delphinidin and cyanidin 3-rutinoside. These anthocyanins are more retained than those which are polyglycosylated and they can be rapidly separated with water–acetonitrile–formic acid (81:9:10) as the mobile phase. Fig. 2 shows the chromatograms obtained. Identification of the separated solutes was carried out by comparison with the retention of standard solutes; the observed elution order is consistent with the hydrophobicity order as described in previously published separations [11,16,17,19–22,26,29,31]. Table I lists the identified anthocyanins together with the selectivity  $\alpha$  towards cyanidin 3-glucoside, which was selected as a reference solute, and  $\log \alpha$ .

It must be pointed out that replacement of one sugar by another results in the same variation of  $\log \alpha$  value, whatever anthocyanin is considered. For example, a change from galactose to glucose yields the same shift in  $\log \alpha$  whatever Pg, Cy or Pt are considered. In Fig. 3  $\log \alpha$  values for anthocyanins are plotted against the anthocyanidins arranged in order of increasing hydrophobicity. With this representation, the galactosides line is parallel to the glucosides line, shifted by  $\Delta \log \alpha = 0.11$ . This behaviour is valid for the four lines drawn and provides a valuable means of accurately predicting an individual anthocyanin retention time. Moreover, retention times of all the anthocyanins having the same glycoside can be found from the retention of one of them and from a known plot corresponding to another glycoside group. This mode of identification may only be approximate but it provides useful guidelines for further studies. Use of a gradient precludes advantage being taken of this phenomenon.

*Redcurrant, raspberry and elderberry*

The acetonitrile content of the above-mentioned mobile phase is too high to permit the resolution of the anthocyanins from these fruits. A mixture of lower elution strength [water–acetonitrile–formic acid (84:6:10, v/v/v)] is convenient, as shown in Fig. 4. Peak identification is more difficult as the glycoside part of the anthocyanins from these fruits is constituted by diholosides or triholosides.

Reports on HPLC separations in this area are scarce, with the exception of the work of Bronnum-Hansen and Hansen [18] on elderberries and Spanos and Wrolstad [29] on raspberries. Cyanidin 3-rutinoside is the only standard solute commercially available and we had to perform semi-preparative chromatography with subsequent acid hydrolysis of the isolated fractions. Partial hydrolysis first cleaves the carbohydrate–carbohydrate bond and then the aglycone–carbohydrate bond, while complete hydrolysis yields the aglycone moiety together with the different carbohydrates that constitute the anthocyanins.

Table II lists the fragments obtained by partial hydrolysis of the different heterosides. The number of identified fragments and the hydrolysis kinetics yield information for the further identification of the anthocyanin of interest.

*Redcurrant anthocyanins.* Eleven peaks are present in the chromatogram of the

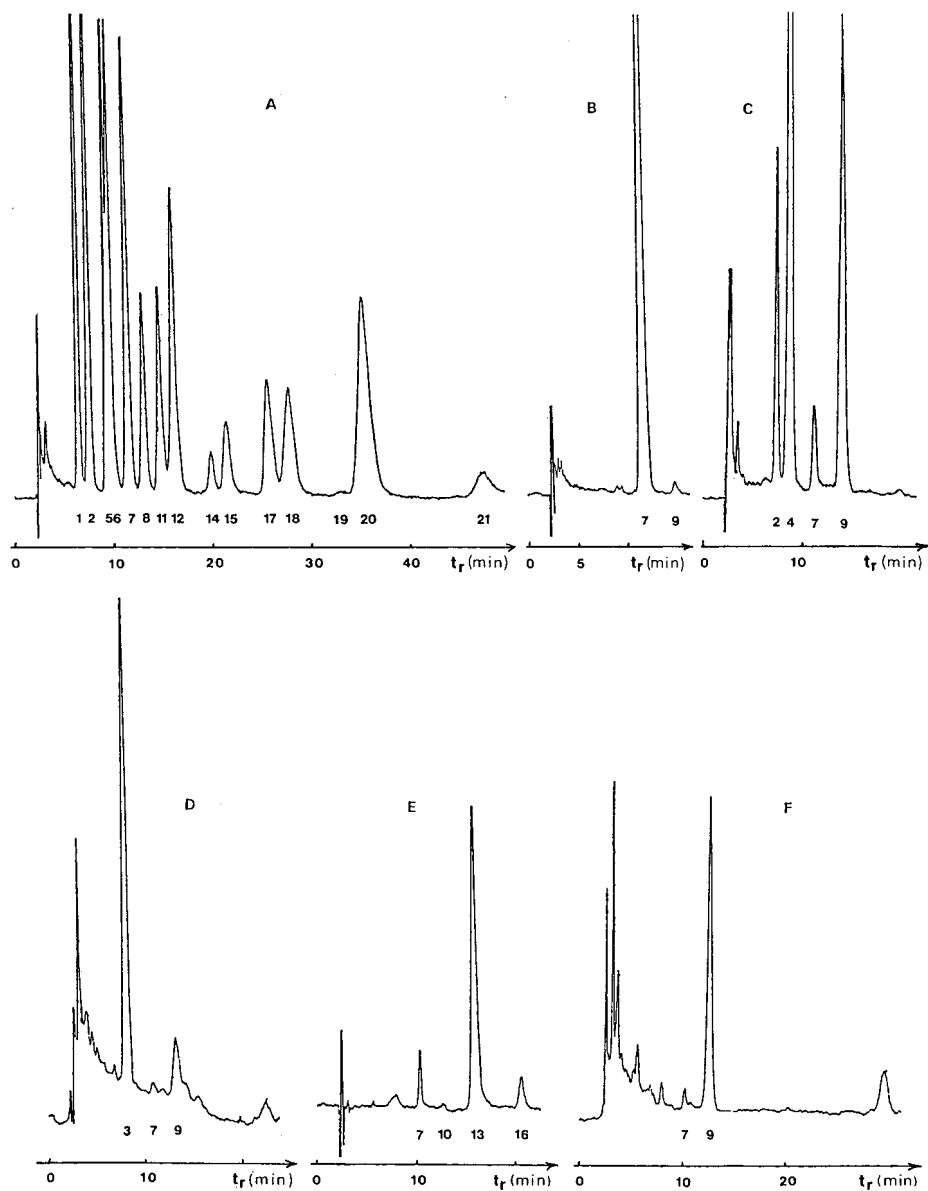


Fig. 2. Chromatograms of fruit juices. (A) Bilberry; (B) blackberries; (C) blackcurrant; (D) morello cherry; (E) strawberry; (F) cherries. Mobile phase: water-acetonitrile-formic acid (81:9:10, v/v/v). See Table I for peak identification.

anthocyanins from this fruit, but we are only interested in the five major peaks 6, 8, 9, 10 and 11. Peaks 9 and 11 were identified as cyanidin 3-glucoside and cyanidin 3-rutinoside, respectively, by comparison with authentic samples. The three others were submitted to preparative chromatography and hydrolysis. Chromatograms

TABLE I  
 ANTHOCYANINS IDENTIFIED IN FIGS. 2 AND 3

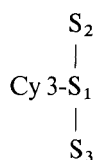
$\alpha = \frac{t'_r}{t'_{r(\text{Cy 3-glu})}}$  with  $t'_r = (t_r - t_0)$ , where  $t_r$  = retention time of a solute and  $t_0$  = retention time of an unretained compound.

Peak No.	Abbreviation <sup>a</sup>	$\alpha$	Log $\alpha$
1	Dp 3-gala	0.456	-0.341
2	Dp 3-glu	0.578	-0.238
3	Cy 3-glu-ruti	0.676	-0.170
4	Dp 3-ruti	0.706	-0.151
5	Cy 3-gala	0.772	-0.112
6	Dp 3-ara	0.814	-0.089
7	Cy 3-glu	1	0
8	Pt 3-gala	1.17	0.070
9	Cy 3-ruti	1.29	0.110
10	Pg 3-gala	1.29	0.110
11	Cy 3-ara	1.35	0.130
12	Pt 3-glu	1.51	0.179
13	Pg 3-glu	1.66	0.219
14	Pn 3-gala	1.92	0.283
15	Pt 3-ara	2.09	0.320
16	Pg 3-ara	2.27	0.355
17	Pn 3-glu	2.56	0.408
18	Mv 3-gala	2.79	0.445
19	Pn 3-ara	3.36	0.527
20	Mv 3-glu	3.61	0.557
21	Mv 3-ara	4.93	0.693

<sup>a</sup> Dp = Delphinidin, Cy = cyanidin, Pt = petunidin, Pg = pelargonidin, Pn = peonidin, Mv = malvidin, glu = glucose, gala = galactose, ara = arabinose, ruti = rutinose.

obtained with the anthocyanin corresponding to peak 8 are displayed in Fig. 5. To shorten the chromatographic run time, gradient elution was performed from the 25th to the 33rd minute, the acetonitrile content being increased from 9% to 25%. The anthocyanin retention times are unchanged as they are eluted before the gradient delay time.

At the very beginning of the hydrolysis, cyanidin and three intermediate anthocyanins are formed, which could be easily identified as (in order of elution) cyanidin 3-sophoroside, cyanidin 3-glucoside and cyanidin 3-rutinoside. According to Table II, the structure of the anthocyanin which yields three intermediates by hydrolysis and the aglycone moiety of which is cyanidin, corresponds to



Therefore the fragment Cy 3-S<sub>1</sub> is obviously cyanidin 3-glucoside, Cy 3-S<sub>1</sub>-S<sub>2</sub> is

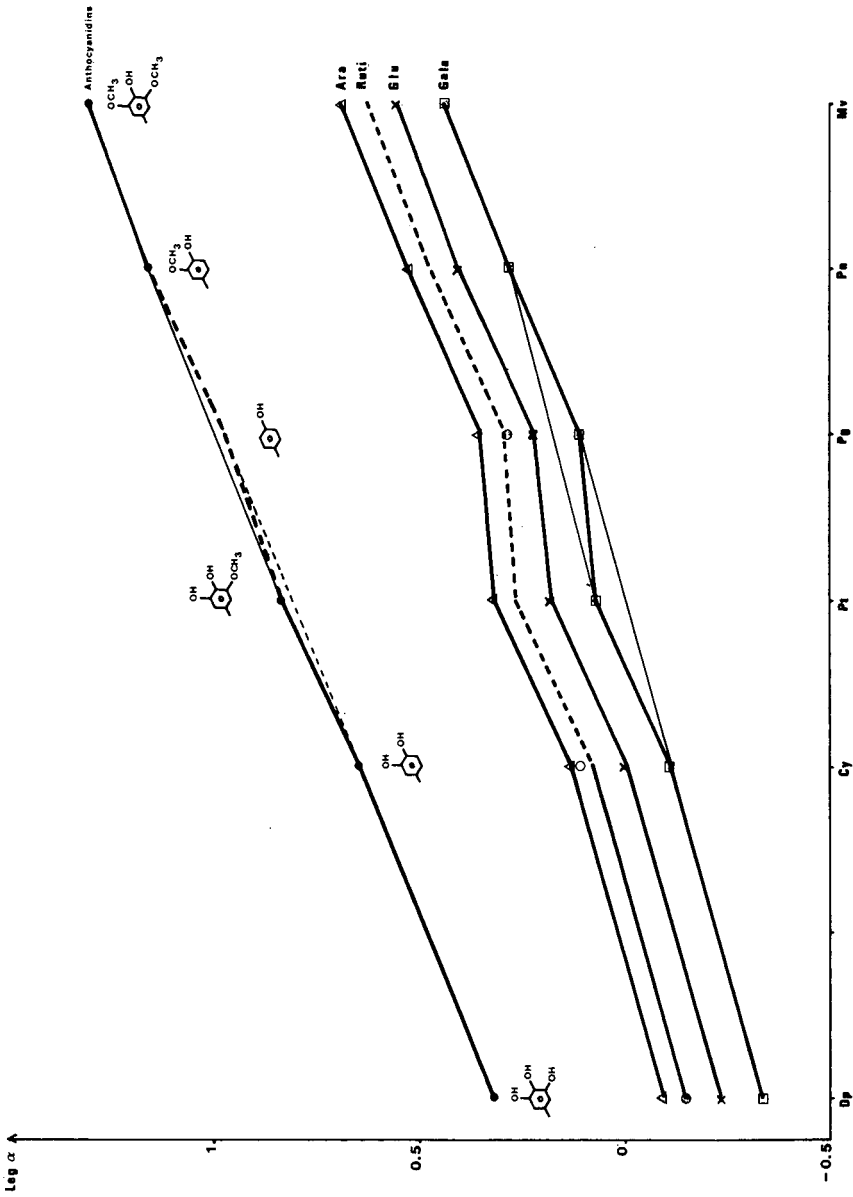


Fig. 3. Log  $\alpha$  of anthocyanins obtained by associating each glycoside with each anthocyanidin encountered. Abscissa: 2 units correspond to an OH loss and 1 unit to an OCH<sub>3</sub> gain. Mobile phase: water-acetonitrile-formic acid (81:9:10, v/v/v). Dp = delphinidin (R = R' = OH); Cy = cyanidin (R = R' = OH, R'' = H); Pt = petunidin (R = R' = OH, R'' = OCH<sub>3</sub>); Pg = pelargonidin (R = R' = H, R'' = OH); Pn = peonidin (R = OCH<sub>3</sub>, R' = OH, R'' = H); Mv = malvidin (R = R'' = OCH<sub>3</sub>, R' = OH).



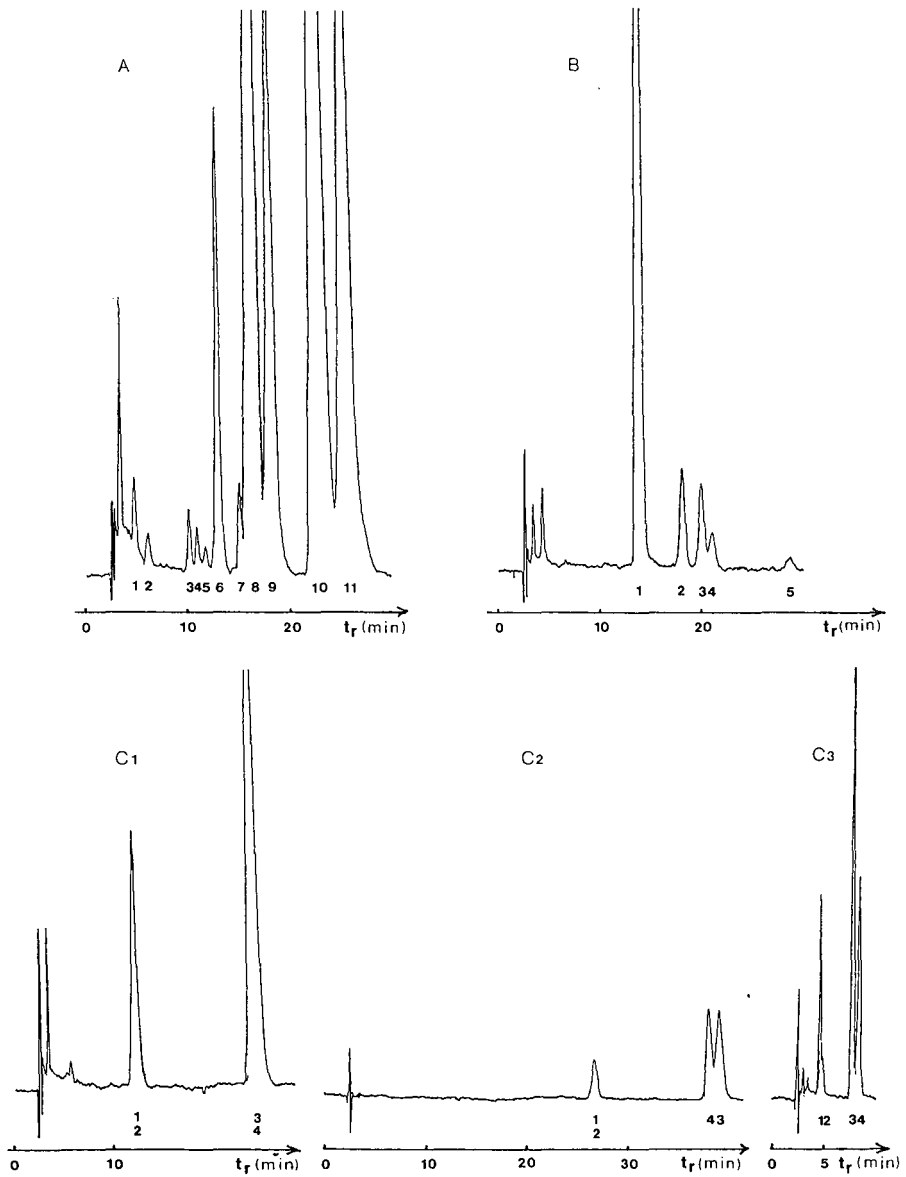


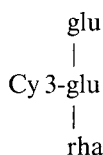
Fig. 4. Chromatograms of fruit juices. (A) Redcurrant; (B) raspberry. Mobile phase: water-acetonitrile-formic acid (84:6:10, v/v/v). (C) Elderberry: (C<sub>1</sub>) elution with the mobile phase used for A and B; (C<sub>2</sub>) elution with a linear gradient from 3 to 6% acetonitrile in acidic medium (10% formic acid) in 20 min and 10 min isocratic with 6% acetonitrile; (C<sub>3</sub>) isocratic elution with 10% acetonitrile in acidic medium (10% formic acid). See Table III for peak identification.

TABLE II  
FRAGMENTS OBTAINED BY PARTIAL ACID HYDROLYSES OF THE DIFFERENT HETERO-SIDES

Heteroside	Anthocyanidic fragments obtained	No. of intermediates	
3-Monoside Ag 3-S <sup>a</sup>	Ag	0	
3-Bioside Ag 3-S <sub>1</sub> S <sub>2</sub>	Ag 3-S <sub>1</sub> + Ag	1	
3,5-Bioside Ag 3-S <sub>1</sub> , 5-S <sub>2</sub>	Ag 3-S <sub>1</sub> + Ag 5-S <sub>2</sub> + Ag	2	
3-Trioside	Ag 3-S <sub>1</sub> S <sub>2</sub> S <sub>3</sub>	Ag 3-S <sub>1</sub> S <sub>2</sub> + Ag 3-S <sub>1</sub> + Ag	2
	$\begin{array}{c} S_2 \\   \\ Ag\ 3-S_1 \\   \\ S_3 \end{array}$	Ag 3-S <sub>1</sub> S <sub>2</sub> + Ag 3-S <sub>1</sub> S <sub>3</sub> + Ag 3-S <sub>1</sub> + Ag	3
3-Bioside, 5-monoside: Ag 3-S <sub>1</sub> S <sub>2</sub> , 5-S <sub>3</sub>	Ag 3-S <sub>1</sub> , 5-S <sub>3</sub> + Ag 3-S <sub>1</sub> S <sub>2</sub> + Ag 5-S <sub>3</sub> + Ag 3-S <sub>1</sub> + Ag	4	

<sup>a</sup> Ag = aglycone; S = sugar.

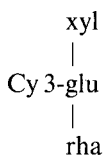
cyanidin 3-sophoroside and Cy 3-S<sub>1</sub>-S<sub>3</sub> is cyanidin 3-rutinoside. Peak 8 in the redcurrant chromatogram is



The amount of Cy 3-sophoroside produced is higher than that of Cy 3-rutinoside, which indicates that the 1-6 glu-rha bond is easier to cleave than the 1-2 glu-glu bond.

Further, the small amount of Cy 3-rutinoside produced decreases much faster than the amount of sophoroside and the corresponding peaks on the chromatograms remain small. TLC of the hydrolysis products reveals the presence of glucose and rhamnose and makes the identification complete.

TLC was utilized for the identification of redcurrant peak 10 and elderberry peak 1. Redcurrant peak 10 yields two intermediates, cyanidin 3-glucoside and cyanidin 3-rutinoside. Conversely, from TLC data three carbohydrates were identified: glucose, xylose and rhamnose. These results come from the fact that cyanidin 3-glucoside and cyanidin 3-sambubioside are eluted simultaneously. With a mobile phase of lower elution strength (3-6% acetonitrile gradient within 20 min) these two solutes were separated and the peak 10 was identified as:



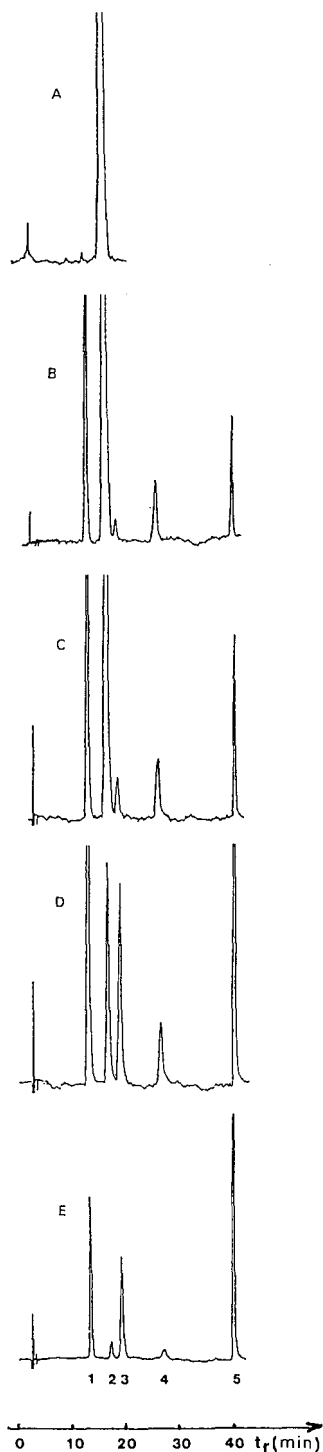


Fig. 5. Results of partial hydrolysis of anthocyanin corresponding to peak 8 of redcurrant. (A) Initial product; (B) hydrolysis time 1 min; (C) 2 min; (D) 5 min; (E) 10 min. Mobile phase: formic acid content constant (10%); from 0 to 25 min, water–acetonitrile–formic acid (84:6:10); from 25 to 35 min, linear gradient from 6 to 25% acetonitrile; from 35 to 45 min, water–acetonitrile–formic acid (65:25:10). Peak identification: (2) Cy 3-glu(glu)(rha) → (1) Cy 3-glu–glu + (4) Cy 3-glu–rha → (3) Cy 3-glu → (5) cyanidine.

The above mobile phase was used when xylose was evidenced by TLC.

All anthocyanins identified from redcurrant, raspberry and elderberry are listed in Table III.

*Raspberry and elderberry anthocyanins.* The same approach as above allowed the identification of cyanidin 3-sophoroside from raspberry. This result is consistent with the report of Spanos and Wrolstad [29]. Peak 4 could not be separated in a sufficient amount by preparative chromatography to allow its identification. Nevertheless, considering Spanos and Wrolstad's studies, it was assumed to be pelargonidin 3-sophoroside. This assumption agrees with retention diagrams, which are discussed below.

TABLE III

ANTHOCYANINS OF REDCURRANT, RASPBERRY AND ELDERBERRY (*cf.*, FIG. 4) WITH IDENTIFICATION OF THE FRAGMENTS OBTAINED BY ACID HYDROLYSIS WHEN NECESSARY

Fruit	Peak No.	Complete hydrolysis		Partial hydrolysis, intermediate anthocyanins <sup>a</sup>	Anthocyanin <sup>a</sup>
		Sugar (TLC)	Anthocyanidin (HPLC)		
Redcurrant	6	Glu + trace of rha	Cy	Cy 3-glu + unidentified intermediate anthocyanin	Cy 3-glu-glu (Cy 3-sopho) + unidentified minor anthocyanin
	8	Glu + rha	Cy	Cy 3-glu-glu Cy 3-ruti Cy 3-glu	glu   Cy 3-glu   rha (Cy 3-2 <sup>G</sup> glu-ruti)
	9	—	—	—	Cy 3-glu xyl
	10	Glu + rha + xyl	Cy	Cy 3-ruti Cy 3-sam Cy 3-glu	Cy 3-glu   rha (Cy 3-2 <sup>G</sup> xyl-ruti)
	11	—	—	—	Cy 3-ruti
	Raspberry	1	Glu	Cy	Cy 3-glu
2		—	—	—	Cy 3-2 <sup>G</sup> glu-ruti
3		—	—	—	Cy 3-glu
4		—	—	—	Pg 3-sopho
5		—	—	—	Cy 3-ruti
Elderberry	1	Glu + xyl	Cy	Cy 3,5-diglu Cy 3-glu Cy 3-sam	Cy 3-sam, 5-glu
	2	—	—	—	Cy 3,5-diglu
	3	Glu + xyl	Cy	Cy 3-glu	Cy 3-sam
	4	—	—	—	Cy 3-glu

<sup>a</sup> Rha = rhamnose, xyl = xylose, sopho = sophorose, sam = sambubiose.

In contrast to Spanos and Wrolstad, we could not detect any pelargonidin 3-glucoside rutinoside and pelargonidin 3-glucoside. This may be due to the raspberry variety.

Hydrolysis and subsequent TLC of elderberry anthocyanins indicated the presence of xylose. In spite of the use of an acetonitrile gradient (3–6% acetonitrile within 20 min), we could not separate Cy 3-sam 5-glu from Cy 3,5-diglu. This separation was performed by Bronnum-Hansen and Hansen [18] with a tetrahydrofuran (THF) gradient in 0.05 M phosphoric acid (pH 1.8) from 1 to 40% THF within 15 min. From the solubility parameter difference between THF and acetonitrile, it seems difficult to achieve such a good separation with acetonitrile.

### *Retention behaviour*

Table IV gives the observed retentions of the identified anthocyanins and anthocyanidins as the selectivity  $\alpha$  towards Cy 3-glu, which was selected as a reference compound. Many solutes coelute and water–acetonitrile–formic acid (84:6:10) does not permit complete resolution.

### *Contribution of glycosides to anthocyanin retention*

A graph similar to that in Fig. 3 was constructed from the results obtained with mobile phase I (6% acetonitrile). The lines connecting the different aglycones and those connecting the anthocyanins exhibiting the same glucoside moiety are parallel (*cf.*, Fig. 6). The slopes of the anthocyanidins lines are slightly steeper than those corresponding to the anthocyanins.

The observed data can be interpreted with the aid of the general treatment of fragmental constants derived by Rekker and Kort [35]. Retention characteristics in RP-HPLC depend on the hydrophobicity and can be determined by considering each part of the molecule of a given solute and taking in account its hydrophobic properties,  $f_i$ . The hydrophobicity of a molecule is the sum of the different hydrophobic fragment constants and the intramolecular effects  $f_j$ . Following Rekker and Kort's theory, there should be a linear relationship between  $\log \alpha$  and the hydrophobicity of the solute.

Let  $P$  be the partition coefficient of a solute between organic and aqueous phases and  $k'$  the capacity factor:

$$\log P = \sum_i f_i + \sum_j f_j \quad (1)$$

$$\log k' = A \log P + B \quad (2)$$

where  $A$  and  $B$  are constants for a given chromatographic system.

$$\alpha = \frac{k'}{k'_{\text{ref}}}$$

where  $k'_{\text{ref}}$  is the capacity factor of the reference solute (cyanidin 3-glucoside).

$$\log \alpha = \log k' - \log k'_{\text{ref}} \quad (3)$$

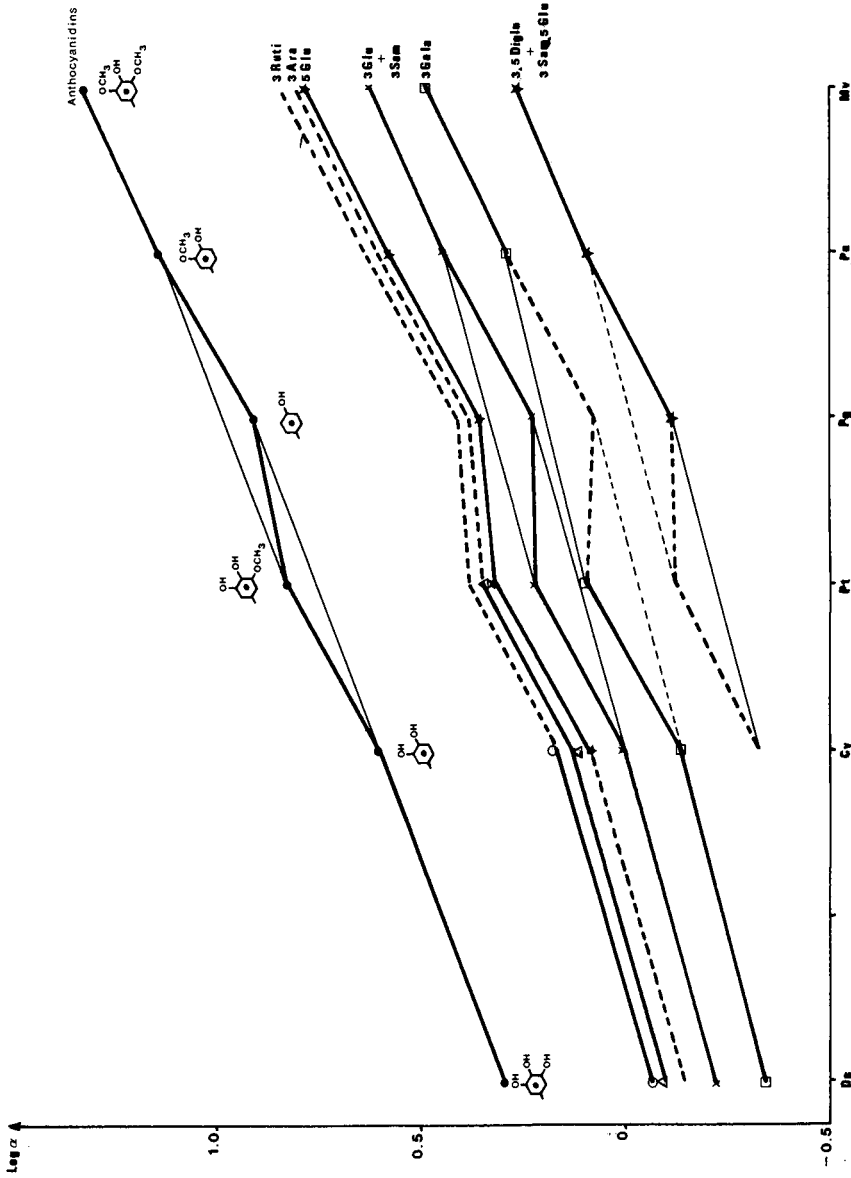


Fig. 6.  $\text{Log } \alpha$  of anthocyanins obtained by associating each glycoside with each anthocyanidin encountered. Abscissa, 2 units corresponds to an OH loss and 1 unit to an  $\text{OCH}_3$  gain. Mobile phase: water-acetonitrile-formic acid (84:6:10).

TABLE IV  
RETENTION BEHAVIOUR OF THE IDENTIFIED ANTHOCYANINS

Mobile phase: water-acetonitrile-formic acid (84:6:10).

Anthocyanin	a <sup>a</sup>	b <sup>b</sup>	c <sup>c</sup>	$\alpha = \frac{t'_r}{t'_{r(\text{Cy 3-glu})}}$	Log $\alpha$
Dp 3-gala		×		0.45	-0.35
Cy 3,5-diglu	×			0.47	-0.33
Cy 3-sam, 5-glu			×	0.47	-0.33
Dp 3-glu		×		0.59	-0.23
Cy 3-sopho			×	0.66	-0.18
Cy 3-gala	×			0.73	-0.14
Pg 3,5-diglu		×		0.75	-0.12
Dp 3-ara		×		0.80	-0.10
Dp 3-ruti		×		0.84	-0.07
Cy 3-(2 <sup>G</sup> glu-ruti)			×	0.91	-0.04
Cy 3-glu	×			1	0
Cy 3-sam			×	1.00	0.00
Pg 3-sopho		×		1.05	0.02
Cy 5-glu	×			1.21	0.08
Pn 3,5-diglu	×			1.22	0.09
Pt 3-gala		×		1.22	0.09
Cy 3-ara			×	1.30	0.11
Cy 3-(2 <sup>G</sup> xyl-ruti)		×		1.35	0.13
Cy 3-ruti	×			1.52	0.18
Pt 3-glu		×		1.67	0.22
Pg 3-glu	×			1.66	0.22
Mv 3,5-diglu	×			1.80	0.26
Delphinidine			×	1.95	0.29
Pn 3-gala		×		1.96	0.29
Pt 3-ara		×		2.17	0.34
Pg 5-glu	×			2.30	0.36
Pn 3-glu	×			2.67	0.43
Cy 3-L-rha	×			2.68	0.43
Mv 3-gala		×		3.06	0.49
Pn 5-glu	×			3.80	0.58
Cyanidine	×			3.98	0.60
Mv 3-glu	×			4.17	0.62
Mv 5-glu	×			6.00	0.78
Petunidine	×			6.6	0.82
Pelargonidine	×			8.0	0.90
Paeonidine	×			13.4	1.13
Malvidine	×			20.4	1.31

<sup>a</sup> Standards and their products from partial hydrolysis.

<sup>b</sup> Identified through a comparison with literature.

<sup>c</sup> Isolated through semi-preparative HPLC and identified through a thermal fragmentation followed by analytical chromatography of the products obtained.

From eqns. 1-3, we can write

$$\log \alpha = A \left( \sum_i f_i + \sum_j f'_j \right) - A \log P_{ref} \quad (4)$$

where  $A \log P_{\text{ref}}$  is constant under fixed analysis conditions.

To evaluate the hydrophobicity of a single anthocyanin, we can consider the two fragments: aglycone (Ag) and glycoside (S):

$$\log \alpha = A(f_{\text{Ag}} + f_{\text{S}} + f'_{\text{Ag-S}}) - A \log P_{\text{ref}} \quad (5)$$

With the aglycone,

$$\log \alpha_{\text{Ag}} = A(f_{\text{Ag}} - \log P_{\text{ref}}) \quad (6)$$

and we can write

$$\log \alpha - \log \alpha_{\text{Ag}} = A(f_{\text{S}} + f'_{\text{Ag-S}}) \quad (7)$$

This difference is represented in Fig. 6 by the distance between the Ag-S anthocyanin and the related aglycone Ag. It has been observed experimentally that it is constant for all the aglycones, as evidenced by the constant shift between the lines. From eqn. 7 it is obvious that the intramolecular effect  $f'_{\text{Ag-S}}$  is not related to the aglycone species. This can be explained as follows: the different anthocyanidins exhibit distinctive substituents (H, OH, OCH<sub>3</sub>) which are far from the Ag-S bond and as a consequence it may be guessed that the aglycone-sugar interaction is not influenced by these groups. In this mode the effect is identical whatever the aglycone considered. In consequence,  $f_{\text{S}} + f'_{\text{Ag-S}}$  is characteristic of the sugar.

We can write

$$\Delta S = A(f_{\text{S}} + f'_{\text{Ag-S}}) \quad (8)$$

and we can consider it as the sugar contribution to the anthocyanin retention:

$$\log \alpha = \log \alpha_{\text{Ag}} + \Delta S \quad (9)$$

The determination of  $\Delta S$  from available anthocyanins allows the prediction of the retention characteristics of unknown or unavailable anthocyanins.

When many sugars  $S_1, S_2, S_3$ , etc., are involved in the glucoside structure, then  $\Delta S = \Delta S_1 + \Delta S_2 + \Delta S_3 \dots$ , where  $\Delta S_1$  is the contribution of the first sugar bonded to an anthocyanidin (it is a glucose molecule in every case),  $\Delta S_2$  that of the second sugar fixed either on  $S_1$  or in the 5-position on the anthocyanidin and  $\Delta S_3$  that of the third sugar also bonded to  $S_1$  or in the 5-position, etc.

In Fig. 6,  $\Delta S_1$  is represented by the distance between the points corresponding to the aglycone Ag and to the anthocyanin Ag  $S_1$ ,  $\Delta S_2$  by the distance between Ag glu and Ag glu  $S_2$  and  $\Delta S_3$  by the distance between Ag glu  $S_2$  and Ag glu  $S_2 S_3$ . As already mentioned, the aglycone line has a slightly steeper slope than the anthocyanin line and  $\Delta S_1$  is different from delphinidin to malvidin.

Table V gives the values of  $\Delta S_1, \Delta S_2$  and  $\Delta S_3$  obtained from the chromatographic behaviour of cyanidin. Fig. 7 displays the  $\Delta S$  values of all the glycosides encountered. Parallelism of the segments corresponding to the bonding of a third identical sugar on different anthocyanins (*e.g.*, the segments sam-xyl ruti and



TABLE V  
CONTRIBUTION OF SUGARS TO ANTHOCYANIN RETENTION

Sugar	$\Delta S_1$	$\Delta S_2$	$\Delta S_3$
3-Glucose	-0.60	-0.18	-0.23
3-Xylose	0	0	-0.05
3-L-Rhamnose	-0.17	0.18	0.12
5-Glucose	-0.52	-0.34	-0.34
3-Galactose	-0.74		
3-Arabinose	-0.49		

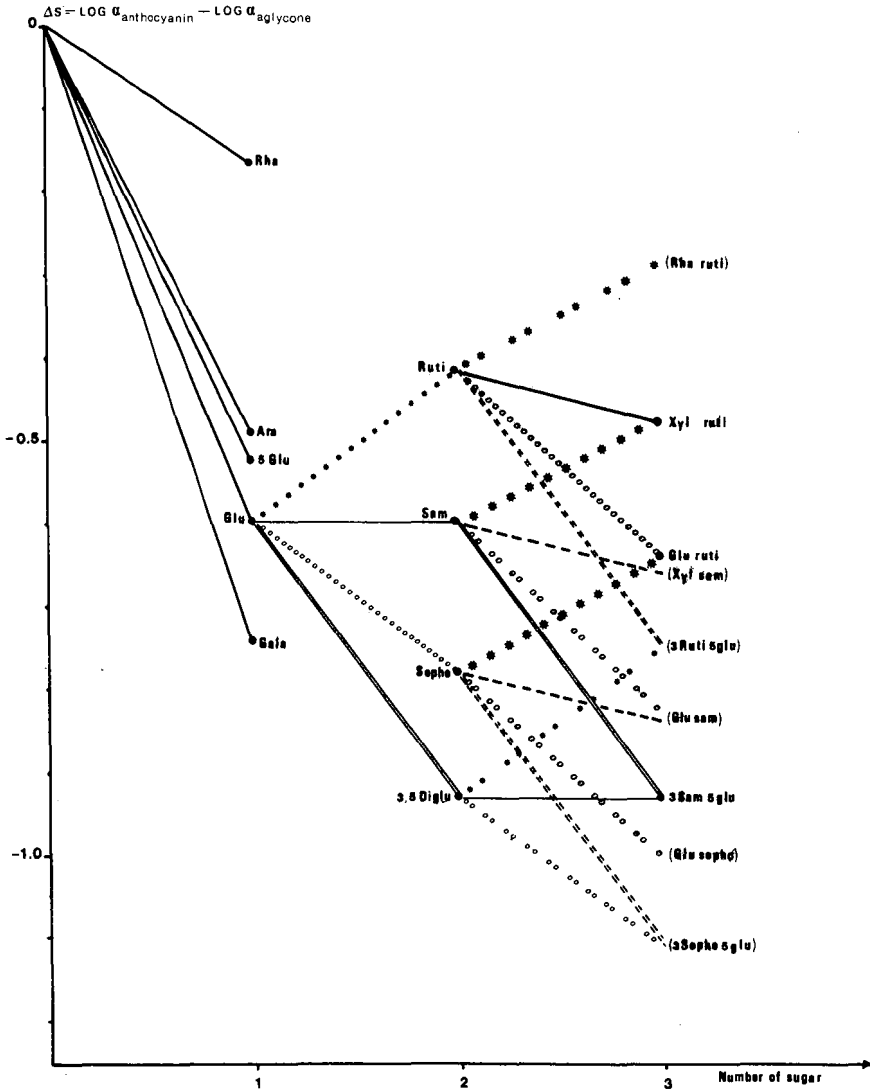


Fig. 7. Sugar contribution to the anthocyanin retention. Mobile phase: water-acetonitrile-formic acid (84:6:10). The glycosides in parentheses do not correspond to experimental points but were deduced from the other points by the dotted segments.

sopho–glu ruti). From the plots, the prediction of the retention characteristics of other triholosides not previously encountered in the experiments (glu–sopho, glu–sam, 3–ruti–5–glu, etc.) is straightforward.

From Table V and Fig. 7, the following comments can be made:

(a) With every sugar  $\Delta S_1$  is always smaller than  $\Delta S_2$ , and the addition of a sugar to a monoglycosylated anthocyanin has much less effect on retention than adding a sugar to an aglycone. For rhamnose the effect is even the reverse. This phenomenon can easily be explained (see eqn. 8):

$$\Delta S_1 = A(f_{S_1} + f'_{Ag-S_1})$$

The presence of the glucoside  $S_1$  decreases the hydrophobicity of the  $Ag-S_1$  molecule (negative value of  $f_S$ ) with the consequence of a decrease in retention. On the other hand, hydrophobicity is increased by the interactions between polar groups (positive value of  $f'_{Ag-S}$ ) that increase retention and act in the reverse direction to the glucoside moiety. However,  $|f_{S_1}| > |f'_{Ag-S_1}|$  and  $\Delta S_1$  is always negative (decrease in retention).

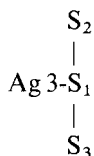
For the same sugar added to the first one:

$$\Delta S_2 = A(f_{S_2} + f'_{AgS_1-S_2}) \quad (f_{S_1} = f_{S_2})$$

The interaction  $AgS_1-S_2$  is logically stronger than the  $Ag-S_1$  interaction,  $f'_{AgS_1-S_2} > f'_{Ag-S_1}$  and the effect of  $S_2$  on retention is less important than that of  $S_1$ .

With rhamnose,  $|f'_{Agglu-rha}| > |f_{rha}|$  and the  $\Delta S_2$  value is positive, *i.e.*, rutinoides are eluted after glucosides.

(b) On the other hand, the third sugar molecule  $S_3$  has a slightly greater effect than the second sugar  $S_2$  in the case of the ramified structure:



Interactions between two sugars look stronger in a diglycoside than in a triglycoside molecule.

(c) The addition of a glucose in the 5-position to an aglycone leads to a decrease in  $\log \alpha$  that is greater than that given by the same addition to anthocyanin glycosylated in the 3-position (compare the values in the fourth line in Table V). Therefore, an interaction would exist between a sugar in the 3-position and glucose in the 5-position.

(d) A modification of the mobile phase such as an increase in the acetonitrile content leads to a decrease in  $\Delta S$  that is greater for diosides and triosides than for monosides (*cf.*, Figs. 7 and 8) and the elution order is changed: with 9% acetonitrile, rutinoides are eluted after arabinosides whereas with 6% acetonitrile they are eluted first.

The results are in agreement with Bittour's work [36] on the coefficient  $a$  in the relationship  $\log k' = a\varphi^n + b$ , where  $\varphi$  represents the volume percentage of water in

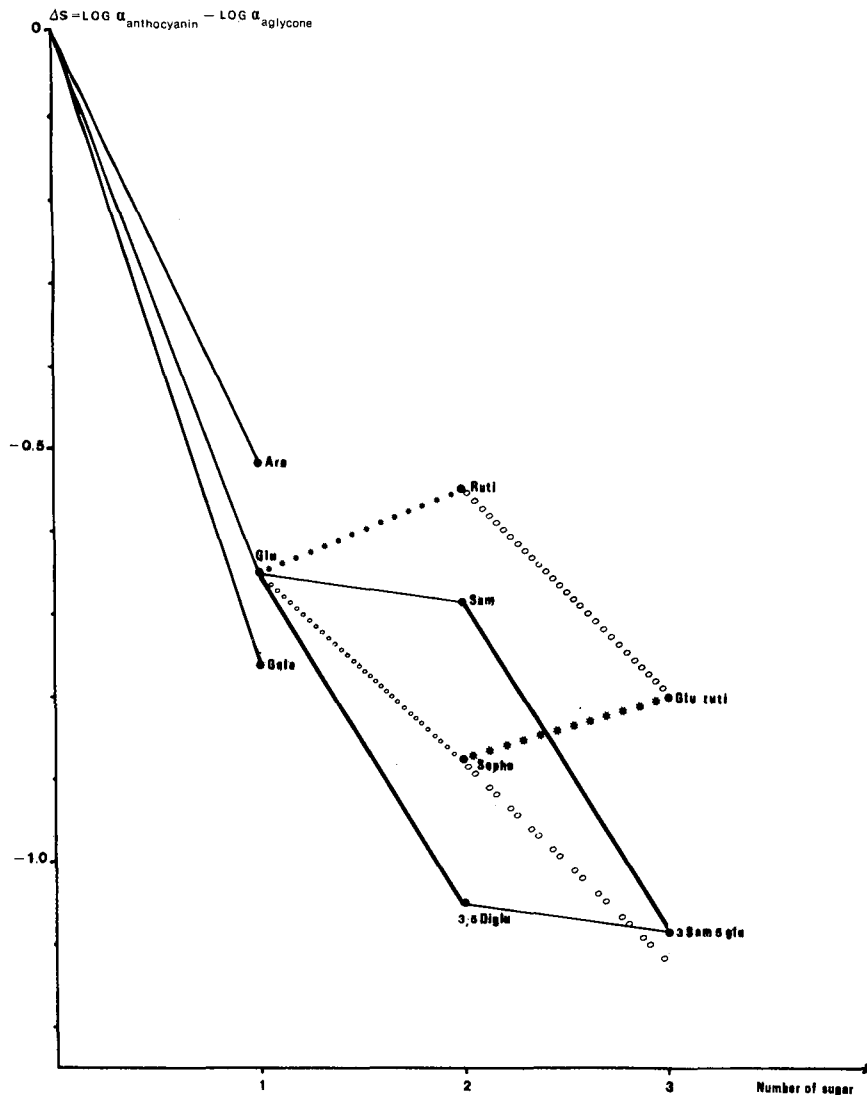


Fig. 8. Sugar contribution to anthocyanin retention. Mobile phase: water-acetonitrile-formic acid (81:9:10).

the mobile phase. She reported a linear variation of  $a$  with the molar volume of solutes. In other words the retention variations due to an increase in the acetonitrile content are higher for large than for small molecules. This allowed us to separate cyanidin 3-glucoside from cyanidin 3-sambubioside by using different acetonitrile contents. When the acetonitrile content is less than 6%, elution is very slow, and we used a slow gradient from 3 to 6% in 20 min, the 6% content then being maintained until the elution was completed. In this instance cyanidin 3-glucoside appears before cyanidin 3-sambubioside (*cf.*, Fig. 4C<sub>2</sub>). Experiments with an acetonitrile content higher than

6% were also performed and good results were obtained with 10% acetonitrile. The elution order is then reversed when compared with the previous results (*cf.*, Fig. 4C<sub>3</sub>).

#### *Contribution of aglycone moiety to anthocyanin retention*

In eqn. 9 this contribution is denoted as  $\log \alpha_{AB}$ , and the experimental values are given in Table 4. The plot in Fig. 6 shows that the addition of a hydroxyl group to pelargonidin, cyanidin or peonidin leads to the same variation,  $\Delta(\text{OH})$ , of  $\log \alpha$ . The corresponding segments are colinear or parallel. The same effect occurs with addition of a methoxy group to cyanidin or pelargonidin [ $\Delta(\text{OCH}_3)$  variation of  $\log \alpha$ ]. However, this does not account well for such an addition to peonidin.

This is also valid for the lines corresponding to anthocyanins and is of obvious practical interest. The possibilities of deducing the retention values of one anthocyanin from another are thus increased. With 3-glucosides, the values obtained are  $\Delta(\text{OH}) = -0.23$  and  $\Delta(\text{OCH}_3) = 0.22$ .

With the same anthocyanins which were chromatographed with the 9% acetonitrile mobile phase (see Fig. 3), the  $\Delta(\text{OH})$  value is nearly the same ( $-0.24$ ) whereas  $\Delta(\text{OCH}_3)$  is slightly lower (0.18). This result is in agreement with Bitteur's data: an increasing acetonitrile concentration has more effect upon the largest mole which contains  $\text{OCH}_3$  and then  $\Delta(\text{OCH}_3)$  is lowered. As OH is small, this behaviour is not shown by  $\Delta(\text{OH})$ .

#### CONCLUSION

From this study a better understanding of the retention of anthocyanins has been obtained. The experimental results explained by Rekker's theory established that the retention of these compounds is due to two independent factors, one specific to the anthocyanidine and the other to the sugar. These two factors were studied and rules governing the chromatography of anthocyanins have been established and it is now possible to predict the retention of any compound in this family, either graphically or by calculation.

Now, with the identification of the peaks in the redcurrant chromatogram, the anthocyanidine profiles of most common red fruits are known and HPLC analysis is therefore a suitable method for determining which red fruit has been used in the preparation of a particular food product.

#### REFERENCES

- 1 T. Swain, in T. A. Geissman (Editor), *The Chemistry of Flavonoid Compounds*, Pergamon Press, New York, 1962, p. 513.
- 2 J. B. Harborne and E. Hall, *Phytochemistry*, 3 (1964) 453.
- 3 J. B. Harborne, *Comparative Biochemistry of the Flavonoids*, Academic Press, London, New York, 1967, p. 1.
- 4 J. van Buren, in A. C. Hulme (Editor), *The Biochemistry of Fruits and Their Products*, Academic Press, London, 1970, p. 278.
- 5 J. Oydvin, *Hortic. Res.*, 14 (1974) 1.
- 6 E. D. Dekazos, *J. Food Sci.*, 35 (1970) 237.
- 7 F. J. Francis, *J. Food Sci.*, 50 (1985) 1640.
- 8 R. E. Wrolstad and B. Struthers, *J. Chromatogr.*, 55 (1971) 405.
- 9 B. M. Barritt and L. C. Torre, *J. Chromatogr.*, 75 (1973) 151.

- 10 J. Le Lous, B. Majoie, J. L. Moriniere and E. Wulfert, *Ann. Pharm. Fr.*, 8-9 (1975) 393.
- 11 M. Williams, G. Hrazdina, M. M. Wilkinson, J. G. Sweeny and G. A. Jacobucci, *J. Chromatogr.*, 155 (1978) 389.
- 12 A. L. Camire and F. M. Clydesdale, *J. Food Sci.*, 44 (1979) 920.
- 13 N. Akavia, D. Strack and A. Cohen, *Z. Naturforsch., Teil C*, 36 (1981) 378.
- 14 L. P. McCloskey and L. S. Yengoyan, *Am. J. Enol. Vitic.*, 4 (1981) 25.
- 15 K. van de Castele, H. Geiger, R. de Loose and C. F. van Sumere, *J. Chromatogr.*, 259 (1983) 291.
- 16 A. Baj, E. Bombardelli, B. Gabetta and E. M. Martinelli, *J. Chromatogr.*, 279 (1983) 365.
- 17 S. Asen and R. Griesbach, *J. Am. Soc. Hortic. Sci.*, 5 (1983) 845.
- 18 K. Bronnum-Hansen and S. H. Hansen, *J. Chromatogr.*, 262 (1983) 385.
- 19 J. Kärppä, N. Kallio, I. Peltonen and R. Linko, *J. Food Sci.*, 49 (1984) 634.
- 20 J. P. Roggero, B. Ragonnet and S. Coen, *Vignes Vins*, 327 (1984) 38.
- 21 O. M. Andersen, *J. Food Sci.*, 50 (1985) 1230.
- 22 R. G. Goldy, W. E. Ballinger and E. P. Maness, *J. Am. Soc. Hortic. Sci.*, 6 (1986) 955.
- 23 V. Hong and R. E. Wrolstad, *J. Assoc. Off. Anal. Chem.*, 2 (1986) 199.
- 24 G. M. Sapers, K. B. Hicks, A. M. Burgher, D. L. Hargrave, S. M. Sondey and A. Bilyk, *J. Am. Soc. Hortic. Sci.*, 6 (1986) 945.
- 25 V. Hong and R. E. Wrolstad, *J. Assoc. Off. Anal. Chem.*, 2 (1986) 208.
- 26 G. Mazza, *J. Food Sci.*, 5 (1986) 1260.
- 27 J. Raynal, C. Ginestet, J. M. Souquet and M. Moutounet, *Journ. Int. Études Polyphénols, Montpellier*, (1986) 482.
- 28 G. M. Sapers and D. L. Hargrave, *J. Am. Soc. Hortic. Sci.*, 1 (1987) 100.
- 29 G. A. Spanos and E. R. Wrolstad, *J. Assoc. Off. Anal. Chem.*, 6 (1987) 1036.
- 30 F. Siewek, R. Galensa and K. Herrmann, *Z. Lebensm.-Unters.-Forsch.*, 179 (1984) 315.
- 31 E. Verette, *Thésis*, Faculté de Pharmacie, Montpellier, 1984.
- 32 H. Engelhardt, B. Dreyer, H. Schmidt, *Chromatographia*, 16 (1982) 11.
- 33 P. Ribereau-Gayon, *Les Composés Phénoliques des Végétaux*, Dunod, Paris, 1968, p. 149.
- 34 C. Andary, J. L. Roussel, J.-P. Rascol and G. Privat, *J. Chromatogr.*, 303 (1984) 312.
- 35 F. R. Rekker and H. M. Kort, *Eur. J. Med. Chem.*, 6 (1979) 479.
- 36 S. Bittour, *Thésis*, Université Pierre et Marie Curie, Paris, 1986.



## **Solid-phase reagent containing the 3,5-dinitrophenyl tag for the improved derivatization of chiral and achiral amines, amino alcohols and amino acids in high-performance liquid chromatography with ultraviolet detection**

A. J. BOURQUE and IRA S. KRULL\*

*Department of Chemistry and The Barnett Institute, 341 Mugar Building, Northeastern University, 360 Huntington Avenue, Boston, MA 02115 (U.S.A.)*

(Manuscript received August 1st, 1990)

---

### ABSTRACT

A solid-phase reaction technique is described for improved derivatization of aliphatic amines, amino alcohols and amino acids. A polymeric activated ester is used for the immobilization of the 3,5-dinitrobenzoyl group, which can then be used for derivatizations of strong or weak nucleophiles, while avoiding solution-phase derivatization conditions. The reagent is easily prepared and can be regenerated after use to attain its original reactivity. The resulting chromatograms are free of system peaks due to excess derivatizing reagent, and sample handling is kept to a minimum. The reagent can be used in conjunction with both reversed- and normal-phase chromatography and can be used for off-line gas chromatographic or high-performance liquid chromatographic (HPLC) derivatizations. In addition, the reagent can be used on-line for derivatization in HPLC. Since the labelling reagent is a strong  $\pi$ -acid, chiral substrates can be derivatized and separated on a Pirkle-type  $\pi$ -donor column. The confirmation and quantitation of amphetamine in urine was accomplished using a polymer containing two labelling moieties, *p*-nitrobenzoyl and 3,5-dinitrobenzoyl. The derivatization and separation of chiral and achiral amines, amino alcohols and amino acids is described.

---

### INTRODUCTION

Amine-containing compounds are used in the synthesis of a majority of chiral and achiral pharmaceutically important compounds. The precursors and final products must be chemically and optically pure to assure high yield and purity of the final product. However, the analysis of aliphatic amines and amino acids is complicated by ionization of the amino functionality and poor chromatographic behavior on silica-based supports. The usual methodology for trace analysis of amines involves a homogeneous solution-based derivatization procedure, whereby a chromophore or electrophore is introduced, thus increasing the chromatographic performance, detectability and, at times, the volatility of the analyte [1]. Such derivatization procedures can be unwieldy, requiring time and effort and introducing many steps where analyte losses can occur. The resulting chromatograms are further complicated by excess or hydrolyzed derivatization reagents. Without suitable sample treatment

after the derivatization step, these reagents can contaminate the system, interfere with ultimate quantitation, and reduce the efficacy and lifetime of the chromatographic column. Such arguments are applicable to gas chromatography (GC), as well as to high-performance liquid chromatography (HPLC).

Over the past decade, solid-phase reagents have become increasingly popular for the facile conversion of analytes to more detectable species. These methods have largely been enzyme based, whereby an enzyme–substrate reaction produces an electrochemically or optically detectable species [2,3], or based on organic chemistry, whereby an immobilized activated site is reacted with a sufficiently electrophilic or nucleophilic substrate [4–7]. The advantages of performing these solid-phase reactions have been well covered in the literature [8,9]. Some of the more notable advantages include:

(1) Only the amount of reagent that reacts with the analyte is used. This yields chromatograms which are free of excess derivatizing reagent and allows the same batch of polymer to be used many times before efficacy of derivatization becomes a concern.

(2) More selective conversion of the analyte to the desired derivatives, yielding: (a) less complex chromatograms with higher signal-to-noise ratios and (b) functional group discrimination which is often not possible in solution phase derivatization without the use of blocking groups.

(3) Improved stability of the solid-phase reagents over time compared with the analogous solution-phase reagent.

(4) Trace analysis of analytes is facilitated by high local concentrations of the derivatizing reagent. These concentrations in solution would likely exceed the solubility of the derivatization reagent.

(5) Solid-phase derivatizations often allow for a higher percentage of conversions [10].

(6) The use of co-immobilized reagents allows for the quantitation and confirmation of analyte presence within a single chromatographic run. This methodology has been proven invalid for solution-phase derivatization, due to kinetic effects and the possibility of cross-reactions between the derivatization reagents in solution.

The resolution of optical isomers by HPLC is recognized as being the most sensitive technique available for unequivocal determination of enantiomeric composition [11]. The importance of this technique cannot be understated, in that about 25% of all pharmaceuticals dispensed between 1959 and 1980 contained at least one chiral center and the pharmacological activity of the enantiomers is often very different [12,13]. One need only be reminded of the thalidomide tragedy to understand the importance of absolute knowledge of enantiomeric excess for any given pharmaceutical [14]. Chiral molecules that lack chromophoric ligands generally require derivatization for visualization by UV–fluorescence detection. For physical resolution of chiral molecules, at least three points of interaction between the chiral analyte and the chiral selector are necessary, while one of these interactions must be steric in nature [15]. Thus, derivatization, which enhances the detectability of the analyte, can also be used to introduce a specific site for interaction with the brush-type Pirkle chiral columns. The usual treatment is to introduce a  $\pi$ -donor (naphthyl) or  $\pi$ -acceptor (3,5-dinitrophenyl) moiety to the molecule being analyzed [16–18]. Columns are commercially available, designed specifically to be used for such derivatized analytes.

We have synthesized two polymers which contain activated ester moieties. The



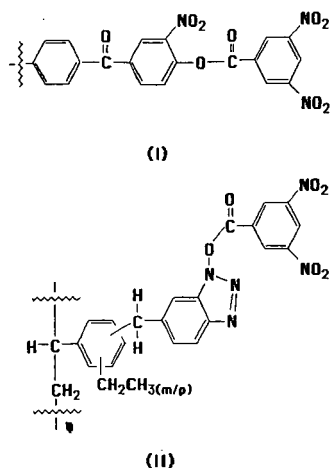


Fig. 1. Structure of polymeric reagents. (I) Polymeric benzophenone-DNB, (II) polymeric benzotriazole-DNB.

first polymer (I, Fig. 1) was prepared from 200–400 mesh polystyrene beads cross-linked with 4% divinylbenzene (DVB). We modified the polymer to obtain an *o*-nitrophenol to which various acid chloride–chloroformate moieties could be attached. The second polymer (II, Fig. 1) was based on ethylvinylbenzene (EVB) cross-linked with DVB, in which a hydroxybenzotriazole functionality had been introduced. The two polymers showed remarkably different reaction kinetics due to their different activated linkages and polymeric supports. These reagents could be used off-line or on-line, pre-column, for real- or delayed-time derivatizations of sufficiently nucleophilic analytes, such as amines and amine analogues. The derivatives had enhanced sensitivity to absorbance detection due to the addition of a chromophoric label. The dinitrophenyl derivatives were amenable to reductive electrochemical detection, as well as photochemical dissociation and reduction of the cleaved aromatic nitro groups to nitrite, which could then be detected electrochemical in an oxidative mode [19]. Thus, three possible modes of detection were possible; a significant advantage in confirmation of the analyte in a complex matrix over detection of the underivatized analyte. Other detector labels (fluorenyl, *o*-acetylsalicyloyl and *p*-nitrobenzoyl) can be attached to the polymeric reagents to yield different chromatographic and detector selectivity to the derivatized analyte.

These different polymers can be mixed to form a known amount of each label per gram of the mixed polymer. Derivatization of a single analyte produced a characteristic profile of derivatives having known retention times and detector responses. This efficiently solved the problem of co-elution of a matrix component with the analyte of interest since the likelihood of matrix co-elution with both derivatives was minimal [20].

In this paper, the simultaneous determination of amphetamine in urine using a 1:1 molar mix of immobilized *p*-nitrobenzoyl and 3,5-dinitrobenzoyl (DNB) moieties is shown. Both derivatives eluted well-resolved from the matrix, without any extraction/matrix work-up involved. The simultaneous analysis and confirmation

within a 5-min chromatographic run exemplifies the utility of solid-phase derivatization methodology for analyses in complex matrices.

## EXPERIMENTAL

### *Materials*

A LiChrosorb 5- $\mu\text{m}$  particle size,  $\text{C}_{18}$  column (EM Science, Cherry Hill, NJ, U.S.A.), 250 mm  $\times$  4.6 mm I.D., was used for the hydrolysis analysis and analysis of achiral derivatives. For chiral separations Supelcosil LC-(*R*)-Naphthyl Urea/LC-(*S*)-Naphthyl Urea, 250 mm  $\times$  4.6 mm I.D. columns (Supelco, Bellefonte, PA, U.S.A.) were used. 3,5-Dinitrobenzoyl chloride (DNBCl) and other reagents were obtained from Aldrich (Milwaukee, WI, U.S.A.). Amino acids and amino acid methyl esters were purchased from Sigma (St. Louis, MO, U.S.A.). The dinitrobenzamide (DNBa) standards were synthesized following literature procedures [21,22]. Polymeric supports were purchased from Fluka (polystyrene cross-linked with 4% DVB, 200–400 mesh), and from Waters (Milford, MA, U.S.A.; Porapak Q; 57% DVB, 38.6% EVB, *meta/para* ratio 2.5:1, 100–120 mesh) [23]. Amphetamine sulphate and norephedrine HCl were donated by Thomas Doyle (FDA, Washington DC, U.S.A.). HPLC solvents were obtained from EM Science, as their Omnisolv grade. All solvents were filtered through a 0.45- $\mu\text{m}$  membrane (PTFE, Millipore, Bedford, MA, U.S.A.; Nylon 66, Supelco) and degassed under vacuum before use.

### *Apparatus*

The HPLC system consisted of a Waters Model 6000A pump, a Rheodyne Model 7125 injection valve (Rheodyne, Cotati, CA, U.S.A.) and a UV Monitor III (LDC Milton Roy, Riviera Beach, FL, U.S.A.). Data acquisition was performed using Rainin Dynamax DA (Rainin Instruments, Berkeley, CA, U.S.A.) through a Macintosh Plus personal computer (Apple Computers, Cupertino, CA, U.S.A.). At times, data was collected from a Hitachi D-2000 Chromatointegrator (Hitachi Instruments, Naka Works, Mito City, Japan).

Physical and spectral characterization of the derivatives, used to characterize the kinetics and thermodynamics of the polymeric reagent with various analyte classes, included a Varian Model XL-300 NMR Spectrometer (Varian, Palo Alto, CA, U.S.A.), a Perkin-Elmer Model 599B infrared spectrophotometer (Perkin-Elmer, Analytical Instruments, Norwalk, CT, U.S.A.), a Thomas Hoover capillary melting point apparatus (Arthur H. Thomas, Philadelphia, PA, U.S.A.), a Milton Roy Model Spectronic 1201 scanning UV–VIS spectrophotometer (Milton Roy, Analytical Products Division, Rochester, NY, U.S.A.) and a Nuclide magnetic sector mass spectrometer (Nuclide, State College, PA, U.S.A.). Elemental analyses of the polymeric reagents were performed at Galbraith Laboratories (Knoxville, TN, U.S.A.). Solvents removal under reduced pressure was performed on a Buchi RotoVap (VWR Scientific, Boston, MA, U.S.A.).

### *Synthesis of analytical standards of amines, amino alcohols and amino acids*

All DNBa-standard derivatives were characterized via  $^1\text{H}$  NMR and electron-impact mass spectrometry (EI–MS) and were determined to be the expected structures.

*Amines.* DNBa standards of primary and secondary amines were prepared via

solution-phase derivatization of the amine with pyridine-catalyzed DNBCl according to literature procedures [21].

*Amino alcohols.* Standards of primary and secondary amino alcohols were prepared via solution-phase derivatization of the amine functionality with triethylamine (TEA)-catalyzed DNBCl according to literature procedures [22].

*Amino acids.* For achiral, reversed-phase (RP) analysis of amino acids using solid-phase derivatization, only the amine functionality was modified. Synthesis of the derivatives required temporary protection of the carboxylic acid group, while the amine group was acylated with DNBCl. The standards were prepared following a modification of a literature procedure, in which the electrophilic reagent, trityl chloride, was replaced with DNBCl [24].

*Amino acid methyl esters.* The methyl esters of some of the amino acids used were purchased as the methyl ester hydrochlorides. Others were synthesized in our laboratory using the amino acid and dry methanol-HCl or BF<sub>3</sub>-methanol (50:50, w/w) according to literature procedures [22].

#### *Synthesis of the polymeric benzophenone and polymeric hydroxybenzotriazole*

*Polymeric benzophenone.* Polystyrene-divinylbenzene was washed with acetonitrile (ACN) using a Soxhlet apparatus for 48 h to remove monomeric impurities which would leach from the polymer and complicate the chromatograms of the derivatives. The modification of the polystyrene followed a literature procedure [25]. The analytical label was covalently attached to the polymeric phenol intermediate, via the acid chloride, using pyridine as a nucleophilic catalyst [25].

*Polymeric benzotriazole.* The second polymeric reagent contained an immobilized hydroxybenzotriazole functionality. This polymeric hydroxybenzotriazole was synthesized from an EVB-DVB polymer following a literature procedure [26]. Addition of the analytical label to the polymeric hydroxybenzotriazole intermediate was identical to that of the polymeric benzophenone.

#### *Physical characterization of the polymeric activated esters*

*Hydrolysis of polymeric benzophenone activated ester.* A hydrolysis procedure was used to quantitatively cleave the analytical label from the polymer. The benzoic acid generated was quantitated via HPLC using external-standard calibration. A 200-mg amount, weighed to the nearest 0.1 mg, was hydrolyzed by suspension in 2 ml of 2 M KOH and 3 ml of dimethylformamide (DMF). The suspension was heated with stirring to 60°C for 30 min. The solution was then acidified (pH 3) using concentrated HCl, and the polymer was filtered directly into a 25-ml volumetric flask. The solution was made to the mark with ACN-water (30:70) and analyzed by RP-HPLC (Table I).

*Hydrolysis of polymeric benzotriazole-DNB.* The characterization of the benzotriazole labelled with *o*-acetylsalicyloyl chloride was via a similar hydrolysis procedure [6] (Table I).

*Elemental analysis of polymeric benzophenone and polymeric benzotriazole.* Elemental analyses of both polymers were performed at Galbraith Laboratories (Table I).

#### *Regeneration of the polymeric reagents*

Since both polymeric reagents swell in ACN it was often sufficient to wash the

TABLE I  
QUANTITATIVE DATA FOR POLYMERIC REAGENTS

---

<i>Benzophenone elemental analysis</i>				
Polystyrene-DVB	91.88% C,	8.02% H		
Polymeric phenol	77.00% C,	5.93% H,	2.67% N,	10.30% O
Tagged phenol	71.82% C,	5.12% H,	4.46% N,	14.56% O
<i>Benzophenone elemental analysis results<sup>a</sup></i>				
	1.91 ± 0.02 mequiv. phenol/g of polymer			
	0.64 ± 0.02 mequiv. label/g of polymer			
<i>Benzophenone hydrolysis results<sup>b</sup></i>				
	0.62 ± 0.02 mequiv. label/g of polymer			
<i>Benzotriazole hydrolysis results<sup>c</sup></i>				
	0.31 ± 0.01 mequiv. label/g of polymer			

---

<sup>a</sup> Based on increase in nitrogen, less than 0.014 mequiv. Cl<sup>-</sup> found, indicating near quantitative conversion of intermediate to the polymeric phenol.

<sup>b</sup> Hydrolysis was performed on polymer acylated with benzoyl chloride due to instability of the 3,5-dinitrobenzoate anion to the hydrolysis conditions.

<sup>c</sup> Hydrolysis was performed on polymer tagged with *o*-acetylsalicyloyl chloride.

reagent with several aliquots of ACN, allowing each aliquot to sit for 60 s to allow for impurities to diffuse out of the pores of the polymer. Occasionally, an overnight Soxhlet extraction was performed using ACN to thoroughly clean the polymer. The polymer was then dried and acylated with DNBCl to yield the final tagged reagent.

#### *Solid-phase on-line derivatization*

Only the polymeric benzophenone-DNB reagent was used on-line, due to the instability of the polymeric benzotriazole-DNB reagent to water. The on-line reactor was assembled from stainless-steel hardware (27 mm × 2.2 mm I.D., 0.2- $\mu$ m frits). Similar-dimension columns are commercially available for facile in-house packing of guard columns from Upchurch Scientific (Oak Harbor, WA, U.S.A.). The reactor was attached to an injector through the injection-loop ports (ports 1 and 4, Rheodyne Model 7010), and this configuration was used as a switching valve [5]. The analyte was injected and allowed to pass through the reactor for real-time, on-line derivatization, or was switched to a bypass mode to trap the analyte to attain longer reaction times (Fig. 2). The reactor was attached to the switching valve using 15 cm of small bore (0.009 in. I.D.) stainless-steel tubing. It could then be lowered into a thermostated hot water reservoir to increase the temperature of the reaction.

*Reversed-phase derivatization.* The derivatization of nucleophiles in aqueous organic solvents on-line, was complicated by the reactivity of the polymer. A dual-pump apparatus was configured such that only anhydrous organic solvent passed through the reactor. A mixing tee was placed after the reactor and before the analytical column, where the strength of the final eluent was adjusted through proportioning of the pumps (Fig. 2). The derivatization solvent was ACN or tetrahydrofuran (THF) and the aqueous solvent was generally ACN-water (10:90) or THF-water (10:90). A mixture of three amines (morpholine, *n*-propylamine and *n*-butylamine; 20 ppm each), was derivatized on-line using the dual-pump system. The derivatization of amines was tested in two different anhydrous organic eluents, THF-ACN (1:1) and ACN (Fig. 3).

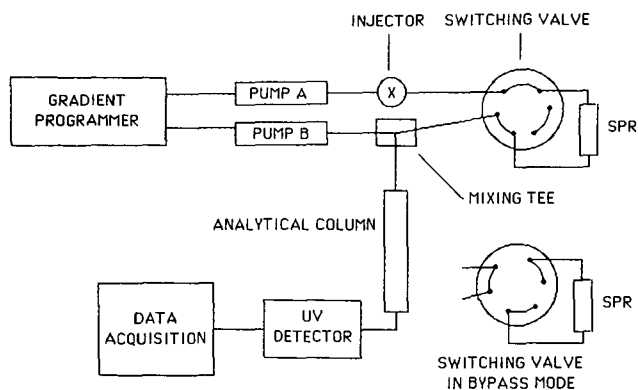


Fig. 2. Diagram of dual-mobile-phase HPLC system. Pump A contains anhydrous ACN, pump B contains ACN-water (10:90). Column, LiChrosorb 5  $\mu\text{m}$  C<sub>18</sub> cartridge, 125  $\times$  4.0 mm I.D.

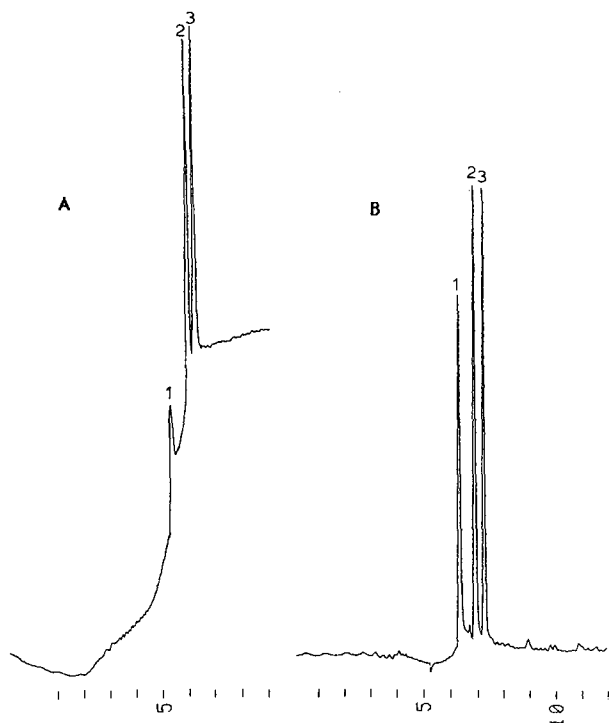


Fig. 3. On-line derivatization of (1) morpholine, (2) propylamine and (3) butylamine using two mobile phases. (A) THF-ACN (1:1); (B) ACN. Both systems are split mobile-phase gradients in which only pure organic flows through the on-line reactor. Conditions: injection volume, 20  $\mu\text{l}$ ; column, LiChrosorb 5  $\mu\text{m}$  C<sub>18</sub> cartridge, 125  $\times$  4.0 mm I.D.; pump A: 100% organic; pump B: 10% organic. Gradient No. 8, 5-85% A over 5 min. Retention time in min.

*Normal-phase derivatization.* The derivatization of amines and amine analogues in normal-phase was expected to be more facile than in reversed-phase due to the lack of water in the mobile phase. However, since the reactivity of the polymer was enhanced at elevated temperatures (50–80°C), the reactor had to be protected from alcohols as well. Reactions were accomplished using a single programmable pump (Waters, Model 590) with flow-programmed step gradient. The analyte flowed through the reactor at 0.1 ml/min and was then stepped up to higher flow-rates at the rate of 1 ml increments every ten seconds, to a final flow-rate of 3.1 ml/min. The reactor column was placed in a hot water bath to equilibrate 2 min before injection of the analyte, and was removed from the bath after 4 min to prolong its lifetime. Analysis of the enantiomers of amphetamine was accomplished in <20 min from injection to derivatization, separation and detection of the on-line formed derivatives (Fig. 4).

*Solid-phase off-line derivatizations*

An amount of the polymeric reagent was added to a Pasteur pipet which had been scored and broken *ca.* 5 cm above the tapered section. The tapered end was plugged with a small amount of tissue paper which kept the polymer bed intact, and filtered any particulates from the final solution containing the derivatives. A volume of analyte (30–100  $\mu$ l) was added to a fixed mass of the polymer (30–150 mg) such that the

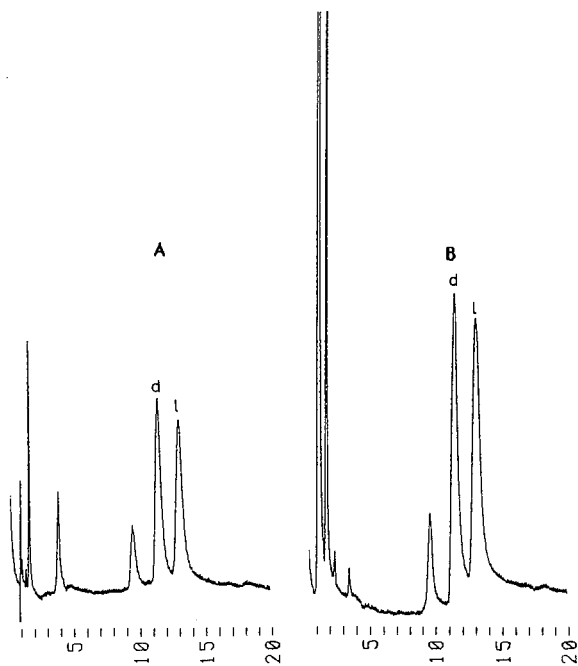


Fig. 4. On-line derivatization and separation of the enantiomers of amphetamine. (A) Injection of 75 ppm of the standard amphetamine-3,5-dinitrobenzamide; (B) injection of 100 ppm amphetamine free base in ACN-DCM (1:1) with 0.05% TEA added. Real-time derivatization at 72°C in a mobile phase of hexane-DCM-THF (70:27:3). Derivatization occurred at 0.1 ml/min for 40 s. The flow-rate was increased in increments of 1 ml every 10 s to a final flow-rate of 3.1 ml/min. Conditions: injection volume, 10  $\mu$ l; column, Supelco 5  $\mu$ m, LC-(R)-Naphthyl Urea 250  $\times$  4.6 mm I.D. Retention time in min.

polymer was wetted without the analyte reaching the tissue plug. The solid-phase reaction was allowed to proceed for an amount of time determined by the kinetics of the substrate, and was washed with 500  $\mu$ l ACN. The eluent was then diluted with water to match the mobile phase. For normal-phase work, the derivatives were eluted from the reactor using 1 ml of the mobile phase. For normal-sensitivity work (ppm and above), 20  $\mu$ l of the final solution was injected into the HPLC. After each derivatization, the polymer was removed from the cartridge, the tissue paper replaced, and the reactor filled with fresh polymer. The used polymer was placed aside to be regenerated.

#### Optimization of off-line derivatization conditions

*Time and temperature.* Typical primary and secondary amine substrates were used to characterize the kinetics of the solid-phase reagents with amines. Thus, a 200-ppm solution of *n*-butylamine in ACN and a 200-ppm solution of diethylamine in ACN were used as test substrates to determine the dependence of percent derivatization as a function of time. Each analyte was derivatized separately, off-line for different intervals, and the product obtained was compared to the external standard that had been synthesized and characterized. The percent conversion of the amine to the amide was quantitated. Reaction time intervals were 5, 10, 20, 40 and 80 s. A 30  $\mu$ l volume of the amine solution was injected onto 70 mg of the polymeric reagent,

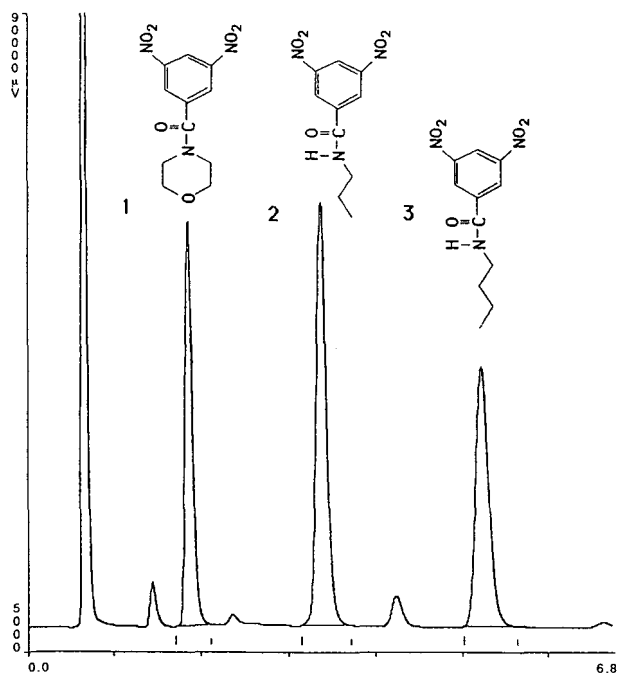


Fig. 5. Analysis of amines using off-line derivatization. Derivatives in order of elution: 1 = morpholine-DNBa, 2 = *n*-propyl-DNBa, 3 = *n*-butyl-DNBa. Conditions: 20 ppm each in ACN, 30  $\mu$ l  $\times$  70 mg polymeric benzophenone-DNB; 1 min at RT, elute to 1 ml ACN, inject 10  $\mu$ l. Column, LiChrosorb 5  $\mu$ m C<sub>18</sub> cartridge, 125  $\times$  4.0 mm I.D., ACN-water (50:50) at 1.5 ml/min. Retention time in min.

and the reaction was quenched with 200  $\mu\text{l}$  of ACN–water (80:20), which was adjusted to a concentration of 2 mM  $\text{HNO}_3$ . Quantitation of percent conversion was performed as before. The off-line derivatization of three amines was performed (Fig. 5).

The same experiment was performed using a base catalyst. An equimolar amount of TEA was added to the 200-ppm solution of *n*-butylamine–diethylamine in pure ACN. The identical study was performed using a 4 mM  $\text{HNO}_3$  quenching solution (Fig. 6).

An analogous experiment was performed using the polymeric benzotriazole–DNB reagent. Since nearly quantitative conversion of the amine, in the presence of a base catalyst, to the 3,5-dinitrobenzamide (DNBa) occurred at room temperature (RT) in  $\leq 60$  s with both polymeric reagents, no temperature optimizations were performed.

#### *Concentration of base catalyst vs. amine concentration*

The amount of TEA used as a base catalyst was varied from 0.5 to 2 equiv. vs. *n*-butylamine concentration. Derivatization conditions were identical to those used for the optimization of time.

#### *pH. study vs. percent derivatization*

For partially or wholly aqueous solutions, the pH of the solution was an important factor, since ionization of the analyte rendered the amine functionality non-nucleophilic. Eight buffers were prepared by adjusting the pH of a 50-ml aliquot of 0.4 M  $\text{H}_3\text{BO}_3$  to the pH of interest using 0.5 M KOH and diluting to a 100 ml volumetric. Thus, 0.2 M  $\text{H}_3\text{BO}_3$  buffers with pH values between 7.0 and 10.0 in 0.5 pH increments were prepared. A 400-ppm solution of *n*-butylamine was prepared and 25-ml aliquots of the amine solution were mixed with 25-ml aliquots of the appropriate buffer solution to prepare the final analyte solution. The final composition was 200 ppm *n*-butylamine in ACN–0.1 M borate buffer (50:50) at different pH values. Derivatization conditions and quantitation of percent conversion were identical to those used for the optimization of time. No analogous pH study was performed with the polymeric benzotriazole–DNB reagent.

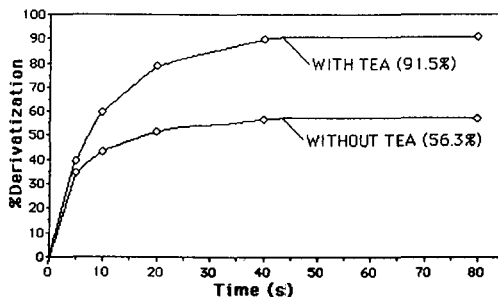


Fig. 6. Percentage of derivatization vs. time of butylamine with polymeric benzophenone–DNB in ACN with and without equimolar TEA present. Conditions: 30  $\mu\text{l}$  of 200 ppm in ACN  $\times$  70 mg polymeric benzophenone–DNB; 2 min at RT, elute with 500  $\mu\text{l}$  ACN, dilute with 500  $\mu\text{l}$  water; injection volume, 10  $\mu\text{l}$ ; column, LDC–Milton Roy 3  $\mu\text{m}$  Spherisorb ODS-II, 100  $\times$  4.0 mm I.D., ACN–water (50:50) at 1.5 ml/min.



### Percent derivatization vs. amine concentration

The working range of amine concentrations over which the percent derivatization remained constant was determined. Solutions of *n*-butylamine were prepared in the concentration range of 500 ppb<sup>a</sup> to 20 000 ppm. No base catalyst was used. Derivatizations and quantitation using the polymeric benzophenone-DNB were performed as before.

### Derivatization protocol for amines, amino alcohols, amino acids and amino acid methyl esters using both polymeric reagents

**Amines.** Amines as the free base were weighed or injected into a volumetric flask containing ACN and an equimolar amount of TEA. The TEA had to be specially treated to remove 1° and 2° amine impurities, which otherwise complicated the chromatograms [27]. Amines as the hydrochloride or sulphate were prepared in ACN-0.05 M NaOH (80:20). For derivatization of these solutions followed by normal-phase chromatography, the water was trapped using 500 mg of anhydrous Na<sub>2</sub>SO<sub>4</sub>, which was placed below the polymer bed in the off-line reactors. Thus, the derivative and solution were made anhydrous as they eluted from the reactor. The comparison of percent derivatization vs. time for both polymers is given in Fig. 7. Quantitation was performed using peak areas (Table II).

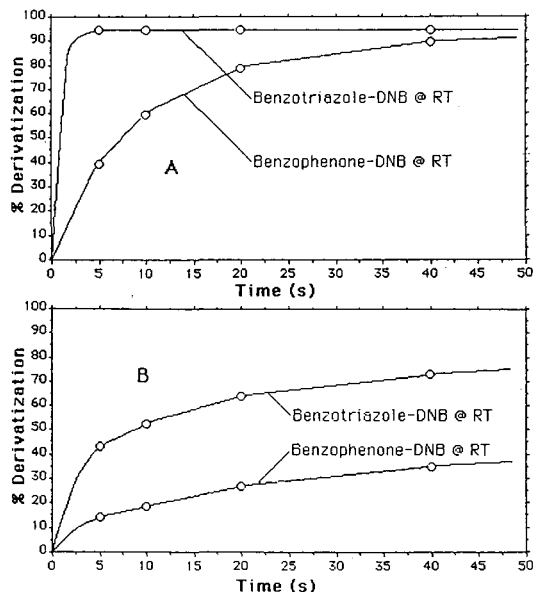


Fig. 7. Time dependence of derivatization of *n*-butylamine and diethylamine with the two polymeric reagents. (A) Kinetic curve for *n*-butylamine, (B) kinetic curve for diethylamine. Conditions: 200 ppm *n*-butylamine-diethylamine in ACN with equimolar TEA. 30  $\mu$ l  $\times$  70 mg polymeric benzophenone-DNB, 50  $\mu$ l  $\times$  30 mg polymeric benzotriazole-DNB; 2 min at RT, elute with 500  $\mu$ l ACN, dilute with 500  $\mu$ l water. Chromatography, injection volume, 20  $\mu$ l; LiChrosorb 5  $\mu$ m C<sub>18</sub>, 125  $\times$  4.0 mm I.D., ACN-water (50:50) at 1.5 ml/min.

<sup>a</sup> Throughout the article, the American billion (10<sup>9</sup>) and trillion (10<sup>12</sup>) is meant.

TABLE II

ENANTIOMERIC PURITY OF AMINES<sup>a,c</sup>

Sample	<i>d</i> (%)	<i>l</i> (%)
(±)-1-amino-1-phenylpropane <sup>b</sup> (lot KM63206KM)	50.45 ± 0.05	49.55 ± 0.05
( <i>R</i> )-(+)-1-amino-1-phenylethane <sup>c</sup> (lot AP03909TM)	98.86 ± 0.04	1.14 ± 0.04
( <i>S</i> )-(−)-1-amino-1-phenylethane <sup>c</sup> (lot 00901JP)	1.95 ± 0.16	98.05 ± 0.16
( <i>R</i> )-(+)-1-amino-1-(1-naphthyl)ethane <sup>d</sup> (lot 03424HM)	99.11 ± 0.05	0.89 ± 0.05
( <i>S</i> )-(−)-1-amino-1-(1-naphthyl)ethane <sup>d</sup> (lot 88F0342)	0.78 ± 0.07	99.22 ± 0.07

<sup>a</sup> 40  $\mu$ l amine solution  $\times$  80 mg benzophenone-DNB, 2 min at RT, elute to 1 ml with mobile phase, LC-(*S*)-Naphthyl Urea column, 250  $\times$  4.6 mm I.D., 20  $\mu$ l  $\times$  0.016 a.u.f.s. at 254 nm.

<sup>b</sup> Hexane-DCM-methanol (90:7:3) at 1 ml/min.

<sup>c</sup> Hexane-DCM-methanol (80:15:5) at 2 ml/min.

<sup>d</sup> Hexane-DCM-methanol (70:25:5) at 2 ml/min.

<sup>e</sup> All amines purchased through Aldrich.

*Amino alcohols.* The amino alcohols were dissolved in ACN containing equimolar TEA. For reversed-phase work, the derivatives were eluted from the off-line reactor with 500  $\mu$ l of ACN and diluted with water prior to injection (Fig. 8). For normal-phase chromatography, the derivatives were eluted from the off-line reactor using 1 ml of the mobile phase.

*Amino acids.* The amino acids were dissolved in ACN-0.05 *M* NaOH (80:20). This allowed the amine functionality to remain as the free base and provided good wetting and swelling properties for the polymer. Derivatization was as above for the amines, and separation was performed on a C<sub>18</sub> column with 0.1% trifluoroacetic acid (TFA) added for pH suppression (Fig. 9).

*Amino acid methyl esters.* The methyl esters of the amino acids studied were either synthesized using BF<sub>3</sub>-methanol or methanol-HCl(g), or were purchased as the hydrochloride salt and were neutralized in 0.1 *M* NaOH. The solution was made partially organic (ca. 12%), and the analyte was extracted using a solid-phase technique. The preparation of a 200-ppm solution of the methyl ester of phenylalanine was as follows: 24.1 mg of the hydrochloride was weighed directly into a 5-ml Reacti-vial and 2 ml of 0.1 *M* NaOH was added. A 0.250 ml volume of ACN was added

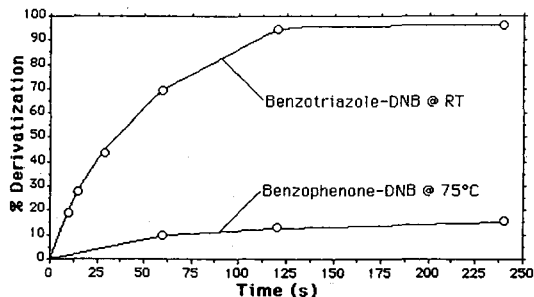


Fig. 8. Time dependence of derivatization of ethanolamine with both polymers. Same conditions as Fig. 7, except separation was performed on a Spherisorb 3  $\mu$ m CN 100  $\times$  4.6 mm I.D., ACN-water (50:50) at 1.5 ml/min.

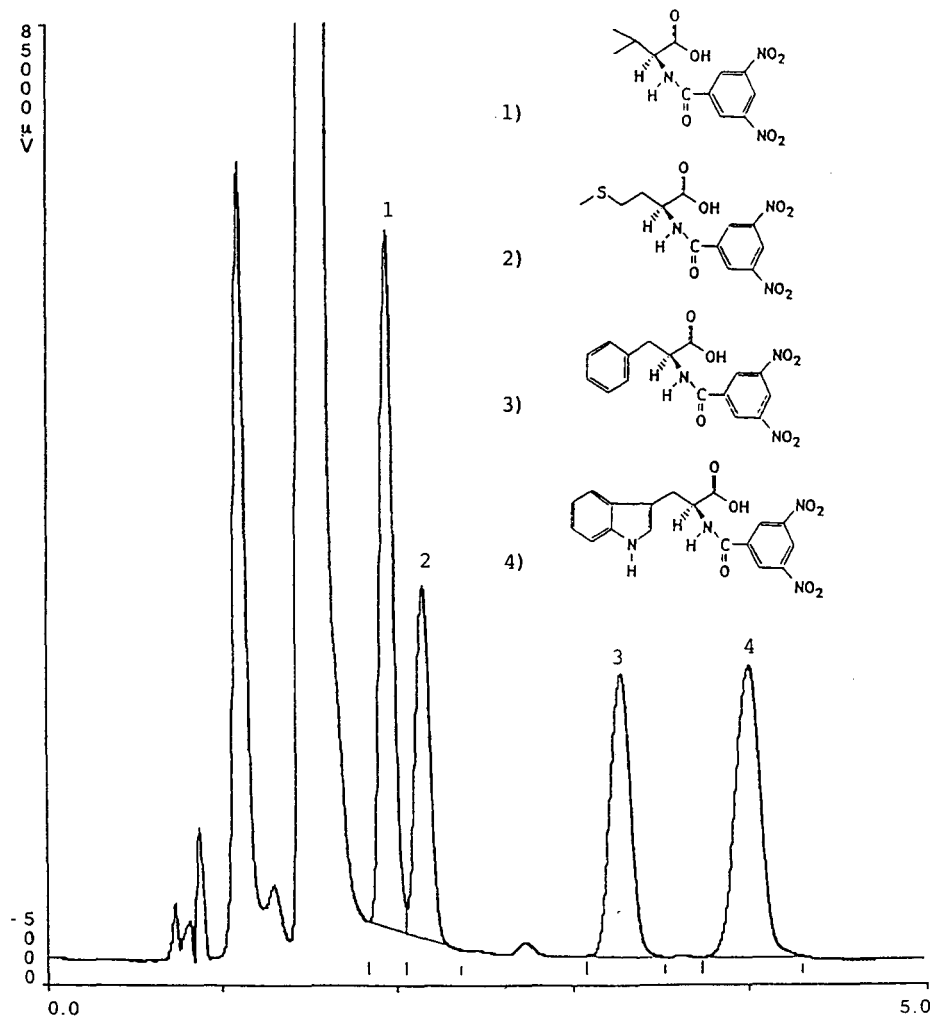


Fig. 9. Derivatization of (1) valine; (2) methionine; (3) phenylalanine; and (4) tryptophan dissolved in ACN-0.05 *M* NaOH (80:20). Conditions: 50  $\mu$ l (200 ppm each)  $\times$  30 mg polymeric benzotriazole-DNB; 2 min at RT, elute to 500  $\mu$ l ACN, dilute with 500  $\mu$ l water; injection volume, 20  $\mu$ l; column, Spherisorb 3  $\mu$ m CN 100  $\times$  4.6 mm I.D., ACN-water (20:80) (0.1% TFA). Retention time in min.

to aid in the dissolution of the free base. The solution was taken up in a 5-ml gastight syringe and passed over an RP-C<sub>18</sub> Sep-Pak cartridge which had been conditioned with 3 ml of ACN and 1 ml of distilled water. The eluate was discarded and the cartridge washed with 1 ml of distilled water. The amino acid methyl ester was eluted into a 100-ml volumetric flask with two 5-ml aliquots of pure ACN. The solution was made equimolar with TEA and the volumetric flask was brought to the mark. Derivatization of this solution was identical to that of a free amine in ACN (Figs. 10 and 11). Quantitation was performed using peak areas (Tables III and IV).

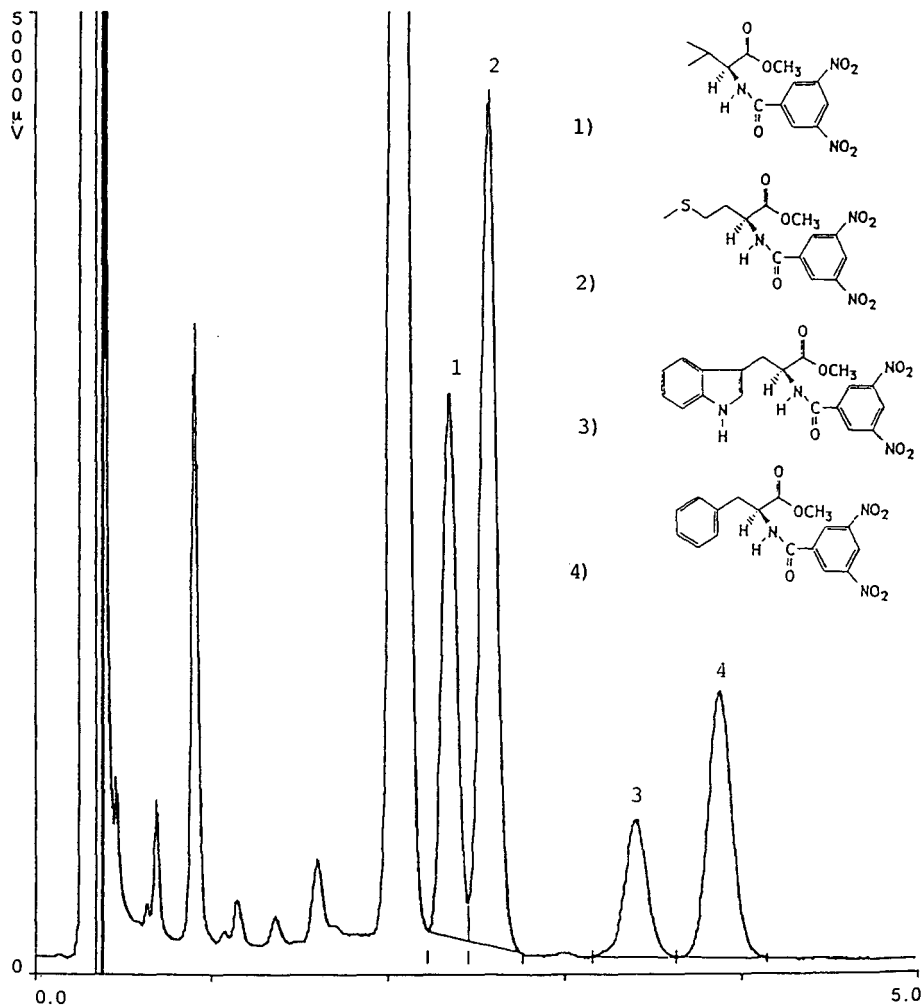


Fig. 10. Derivatization of the methyl esters of (1) valine; (2) methionine; (3) tryptophan; and (4) phenylalanine. Conditions: 100  $\mu$ l (100 ppm each)  $\times$  60 mg polymeric benzotriazole-DNB; 2 min at RT, elute to 500  $\mu$ l ACN, dilute with 500  $\mu$ l water; injection volume, 20  $\mu$ l; column, LiChrosorb 5  $\mu$ m C<sub>18</sub>, 125  $\times$  4.0 mm I.D., ACN-water (45:55) at 2.5 ml/min. Retention time in min.

#### Single-blind chiral analysis of amphetamine

The enantiomeric ratio of amphetamine isomers was determined in five samples, spiked with varying ratios of *d*- and *l*-amphetamine. The samples were prepared from the pure enantiomers of amphetamine sulphate, which was dissolved in ACN-0.25 M KOH (50:50). Unknown ratios of *d*- and *l*-amphetamine were prepared by adding different amounts of the two stock solutions to a third vial. The authors had no previous knowledge of the enantiomeric compositions.

Determination of the enantiomeric composition was via derivatization and chromatographic analysis of the samples. Five samples were analyzed by injecting

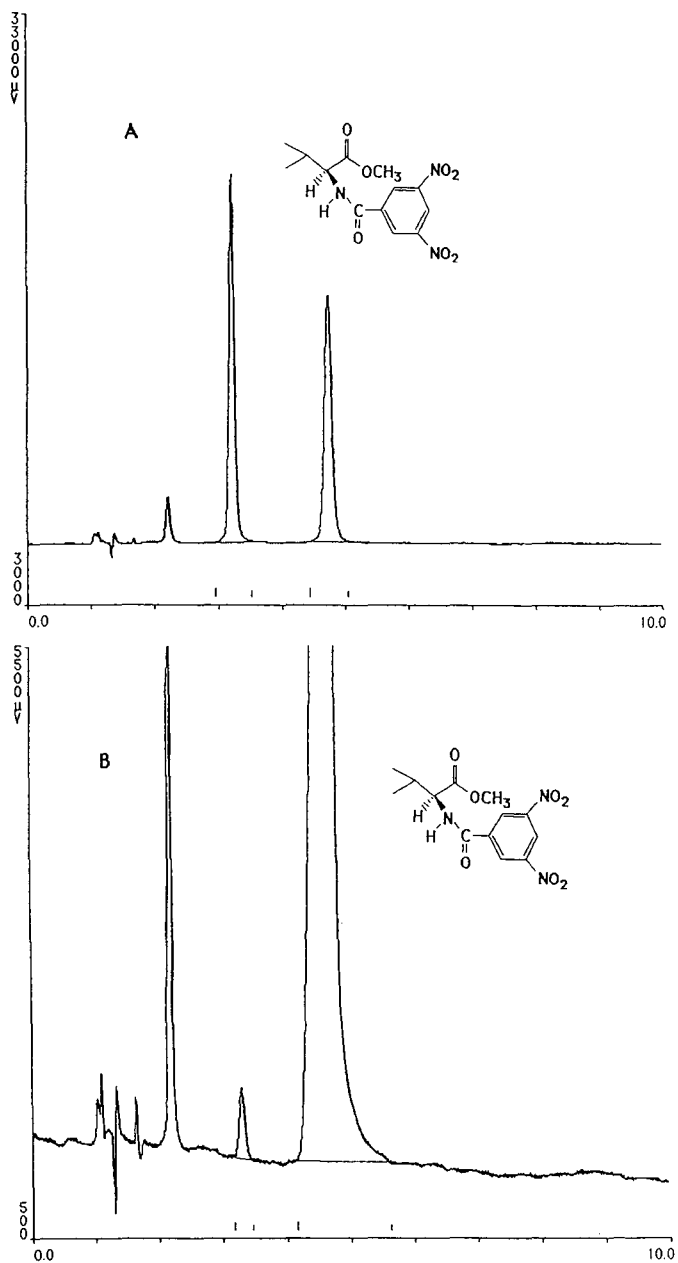


Fig. 11. Chiral separation of *d*- and *l*-valine methyl esters as the off-line formed 3,5-dinitrobenzamide. (A) 1 pptt *d,l*-Valine showing 50:50 composition by area; (B) 2 pptt *l*-valine showing  $0.18 \pm 0.02\%$  enantiomeric contamination of the *d*-isomer. Conditions:  $20 \mu\text{l} \times 30 \text{ mg}$  polymeric benzophenone-DNB, 3 min at RT, elute to 1 ml with mobile phase, injection volume  $20 \mu\text{l}$ . Chromatography,  $5 \mu\text{m}$  LC-(*S*)-Naphthyl Urea  $250 \times 4.6 \text{ mm}$  I.D., hexane-DCM-methanol (90:5:5) at 3.0 ml/min. Retention time in min.

TABLE III  
CHROMATOGRAPHIC FIGURES OF MERIT FOR THE AMINO ACID DERIVATIVES<sup>a</sup>

Compound as 3,5-DNBa (methyl ester)	Column efficiency ( <i>N</i> ) <sup>f</sup>	<i>k'</i> [( <i>t<sub>r</sub></i> - <i>t<sub>0</sub></i> )/ <i>t<sub>0</sub></i> ]	$\alpha$ ( <i>k'<sub>2</sub></i> / <i>k'<sub>1</sub></i> )
<i>Phenylalanine</i> <sup>b</sup>			
<i>d</i> -form	7780	2.12	1.38
<i>l</i> -form	7610	2.92	
<i>Alanine</i> <sup>c</sup>			
<i>d</i> -form	7820	0.95	1.66
<i>l</i> -form	7580	1.75	
<i>Valine</i> <sup>d</sup>			
<i>d</i> -form	7590	2.21	1.68
<i>l</i> -form	7510	3.72	
<i>Tryptophan</i> <sup>e</sup>			
<i>d</i> -form	8540	1.49	1.74
<i>l</i> -form	7630	2.59	

<sup>a</sup> 40  $\mu$ l  $\times$  80 mg benzophenone-DNB, 3 min at RT, elute to 1 ml with mobile phase. Supelco LC-(S)-Naphthyl Urea column, 250  $\times$  4.6 mm I.D., 20  $\mu$ l  $\times$  0.004 a.u.f.s.

<sup>b</sup> Hexane-DCM-methanol (75:23:2) at 2 ml/min.

<sup>c</sup> Hexane-DCM-methanol (70:25:5) at 2 ml/min.

<sup>d</sup> Hexane-DCM-methanol (90:5:5) at 3 ml/min.

<sup>e</sup> Hexane-DCM-methanol-ACN (70:22:5:3) at 2 ml/min.

<sup>f</sup> *N* = number of plates.

70  $\mu$ l of the amine solution onto 150 mg of the polymeric benzophenone-DNB reagent, allowing the reaction to occur at RT for 60 s and eluting the derivative to 0.7 ml with 100% THF. Four derivatizations were performed with 2-3 injections per derivatization. Determination of enantiomeric composition was performed using peak areas (Table V).

TABLE IV  
ENANTIOMERIC PURITY OF AMINO ACIDS<sup>a</sup>

Amino acid	<i>d/l</i>	<i>d</i>	<i>l</i>
Phenylalanine <sup>b</sup>	(49.95/50.05) $\pm$ 0.03	99.15 $\pm$ 0.02	99.62 $\pm$ 0.02
Alanine <sup>c</sup>	(50.01/49.99) $\pm$ 0.04	98.90 $\pm$ 0.05	97.90 $\pm$ 0.05
Valine <sup>d</sup>	(50.21/49.79) $\pm$ 0.10	-- <sup>f</sup>	99.82 $\pm$ 0.02
Tryptophan <sup>e</sup>	(49.99/50.01) $\pm$ 0.01	100.00 $\pm$ 0.00	100.00 $\pm$ 0.00

<sup>a</sup> 40  $\mu$ l sample  $\times$  80 mg polymeric benzophenone-DNB, 1 min at RT, elute to 1 ml with mobile phase. Supelco LC-(S)-Naphthyl Urea column, 250  $\times$  4.6 mm I.D., 20  $\mu$ l  $\times$  0.004 a.u.f.s. at 254 nm.

<sup>b</sup> Hexane-DCM-methanol (75:23:2) at 2 ml/min.

<sup>c</sup> Hexane-DCM-methanol (70:25:5) at 2 ml/min.

<sup>d</sup> Hexane-DCM-methanol (90:5:5) at 3 ml/min.

<sup>e</sup> Hexane-DCM-methanol-ACN (70:22:5:3) at 2 ml/min.

<sup>f</sup> *d*-Enantiomer not analyzed.

TABLE V  
SINGLE-BLIND SPIKED AMPHETAMINE ANALYSIS<sup>a</sup>

Sample	Spiked composition (%)	Determined (%)	R.S.D. (%)	RE <sup>b</sup> (%)
<i>5-119-1</i>				
<i>d</i> -form	65.0	64.7 ± 0.2	0.3	-0.6
<i>l</i> -form	35.0	35.3 ± 0.2	0.6	+0.9
<i>5-119-2</i>				
<i>d</i> -form	75.0	73.4 ± 0.5	0.7	-2.1
<i>l</i> -form	25.0	26.6 ± 0.5	1.9	+6.4
<i>5-119-3</i>				
<i>d</i> -form	50.0	50.5 ± 0.3	0.6	+1.0
<i>l</i> -form	50.0	49.5 ± 0.3	0.6	-1.0
<i>6-13-2</i>				
<i>d</i> -form	65.0	64.6 ± 0.4	0.6	-0.6
<i>l</i> -form	35.0	35.4 ± 0.4	1.1	+1.1
<i>6-13-3</i>				
<i>d</i> -form	50.0	50.1 ± 0.2	0.4	+0.2
<i>l</i> -form	50.0	49.1 ± 0.2	0.4	-0.2

<sup>a</sup> 70  $\mu$ l amine solution  $\times$  150 mg polymeric benzophenone-DNB, 1 min at RT, elute to 1 ml with mobile phase hexane-ethanol (97:3) at 3 ml/min. Supelco LC-(R)-Naphthyl Urea column, 250  $\times$  4.6 mm I.D., 5  $\mu$ m; 10  $\mu$ l injection  $\times$  0.016 a.u.f.s. at 254 nm.

<sup>b</sup> Relative error (% RE) = [(found - spiked)/spiked]  $\cdot$  100%.

#### *Single-blind achiral analysis of amphetamine in urine using a mixed-bed reactor*

A solution of amphetamine sulphate was spiked into a urine sample (0.1 M NaOH) to a representative concentration of levels found when the substance is abused [28]. The presence of amphetamine in the sample was shown by derivatization with the polymeric benzotriazole-DNB reagent. The derivative retention time matched that of the standard amphetamine-DNBa which had been synthesized earlier. The presence of amphetamine was confirmed by the use of a second labelling reagent, *p*-nitrobenzoyl (pNB). The polymer was tagged with this reagent and used as above to prove the identity of the amphetamine derivative peak, again compared to the retention time of the standard amphetamine-pNBa. To quantitate the amount of amphetamine present in the spiked samples both polymers were simultaneously used. A 1:1 mixture of the two polymeric reagents (pNB-DNB) was prepared and the sample again derivatized. This time, two derivative peaks were formed, indicating reaction of the amphetamine with both polymeric reagents (Fig. 12). A calibration curve of amphetamine from 5 to 50 ppm was prepared in a urine matrix which had been adjusted to contain 60% ACN. Three single-blind spiked samples were prepared in the same manner at concentrations within the standard curve. The standard curve and samples were derivatized using 100  $\mu$ l sample *vs.* 60 mg of the 1:1 labelled polymeric benzotriazoles. Both derivatives were used to quantitate the concentration of amphetamine present (Table VI).

#### *Single-blind analysis of amino acid enantiomeric composition*

To further validate the method with a different class of analyte, an experiment was performed with a known amount of phenylalanine of unknown enantiomeric

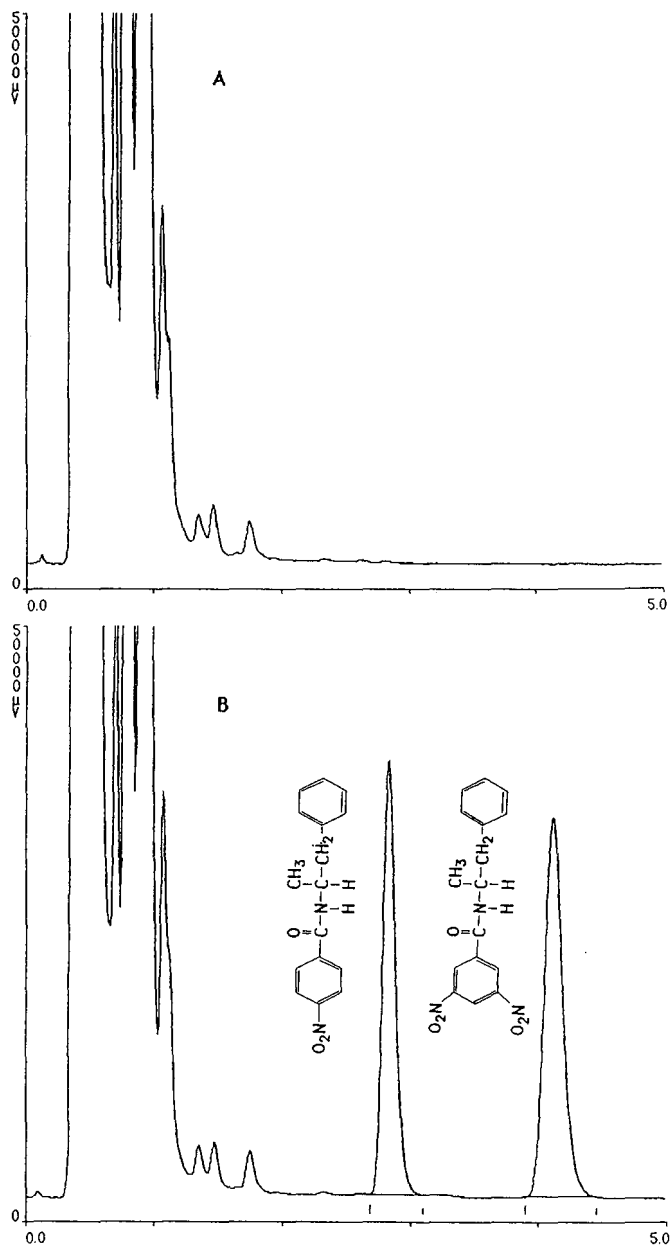


Fig. 12. Mixed-bed derivatization of amphetamine in urine. (A) Urine blank derivatized with polymeric benzotriazole-(pNB/DNB) (1:1); (B) spiked sample (35 ppm) derivatized with polymeric benzotriazole-(pNB/DNB) (1:1). Conditions: derivatization, 100  $\mu$ l sample  $\times$  60 mg polymeric benzotriazole; 2 min at RT, elute with 500  $\mu$ l ACN, dilute with 500  $\mu$ l 0.05 *M* NaOH, injection volume 20  $\mu$ l. Chromatography, LiChrosorb 5  $\mu$ m C<sub>18</sub>, 125  $\times$  4.0 mm I.D., ACN-water (50:50) adjusted to 0.05% (v/v) NH<sub>4</sub>OH at 2.0 ml/min. Retention time in min.



TABLE VI

SINGLE-BLIND SPIKED AMPHETAMINE ANALYSIS USING POLYMERIC MIXED BED REACTOR OFF-LINE<sup>a</sup>

Sample	Spiked concentration (ppm)	Determined (ppm)			
		pNP-amphetamine	RE (%)	DNP-amphetamine	RE (%)
8-84-1	32.3	33.0 ± 0.4	+2.2	34.0 ± 0.5	+5.2
8-84-2	28.2	28.7 ± 0.3	+1.6	29.8 ± 0.8	+5.6
8-84-3	40.4	40.9 ± 0.1	+1.3	42.8 ± 0.5	+5.9

<sup>a</sup> 100  $\mu$ l sample  $\times$  60 mg (pNP/DNB)-benzotriazole (1:1), 2 min at RT, elute with 0.5 ml ACN, dilute with 0.5 ml 0.05 M NaOH, ACN-water (50:50) adjusted to 0.05% (v/v) NH<sub>4</sub>OH at 2 ml/min, 125  $\times$  4.0 mm I.D. LiChrosorb 5  $\mu$ m C<sub>18</sub>, 20  $\mu$ l injection  $\times$  0.016 a.u.f.s. at 254 nm.

composition. The experiment simulated a real-world analysis to determine enantiomeric purity of a lot of amino acid. It was necessary to prepare the methyl ester of the amino acid for chiral recognition. Thus, each lot was alkylated using 2 ml BF<sub>3</sub>-methanol (50:50, w/w) and 20 ml of anhydrous methanol at 70°C for 30 min. The methanol was evaporated under reduced pressure and the residue dissolved in 5 ml of 5 M KOH. The KOH was extracted with 5  $\times$  1 ml aliquots of dichloromethane (DCM), and the DCM extracts were combined and dried over Na<sub>2</sub>SO<sub>4</sub> directly into a 10-ml volumetric flask. The Na<sub>2</sub>SO<sub>4</sub> was washed with a 5-ml aliquot of ACN, and the volumetric flask was brought to the mark with DCM. A 40- $\mu$ l sample of this solution was injected onto 80 mg of the polymeric benzophenone-DNB reagent, and after 3 min at RT the derivative was washed from the reactor cartridge with 1 ml THF-hexane (15:85). A 20- $\mu$ l sample was injected. Separations were performed on a 5- $\mu$ m LC-(S)-Naphthyl Urea 250  $\times$  4.6 mm I.D. column using hexane-DCM-methanol (75:23:2) at 1.5 ml/min. The ratio of enantiomers was determined via area counts of the two enantiomers (Table VII).

TABLE VII

SINGLE-BLIND SPIKED PHENYLALANINE ANALYSIS<sup>a</sup>

Sample	Spiked comp. (%)	Determined (%)	R.S.D. (%)	RE (%)
6-73-2				
<i>d</i> -form	33.6	33.3 ± 0.3	0.9	-0.9
<i>l</i> -form	66.4	66.7 ± 0.3	0.4	+0.5
6-74-1				
<i>d</i> -form	11.2	11.1 ± 0.4	3.6	-0.9
<i>l</i> -form	88.8	88.9 ± 0.4	0.4	+0.1
6-74-2				
<i>d</i> -form	11.2	11.2 ± 0.2	1.6	-
<i>l</i> -form	88.8	88.8 ± 0.2	0.2	-

<sup>a</sup> 40  $\mu$ l sample  $\times$  80 mg polymeric benzophenone-DNB, 3 min at RT, to 1 ml of THF-hexane (15:85), hexane-DCM-methanol (75:23:2) at 3 ml/min. Supelco LC-(S)-Naphthyl Urea column, 250  $\times$  4.6 mm I.D., 20  $\mu$ l injection  $\times$  0.004 a.u.f.s. at 254 nm.

*Comparison of chiral resolution of urea vs. amide derivatives of d,l-norephedrine*

The 3,5-dinitrobenzamide and 3,5-dinitrophenylurea derivatives of *d,l*-norephedrine were synthesized via the solution-phase reactions of *d,l*-norephedrine with

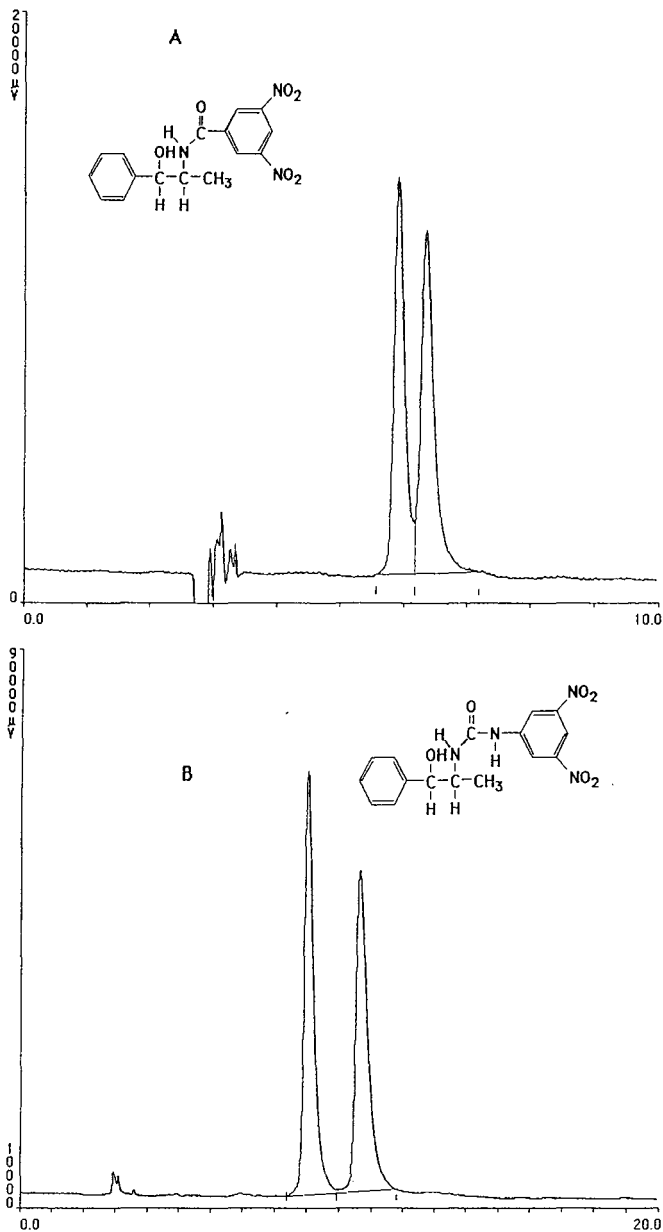


Fig. 13. Comparison of chiral resolution of the standards of the (A) 3,5-dinitrobenzamide and the (B) 3,5-dinitrophenylurea of *d,l*-norephedrine. Conditions: 40 ppm each in mobile phase, injection volume 10  $\mu$ l. Chromatography, 5- $\mu$ m LC-(*S*)-Naphthyl Urea 250  $\times$  4.6 mm I.D., methyl-*tert*-butyl ether (MtBE)-ACN-methanol (92:7:1) at 1.0 ml/min. Retention time in min.

3,5-dinitrophenylacetylazide (DNPAA) and DNBCl, respectively. The dinitrophenyl-urea was formed by decomposition of the DNPAA at 80°C in toluene to form dinitrophenylisocyanate *in situ* [29]. The *d,l*-norephedrine was added to this solution and allowed to react for 30 min. The urea was isolated by rotary evaporation and recrystallized from methanol–water. The derivatives were purified via recrystallization and a 40-ppm solution of each was prepared in the mobile phase. The chiral resolution of each under identical separation conditions was determined (Fig. 13).

## RESULTS AND DISCUSSION

We describe here a solid-phase approach for the derivatization of nucleophiles for improved separation and detection in HPLC with UV detection. Two polymeric reagents have been prepared by modifying commercially available polymeric supports. The first polymeric reagent contained an *o*-nitrobenzophenone activated ester linkage which had been proven useful for on- and off-line derivatizations of amines and related nucleophiles. The second polymeric reagent contained a benzotriazole ester, which was > 2 orders of magnitude more reactive towards nucleophiles [25]. This was due to the polymeric matrix which differed from the first reagent in structure as well as mesh size, surface area and possibly pore size. This reagent allowed for enhanced derivatization of less nucleophilic species, such as amino acids and amino alcohols. It was, however, sensitive to moisture and could not be used on-line for HPLC derivatizations [6]. A comparison of the reactivity of the two polymers is made in this paper, but we have not compared specific rate constants. We are currently synthesizing new batches of both polymers from the same polystyrene–divinylbenzene matrix and a true comparison of rate constants is forthcoming [30].

### *Synthesis/characterization of derivatives*

For true calculations of the percent conversion of analytes, the expected derivatives from the solid-phase reactions with amine substrates were synthesized on a preparative scale. This allowed knowledge of the chromatographic behavior of the derivatives, as well as the efficiency of conversion of analyte to derivative. The derivatives of amines, amino acids and amino alcohols were synthesized via solution phase techniques and then characterized for physical and spectral purity. Derivatives which contained a secondary amide, obtained from a primary amine analogue, had a maximum at 207 nm. Those containing a tertiary amide, had a maximum at 233 nm. For HPLC determinations, the UV wavelength used was 254 nm, which provided good sensitivity for both 2° and 3° amides.

### *Characterization of the polymeric reagents*

*Hydrolysis.* The polymers were characterized via a hydrolysis procedure, which quantitatively hydrolyzed the ester groups, as well as by elemental analysis. The hydrolysis procedure afforded the absolute amount of analytical label covalently attached to the polymeric benzophenone or the polymeric hydroxybenzotriazole. The benzoic acid released from the polymers under high pH conditions, was quantitated via HPLC using external standard calibration. The hydrolysis procedure for the benzophenone was performed with a benzoyl, not 3,5-dinitrobenzoyl, moiety attached to the polymer. A significant amount of the 3,5-dinitrobenzoate anion underwent

decarboxylation under conditions of the experiment. Unsubstituted benzoyl chloride (BCl) was used to tag the polymer under the assumption that the two different acid chlorides would add to the polymer to the same extent. The BCl-tagged polymer was hydrolyzed and the benzoic acid generated, then quantitated. The recovery of benzoic acid from the hydrolysis procedure was constant at  $96.1 \pm 0.4\%$ , from 30 min to 2 h. This suggested that none of the benzoic acid released from the polymer was lost. The amount of benzoic acid found was a true representation of the amount originally covalently attached to the polymer (Table I).

The polymeric hydroxybenzotriazole was tagged with *o*-acetylsalicyloyl chloride, washed and dried prior to the loading determination. The hydrolysis procedure was performed previously and included a liquid-liquid extraction procedure [6]. The amount obtained for the polymeric hydroxybenzotriazole was roughly one half of the loading of the polymeric benzophenone (Table I).

*Elemental analysis.* The elemental analysis of the polymeric benzophenone was performed on the virgin polystyrene, the intermediate polymeric phenol and the final reagent which had been acylated with DNBCl. Though the reactivity of the polymers acylated with BCl and DNBCl would be expected to be different due to the inductive effects of the nitro groups in the 3,5-DNB label, the two acid chlorides added to the polymer in nearly equivalent amounts as indicated by the agreement between hydrolysis and elemental analysis data (Table I). The quantitative conversion of the polymeric *p*-chloro intermediate to the benzophenone was indicated by the lack of chlorine. From the difference in nitrogen content in the starting polystyrene and the polymeric benzophenone intermediate, the absolute loading possible, if all polymeric benzophenone sites were converted to the active ester, was calculated to be 1.9 mmol/g. The difference in nitrogen content between the polymeric phenol and the final analytical reagent gave the amount of label which was covalently attached to the solid-phase reagent. The elemental analysis data indicated 30% of the phenol sites were esterified. The reason for the unlabelled sites may be a combination of incomplete acylation of accessible phenol sites, hydrolysis of the activated ester during the washing procedure, and phenol sites within the pores of the polymer which were sterically inaccessible to the DNBCl. The loading obtained, however, still created a local molar excess of labeling reagent of >350-fold for ppm concentrations of analyte.

The elemental analysis of the polymeric hydroxybenzotriazole reagent was performed using only the starting polystyrene and the final reagent tagged with an *o*-acetylsalicyloyl group [6]. The percentage of each element was calculated based on the hydrolysis data of 0.31 mequiv. *o*-acetylsalicyloyl/g polymer. The calculated percentages matched closely the actual percentages of each element present, which suggested agreement between hydrolysis data and elemental analysis data for the polymeric hydroxybenzotriazole (Table I).

#### *Regeneration of polymeric reagents*

Regeneration of the polymeric reagents was accomplished by washing with ACN, and retagging with DNBCl. After >50 regenerations, the polymeric benzophenone-DNB still acylated butylamine to over 90% completion in <60 s. After two years, the polymeric hydroxybenzotriazole was washed with ACN and tagged. The reagent showed very high reactivity for amines, amino alcohols and amino acids. This corroborated our theory that the polymeric intermediates were totally regenerable and only the final tagging reaction need be repeated.

### *On-line derivatization*

Only the polymeric benzophenone–DNB was used on-line for real-time or delayed conversion of the amine analogues to the corresponding amides. The solvent used for on-line derivatizations was the mobile phase or, at times, a single component of the mobile phase. The solvents used for optimal percent derivatizations had to be chosen with the separation scheme in mind. Again, ACN-, THF- and DCM-containing mobile phases offered the highest percent of conversions. Not unexpectedly, the solvents which yielded the highest percent of conversions, also led to increased reactor bleed and reduced lifetime. The average useful analytical lifetime of the reactor was one day's work; the reactor had to be dismantled and repacked at the beginning of each day for efficient, reproducible results.

For on-line derivatizations in reversed-phase solvents, a dual-mobile-phase system was configured in which only anhydrous organic solvent flowed through the reactor (Fig. 2) [5]. This was necessary due to the reduced lifetime of the polymeric benzophenone–DNB in aqueous solutions. The analytes were injected in pure ACN and were passed through the reactor at low flow-rates and elevated temperatures. The derivatives formed on-line were preconcentrated on the head of the analytical column by forming an initially weak isocratic mobile phase. When the derivatives had left the reactor column, the gradient was increased to remove the derivatives from the analytical column. In this manner, all band broadening contributions prior to the analytical column were negated. While in theory very large injection volumes could be used, only 20- $\mu$ l injections were attempted. The on-line derivatization of three amines, morpholine, *n*-propylamine and *n*-butylamine, was performed using two different solvent systems. The first was a 1:1 mixture of ACN and THF. The anhydrous organic contained a 1:1 mixture of these solvents, and the aqueous pump contained 10% of the 1:1 organic mixture. This was done because of the difference in reactivity in THF compared to ACN. The derivatives were more easily formed in solvents which were partially or wholly ACN (Fig. 3).

For normal-phase on-line derivatizations, a single pump was configured due to the inability of the system to effectively precipitate the derivatives at the head of the chiral column. The polymeric benzophenone–DNB was more stable towards normal-phase solvents due to their non-polar, anhydrous nature. It was found that the polymeric benzophenone–DNB effectively acylated alcohols which were used as polar modifiers, and these had to be substituted with other non-nucleophilic polar modifiers. The amount of time the reaction was allowed to continue could be chosen through a choice of flow-rate in real-time derivatizations, or the amount of time the analyte was allowed to reside within the reactor under bypass conditions (Fig. 2). The real-time derivatizations gave less baseline disturbance and more symmetric peak shapes. The baseline disturbance was understandable, since a small amount of analytical label was constantly bleeding through the system due to the instability of the reagent. To switch the reactor on- and off-line, caused a break in this constant bleed. The better symmetry of the peaks was due to reduced diffusion within the reactor under steady flow conditions. When the analyte was trapped, the heat from the water bath caused thermal convection inside the reactor which led to diffusional band broadening. Interestingly, less reactive polymeric reagents yielded more symmetric derivative peaks in the bypass mode than for real-time conversions [31]. With less reactive polymers, diffusional band broadening was not as important as reaction band broadening. While

less reactive, these polymeric reagents proved useful for the on-line conversion of many pharmaceutically important amines [32]. Another factor in the symmetry of the derivative peaks was the kinetics of reaction. Slow reaction kinetics with a moving analyte will lead to what is termed, "reaction band broadening" which means that the analyte plug experiences derivatization throughout the length of the polymeric reactor, instead of instantaneous derivatization. This would appear most noticeably for real-time derivatizations at higher flow-rates or, as mentioned, with less reactive polymers [33]. This was noticed for the injected amphetamine *vs.* the injected standard, amphetamine-DNBa (Fig. 5). The standard had some asymmetry due to void volume and eddy diffusion band broadening, but the derivative peak tailed more so, indicating reaction band broadening had also occurred.

For on-line derivatizations, the temperature of reaction was raised to enhance the rates. Since kinetics are based on activation energy, concentration of reactants and temperature, higher temperatures yielded higher overall conversions. The increase in temperature had a two-fold effect; it raised the energy of the reactants closer to the activation energy of the tetrahedral intermediate, and it decreased the viscosity of the solution, increasing mass transfer to and from the active ester sites. For on-line studies, derivatization temperatures of 50–70°C were used, depending on the mobile phase. The optimal temperature was chosen by allowing the injected analyte to flow through the reactor at low flow-rates and determining the increase in derivatization with increases in temperature.

#### *Optimization of off-line derivatization conditions*

*Solvent.* The solvent must be a polar, aprotic, non-nucleophilic solvent of low viscosity to properly stabilize the tetrahedral adduct formed upon nucleophilic addition to the carbonyl carbon. The solvent must be compatible with the separation scheme and the detection mode. The solvent must also swell the polymer, to allow for better mass transfer of analyte into the pores of the polymer. The optimum solvent for derivatization of primary and secondary amines was determined to be ACN [6].

*Temperature and time.* The proper amount of time was determined for amines by plotting the percentage of analyte converted *vs.* time. The carbonyl carbon of the ester linkage is highly activated towards nucleophilic attack, due to the *ortho*-nitro group and the *para*-carbonyl group in the polymeric phenol, which act to delocalize the negative charge on the leaving group. However, activation of the carbonyl center now was due largely to the inductive effect of the two nitro groups in the analytical label. This was determined by a comparison of the reactivity of the same polymeric benzophenol which had been tagged with other reagents such as 9-fluorenylchloroformate and *o*-acetylsalicyloyl chloride. These polymeric reagents were less activated due to the structure of the labelling moiety, and yielded lower percent of derivatizations. Under ambient temperature conditions, the polymeric benzophenone-DNB reacted with a 200-ppm concentration of *n*-butylamine to more than 90% completion within 60 s. This was convenient, and thus, no attempts at optimizing reaction temperature were performed.

The same optimization of time was performed with identical substrate and solvent conditions. The polymeric hydroxybenzotriazole-DNB reagent was more reactive than the polymeric benzophenone-DNB. The rate of acylation of a primary amine, *n*-butylamine, could not be measured at RT. A 10-s derivatization yielded 95%

conversion, while a 5-s derivatization yielded 96%. The reaction was assumed to occur instantaneously. The reaction of diethylamine was slower due to steric hindrance of the nucleophilic center, conversion was 48% in 5 s.

#### *Effect of base catalyst on percent conversions*

The kinetic plot of percent conversion vs. time asymptoted to a constant value after reaching 50% conversion (Fig. 6). At this point, the hydrogen ion generated during the final stage of the addition-elimination reaction was protonating unreacted amines. Addition of TEA scavenged this proton, allowing the reaction to proceed to completion [34]. TEA also deprotonated any residual phenol sites, thus removing a source of hydrogen bonding and possible loss of analyte due to ion-pair formation. This was first noticed when *n*-butylamine and diethylamine were derivatized simultaneously. *n*-Butylamine proceeded to a higher percent conversion, while the percent conversion of diethylamine was reduced. Addition of TEA allowed for the derivatization of three amines simultaneously, without any interaction between the analytes (Fig. 5). Concentrations of the base catalyst in greater than an equimolar amount gave no higher percent derivatizations, but were deleterious due to derivatization of impurities in the TEA. For aqueous derivatizations, the pH was adjusted with hydroxide, which kept the analyte as the free amine. The only drawback was that the analytes and hydroxide were now competing for the same active ester sites. The high molar excess of the derivatizing reagent assured that at pH 11 or lower, this was not a major factor.

#### *pH dependence of derivatization*

The pH dependence was determined using partially aqueous solutions. Borate buffer was adjusted to appropriate pH values and mixed with an equal amount of ACN. The derivatization maximum, 70%, occurred at pH 9.5. At pH 7 the analyte was partially protonated and non-nucleophilic, while at higher pH values there may have been competition of the amine with hydroxide for the active ester sites, and/or alkaline hydrolysis of the derivatized analyte.

#### *Linearity of derivatization with substrate concentration*

Theoretically, the reproducibility of the percentage of derivatization should remain constant, regardless of the concentration of amine. This was true when the polymeric ester was in large molar excess. For 30  $\mu$ l of 200 ppm *n*-butylamine, the immobilized reagent (70 mg) was in 366-fold excess. This was important for standard addition experiments, where additional analyte added must produce a linear response. The linear range of *n*-butylamine was from 10 parts per thousand (ppth) to the detection limit, which for amines derivatized precolumn, off-line, was 1 ppm. Above 10 ppth, the percent derivatization began to drop. The polymer became the limiting reagent at this concentration.

#### *Derivatization characteristics*

*Detection limits.* The high limit of detection was due to the dilution of the analyte as it was extracted from the polymeric matrix, off-line. The injection volume was 20  $\mu$ l; a larger injection volume would have allowed lower concentrations to be detected. A larger amount of analyte injected onto a larger mass of polymer would have

accomplished the same feat. Solid-phase extraction of the analyte using ion-exchange sorbents or ion-pair formation using hexanesulphonic acid and hydrophobic ( $C_{18}$ ) solid-phase extraction could also be used to lower detection limits [35]. Evaporation of the solvent after elution from the solid-phase derivatization cartridge was considered, but this usually leads to a loss in precision. A detection limit of approximately 1 ppm was deemed appropriate for most applications.

#### *Optimization of analyte/reagent ratios*

Ideally, the polymer should remain in at least 40-fold molar excess if derivatization of the analyte is dependent only on concentration of the analyte. When performing off-line reactions, the polymer bed should not be completely wetted with the sample. If this occurred, some of the analyte would be absorbed by the tissue plug and reproducibility of the method would suffer. The ratio of injected volume to mass of polymer used was different for the two polymers and was a function of surface area. The ratio of volume to mass in  $\mu\text{l}/\text{mg}$  for the two polymers was 1:2 for the polymeric benzophenone-DNB and 1.7:1 for the polymeric benzotriazole-DNB. The higher surface area of the polymeric benzotriazole reagent allowed for a smaller mass to adsorb a larger volume of injected analyte.

#### *Reproducibility of the method*

For derivatization off-line of analyte concentrations at  $10 \times$  the detection limit, the reproducibility of derivatization was good. The percent relative standard deviation (R.S.D.) of peak areas obtained was in most cases less than 5%. This, in conjunction with a 2% R.S.D. for injection from a fixed-loop injector, gave good reproducibility for injection volumes of  $\geq 10 \mu\text{l}$ . Thus, reproducibility of the entire method was  $\leq 7\%$  R.S.D.

#### *Achiral analyses*

*Amines.* The achiral analysis of amines was shown for three amines derivatized off-line (Fig. 5). Aliphatic amines are not easily analyzed by HPLC in the absence of derivatization due to their poor molar absorptivity, ionization at neutral pH and poor behavior on silica-based supports. The facile derivatization of these analytes using solid-phase reagents solved these problems, and the final derivatives could be easily detected to low ppm levels. Comparison of the reaction of *n*-butylamine and diethylamine with the two polymers indicated their difference in relative reactivity (Fig. 7).

*Amino alcohols.* Amino alcohols had even less desirable qualities for separation and detection than amines. This was due to the increased intramolecular hydrogen bonding, high water solubility and lower vapor pressure. Thus, even GC analyses are not effective in the absence of derivatization. The polymeric benzophenone-DNB reagent reacted slowly with these compounds, due to intramolecular hydrogen bonding which slowed mass transfer to the polymeric surface. For a homologous series of amino alcohols this meant that the nucleophilicity of the amine group increased as the carbon chain separating the alcohol oxygen and the amine increased. This was due to inductive effects of the electronegative oxygen, which removed electron density from the nitrogen atom. However, viscosity increased with chain length, due to intramolecular hydrogen bonding, which was possible when the chain length was  $> 3$ .



The polymeric benzophenone-DNB accomplished a 15% derivatization of ethanolamine at 75°C for 10 min, while the polymeric benzotriazole-DNB accomplished a 96% conversion in under 2 min at RT (Fig. 8).

*Amino acids.* Amino acids were slow to undergo derivatization with either reagent due to their zwitterionic nature at neutral pH. For most amino acids, at pH 10 the carboxyl group was ionized, leaving the amine group unprotonated and nucleophilic. However, the hydration sphere around the carboxyl group slowed mass transfer to the polymer, and electron induction from the carboxyl group lowered the nucleophilicity of the amine. Methionine and phenylalanine were dissolved in ACN-0.05 M NaOH (80:20) and reacted with both polymeric reagents. The polymeric benzophenone-DNB reagent derivatized both amino acids 2% in 2 min at RT while the polymeric benzotriazole-DNB reagent derivatized both amino acids *ca.* 25%. The separation of valine, methionine, phenylalanine and tryptophan, derivatized using the polymeric benzotriazole-DNB reagent off-line, showed a hydrolysis peak due to reaction of the hydroxide ions (Fig. 9). The hydrolysis product, 3,5-dinitrobenzoate anion, was retained due to pH suppression of the mobile phase. Use of a gradient would have yielded better resolution and smaller peak volumes; isocratic conditions, however, were sufficient.

*Amino acid methyl esters.* The derivatization of amino acid methyl esters yielded higher percent derivatizations, since the amine group was more accessible. The methyl ester hydrochlorides were neutralized, solid-phase extracted from solution, and eluted into ACN. Using the polymeric benzotriazole-DNB for 2 min at RT, the percent derivatization of phenylalanine and methionine was 75%. A better separation from early-eluting compounds was obtained, since the methyl esters were more hydrophobic. In addition, the hydrolysis peak was not as severe since there was no pH suppression (Fig. 10). The hydrolysis peak was removed in subsequent analyses by using a mobile phase with ACN-water (45:55) adjusted to 0.05% (v/v) NH<sub>4</sub>OH. Again, a gradient system would be necessary for analysis of all amino acids, and these amino acid methyl esters were chosen to show efficacy of the methodology.

### *Chiral analyses*

The derivatization of chiral analytes with an achiral  $\pi$ -acid label, allowed for direct chiral recognition on Pirkle brush-type stationary phases [16-18]. All chiral work was performed in normal phases, because solvation of the chiral analytes with water obscured the 1:1 (analyte-stationary phase), 3-point molecular recognition. The use of a  $\pi$ -acid-labelled analyte and a  $\pi$ -base stationary phase, offers higher resolution of enantiomers than the opposite logic. In addition,  $\pi$ -acid derivatizing reagents are more powerful acylating reagents, and allow for facile conversions of weak nucleophiles. Thus, the use of a  $\pi$ -acid immobilized reagent seemed justified.

The off-line derivatization of chiral amines was accomplished using the polymeric benzophenone-DNB to exemplify the usefulness of the analytical methodology.  $\alpha$  Values for some substrates were as high as 1.8 and this recognition allowed for sensitive measurements of enantiomeric excess. Although all chiral amines analyzed were less than 100% optically pure, most contained less than 1% of the other isomer (Table II). The 3,5-dinitrobenzamides of secondary amines have no proton on the amide nitrogen and it appeared that this hydrogen bonding with the stationary phase was important for chiral recognition. None of the secondary amines were baseline

resolved as the 3,5-dinitrobenzamides. Generally, these compounds were reacted with 3,5-dinitrophenylisocyanate in solution to form a dinitrophenyl urea [29]. The separation of *d,l*-norephedrine as the 3,5-dinitrobenzamide vs. the 3,5-dinitrophenyl urea derivative gave an indication of the effect of the urea's enhanced recognition (Fig. 13).

Derivatives of the amino alcohols did not separate well, due to the achiral interactions of the alcohol group with the stationary phase.  $\alpha$  Values ranged from 1.0 to 1.2. The compounds studied did not contain an aromatic center, which enhances the recognition through  $\pi$ - $\pi$  interactions and increased steric bulk of the ligand. The distance of the chiral center from the site of acylation also had a profound effect on the recognition. As the chiral site moved further from the  $\pi$ -acid label, recognition became less due to a poorer fit of the necessary sites of interaction with the stationary phase (*i.e.*, dipole interaction, hydrogen bonding and steric fit).

Chiral recognition of amino acid methyl esters was enhanced due to dipole interaction of the carbonyl group adjacent to the chiral carbon. Only tryptophan methyl ester was found to be 100% optically pure (Tables III and IV). The detection limit of enantiomeric excess was assumed to be  $\leq 0.1\%$  based on the detection limit of *d*-valine methyl ester, which showed 0.18% optical impurity. This allowed for approximately 0.06% to be detected at a signal-to-noise ratio of 2 (Fig. 11). The separation values for many of the amino acid methyl esters were comparable to values obtained with similar chiral stationary phases [36,37].

#### *Single-blind spiked chiral analysis of amphetamine*

Artificial spiked samples in ACN-0.1 M NaOH (50:50) of *d,l*-amphetamine sulphate were prepared at different enantiomeric compositions. Analysis of the samples involved injection of the analyte solution onto the polymeric benzophenone-DNB off-line, and elution of the derivatives after a set amount of time. Injection of the solution containing the derivatives yielded the enantiomeric ratio of the amphetamine enantiomers from peak areas (Table V).

#### *Single-blind achiral analysis of amphetamine in urine using a mixed-bed reactor*

The analysis of amphetamine spiked into urine was accomplished using a 1:1 molar mix of polymeric benzotriazole-(pNB/DNB) off-line. Quantitation was performed via comparison to an external-standard calibration plot which was obtained from known amounts of amphetamine, spiked into the same urine matrix. The pNB derivative of amphetamine was more accurate than the DNB derivative, possibly due to matrix coelution. This possibility was negated since there was no peak present in the blank at that retention time. Also, the standard curve should have accounted for that problem, since it was prepared in the same matrix. We are uncertain as to the determinant error. Numbers for each derivative were within an acceptable percent relative error of the true amount (Table VI and Fig. 12).

#### *Single-blind analysis of enantiomeric composition of phenylalanine*

This experiment was designed to show the validity of the approach to a real-world lot of amino acid which could be used for pharmaceutical preparations or peptide synthesis. It also proved a lack of racemization inherent in the methodology. The phenylalanine was alkylated, extracted and derivatized off-line using the

polymeric benzophenone-DNB reagent. Chiral analysis was performed using peak areas of the enantiomers. Excellent agreement was seen between the spiked ratios and those determined using off-line solid-phase derivatization followed by chiral chromatography (Table VII).

## CONCLUSIONS

We described two polymeric reagents useful for the conversion of nucleophilic substrates to more detectable species for HPLC-UV detection. These derivatives were amenable to reversed- or normal-phase chromatography, and the polymers generated derivatives which were amenable to Pirkle-type enantioselective separations. In previous work, the derivatives had been engineered to contain a chiral center, in which case derivatives of enantiomeric analytes were separated as diastereomers on achiral stationary phases [7]. This approach was shown to be a viable alternative to solution-phase derivatizations for indirect enantiomeric recognition. However, the preferred approach to analysis of chiral analytes is direct enantiomeric recognition on a chiral stationary phase, and the use of a polymeric reagent which imparted an achiral tag to the analyte has now allowed for this. Sensitive, facile determinations of enantiomeric excess for chiral analytes has been shown possible using these solid-phase reagents. The use of a polymer containing more than one labelling moiety yielded additional information about an analyte in a complex matrix. Future work will include the detection of catecholamine metabolites in serum and/or urine to further exemplify the utility of the methodology.

## ACKNOWLEDGEMENTS

This work was supported, in part, by an unrestricted grant from Pfizer, Inc., Pfizer Central Research, Analytical Research Department (G. Forcier and K. Bratin), Groton, CT, an NIH-Biomedical Research Support Grant to Northeastern University (S. Fine), No. RR07143, Department of Health and Human Resources (DHHS), and a research and development contract from Supelco, Inc. (J. Crissman and B. Feibush), Division of Rohm & Haas Corporation, State College, PA. The Dynamax software system for chromatographic data acquisition, storage and manipulation was donated to NU from Rainin Instruments, Inc., Berkeley, CA (D. Schmidt, Jr.). We are grateful for all of the financial and instrumental support provided the University in pursuit of the work described.

Various colleagues at Northeastern University have collaborated with the authors in method development and validation. Single-blind spiked samples were prepared by J. R. Mazzeo and F.-X. Zhou. Special gratitude is due to C.-X. Gao for synthesis of the polymeric benzotriazole reagent. Some of the amino alcohol and amino acid dinitrobenzamide standards were prepared by S. Lin. Other colleagues who have shown interest and who have contributed to the work through discussions include C.-X. Gao and S. C. Krzysko. Many thanks are due to Thomas Doyle of the FDA in Washington DC for stimulating correspondence, as well as donation of some of the pharmaceuticals.

This is publication number (455) from The Barnett Institute at Northeastern University.

## REFERENCES

- 1 J. F. Lawrence and R. W. Frei, *Chemical Derivatization in Liquid Chromatography*, Elsevier, Amsterdam, 1977.
- 2 G. G. Guilbault, *Analytical Uses of Immobilized Enzymes*, Marcel Dekker, New York, Basel, 1984.
- 3 S. T. Colgan and I. S. Krull, in I. S. Krull (Editor), *Reaction Detection in Liquid Chromatography*, Marcel Dekker, New York, 1986, p. 227.
- 4 M. V. Shambhu and G. A. Digenis, *J. Chem. Soc. Chem. Comm.*, (1974) 619.
- 5 S. T. Colgan, I. S. Krull, C. Dorschel and B. Bidlingmeyer, *J. Chromatogr. Sci.*, 26 (1988) 501.
- 6 C.-X. Gao, T.-Y. Chou, S. T. Colgan, I. S. Krull, C. Dorschel and B. Bidlingmeyer, *J. Chromatogr. Sci.*, 26 (1988) 449.
- 7 T.-Y. Chou, C.-X. Gao, N. Grinberg and I. S. Krull, *Anal. Chem.*, 61 (1989) 1548.
- 8 L. Nondek, R. W. Frei and U. A. Th. Brinkman, *J. Chromatogr.*, 282 (1983) 141.
- 9 C.-X. Gao and I. S. Krull, *Biochromatogr.*, 4 (1989) 222.
- 10 J. M. Rosenfeld, Y. Shahin and E. Y. Osei-Twum, *Anal. Chem.*, 58 (1986) 3044.
- 11 R. W. Souter, *Chromatographic Separations of Stereoisomers*, CRC Press, Boca Raton, FL, 1985, Ch. 3.
- 12 D. E. Drayer, in I. W. Wainer and D. E. Drayer (Editors), *Drug Stereochemistry*, Marcel Dekker, New York, 1988, p. 209.
- 13 M. F. Balandrin, J. A. Klocke, E. S. Wurtele and W. H. Bolliger, *Science (Washington D.C.)*, 228 (1985) 1154.
- 14 H. Ockenfels and F. Kohler, *Experientia*, 26 (1970) 1236.
- 15 C. E. Dalgleish, *J. Chem. Soc.*, 37 (1952) 3940.
- 16 W. H. Pirkle and D. W. House, *J. Org. Chem.*, 44 (1979) 1957.
- 17 W. H. Pirkle and J. M. Finn, *J. Org. Chem.*, 46 (1981) 2935.
- 18 W. H. Pirkle and T. C. Pochapsky, in J. C. Giddings, E. Grushka and P. R. Brown (Editors), *Advances in Chromatography*, Vol. 27, Marcel Dekker, New York, 1987, Ch. 3.
- 19 M.-Y. Chang, L.-R. Chen, X.-D. Ding, C. M. Selavka, I. S. Krull and K. Bratin, *J. Chromatogr. Sci.*, 25 (1987) 460.
- 20 C.-X. Gao, D. Schmalzing and I. S. Krull, *Biomed. Chromatogr.*, in press.
- 21 R. L. Shriner, R. C. Fuson, D. Y. Curtin and T. C. Morrill, *The Systematic Identification of Organic Compounds*, Wiley, New York, 6th ed., 1980, Ch. 6.
- 22 D. Knapp, *Handbook of Analytical Derivatization Reagents*, Wiley, New York, 1979.
- 23 G. E. Pollock, D. O'Hara and O. L. Hollis, *J. Chromatogr. Sci.*, 22 (1984) 343.
- 24 K. Barlos, D. Papajoannou and D. Theodoropoulos, *J. Org. Chem.*, 47 (1982) 1324.
- 25 B. J. Cohen, H. Karoly-Hafeli and A. J. Patchornik, *J. Org. Chem.*, 49 (1984) 924.
- 26 R. Kalir, A. Warshawsky, M. Fridkin and A. J. Patchornik, *Eur. J. Biochem.*, 9 (1975) 55.
- 27 K. B. Wiberg, *Laboratory Technique in Organic Chemistry*, McGraw-Hill, New York, 1960, p. 248.
- 28 E. R. Barnhart (Editor), *Physicians' Desk Reference*, Medical Economics, Co., Oradell, 39th ed., 1985, p. 1960.
- 29 W. H. Pirkle, G. Mahler and M. H. Hyun, *J. Liq. Chromatogr.*, 9 (1986) 443.
- 30 A. J. Bourque and I. S. Krull, in preparation.
- 31 C.-X. Gao, T.-Y. Chou and I. S. Krull, *Anal. Chem.*, 61 (1989) 1538.
- 32 C.-X. Gao and I. S. Krull, *J. Pharm. Biomed. Anal.*, 7 (1989) 1183.
- 33 L. Nondek, U. A. Th. Brinkman and R. W. Frei, *Anal. Chem.*, 55 (1983) 730.
- 34 T. H. Lowry and K. S. Richardson, *Mechanism and Theory in Organic Chemistry*, Harper & Row, New York, 2nd ed., 1981, p. 645.
- 35 R. M. Patel, J. R. Benson and D. Hometchko, *LC · GC*, 8 (1990) 152.
- 36 N. Oi, M. Nagase, Y. Inda and T. Doi, *J. Chromatogr.*, 259 (1983) 487.
- 37 N. Oi, M. Nagase, Y. Inda and T. Doi, *J. Chromatogr.*, 265 (1983) 111.

CHROM. 22 801

## **Automated phenylthiocarbamyl amino acid analysis of carboxypeptidase/aminopeptidase digests and acid hydrolysates<sup>a</sup>**

RICHARD S. THOMA and DAN L. CRIMMINS\*

*Howard Hughes Medical Institute, Core Protein/Peptide Facility, Washington University School of Medicine, 660 South Euclid, Box 8045, St. Louis, MO 63110 (U.S.A.)*

(Received July 24th, 1990)

---

### ABSTRACT

A fully automated exopeptidase digestion procedure for the partial determination of N- and C-terminal peptide/protein sequence is described. The digestion of various substrates with aminopeptidase M, carboxypeptidase A, P or Y was accomplished with the Varian 9090 autosampler's robotic automix routines. The released free amino acids, in addition to free amino acids from acid hydrolysates, were derivatized with phenylisothiocyanate in an automated fashion and subsequently chromatographed on a C<sub>18</sub> column for separation and quantitation. The advantages of automating this precolumn phenylisothiocyanate derivatization are the virtual elimination of sample manipulation errors and very reproducible data due to the precise control of the reaction conditions both of which, facilitate the interpretation of the exopeptidase reaction kinetic data.

---

### INTRODUCTION

Analysis of C- and N-terminal sequences using exopeptidases can provide important information about the primary structure of proteins and peptides. Methods involving the digestion of a protein or peptide with carboxypeptidases and aminopeptidases and subsequent identification of the released amino acids by reversed-phase high-performance liquid chromatography (RP-HPLC) have been employed for such analysis [1,2]. Presently, enzymatic digestion using a carboxypeptidase is the most common method for obtaining C-terminal sequence, although recent work using C-terminal chemical modification appears promising [3,4]. Carboxypeptidase A (CPA) [5,6], P (CPP) [7] and Y (CPY) [8] are all used to obtain C-terminal sequence. The number of amino acids sequenced and the rate at which proteolysis occurs is substrate specific. Each carboxypeptidase has a distinct pH optimum, *i.e.*, pH 7.8 for CPA [6], pH 6.0 for CPY [8] and pH 3.7 for CPP [7]. For all three carboxypeptidases, proteolysis drastically slows when a proline residue is encountered. Classical Edman

---

<sup>a</sup> Portions of this work have been presented at the 9th International Symposium on HPLC of Proteins, Peptides and Polynucleotides, Philadelphia, PA, November 6–8, 1989. The majority of the papers presented at this symposium have been published in *J. Chromatogr.*, Vol. 512 (1990).

degradation chemistry is the preferred procedure for obtaining N-terminal sequence [9]. Situations arise however, where labile amino acids {*e.g.*, tyrosine-sulfate (Y[SO<sub>3</sub>]) and methionine-sulfoxide (M[O])} exhibit poor recovery after exposure to the chemistry of the sequencing reaction. In these cases, exopeptidase digestion can be performed, such as with aminopeptidase M (APM) [10].

All exopeptidase reactions require extensive sample manipulation during the digestion and subsequent residue analysis. Since the rate of the digestion reaction is residue specific, precise timed removal of the aliquots is often crucial and may require 5–10 aliquots to obtain reliable sequence information. For each aliquot then, the reaction must first be quenched and then prepared for HPLC analysis. It is apparent that sample manipulation alone, is a major source of error in manual exopeptidase digestion reactions. Several other potential sources of error associated with amino acid analysis are: (i) the derivatization reaction and the derivative stability; (ii) the procedure used to hydrolyze the samples, *e.g.*, acid hydrolysis or proteolysis; (iii) reagent and sample purity; and (iv) the chromatographic system used for peak identification and quantitation [11,12].

We present data which shows that free amino acids obtained from acid hydrolysates can be reproducibly and quantitatively derivatized with phenylisothiocyanate (PITC) in an automated fashion using a heptane extraction procedure [13] to remove excess PITC. In addition, exopeptidase digests (CPA, CPP, CPY and APM) are automated and the liberated amino acids derivatized as above, thereby minimizing sample manipulation errors frequently encountered with these reactions. Automating this entire procedure aided in the interpretation of the resulting kinetic data. Furthermore, the relevant reaction parameters can be tested, *e.g.*, enzyme/substrate ratio, incubation time, simply by programming the 9090 autosampler for overnight runs thus allowing for “next-day” optimization. Several other researchers have successfully automated the precolumn derivatization procedure primarily for hydrolysates using PITC [14–17], 9-fluorenylmethyl chloroformate (FMOC-Cl) [18–23], *o*-phthaldehyde (OPA) [22,23] and 5-dimethylaminonaphthalene-1-sulfonyl chloride (Dns-Cl) [24].

## EXPERIMENTAL

### *Chemicals and reagents*

CPY (lot No. 851101092) and APM (lot No. 840629002) were Pierce (Rockford, IL, U.S.A.) products and Boehringer Mannheim (Indianapolis, IN, U.S.A.) was the supplier for CPA (lot No. 11201822-22) and CPP (lot No. 10109521-01). Peptides and proteins were purchased from Sigma (St. Louis, MO, U.S.A.) or Peninsula Labs. (Belmont, CA, U.S.A.) and used without further purification. Radio-labeled [<sup>3</sup>H]-proline (30.8 Ci/mmol) and [<sup>3</sup>H]leucine (153 Ci/mmol) were purchased from New England Nuclear (Boston, MA, U.S.A.). The sources of HPLC columns and solvents, amino acid reagents, water purification and additional materials have been described [25,26].

### *HPLC instrumentation and chromatography*

Chromatographic hardware included an Applied Biosystems (Foster City, CA, U.S.A.) 130A separation system (254-nm amino acid analysis) and a Varian (Walnut

Creek, CA, U.S.A.) 9090 autosampler. Data were acquired and analyzed as previously described [25,26]. Radioactivity was determined using a Beckman (Fullerton, CA, U.S.A.) LS7000 scintillation counter.

The solvent program used to effect separation of the phenylthiocarbamyl (PTC) amino acids was a two-step gradient of 7 to 30% B in 10 min followed by 30 to 58% B in the next 10 min at a flow-rate of 0.3 ml/min and column temperature of 37°C with mobile phases 50 mM sodium acetate, pH 5.4 (A) and acetonitrile–water (70:30, v/v) (B).

#### *Exopeptidase digestions*

For each digest one of the following exopeptidase solutions was prepared: CPA (1.0 µg/µl in 0.025 M ammonium bicarbonate, pH 7.8), CPP (0.01 units/µl in 0.1 M acetic acid, pH 4.0), CPY (0.1 µg/µl in 0.025 M ammonium acetate, pH 6.0) or APM (0.01 µg/µl in 0.1 M sodium phosphate, pH 7.0). The reaction was automated using the Varian 9090 autosampler as outlined in Fig. 1B and Table I. Manual digestion reactions were performed under identical conditions to that of the automated procedure. The reaction was started by adding 10 µl of the exopeptidase solution to 90 µl peptide/protein (5–15 µg) solution (same buffer as exopeptidase). Aliquots of 5 µl of the reaction mixture were removed at seven time points (3.5, 6.5, 10.5, 16.5, 25.5, 42.5 and 74.5 min) over 1.5 h. Reactions were quenched by adding 2 µl 1 M HCl (CPA, CPY or APM) or 1 M NaOH (CPP). The resulting solutions were then subjected to precolumn PITC derivatization and amino acid analysis as described below.

#### *Amino acid analysis*

Samples containing norleucine as internal standard were acid hydrolyzed in the vapor phase and derivatized with PITC with slight modifications [25,26] of established procedures [11,27,28]. To a 5–10-µl sample of hydrolysate or exopeptidase digest aliquot was added 40 µl methanol–triethylamine (TEA) (8:1, v/v) followed by 5 µl PITC and incubated for 20 min at room temperature. Excess PITC was extracted with 2 × 15 µl of heptane [13] and the aqueous phase containing the PTC amino acids was diluted with 2 × 40 µl mobile phase A–acetic acid (100:3, v/v) prior to injection (Fig. 1A and Table I).

## RESULTS AND DISCUSSION

#### *Automated PITC derivatization of acid hydrolysates*

Reagent addition, mixing and extraction with the automix feature of the Varian 9090 autosampler permits the amino acid derivatization steps to be automated with no increase in total analysis time. Fig. 1A and Table I present a schematic of the various automix steps and the autosampler programming, respectively, for amino acid analysis. The derivatization procedure follows standard PITC precolumn reaction conditions as outlined in earlier publications [11,27,28] with two modifications. First, there is no provision to dry the sample to remove excess PITC. Heptane has been reported to efficiently extract excess PITC in a manual procedure [13] thus generating a two-phase system. Analogous procedures have been successfully automated for FMOC-Cl precolumn derivatization to remove excess reagent and by-products [18–21]. In our system, the heptane/PITC extract separates to the top layer after

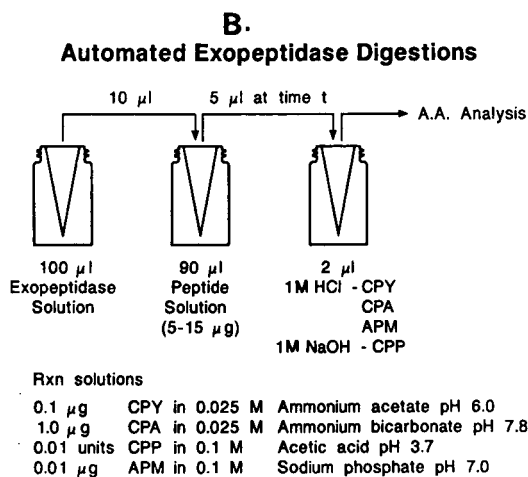
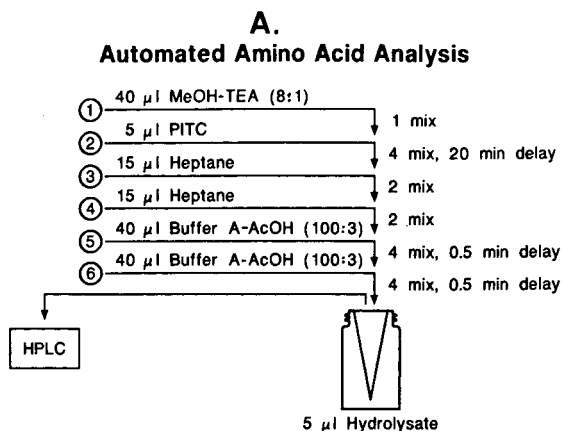


Fig. 1. Schematic layout of the automated derivatization and digestion procedure using the Varian 9090 autosampler. (A) Automated amino acid analysis; (B) automated exopeptidase digestions. See Table I for autosampler programming. MeOH = Methanol; TEA = triethylamine; AcOH = acetic acid; A.A. = amino acid; Rxn = reaction.

thorough mixing with the aqueous solution. This is fortunate since the injection needle adds or removes sample only from the bottom of the vial and thus the PITC in the organic phase will not be injected onto the column. The second modification to the standard PITC reaction conditions required the partial neutralization of TEA and dilution of methanol (Fig. 1A and Table I) which are normally removed from the reaction mixture *in vacuo* [11,27,28]. Failure to dilute these reaction constituents resulted in aberrant chromatography, particularly in the first half of the chromatogram (data not shown). The addition of mobile phase A-acetic acid (Fig. 1A and Table I) completely eliminated this problem and produced an acceptable chromatogram (Fig. 2A). The relative elution order for the PTC amino acids (Fig. 2A) is in



TABLE I  
PROGRAMMING THE VARIAN 9090 AUTOSAMPLER

Sequence line	Method	Position	Next sampling time (min)	Automix
<i>Exopeptidase digestion<sup>a</sup></i>				
1	11	2-1	1.0	D
2	12	1-2	1.0	E
3	13	1-3	2.0	E
4	14	1-4	4.0	E
5	15	1-5	7.0	E
6	16	1-6	15.0	E
7	17	1-7	30.0	E
8	18	1-8	--	E
<i>Amino acid analysis</i>				
9	1	1-1 <sup>b</sup> /1-8	9.0	FABBCC
10	0			

	Automix	Position	Delay time (min)	Transfer volume ( $\mu$ l)	Mix cycles
<i>Automix routines<sup>c</sup></i>					
PITC	A	3-1	20.0	5	4
Heptane	B	3-2	--	15	2
Buffer A-acetic acid (100:3)	C	3-3	0.5	40	4
Exopeptidase	D	2-2	--	10	2
Reaction vial	E	2-1	--	5	0
Methanol-triethylamine (8:1)	F	2-5	--	40	1

<sup>a</sup> The ABI 130 was "double-programmed" so that at the start of the exopeptidase reaction the HPLC was subjected to a 90-min wash cycle. After this mock run, the HPLC system was then ready to accept the first sample (standard H control). Every 43 min thereafter, an exopeptidase aliquot was injected until all seven time points were analyzed. Thus, the total time required to analyze the automated exopeptidase reaction including subsequent PTC-amino acid analysis was about 7 h.

<sup>b</sup> Position 1-1 contains standard H and no enzyme is added to the vial.

<sup>c</sup> The configuration set-up for the autosampler was: tube volume = 0  $\mu$ l; wash cycle volume = 40  $\mu$ l; viscosity factor = 1; and air displacement by the syringe was used to mix the liquids.

agreement with previous data [11,27,28] and up to 90  $\mu$ l out of the 130  $\mu$ l in the aqueous phase can be chromatographed without a serious loss of resolution.

It was important to demonstrate that the PTC-amino acids were quantitatively recovered in the aqueous phase. To this end, [<sup>3</sup>H]leucine and [<sup>3</sup>H]proline were individually added to a standard H mixture and derivatized by the automated procedure. The autosampler was programmed for a 0- $\mu$ l injection so that the two layers could be independently analyzed for radioactivity. Table II shows that more than 98% of the <sup>3</sup>H derivatives was recovered in the aqueous phase. Furthermore, these [<sup>3</sup>H] PTC-amino acids were found to coelute with their corresponding unlabelled counterparts (data not shown).

Prior to the exopeptidase experiments, it was necessary to investigate the

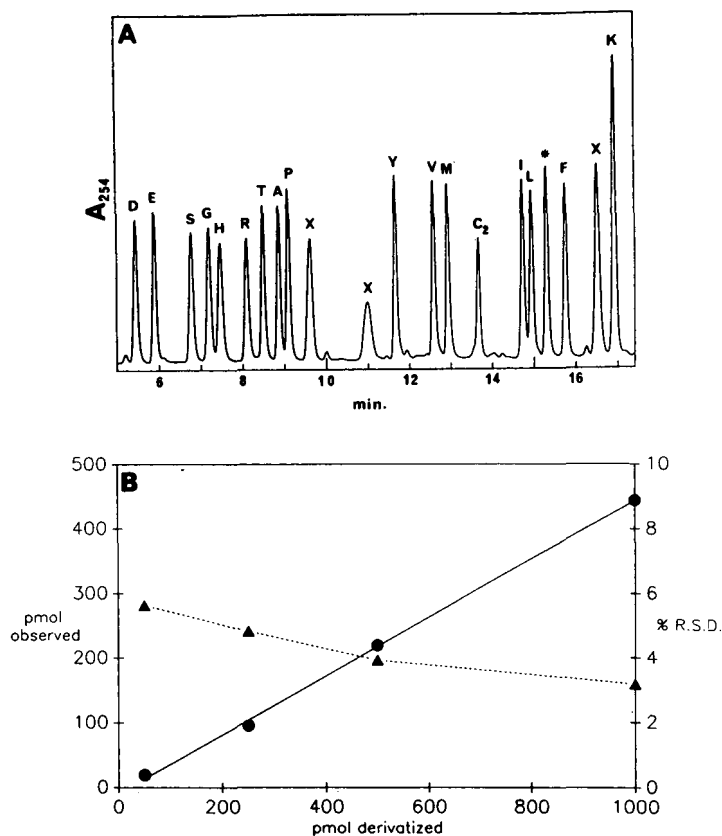


Fig. 2. Chromatogram of PTC-amino acids, and injection linearity and percent relative standard deviation (% R.S.D.) for the automated precolumn PITC derivatization procedure. (A) Chromatogram of PTC-amino acids (Pierce standard H) derivatized at 250 pmol/amino acid and injected at 96 pmol/amino acid monitored at 254 nm (200 mV full scale). The standard single-letter code for the amino acids is used; C<sub>2</sub> = cystine; \* = norleucine; X = reagent-associated peaks. (B) Injection linearity and % R.S.D. for four different standard H concentrations (pmol derivatized) of 50, 250, 500 and 1000 pmol/amino acid. Twelve individual analyses were made at each concentration and both the average observed pmol/amino acid and % R.S.D. were then calculated. ●—● = Average pmol/amino acid observed; ▲—▲ = % R.S.D. for each standard H concentration.

reproducibility of the automated precolumn PITC derivatization procedure and subsequent chromatography and data quantitation. Twelve separate standard H samples each, at four decreasing concentrations (1000, 500, 250 and 50 pmol/amino acid) were subjected to this procedure. Fig. 2B (filled circles) shows the mean result for all 16 amino acids at each of the four concentrations. All four averaged concentrations fall on the expected line when exactly 50  $\mu$ l of the aqueous layer is injected which also indicates that the 50- $\mu$ l loop used in the 9090 autosampler was completely filled. Fig. 2B (filled triangles) also shows the percent relative standard deviation (% R.S.D.) for each of the four concentrations. There was a slightly greater variation from run to run when less material was taken for analysis, 5.63% R.S.D. (50 pmol) vs. 3.18%

TABLE II  
RECOVERY OF TWO PTC-AMINO ACIDS AFTER HEPTANE EXTRACTION

Extraction with heptane (and radioactivity analysis of each phase) as described in Experimental and as illustrated in Fig. 1A and Table I. Five independent samples (100 000 cpm) were analyzed and the average % cpm for each phase calculated, with the range of all five determinations shown in parentheses for the aqueous phase.

	% cpm	
	Aqueous	Organic
[ <sup>3</sup> H]Leucine	98.8 (97.3-99.6)	1.2
[ <sup>3</sup> H]Proline	98.9 (98.5-99.6)	1.1

R.S.D. (1000 pmol). These values are in the range reported for other automated precolumn derivatization procedures [17,19-23]. The % R.S.D. for each of the individual 16 amino acids were determined at each concentration and two of these (50 pmol/amino acid and 1000 pmol/amino acid) are shown in Table III. Not

TABLE III  
PERCENT RELATIVE STANDARD DEVIATION (% R.S.D.) FOR 50 AND 1000 PMOL DERIVATIZED STANDARDS

Twelve separate standard H samples at the indicated concentration were derivatized as described in Experimental and as illustrated in Fig. 1A and Table I. The standard single-letter code for the amino acids is used and the % R.S.D. was calculated for an individual amino acid at a given concentration from these twelve analyses. See also Fig. 2B (filled triangles) for a global average % R.S.D. for other standard H concentrations.

Amino acid	% R.S.D.	
	50 pmol	1000 pmol
D	5.32	2.58
E	4.27	2.28
S	5.05	2.97
G	5.09	2.91
H	4.35	3.43
R	5.50	2.83
T	5.25	3.44
A	5.26	2.67
P	5.51	2.91
Y	5.02	3.95
V	5.36	3.58
M	5.16	2.90
I	6.20	3.47
L	7.98	3.09
F	6.15	3.13
K	8.61	4.66
Average	5.63	3.18

surprisingly, the % R.S.D. for a given amino acid at the 50-pmol level was greater than at 1000-pmol level. The lysine % R.S.D. was noticeably higher for both, which may be due to incomplete reaction at the two potential reactant sites or a recovery problem in the heptane extraction step. The leucine % R.S.D. at the 50-pmol level was appreciably higher than the average. It is unlikely however, that this is the result of the heptane extraction step (Table I).

Peptides and proteins were acid hydrolyzed and the resulting free amino acids derivatized by the automated procedure. Table IV shows the amino acid analysis for three peptides, Leu-enkephalin, bradykinin and angiotensin I and three proteins, myoglobin, concanavalin A and lysozyme. No major differences between the observed

TABLE IV

## AUTOMATED PTC-AMINO ACID ANALYSIS OF PEPTIDE AND PROTEIN ACID HYDROLYSATES

Samples were hydrolyzed as described in Experimental and derivatized as described in the legend to Table III. The amount of sample hydrolyzed was 0.9  $\mu$ g Leu-enkephalin; 2.0  $\mu$ g bradykinin; 2.1  $\mu$ g angiotensin I; 2.7  $\mu$ g myoglobin; 4.2  $\mu$ g concanavalin A; and 2.3  $\mu$ g lysozyme. The standard single-letter code for the amino acids is used and the values corresponding to the observed number of residues are given in parentheses. C and W were not determined. The peptide hydrolysates were diluted/injected such that 1 residue corresponds to about 250 pmol and for the proteins, 1 residue corresponds to about 25 pmol.

Leu-enkephalin			Bradykinin			Angiotensin I		
G	2.0	(2)	S	0.88	(1)	D	1.1	(1)
Y	1.0	(1)	G	0.98	(1)	H	2.1	(2)
L	0.98	(1)	R	2.2	(2)	R	1.1	(1)
F	0.99	(1)	P	2.9	(3)	P	0.97	(1)
			F	2.0	(2)	Y	0.90	(1)
						V	0.99	(1)
						I	0.94	(1)
						L	1.0	(1)
						F	1.0	(1)
Myoglobin			Concanavalin A			Lysozyme		
D/N	10.5	(10)		31.1	(32)		22.1	(21)
E/Q	19.6	(19)		12.4	(12)		5.6	(5)
S	4.8	(5)		28.0	(31)		8.6	(10)
G	14.9	(15)		16.1	(16)		11.4	(12)
H	10.9	(11)		6.1	(6)		1.1	(1)
R	2.3	(2)		6.5	(6)		11.7	(12)
T	6.6	(7)		17.5	(19)		6.5	(7)
A	15.3	(15)		18.4	(19)		11.9	(12)
P	4.3	(4)		10.3	(11)		2.0	(2)
Y	1.8	(2)		6.6	(7)		2.7	(3)
V	6.8	(7)		16.2	(16)		5.9	(6)
M	2.3	(2)		1.8	(2)		2.2	(2)
I	7.6	(9)		13.2	(15)		5.5	(6)
L	16.6	(17)		18.8	(18)		8.0	(8)
F	6.8	(7)		10.7	(11)		3.1	(3)
K	17.5	(19)		12.2	(12)		6.0	(6)

and expected values were found for any of the six samples. The 9090 autosampler was able to perform all the necessary manipulations for the analysis of acid hydrolysates except for the hydrolysis step [14,17].

#### *Automated exopeptidase digestions*

Automated exopeptidase digestions were performed using the automix feature of the Varian 9090 autosampler. Fig. 1B and Table I present a schematic of the automix steps prior to amino acid analysis and the autosampler programming, respectively. The 9090 transfers 10  $\mu$ l of the exopeptidase solution (CPA, CPP, CPY or APM) to another vial containing the substrate to start the reaction. Samples (5  $\mu$ l) are then removed at seven different time points and the reaction was quenched with 2  $\mu$ l 1 M HCl (CPA, CPY or APM) or 2  $\mu$ l 1 M NaOH (CPP). Programming steps for the 9090 autosampler are sequential so that the next sampling time (min) of 1.0, 1.0, 2.0, 4.0, 7.0, 15.0 and 30.0 (Table I) translates to 3.5, 6.5, 10.5, 16.5, 25.5, 42.5 and 74.5-min aliquots in real time. A feature of the 9090 autosampler is that transfers must be directed to a single target vial and at the end of all transfers an injection must occur. For the exopeptidase digests, the reaction is quenched by transferring aliquots from the reaction vial to a third vial containing the quenching agent. We defeated the injection command, which would have resulted in sample loss, by programming 0- $\mu$ l injections after the addition of exopeptidase to the substrate and after the reaction aliquot was transferred to the quenching solution. Each timed aliquot remained in the presence of acid or base until all seven were sampled after which, PITC derivatization proceeded as above. Since each aliquot was derivatized and then immediately chromatographed, the stability of the PTC derivatives was not a concern [11,12].

Examples of several peptide digests are presented to demonstrate the utility of the 9090 autosampler for exopeptidase digests (Figs. 3 and 4). All digests were designed so that the release of one amino acid would be equivalent to 100–400 pmol. Fig. 3A shows a typical CPY digestion of angiotensin I. From these kinetic data, one would predict a C-terminal sequence of F–H–L–COOH, in perfect agreement with this peptide's known sequence. In this example all three amino acids were cleaved at a steady rate resulting in simple interpretation of the kinetic data. Often, C-terminal predictions become more difficult as the number of liberated residues increases. The CPY digestion of renin substrate tetradecapeptide (Fig. 3B) provides such an example by showing the rapid cleavage for the first five C-terminal amino acids. S, Y, V and two residues of L all appear to be cleaved almost simultaneously from the peptide. Careful inspection of the first 20 min of the digestion profile indicated that S is the first amino acid cleaved (data not shown). After S however, no additional sequence could be unambiguously assigned. Decreasing the CPY concentration did not improve this situation.

Fig. 3 C–F shows more examples of peptide digests using other carboxypeptidases. CPA digested two amino acids (I–V–COOH) for gonadotropin releasing hormone (14–26) as illustrated in Fig. 3C and two amino acids (F–M–COOH) for Met-enkephalin (Fig. 3D). In both cases, further digestion was impeded when the enzyme encountered an unfavorable residue [5]. Examples for CPP digestion are shown in Fig. 3E for angiotensin I (F–H–L–COOH) and Fig. 3F for dynorphin A (1–6) (F–L–R–COOH). Again, the rate of cleavage was affected by specific residues [7]. For all the examples presented in Fig. 3 C–F, increasing the enzyme concentration did not materially change the results.

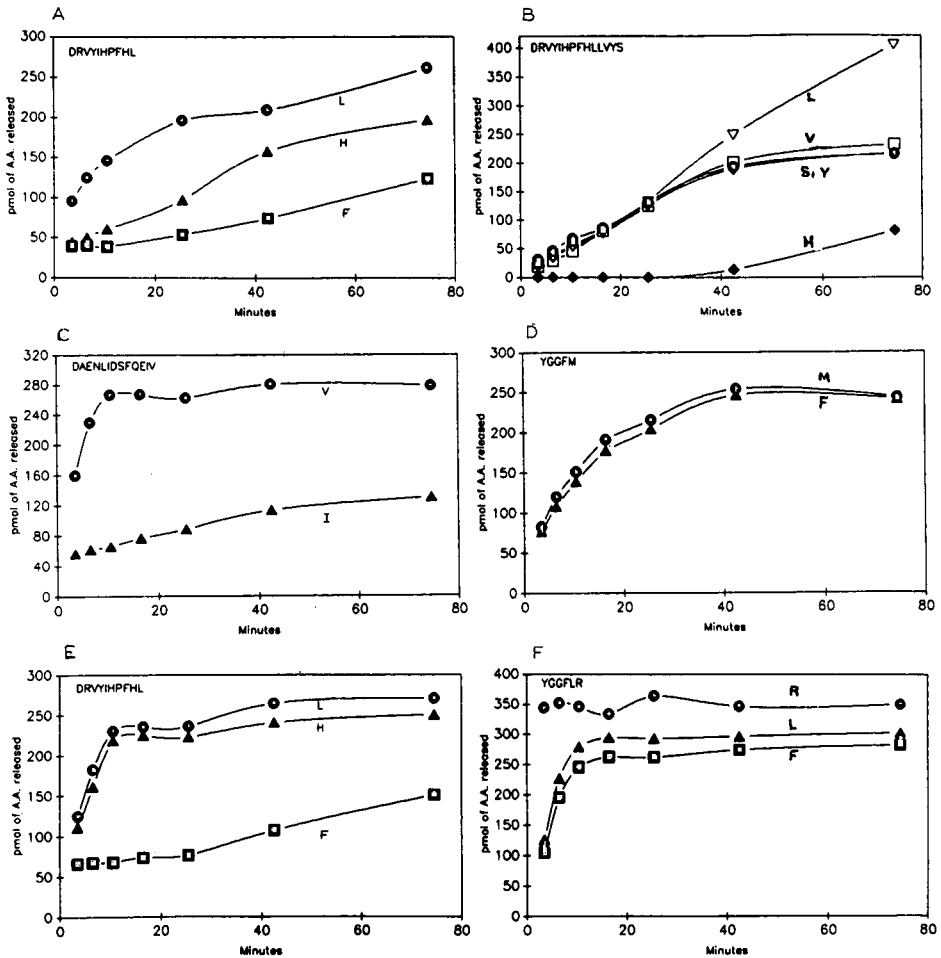


Fig. 3. Kinetic analysis of released amino acids from automated carboxypeptidase digestion of six peptides. (A) Angiotensin I (CPY); (B) renin substrate tetradecapeptide (CPY); (C) human pre-pro-gonadotropin releasing hormone (14-26) (CPA); (D) Met-enkephalin (CPA); (E) angiotensin I (CPP); (F) dynorphin A (1-6) (CPP). The order of released amino acids is indicated by the following symbols: ● = 1st; ▲ = 2nd; ■ = 3rd; ▼ = 4th; ◆ = 5th. Filled symbols indicate a positive sequence assignment while open symbols indicate that this residue could not be assigned in the sequence. The sequence of the peptide, using the standard single-letter code, is located in the top left corner of each plot.

N-Terminal sequencing was accomplished using APM. Fig. 4A presents the kinetic plot of an APM digest of the peptide adrenocorticotrophic hormone (1-10). For this reaction, eight amino acids were released yielding a tentative prediction of  $\text{NH}_2\text{-S-(S, Y)-M-(E, H, R, F)}$ . It becomes increasingly difficult to assign sequence when either multiples of a given residue are released or the total number of liberated residues exceeds about 5.

Peptides with modified amino acids, *e.g.*,  $\text{Y}[\text{SO}_3]$  and  $\text{M}[\text{O}]$  are known to quantitate poorly, if at all, after standard acid hydrolysis [29]. Exopeptidase digestions

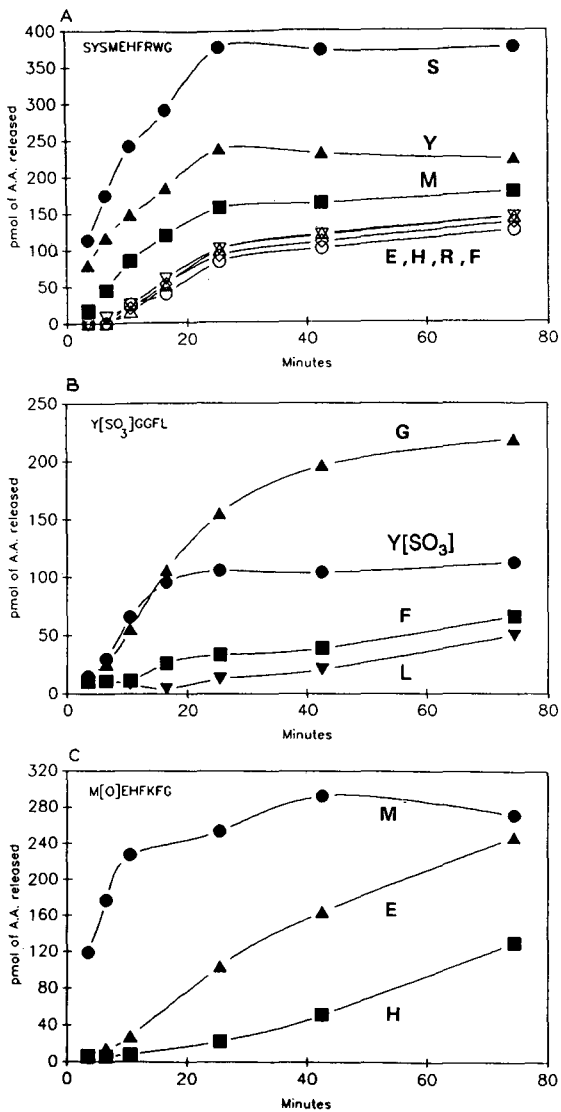


Fig. 4. Kinetic analysis of released amino acids from automated aminopeptidase digestion of three peptides. (A) Adrenocorticotrophic hormone (1-10) (APM); (B) Leu-enkephalin (Y[SO<sub>3</sub>]) (APM); (C) adrenocorticotrophic hormone (4-10) (M[O]) (APM). See Fig. 3 for symbol designation.

provide an alternate means of sequencing and potentially quantitating these residues. Fig. 4B demonstrates an almost complete digest of Leu-enkephalin (Y[SO<sub>3</sub>]) with APM yielding a predicted sequence of NH<sub>2</sub>-Y[SO<sub>3</sub>]-G-G-F-L. In this instance, the concentration of peptide was approximately 100 pmol. Fig. 4C shows the analysis of the modified amino acid M[O] in the peptide adrenocorticotrophic hormone (4-10) (M[O]) after digestion with APM. Sequence prediction for this reaction was NH<sub>2</sub>-M[O]-E-H.

A total of six peptides were digested with each of the four exopeptidases CPA, CPP, CPY and APM by either the fully automated procedure (both digestion and amino acid analysis) or in the totally manual mode (both digestion and amino acid analysis). Table V presents these results for the total number of released amino acids for a specific substrate-enzyme pair and the number of residues unambiguously assigned to the sequence is given in parentheses for each mode of analysis. The number of amino acids cleaved per peptide varied from 0 to 10 and the number of positive assignments ranged from 0 to 4 residues. The results derived from any automated procedure must, as a minimum, be the equal of those obtained from a manual analysis if the automated procedure is to gain acceptance. Furthermore, the automated procedure should be less labor intensive than the manual counterpart and also allow for both rapid analysis and optimization. The data listed in Table V clearly show that the automated exopeptidase procedure (97 total released residues and 36 total positive sequence assignments) is comparable to the manual procedure (89 total released residues and 33 total positive sequence assignments). We interpret this to mean that the automated procedure performs as well as the more labor intensive manual procedure.

It should be emphasized that in the course of this investigation, no attempt was made to use "ideal" substrates which may yield extended sequence information. Rather, we surveyed a broad spectrum of substrates and exopeptidases to evaluate the general utility of the automated procedure. In this regard, our preliminary experiments with automated protein-exopeptidase reactions were not very successful. Few if any residues were liberated for the six proteins tested (myoglobin,  $\beta$ -casein, cytochrome *c*, concanavalin A,  $\beta$ -lactoglobulin and lysozyme) when using the above four exopeptidases. This may be due to poorly accessible termini and future experiments will include the use of denaturants in an attempt to force the reaction. Lastly, in this initial investigation we decided to analyze samples at what we considered to be a comfortable minimum level of 50 to 100 pmol. This amount of material is in the range reported [11,27,28] for successful, routine PITC derivatization. It is fully anticipated that if

TABLE V  
NUMBER OF AMINO ACIDS CLEAVED COMPARING MANUAL (M) VERSUS AUTOMATED (A) EXOPEPTIDASE SEQUENCING

The six peptides were digested with the four exopeptidases as described in Experimental either in the totally automated mode (both digestion and amino acid analysis) or totally manual mode (both digestion and amino acid analysis). The total number of released residues for a specific substrate/enzyme pair is listed and the values in parentheses correspond to the number of correct sequence assignments from this total number of released residues.

Peptide	CPA		CPP		CPY		APM	
	M	A	M	A	M	A	M	A
Renin substrate tetradecapeptide	8(1)	7(0)	6(1)	7(2)	7(1)	7(3)	6(0)	6(0)
Angiotensin I	3(3)	3(3)	3(3)	4(2)	3(3)	3(3)	10(0)	10(0)
Adrenocorticotrophic hormone (1-10)	2(2)	4(1)	8(2)	8(1)	2(0)	2(2)	8(2)	8(1)
Dynorphin A (1-6)	0(0)	0(0)	4(2)	3(1)	3(3)	3(3)	6(2)	6(2)
Bradykinin	0(0)	0(0)	2(2)	4(4)	2(2)	3(3)	1(0)	2(0)
Gonadotropin releasing hormone	3(2)	2(2)	0(0)	0(0)	2(2)	5(3)	0(0)	0(0)



greater sensitivity is required, e.g., Fmoc-Cl [14–17], OPA [22,23] and Dns-Cl [24], these derivatization procedures could be incorporated into the automated exopeptidase protocol.

#### ACKNOWLEDGEMENTS

We thank Dave McCourt (HHMI) for his contributions in improving the chromatography of the PTC-amino acids and Jan Tschida, John Simpson, Terry Sheehan and Anton Mayer (Varian Associates) for their interest in this work.

#### REFERENCES

- 1 G. Allen, in T. S. Work and R. H. Burdon (Editors), *Sequencing of Proteins and Peptides*, Elsevier, Amsterdam, 1986, pp. 38–42, 228–230.
- 2 R. P. Ambler, *Methods Enzymol.*, 25 (1972) 143–154.
- 3 D. H. Hawke, H. W. Lahm, J. E. Shively and C. W. Todd, *Anal. Biochem.*, 166 (1987) 298–307.
- 4 D. J. Strydom, *Anal. Biochem.*, 174 (1988) 679–686.
- 5 R. P. Ambler, *Methods Enzymol.*, 25 (1972) 262–272.
- 6 G. Gimenez-Gallego and K. A. Thomas, *J. Chromatogr.*, 409 (1987) 299–304.
- 7 H. S. Lu, M. L. Klein and P. H. Lai, *J. Chromatogr.*, 447 (1988) 351–364.
- 8 R. Hayashi, *Methods Enzymol.*, 47 (1977) 84–93.
- 9 M. W. Hunkapillar, R. M. Hewick, W. J. Dreyer and L. E. Hood, *Methods Enzymol.*, 91 (1983) 399–413.
- 10 A. Light, *Methods Enzymol.*, 25 (1972) 253–262.
- 11 S. A. Cohen and D. J. Strydom, *Anal. Biochem.*, 174 (1988) 1–16.
- 12 D. Atherton, in T. E. Hugli (Editor), *Techniques in Protein Chemistry*, Academic Press, San Diego, CA, 1989, pp. 273–283.
- 13 A. S. Inglis, N. A. Bartone and J. Finlayson, *J. Biochem. Biophys. Meth.*, 15 (1988) 249–254.
- 14 K. A. West and J. W. Crabb, in J. J. Villafranca (Editor), *Current Research in Protein Chemistry: Techniques, Structure and Function*, Academic Press, San Diego, CA, 1990, pp. 37–48.
- 15 M. Meys, T. Wheat and S. A. Cohen, presented at 9th International Symposium on HPLC of Proteins, Peptides and Polynucleotides, Philadelphia, PA, November 6–8, 1989.
- 16 S. A. Cohen, M. Meys, D. Wittmer, T. Wheat, P. Pino and W. Fuchs, presented at 3rd Symposium Protein Society, Seattle, WA, July 29–August 2, 1989.
- 17 K. A. West and J. W. Crabb, presented at 3rd Symposium Protein Society, Seattle, WA, July 29–August 2, 1989.
- 18 T. L. Sheehan, A. G. Mayer and T. Wehr, presented at 7th International Symposium on HPLC of Proteins, Peptides and Polynucleotides, Washington, DC, November 2–4, 1987.
- 19 R. Cunico, A. G. Mayer, C. T. Wehr and T. L. Sheehan, *Biochromatogr.*, 1 (1986) 6–14.
- 20 B. Gustavsson and I. Betner, *J. Chromatogr.*, 507 (1990) 67–77.
- 21 I. Betner and P. Foldi, *LC · GC*, 6 (1988) 832–840.
- 22 R. Schuster, *J. Chromatogr.*, 431 (1988) 271–284.
- 23 D. T. Blankenship, M. A. Krivanek, B. L. Ackermann and A. D. Cardin, *Anal. Biochem.*, 178 (1989) 227–232.
- 24 M. Simmaco, D. DeBiase, D. Barra and F. Bossa, *J. Chromatogr.*, 504 (1990) 129–138.
- 25 D. L. Crimmins, J. Gorka, R. S. Thoma and B. D. Schwartz, *J. Chromatogr.*, 443 (1988) 63–71.
- 26 D. L. Crimmins, R. S. Thoma, D. W. McCourt and B. D. Schwartz, *Anal. Biochem.*, 176 (1989) 255–260.
- 27 B. A. Bidlingmeyer, S. A. Cohen and T. L. Tarvin, *J. Chromatogr.*, 336 (1984) 93–104.
- 28 R. L. Heinrikson and S. C. Meredith, *Anal. Biochem.*, 136 (1984) 65–74.
- 29 A. N. Glazer, R. J. Delange and D. S. Sigman, in T. S. Work and E. Work (Editors), *Chemical Modification of Proteins*, Elsevier, Amsterdam, 1985, pp. 27 and 52.



## **Breakthrough curves of insulin, [D-Phe<sup>6</sup>]-Gonadotropin-releasing hormone and phenylalanine methyl ester on copolymers of alkylacrylate and divinylbenzene**

P. SLONINA\*

*Berlin-Chemie AG, Glienicker Weg 125, 1199 Berlin (G.D.R.)*

and

A. SEIDEL\*

*Academy of Sciences, Institute of Physical Chemistry, Rudower Chaussee 5, 1199 Berlin (G.D.R.)*

(First received December 19th, 1989; revised manuscript received August 7th, 1990)

---

### ABSTRACT

Copolymers of alkylacrylate and divinylbenzene were characterized by analysing breakthrough curves of different biologically active substances for various mobile phase velocities, ionic strengths and solute and solvent concentrations. Effective surface diffusivities and adsorption equilibrium constants were determined with nonlinear regression methods by matching the experimental curves with the theoretical curves according to Babcock *et al.*'s solution.

---

### INTRODUCTION

The importance of porous organic polymer phases in the adsorption chromatography of biologically active substances is increasing in comparison with reversed-phase silica materials [1–5]. Polymers possess higher chemical stability and their structures and surface characteristics can be modified in a convenient way [6].

Porous copolymers of divinylbenzene and alkylacrylate with variable carbon chain lengths are chromatographic supports [copolymers, acrylate, ester (CAE) supports] with a specific surface area between 250 and 400 m<sup>2</sup>/g. They are stable in the pH range 1–10, possess a high quenching stability and are pressure resistant up to 5 MPa. They are preferably applied in the medium and normal pressure range [7].

The mechanism of a chromatographic separation process is essentially influenced by the mass transfer properties and the equilibrium parameters of the system under consideration. Experimental methods for determining diffusivities of mass transport in porous media and adsorption equilibrium constants have been briefly reviewed [8]. Mainly pulse chromatographic techniques are applied, but the same

---

\* Present address: Forschungsinstitut für Balneologie und Kurortwissenschaften, 9933 Bad Elster (G.D.R.).

information can be obtained from frontal chromatographic experiments. The latter method was used in this work to characterize the above-mentioned adsorbents.

#### ANALYSIS OF FRONTAL CHROMATOGRAPHIC EXPERIMENTS

In these experiments, the input into a column filled with adsorbent is a step function. The analysis of the experiments is usually accomplished by adjusting parameters to match experimental breakthrough curves (BTC) with the theoretical curves. The theoretical description of adsorption from a flow through a bed of solid particles under isothermal conditions and at a constant superficial velocity based on mass balances has been developed by several workers [9-11]. Assuming axial dispersion, mass transport from the bulk phase to the external surface of the particles (film diffusion) and diffusion in the particles to be the rate-determining steps, the particles to be spherical and the adsorption isotherm to be linear, the following system of partial differential equations can be derived:

Mass balance of the bulk phase:

$$D_{ax} \cdot \frac{\partial^2 c_L}{\partial h^2} - w \cdot \frac{\partial c_L}{\partial h} - \beta \cdot \frac{3}{R} \cdot \frac{1 - \varepsilon}{\varepsilon} (c_L - c_{p|R}) = \frac{\partial c_L}{\partial t} \quad (1)$$

Mass balance of the solid phase:

$$D_S \left( \frac{\partial^2 q}{\partial r^2} + \frac{2}{r} \cdot \frac{\partial q}{\partial r} \right) + D_P \left( \frac{\partial^2 c_P}{\partial r^2} + \frac{2}{r} \cdot \frac{\partial c_P}{\partial r} \right) = \frac{\partial q}{\partial t} + \varepsilon_P \cdot \frac{\partial c_P}{\partial t} \quad (2)$$

where  $D_S$  is the surface diffusivity and  $D_P$  is the pore diffusivity. Defining an effective surface diffusivity as

$$D_{S,E} = \frac{D_S K + D_P}{K + \varepsilon_P} \quad (3)$$

eqn. 2 can be simplified to

$$D_{S,E} \left( \frac{\partial^2 q}{\partial r^2} + \frac{2}{r} \cdot \frac{\partial q}{\partial r} \right) = \frac{\partial q}{\partial t} \quad (4)$$

This equation is equivalent to

$$D_{P,E} \left( \frac{\partial^2 c_P}{\partial r^2} + \frac{2}{r} \cdot \frac{\partial c_P}{\partial r} \right) = \frac{\partial q}{\partial t} \quad (5)$$

with an effective pore diffusivity

$$D_{P,E} = K D_{S,E} \quad (6)$$

The linear adsorption isotherm:

$$q = K c_P \quad (7)$$

Initial conditions:

$$c_L(0, h) = 0 \quad (8)$$

$$q(0, r, h) = 0 \quad (9)$$

Boundary conditions:

$$c_L(t, 0) = c_{LE} \quad (10)$$

$$c_L(t, \infty) = 0 \quad (11)$$

$q(t, R, h)$  given by

$$\frac{\partial \bar{q}}{\partial t}(t, h) = \beta \cdot \frac{3}{R} \left[ c_L(t, h) - \frac{q(t, R, h)}{K} \right] \quad (12)$$

with

$$\bar{q}(t, h) = \frac{3}{R^3} \int_0^R q(t, r, h) r^2 dr \quad (13)$$

$$q(t, 0, h) \neq \infty \quad (14)$$

In the case of a non-linear adsorption isotherm, the above system of equations has to be solved numerically. For a linear isotherm, a simple approximate solution was derived by Babcock *et al.* [10], extending the work of Rosen [9]. After rearrangement this solution is

$$\frac{c_L}{c_{LE}}(t, H) = \frac{1}{2}(1 - \operatorname{erf} \tau) \quad (15)$$

with

$$\tau = \frac{t_m - t}{2 \sqrt{\frac{H}{w} \left[ \frac{1 - \varepsilon}{\varepsilon} \cdot K^2 \cdot \frac{R^2}{15 D_{\text{tot}}} + \left( 1 + K \cdot \frac{1 - \varepsilon}{\varepsilon} \right)^2 \frac{D_{\text{ax}}}{w^2} \right]}} \quad (16)$$

and

$$t_m = \frac{H}{w} \left( 1 + K \cdot \frac{1 - \varepsilon}{\varepsilon} \right) \quad (17)$$

$D_{\text{tot}}$  is connected with  $D_{\text{s,E}}$  and  $\beta$  in the following way:

$$\frac{R^2}{15 D_{\text{tot}}} = \frac{R^2}{15 D_{\text{s,E}}K} + \frac{R}{3\beta} \quad (18)$$

The solution to calculate the BTC contains four free parameters: the axial dispersion coefficient  $D_{\text{ax}}$ , the film diffusion coefficient  $\beta$ , the effective surface diffusivity  $D_{\text{s,E}}$  and the adsorption equilibrium constant  $K$ .

The contributions of surface diffusion, film diffusion and axial dispersion to the total mass transfer resistance can be expressed as

$$R_{\text{Eff}} = 100 \cdot \frac{B_1}{B_1 + B_2 + B_3} \quad (19)$$

$$R_{\text{F}} = 100 \cdot \frac{B_2}{B_1 + B_2 + B_3} \quad (20)$$

$$R_{\text{ax}} = 100 \cdot \frac{B_3}{B_1 + B_2 + B_3} \quad (21)$$

with

$$B_1 = \frac{1 - \varepsilon}{\varepsilon} \cdot K \cdot \frac{R^2}{15 D_{\text{s,E}}} \quad (22)$$

$$B_2 = \frac{1 - \varepsilon}{\varepsilon} \cdot K^2 \cdot \frac{R}{3\beta} \quad (23)$$

$$B_3 = \left(1 + K \cdot \frac{1 - \varepsilon}{\varepsilon}\right)^2 \frac{D_{\text{ax}}}{w^2} \quad (24)$$

According to Babcock *et al.* [10], the above approximate solution (eqn. 15) is applicable if

$$3 \cdot \frac{D_{\text{s,E}}}{R^2} \cdot \frac{H}{w} \cdot K \cdot \frac{1 - \varepsilon}{\varepsilon} > 2 \quad (25)$$

A further restriction is given in ref. 12, where an exact solution of the problem under consideration is derived. Eqn. 15 holds only for large Peclet numbers ( $Pe = Hw/D_{\text{ax}}$ ). The same limit results from the fact that eqns. 10 and 11 are not adequate boundary conditions in the presence of axial dispersion [13]. Thus eqn. 15 does not hold for cases with large dispersion effects transforming the S-shaped BTC to an exponential curve valid for a perfectly mixed column.

### Determination of parameters

It is possible to determine  $D_{ax}$  from independent experiments as described below. Then only the overall mass transfer parameter  $D_{tot}$  and the equilibrium constant  $K$  have to be deduced from the experimental BTC. Standard non-linear parameter estimation procedures [14] can be used to calculate  $K$  and  $D_{tot}$ , minimizing the following standard deviation:

$$\sigma = \sqrt{\frac{1}{N-2} \sum_{i=1}^N (c_{Lth i} - c_{Lex i})^2} \quad (26)$$

The two parameters  $D_{S,E}$  and  $\beta$  cannot be determined separately by analysis of a single BTC. However, to determine  $D_{S,E}$  from  $D_{tot}$  with eqn. 18, an independent estimation of the film diffusion coefficient  $\beta$  using literature correlations is possible.

### Axial dispersion

As reported [8], the influence of axial dispersion on the course of BTC is frequently underestimated. For the case that no mass transfer occurs ( $\beta = 0$ ), eqn. 1 with the initial and boundary conditions given in eqns. 8, 10 and 11 has the following well known analytical solution (e.g., [15]):

$$\frac{c_L}{c_{LE}}(t, H) = \frac{1}{2} \left[ \operatorname{erfc} \left( \frac{H - wt}{2\sqrt{D_{ax}t}} \right) + \exp \left( \frac{Hw}{D_{ax}} \right) \operatorname{erfc} \left( \frac{H + wt}{2\sqrt{D_{ax}t}} \right) \right] \quad (27)$$

Like eqn. 15, due to the incorrect boundary conditions (eqns. 10 and 11), eqn. 27 is also valid only for small dispersion effects. Using numerical methods of solving eqns. 1 and 8 with the correct boundary conditions [13]:

$$c_L(t, 0) = c_{LE} + \frac{D_{ax}}{w} \cdot \frac{\partial c_L}{\partial h}(t, 0) \quad (28)$$

$$\frac{\partial c_L}{\partial h}(t, H) = 0 \quad (29)$$

it was determined that eqn. 27 is applicable if  $Pe > 20$  [16].

### Film diffusion

There are several correlations for calculating film diffusivities  $\beta$ . In this work the correlation of Gnielinski [17] was used. This correlation takes into account the porosity of the fixed bed and allows for contributions of laminar and turbulent flow to the mass transfer:

$$\beta = \frac{D_L}{2R} \cdot Sh_b \quad (30)$$

with

$$Sh_b = [1 + 1.5(1 - \varepsilon)]Sh_p$$

$$Sh_p = 2 + \sqrt{Sh_L^2 + Sh_T^2}$$

$$Sh_L = 0.644 \sqrt[3]{Sc} \sqrt{Re}$$

$$Sh_T = \frac{0.037 Re^{0.8} Sc}{1 + 2.443 Re^{-0.1} (Sc^{0.666} - 1)}$$

$$Re = \frac{w \cdot 2R}{\nu_L}$$

$$Sc = \frac{\nu_L}{D_L}$$

## EXPERIMENTAL

In a  $9.5 \times 0.9$  cm I.D. column, breakthrough curves on a CAE support (particle diameter 50–63  $\mu\text{m}$ , mean particle diameter  $2R = 55 \mu\text{m}$ ,  $\varepsilon = 0.45$ ,  $\varepsilon_p = 0.54$ ) for three biologically active substances given in Table I were determined at  $25^\circ\text{C}$ . No aggregates were formed under the experimental conditions studied. As the elutropic strength of solvents in the application of the considered support corresponds to the order well known from chromatography on reversed-phase silica and other polymers (methanol < ethanol < acetonitrile [18–21]), a mixture of acetonitrile and phosphoric acid (0.01  $M$ ) was used as the eluent. UV detection at 205 nm was employed.

The following experimental conditions were varied: interstitial velocity  $w = 11.64 \cdot 10^{-5}$ – $34.9 \cdot 10^{-5}$  m/s (this corresponds to a flow-rate between 12 and 36 ml/h), solute concentration  $c_{LE} = 0.025$ – $0.5$  g/l, ionic strength (NaCl)  $I = 0$ – $0.6$  and solvent (acetonitrile) concentration  $c_S = 8.25$ – $29.5$  vol.-%.

TABLE I  
SOLUTES USED

The purity of all solutes was >95%.

Solute	$M$ (g/mol)	$10^{10} D_L$ ( $\text{m}^2/\text{s}$ )
Insulin <sup>a</sup>	5800	1.4
D-Phe <sup>6</sup> -gonadotropin-releasing hormone (D-Phe <sup>6</sup> -GnRH) <sup>b</sup>	1400	3.0
Phenylalanine methyl ester (Phe-OMe) <sup>c</sup>	179	6.0

<sup>a</sup> Pig pancreas, gel chromatography, crystallized.

<sup>b</sup> Synthesized chemically, purified by ion exchange.

<sup>c</sup> Synthesized chemically.



Prior to the analysis of the BTC of the given substances on CAE support, the effect of axial dispersion was studied in independent experiments. BTC with inert non-porous glass beads of comparable particle size were measured in the same column for all three substances and different interstitial velocities. This was deemed necessary, as available correlations for determining  $D_{ax}$  have been verified only for larger particles.

## RESULTS AND DISCUSSION

Fig. 1 shows experimental BTC for the three solutes investigated on the non-porous material for typical experimental conditions. The time scale is normalized according to eqn. 17 by  $t_m = H/w$ .

Obviously there is a considerable deviation from the plug flow behaviour due to dispersion effects. This effect has to be evaluated accurately in analysing BTC on porous polymer phases. The axial dispersion coefficients  $D_{ax}$  can be obtained with non-linear regression methods calculating theoretical BTC with eqn. 27. We considered a graphical matching of the experimental curves to a set of theoretical curves to be sufficient to calculate  $D_{ax}$ . In Table II, determined axial dispersion coefficients and the film transfer coefficients  $\beta$  calculated with eqn. 30 are summarized. All Peclet numbers are  $> 200$ .

With the quantitative knowledge of the effects of axial dispersion and film diffusion, the experimental BTC on the porous CAE phases could be analysed with eqns. 15 and 18. In order to determine the adsorption equilibrium constants  $K$  and the effective surface diffusivities  $D_{s,E}$ , the standard deviation between the theoretical and experimental curves (eqn. 26) was minimized using the method of Marquardt [14]. The sensitivity of  $\sigma$  to changes in  $K$  was more pronounced than that to changes in  $D_{s,E}$  and  $K$  could be determined more reliably. All values of  $\sigma$  were  $< 0.01$ . The validity of eqn. 25 was checked for all parameters optimized.

The obtained adsorption equilibrium constants and effective surface diffusivities for insulin at different interstitial velocities are given in Table III. The results indicate the necessary independence of the adsorption equilibrium constant on the interstitial

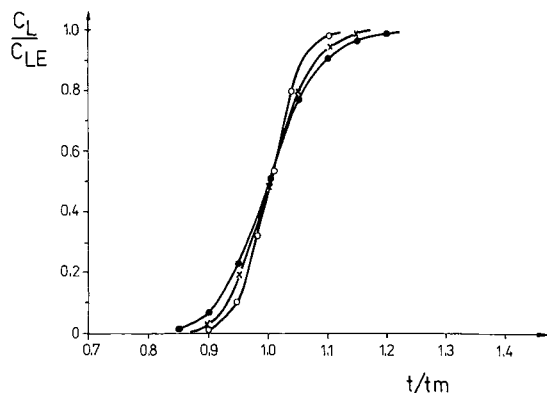


Fig. 1. BTC on non-porous material for (○) Phe-OMe, (●) insulin and (×) D-Phe<sup>6</sup>-GnRH,  $w = 11.64 \cdot 10^{-5}$  m/s; other experimental conditions in Table II.

TABLE II

## AXIAL DISPERSION COEFFICIENTS AND FILM DIFFUSION COEFFICIENTS

 $c_{LE} = 0.1 \text{ g/l}; I = 0.1; c_s = 29.5 \text{ vol.-% (insulin), } 27 \text{ vol.-% (D-Phe}^6\text{-GnRH), } 8.25 \text{ vol.-% (Phe-OMe).}$ 

Solute	$10^5 w \text{ (m/s)}$	$10^8 D_{ax} \text{ (m}^2\text{/s)}$	$10^5 \beta \text{ (m/s)}^a$
Insulin	11.64	3.3	1.39
Insulin	13.43	3.9	1.42
Insulin	18.38	5.3	1.51
Insulin	23.51	6.7	1.58
Insulin	34.94	10.1	1.73
D-Phe <sup>6</sup> -GnRH	11.64	2.0	2.76
Phe-OMe	11.64	1.1	5.20

<sup>a</sup>  $v_L$  in eqn. 30 was taken to be  $10^{-6} \text{ m}^2\text{/s}$  for all solutes and independent of solute, solvent and salt concentrations.

velocity. The same holds for the effective surface diffusivities in the frame of the usual uncertainties of such intraparticle mass transfer parameters. The tendency of the course of  $D_{s,E}$  might be due to not completely reliable  $\beta$  values being obtained using eqn. 30.

Table III also gives the contributions of surface diffusion, film diffusion and axial dispersion to mass transfer resistance (eqns. 19–24). Under the experimental conditions of this study film diffusion has the least resistance to mass transfer compared with intraparticle diffusion and axial dispersion. However, all three effects are significant for the course of the BTC.

Table IV compares the results for the three different solutes. As with the molecular diffusivities (Table I), the effective surface diffusivities have a reciprocal dependence on the molecular weights of the solutes. The difference between the effective surface diffusivities and the molecular diffusivities is approximately two orders of magnitude. The BTC for the three solutes on CAE support are shown in Fig. 2. The good representation of the measured data by eqn. 15 can be seen. In Fig. 2 the time is divided by  $t_m$  (eqn. 17). At this time the breakthrough would occur without mass transfer limitations. In the time scale  $t/t_m$  differences in the solutes with regard to mass transfer become obvious. The lowest effective surface diffusivity for insulin leads to the

TABLE III

## BTC FOR INSULIN

 $c_{LE} = 0.1 \text{ g/l}; I = 0.1; c_s = 29.5 \text{ vol.-%.}$ 

$10^5 w \text{ (m/s)}$	$K$	$10^{12} D_{s,E} \text{ (m}^2\text{/s)}$	$R_{Eff}$	$R_F$	$R_{ax}$
11.64	3.82	2.37	41.4	52.4	6.2
13.43	3.77	2.55	39.9	53.5	6.6
18.38	3.77	2.98	35.8	56.5	7.7
23.51	3.82	3.21	31.8	59.8	8.4
34.94	3.86	3.40	25.4	65.6	9.0

TABLE IV

RESULTS FOR INSULIN, D-Phe<sup>6</sup>-GnRH AND Phe-OMe

$w = 11.64 \cdot 10^{-5}$  m/s;  $c_{LE} = 0.1$  g/l;  $I = 0.1$ ;  $c_S = 29$  vol.-% (insulin), 27 vol.-% (D-Phe<sup>6</sup>-GnRH), 8.25 vol.-% (Phe-OMe).

Solute	$K$	$10^{12} D_{S,E}$ (m <sup>2</sup> /s)
Insulin	5.53	1.77
D-Phe <sup>6</sup> -GnRH	4.65	4.04
Phe-OMe	5.53	6.63

earliest breakthrough of this substance. For comparison, in Fig. 2 the insulin BTC on non-porous material from Fig. 1 is also shown once more.

#### *Influence of solute concentration on $D_{S,E}$ and $K$*

Table V shows the effective surface diffusivities and the adsorption equilibrium constants for insulin and D-Phe<sup>6</sup>-GnRH as a function of the solute concentration in the eluent for two different ionic strengths. Obviously both parameters are independent of the solute concentration. For the effective surface diffusivities this is also demonstrated by some results presented in the normalized time scale in Fig. 3. The obtained independence of equilibrium constants of solute concentration as required by eqn. 7 justifies the application of Babcock *et al.*'s solution.

#### *Influence of ionic strength in the eluent on $D_{S,E}$ and $K$*

From the results in Table V it can be further concluded that in the range of measurements the effective surface diffusivity is not sensitive to changes in the ionic strength in the eluent. This is corroborated over a broader range of ionic strength for D-Phe<sup>6</sup>-GnRH in Table VI and Fig. 4. In Fig. 4 the BTC for different ionic strengths almost coincide on the normalized time scale and can be calculated with a value for  $D_{S,E}$  averaged from the corresponding results given in Table VI.

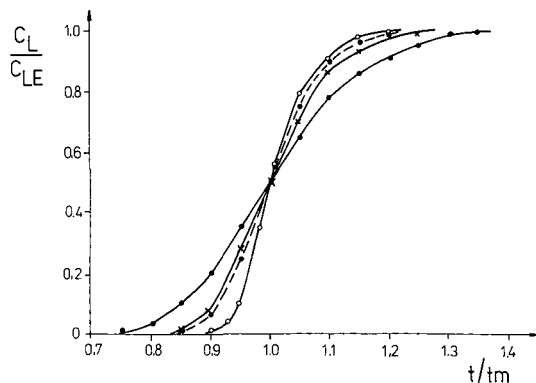


Fig. 2. BTC on CAE supports for (○) Phe-OMe, insulin (●—●) and D-Phe<sup>6</sup>-GnRH (×) and for insulin on non-porous material (●---●).  $w = 11.64 \cdot 10^{-5}$  m/s; other experimental conditions in Tables II and IV.

TABLE V  
INFLUENCE OF SOLUTE CONCENTRATION

$w = 11.64 \cdot 10^{-5}$  m/s;  $c_s$  (insulin) = 27 vol.-% ( $I = 0$ ), 29 vol.-% ( $I = 0.1$ );  $c_s$  (D-Phe<sup>6</sup>-GnRH) = 24 vol.-% ( $I = 0$ ), 27 vol.-% ( $I = 0.1$ ).

Solute	$c_{LE}$ (mg/ml)	$I = 0$		$I = 0.1$	
		$K$	$10^{12}D_{S,E}$ (m <sup>2</sup> /s)	$K$	$10^{12}D_{S,E}$ (m <sup>2</sup> /s)
Insulin	0.025	3.96	2.26	—	—
	0.050	3.91	2.31	5.25	1.80
	0.075	3.72	2.41	—	—
	0.1	3.72	2.39	5.53	1.77
	0.2	—	—	5.67	1.70
	0.5	—	—	5.02	1.91
D-Phe <sup>6</sup> -GnRH	0.025	4.83	3.89	4.47	4.18
	0.050	4.93	3.84	4.79	3.93
	0.075	4.74	3.96	4.79	3.95
	0.1	4.51	4.10	4.65	4.04

The addition of salt to the mobile phase increases the equilibrium constants of D-Phe<sup>6</sup>-GnRH for an ionic strength between 0 and 0.2 (Table VI) due to the known increase in available adsorbent surface for the solute according to the Stern–Guy–Chapman theory [22]. This confirms known results for other systems [18–21]. Above  $I = 0.2$  the equilibrium constants remain constant.

#### Influence of solvent concentration on $D_{S,E}$ and $K$

Table VII contains equilibrium constants and effective surface diffusivities for acetonitrile concentrations determined to be most effective for chromatography of the solutes investigated on CAE supports. From the results it is obvious that the influence of solvent concentration in the eluent on intra-particle mass transfer is small. This is

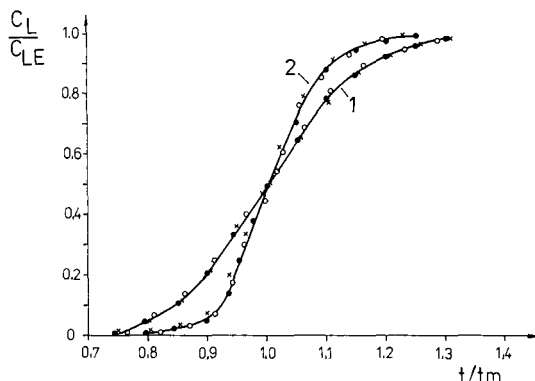


Fig. 3. BTC for (1) insulin and (2) D-Phe<sup>6</sup>-GnRH for  $I = 0$  and different solute concentrations (●)  $c_{LE} = 0.025$  g/l; (×)  $c_{LE} = 0.05$  g/l; (○)  $c_{LE} = 0.1$  g/l. Solid lines, calculated with averaged diffusivities  $D_{S,E}(1) = 2.32 \cdot 10^{-12}$  m<sup>2</sup>/s,  $D_{S,E}(2) = 3.98 \cdot 10^{-12}$  m<sup>2</sup>/s. Experimental conditions in Table V.

TABLE VI

$D_{S,E}$  AND  $K$  FOR THE ADSORPTION OF D-Phe<sup>6</sup>-GnRH AS A FUNCTION DEPENDENCE ON IONIC STRENGTH

$w = 11.64 \cdot 10^{-5}$  m/s;  $c_{LE} = 0.1$  g/l;  $c_S = 27$  vol.-%.

Ionic strength, I	$K$	$10^{12} D_{S,E}$ (m <sup>2</sup> /s)
0	3.35	4.70
0.1	4.65	4.04
0.2	5.25	3.22
0.4	5.25	3.23
0.6	5.21	3.27

TABLE VII

INFLUENCE OF SOLVENT CONCENTRATION

$w = 11.64 \cdot 10^{-5}$  m/s;  $c_{LE} = 0.05$  g/l;  $I = 0$ .

Solute	$c_S$ (Vol.-%)	$K$	$10^{12} D_{S,E}$ (m <sup>2</sup> /s)
Insulin	27	3.91	2.31
	28	3.08	2.82
	29.5	1.83	3.84
D-Phe <sup>6</sup> -GnRH	22	6.45	2.70
	24	4.93	3.84
	26	3.03	5.18
	27	2.71	5.59

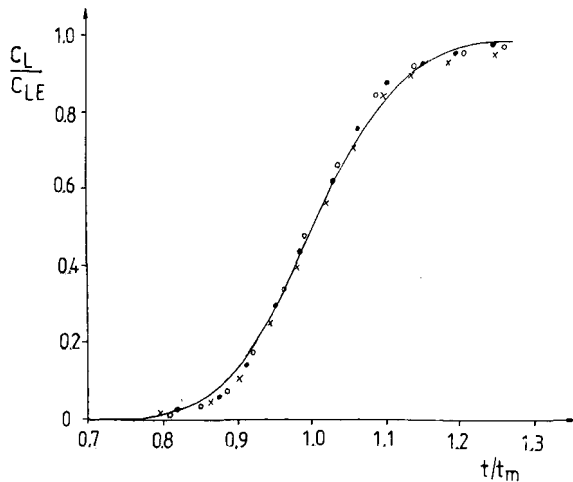


Fig. 4. BTC for D-Phe<sup>6</sup>-GnRH at different ionic strengths. (●)  $I = 0$ ; (×)  $I = 0.1$ ; (○)  $I = 0.4$ . Solid line, calculated with an averaged diffusivity  $D_{S,E} = 3.84 \cdot 10^{-12}$  m<sup>2</sup>/s. Experimental conditions in Table VI.

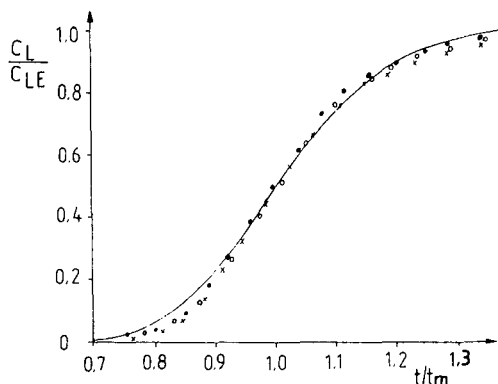


Fig. 5. BTC for insulin at different solvent concentrations. (●)  $c_s = 27$  Vol.-%; (×)  $c_s = 28$  vol.-%; (○)  $c_s = 29.5$  vol.-%; solid line, calculated with an averaged diffusivity  $D_{s,E} = 2.99 \cdot 10^{-12} \text{ m}^2/\text{s}$ . Experimental conditions in Table VII.

illustrated in Fig. 5, where experimental data for insulin with different solvent concentrations are compared on the normalized time scale with a BTC calculated using an averaged  $D_{s,E}$ . The adsorption equilibrium constants decrease considerably with increasing solvent concentration. The enhanced solubility of the solutes reduces their adsorbability.

## CONCLUSIONS

The determination of effective diffusivities and of adsorption equilibrium constants for chromatographic supports requires a careful analysis of all mass transfer resistances existing in both the mobile and the stationary phases. Axial dispersion and film diffusion were found to have a large influence on the course of measured breakthrough curves of three biologically active substances on porous copolymers of alkylacrylate and divinylbenzene. The axial dispersion coefficient could be determined from independent experiments with non-porous material. The film diffusion coefficient was estimated from an available correlation. Using Babcock *et al.*'s approximate solution from the experimental breakthrough curves adsorption equilibrium constants and effective surface diffusivities were calculated. As assumed in the applied model, the adsorption equilibrium constants of the investigated solutes proved to be independent of solute concentration but increased with increasing salt concentration and decreasing solvent concentration. Within the range of investigations the diffusivities were found to be not very sensitive to changes in solute, salt and solvent concentrations in the eluent.

## SYMBOLS

$c_L$	bulk phase concentration
$c_{LE}$	bulk phase concentration at column entry
$c_P$	liquid phase concentration in the pores

$c_s$	solvent concentration
$D_{ax}$	axial dispersion coefficient
$D_p$	pore diffusivity
$D_{p,E}$	effective pore diffusivity (eqn. 6)
$D_s$	surface diffusivity
$D_{s,E}$	effective surface diffusivity (eqn. 3)
$D_L$	molecular diffusivity
$D_{tot}$	mass transfer coefficient, defined in eqn. 18
$h$	axial distance
$H$	column length
$I$	ionic strength
$K$	adsorption equilibrium constant
$N$	number of data
$Pe$	Peclet number, $Pe = Hw/D_{ax}$
$q$	solid phase concentration
$r$	radial distance
$R$	particle radius
$R_{ax}$	contribution of axial dispersion to mass transfer resistance (eqn. 21)
$R_{Eff}$	contribution of surface diffusion to mass transfer resistance (eqn. 19)
$R_F$	contribution of film diffusion to mass transfer resistance (eqn. 20)
$Re$	Reynolds number (eqn. 30)
$Sc$	Schmidt number (eqn. 30)
$Sh$	Sherwood number (eqn. 30)
$t$	time
$t_m$	characteristic time, defined in eqn. 17
$w$	interstitial velocity
$\beta$	film diffusion coefficient
$\varepsilon$	bed porosity, $1 - V_{solid}/V_{total}$
$\varepsilon_p$	intra-particle porosity
$\sigma$	standard deviation, defined in eqn. 26
$\nu_L$	kinematic viscosity
$\tau$	defined in eqn. 16

### *Subscripts*

ex	experimental value
th	theoretical value
b	bed
L	laminar
P	particle
T	turbulent

### *Superscript*

—	average value (bar over symbol)
---	---------------------------------

### ACKNOWLEDGEMENTS

The synthesis and supply of the CAE supports by Dr. K. Haeupke (Chemie-kombinat, Bitterfeld, G.D.R.) is gratefully acknowledged, as are the critical comments of the reviewers.

## REFERENCES

- 1 Z. Iskandarani and D. J. Pietrzyk, *Anal. Chem.*, 51 (1981) 439.
- 2 T. McRae, R. P. Gregson and R. J. Quinn, *J. Chromatogr. Sci.*, 20 (1982) 475.
- 3 M. J. Cope and I. E. Davidson, *Analyst (London)*, 112 (1987) 417.
- 4 P. Hanai, Y. Arai, M. Kiruhawa, K. Nogushi and Y. Anagihara, *J. Chromatogr.*, 249 (1985) 323.
- 5 J. V. Dawkins, W. P. Gabott, L. L. Lloyd, J. A. McCornville and F. P. Warner, *J. Chromatogr.*, 452 (1988) 145.
- 6 J. P. Benson and D. J. Woo, *J. Chromatogr. Sci.*, 22 (1984) 386.
- 7 P. Slonina and K.-D. Kaufmann, *Z. Chem.*, submitted for publication.
- 8 H. W. Haynes, *Cat. Rev. Sci. Eng.*, 30 (1988) 563.
- 9 J. B. Rosen, *J. Chem. Phys.*, 20 (1952) 387.
- 10 R. E. Babcock, D. W. Green and R. H. Perry, *AIChE J.*, 12 (1966) 922.
- 11 S. Masamune and J. M. Smith, *AIChE J.*, 11 (1965) 34.
- 12 A. Rasmuson and I. Neretnieks, *AIChE J.*, 26 (1980) 686.
- 13 P. V. Danckwerts, *Chem. Eng. Sci.*, 2 (1953) 1.
- 14 D. W. Marquardt, *J. Soc. Appl. Math.*, 11 (1963) 431.
- 15 P. Cornel, H. Sontheimer, R. S. Summers and P. V. Roberts, *Chem. Eng. Sci.*, 41 (1986) 1801.
- 16 A. Seidel, *Chem. Eng. Sci.*, in press.
- 17 V. Gnielinski, *Verfahrenstechnik*, 12 (1978) 363.
- 18 D. J. Pietrzyk and C. H. Chu, *Anal. Chem.*, 49 (1977) 757.
- 19 D. J. Pietrzyk and C. H. Chu, *Anal. Chem.*, 49 (1977) 860.
- 20 C. H. Chu and D. J. Pietrzyk, *Anal. Chem.*, 46 (1974) 330.
- 21 L. R. Snyder and J. J. Kirkland, *Introduction to Modern Liquid Chromatography*, Wiley, New York, 1979.
- 22 F. Cantwell and S. Puon, *Anal. Chem.*, 51 (1979) 623.



## Alternative mobile phases for the reversed-phase high-performance liquid chromatography of peptides and proteins

BENNY S. WELINDER\*

*Hagedorn Research Laboratory, DK-2820 Gentofte (Denmark)*

and

HANS H. SØRENSEN

*Novo Nordisk A/S, DK-2820 Gentofte (Denmark)*

(First received March 20th, 1990; revised manuscript received July 20th, 1990)

---

### ABSTRACT

The use of a high content of acetic acid as mobile phase additive for the reversed-phase high-performance liquid chromatography (RP-HPLC) of several proteins and extracts of biological tissues was evaluated for a divinylbenzene (DVB)-based stationary phase, and the separations obtained with acetic acid gradients in acetonitrile, isopropanol or water were compared with classical polypeptide RP-HPLC on silica  $C_4$  with trifluoroacetic acid (TFA)-acetonitrile. The separation patterns for recombinant derived interleukin- $1\beta$  (IL- $1\beta$ ) on the  $C_4$  column eluted with TFA-acetonitrile and the DVB column eluted with acetic acid-acetonitrile were similar, but only the polymeric column was able to separate the components present in an iodinated IL- $1\beta$  preparation. Neither eluent had any harmful effect on the biological activity of IL- $1\beta$  isolated after RP-HPLC.

Several standard proteins could be separated when the polymeric column was eluted with acetic acid gradients in acetonitrile, isopropanol or water and, although the separation efficiency with acetic acid in water was lower than that in combination with classical organic modifiers, insulin, glucagon and human growth hormone (hGH) were eluted as sharp, symmetrical peaks. The recoveries of insulin and hGH were comparable for all three mobile phases (80–90%).

The separation patterns obtained from a crude acetic acid extract of a normal and a diabetic, human pancreas analysed using acetic acid gradients with or without organic modifiers were found to be similar and comparable to those obtained on a silica  $C_4$  column eluted with an acetonitrile gradient in TFA. The principal differences resulted from the use of different UV wavelengths (215 nm for TFA-acetonitrile, 280 nm for acetic acid).

Acetic acid extracts of recombinant derived hGH-producing *Escherichia coli* were separated on the DVB column eluted with an acetic acid gradient in water. Although the starting material was a highly complex mixture, the hGH isolated after this single-step purification was surprisingly pure (as judged by sodium dodecyl sulphate-polyacrylamide gel electrophoresis).

Consequently several (pure) polypeptides and complex biological samples were separated on a polymeric stationary phase eluted with acetic acid gradients in water without the use of organic modifiers.

---

### INTRODUCTION

Reversed-phase high-performance liquid chromatography (RP-HPLC) is based on modulation of the hydrophobic binding forces between a stationary phase and

hydrophobic domains in the sample molecules. The sample molecules are bound to alkyl or phenyl groups anchored to a solid matrix, and the chromatographic process is performed by adding substances with greater affinity for these ligands to the mobile phase. Organic modifiers such as acetonitrile, methanol, ethanol or propanol have been the most popular mobile phase additives, but the use of butanol, tetrahydrofuran and acetone has also been reported.

In RP-HPLC peptide and protein analyses, the binding between the ligand and the hydrophobic domains can often be eliminated with a narrow shift in the concentration of organic modifiers and at a relatively low level of these modifiers (*e.g.*, less than 50% acetonitrile) and if no secondary binding phenomena are involved, the chromatography may result in elution of the polypeptide molecules in narrow peaks with good recoveries.

With increasing hydrophobicity of protein molecules, the binding forces gradually increase to the point where addition of up to 90% of organic modifier is insufficient for elution from the stationary phase. Such insufficient mobile phase competition normally leads to chromatograms that show broad peaks with non-ideal shapes, in combination with severely reduced recoveries, a situation often seen after RP-HPLC of membrane proteins.

We have recently published an RP-HPLC analysis of sodium dodecyl sulphate (SDS)-solubilized membrane proteins from human erythrocyte ghosts using a polymeric stationary phase with phenyl ligands, eluted with acetonitrile-acetic acid [1]. Several membrane proteins with molecular weight (MW) > 100 000 dalton were eluted with very good recoveries, and this observation lead us to the hypothesis that less hydrophobic sample molecules, *e.g.*, small proteins, could perhaps be eluted at low modifier concentrations from selected reversed-phase stationary phases after addition of acetic acid to the mobile phase, perhaps even without the use of organic modifiers.

In this work, we characterized a polymeric phenyl-based stationary phase using gradients of acetic acid in water, isopropanol or acetonitrile. A number of polypeptides, and also highly heterogeneous extracts of biological tissues, were eluted without the use of classical organic modifiers and the recoveries and biological activities of selected polypeptides were measured. The separation pattern without organic modifier was compared with that obtained after eluting similar samples from a classical silica-based stationary phase (Nucleosil C<sub>4</sub>) with a widely used mobile phase [trifluoroacetic acid (TFA)-acetonitrile].

## EXPERIMENTAL

### HPLC

Commercially available HPLC equipment and columns were used throughout.

*Pumps.* M6000A, M510, M45, M590 (Waters Assoc.), Spectra-Physics SP 8700 and Gynkotek 300C pumps were used.

*Sample injectors.* U6K, WISP 710A and 712B (Waters Assoc.), and Model 7125 (Rheodyne) types were employed.

*UV-detectors.* M440 Lambda Max (Waters Assoc.), Hitachi L4200, Linear UVIS 200 and Pye Unicam UV detectors were used.

*Integrators.* These were M730, M840 (Waters Assoc.), Hitachi L2500 and Hewlett-Packard 3390A.

*Gradient Controllers.* M660, M720 and M840 (Waters Assoc.), Gynkotek 250B and Spectra-Physics SP8700 were used.

*Chemicals.* Acetonitrile, methanol and isopropanol were obtained from Rathburn (HPLC grade S), acetic acid (analytical-reagent grade) from Merck. All other chemicals were of analytical-reagent, sequential or similar purity. Water was obtained from a Millipore Milli-Q apparatus. All mobile phases were filtered through a 0.45- $\mu\text{m}$  Millipore filter and degassed before use. During chromatography, the mobile phases were degassed continuously with helium sparking or by passage through an ERMA ERC 3310 degasser.

*Columns.* A TSK Phenyl 5PW RP+ column (75  $\times$  4.0 mm I.D.) was obtained from Tosoh, a Nucleosil 300  $\text{\AA}$  C<sub>4</sub> (5  $\mu\text{m}$ ) column (250  $\times$  4.0 mm I.D.) from Macherey-Nagel and a Pentax PEC 102 column (100  $\times$  7.5 mm I.D.) from Pentax. Dynosphere PD-102-RE was used in prepacked columns (250  $\times$  4.0 mm I.D.) or obtained as a packing material from Dyno Particles. Columns of I.D. 4.6 mm, 8.0 mm and 16.0 mm and various lengths were slurry-packed in methanol (maximum pressure 150 bar) in our laboratory.

*HPLC separation.* All separations were performed at room temperature except for the Nucleosil separations with TFA-acetonitrile, which were carried out at 45°C. Detailed descriptions of the mobile phases and gradients used are given in the figure legends. Recoveries were calculated by comparing the area under the UV-curve after gradient elution of the specific column with that obtained after bypassing the column with 1.5-m PTFE capillary tubing.

#### *Sodium dodecyl sulphate-polyacrylamide gel electrophoresis (SDS-PAGE)*

SDS-PAGE was performed in a Pharmacia Phast Gel apparatus with 8–25% gradient gels. Electrophoresis and silver staining were performed as described by the manufacturer (Pharmacia Bulletin, Nos. 110 and 210).

#### *Samples*

Interleukin-1 $\beta$ , insulin (crystalline, porcine and highly purified human), human proinsulin and human growth hormone were obtained from Novo Nordisk. Other polypeptides were purchased from Sigma or Aldrich.

Pancreatic glands were obtained from the University Hospital, Copenhagen. From normal individuals classified as kidney donors, the pancreas was removed and frozen shortly after death. Only smaller parts of the pancreas were available from this category. From IDDM patients (insulin-dependent diabetics, age and diabetes duration unknown), the whole pancreas was removed after the ischaemia time (6–8 h according to the Danish death criteria). The pancreatic glands were kept frozen (*ca.* –30°C) after removal.

Before extraction, the pancreatic tissue was lyophilized and ground to a coarse powder. As 3 *M* acetic acid was found to be the optimum concentration for pancreas extraction (B. Hansen and S. Linde, unpublished results), the tissue was lyophilized before extraction in order to avoid any uncontrolled dilution of the acetic acid concentration in the added extraction medium. Up to 40 g of lyophilized pancreas powder were mixed with 200 ml of 3 *M* acetic acid, minced in a Warring Blender for *ca.* 1 min and extracted under magnetic stirring for 60 min. All operations were performed at 4°C. The extract was centrifuged at 4°C for 20 min in a Sorvall RC-5 cooled

centrifuge (25 000 g), the supernatant decanted and the tissue re-extracted twice under similar conditions.

The crude acetic acid extracts were analysed as such, or after lyophilization. Especially the diabetic extracts were difficult to lyophilize; the residue often had an oily appearance, probably owing to the presence of lipids in the crude extract.

#### *Gel chromatography*

Lyophilized acetic acid extracts were separated on a 90 × 2.5 cm I.D. Sephadex G-50 column eluted at 4°C with 3 M acetic acid at a flow-rate of *ca.* 20 ml/h. The column eluate was monitored continuously at 280 nm (Uvicord II) and 15-min fractions were collected in an LKB 7000 Ultrarac fraction collector. A 200-mg amount of lyophilized sample was dissolved in *ca.* 25 ml of 3 M acetic acid and filtered [coarse filter-paper, followed by filtration on Millipore filters (5, 1.2, 0.8 and finally 0.45 μm)] before application.

Gel chromatography of 100 mg of crystalline porcine insulin, performed under similar conditions, resulted in the separation of the b-component [primarily containing the covalent insulin dimer (12 000 dalton) and proinsulin (9000 dalton)] and the c-component (containing insulin peptide and insulin-like material, MW 6000 dalton).

The components in the acetic acid extracts obtained after gel chromatography were collected into two fractions: peak I (the main peak, MW > 6000 dalton) and peak II (the smaller peak with elution volume greater than the main peak, MW *ca.* 6000 dalton). Peak I and II material was isolated from the column eluate by lyophilization.

#### *Protein determination*

The protein content in the extracts was measured using the Coomassie Brilliant Blue protein assay (Bio-Rad Labs.) with bovine serum albumin as a standard, as described by the manufacturer. Before analysis, the extracts were diluted to 0.1 M acetic acid.

#### *Insulin determination*

Insulin radioimmunoassays (RIAs) were carried out essentially as described [2] using a monoiodinated insulin tracer obtained from Novo-Nordisk.

#### *Amino acid sequencing*

Amino acid sequencing was performed using a gas-phase sequencer (Applied Biosystems 475) equipped with an on-line Model 120A PTH analyser and a Model 900A data module. The sequence data were compared with published amino acid sequences in a database [Genetics Computer Group, UVGCG NRBF Protein, version 6.0 (April 89)].

## RESULTS

Interleukin-1β (IL-1β), a 17 400-dalton polypeptide with two free SH groups, is a "sticky" molecule which binds so strongly to several silica-based C<sub>18</sub> and C<sub>8</sub> columns that the use of TFA-acetonitrile as the mobile phase was insufficient for elution and/or separation [3]. Only a C<sub>4</sub> column was found to be useful for TFA-acetonitrile-

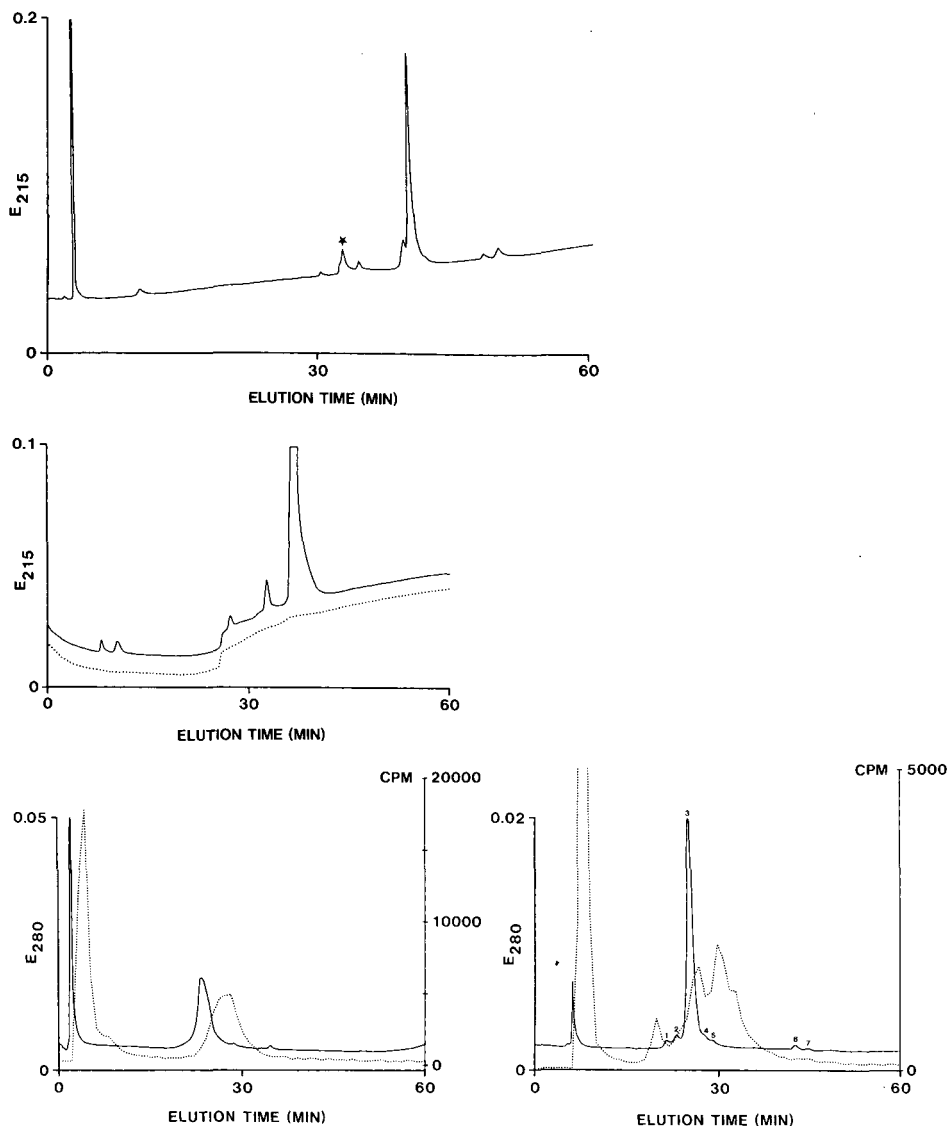


Fig. 1. Upper: RP-HPLC of 25  $\mu\text{g}$  of IL-1 $\beta$  using a 250  $\times$  4.0 mm I.D. Nucleosil 300  $\text{\AA}$  C<sub>4</sub> column eluted at 45°C with an acetonitrile gradient (10  $\rightarrow$  50% linearly during 60 min) in 0.05% TFA. Flow-rate, 1.0 ml/min. The peak marked with an asterisk is a "ghost" peak. Middle: HPLC of 25  $\mu\text{g}$  of IL-1 $\beta$  (solid curve) using a 100  $\times$  7.5 mm I.D. Pentax PEC 102 hydroxyapatite column eluted with a linear phosphate gradient [0.01 M Na<sub>2</sub>HPO<sub>4</sub>-0.3 mM CaCl<sub>2</sub> (pH 6.8)  $\rightarrow$  0.4 M Na<sub>2</sub>HPO<sub>4</sub>-0.0075 mM CaCl<sub>2</sub> (pH 6.8)] during 45 min followed by 15-min isocratic elution with the final buffer. Flow-rate, 0.5 ml/min. Dotted curve, blind injection. Lower left: RP-HPLC of 50  $\mu\text{g}$  of IL-1 $\beta$  (solid curve) and [<sup>125</sup>I]IL-1 $\beta$  (dotted curve) using a 75  $\times$  4.0 mm I.D. TSK Phenyl 5PW RP+ column eluted with 24% acetic acid-12% acetonitrile isocratically for 10 min, thereafter  $\rightarrow$  30% acetic acid-30% acetonitrile linearly during 35 min, and then to 40% acetic acid-60% acetonitrile linearly during 15 min. Flow-rate, 0.5 ml/min. Lower right: RP-HPLC of 25  $\mu\text{g}$  of IL-1 $\beta$  (solid curve) and [<sup>125</sup>I]IL-1 $\beta$  (dotted curve) using a 250  $\times$  4.6 mm I.D. Dynosphere PD-102-RE column eluted with an acetic acid-acetonitrile gradient (27% acetic acid-21% acetonitrile  $\rightarrow$  32% acetic acid-36% acetonitrile linearly during 60 min). Flow-rate, 0.5 ml/min.

based RP-HPLC of this polypeptide (Fig. 1, upper). In addition, a fairly good separation was obtained when a hydroxyapatite column was eluted with a phosphate gradient (Fig. 1, middle), but in order to optimize further the separation between native IL-1 $\beta$  and closely related IL-1 $\beta$ -like impurities, a polymeric phenyl column (TSK Phenyl 5PW RP+) was eluted with an acetic acid-acetonitrile gradient (found to be useful for the separation of very hydrophobic SDS-solubilized membrane proteins from erythrocyte ghosts [1]). Under these conditions, purified recombinant-derived IL-1 $\beta$  was separated in a main component and a few minor constituents (Fig. 1, lower left, solid curve), but a better separation was obtained when another polymeric phenyl-based column, Dynosphere PD-102-RE, was eluted with the same mobile phase (Fig. 1, lower right, solid curve). A major component, constituting 90–95% of the sample material, was separated from six minor contaminants. The peak shape and separation capacity of this system were superior to those obtained using the above-mentioned C<sub>18</sub>/C<sub>8</sub> and hydroxyapatite systems, and slightly better than that obtained using the silica-based C<sub>4</sub> columns eluted with TFA-acetonitrile (*cf.*, Fig. 1, upper).

For further evaluation of the selectivity of the two polymeric stationary phases eluted with acetic acid-acetonitrile a [<sup>125</sup>I]IL-1 $\beta$  preparation containing *ca.* 1 atom I/mol IL-1 $\beta$  was applied to the columns. Using the TSK Phenyl column [<sup>125</sup>I]IL-1 $\beta$  was eluted as a single component, partially separated from native IL-1 $\beta$  (Fig. 1, lower left, dotted curve), whereas four major [<sup>125</sup>I]IL-1 $\beta$  components were separated using the Dynosphere PD-102-RE column (Fig. 1, lower right, dotted curve).

As the separation of native IL-1 $\beta$  using the TFA-acetonitrile-C<sub>4</sub> system was comparable to that obtained on the Dynosphere column, [<sup>125</sup>I]IL-1 $\beta$  was analysed under conditions similar to those used in Fig. 1, upper. However, the radioactivity was eluted as a single component with a similar retention time to native IL-1 $\beta$  [3]. Similar results were obtained when [<sup>125</sup>I]IL-1 $\beta$  was analysed on the hydroxyapatite column [3]. The recoveries of IL-1 $\beta$  and iodinated IL-1 $\beta$  from the Dynosphere PD-102-RE column were found to be identical (*ca.* 80%).

In order to evaluate the potential harmful influence of acetic acid-acetonitrile on the biological activity of IL-1 $\beta$ , the column eluates containing components 1–7 shown in Fig. 1, lower right, were exchanged with RPMI 1640 and the content of IL-1 $\beta$  (ELISA assay) and the biological activities in the leukocyte activating factor (LAF) assay were determined as described [4]. The specific biological activity of the main component (marked "3") was found to be slightly higher than that of native IL-1 $\beta$  and those of the six minor components slightly reduced or similar to those in native IL-1 $\beta$  (Table I), indicating that the chromatographic procedure had no deleterious influence on the resulting specific biological activity. The specific biological activity of the main peaks isolated after hydroxyapatite chromatography (Fig. 1, middle) and also after RP-HPLC on Nucleosil C<sub>4</sub> eluted with TFA-acetonitrile (Fig. 1, upper) were determined in parallel, and found to be comparable to that of native IL-1 $\beta$  and IL-1 $\beta$  which had been incubated for 60 min in 0.085% TFA–80% acetonitrile (Table I).

For further characterization of the Dynosphere column, a number of commercially available peptides and proteins were eluted with three different mobile phases of acetic acid gradients in acetonitrile (Fig. 2, upper curve) in isopropanol (Fig. 2, middle curve) and in water (Fig. 2, lower curve). In the three experiments the column was

TABLE I

SPECIFIC BIOLOGICAL ACTIVITIES OF INDIVIDUAL FRACTIONS OBTAINED AFTER RP-HPLC OF PURIFIED IL-1 $\beta$  IN ACETIC ACID-ACETONITRILE (SEE FIG. 1, LOWER RIGHT), ON A HYDROXYAPATITE COLUMN (SEE FIG. 1, MIDDLE) OR ON A SILICA C<sub>4</sub> COLUMN ELUTED WITH TFA-ACETONITRILE (SEE FIG. 1, UPPER).

Before analysis in the ELISA and LAF assay (performed as described [4]), the solvents in the RP-column eluate were exchanged with RPMI 1640 on NAP-5 columns.

Fraction	Peak No.	Units/mg ( $\times 10^{-8}$ )
From Fig. 1, lower right	1	2.9
	2	3.5
	3	6.8
	4	3.6
	5	4.5
	6	4.6
	7	5.6
From Fig. 1, middle	Main peak	7.9
From Fig. 1, upper	Main peak	7.2
Native IL-1 $\beta$		5.7
Native IL-1 $\beta$ desalted in RPMI		5.0
Native IL-1 $\beta$ after 60 min in 0.085% TFA-80% acetonitrile		4.6

eluted with linear 60-min gradients. Although it was observed that the efficiency gradually decreased when acetonitrile was replaced with isopropanol and acetic acid (most clearly seen in the chromatographic behaviour of  $\beta$ -lactoglobulin in the three mobile phases), it was also found that insulin could be eluted as a narrow peak with an acetic acid gradient, similarly to the behaviour of the much more hydrophobic human growth hormone (hGH, MW 22 000 dalton).

The elution of 2 mg of crystalline porcine insulin from a 16.0 mm I.D. Dynosphere PD-102-RE column using essentially the same three mobile phases in similar gradients is shown in Fig. 3, left. Under these conditions, the elution strength of acetic acid is lower than that of acetonitrile and isopropanol. The chromatograms are similar with respect to the peak shape of the main component (insulin peptide), but the insulin-like contaminants are better separated from the main component in the acetic acid gradient. The recovery of crystalline insulin was measured for the three mobile phases and found to be 86% (acetonitrile), 76% (isopropanol) and 85% (acetic acid in water).

Biosynthetic hGH analysed under similar conditions to crystalline insulin eluted as a single component in all three mobile phases (chromatograms not shown), and the recoveries were found to be 76% (acetonitrile), 85% (isopropanol) and 90% (acetic acid in water).

In order to investigate the separation capacity of the Dynosphere PD-102-RE column for complex biological samples, an acetic acid extract of a normal human pancreas (removed and frozen immediately after death) was analysed using the above three mobile phases. Pancreatic tissue was extracted as described under Experimental and, after centrifugation, the aqueous extract was isolated from residual tissue and a lipid layer. A 200- $\mu$ l volume of this raw extract, containing *ca.* 3 mg of protein, was applied to a 180  $\times$  16.0 mm I.D. Dynosphere column and eluted at 4.0 ml/min with a

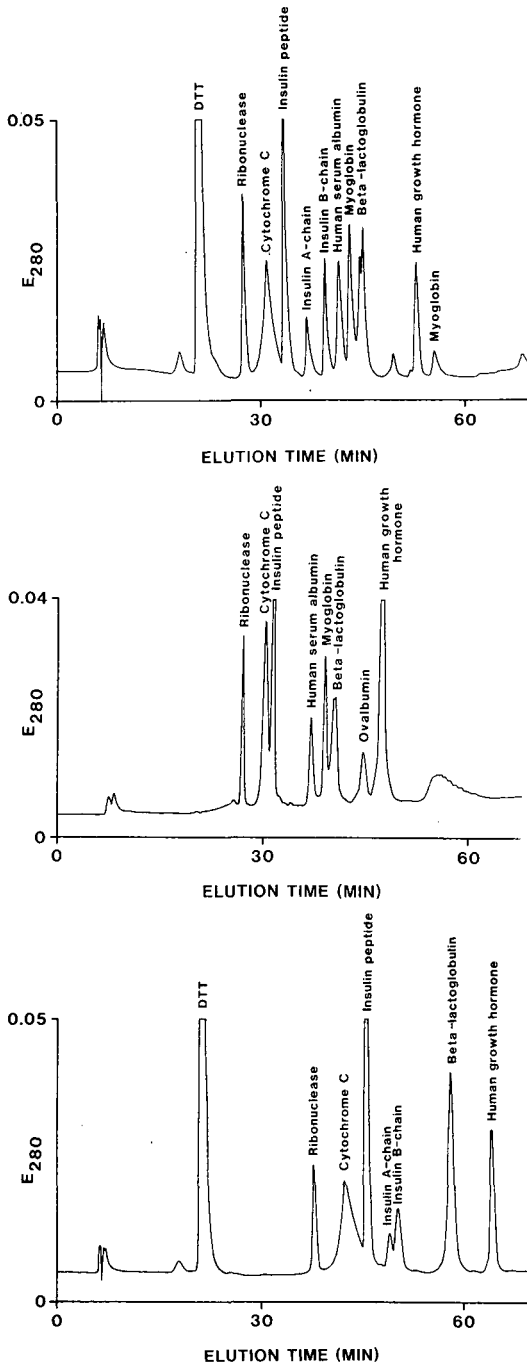


Fig. 2. Separation of a number of "standard proteins" using a  $250 \times 4.6$  mm I.D. Dynosphere PD-102-RE column eluted with a linear gradient (25% acetic acid–15% acetonitrile  $\rightarrow$  40% acetic acid–60% acetonitrile during 60 min followed by 10 min isocratically at 40% acetic acid–60% acetonitrile (upper), 25% acetic acid–15% isopropanol  $\rightarrow$  40% acetic acid–60% isopropanol during 60 min followed by 10 min isocratically at 40% acetic acid–60% isopropanol (middle) or 37.5  $\rightarrow$  90% acetic acid during 60 min followed by 10 min isocratically at 90% acetic acid). Sample amount, 20–50  $\mu$ g; only the individual proteins indicated in the three panels were applied in each analysis. Flow-rate, 0.5 ml/min.



60-min linear gradient (Fig. 3, right). Apart from the already observed difference in elution strength between the three mobile phases, the overall elution patterns of this complex mixture were comparable in the three cases.

RP-HPLC of three pancreatic polypeptides, insulin, proinsulin and glucagon, eluted with an acetic acid gradient is shown in Fig. 4, left. All polypeptides were eluted as very narrow, symmetrical peaks, and the impurities in crystalline glucagon were very well resolved. Glucagon and insulin were eluted with the same retention time under these conditions, whereas monoiodinated glucagon was separated from the native glucagon (Fig. 4, right). The component that eluted *ca.* 15 min after glucagon is human serum albumin added to the [ $^{125}$ I]glucagon preparation.

To evaluate the usability of the acetic acid-Dynosphere system for the further

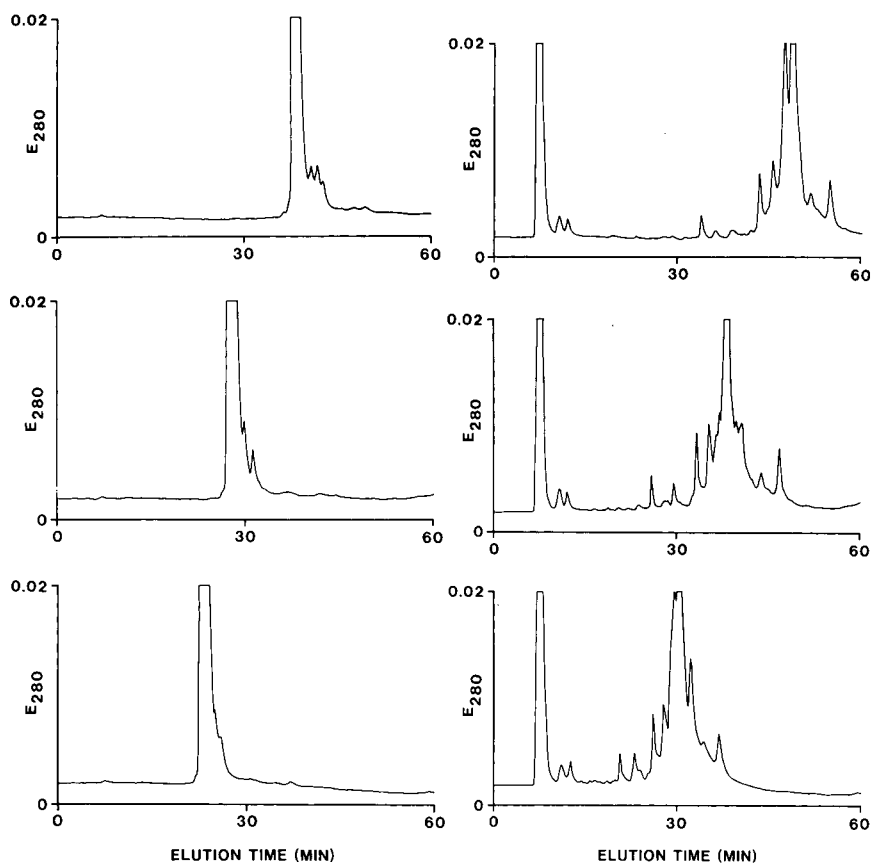


Fig. 3. Left: RP-HPLC of 2 mg of crystalline porcine insulin using a  $180 \times 16.0$  mm I.D. Dynosphere column eluted with acetic acid in water, isopropanol or acetonitrile as organic modifiers. All gradients were linear during 60 min. Flow-rate, 4.0 ml/min. Upper curve: 37.5 acetic acid  $\rightarrow$  90% acetic acid. Middle curve: 25% acetic acid-15% acetonitrile  $\rightarrow$  40% acetic acid-60% acetonitrile. Lower curve: 25% acetic acid-15% isopropanol  $\rightarrow$  40% acetic acid-60% isopropanol. Right: separation of 200  $\mu$ l of crude acetic acid extract of a normal human pancreas using a  $180 \times 16.0$  mm I.D. Dynosphere PD-102-RE column eluted as described for the left panel.

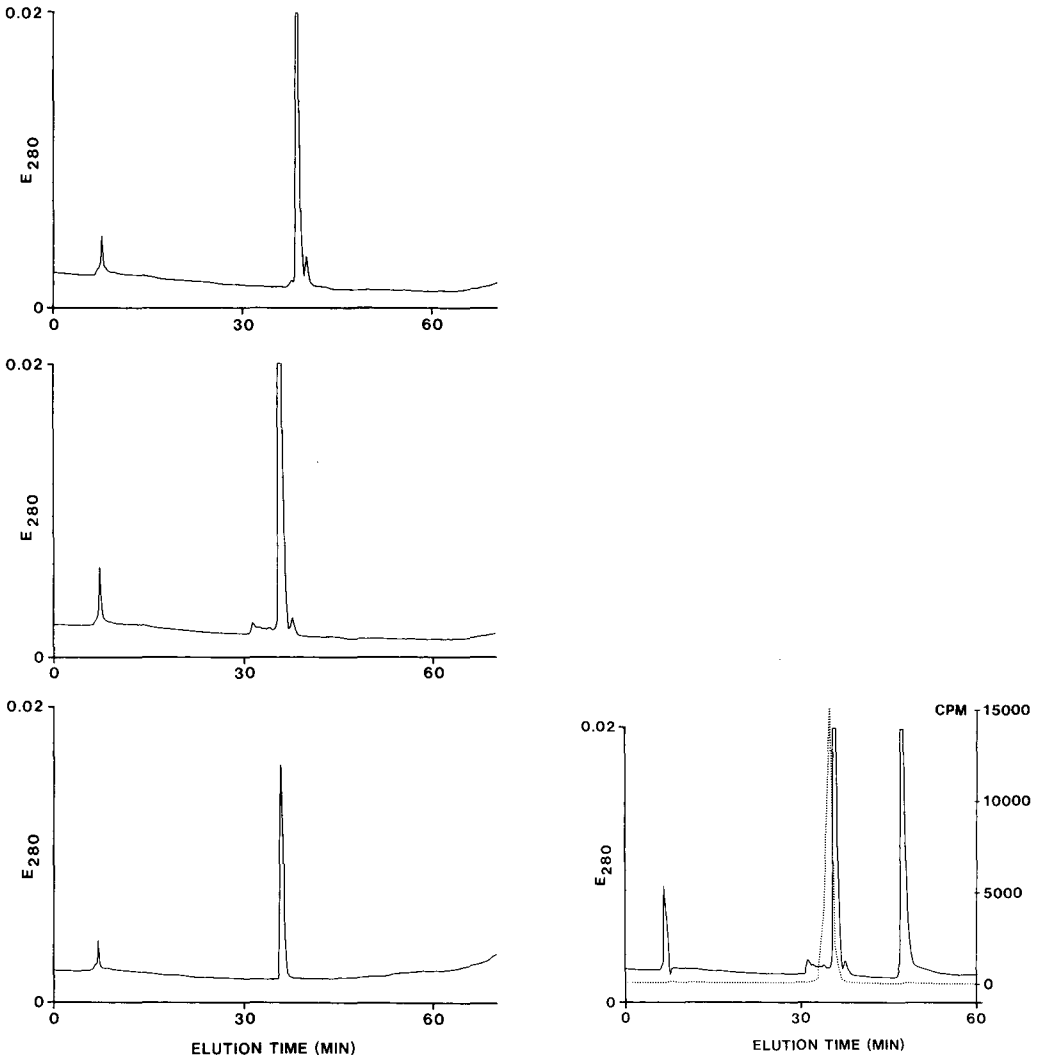


Fig. 4. Left: RP-HPLC of 10  $\mu\text{g}$  of human proinsulin (upper curve), 15  $\mu\text{g}$  of crystalline porcine glucagon (middle curve) and 6  $\mu\text{g}$  of human insulin (lower curve) using a  $280 \times 4.6$  mm Dynosphere PD-102-RE column eluted with a linear acetic acid gradient (37.5 acetic acid  $\rightarrow$  90% acetic acid) during 60 min. Flow-rate, 0.5 ml/min. Right: RP-HPLC of a mixture of 15  $\mu\text{g}$  of crystalline porcine glucagon and *ca.* 35 000 cpm [ $^{125}\text{I}$ ]glucagon. UV registration, solid curve; radioactivity, dotted curve. Stationary and mobile phases as in the left panel.

characterization of acetic acid extracts of normal and diabetic pancreatic glands, another normal and two diabetic pancreatic glands were extracted in 3 M acetic acid and the crude extracts were separated in a 37.5  $\rightarrow$  90% acetic acid gradient (Fig. 5). The chromatograms of the extracts were found to be very different: the proteins extracted from the diabetic pancreata were eluted much earlier than those in the normal pancreas, indicating less hydrophobicity and/or lower molecular weight, and

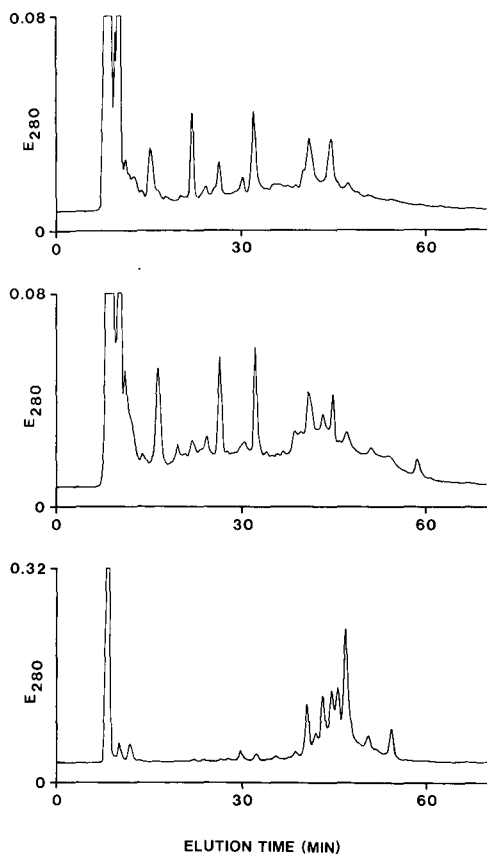


Fig. 5. RP-HPLC of 200  $\mu$ l of crude acetic acid pancreas extract from two human diabetics (upper and middle curves) and a normal human (lower curve) using a 280  $\times$  4.6 mm I.D. Dynosphere column eluted with an acetic acid gradient (37.5 acetic acid  $\rightarrow$  90% acetic acid during 60 min) followed by 10 min isocratically at 90% acetic acid. Flow-rate, 0.5 ml/min.

the amount of extractable peptides/proteins in the crude extracts from the normal pancreatic glands was much higher than in those from diabetics (compare the UV scales).

RP-HPLC of peak I and II material (obtained as described under Experimental) using the Dynosphere-acetic acid system is shown in Fig. 6 (left, normal pancreas; right, diabetic pancreas). The separation of peak I materials from the diabetic pancreas was much less detailed than that of the instantly analysed crude extract (*cf.*, Fig. 5, upper and middle curves), whereas the peak II materials from the normal and the diabetic pancreata were both very well resolved.

In order to compare the above-mentioned separations of the pancreatic extracts (using acetic acid as mobile phase) with a commonly used RP-HPLC polypeptide separation system, peak I and II material were separated on a Nucleosil 300  $\text{\AA}$  C<sub>4</sub> column eluted with TFA-acetonitrile. The separation pattern obtained for peak I and II material from the normal pancreas (Fig. 7, upper left) and the diabetic pancreas

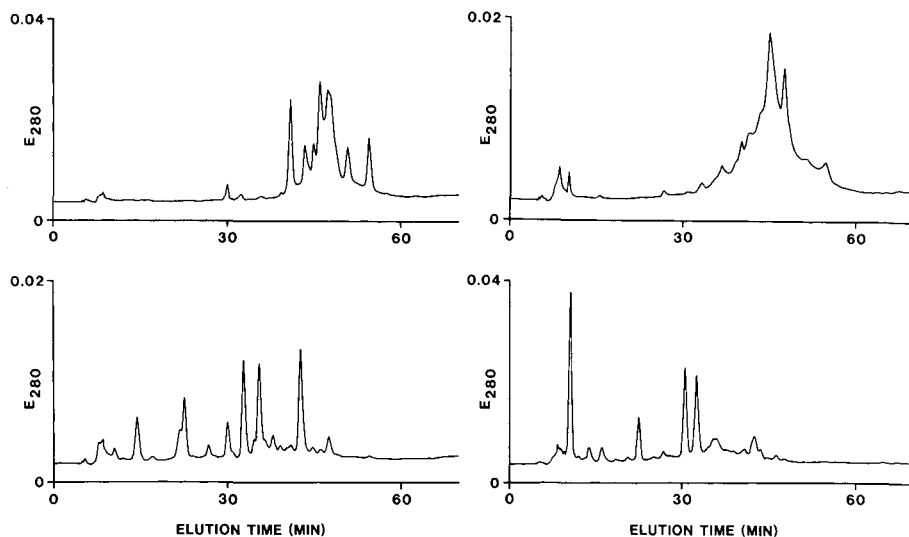


Fig. 6. Left: RP-HPLC of peak I (upper curve) and peak II material (lower curve) from normal human pancreas, redissolved in 3 M acetic acid to 1.0 mg/ml, centrifuged and filtered (0.45  $\mu$ m). 200  $\mu$ l were applied. Stationary and mobile phases as in Fig. 5. Flow-rate, 0.5 ml/min. Right: RP-HPLC of peak I material (upper curve) and peak II material (lower curve) from a diabetic human pancreas. 200  $\mu$ l were applied. All conditions as in Fig. 5.

(Fig. 7, upper right) were more detailed than those obtained with the Dynosphere-acetic acid system (Fig. 6), but the distributions of components throughout the chromatograms in the two highly different RP systems were very similar both for the normal pancreatic extracts (Fig. 6, left, *versus* Fig. 7, upper left) and for the diabetic pancreatic extracts (Fig. 6, right, *versus* Fig. 7, upper right).

The UV absorption of the column eluate from the Nucleosil C<sub>4</sub>-TFA-acetonitrile system was monitored at 215 nm, whereas the eluate from the Dynosphere-acetic acid system had to be monitored at a higher wavelength (280 nm). In order to compare the separations at a similar wavelength, peak I and II material from a diabetic pancreas was separated in the Nucleosil-TFA-acetonitrile system followed by detection at 280 nm (Fig. 7, lower). When these chromatograms are compared with Fig. 6, right, it can be seen that the separation patterns of the same sample in two different RP systems now appear to be very similar.

SDS-PAGE of the first, second and third crude acetic acid extracts of a normal pancreas, shown in Fig. 8, indicated a highly heterogeneous protein-peptide mixture with a molecular weight distribution in the total fractionation range (6000–300 000 dalton).

Finally, a series of crude extracts of recombinant-derived hGH-producing *Escherichia coli* were analysed. The crude bacterium pellet or disrupted bacteria were extracted in acetic acid and separated in the Dynosphere-acetic acid system (Fig. 9 A and B). In both instances, hGH was eluted in the late part of the chromatogram, well separated from all residual sample components. As can be seen from SDS-PAGE of

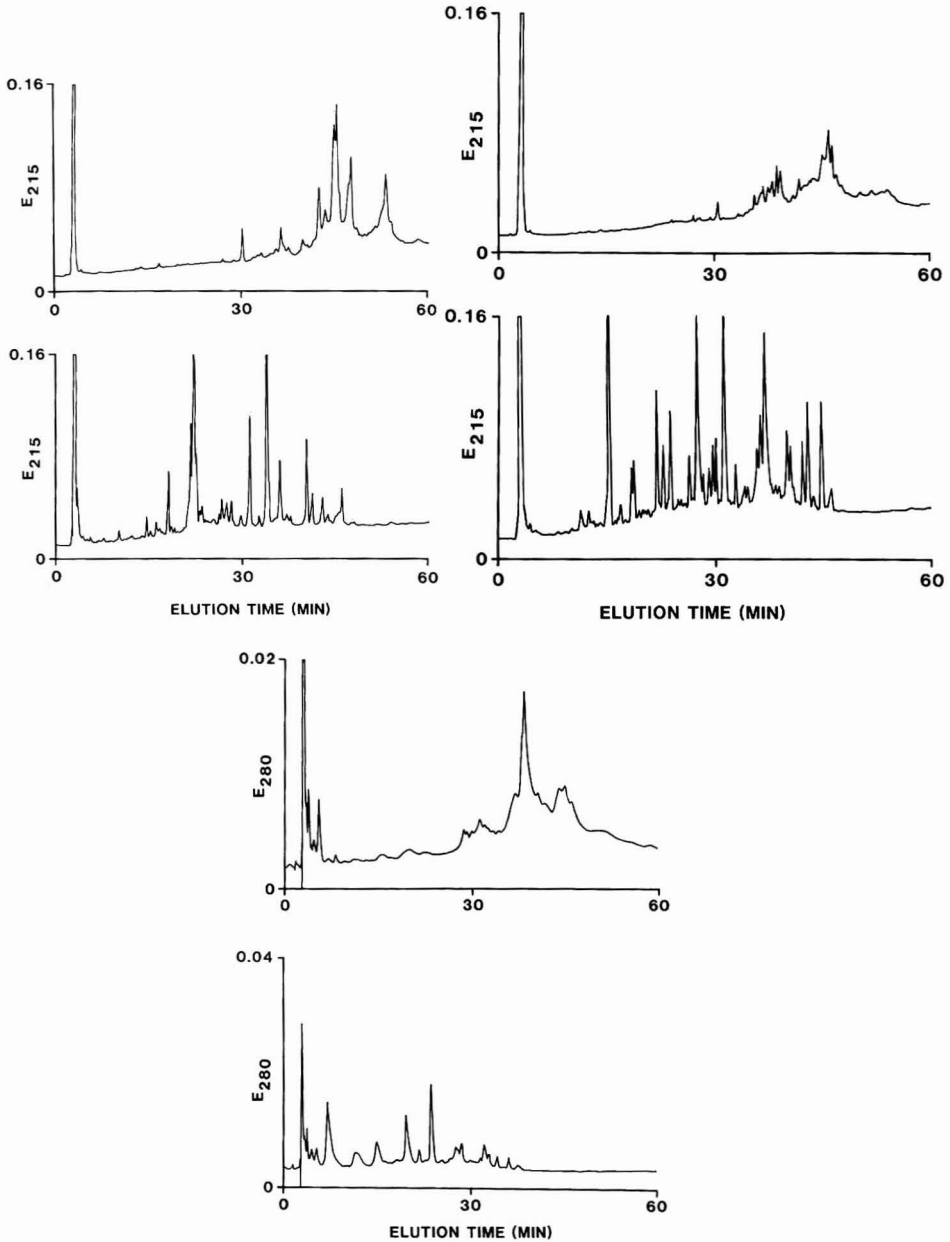


Fig. 7. Top: RP-HPLC of peak I material (upper curve) and peak II material (lower curve) from a normal human pancreas (left) and from a diabetic, human pancreas (right) using a 250 × 4.0 mm I.D. Nucleosil 300 Å C<sub>4</sub> column eluted at 45°C with an acetonitrile gradient (12 → 57% acetonitrile linearly during 60 min) in 0.1% TFA. 50 μl were applied in all analyses. Flow-rate, 1.0 ml/min. Bottom: RP-HPLC of peak I material (upper curve) and peak II material (lower curve) from a diabetic, human pancreas. 200 μl were applied. Stationary and mobile phases as for the top panels. Flow-rate, 1.0 ml/min. UV-registrations, 280 nm.

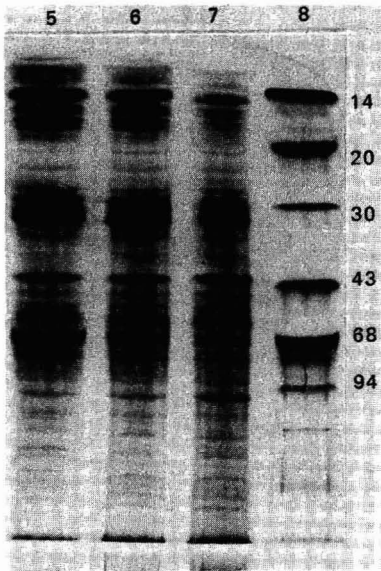


Fig. 8. SDS-PAGE of first, second and third acetic acid extracts of a normal, human pancreas (lanes 5, 6 and 7). Lane 8: molecular weight markers. The figures correspond to the MW in kilodalton.

the isolated hGH fractions, this single-step procedure resulted in a very efficient purification of the hGH preparation (Fig. 9C).

The acetic acid extract of the disrupted hGH *E. coli* bacteria was also analysed in the Nucleosil-TFA-acetonitrile system (Fig. 9D). The separation pattern was similar to that obtained with the Dynosphere-acetic acid system with respect to distribution of the components throughout the chromatogram, but it was also obvious that the peak capacity of the former system is higher.

## DISCUSSION

Hydrophobic peptides and proteins may constitute a major problem in RP-HPLC owing to their high affinity to the stationary phase ligands (whether they are alkyl or phenyl groups), and conventional mobile phase additives (acetonitrile, alcohols) are often unable to break the hydrophobic bindings. Detergents, which may be useful for similar problems in the size exclusion of hydrophobic polypeptides, have hardly ever been reported as mobile phase additives in RP-HPLC, probably because they are almost irreversibly bound to the ligands, thereby totally changing the surface characteristics of the reversed stationary phase.

We have been able to elute a number of erythrocyte ghost membrane proteins with MW > 100 000 dalton with good recovery from a phenyl column using a mobile phase based on a high content of acetic acid plus acetonitrile [1]. The reason for this surprising separation was probably the acetic acid in combination with the stationary phase phenyl groups, which normally binds peptides and proteins less strongly than C<sub>8</sub> and C<sub>18</sub> columns.

We therefore chose the same stationary and mobile phase for the initial charac-

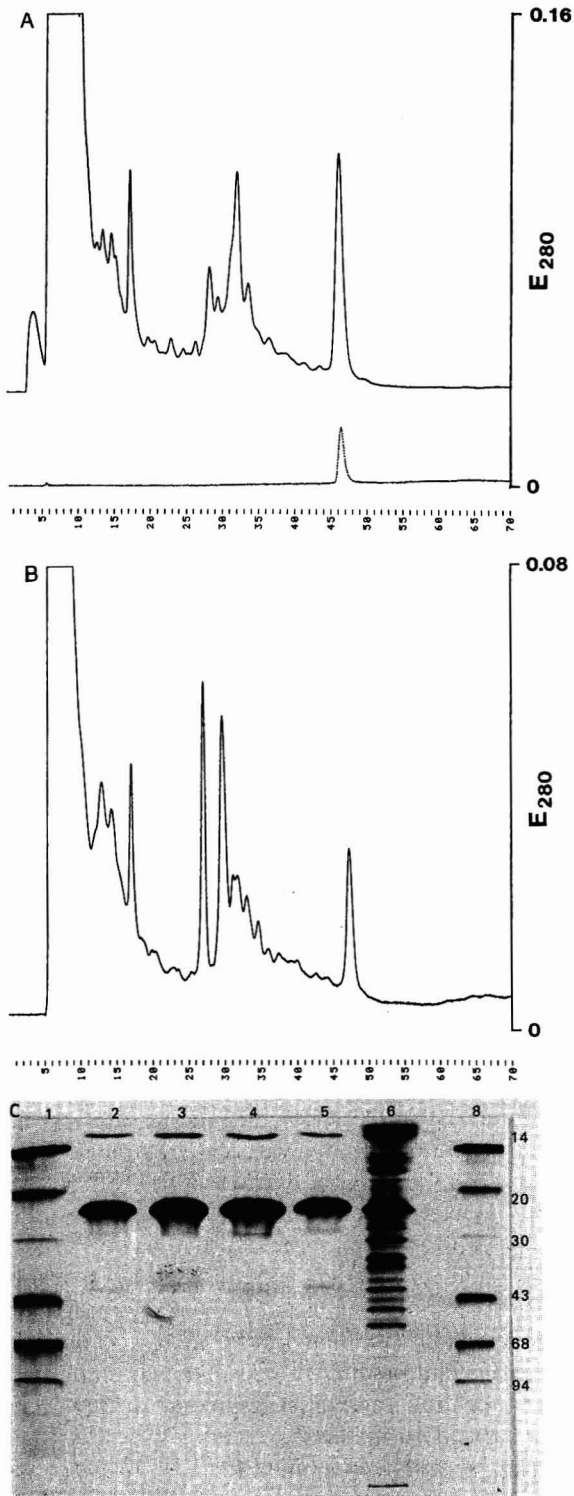


Fig. 9.

(Continued on p. 196)

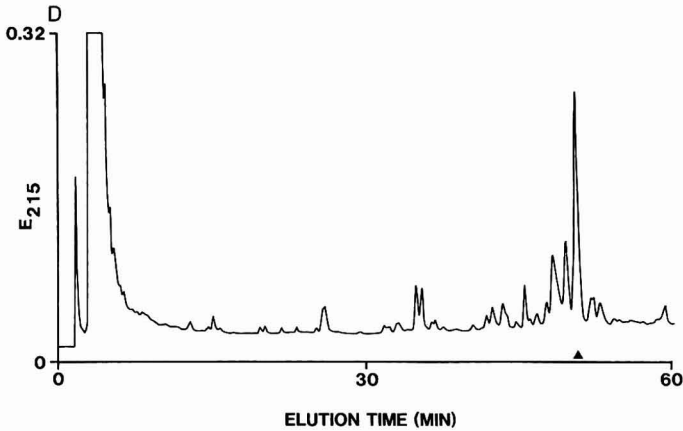


Fig. 9. (A) RP-HPLC of acetic acid extracts of disrupted hGH-producing *E. Coli*. A 0.75-ml bacteria residue pellet was extracted for 2.5 h at 4°C in 50% acetic acid. After centrifugation, the supernatant was diluted 1:1 with distilled water and 1800  $\mu$ l were applied to a 150  $\times$  8.0 mm I.D. Dynosphere PD-102-RE column. Elution was performed with a slightly concave 60-min gradient (37.5  $\rightarrow$  90% acetic acid, Waters Assoc. M660 gradient controller, gradient No. 5) followed by 10 min isocratically at 90% acetic acid (upper curve). The lower curve shows the elution pattern of 50  $\mu$ g of highly purified hGH under similar conditions. Flow-rate, 1.0 ml/min. The numbers on the abscissa are the elution times in minutes. (B) RP-HPLC of hGH-producing *E. Coli* extracted directly with acetic acid. A 0.5-ml bacteria pellet was extracted with 2.5 ml of glacial acetic acid at 4°C for 2.5 h. After centrifugation, the supernatant was diluted with distilled water (1:1.5), and 1000  $\mu$ l were applied to a 150  $\times$  8.0 mm I.D. Dynosphere PD-102-RE column eluted as described for (A). (C) SDS-PAGE of an acetic acid extract of disrupted hGH-producing *E. coli* (lane 6) and of hGH isolated after four individual RP-HPLC separations of this acetic acid extracts using the Dynosphere column under the conditions described for (A) (lanes 2–5, respectively). Lanes 1 and 8: molecular weight markers. The figures correspond to the MW in kilodalton. (D) RP-HPLC of an acetic acid extract of disrupted hGH-producing *E. Coli* using a 250  $\times$  4.0 mm I.D. Nucleosil 300  $\text{Å}$  C<sub>4</sub> column eluted with an acetonitrile gradient (25%  $\rightarrow$  50% acetonitrile linearly during 60 min) in 0.1% TFA. Flow-rate, 1.0 ml/min. The elution volume of biosynthetic human growth hormone is marked with a filled triangle.

terization of IL-1 $\beta$ , which is hydrophobic, but not to such an extent as membrane proteins; we found that the molecule hardly could be eluted from a C<sub>8</sub> column and that it bound irreversibly to a C<sub>18</sub> column [3] whereas TFA-acetonitrile was well suited for the elution of IL-1 $\beta$  from a C<sub>4</sub> column (Fig. 1, upper). Similar observations have been published elsewhere [5].

It was interesting that the TSK Phenyl 5PW RP+ column, found to be excellent for separating erythrocyte ghost membrane proteins, was less suitable for the RP-HPLC of IL-1 $\beta$  (Fig. 1, lower left), whereas another phenyl column, Dynosphere PD-102-RE (based on polymerized divinylbenzene) eluted with the same mobile phase was able to separate the IL-1 $\beta$  preparation much more effectively, with excellent peak shape and good recovery (Fig. 1, lower right). It should be added that the Dynosphere column was found to be considerably less useful for the separation of erythrocyte ghost membrane proteins than the TSK Phenyl 5PW RP+ column [6]. The separations obtained using a silica C<sub>4</sub> column and a Dynosphere column were comparable in the case of IL-1 $\beta$  (Fig. 1, upper and lower right, solid curve). However, [<sup>125</sup>I]IL-1 $\beta$  was eluted as a single component from the C<sub>4</sub> column, whereas four major fractions were separated using the Dynosphere column. [<sup>125</sup>I]IL-1 $\beta$  was also



eluted as a single component from the TSK Phenyl column, illustrating the very different selectivities of the two polymeric phenyl columns (Fig. 1, lower panels, dotted curves) and the C<sub>4</sub> silica column.

Interestingly, the combined effects of acetic acid and acetonitrile and the binding to the reversed stationary phase had no effect on the specific biological activity of the purified IL-1 $\beta$ , which was found (within the experimental variations in the LAF assay) to be equal to that of IL-1 $\beta$  before RP-HPLC (Table I). Further, RP-HPLC in TFA-acetonitrile (Nucleosil C<sub>4</sub>) was also without effect on the resulting specific biological activity, indicating that although IL-1 $\beta$  is a reactive molecule (two free SH groups), it is resistant towards the influence of the harsh mobile phases and the strong binding to the stationary phases, conditions known to be destructive for several other biological active polypeptides [7].

A hydroxyapatite column eluted with a phosphate gradient, a non-RP technique, was able to resolve the IL-1 $\beta$  preparation fairly well, although some tailing was observed for the main fraction (Fig. 1, middle). The specific biological activity of this main fraction was found to be equal to that of native IL-1 $\beta$  (Table I), indicating that hydroxyapatite chromatography should always be considered as a potential alternative for the RP-HPLC of peptides and proteins.

From the characterizations of the Dynosphere column with "standard proteins", insulin and raw pancreas acetic acid extract, it should be noted that in general, the mobile phase based solely on acetic acid was less efficient than those with acetonitrile and isopropanol (Fig. 2). It was most clearly demonstrated in the elution pattern of  $\beta$ -lactoglobulin: the separation of the two chains was distinct with acetonitrile (Fig. 2, upper), indicated with isopropanol (middle) but absent with acetic acid (lower).

However, the peak shape and recovery of hGH and insulin were ideal after elution with acetic acid alone (Fig. 2, lower, and Fig. 3, left). It is especially worth noting that the recovery of the hydrophobic 22 000-dalton hGH in an acetic acid gradient in water was 90%. Glucagon, glucagon-related impurities and monoiodinated glucagon were also well separated in the acetic acid gradient (Fig. 4), whereas glucagon and insulin peptide, in contrast to several acetonitrile-based RP-HPLC systems [8], were found to coelute.

As the separation of the complex pancreatic extract resulted in very comparable chromatograms in all three mobile phases (Fig. 3, right), we concluded that an acetic acid gradient could be used for further characterizing the extracts of the normal and the diabetic human pancreas. The fact that the diabetic pancreas contained less extractable peptides/proteins with considerably lower hydrophobicity and/or molecular weight than the normal pancreas (Fig. 5) may be explained by the fact that the normal pancreatic glands were "fresh" (obtained from persons exposed to sudden death, classified as kidney donors), whereas the diabetic pancreatic glands were removed after the ischaemia time (6–8 h according to the Danish death criteria). The pancreas is loaded with digestive enzymes, and proteolytic cleavage of peptide bonds in this period is very likely to take place.

After Sephadex G-50 chromatography of normal pancreatic extracts in 3 M acetic acid, the amount of material with MW > 6000 dalton (95–98%) was substantially higher than the amount of peptides with MW  $\leq$  6000 dalton (1–2%) [6], indicating that the endocrine pancreas constitutes 1–2% of the total weight of the

pancreas, and that the major digestive enzymes constitutes *ca.* 75% of the total proteins present in the exocrine pancreas.

The fact that hGH was eluted very late in the chromatogram when the Dynosphere column was eluted with an acetic acid gradient in water, in combination with the high recovery for hGH with this mobile phase, makes the system very useful for purification of the crude acetic acid extracts of *E. coli* with the inserted hGH gene [9] (Fig. 9A and B). hGH was very well separated from the majority of co-extracted impurities, and only minor residual contaminants were detected, even when the SDS-PAGE was overloaded (Fig. 9). The fact that the extraction medium (similar to the acetic acid extracts of pancreatic glands) may be applied, directly or after dilution with water, to the RP column, makes this procedure very attractive for preparative purposes.

When the above-mentioned samples (IL-1 $\beta$ , extracts of human diabetic and normal pancreata after Sephadex G-50 chromatography and crude hGH *E. coli* extracts) were analysed using a Nucleosil 300 Å C<sub>4</sub> column eluted with TFA-acetonitrile (Figs. 1, 7 and 9), it is striking that the separation patterns for the two highly different RP systems were very similar in the overall distribution of the separated components. It is normally considered that the  $\pi$ -electrons in the aromatic ring lead to binding characteristics different from those obtained with alkyl groups, but in the systems used in this study, the chromatograms were found to be comparable, especially when the column eluates were monitored at similar wavelengths (Fig. 6, right, and Fig. 7, lower). However, for further studies of similarities and differences, the Dynosphere should be eluted with TFA-acetonitrile and the chromatograms compared with those obtained with acetic acid gradients. The opposite comparison (Nucleosil C<sub>4</sub> eluted with 37.5–90% acetic acid) is hardly realistic owing to potential solubility problems with the silica-based stationary phase.

The reason for the elution strength of acetic acid in this RP situation is not obvious. The use of high concentration of formic acid has been reported for the RP-HPLC of defatted egg yolk proteins, but only present in buffer A [72% formic acid, buffer B being isopropanol-acetonitrile (2:1)] [10]. Formic acid (60%) has been used as a mobile phase additive for the RP-HPLC of water-insoluble polio virus proteins [11] and bovine serum albumin derivatives and other hydrophobic proteins [12], but in these experiments the elution was performed with 10–30% isopropanol in formic acid (60% formic acid being present in both buffer A and buffer B). Formic acid itself, in concentrations up to 100%, eluted only very few proteins, and it was reported that replacing formic acid with acetic acid was unsuccessful, leading to non-ideal peak shapes and reduces recoveries [11]. The separation of  $\beta$ -lactoglobulin, eluted as two components with very good separation, indicates that the separation capacity of the formic acid-isopropanol system is different from that of the Dynosphere-acetic acid system described here, but equal to that obtained when the Dynosphere was eluted with an acetonitrile-containing mobile phase (Fig. 2, upper). The major reason for the differences between the formic acid system and the acetic acid system is probably the use of a C<sub>8</sub> column in the formic acid-isopropanol system [11,12] *versus* a phenyl column in this work. We eluted the Dynosphere column with a formic acid gradient (20  $\rightarrow$  90% formic acid), but recovered virtually none of the proteins and peptides separated in Fig. 2, and the baseline was extremely unstable [6].

In conclusion, we have developed a reversed-phase system which allows sep-

aration of a number of individual peptides/proteins and complicated crude acetic acid extracts of various biological tissues. The separation capacity, peak shapes and recoveries were frequently excellent, and the elution could be performed with acetic acid alone, without the commonly used organic modifiers. Further characterization of extracts of the normal and diabetic human pancreas will be published separately [13].

#### ACKNOWLEDGEMENTS

We thank Ingelise Fabrin, Helle Bojesen-Koefoed and Linda Larsøe for excellent technical assistance, Jens Mølviq for performing the LAF assays and Kim Ry Hejnæs for generous supplies of IL-1 $\beta$  and [<sup>125</sup>I]IL-1 $\beta$ .

#### REFERENCES

- 1 B. S. Welinder, H. H. Sørensen and B. Hansen, *J. Chromatogr.*, 462 (1989) 255.
- 2 O. D. Madsen, L.-I. Larsson, J. H. Rehfeldt, T. W. Schwartz, Å. Lernmark, A. O. Labrecque and D. F. Steiner, *J. Cell. Biol.*, 103 (1986) 2025.
- 3 H. H. Sørensen, unpublished results.
- 4 J. Mølviq, L. Baek, P. Christensen, K. R. Manogue, H. Vlasara, P. Platz, L. S. Nielsen, A. Svejgaard and J. Nerup, *Scand. J. Immunol.*, 27 (1988) 705.
- 5 J. A. Schmidt, P. A. Cameron and G. A. Limjuco, *U.S. Pat.*, 4 770 781, 1987.
- 6 B. S. Welinder, unpublished results.
- 7 B. S. Welinder, in R. Hodges and C. Mant (Editors), *HPLC of Peptides and Proteins: Separation, Analysis and Conformation*, CRS Uniscience, Boca Raton, FL, 1991, in press.
- 8 S. Linde, J. H. Nielsen, B. Hansen and B. S. Welinder, *J. Chromatogr.*, 462 (1989) 243.
- 9 H. Dalbøge, H. H. M. Dahl, J. Pedersen, J. W. Hansen and T. Christensen, *Biotechnology*, 5 (1987) 161.
- 10 D. D. Sheumack and R. W. Burley, *Anal. Biochem.*, 174 (1988) 548.
- 11 J. Heukeshoven and R. Dernick, *J. Chromatogr.*, 326 (1985) 91.
- 12 J. Heukeshoven and R. Dernick, *J. Chromatogr.*, 252 (1982) 241.
- 13 B. S. Welinder and S. Linde, *J. Chromatogr.*, 537 (1991) 201.



## Reversed-phase high-performance liquid chromatographic characterization of acetic acid extracts of the normal and the diabetic human pancreas

BENNY S. WELINDER\* and SUSANNE LINDE

*Hagedorn Research Laboratory, DK-2820 Gentofte (Denmark)*

(First received March 20th, 1990; revised manuscript received July 20th, 1990)

---

### ABSTRACT

The combination of a divinylbenzene-based reversed-phase (RP) column and acetic acid gradients in water as mobile phase described in the accompanying paper was used for characterizing the extractable polypeptides from the normal and the diabetic human pancreas. The pancreas was lyophilized, minced and extracted three times in 3 *M* acetic acid. After mechanical clarification, the raw extracts were applied directly to the RP column. Alternatively, the extracts were lyophilized and subjected to size-exclusion chromatography on Sephadex G-50 in 3 *M* acetic acid. Two fractions with mol. wt. > 6000 dalton (Peak I) or with mol. wt. ≤ 6000 dalton (Peak II) were obtained.

The Sephadex G-50 size-exclusion chromatography and the RP-high-performance liquid chromatographic (HPLC) analyses of the crude extracts from a normal pancreas clearly demonstrated the weight distribution and differences between the exocrine pancreas (containing primarily the major digestive enzymes) and the endocrine pancreas (containing insulin, glucagon, etc.). RP-HPLC analyses of crude extracts from various normal pancreatic glands resulted in very similar UV profiles, whereas those from a number of individual diabetic glands differed. Chromatograms of acetic acid extracts from normal pancreata were similar when analysed before or after lyophilization, whereas lyophilization of acetic acid extracts of diabetic glands resulted in severely obscured chromatograms.

RP-HPLC analyses clearly demonstrated several differences between the diabetic and the normal pancreas. In the crude extracts, the extractable proteins from the diabetic pancreas were shifted towards lower molecular weight and/or hydrophobicity. Further, a peak co-eluting with authentic, human insulin could be demonstrated in the raw extract and in the peak II material from the normal pancreas, whereas virtually no mass signal was seen in the UV-profiles of similar materials from the diabetic gland. This finding was further verified by insulin radioimmunoassay (RIA) performed on the isolated fractions after RP-HPLC of a crude extract from a normal and a diabetic pancreas. The insulin content in the diabetic pancreas was found to be *ca.* 1% of that in the normal pancreas. When authentic glucagon was added to crude extracts from a diabetic pancreas, a single component was found after immediate analysis, but after several hours at room temperature the glucagon was found to be degraded. Added insulin was stable under these conditions.

Similar RP analyses were performed on a silica C<sub>4</sub> column eluted with an acetonitrile gradient in trifluoroacetic acid. Although the chromatograms were more complex than those obtained with acetic acid as mobile phase, they were comparable in outline, and the differences between the normal and the diabetic glands could again be demonstrated.

One of the reasons for the differences between the normal and the diabetic pancreas may be that the normal glands were removed and frozen immediately after death, whereas the diabetic glands were obtained after an ischaemia time of 6 h or more, leaving considerable time for post mortem enzymatic degradation.

The RP-HPLC system is very suitable for these analyses. The acetic acid extracts can be applied directly to the RP column and, after lyophilization, the isolated fractions may be re-analysed [RIA or enzyme-linked immunosorbent assay (ELISA)], or subjected to a second (alternative) RP-HPLC. After such double RP-HPLC purification, almost all major individual components in the peak I and II material from a normal pancreas were sufficiently pure for microsequencing, and identification (based on 30 steps in the gas-phase sequencer and comparing the sequence information obtained with databases) again reflected the distribution of the principal components from the exocrine and the endocrine pancreas in the peak I and II materials.

---

## INTRODUCTION

Extraction of biological samples (tissues, organs or whole organisms), often the first step in many isolation procedures for biopolymers, normally results in extremely complex mixtures of lipids, carbohydrates and proteins/peptides. One of these main groups may be excluded, or favoured, through a proper choice of solvent, *e.g.*, a very polar solvent will solubilize more protein material than lipid, but most often an aqueous extract will contain numerous related compounds in addition to those desired.

Characterization of such raw extracts is normally not performed with general analytical tools (*e.g.*, general protein or carbohydrate analysis) but with analyses specific for a single or a narrow group of compounds, such as biological activity (*e.g.*, enzymatic activity) or antigenicity [enzyme-linked immunosorbent assay (ELISA), radioimmunoassay (RIA), etc.]. In the case of polypeptides, the development of analytical and preparative reversed-phase high-performance liquid chromatography (RP-HPLC) with sensitive, non-specific mass detection (UV, refractive index), or more specific post-column reactions, in the last decade has reached a level where the separation and determination of more than 100 polypeptides in a single chromatographic analysis can be achieved in less than 1 h. Consequently, this technique has been incorporated as a rapid downstream control analysis in the industrial scale extraction of biological materials, such as the production of insulin and growth hormone.

In this work we applied RP-HPLC for the characterization of crude extracts of the normal and the diabetic human pancreas. Acetic acid was chosen as solvent owing to the extremely good solubility of the majority of peptides and proteins from the endocrine pancreas in this solvent [1]. As we recently demonstrated that a polymeric phenyl-based RP column could be eluted with an acetic acid gradient without the use of organic modifiers [2], this system was used for the RP-HPLC characterization of the acetic acid extracts, thereby eliminating the need for solvent exchange or concentration/isolation procedures between extraction and characterization of the solubilized sample material. The UV profiles obtained were compared with those of similar separations using a silica-based RP column eluted with an acetonitrile gradient in trifluoroacetic acid (TFA). Several pancreatic proteins/peptides isolated after the acetic acid extraction and RP-HPLC in acetic acid gradients have been identified after amino acid sequencing, indicating the general applicability of this extraction/analysis system for identification purposes.

## EXPERIMENTAL

The HPLC equipment, columns, samples and all analyses were performed as described in the accompanying paper [2]. Detailed descriptions of the stationary and mobile phases are given in the legends to the figures.

## RESULTS

Fig. 1 (left) shows the elution profile obtained after Sephadex G-50 chromatography of lyophilized acetic acid extracts obtained after the first, second and third

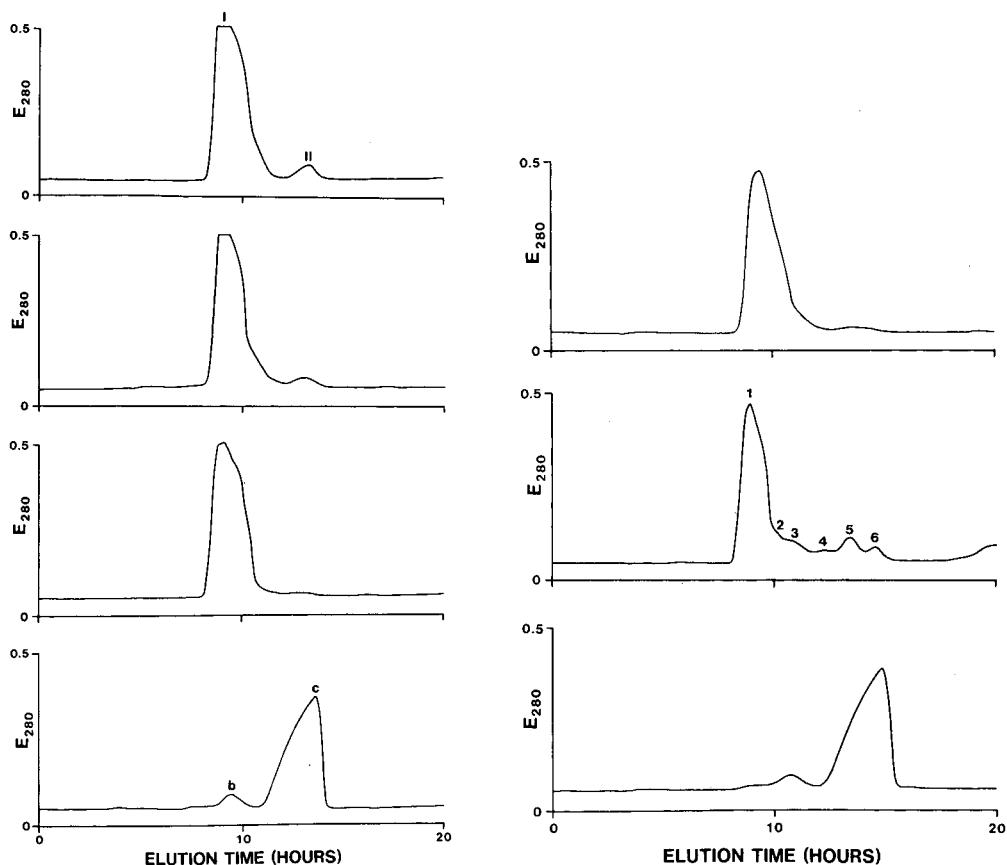


Fig. 1. Left: Sephadex G-50 chromatography of 200 mg of lyophilized material obtained from first, second and third extractions of a normal human pancreas. After lyophilization of the crude acetic acid extracts, the residues were dissolved in 3 *M* acetic acid, centrifuged and filtered. A 95 × 2.5 cm column was eluted at 4°C (ca. 20 ml/hour) with 3 *M* acetic acid. From top to bottom: first, second and third extractions. Peak I and II materials are marked "I" and "II", respectively. Bottom: 100 mg of crystalline, porcine insulin. The b- and c-components are marked accordingly. Right: Sephadex G-50 chromatography of 200 mg of lyophilized acetic acid extract (combined from the first, second and third extractions) of a normal human pancreas (top), a diabetic, human pancreas (middle) and 100 mg of crystalline, porcine insulin (bottom). The elution was performed as described for the left panel.

extractions of a normal human pancreas. In all three extracts, the majority of extractable polypeptides were eluted in the void volume fraction (peak I). A smaller fraction (peak II) with a similar elution volume to insulin peptide (compare to the bottom curve on the left) gradually decreased from the first to the third extraction. A comparison between the Sephadex G-50 profiles obtained from lyophilized acetic acid crude extracts of a normal and a diabetic pancreas is shown in Fig. 1, right. The diabetic extract has a similar distribution in mass between the void volume peak and the residual material with higher elution volume, but whereas only a single peak with molecular weight (MW)  $\leq 6000$  dalton was detected in the extract from a normal pancreas, this region contained two larger and three smaller peaks (marked 2-6), indicating a more heterogeneous distribution of the peptide region in the extract of the diabetic pancreas.

On average, 2-4 mg of peak II material and 50-80 mg of peak I material were obtained after Sephadex G-50 chromatography of 200 mg of lyophilized crude extract of a normal pancreas, indicating a considerable loss of material during the filtrations prior to gel chromatography. The protein concentrations in the extracts showed extremely wide variations, indicating the very heterogeneous sample material. The insulin contents in the crude extracts were equally scattered (Table I).

After sodium dodecyl sulphate-polyacrylamide gel electrophoresis (SDS-PAGE) of crude extracts of a normal and a diabetic pancreas, numerous proteins were distributed throughout the whole separation range (6000-300 000 dalton) in both extracts. SDS-PAGE of peaks I and II also verified that peak II material from a normal and a diabetic pancreas primarily contained peptides with MW similar to or lower than the effective MW fractionation range of the 8-25% gradient gel system (data not shown).

RP-HPLC analyses of the first extract from a normal and a diabetic pancreas, using a Dynosphere PD-102-RE column eluted with an acetic acid gradient, are shown in Fig. 2, upper, and those of the corresponding lyophilized extracts in Fig. 2, lower. For both the crude extracts and the lyophilized extracts, subsequent extrac-

TABLE I

CONTENTS OF PROTEIN AND INSULIN DETERMINED IN THE ACETIC ACID EXTRACTS OF THREE INDIVIDUAL NORMAL AND FIVE INDIVIDUAL DIABETIC HUMAN PANCREATA

The insulin and protein contents are calculated per gram of lyophilized pancreas.

Pancreas	Protein (mg/g)	Insulin ( $\mu$ g/g)
Normal	258	607
	161	463
	81	322
Diabetic	80	37
	59	38
	15	15
	41	19
	53	14



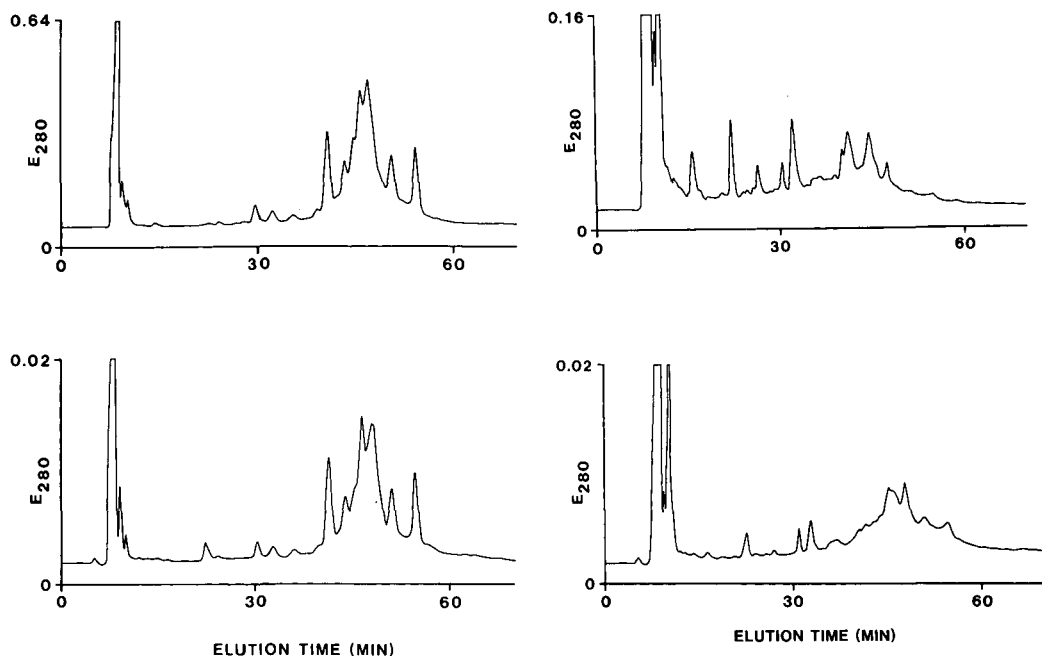


Fig. 2. RP-HPLC of 200  $\mu$ l of crude acetic acid extract of a normal (upper left) and a diabetic human pancreas (upper right) and of the corresponding lyophilized acetic acid extracts solubilized to 1 mg/ml in 3 *M* acetic acid. A 200- $\mu$ l volume was applied in the analysis of this material from a normal (lower left) and a diabetic pancreas (lower right). A 250  $\times$  4.6 mm I.D. Dynosphere PD-102-RE column was eluted at 0.5 ml/min with an acetic acid gradient (37.5  $\rightarrow$  90% acetic acid linearly during 60 min followed by 10 min isocratically at 90% acetic acid).

tions of both glands resulted in similar RP-HPLC profiles at reduced levels (data not shown). When the UV-profiles of normal glands (Fig. 2, left) are compared with those from a diabetic (Fig. 2, right), it can be seen that much less UV-absorbing material was present in the raw extract of the diabetic pancreas (note the different UV scales), and the RP-HPLC profile of the diabetic pancreas is very different from that of a normal pancreas. The diabetic protein distribution is shifted towards earlier elution, indicating lower hydrophobicity and/or molecular weight of the individual sample components. The dominant part in the RP-HPLC profile of the normal pancreas is a group of peaks eluted in the last third of the chromatogram, whereas in the extracts of the diabetic pancreas the impact of this group of peaks is strongly reduced, compared with the earlier eluting peaks, which now are the dominating sample constituents. In addition, lyophilization of the raw acetic acid extracts of a diabetic pancreas led to a considerable reduction in chromatographic separation efficiency (compare the upper and lower curves in Fig. 2, right). The last half of the chromatogram is seriously obscured, and the number of individual components in the whole chromatogram is reduced. In contrast, the RP-HPLC profile of the directly analysed crude extract from a normal pancreas was very similar to that obtained for the lyophilized extract (Fig. 2, left, upper and lower curves).

RP-HPLC analyses of peak I and II material from a normal and a diabetic pancreas are shown in Fig. 3, left and right, respectively. The sample constituents from the extract of the normal pancreas are clearly divided into two groups with different retention times, reflecting the separation according to MW after Sephadex G-50 chromatography, whereas the separation efficiency of the diabetic peak I material (Fig. 3, right, upper curve) was found to be reduced in a similar way to that above for the lyophilized total extract (Fig. 2, right, lower curve). However, the peptide-like peak II material derived from the diabetic pancreas was separated equally efficiently as that from the normal pancreatic extract (Fig. 3, lower curves). Similar results were obtained for other individual peak I and II materials [2], indicating that this reduction in separation capacity of the diabetic material is of a general nature.

Three different normal pancreatic glands (parts of the whole pancreas) were extracted, followed by RP-HPLC of the lyophilized crude acetic acid extracts (Fig. 4, left). It can be seen that the extraction-RP-HPLC analysis procedure resulted in comparable UV profiles: the majority of sample components were found to be present in each of the three different extracts, although limited variations in the significance of the individual peaks were noticed between the different samples. The sample components in the last part of the chromatogram were the most abundant, indicating that the majority of the extracted material consists of peak I material (compare with Fig. 3, left, upper curve). Comparable analyses were performed with three different diabetic pancreatic crude extracts (Fig. 4, right). The first half of the chromatograms differed more than that for similar extracts of normal glands, whereas the last parts of the chromatograms were comparable. However, these last parts of three RP-HPLC traces of the diabetic extracts were still significantly different from those of normal glands (compare with the left panel).

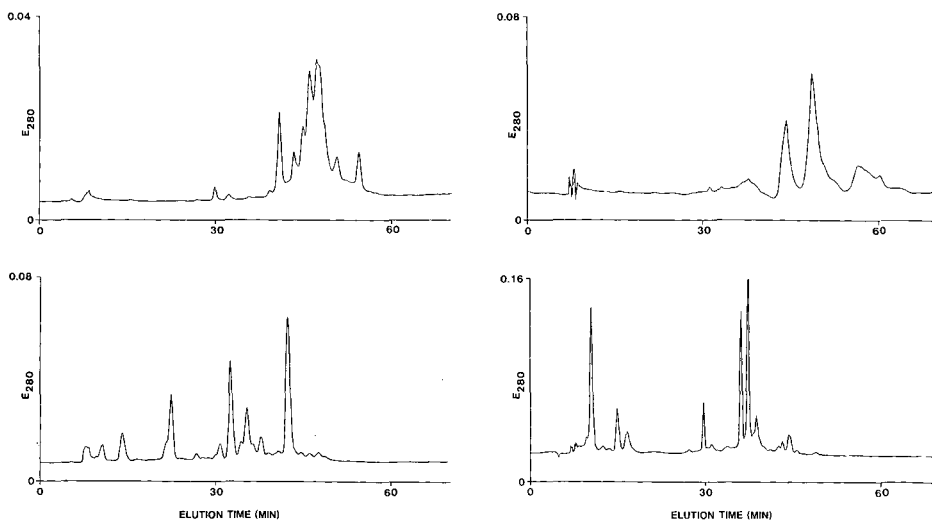


Fig. 3. RP-HPLC of peak I (upper curves) and peak II (lower curves) material (lyophilized crude acetic acid extract after Sephadex G-50 chromatography as described under Experimental), obtained from a normal human (left) and a diabetic human pancreas (right). The sample material was redissolved in 3 M acetic acid to 1 mg/ml, centrifuged and filtered (0.45  $\mu$ m). 200  $\mu$ l of both samples were applied. Stationary and mobile phases as in Fig. 2.

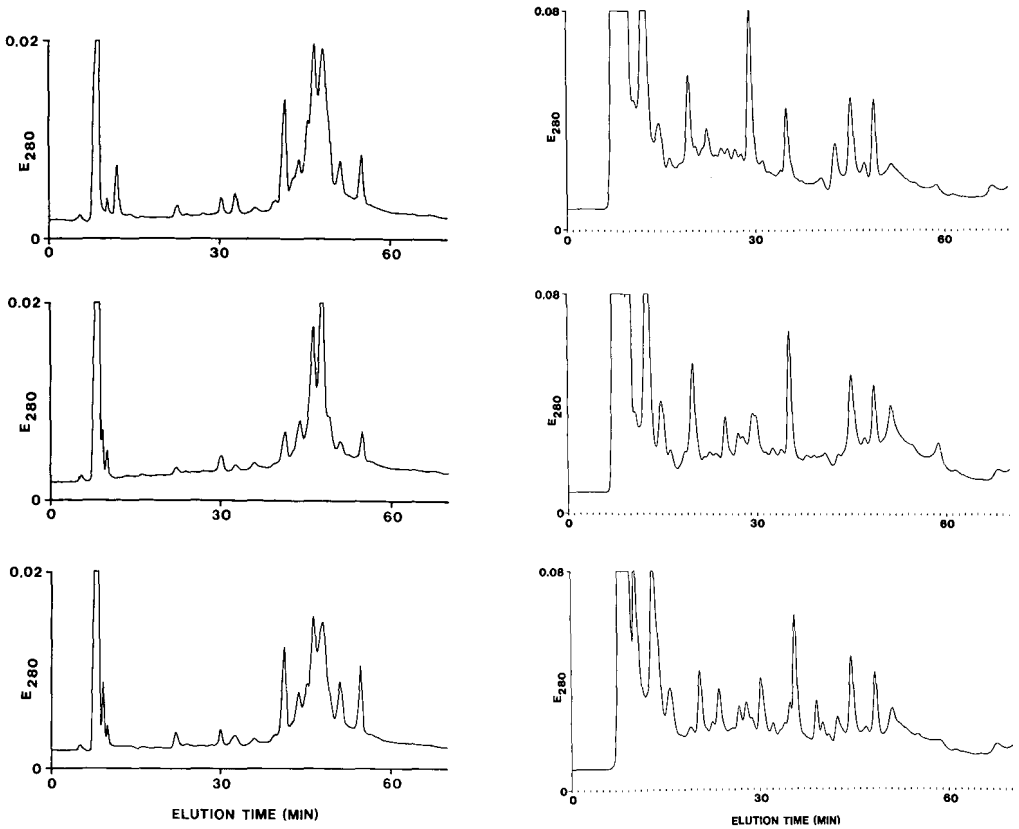


Fig. 4. Left panel: RP-HPLC of lyophilized crude acetic acid extracts of three different normal human pancreatic glands. The lyophilization residues were redissolved to 1 mg/ml in 3 M acetic acid, centrifuged and filtered (0.45  $\mu$ m). 200  $\mu$ l were applied in all analyses. Stationary and mobile phases essentially as in Fig. 2. Right panel: RP-HPLC of 200  $\mu$ l crude acetic acid extracts of three different diabetic, human pancreatic glands. Stationary and mobile phases as in Fig. 2.

In order to compare the separation capacity of the Dynosphere column eluted with an acetic acid gradient with that of a commonly used RP-HPLC system, the crude extracts of a normal and diabetic pancreas were separated on a Nucleosil 300  $\text{\AA}$  C<sub>4</sub> column eluted with an acetonitrile gradient in TFA (Fig. 5). The chromatograms of extracts from a normal pancreas were remarkably similar in the two different systems, again demonstrating the predominant position of the sample components eluted in the last third of the chromatogram (compare Fig. 5, upper, with Fig. 2, left, upper curve). The HPLC profile of the extract from the diabetic pancreas (Fig. 5, lower) was more detailed than obtained after elution of the Dynosphere column with an acetic acid gradient (Fig. 2, right, upper curve) with respect to the components eluted in the first half of the chromatogram, again emphasizing the shift in hydrophobicity and molecular weight compared with the late-eluting main components in extracts of the normal pancreas.

The elution positions of insulin, proinsulin and glucagon in the Dynosphere-

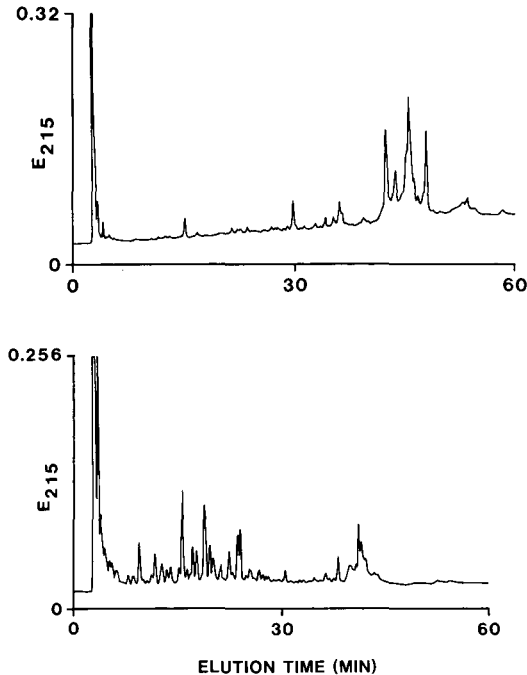


Fig. 5. RP-HPLC of 10  $\mu$ l of the crude acetic acid extract of a normal human (upper) and a diabetic human pancreas (lower) using a 250  $\times$  4.0 mm I.D. Nucleosil 300  $\text{\AA}$  C<sub>4</sub> column eluted at 1.0 ml/min with an acetonitrile gradient (12  $\rightarrow$  57% acetonitrile linearly during 60 min) in 0.1% TFA. Separation temperature: 45°C.

acetic acid RP system were mapped in the normal and the diabetic crude extracts after spiking with small amounts of the authentic hormones (Fig. 6). Insulin and glucagon co-eluted in this system, and the retention times of these two hormones were similar to that of an already existing peak in the extract from the normal pancreas (upper curve), whereas very little UV-absorbing material was present at those positions in the chromatogram of diabetic crude extract where insulin, glucagon and proinsulin were eluted (lower curve).

During these spiking experiments, it was noted that when glucagon was added to the diabetic crude extract, the resulting chromatogram depended on the time spent in the autosampler before the actual column separation: when the glucagon-spiked extract was analysed immediately, a single glucagon-peak was observed (Fig. 7, left, middle curve), but after 15 h, two additional major peaks with shorter retention times than glucagon was observed (Fig. 7, left, lower curve). This was not an effect of instability of the diabetic acetic crude extract as such, since the UV profile of an immediately analysed crude extract was found to be similar to that obtained from the same extract stored at room temperature for 48 h (data not shown).

A similar experiment was performed after addition of crystalline glucagon plus trace amounts of [<sup>125</sup>I]glucagon (Fig. 7, right). Immediate analysis of the tracer alone or added to the diabetic crude extract resulted in a single UV glucagon peak and a radioactivity peak with a slightly reduced retention time (plus a UV peak correspond-

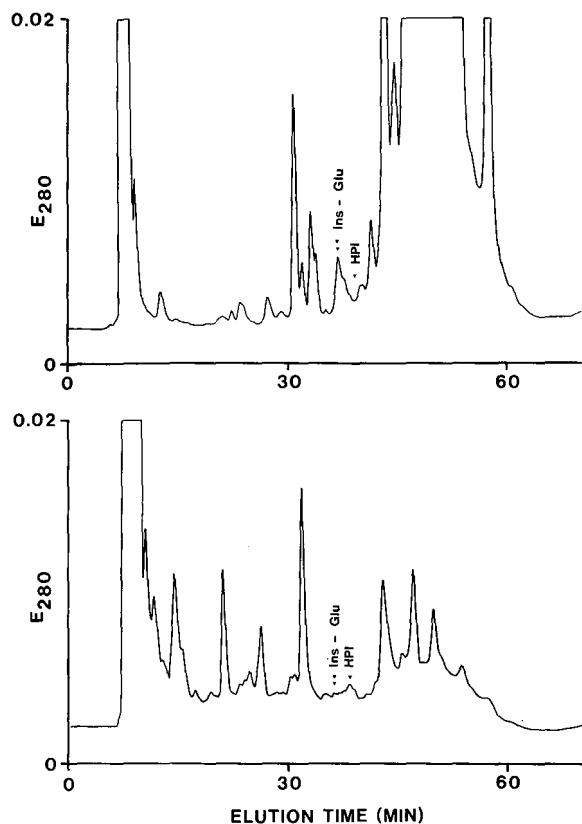


Fig. 6. RP-HPLC of 25  $\mu$ l of crude acetic acid extract from a normal human (upper) and a diabetic human pancreas (lower). The elution positions of human insulin (Ins), porcine glucagon (Glu) and human proinsulin (HPI) are marked with filled triangles. Stationary and mobile phases as in Fig. 2.

ing to the human serum albumin added to the tracer preparation; Fig. 7, right, upper and middle curves). However, after 48 h at room temperature, the crude extract with added glucagon again showed two major UV peaks with markedly reduced retention times, and all the radioactivity was eluted in the first major peak (Fig. 7, right, lower curve). This degradation of glucagon could only be demonstrated in the case of the diabetic crude extract. If glucagon was incubated in crude extract of a normal, human pancreas for 17 h in a WISP autosampler, a single UV glucagon peak was obtained after RP-HPLC. Further, under the conditions causing degradation of added glucagon, insulin added to the diabetic and the normal extracts was found to be totally stable (data not shown).

Although no distinct UV peak with a similar retention time to that of added human insulin could be demonstrated in crude extracts of a diabetic pancreas, a small UV peak, co-eluting with added insulin, was observed when peak II material (assumed to be enriched with polypeptides with  $MW \leq 6000$  dalton) from a diabetic pancreas was analysed. As many insulin dependent diabetes mellitus (IDDM) pa-

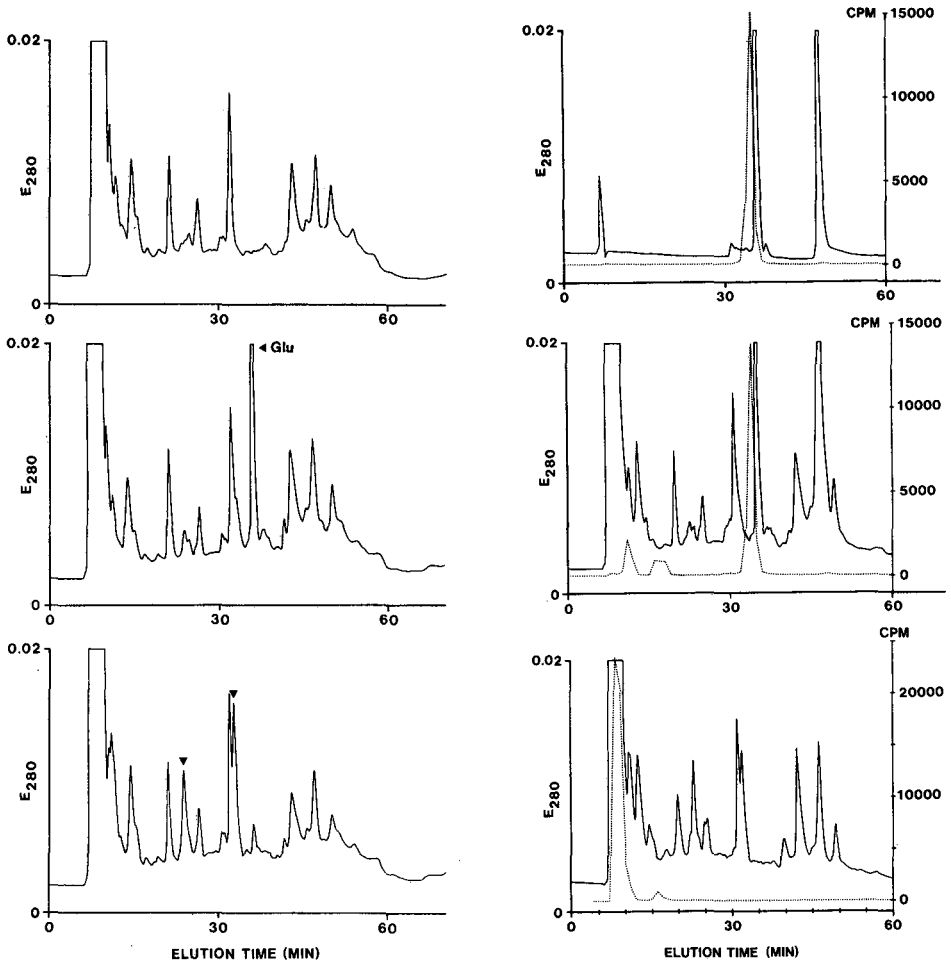


Fig. 7. Left: RP-HPLC of 25  $\mu$ l of crude acetic acid extract from a diabetic human pancreas (upper) and the same extract spiked with 10  $\mu$ g of crystalline, porcine glucagon (Glu) and injected immediately (middle curve) or after 15 h in a WISP autosampler (lower curve). The two major additional peaks formed from the added glucagon are marked with filled triangles. Right: RP-HPLC of 10  $\mu$ g of crystalline, porcine glucagon + ca. 35 000 cpm of [ $^{125}$ I]glucagon (upper curve), of 35  $\mu$ l of crude acetic acid from a diabetic, human pancreas spiked with 10  $\mu$ g of crystalline, porcine glucagon + ca. 35 000 cpm of [ $^{125}$ I]glucagon, analysed immediately (middle curve) or after storage at room temperature for 48 h (lower curve). Solid curves, UV; dotted curves, radioactivity. The large peak in the last part of the chromatograms represents serum albumin added to the [ $^{125}$ I]glucagon tracer preparation. Stationary and mobile phases as in Fig. 2.

tients maintain small amounts of  $\beta$ -cell function after the clinical onset of diabetes mellitus, the nature of this peak was investigated further. RP-HPLC of crude extracts from a normal and a diabetic pancreas was followed by insulin RIA of the isolated fractions, and it could be clearly demonstrated, that small amounts of immunological reactive insulin were present in the diabetic pancreas (Fig. 8). Approximately 1% of the amount of insulin extracted from the normal pancreas could be demonstrated

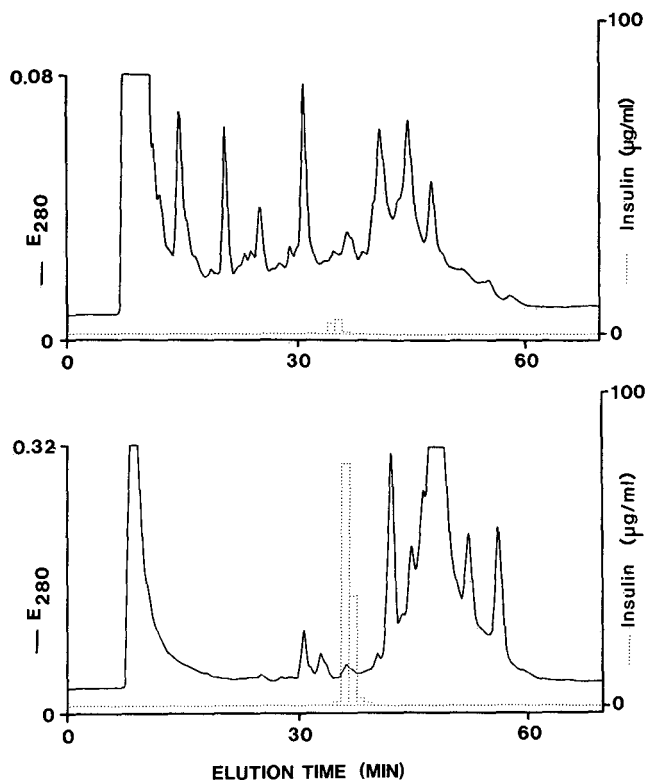


Fig. 8. RP-HPLC of 200  $\mu$ l of raw acetic acid extract of a diabetic human pancreas (upper) and a normal human pancreas (lower). Fractions (1 min) were collected and lyophilized in a Speed Vac concentrator, redissolved and analysed for insulin content (RIA) as described under Experimental. Stationary and mobile phases as in Fig. 2.

after RP-HPLC of the extract of the diabetic gland. The minor content of insulin in the diabetic pancreata was also directly confirmed by insulin RIA of the crude extracts (Table I).

The present acetic acid RP-HPLC system should, in theory, be suitable as an isolation-identification system, owing to the volatile mobile phase. As it is obvious, that the number of sample components demonstrated in the UV profiles of the crude extracts was less than the number of components demonstrated after SDS-PAGE or after silica C<sub>4</sub>-TFA-acetonitrile RP-HPLC, a second purification step, preferably involving a different stationary or mobile phase, would probably be necessary before any sequence analyses.

As a first attempt to make the above-described Dynosphere-acetic acid separations (all performed on a 250  $\times$  4.6 mm I.D. column) a truly preparative isolation system, larger amounts of crude extracts were loaded on a 180  $\times$  16.0 mm I.D. Dynosphere column and eluted with a similar acetic acid gradient at 4.0 ml/min. Almost identical UV profiles were obtained when the 16 mm I.D. column was loaded with up to 10 mg of lyophilized crude extract of a normal pancreas (data not shown). Approximately 5 mg of peak I and 3 mg of peak II material were then separated on

the 16 mm I.D. column, and the major peaks from both separations were collected manually. These individual fractions were then further purified using a Nucleosil 300 Å C<sub>4</sub> column eluted with an acetonitrile gradient in TFA or a TSK Phenyl 5PW RP+ column eluted with an acetonitrile gradient in 100 mM ammonium hydrogencarbonate. In the former instance, the acetic acid column eluate could be loaded directly

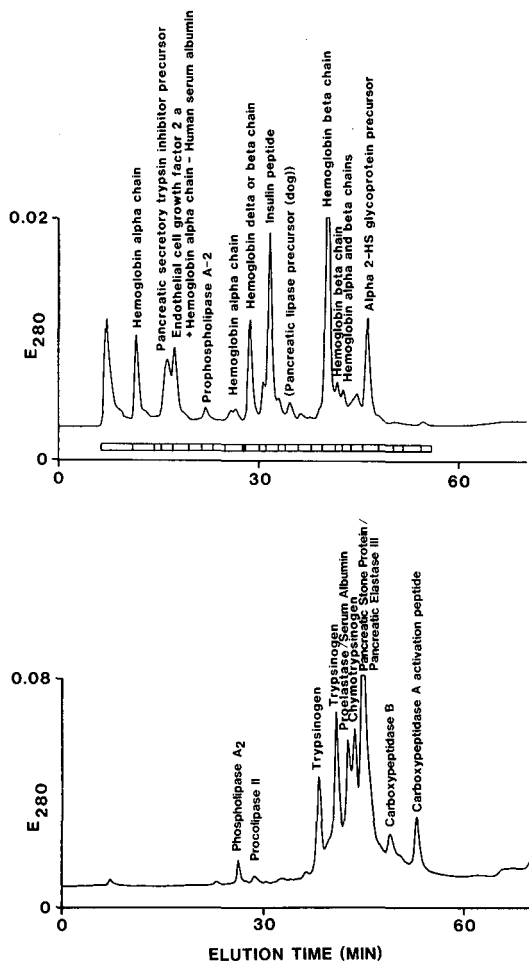


Fig. 9. Upper: RP-HPLC separation of peak II material [redissolved in 3 M acetic acid to 10 mg/ml, centrifuged and filtered (0.45  $\mu$ m)] from a normal human pancreas using a 180  $\times$  16.0 mm I.D. Dynosphere PD-102-RE column eluted at 4.0 ml/min with an acetic acid gradient (37.5  $\rightarrow$  90% acetic acid linearly during 60 min, followed by 10 min isocratically at 90% acetic acid). 275  $\mu$ l (= 2.75 mg of peak II material) were applied, and fractions were collected as indicated above the abscissa. After rechromatography of these fractions (Nucleosil C<sub>4</sub>-TFA-acetonitrile) the major peaks were isolated and subjected to amino acid sequencing. For identification, the sequence information obtained after 30 degradation cycles was compared with published amino acid sequences in a database. Lower: RP-HPLC separation of peak I material from a normal human pancreas using the same stationary and mobile phase. 500  $\mu$ l (= 5 mg of peak I material) were applied, and fractions corresponding to the main peaks were collected. Rechromatography, amino acid sequencing and identification as described for the upper panel.



onto the Nucleosil column (after dilution with one volume of distilled water), whereas lyophilization of the acetic acid column eluate was found to be necessary before analysis in the ammonium hydrogencarbonate system (if the acetic acid was neutralized with ammonia solution, the large amounts of ammonium acetate in the sample seriously disturbed the separation).

The major components obtained after the second purification steps were isolated by lyophilization and subjected to amino acid sequence analyses. Usually 30 degradation cycles were performed, and the sequence information obtained was compared with published sequences in databases for identification. The preliminary results of these analyses are shown in Fig. 9. It should be noted that the database identifications are shown in the figures, although only parts of the sequences have been identified in the actual RP-HPLC fractions. A complete sequence, or a mass spectrometric MW determination of the isolated compounds, might have identified which part of the sample molecule was actually present, but such analyses were not performed in these preliminary identification experiments.

## DISCUSSION

The most frequently published procedure for the extraction of human and animal pancreatic glands utilizes acidified ethanol [3–19]. However, this procedure has been adapted from the industrial-scale extraction of insulin based on the pancreata of slaughterhouse animals, and it is highly specific for insulin and similar pancreatic peptides (glucagon, pancreatic polypeptide, somatostatin, etc.). The most common acidifier in these extractions is sulphuric acid, specially adapted for the porcine pancreas. However, when in the early 1970s we studied the efficiency of this extraction procedure for pancreatic glands from young cattle and humans, we observed a significantly lower yield compared with fresh porcine glands. In the case of young cattle, comparable amounts of insulin were extractable with ethanol acidified with phosphoric acid instead of sulphuric acid, but for human glands similar high yields were obtained only after extraction with 3 *M* acetic acid or 3 *M* acetic acid in 8 *M* urea. The last solvent was extremely efficient: after three successive extractions, virtually only the connective tissue remained in a non-solubilized state, but owing to the overwhelming amount of very different solubilized compounds and the absence of modern HPLC techniques, an isolation procedure for insulin was difficult to design [1].

Today, preparative HPLC is immediately involved in such considerations, but still the choice of the extraction medium for a “general” extraction of pancreatic glands (*i.e.*, extracting the majority of peptides and proteins present) must be carefully considered. Acidified ethanol or similar alcohols are certainly not an obvious choice, as the solubility of proteins is normally limited in this solvent, and the alcohol must necessarily be removed before the extraction medium can be applied to an RP column. A mixture of 3 *M* acetic acid in 8 *M* urea is very powerful solvent for most peptides and proteins, but large volumes of this solvent are hardly the most desirable in a normal RP binding–elution procedure.

The use of 3 *M* acetic acid remains an attractive possibility. The proteolytic enzymes present in large amounts in the exocrine pancreas are inhibited, the solubilizing properties for proteins are equal to that of acetic acid–urea, but the extraction medium is directly compatible with standard RP chromatographic systems. As we

recently have reported the elution of several proteins and peptides, including insulin and glucagon, from a polymeric phenyl column using an acetic acid gradient [2] (*i.e.*, without the use of common organic modifiers), it should be possible to perform the extraction and RP-HPLC separation in essentially the same liquid phase, thereby avoiding any sample manipulations between the extraction and the initial chromatographic purification.

Sephadex G-50 size-exclusion chromatography of the acetic acid pancreatic extract reflects the expected distribution between extractable "peptides" and "proteins": the endocrine part of the pancreas amounts to *ca.* 1–2% (on a weight basis) and the content of the major pancreatic hormone (insulin, MW 6000 dalton) is roughly 25% of that. Approximately 75% of the protein content of the exocrine pancreas consists of the major digestive enzymes (trypsin, chymotrypsin, lipase, amylase, elastase, carboxypeptidase A and B), which, together with serum albumin and haemoglobin (expected to be present in large amounts in extracts of vascularized tissue), contribute to the large void-volume peak I (Fig. 1).

When a normal human pancreas was extracted three times, the RP-HPLC profiles of the extracts were found to be very similar, with the exception of the amount of solubilized material. Lyophilization of these crude acetic acid extracts did not change the UV profiles obtained after RP-HPLC, in contrast to the findings for the diabetic human pancreas, where lyophilization of the crude acetic acid extracts resulted in deterioration of the separation pattern, especially in the last half of the chromatograms (Fig. 2). When the crude extract of a normal pancreas was compared with that of a diabetic pancreas, it was obvious that the diabetic extracts contained considerably less protein/peptide mass, and that the UV profile of solubilized proteins/peptides from a diabetic pancreas was displaced towards lower molecular weight and/or hydrophobicity. This displacement is clearly seen in all three diabetics (Fig. 4, right).

In outline, the extracts of three different normal pancreatic glands were similar (Fig. 4, left), whereas those of three diabetics were less comparable but clearly very different from a normal extract. The observed MW and/or hydrophobicity displacement for the diabetic extract compared with the normal extract was also clearly demonstrated when the RP-HPLC analyses were performed using a Nucleosil C<sub>4</sub> column eluted with the TFA–acetonitrile system (Fig. 5). Although a larger number of sample components were detected in the TFA–acetonitrile system (primarily owing to the use of UV registration at 215 nm instead of 280 nm in the acetic acid systems) [2], the use of these two highly different stationary–mobile phase combinations nevertheless resulted in surprisingly similar chromatograms. The MW and hydrophobicity differences between the extractable proteins and peptides from the normal and the diabetic pancreas could be demonstrated after Sephadex G-50 size-exclusion chromatography and also RP-HPLC with two different stationary–mobile phase combinations. This could reflect the difference in time between clinical death and removal/freezing of the two types of pancreatic tissue. If the pancreas is left at body temperature after death, most of the digestive enzymes present in the exocrine pancreas will be active for hours, resulting in marked cleavage of the pancreatic polypeptides. The finding that glucagon was degraded after incubation with extracts of the diabetic pancreas probably reflects that during the ischaemia time, the proteolytic enzymes in this pancreas were transformed to their active state, in contrast to the conditions in

the normal pancreas (removed and frozen shortly after death), where the majority of the enzymes would be expected to be present as inactive proenzymes.

It might seem surprising that insulin was not degraded under similar conditions. However, it was recently reported that acid saline extracts of the rat submaxillary gland (known to contain large amounts of glucagon-like material) were able to degrade [ $^{125}$ I]glucagon and [ $^{125}$ I]pancreatic polypeptide, whereas [ $^{125}$ I]insulin was left intact. The degradative effect could be inhibited by the addition of thiol proteinase inhibitors, whereas aprotinin had no effect [20]. Further, when pieces of surgically removed human pancreatic glands were left at room temperature for up to 12 h after the dissection, it was found that glucagon was much more susceptible to proteolytic enzymes than insulin and pancreatic polypeptide [21].

Further evidence for the proteolytic degradation is the finding of several serum albumin and globin chain sequences in the peak II material (Fig. 9 upper). Intact globin and human serum albumin would not be expected to appear in a size-exclusion fraction isolated according to a molecular weight of  $\leq 6000$  dalton.

The reason for the markedly reduced RP-HPLC separation efficiency of lyophilized sample material from the diabetic pancreas is not clear. During the extraction and isolation procedures it was noticed that the diabetic pancreas contained considerably more fatty substances than the normal pancreas. After centrifugation of the raw extract, three phases were obtained: pancreatic tissue as precipitate, a top layer consisting primarily of semi-liquid/semi-solid lipids and, in between, a fairly clear, aqueous layer containing the solubilized pancreatic sample material in 3 *M* acetic acid. It was difficult to decant this interphase completely from the lipids, especially when the lipid layer at the top was pronounced, and after lyophilization of the acetic acid crude extracts from the diabetic pancreas the lyophilization residue had an oily appearance, in contrast to those from a normal pancreas, which remained fairly dry after lyophilization. As the sample preparation before RP-HPLC was identical for crude extracts and lyophilized pancreatic extracts (high-speed centrifugation in Eppendorf tubes followed by 0.45- $\mu$ m filtration), the harmful effect can probably be localized to the lyophilization in the presence of lipids.

The general usability of the Dynosphere-acetic acid system for succeeding analyses was illustrated by the insulin RIA analyses performed after lyophilization of collected fractions (Fig. 8) and also by the initial sequence results obtained after a secondary RP purification of the major components in peak I and II material from a normal pancreas. The major digestive enzymes from the exocrine pancreas and the major hormone from the endocrine pancreas (*i.e.*, insulin) were easily identified (Fig. 9). Further sequencing of minor fractions are in progress.

It is worth mentioning, that the extraction and the two RP separations were performed without any isolation steps (lyophilization, precipitation). This procedure should therefore be well suited for isolating components present in very small amounts, where isolation and redissolution may severely reduce the yield before the sample can be transferred to the amino acid sequencer. If the final RP-HPLC is performed in micro-columns, the isolated polypeptide may be collected directly from the outlet tube of the UV photometer onto a glass-fibre disc and transferred to the gas-phase sequencer. The peptide separation efficiency of the present acetic acid system is lower than that of an alkylsilica-TFA-acetonitrile system. However, the polymeric stationary phase utilized here is the first to be eluted with acetic acid gradients

in water, and other existing polymer-based RP columns or future developments in stationary phase design may well increase the selectivity and separation capacity in acetic acid gradients.

For the isolation of pure peptides/proteins from crude extracts containing numerous sample components, more than one RP-HPLC system is often needed. To obtain maximum resolution, it is essential to apply two RP-HPLC methods with different stationary phase and/or mobile phase compositions, and the initial one could well be a polymeric RP column eluted with an acetic acid gradient in water. The reduced sensitivity (due to the inapplicability of low-UV detection) is less inconvenient in the initial part of a purification procedure, and such a system may be cleaned up with strong alkaline and will tolerate a considerably higher number of crude samples than an alkylsilica column, which remains the obvious choice for the second-dimension RP-HPLC.

In conclusion, we have developed an extraction procedure for pancreatic glands and an RP-HPLC analysis system for the characterization of these extracts using the same solvent throughout, thereby allowing a direct characterization and identification (RIA, sequence determinations) of extracted compounds. The resulting UV profiles clearly reflect the different distributions of proteins and peptides in the exocrine and the endocrine pancreas.

The RP chromatograms obtained from a number of normal pancreatic glands were found to be very similar, whereas those from diabetic glands were mutually more different and deviated considerably from the composition of extracts of normal glands. The reason for this discrepancy is probably a much more pronounced post mortem enzymatic decomposition of the pancreatic polypeptides in the diabetic glands, which were removed several hours after clinical death.

Screening experiments with other commercially available polymer-based RP columns and application of the extraction and characterization procedure to the normal human pancreas with similar ischaemia times to the diabetic pancreas, to pancreatic glands obtained from experimental animals with chemically or immunologically induced insulin-dependent diabetes mellitus and to experimental animals with pancreatic tumours are in progress.

#### ACKNOWLEDGEMENTS

We thank Linda Larsø, Helle Bojesen-Koefoed and Ingelise Fabrin for excellent technical assistance, Stephen Bayne for some of the amino acid sequence analyses and Hans H. Sørensen for performing the TFA-acetonitrile RP-HPLC analyses.

#### REFERENCES

- 1 S. Linde and B. Hansen, unpublished results.
- 2 B. S. Welinder and H. H. Sørensen, *J. Chromatogr.*, Chrom. 22742.
- 3 A. K. Tung, J. L. Ruse and E. Cockburn, *Can. J. Biochem.*, 58 (1980) 707.
- 4 V. K. Naithani, G. J. Steffens, H. S. Tager, G. Buse, A. Rubenstein and D. F. Steiner, *Hoppe-Seyler's Z. Physiol. Chem.*, 365 (1984) 571.
- 5 A. M. F. Souza, L. B. Carvalho, E. M. P. Freitas, F. J. C. Aguiar, H. B. Cuitinhos and R. G. Pessoa, *Comp. Biochem. Physiol. B.*, 77 (1984) 595.
- 6 F. Laurent, H. Karmann and P. Mialhe, *Horm. Metab. Res.*, 19 (1987) 134.

- 7 H. Keilacker, R. Hildebrandt, S. Knospe, W. Besch and M. Ziegler, *Exp. Clin. Endocrinol.*, 87 (1986) 3198.
- 8 C. W. Pettinga, *Biochem. Prep.*, 6 (1958) 28.
- 9 T. Tomita, V. Doull, J. R. Kimmel and H. G. Pollock, *Diabetologia*, 27 (1984) 454.
- 10 G. Trump, H. W. Hildemann and G. B. Tebow, *Anal. Biochem.*, 138 (1984) 298.
- 11 Y. Tasaka, Y. Inoue, K. Marumo and Y. Hirata, *Endocrinol. Jpn.*, 31 (1984) 387.
- 12 H. S. Yadawa and Z. Ali, *Indian J. Exp. Biol.*, 14 (1976) 90.
- 13 K. Kimata, M. Horino, A. Tenku, H. Oyama, M. Endoh, M. Matsuki, Y. Nagase, S. Nishida and K. Sano, *Kawasaki Med. J.*, 9 (1983) 61.
- 14 K. Brunfeldt, T. Deckert and J. Thomsen, *Acta Endocrinol.*, 60 (1969) 543.
- 15 C.-D. Agardh, M. A. Lesniak, G. C. Gerritsen and J. Roth, *Metabolism*, 35 (1986) 244.
- 16 J. Zayas, *Biotechnol. Bioeng.*, 27 (1985) 1223.
- 17 Y. Tasaka, K. Marumo, Y. Inoue and Y. Hirata, *Acta Endocrinol.*, 113 (1986) 355.
- 18 J. R. Kimmel and H. G. Pollock, *Diabetes*, 16 (1967) 687.
- 19 J. R. Kimmel, J. Hayden and H. G. Pollock, *J. Biol. Chem.*, 250 (1975) 9369.
- 20 Y. Tasaka, K. Marumo, Y. Inoue and Y. Hirata, *Endocrinol. Jpn.*, 36 (1989) 47.
- 21 Y. Tasaka, S. Inoue, Y. Hirata, F. Hanyu and M. Endo, *Endocrinol. Jpn.*, 28 (1981) 261.



## **Protein–ligand interactions studied on bovine serum albumin with free and polymer-bound Cibacron Blue F3G-A as ligand with reference to affinity partitioning**

GÖTE JOHANSSON\* and MONICA JOELSSON

*Department of Biochemistry, Chemical Centre, University of Lund, Box 124, S-22100 Lund (Sweden)*  
(First received June 15th, 1990; revised manuscript received August 28th, 1990)

---

### ABSTRACT

The interactions in aqueous solutions between bovine serum albumin and the textile dye Cibacron Blue F3G-A, in both the free and polymer-bound forms, were studied using difference spectroscopy and gel chromatography. The polymers used as dye carriers were dextran, Ficoll, hydroxypropyl-starch, poly(vinyl alcohol) and poly(ethylene glycol). The addition of poly(ethylene glycol) to the solutions decreases the number of apparent binding sites on the albumin molecule, whereas this does not occur in the presence of dextran. The results were compared with the influence of polymer-bound dye on the partitioning of albumin in aqueous two-phase systems composed of dextran and poly(ethylene glycol). The partitioning of lactate dehydrogenase, which also interacts with this dye, was studied for comparison.

---

### INTRODUCTION

The use of affinity ligands in the purification of proteins has led to rapid and very selective separation methods. The most common procedure is affinity chromatography, in which the affinity ligand is covalently attached to an insoluble matrix. This gives an adsorbent which selectively binds one or several specific proteins. A closely related technique which has advantages for large-scale processes is based on aqueous (liquid–liquid) two-phase systems. These two-phase systems are obtained by dissolving two polymeric substances [*e.g.*, dextran and poly(ethylene glycol) (PEG)] in water [1,2]. An affinity ligand can be localized to one of the phases by attaching the ligand to the polymer concentrated in this phase [3–5]. By introducing the affinity ligand, the partitioning of ligand-binding proteins changes. In some instances, *e.g.*, glucose-6-phosphate dehydrogenase and phosphofructokinase, the change in the partition coefficient of the enzymes has been as large as 10 000-fold [6].

In systems containing affinity ligands a number of interactions can be envisaged. In general, the specific interaction between a ligand and the (target) protein is the basis for the isolation whereas other kinds of interactions (*e.g.*, ligand–ligand and ligand–polymer) might interfere and reduce the separation capacity and the selectivity. The presence of soluble or cross-linked polymers may also influence the binding strength of the ligand to the target protein.

For both affinity chromatography and affinity partitioning, a useful group of ligands is the textile dyes derived from symmetrical triazine [7]. These dyes can be obtained with a great variety of molecular structures, among which can be found some with a striking affinity for certain enzymes, especially among kinases and dehydrogenases. The interaction between formate dehydrogenase and PEG-bound dyes (Cibacron Blue 3GA and Procion Red HE3B) or NADH was studied by Cordes *et al.* [8] by using ultracentrifugation, fluorescence and affinity partitioning. The dye-polymer-enzyme complexes were shown to have larger dissociation constants in the upper (PEG-rich) phase than in the lower (dextran-rich) phase. In this study, we chose the commonly used ligand Cibacron Blue F3G-A and bovine serum albumin (BSA) as the ligand-binding protein.

## EXPERIMENTAL

### *Chemicals*

Dextran T-500 ( $M_r = 500\,000$ ), dextran T-70 ( $M_r = 70\,000$ ) and Ficoll 400 ( $M_r = 400\,000$ ) were purchased from Pharmacia (Uppsala, Sweden), poly(ethylene glycol) (PEG 8000) ( $M_r = 7000\text{--}9000$ ) from Union Carbide (New York, U.S.A.), hydroxypropyl-starch (HPS) ( $M_r = 35\,000$ ) from Perstorp Biolytica (Lund, Sweden) as Aquaphase PPT and poly(vinyl alcohol) (PVA 14) ( $M_r = 14\,000$ ) from BDH (Poole, U.K.). Cibacron Blue F3G-A was purchased from Serva (Heidelberg, F.R.G.). Bovine serum albumin (BSA) and lactate dehydrogenase (LDH) were obtained from Sigma (St. Louis, MO, U.S.A.). All other chemicals were of analytical-reagent grade.

### *Synthesis of dye-polymer derivatives*

Cibacron Blue F3G-A polymer derivatives were synthesized as described previously [9,10]. The degrees of substitution (moles of dye per mole of polymer) were 1.0 for PEG, 7.6 for dextran, 1.3 for HPS, 20 for Ficoll and 1.1 for PVA.

### *Difference spectra*

Difference spectra were obtained in the visible range by using a Hitachi 100-60 spectrophotometer equipped with 10- or 2-mm cuvettes at 22°C.

### *Gel chromatography*

A column of Sephadex G-100 (17 × 0.9 cm I.D.) was equilibrated with 305  $\mu\text{M}$  Cibacron Blue F3G-A (deactivated by sodium hydroxide and dialysed) in 25 mM sodium phosphate buffer (pH 7.5). A sample (0.5 ml) containing 100  $\mu\text{M}$  BSA in the above solution was applied. Elution was carried out at 22°C with the equilibration solution. Fractions of 0.6 ml were collected and the concentration of Cibacron Blue F3G-A was determined by absorbance measurement at 615 nm after ninefold dilution.

### *Two-phase systems*

The systems were prepared by weighing out the required amounts of stock solutions of dextran 500 and PEG 8000, together with ligand-polymer, buffer, LDH or BSA and water. All polymer concentrations are given as percentages by weight. The partitioned proteins were desalted before use by dialysis. Cibacron Blue F3G-A was deactivated with sodium hydroxide, neutralized and desalted by gel chromatography



on Sephadex G-25. The systems were equilibrated by careful mixing at 22°C for 30 s and the phases settled within 15 min. Samples were withdrawn from the two phases and analysed. The partition coefficient,  $K$ , defined as the ratio of the solute concentrations in the upper and lower phases, was calculated.

### Assays

Albumin was measured by the absorbance at 280 nm and Cibacron Blue F3G-A at 615 nm. When partitioned together, albumin was measured at 233 nm and corrections were made for the influence of the dye. The activity of LDH was determined photometrically at 340 nm according to Bergmeyer [11].

### RESULTS

The interaction between BSA and the ligand Cibacron Blue F3G-A (Cb) was found to be dependent on whether the dye was free (and deactivated) or bound to a water-soluble polymer. In the latter instance the kind of polymer used as the ligand

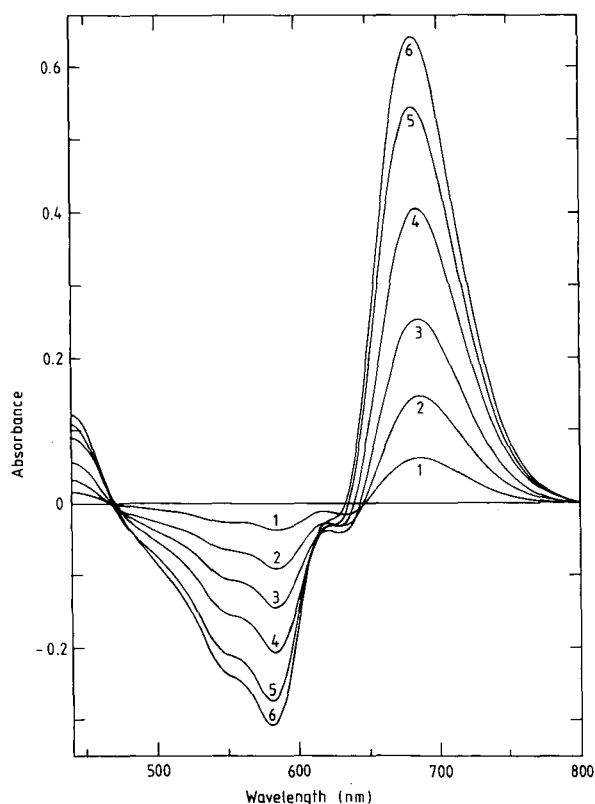


Fig. 1. Difference spectra of Cibacron Blue-PVA ( $795 \mu M$  dye) in the presence of various concentrations of BSA: 1 = 36; 2 = 91; 3 = 181; 4 = 363; 5 = 725; 6 = 1450  $\mu M$ . The solutions contained 25 mM sodium phosphate buffer (pH 7.5). The measurements were carried out with a 0.2-cm cuvette. Temperature, 22°C.

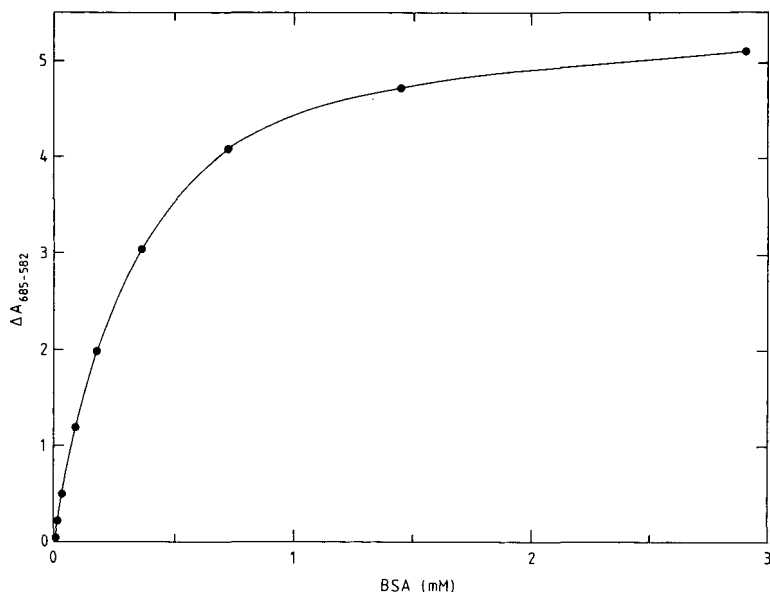


Fig. 2. Difference absorbance of Cibacron Blue PVA with BSA between 685 and 582 nm. The values were recalculated to a 1-cm path length.

carrier was important. This was studied in this work by using difference spectroscopy and also, in a few instances, gel chromatography.

#### *Difference spectra*

The type of spectra obtained when the absorbance of mixtures of dye and albumin was measured against a dye solution (of the same concentration) can be seen in Fig. 1. By following the difference in absorbance between two peaks (at two wavelengths) as a function of the concentration of albumin (or other dye-binding substance), curves of the type shown in Fig. 2 were obtained. From the limiting value, obtained by inverse plots [12], which, because of the excess of albumin, are assumed to represent the fully bound dye, the number of moles of dye bound per mole of albumin and the number of moles of free (unbound) dye can be calculated. These relationships for Cb attached to PEG and PVA are shown in Fig. 3. From this kind of experiment, the influence of the carrier molecule on the dye-protein interaction was studied. In the case of (non-polymer-bound) Cb it was difficult to determine the limiting absorbance difference. The apparent maximum number,  $\nu_{\max}$ , of ligand molecules bound per albumin molecule was in the range 3.5–4.5. Both PEG and PVA as ligand carriers gave a distinct value of  $\nu_{\max} = 2$  (Fig. 3). When the dye was bound to HPS and Ficoll the binding number increased over the whole concentration range studied and values exceeding 3 and 4, respectively, were observed (Table I). Also in the case of Cb-dextran no saturation was observed and the apparent binding number could take values of at least 2 units. The addition of PEG in several instances caused a decrease in the  $\nu_{\max}$  value whereas dextran did not have any noticeable effect (Table I).

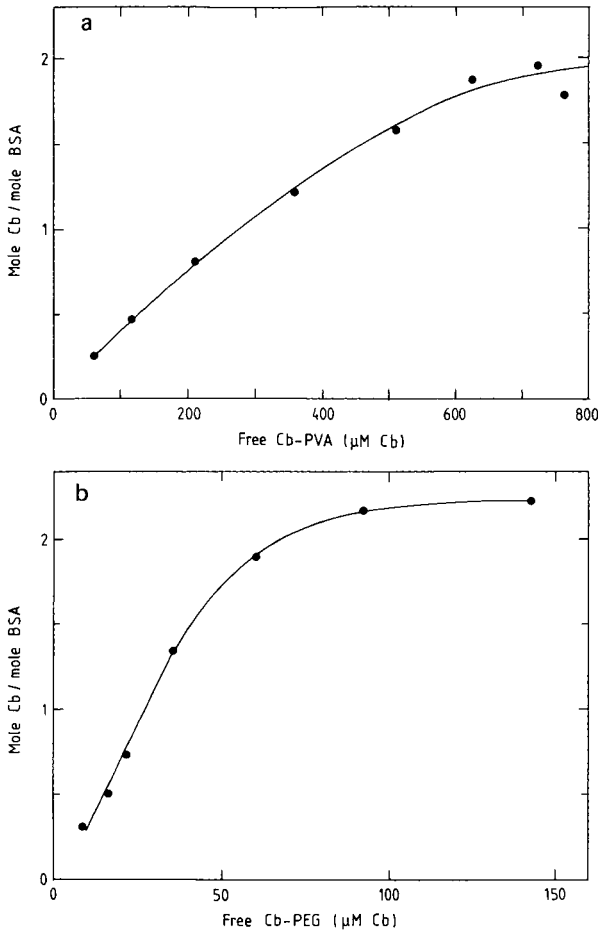


Fig. 3. Molar binding of two Cibacron Blue-polymers to BSA as a function of the concentration of free Cibacron Blue-polymer. (a) Cibacron Blue-PVA; (b) Cibacron Blue-PEG. The solutions contained 25 mM sodium phosphate buffer (pH 7.5). Temperature, 22°C.

*Relative binding strength*

The concentration of free (non-albumin-bound) dye necessary to obtain half saturation was in most instances within the range 20–150 μM. An exception was Cb-PVA with a value of 300 μM (Table I). To determine the relative binding strengths of the first bound ligand molecules, the concentrations of free Cb (deactivated or polymer-bound) in equilibrium with the 1:1 dye-albumin complex were compared. This dye concentration increased in the following order of ligand carriers: PEG < Ficoll = HPS < dextran < PVA, corresponding to a decrease in binding strength in the same order. The respective concentrations of polymer-bound dye were 15, 60, 62, 100 and 125 μM. For the dye itself the value was in the range 4–12 μM. The presence of polymers in some instances affected the binding as determined for Cb and polymer-bound dye. Dextran (10 or 5%) did not change the binding strength noticeably, while it

TABLE I

APPARENT NUMBER OF BINDING SITES,  $v_{\max}$ , ON BSA AND THE CONCENTRATION OF FREE Cb-POLYMER,  $C_{1/2}$ , NECESSARY TO ACHIEVE HALF SATURATION VALUES DETERMINED FROM DIFFERENCE SPECTROSCOPY

Temperature, 22°C.

Ligand	Solvent	$v_{\max}$	$C_{1/2}$ ( $\mu\text{M}$ )
Cb	Water	3.5–4.5	35–85
	10% PEG 8000	2.5	70
	10% dextran 70	3.0–3.5	20
Cb-PEG	Water	2.2	28
	10% PEG 8000	1.1	51
	5% dextran 70	2.1	31
Cb-PVA	Water	2.1	300
Cb-HPS	Water	> 3	100–120
Cb-Ficoll	Water	> 4	> 100
	10% PEG 8000	2	85
Cb-dextran	Water	> 2	100–150
	4% PEG 8000	> 1	175

was reduced in the presence of PEG (10 or 4%) 2–3-fold ( $30 \mu\text{M}$  for the dye and  $45 \mu\text{M}$  for Cb-PEG).

#### Association of Cb with polymers

The interaction between the dye (in hydroxyl form) and various polymers in aqueous solution could also be studied by difference spectrophotometry at levels up to

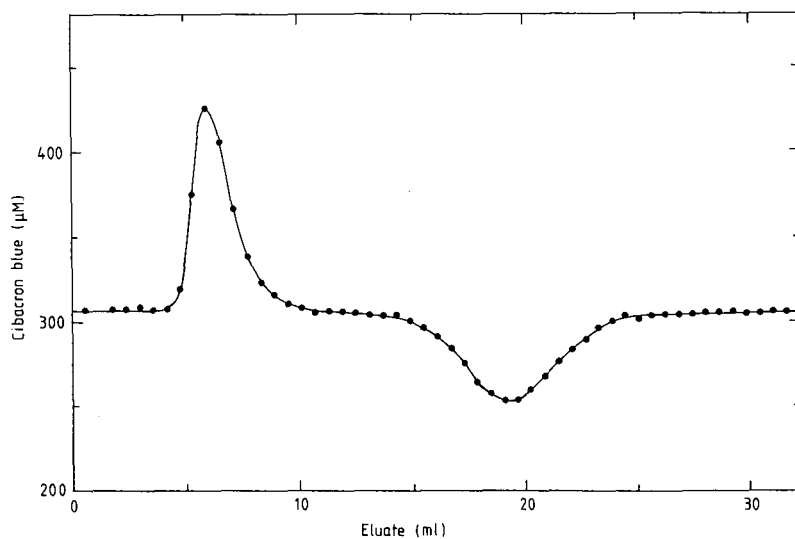


Fig. 4. Gel chromatography of BSA (50 nmol) on Sephadex G-100 equilibrated with  $305 \mu\text{M}$  deactivated Cibacron Blue in  $25 \text{ mM}$  sodium phosphate buffer (pH 7.5). Temperature, 22°C.

TABLE II

PARTITIONING OF DEACTIVATED CIBACRON BLUE F3G-A (Cb), Cb-PEG AND BSA IN 5.2% DEXTRAN 500, 3.8% PEG 8000 AND 25 mmol SODIUM PHOSPHATE BUFFER PER kg SYSTEM (pH 7.5)

Temperature, 22°C.

Concentration ( $\mu\text{mol/kg}$ )	$K$		
	Cb	Cb-PEG	BSA
10	3.17		
50	3.47		
250	3.77		
1050	4.04		
5250	4.54		
15		4.80	
60		5.69	
300		6.83	
600		7.22	
900		7.60	
29			1.10
74			1.05
147			1.01

150 g/l of polymer. The apparent amount of dye bound per gram of polymer was a linear function of the concentration of free dye. The strongest interaction was found for PVA, *i.e.*, 75  $\mu\text{mol}$  of dye per gram of polymer at a 100  $\mu\text{M}$  concentration of free dye. Corresponding values for Ficoll, HPS and PEG were 11, 1.4 and 1.1  $\mu\text{mol/g}$ , respectively. Dextran showed only weak spectral shifts on Cb and no tendency for saturation could be seen.

#### *Gel chromatography*

The number of Cb molecules binding to one molecule of albumin was also determined by gel chromatography on Sephadex G-100 (Fig. 4). The value was found to be 5.2 when the concentration of dye was 305  $\mu\text{M}$ . In a similar experiment with Cb-PEG (200  $\mu\text{M}$ ) on Sephadex G-200, the positive and negative peaks were not fully separated. A careful estimation gave a binding number of *ca.* 3.

#### *Two-phase partitioning*

The partitioning between the two aqueous phases of a PEG-dextran system was studied for BSA, free ligand (Cb) and PEG-bound ligand (Cb-PEG). Table II gives the partitioning of Cb at various concentrations. The Cb favoured the upper, PEG-rich, phase with a partition coefficient  $K = 3-4.5$ . When the dye was attached to PEG the  $K$  value increased by a factor of 1.7 ( $K = 4.8-7.6$ ) (Table II). The partitioning of the BSA was nearly equal between the two phases with  $K = 1.0-1.1$  (Table II).

#### *Co-partitioning of albumin with Cb or Cb-PEG*

The partitioning of Cb was affected by the presence of BSA in the system (Fig. 5). With an excess of albumin the dye, assumed to be in a 1:1 complex with the protein,

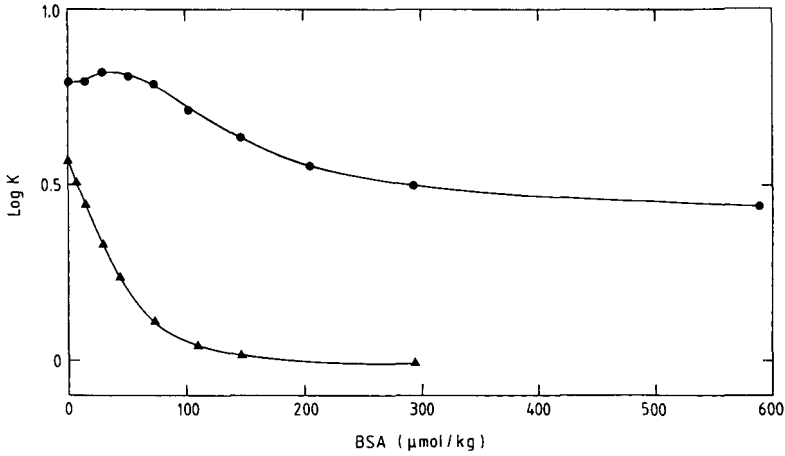


Fig. 5. Partition coefficients,  $K$ , of (▲) Cibacron Blue F3G-A (deactivated) and (●) PEG-bound Cibacron Blue as a function of the concentration of BSA in aqueous two-phase systems. The composition of the systems was 5.2% dextran 500, 3.8% PEG 8000, 25 mmol/kg sodium phosphate buffer (pH 7.5), 0.25 mmol/kg Cibacron Blue or Cb-PEG and various amounts of BSA. Temperature, 22°C.

showed the same partition coefficient as the free albumin. On the other hand, when the Cb was bound to PEG (Fig. 5), the 1:1 complex had  $K \approx 2.5$  ( $\log K = 0.4$ ). By taking the concentration of albumin necessary to reach half saturation as a measure of the relative binding strength, the curves indicate that the dye itself interacted around five times more strongly with BSA than did the PEG-linked dye.

The extraction curve for albumin (of constant concentration) with increasing

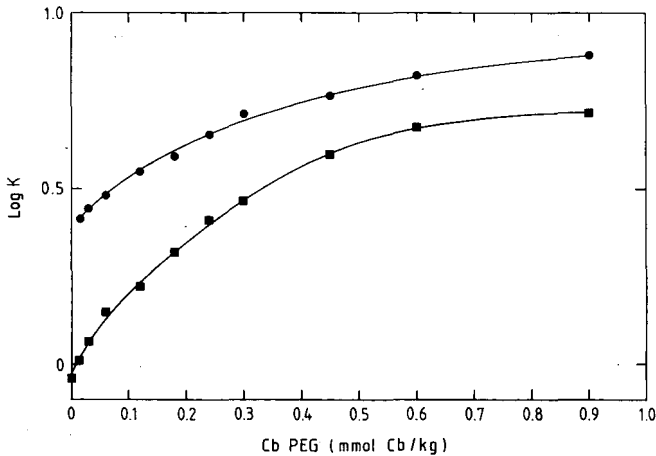


Fig. 6. Partition coefficients,  $K$ , of (■) BSA and (●) Cb-PEG when partitioned together in a two-phase system containing 5.2% dextran 500, 3.8% PEG 8000, 25 mmol/kg sodium phosphate buffer (pH 7.5), 147  $\mu$ mol/kg BSA and various amounts of Cb-PEG. Temperature, 22°C.

TABLE III

## PARTITION OF Cb-POLYMERS AND DEACTIVATED Cb WITHOUT AND WITH AN EXCESS OF BOVINE SERUM ALBUMIN

The partition coefficients,  $K_{Cb}$ , of Cb (polymer-bound or not) in the presence of excess of BSA are extrapolated values. Two-phase systems as in Fig. 5.

Cb carrier	$K_{Cb}$	
	Free	In excess of BSA
None	3.17	0.95
PEG	6.83	2.82
PVA	6.87	5.0-6.3
HPS	3.61	1.20
Ficoll	12.0	5.01
Dextran	0.066	0.018

amounts of Cb-PEG is shown in Fig. 6. The  $K$  value of albumin approaches 6.3 ( $\log K = 0.80$ ), which should be the partition coefficient of the saturated Cb-PEG-protein complex. The co-partitioning of Cb-PEG is also shown in Fig. 6.

*Partitioning of various Cb polymers*

The partition coefficients of a number of Cb polymers in excess of albumin are summarized in Table III. The  $K$  value of the complex was higher for PVA and Ficoll than PEG as ligand carrier. Dextran, giving a complex which favours the lower phase, was more than three times as potent as PEG. While the degree of substitution for Ficoll and dextran is  $> 1$  (20 and 7.6, respectively), they may form complexes with several binding points to the same albumin molecule or bridges between several protein molecules.

*Partitioning of lactate dehydrogenase (LDH)*

Partitioning of LDH from rabbit muscle was studied for comparison (Fig. 7). The most effective extractors (to opposite phases) were Cb-Ficoll and Cb-dextran, respectively. The estimated maximum changes in the logarithm of the partition coefficient,  $\Delta \log K_{max}$ , are summarized in Table IV. Cb-Ficoll showed the largest shift in  $\log K$  (0.99 units) for LDH. The power of extraction should, however, be related to the partitioning of the polymer-bound dye. For this comparison we introduce the effectivity number,  $\varepsilon$ , i.e., the relative value  $\Delta \log K_{max,LDH} / \log K_{ligand}$ . The  $\varepsilon$  value ranged from 1.4 to 2.4 with the highest value for dye-HPS (Table IV).

*Model for affinity partitioning*

The partitioning of a protein between the two aqueous phases containing a polymer-bound ligand can be calculated from the assumed number of binding sites and dissociation constants. We present here an extended version of the well known model for affinity partitioning suggested by Flanagan and Barondes [13], assuming that the protein has two binding sites for the ligand when it is in the upper phase and three binding sites in the lower phase. The dependence of  $\log K$  on the total concentration of ligand-polymer is derived as follows.

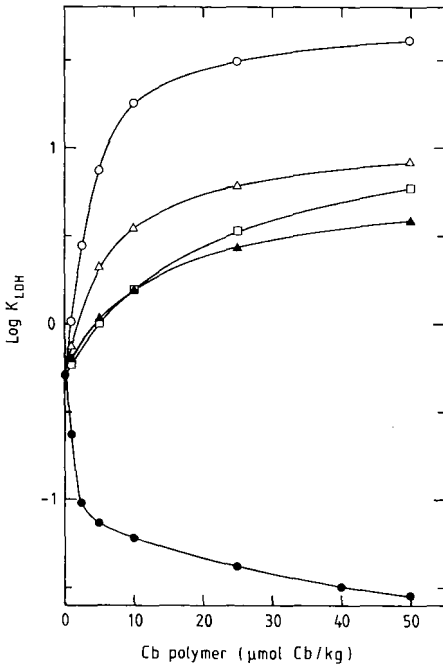


Fig. 7. Partition coefficients,  $K_{LDH}$ , of lactate dehydrogenase (12–15 U/kg) in the same system as in Fig. 5 but with various concentrations of Cibacron Blue-polymer derivatives:  $\square$  = Cb-PEG;  $\blacktriangle$  = Cb-PVA;  $\circ$  = Cb-Ficoll;  $\triangle$  = Cb-HPS;  $\bullet$  = Cb-dextran.

With a total concentration  $C_P$  of the protein in a system with a volume ratio (top/bottom)  $V$ , the free protein has a partition coefficient  $K_P$  and the ligand-PEG a partition coefficient  $K_L$ . The dissociation constants in the top phase,  $k_{t1}$  and  $k_{t2}$ , are defined by

$$k_{t1}[PL]_t = [P]_t[L]_t \quad (1)$$

$$k_{t2}[PL_2]_t = [PL]_t[L]_t \quad (2)$$

TABLE IV

PARTITION OF Cb-POLYMERS AND THEIR MAXIMUM EFFECT ON THE PARTITION OF LACTATE DEHYDROGENASE ( $\Delta \text{LOG } K_{LDH, \text{max}}$ )

Two-phase systems as in Fig. 5. The effectivity number,  $\epsilon$ , of polymer molecules bound per enzyme molecule was calculated as  $\epsilon = \log K_{LDH, \text{max}} / \log K_{Cb\text{-polymer}}$ .

Cb carrier	$\text{Log } K_{Cb\text{-polymer}}$	$\text{Log } K_{LDH, \text{max}}$	$\epsilon$
PEG	0.88	1.52	1.7
PVA	0.84	1.14	1.4
HPS	0.56	1.34	2.4
Ficoll	1.08	2.07	1.9
Dextran	-1.18	-1.85	1.6



and the three constants in the bottom phase,  $k_{b1}$ ,  $k_{b2}$  and  $k_{b3}$ , are defined by

$$k_{b1}[PL]_b = [P]_b[L]_b \quad (3)$$

$$k_{b2}[PL_2]_b = [PL]_b[L]_b \quad (4)$$

$$k_{b3}[PL_3]_b = [PL_2]_b[L]_b \quad (5)$$

where  $[P]_i$ ,  $[PL]_i$  and  $[PL_2]_i$  are the concentrations of the protein, monoligand protein and diligand protein, respectively, in the top phase ( $i = t$ ) and bottom phase ( $i = b$ ).  $[PL_3]_b$  is the triligand protein present only in the bottom phase.

The total concentrations of protein,  $C_{p,i}$ , in the top phase can be written as a function of  $[L]_i$ :

$$C_{p,t} = [P]_t \left\{ 1 + \frac{[L]_t}{k_{t1}} + \frac{[L]_t^2}{k_{t1}k_{t2}} \right\} = [P]_t Q \quad (6)$$

and the total protein concentration,  $C_{p,b}$ , in the bottom phase as

$$C_{p,b} = [P]_b \left\{ 1 + \frac{[L]_b}{K_L k_{b1}} + \frac{[L]_b^2}{K_L^2 k_{b1} k_{b2}} + \frac{[L]_b^3}{K_L^3 k_{b1} k_{b2} k_{b3}} \right\} = [P]_b R \quad (7)$$

The protein concentration in the top phase can also be expressed as the overall concentration of protein:

$$[P]_t = \frac{C_p(1 + V)}{VQ + R/K_p} \quad (8)$$

The overall partition coefficient for the protein,  $K_{tot}$ , will then be

$$K_{tot} = \frac{C_{p,t}}{C_{p,b}} = \frac{[P]_t}{[P]_b} \cdot \frac{Q}{R} = K_p \cdot \frac{Q}{R} \quad (9)$$

In the same way, the total concentration of ligand in the top phase,  $C_{L,t}$ , and in the bottom phase,  $C_{L,b}$ , can be expressed as functions of  $[L]_i$ :

$$C_{L,t} = [L]_t + \frac{[P]_t}{k_{t1}} \cdot [L]_t + \frac{2[P]_t}{k_{t1}k_{t2}} \cdot [L]_t^2 \quad (10)$$

$$C_{L,b} = \frac{[L]_b}{K_L} + \frac{[P]_b}{k_{b1}} \cdot \frac{[L]_b}{K_L} + \frac{2[P]_b}{k_{b1}k_{b2}} \cdot \frac{[L]_b^2}{K_L^2} + \frac{3[P]_b}{k_{b1}k_{b2}k_{b3}} \cdot \frac{[L]_b^3}{K_L^3} \quad (11)$$

The overall concentration of ligand,  $C_L$ , in the system is then

$$C_L = \frac{1}{1 + V} (VC_{L,t} + C_{L,b}) \quad (12)$$

TABLE V

SETS OF DISSOCIATION CONSTANTS WHICH GIVE GOOD CURVE FITTING FOR THE EXTRACTION CURVES IN FIG. 7

Cb-polymer	Dissociation constant (mM)				
	$k_{t1}$	$k_{b1}$	$k_{t2}$	$k_{b2}$	$k_{b3}$
PVA	0.006	0.003	0.02	0.01	0.2
PEG	0.007	0.007	0.035	0.035	3
Ficoll	0.0013	0.0013	0.003	0.003	0.018
HPS	0.003	0.004	0.006	0.008	0.2
Dextran	0.00025	0.00125	0.00025	0.00125	0.1

As the overall partition coefficient,  $K_{tot}$ , of protein cannot be expressed explicitly as a function of  $C_L$ , both of these values were calculated for a series of values of  $[L]_t$  via eqns. 9 and 12. By using  $V = 1$ ,  $C_p = 0.15$  mM,  $K_L = 6.3$  and  $K_p = 1.0$ , which correspond to the conditions for the experiment in Fig. 6, a good fit was obtained by using the following values for the dissociation constants:  $k_{t1} = 0.025$  mM,  $k_{t2} = 0.1$  mM,  $k_{b1} = 0.01$  mM,  $k_{b2} = 0.04$  mM and  $k_{b3} = 10$  mM. Corresponding  $k$  values in the top and bottom phases were chosen to be in the ratio 2.5:1. For the case when only one binding site is assumed in the top phase and two in the bottom phase, the same equations can be used if only the  $[L]_t^2$  terms in eqns. 6 and 10 and the  $[L]_b^3$  terms in eqns. 7 and 11 are omitted. In this event good curve fitting was obtained with  $k_{t1} = 0.1$  mM,  $k_{b1} = 0.16$  mM and  $k_{b2} = 1.2$  mM.

When the above model (with two binding sites in the top phase) was applied to the experimental data for the partitioning of LDH (Fig. 7), excellent fits were obtained by using the sets of dissociation constants summarized in Table V. The values used indicate that the first dissociation constant for LDH-dye-polymer may well be approximately the same in both the bottom and top phases with the exception of the complex with dye-dextran. In the latter instance the curve fitting indicates a fivefold stronger complex in the top (PEG-rich) phase than in the bottom (dextran-rich) phase.

## DISCUSSION

The apparent number of binding sites on the albumin molecule for Cb (in water) found in this work (3.5–4.5 spectroscopically, 5.2 by gel filtration) is close to the value of 3.4 found by Antoni *et al.* [14] by using difference spectroscopy but considerably higher than the value of 2.0 reported by Ling and Mattiasson [15] using partitioning in aqueous two-phase systems and equilibrium dialysis. The higher value obtained by using gel filtration could be explained by assuming sandwich binding (one dye molecule associating with one albumin-bound dye molecule), which may not necessarily be reflected in the difference spectrum.

Covalent binding of the dye to the polymers PEG and PVA reduces the number of available binding sites on the albumin molecule. This might be due to unfavourable interaction between the attached polymer chain and that part of the surface of the protein molecule which surrounds one of the binding sites. The effect of polymers is

striking. While addition of bulk dextran had a small influence on the number of bound Cb and Cb-PEG and on the binding strength, both parameters were reduced by the addition of PEG. This indicates that the polymer influences the conformation of the albumin molecule in such way that one of the binding sites drastically lowers its dye-binding ability.

Another possible explanation for the reduced binding could be that one of the elements of the Cb molecule, *e.g.*, the hydrophobic parts, interacts with the polymer chains. If so, contact points (on the dye molecule) for the protein may be masked. Depending on the relative importance of these contact points for the binding strength to the various site on BSA, the weakening of the interaction could be influenced more or less drastically by the presence of polymers such as PEG or PVA.

Polymer-bound triazine dyes have been used as affinity ligands for the isolation of proteins by partitioning between the aqueous phases of dextran-PEG-water two-phase systems. The results obtained here point toward the possibility that proteins, in this instance albumin, do not have to expose the same number of binding sites in the two phases. Earlier models for affinity partition have been based on the assumption of the same  $v_{max}$  in both phases. In the model presented above it is assumed that the protein has one more binding site in the bottom than in the top phase. If only one binding site is assumed in the top phase the albumin has to bind Cb-PEG more strongly (1.6-fold) in the top compared with the bottom phase. With two binding sites

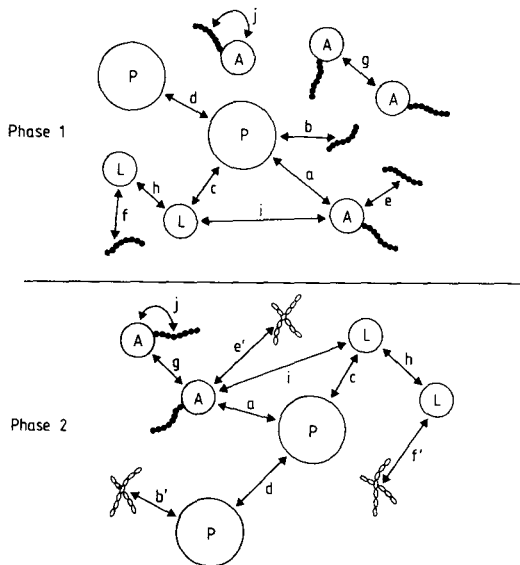


Fig. 8. Scheme of some important interactions which take place in the aqueous two-phase systems containing two polymers mainly concentrated in opposite phases. P, Protein; A, polymer-bound ligand; L, free ligand. The indicated interactions are (a) protein to polymer-bound ligand; (b) and (b') protein to phase-forming polymer; (c) protein to free ligand; (d) protein to protein; (e) and (e') polymer-bound ligand to phase-forming polymer; (f) and (f') free ligand to phase-forming polymer; (g) self-interaction between polymer-bound ligand; (h) self-interaction between free ligand; (i) polymer-bound ligand to free ligand; (j) between polymer bound ligand and its carrier polymer.

in the top phase the binding might be stronger in the bottom phase, as indicated by the binding experiments, by 2.5-fold (for the first constant). In this instance the third binding constant in the bottom phase was without any influence.

The partition experiments also gave the partition coefficients of the minimum complex and of the fully substituted albumin complex (Figs. 5 and 6). As the latter value is greater than the former, it can be concluded that the number of binding sites (in the top phase) must be larger than unity. The two-phase system studied here has phases that contain considerable amounts of both polymers, 5.70% PEG and 1.05% dextran in the top phase and 1.85% PEG and 9.46% dextran in the bottom phase [1] and therefore the "polymer effect" may not be as pronounced as in systems with higher polymer concentrations where the polymers have a more one-sided partition to one phase each.

The curve fitting in Table V indicates that the dye-protein interaction, in the case of LDH, is strongly dependent on the choice of ligand-carrying polymer. The first dissociation constants (in the top and bottom phases) show that the most effective binding is obtained with dextran whereas PEG, which is the most commonly used ligand carrier, gave the lowest binding.

Aqueous two-phase systems applied for affinity partitioning of proteins involve a great number of molecular interactions. The possible 1:1 interactions (between two molecular species) are summarized in Fig. 8. To achieve a good affinity extraction into the top phase, in which the polymer-bound ligand is concentrated, the protein-ligand interaction (a) should be stronger in the top phase and the ligand-ligand (g), ligand-polymer (e) and ligand-carrier polymer (j) interactions should be as small as possible in this phase. These interactions all contribute to the apparent dissociation constants of the protein-ligand-polymer complex. By obtaining a deeper understanding of these factors, more selective and effective separation methods based on affinity ligands may be formulated, *e.g.*, two-phase systems with other polymers than those used today.

## CONCLUSIONS

The association of Cibacron Blue F3G-A to serum albumin is influenced both by the binding of the dye to a polymer and by the presence of bulk polymers in an aqueous solution. Both the number of binding sites and the dissociation constants are affected. The kind of polymers used to obtain aqueous polymeric two-phase systems for the affinity partitioning of proteins may therefore be critical.

## ACKNOWLEDGEMENTS

This work was supported by grants from the Technical Research Council of the National Swedish Board for Technical Development (STUF) and the Magn. Bergvalls Foundation.

## REFERENCES

- 1 P.-Å. Albertsson, *Partition of Cell Particles and Macromolecules*, Wiley, New York, 3rd ed., 1986.
- 2 H. Walter and G. Johansson, *Anal. Biochem.*, 155 (1986) 215.
- 3 S. D. Flanagan and S. H. Barondes, *J. Biol. Chem.*, 250 (1975) 1484.

- 4 G. Takerkart, E. Segard and M. Monsigny, *FEBS Lett.*, 42 (1974) 218.
- 5 G. Johansson, *J. Biotechnol.*, 3 (1985) 11.
- 6 G. Johansson and M. Andersson, *J. Chromatogr.*, 303 (1984) 39.
- 7 P. D. G. Dean and D. H. Watson, *J. Chromatogr.*, 165 (1979) 301.
- 8 A. Cordes, J. Flossdorf and M.-R. Kula, *Biotechnol. Bioeng.*, 30 (1987) 514.
- 9 G. Johansson and M. Joelsson, *Biotechnol. Bioeng.*, 27 (1985) 621.
- 10 G. Johansson and M. Joelsson, *J. Chromatogr.*, 411 (1987) 161.
- 11 H. U. Bergmeyer, *Methoden der enzymatischen Analyse*, Vol. 1, Verlag Chemie, Weinheim, 2nd ed., 1970, p. 441.
- 12 S. Subramanian, *Crit. Rev. Biochem.*, 16 (1984) 169.
- 13 S. D. Flanagan and S. H. Barondes, *J. Biol. Chem.*, 250 (1975) 1484.
- 14 G. Antoni, M. C. Casagli, M. Bigio, G. Borri and P. Neri, *Ital. J. Biochem.*, 31 (1982) 100.
- 15 T. G. I. Ling and B. Mattiasson, *J. Chromatogr.*, 252 (1982) 159.



CHROM. 22 800

## High-performance liquid chromatographic analysis of the (cyanoaquo) stereoisomers of several putative vitamin B<sub>12</sub> precursors

SUSAN H. FORD\*, JEAN GALLERY, ALVA NICHOLS and MURRAY SHAMBEE

*Chicago State University, Department of Chemistry and Physics, 95th Street at King Drive, Chicago, IL 60628 (U.S.A.)*

(First received April 10th, 1990; revised manuscript received August 30th, 1990)

---

### ABSTRACT

The cyanoaquo and aquocyano stereoisomers of several putative vitamin B<sub>12</sub> precursors are reversibly formed and can be separated using analytical high-performance liquid chromatographic methods. The behavior of these stereoisomers varies somewhat depending on the type of column used and the chromatographic conditions employed. Both reversed-phase and ion-exchange columns can be used to observe the reversible formation and separation of the stereoisomers of (H<sub>2</sub>O,CN)cobyric acid, cobinamide and the cobinic acid pentaamide-1, -2 and -3 structural isomers. The greatest differences in retention times are seen when the pH of the eluting buffer is less than 4.0 and the buffer contains no KCN.

---

### INTRODUCTION

Cyanocobalamins (vitamin B<sub>12</sub>), and other cobamides, have been the primary focus of interest in most areas of corrinoid research due to their functions as the important coenzyme partners in many critical enzyme-catalyzed reactions in both eucaryotic and procaryotic organisms [see, for example, reviews such as refs. 1 and 2]. This nexus of interest has resulted in several papers in recent years showing how high-performance liquid chromatography (HPLC) could be used to separate and/or identify cobamides found in mammalian or bacterial materials [3–6].

Cobalamin contains not only the corrin ring and attendant side chains, but the  $\alpha$ -side “nucleotide loop” connected to the ring at side chain *f* and is thus known as a “complete” corrinoid. The “incomplete” corrinoids do not have the  $\alpha$ -side “nucleotide” loop, but do contain the complete corrin ring and attendant side chains. These compounds are of interest as precursors to the cobamides in microorganisms [7], and may occasionally function as coenzymes or activators in bacteria since Co $\beta$ -methylcobyric acid acts as a coenzyme in *Clostridium thermoaceticum* [8], and, not only methylcobalamin, but also diaquocobinamide activates the methylreductase system in extracts of *Methanobacterium bryantii* [9]. In a purely chemical sense, however, the “incomplete” corrinoids have been especially useful in studying the redox and other functions of the corrin ring and complexed cobalt atom [10,11]. Recent publications

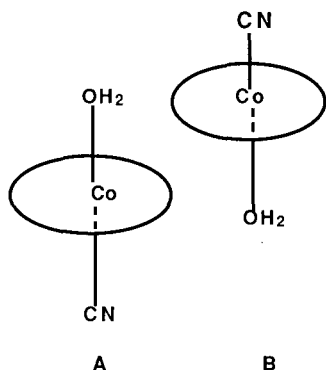


Fig. 1. Abbreviated corrinoid structure showing only the relationship between the CN and H<sub>2</sub>O cobalt atom ligands and the corrin ring plane. A =  $\alpha$ -cyano, $\beta$ -aquo; B =  $\alpha$ -aquo, $\beta$ -cyano.

have shown the usefulness of one of these "incomplete" corrinoids, cobinamide, as a dehalogenating agent for environmental contaminants such as lindane and C-1 polychlorinated hydrocarbons [12,13]. In addition, the incomplete corrinoids can serve as models for the "base-off" cobamides, the forms in which many of the biologically active corrins function as coenzymes [14,15].

Structurally, the "incomplete" corrinoids are nearly unique in that they can exhibit stereoisomerism which is not usually seen with the "complete" corrinoids, except at very low pH for cobalamin [16] and in the case of the phenolyl and cresolyl cobamides recently identified in *Sporomosa ovata* [17]. The cyanoaquo-"incomplete" corrinoids may show either [ $\alpha$ -cyano, $\beta$ -aquo] or [ $\alpha$ -aquo, $\beta$ -cyano] structures (see Fig. 1). This fact was reported in a series of papers by Friedrich and co-workers in the late 1960s [18–20]. These authors showed that the stereoisomers of cobyric acid were thermally unstable and yet clearly distinguishable under the right experimental conditions.

<sup>13</sup>C NMR studies of the aquo<sup>13</sup>CN- and aquo<sup>13</sup>CH<sub>3</sub>-cobinamide stereoisomers have been reported showing small differences in the chemical shifts of the two isomers [10,21]. In addition several reports in the literature have noted the presence of separably identifiable stereoisomers of aquocyano-cobinamide upon HPLC analysis, but none of these reports revealed further investigation of this phenomenon [3,5,6].

In this paper we show how HPLC can be used to distinguish and analyze the cyanoaquo stereoisomers of several different incomplete corrinoids, including cobinamide, cobyric acid, and three isomeric cobinic acid pentaamides, compounds of useful interest in many areas of chemistry.

## EXPERIMENTAL

Whatman DE-53 (high-capacity DEAE) and CM-52 ion-exchange celluloses were purchased from Whatman. Dowex AG-1X2 and cyanocobalamin (vitamin B<sub>12</sub>) were purchased from Sigma. All solvents used for HPLC were of HPLC-grade purity, and water used for preparation of aqueous solvents was distilled, deionized in a Millipore system, filtered through an 0.2- $\mu$ m membrane, then degassed. All other



solvents and chemicals were of reagent grade. Phenol used for desalting of corrinoids was prepared fresh at 91% (v/v) using liquified reagent-grade crystals and distilled, deionized water. Small quantities of cobyric acid and cobinamide in their cyanoaquo forms and of aquocobalamin to use as standards were kindly supplied by H. C. Friedmann.

*Preparation of cobinic acid pentaamide isomers, cobyric acid and cobinamide*

Three isomeric cobinic acid pentaamides of known structure were prepared as follows:

A 5-g amount of vitamin B<sub>12</sub> was incubated for 4 h in 500 ml 1 M HCl at 37°C. After incubation, the solution was neutralized with 5 M NaOH, desalted by phenol extraction [22], and the resulting corrinoid mixture separated on Dowex AG-1X2 as described by Anton *et al.* [23]. The purified cobamic acid pentaamides-1, -2 and -3 as described by these authors were then individually desalted by phenol extraction, crystallized, and the nucleotide was removed from each by the method of Renz [24]. Purification of the individual cobinic acid pentaamides resulting was by chromatography on DE-53 (acetate) columns (Whatman) equilibrated in 0.05% aqueous HCN; 0.08% acetic acid in 0.05% aq. HCN was the eluting solvent. Yields and cobinic acid pentaamide isomer characteristics are given in the text. To remove contaminating heavy metals, the cobinic acid pentaamides were passed through columns of Chelex 100 (Sigma) as suggested by Bratt and Hogenkamp [25], with 0.1 M KCN being used as the eluting solvent, then each isomer was desalted by phenol extraction and dried to a powder or glass. This treatment results in the cyanoaquo form of the incomplete corrinoids as evidenced by a color change from purple to red, and the shift of the  $\gamma$  absorption band in the electronic spectrum from 367 to 352–354 nm. Natural abundance <sup>13</sup>C NMR (proton decoupled) was performed on the cobinic acid pentaamide isomers in <sup>2</sup>H<sub>2</sub>O using a Nicolet spectrophotometer, with a 16- $\mu$ s pulse, 1.0-s pulse delay, tetramethylsilane as external standard and methanol as internal standard to determine precise chemical shift.

Cobyric acid was prepared from vitamin B<sub>12</sub> as described by Renz [24] with the modifications in final product purification previously published [7]. Cobinamide was available from these preparations as a major side product.

Preparation of the Co $\beta$ -adenosyl forms of cobyric acid and of the cobinic acid pentaamides was as previously described [26]. In these preparations, the cyanoaquo-cobinic acid pentaamide or cyanoaquocobyric acid was dissolved in deoxygenated distilled/deionized water (1 mg/2 ml). Argon or nitrogen gassing of the solution was used to maintain the oxygen-free atmosphere of the solution. A crystal of cobalt nitrate was added as catalyst [27] and the solution was continuously stirred. After sealing the solution in a vial, and continuing gassing via a septum, a 10-fold molar excess of aq.(deoxygenated) NaBH<sub>4</sub> was added via syringe. The color of the solution turned dark grey and gas was given off. The solution was transferred to the dark room, where a 1.5 fold molar excess of 5'-iodo-5'-deoxyadenosine (Aldrich) in 1.0 ml deoxygenated water was injected. After stirring an additional 15 min at room temperature in the dark, excess borohydride was destroyed by addition of 2.0 ml 1 M acetic acid, and the solution was phenol extracted. Final purification was via preparative high voltage paper electrophoresis (0.05 M acetate buffer, pH 4.5). Due to their light-sensitivity, the Co $\beta$ -adenosyl corrinoids were stored frozen, desiccated and protected from the light, and were handled only in the dark room in the presence of a red safety lamp.

### Analytical HPLC

Analytical HPLC was performed using a Waters system with dual Model 501 high-pressure pumps, an automated gradient controller and a Model 441 fixed-wavelength absorbance detector with a 365-nm filter. A Kipp and Zonen Model BD41 flatbed recorder was used to record absorbance data. Peak area was used to estimate the percent of individual components in mixtures and when corrinoid stereoisomers clearly separated during chromatography. Two different types of columns, ion exchange (Waters  $-\text{NH}_2$  or Whatman Partisil-5-SAX), and reversed-phase (Waters  $\mu$ Bondapak  $\text{C}_{18}$  or Alltech Adsorbosphere  $\text{C}_{18}$ ), were used. An RCSS CN guard column was employed for the ion-exchange experiments, and an RCSS  $\text{C}_{18}$  guard column for the reversed-phase experiments.

With ion exchange, pyridine acetate buffers in water–tetrahydrofuran (96:4) [3] at 80 mM or less concentration and pH ranges from about 6.0 to 3.5 were used as described in the text, whereas with reversed-phase columns, methanol–aqueous acetic acid [6] or pyridine acetate buffers mixed with 30% or less acetonitrile were employed. All columns used except the Whatman Partisil-5-SAX were 25 cm  $\times$  4.6 mm I.D.; the Partisil column was 10 cm  $\times$  4.6 mm I.D. Corrinoids were dissolved in HPLC-grade water and filtered via syringe using an 0.2- $\mu\text{m}$  PTFE or nylon membrane before injection. Amounts of incomplete corrinoids injected ranged from 1–10 nmoles in 20  $\mu\text{l}$  HPLC-grade water or HPLC-grade water containing 0.01% KCN, depending on the experiment. A maximum of 15 nmol were used in one experiment when corrinoid isomers were collected from the analytical column.

### Additional analytical and preparative techniques

Analytical electrophoresis was performed on paper using buffers and techniques previously described [26]. Determination of the  $\text{p}K_a$  value for each of the cobinic acid pentaamide isomers was essentially as suggested by Anton *et al.* [23] for the cobamic acids using corrinoid migration on paper electrophoresis in buffers of varying pH with  $\text{B}_{12}$  as an external standard. To substantiate the electrophoretically determined  $\text{p}K_a$  values, cobinic acid pentaamide-2 was also titrated by standard analytical means, and the  $\text{p}K_a$  value determined from the titration plot.

Analytical thin-layer chromatography (TLC) was performed on silica gel 60-coated (0.2 mm thickness) plastic plates (E. Merck, Darmstadt, F.R.G.), and preparative TLC was run on glass-backed plates of the same material from E. Merck, layer thickness 2 mm. Solvents used for both analytical and preparative TLC were those described in ref. 28. Analytical ascending paper chromatography was performed using Whatman No. 1 paper in solvent systems E, H and I as described by Bernhauer *et al.* [29]. Visible and UV absorbance spectra were recorded using a Perkin-Elmer Lambda 3B UV–VIS spectrophotometer with 1-ml quartz cells (10 mm light path) and a PE R100A recorder. Concentrations of incomplete corrinoids in solution were calculated using published molar extinction values [17,30], or, in the case of cobinic acid pentaamide-2, using our own experimentally determined values (Table I).

TABLE I

YIELDS AND PHYSICAL/CHEMICAL CHARACTERISTICS OF SEVERAL COMPLETE AND INCOMPLETE CORRINOID ACIDS PREPARED FROM CYANOCOBALAMIN

	Corrinoid					
	Cobamic acids <sup>a</sup>			Cobinic acids <sup>b</sup>		
	1 <sup>c</sup>	2 <sup>d</sup>	3 <sup>e</sup>	1 <sup>c</sup>	2 <sup>d</sup>	3 <sup>e</sup>
Yield (%) <sup>f</sup>	6.7(7.1)	9.4(15.1)	6.9(9.0)	35	73	51
Overall yield	—	—	—	2.4	6.9	3.5
pK <sub>a</sub> <sup>g</sup>	5.10 ± 0.11	4.52 ± 0.07	4.62 ± 0.07	3.30 ± 0.01	3.39 ± 0.01	3.34 ± 0.01

Corrinoid	Electronic spectrum: λ (nm) (ε <sub>M</sub> ) <sup>h</sup>			
	α	β	γ	UV <sub>max</sub>
Cobyric acid-dicyano-	578(8950)	539(7950)	367(28 100) <sup>i</sup>	314(11 150), 260 <sup>k</sup> (18 200)
-Coβ-adenosyl	466(10 300) <sup>j</sup>		351(18 050)	315 and 304(17 350), 262(37 800)
Cobinic acid-1 <sup>c</sup> -dicyano-	580 <sup>l</sup>	540(6650)	368 <sup>l</sup>	311(13 400), 260 <sup>k</sup> (28 550)
-Coβ-adenosyl	465(8250) <sup>j</sup>		349 <sup>k</sup> (15 750)	313(21 500), 262(45 300)
Cobinic acid-2 <sup>d</sup> -dicyano-	579(8300)	539(7000)	367(25 000)	313(13 950), 255 <sup>k</sup> (36 600)
-Coβ-adenosyl	460(10 250) <sup>j</sup>		349 <sup>k</sup> (15 250)	315(26 100), 261(56 000)
Cōbinic acid-3 <sup>e</sup> -dicyano-	579 <sup>l</sup>	539(6900)	367 <sup>l</sup>	311(12 600), 259 <sup>k</sup> (25 800)
-Coβ-adenosyl	462(8100) <sup>j</sup>		347 <sup>k</sup> (11 600)	315 and 303(20 800), 262(39 800)

<sup>a</sup> Prepared per Anton *et al.* [23] by mild acid hydrolysis of cyanocobalamin.<sup>b</sup> In the cyanoaquo form.<sup>c</sup> Isomer 1 is the [a,b,c,e,g]pentaamide [23].<sup>d</sup> Isomer 2 is [a,c,d,e,g]pentaamide [23].<sup>e</sup> Isomer 3 is [a,b,c,d,g]pentaamide [23].<sup>f</sup> The yields shown in parentheses are those reported by Anton *et al.* [23].<sup>g</sup> Cobamic acid pK<sub>a</sub> values are as reported in ref. 23.<sup>h</sup> ε<sub>M</sub> = Molar extinction. Values in l/mol · cm. Extinctions are rounded off to the nearest 50.<sup>i</sup> Very close to those values reported in ref. 30.<sup>j</sup> No clear maximum above 500 nm.<sup>k</sup> Shoulder.<sup>l</sup> Extinctions were determined for cobinic acid-2 by weight; the standard values determined for -2 at the α and γ bands were assumed for -1 and -3 as well and were used in these calculations.

## RESULTS AND DISCUSSION

*Preparation/characterization of cobinic acid isomers*

The yields and certain characteristics of the isomeric cobinic acid pentaamides-1, -2 and -3 are summarized in Table I. The intermediate compounds prepared initially from cyanocobalamin were the cobamic acid pentaamide isomers arising from the hydrolysis of the propionamide groups at corrin ring positions *b*, *d* and *e* originally described by Anton *et al.* [23]. The location on the corrin ring of each free carboxylic acid in the cobamic series was determined by these authors using <sup>13</sup>C NMR; two recent papers substantiate these designations and complete the unambiguous isomer assignments using 1- and 2-dimensional NMR [31,32].

Since the cobinic acids were prepared from the cobamic acids by removal of the  $\alpha$ -side nucleotide loop using the mild conditions of Renz [24], we have assumed that the location of the cobinic acid pentaamide free acid group in each case is identical with that of the cobamic acid from which it was derived. Such an assumption seems warranted by two facts. First, Brown and Peck-Siler [10] observed that when [ $^{13}\text{C}$ ]methylcobalamin was converted to [ $^{13}\text{C}$ ]methylcobinamide via the same method of nucleotide removal that we used, no structural changes in the corrinoid except those anticipated by nucleotide removal were identified using NMR. Second, our own preliminary  $^{13}\text{C}$  NMR work on the cobinic acid pentaamide isomers [33] has given spectra which can be correlated fairly easily with the spectra of the cobamic acids from which they were derived [23,31,32]. This is especially true in the area of the downfield carbon resonances (carbonyl, imine and pyrrole), where isomeric variations are likely to be seen.

It is interesting to note that the cobinic acid pentaamide-2 analogue prepared by us via the procedure of ref. 23 followed by that of ref. 24, is identical by HPLC, TLC, analytical electrophoresis and analytical ascending chromatography to the only cobinic acid pentaamide we reported previously [7] as derivable in significant amounts from the mild acid hydrolysis of cobinamide. In addition, hydrolysis of the amide group at ring position *b* in cobalamin, to give cobamic acid pentaamide-2 (cobamic acid [*a,c,d,e,g*]pentaamide), was the easiest to accomplish, i.e. gave the highest yield reported by Anton *et al.* [23]. Thus the removal of the amide group at position *b* on the corrin ring when hydrolysis is accomplished under mild conditions using acid appears to be especially facile.

As is shown in Table I, the  $\text{p}K_{\text{a}}$  values for the cobinic acid pentaamides are from 1–1.5 pH units lower than those for the corresponding cobamic acid pentaamides. The apparent effect of these differences on separation of the cobinic acid pentaamide-1, -2 and -3 structural isomers compared to separation of the cobamic acid pentaamide isomers by HPLC is discussed in the next section.

Fig. 2 illustrates the complete electronic absorption spectrum of the  $\text{Co}\beta$ -adenosyl and dicyano forms of cobinic acid pentaamide-2. In addition, the major absorption bands in the electronic spectra of the  $\text{Co}\beta$ -adenosyl and dicyano forms of cobyric acid and of the three the cobinic acid pentaamide structural isomers are listed on Table I along with the molar extinction coefficient for each major band. As can be seen from this list, the dicyano-forms have the same band locations, but slightly different extinctions, whereas the  $\text{Co}\beta$ -adenosyl forms exhibit somewhat different locations of the  $\beta$  bands, and variation in almost every extinction value.

#### *HPLC analysis of cobinic acid pentaamide isomers*

Fig. 3 illustrates a typical data print-out from ion-exchange HPLC of the cyanoaquocobinic acid pentaamide isomers and cobyric acid. Tables II–IV summarize the results when the behavior of the cobinic acid pentaamide isomers on HPLC was compared to the behavior of cyanocobalamin, aquocobalamin, cobinamide, cobyric acid and the cobamic acid pentaamides-1, -2 and -3. Table II shows, for example, that when using an ion-exchange column and in the absence of KCN in the buffer, the incomplete corrinoids in their cyanoaquo-forms all exhibited two components, in a pH-dependent manner, whereas the complete corrinoids uniformly showed but one component at all pH values tested. In those cases where the components were

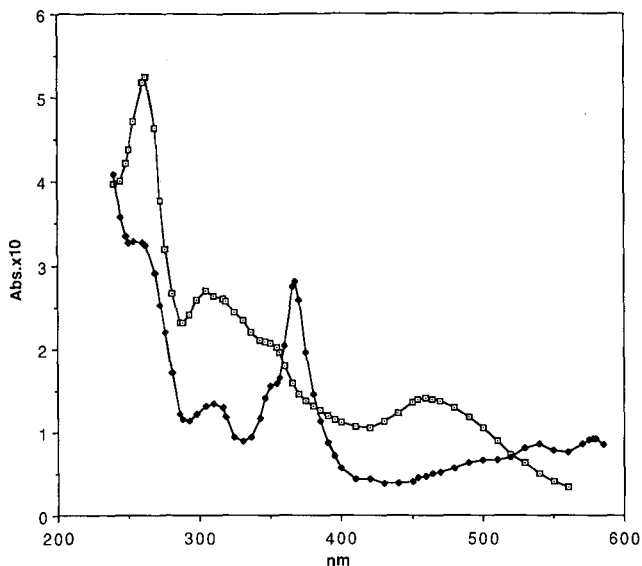


Fig. 2. Electronic absorption spectrum of cobinic acid [a,c,d,e,g]pentaamide, 11.2  $\mu$ M.  $\square$  = Co $\beta$ -adenosyl- (neutral pH, water);  $\blacksquare$  = dicyano- (pH > 10, 0.1 M aq. KCN).

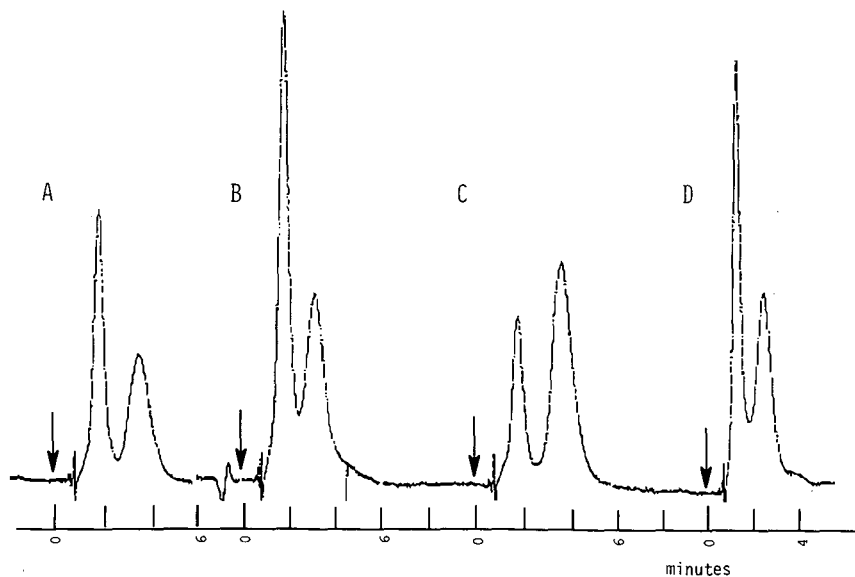


Fig. 3. Typical HPLC behavior of cyanoquo stereoisomers of the cobinic acid pentaamides and cobyrinic acid. Whatman Partisil 5-SAX column, 80 mM pyridine acetate buffer (in water-tetrahydrofuran, 96:4) pH 3.58; 2.0 ml/min., 365 nm filter on detector, 0.05 a.u.f.s. The arrows indicate injection points in time plot. (A) Cobinic acid[a,b,c,e,g]pentaamide (4.9 nmol/20  $\mu$ l); (B) cobinic acid[a,c,d,e,g]pentaamide (6.5 nmol/20  $\mu$ l); (C) cobinic acid[a,b,c,d,g]pentaamide (4.9 nmol/20  $\mu$ l); (D) cobyrinic acid (4.6 nmol/20  $\mu$ l).

TABLE II  
ION-EXCHANGE HPLC OF INCOMPLETE CORRINOIDS

Partisil-5-SAX column 10 cm × 4.6 mm I.D.; isocratic; eluting buffer: 80 mM pyridine acetate in water-tetrahydrofuran (96:4) at the pH indicated; + KCN = addition of 0.02% KCN (all corrinoids were pre-treated with 0.02% KCN when KCN was used in the buffer); 1.0 ml/min pump rate.

Corrinoid	Retention time (min) (component % of total)					
	Buffer pH 3.62		Buffer pH 4.40		Buffer pH 6.05	
	-KCN	+KCN <sup>a</sup>	-KCN	+KCN <sup>a</sup>	-KCN	+KCN <sup>a</sup>
Cyanocobalamin	3.5(100)	3.6(100)	3.5(100)	3.8(100)	3.8(100)	3.6(100)
Aquocobalamin	2.7(100)	3.6(100)	2.6(100)	—	3.5(100)	—
Cobamic acid-1 <sup>b</sup>	—	—	4.6(100)	4.1(100)	—	5.5(100)
-2	—	—	6.0(100)	4.6(100)	—	5.1(100)
-3	—	—	6.9(100)	4.7(100)	—	5.2(100)
Cobinamide	2.6(68)	3.0(100)	2.6(—) <sup>c</sup>	3.0(100)	4.3(—) <sup>c</sup>	3.2(100)
	3.7(32)		3.0(—)		4.7(—)	
Cobinic acid-1 <sup>b</sup>						
cyanoaquo	3.2(49)	3.7(100)	4.5(100)	3.8(100)	4.5(100)	4.4(100)
	4.9(51)					
Coβ-adenosyl	6.2 <sup>d</sup>					
Cobinic acid-2						
cyanoaquo	3.0(56)	3.5(100)	4.0(100)	3.8(100)	3.1(49)	3.9(100)
	4.3(44)				4.0(51)	
Coβ-adenosyl	5.4 <sup>d</sup>					
Cobinic acid-3						
cyanoaquo	3.2(30)	3.7(100)	4.2(—) <sup>c</sup>	3.8(100)	3.9(—) <sup>c</sup>	4.1(100)
	5.0(70)		4.8(—)		4.3(—)	
Coβ-adenosyl	5.9 <sup>d</sup>					
Cobyric acid						
cyanoaquo	2.7(52)	3.4(100)	3.4(100)	3.5(100)	3.5(—) <sup>c</sup>	3.7(100)
	3.8(48)				3.8(—)	
Coβ-adenosyl	3.6 <sup>d</sup>					

<sup>a</sup> Cobamic acids were in the cyano form; when the buffer contained KCN, each incomplete corrinoid was converted to its dicyano form which appeared as a single peak.

<sup>b</sup> For structural designations and systematic names see Table I.

<sup>c</sup> Components not clearly enough separated to calculate percentages.

<sup>d</sup> Single broad peak; 2.0 ml/min pump rate.

sufficiently separated, the percent of each component was calculated by integrating the area under the curve. For all of the cobinic acid pentaamide isomers, cobinamide and cobyric acid, the best separation of the two stereoisomers in each case occurred when the pH was below 4, but only when KCN was absent from the buffer. In the presence of KCN in the buffer, a single corrinoid form was stabilized and only one component was found for each of the incomplete corrinoids, presumably that of the dicyano-corrinoid, and its retention time was approximately half way between those of the two cyanoaquo stereoisomers. In some experiments, when dicyanocobinic acid pentaamide was injected, and buffer without KCN was used, a small peak of intermediate retention time, along with peaks corresponding to the two cyanoaquo stereoisomers, was observed. This component appeared as a minor constituent, with variations in

TABLE III  
REVERSED-PHASE HPLC OF INCOMPLETE CORRINOIDS

An Alltech Adsorbosphere C<sub>18</sub> 25 cm × 4.6 mm I.D. column was used throughout. Isocratic conditions: acetonitrile–80 mM pyridine acetate (30:70) in water–tetrahydrofuran (96:4) pH 3.6 buffer (buffer A); 1.0 ml/min. Gradient conditions: 10-min linear gradient, starting at acetonitrile–buffer A (5:95), ending at acetonitrile–buffer A (30:70); 2.0 ml/min.

Corrinoid	Retention time (min) (component % of total)	
	Isocratic	Gradient
Cyanocobalamin	3.1(100)	5.8(100)
Aquocobalamin	6.9(100) <sup>a</sup>	—
Cobamic acids-1, -2 and -3 <sup>b</sup>	3.2–3.3(100) <sup>c</sup>	6.9(100) <sup>c</sup>
Cobinamide	5.6(55)	7.4(61)
	6.3(45)	9.9(39)
Cobinic acid-1 <sup>b</sup>		
cyanoaquo	5.8(47)	8.1(47)
	6.6(53)	10.6(53)
Coβ-adenosyl	3.9 <sup>d</sup>	
Cobinic acid-2		
cyanoaquo	5.7(48)	7.7(51)
	6.3(52)	9.9(49)
Coβ-adenosyl	3.8 <sup>d</sup>	
Cobinic acid-3		
cyanoaquo	5.8(25)	8.2(17)
	6.5(75)	10.9(83)
Coβ-adenosyl	3.9 <sup>d</sup>	
Cobyric acid		
cyanoaquo	5.4(42)	6.2(60)
	6.0(58)	9.2(40)
Coβ-adenosyl	3.4 <sup>d</sup>	

<sup>a</sup> Broad peak.

<sup>b</sup> For structural designations and systematic names see Table I.

<sup>c</sup> All three isomers had indistinguishable retention times under these conditions.

<sup>d</sup> 2.0 ml/min pump rate; very sharp peak.

retention time and amount observed, but seemed to correspond to the dicyano-form. The appearance of this component is in keeping with the observations of Reenstra and Jencks [16] who reported that the dicyano-form of cobalamin (in its “base-off” form at low pH) was the obligate intermediate in the reversible formation of the cyanoaquo-cobalamin stereoisomers. It should be noted here that our experiments showed this behavior when either ion-exchange or reversed-phase columns were used. It is puzzling that although Stupperich *et al.* [6] mentioned the problem of multiple peaks when dicyanocobinamide was injected in a reversed-phase column without KCN present in the buffer, Jacobsen *et al.* [5] reported only a single component with a very short retention time under similar conditions. The observation of a single component for dicyanocobinamide in the latter case was probably due to the fortuitous choice of buffer pH and ionic strength, since formation of the cyanoaquo stereoisomers from the dicyano form is rapid and facile under almost all of the large number of experimental conditions we tested unless KCN was present in the buffer.

TABLE IV

## REVERSED-PHASE HPLC OF INCOMPLETE CORRINOIDS FOLLOWED BY TLC OR HPLC OF COLLECTED STEREOISOMERS

HPLC conditions: Waters  $\mu$ Bondapak C<sub>18</sub> column; solvent methanol-17 mM acetic acid (40:60), isocratic, 1.0 ml/min; fractions were collected directly from the detector outflow and immediately dried under a stream of nitrogen. TLC was run on analytical silica gel plates in 2-propanol-28% NH<sub>4</sub>OH-water (7:1:2) [28] using corrinoid solutions reconstituted from the HPLC-derived powders. I and II refer to the original HPLC order of elution: I = faster component, II = slower component.

Corrinoid <sup>b</sup>	Retention time (min) (component % of total)		$R_F$ , TLC	
	Original HPLC	Second HPLC <sup>a</sup>	I	II
Cobinamide	I 7.6(65)	I 7.7(59) 9.4(41)	0.57 0.14	0.54 0.14 0.10
	II 9.5(35)	II 8.3(45) 10.1(55)		
Cobinic acid-1 <sup>c</sup>	I 6.9(53)	I 7.6(54) 10.8(46)	0.62 0.28 0.095	0.62 0.28 0.069
	II 8.6(47)	II 8.3(47) 10.3(53)		
Cobinic acid-2	I 7.5(58)	I 8.5(60) 11.4(40)	0.49 0.40 0.22	0.59 0.23
	II 10.1(42)	II 9.1(29) 13.3(68)	0.034	0.052
Cobinic acid-3	I 9.5(34)	I 10.2(27) 14.2(73)	0.54 0.22	0.53 0.19
	II 12.8(66)	II 10.0(19) 13.3(81)		
Cobyric acid	I 5.7(49)	I 6.5(49) 7.7(51)	0.38 0.11	0.39 0.13
	II 7.1(51)	II 6.3(46) 7.8(54)		

<sup>a</sup> HPLC fractions for reinjections were prepared from the original HPLC-derived powders by addition of HPLC-grade water. Conditions for rerun were exactly the same as in the original HPLC runs.

<sup>b</sup> All incomplete corrinooids were in their cyanoquo forms.

<sup>c</sup> For cobinic acid pentaamide structural designations see Table I.

Table II also illustrates the problem of separating the three isomeric cobinic acid pentaamides from each other based on their  $pK_a$  values using ion-exchange chromatography. Unlike the cobamic acid isomers which have  $pK_a$  values differing by 0.1 up to 0.5 pH units (see Table I), and which are separable in mixtures via HPLC on an ion-exchange or a reversed-phase column [3], the cobinic acid pentaamide isomers have  $pK_a$  values differing by less than 0.1 pH unit, and mixtures are not clearly separable on an ion-exchange or reversed-phase column, even with changes in buffer pH and/or ionic strength, using isocratic or gradient elutions.

Table III illustrates the behavior of the cyanoquo stereoisomers on a reversed-phase column using an aqueous buffer and an organic solvent mixture for elution. Clear separation of the isomers occurred under both isocratic and gradient conditions,



although the gradient gave a greater difference in retention times for the two stereoisomers for each. In the case of the cobinic acid pentaamide-3, however, the separation was complicated by a large column hold up, which required a 100% methanol wash to remove.

Data are shown in Tables II and III illustrating the behavior of the Co $\beta$ -adenosyl forms of the cobinic acid pentaamide isomers as well as of cobyric acid. The Co $\beta$ -adenosyl-corrinoids are assumed to be the forms in which the corrins exist in the biosynthetic sequence in producer microorganisms, as well as the form involved in many important metabolic transformations [1,2]. The reversed-phase (C<sub>18</sub> column) HPLC data have been reported on the behavior of Co $\beta$ -adenosylcobinamide [5], and this work was not repeated here. Our data support the assertion that, in contrast to the cyanoaquo forms, the Co $\beta$ -adenosyl-forms of the incomplete corrinoids do not isomerize during HPLC, at least under the various experimental conditions we employed (see Tables II and III).

Table IV shows the results of collection of the separate stereoisomers from the HPLC (reversed-phase) column, then reinjection of each on the same column under the same conditions, and TLC analysis of each component. As can be seen from Table IV, reinjection of each stereoisomer again gave two stereoisomers, as one might predict from the thermal instability of the cyanoaquo stereoisomers as described by Friedrich and co-workers [18–20]. The same sort of behavior was seen on TLC, in cyanide-free solvents. In fact, more than two spots were seen in several cases, possibly corresponding to intermediate forms, or the dicyano- or the diaquocorrinoid in each case. It should be noted that the relative concentrations of methanol and 17 mM acetic acid used in these experiments differed from those reported by Stupperich *et al.* [6]. Their methanol–acetic acid (24:76) solvent mixture did not give a sharp separation of the cobinic acid pentaamide isomers, however, a 40:60 or 50:50 mixture was serviceable.

To summarize the results illustrated on Table IV, the reinjected solutions showed two components, as expected, but the percent of each was either unchanged or slightly enriched in the component with the longer retention time.

In keeping with the nomenclature system devised by Friedrich and Nordmeyer [18,19] for cobyric acid using low-pressure column chromatography at 3°C, it seems plausible to designate the chromatographically slower component (longer retention time on HPLC) as the  $\alpha$ -cyano, $\beta$ -aquo (Fig. 1A) stereoisomer, and the faster component (shorter retention time) as the  $\alpha$ -aquo, $\beta$ -cyano (Fig. 1B) stereoisomer. Friedrich and coworkers [20,34] as well as others have studied the formation of the Co-methyl corrinoids of cobyric acid and cobinamide. This work has led to confusing results [see especially, discussion in ref. 10]. Some authors have found *only* the Co $\beta$ -alkyl form of cobinamide upon reductive alkylation of cobinamide [10,35], whereas others [20,34] have found *mixtures* of the Co $\beta$ /Co $\alpha$ -methyl incomplete corrinoids under the same synthetic conditions. Fanchiang *et al.* [36] found that when Co $\beta$ -methylcobalamin transfers the methyl group to diaquocobinamide, only the  $\beta$  isomer is formed. This work appears to show that the Co $\beta$ -methylcorrinoids are much more thermally stable to isomerization than the cyanoaquo forms, as was shown by Friedrich and co-workers [20,34] who reported that temperatures up to 80°C and the addition of CO gas was required for *complete isomerization* of the Co-methyl (incomplete) corrinoids. This is, of course, in contrast to the isomerization of the cyanoaquo forms, which occurs easily at room temperature.

Component percent composition data in Tables II–IV also illustrate interesting differences in stereoisomer formation among the various incomplete corrinoids tested. Cyanoaquocobinamide exhibits (Table III) an approximately equal mixture of the two stereoisomers with a slight excess of the faster ( $\beta$ -cyano) component during isocratic reversed-phase HPLC using acetonitrile–pyridine acetate buffer at pH 3.61. In contrast, upon isocratic reversed-phase (using methanol–acetic acid) or ion-exchange HPLC at pH 3.61, or reversed-phase HPLC using a gradient, cyanoaquobinamide shows an increase in ratio of  $\beta$ -cyano/ $\alpha$ -cyano to 2:1. This is in contrast to the results of Brown and Hakimi [21] who found, using  $^{13}\text{C}$  NMR, a 2:1 ratio of  $\alpha$ -cyano/ $\beta$ -cyano isomers when  $\text{K}^{13}\text{CN}$  was added to diaquocobinamide, and of Reenstra and Jencks [16] who reported a similar ratio of  $\alpha$ - to  $\beta$ -cyano isomers for “base off” cyanoaquocobalamin, but agrees with the results of Stupperich *et al.* [17] who found nearly equal quantities of the cyanoaquo/aquocyno stereoisomers of the phenolyl- and cresolylcobamides in *Sporomosa ovata*. Brown and Peck-Siler [10] attribute the higher percent of the  $\alpha$ -cyano isomer to thermodynamic control of product ratio, finding a nearly 100% preponderance of the  $\beta$ - $^{13}\text{C}$  $\text{H}_3$  cobinamide when the formation of the methylaquo-stereoisomeric pairs is under kinetic control.

The ratio of the two aquocyno stereoisomers for cobinic acid pentaamides-1 and -2, and cobyric acid using both reversed-phase and ion-exchange columns approximates 1:1, however, cobinic acid pentaamide-3 shows a marked predominance of the slower ( $\alpha$ -cyano) component with ratios of 2:1 to 4:1,  $\alpha/\beta$ . According to Brown and co-workers [10,21] this shows a greater thermal stability of the  $\alpha$ -cyano stereoisomer. This may be due to the interaction of the free  $-\text{COOH}$  at position *e* with the cyano group to stabilize it, since the *e* carboxyl is on the  $\alpha$ -side of the corrin ring. Interestingly, Brown and Peck-Siler [10] found an interaction between  $\alpha$ -side benzimidazole B3  $-\text{N}$ , and the *e* side chain  $-\text{NH}$  in the “base off” benzimidazole deprotonated form of cobalamin.

#### ACKNOWLEDGEMENT

This work was supported by grant S06-GM08043 from NIH.

#### REFERENCES

- 1 F. Wagner, *Ann. Rev. Biochem.*, 35 (1966) 405.
- 2 D. Dolphin (Editor), *B-12, Vol. 2, Biochemistry and Medicine*, Wiley, New York, 1982.
- 3 M. Binder, J. F. Kolhouse, K. C. VanHorne and R. H. Allen, *Anal. Biochem.*, 125 (1982) 253.
- 4 W. B. Whitman and R. S. Wolfe, *Anal. Biochem.*, 137 (1984) 261.
- 5 D. W. Jacobsen, R. Green, E. V. Quadros and Y. D. Montejano, *Anal. Biochem.*, 120 (1982) 394.
- 6 E. Stupperich, I. Steiner and M. Rühlemann, *Anal. Biochem.*, 155 (1986) 365.
- 7 S. H. Ford, *Biochim. Biophys. Acta*, 841 (1985) 306.
- 8 L. Ljungdahl, E. Irlon and H. G. Wood, *Biochemistry*, 4 (1965) 2771.
- 9 W. B. Whitman and R. S. Wolfe, *J. Bacteriol.*, 164 (1985) 165.
- 10 K. L. Brown and S. Peck-Siler, *Inorg. Chem.*, 27 (1988) 3548.
- 11 B. P. Hay and R. G. Finke, *J. Am. Chem. Soc.*, 109 (1987) 8012.
- 12 T. S. Marks, J. D. Allpress and A. Maule, *Appl. Env. Microbiol.*, 55 (1989) 1258.
- 13 U. E. Krone, R. K. Thauer and H. P. C. Hogenkamp, *Biochemistry*, 28 (1989) 4908.
- 14 S. Ragsdale, P. A. Lindahl and E. Münck, *J. Biol. Chem.*, 262 (1987) 14289.
- 15 T. G. Pagano, P. G. Yohannes, B. P. Hay, J. R. Scott, R. G. Finke and L. G. Marzilli, *J. Am. Chem. Soc.*, 111 (1989) 1484.

- 16 W. W. Reenstra and W. P. Jencks, *J. Am. Chem. Soc.*, 101 (1979) 5780.
- 17 E. Stupperich, H. J. Eisinger and B. Krätler, *Eur. J. Biochem.*, 186 (1989) 657.
- 18 W. Friedrich, *Z. Naturforsch. B.*, 21 (1966) 595.
- 19 W. Friedrich and J. P. Nordmeyer, *Z. Naturforsch. B.*, 23 (1968) 1119.
- 20 W. Friedrich and R. Messerschmidt, *Z. Naturforsch. B.*, 24 (1969) 465.
- 21 K. L. Brown and J. M. Hakimi, *Inorg. Chem.*, 23 (1984) 1756.
- 22 H. A. Barker, R. D. Smyth, H. Weissbach, H. Munch-Peterson, J. I. Toohey, J. N. Ladd, G. E. Volcani and R. N. Wilson, *J. Biol. Chem.*, 235 (1960) 181.
- 23 D. L. Anton, H. P. C. Hogenkamp, T. E. Walker and N. A. Matwiyoff, *J. Am. Chem. Soc.*, 102 (1980) 2215.
- 24 P. Renz, *Methods Enzymol.*, 18c (1971) 82.
- 25 G. T. Bratt and H. P. C. Hogenkamp, *Arch. Biochem. Biophys.*, 218 (1982) 225.
- 26 S. H. Ford and H. C. Friedmann, *Arch. Biochem. Biophys.*, 175 (1976) 121.
- 27 D. Dolphin, *Methods Enzymol.*, 18c (1971) 43.
- 28 T. Toraya, E. Krodell, A. S. Mildvan and R. H. Abeles, *Biochemistry*, 18 (1979) 417.
- 29 K. Bernhauer, B. Becher, G. Gross and G. Wilharm, *Biochem. Z.*, 332 (1960) 562.
- 30 R. Bonnett, J. M. Godfrey and D. G. Redman, *J. Chem. Soc.*, (1969) 1163.
- 31 T. G. Pagano and L. G. Marzilli, *Biochemistry*, 28 (1989) 7213.
- 32 H. M. Marques, D. C. Scooby, M. Victor and K. L. Brown, *Inorg. Chim. Acta*, 162 (1989) 151.
- 33 S. H. Ford and B. Williams, unpublished results.
- 34 W. Friedrich and J. P. Nordmeyer, *Z. Naturforsch. B.*, 24 (1969) 588.
- 35 O. Müller and G. Müller, *Biochem. Z.*, 337 (1963) 179.
- 36 Y. T. Fanchiang, G. T. Bratt and H. P. C. Hogenkamp, *Proc. Natl. Acad. Sci. U.S.A.*, 81 (1984) 2698.



## Elimination of peak splitting in the liquid chromatography of the proline-containing drug enalapril maleate

JAROSLAV ŠALAMOUN\* and KAREL ŠLAIS

Institute of Analytical Chemistry, Kounicova 82, 611 42 Brno (Czechoslovakia)

(First received April 23rd, 1990; revised manuscript received July 30th, 1990)

---

### ABSTRACT

Enalapril maleate contains alanylproline dipeptide and can be split into two or more peaks when separated by reversed-phase liquid chromatography. The dependence of the shape, retention or width of peaks of enalapril and its impurities on temperature, pH, ionic strength and presence of ion-pairing compounds was studied. The optimum separation conditions involve a state where the rotational rates are much higher than that of the separation process, *i.e.*, at a higher temperature and lower pH. Enalapril is eluted as a single peak even at room temperature at higher concentrations of both cetyltrimethylammonium bromide and sodium dodecyl sulphate in the mobile phase.

---

### INTRODUCTION

Enalapril maleate ((*S*)-1-{N-[1-(ethoxycarbonyl)-3-phenylpropyl]-L-alanyl}-L-proline, (*Z*)-2-butenedioate (1:1) salt, ENM) [1] is a salt of enalapril (EN) and maleic acid (MA). EN is a pro-drug which is hydrolysed to enalaprilate (DIAC), acting as an inhibitor of enzyme angiotensin convertase. It is indicated for the treatment of renovascular hypertension. There are two major potential impurities in the substance besides the parent compound: DIAC, the free acid produced by hydrolysis of EN, and diketopiperazine (DKP), a cyclization product [1]. The structures of these compounds are shown in Fig. 1.

The configuration of a peptide bond can be either *trans* or *cis* [2] (Fig. 2). Nearly all amino acid residues in proteins are in the *trans* configuration, in which steric repulsion is minimized. With proline, the *cis* configuration is likely to occur as the *trans* configuration because the amide nitrogen is part of a ring.

Recently, reversed-phase liquid chromatography of some proline-containing dipeptides [3] and medium-sized peptides [4] has been studied. It was shown that the peak shape is dependent on temperature, flow-rate and pH. Some chromatographic properties of ENM were published by Ip and Brener [1] but more detailed studies are still lacking.

The presence of both a cationic surfactant and an alkane sulphonate in the mobile phase at concentrations close to saturation causes the formation of a liquid ionic multilayer. This was confirmed by the decrease in the void volume of the column [5–7].

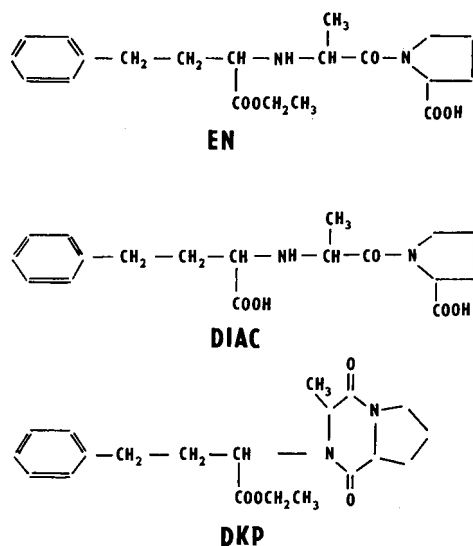


Fig. 1. Structural formulae of EN and its impurities DIAC and DKP.

In this work, the influence of temperature, pH, ionic strength and the presence of cetyltrimethylammonium bromide (CTAB) and sodium dodecyl sulfate (SDS) on the chromatographic behaviour and especially the peak shape and width of ENM and its impurities was studied in order to suppress the negative manifestation of conformational changes of EN and to elute it as a single peak.

#### EXPERIMENTAL

Enalapril maleate [99% by high-performance liquid chromatography (HPLC)], DIAC (98%) and DKP (95%) were prepared in Research Institute of Pure Chemicals (Lachema, Brno, Czechoslovakia). SDS was obtained from Lachema and acetonitrile (LiChrosolv) and CTAB from Merck (Darmstadt, F.R.G.). All other chemicals were of analytical-reagent grade.

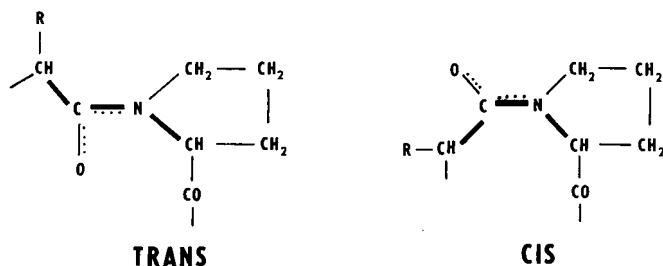


Fig. 2. Configurations around peptide bonds involving proline. The peptide bond interconverts between *trans* and *cis* configurations.

Chromatographic separations were performed on a Hewlett-Packard (Palo Alto, CA, U.S.A.) equipped with a Model 7125 10- $\mu$ l six-port injection valve (Rheodyne, Cotati, CA, U.S.A.) and a Model 1040 diode-array detector (Hewlett-Packard). The analytical columns used were 250  $\times$  4 mm I.D., packed with Silasorb

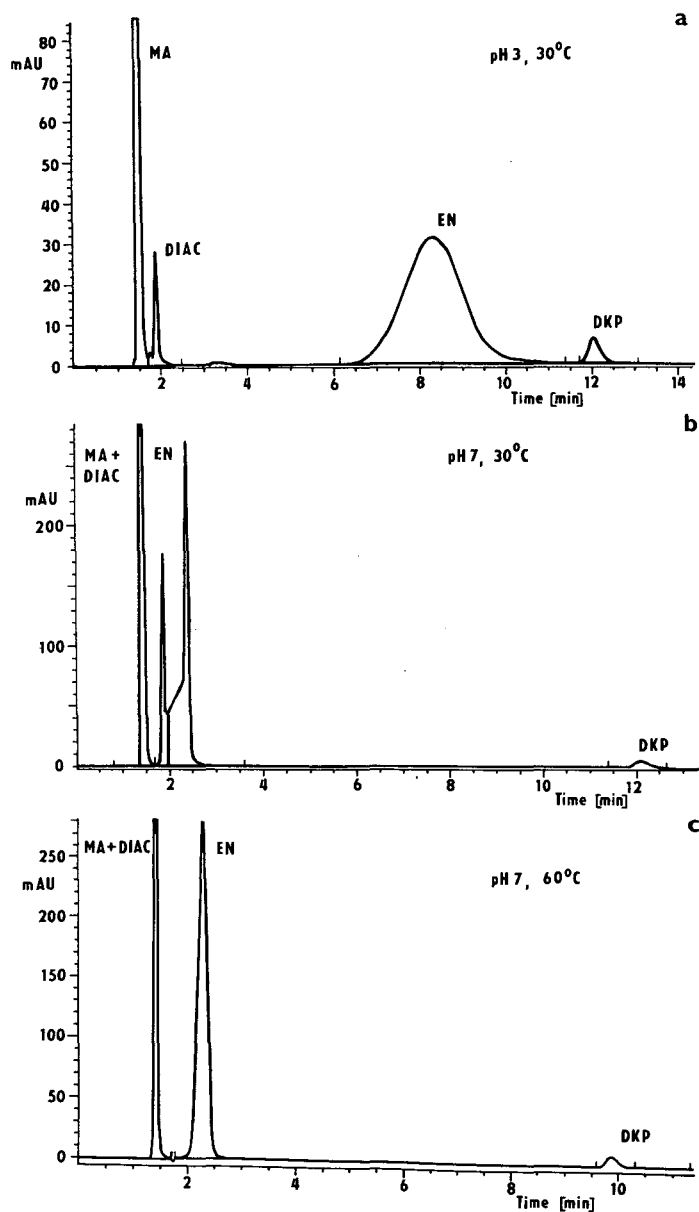


Fig. 3. Effects of pH and temperature on the elution of EN, DIAC and DKP. Mobile phase, 0.05 *M* phosphate buffer (pH 7.0 and 3.0)-acetonitrile (7:3, v/v); column temperature, 30 and 60°C; column packing, Silasorb C<sub>18</sub>; flow-rate, 1.5 ml/min; volume injected, 10  $\mu$ l; sample, ENM and DIAC (0.5 mg/ml) and DKP (0.05 mg/ml); detection, UV, 215 nm.

SPH C<sub>18</sub>, 7.5  $\mu$ m (Lachema), and 100  $\times$  4.6 mm I.D., packed with Spherisorb ODS, 5  $\mu$ m (Philips Analytical, Cambridge, U.K.).

## RESULTS AND DISCUSSION

### *Influence of various parameters on chromatographic behaviour*

*Influence of pH.* At lower pH of the mobile phase, the C–N bond loses its partially double-bond character, which restricts free rotation around the peptide bond owing to partial protonation of the imide group on proline [8]. The increase in the relaxation rate of isomerization of proline containing peptides results in a better peak shape in LC [3]. As far as DKP is concerned, its peak shape and retention are not seriously dependent on either pH or temperature because of the cyclic character of the molecule and because of the amino group being sterically blocked and shielded even from interactions with silanol groups. The influence of pH of the mobile phase on peak shape is illustrated in Fig. 3a and b, which show chromatograms obtained at pH 3 and 7. At higher pH, EN is cleaved into two peaks corresponding to the two conformational isomers. At pH 3 the rate of isomerization is higher and ultimately both isomers are eluted as a single broad peak. The dissociation of the EN carboxylic group is also lower and the hydrophobic interactions increase.

The most significant differences in the retention (Fig. 4) of all the compounds occur at lower pH values of the mobile phase. With decreasing pH, EN changes its net charge from negative to positive at pH 4.2 (its isoelectric point) [9]. Residual highly acidic sites of a silica-based reversed-phase stationary phase [10] interact with the positively charged molecule of EN and increase its retention. In such a way the ion-exchange mechanism significantly influences the retention of EN. With regard to the working pH range of the stationary phase and the resolution of MA and DIAC peaks, we chose pH 3 as the optimum.

*Influence of temperature.* The rate of isomerization rises with increasing temperature as the activation energy of the peptide bond in the molecule containing

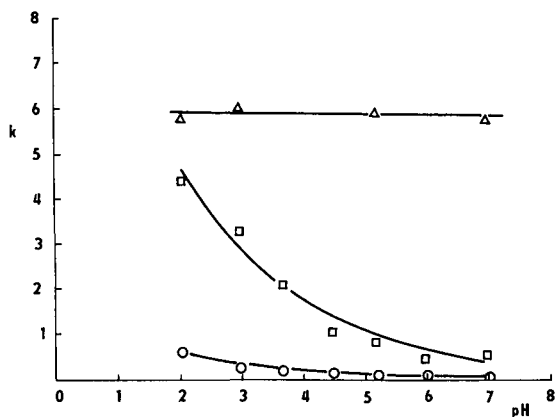


Fig. 4. Dependence of capacity factor ( $k$ ) on pH for ( $\square$ ) EN, ( $\circ$ ) DIAC and ( $\triangle$ ) DKP. The pH of the phosphonate buffer varied from 2 to 7. The retention time of the first-eluted peak (MA) was used for the calculation of  $k$ . Column temperature, 60°C; other conditions as in Fig. 3.



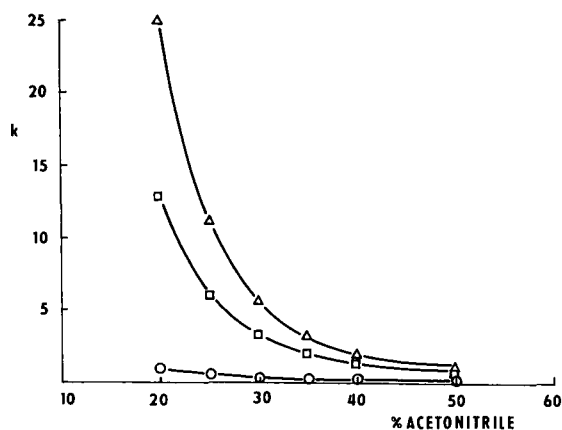


Fig. 5. Dependence of capacity factor ( $k$ ) of (□) EN, (○) DIAC and (△) DKP on acetonitrile concentration in the mobile phase. 0.05 M phosphate buffer (pH 3) was used for mobile phase preparation. Column temperature, 60°C; other conditions as in Fig. 3.

alanylproline is relatively high, *ca.* 20 kcal/mol [3]. The influence of temperature on the retention of chromatographed compounds is not significant, but the peak shape can be improved (Fig. 3).

*Influence of organic solvent concentration.* The retentions of solutes increase with decreasing organic solvent concentration; see Fig. 5, where the dependence of capacity factor ( $k$ ) on acetonitrile concentration in the mobile phase is shown.

*Influence of phosphate buffer concentration.* The concentration of buffer in the mobile phase plays a more significant and a different role in the separation of all the solutes studied (Fig. 6) in comparison with the above-described influence of the concentration of the organic modifier. A low buffer ionic strength allows an increase in interactions of the positively charged molecule of EN (at pH 3) with the negatively

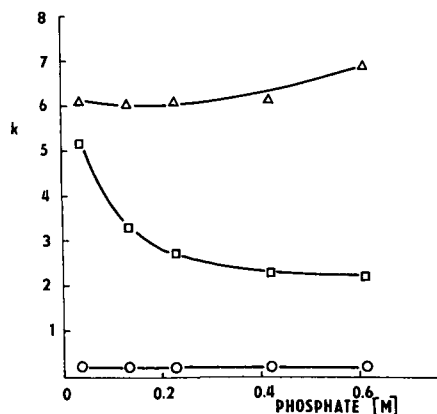


Fig. 6. Dependence of capacity factor ( $k$ ) of (□) EN, (○) DIAC and (△) DKP on phosphate buffer (pH 3) concentration. Column temperature, 60°C; other conditions as in Fig. 3.

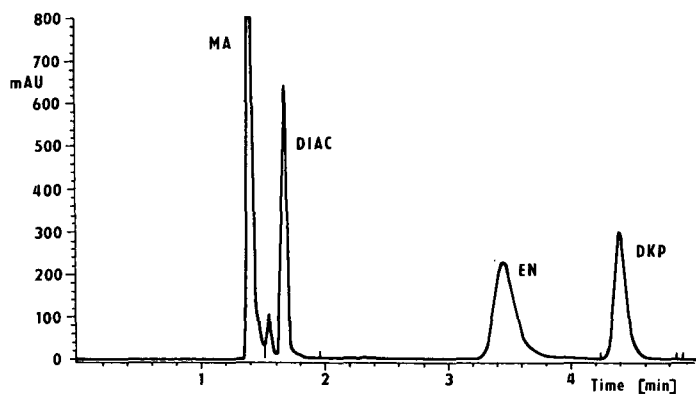


Fig. 7. Chromatogram of ENM, DIAC and DKP under the optimum conditions. Mobile phase, 0.05 *M* phosphate buffer (pH 3)–acetonitrile (6:4, v/v); column temperature, 60°C; concentration of compounds, 0.5 ml/min; other conditions as in Fig. 3.

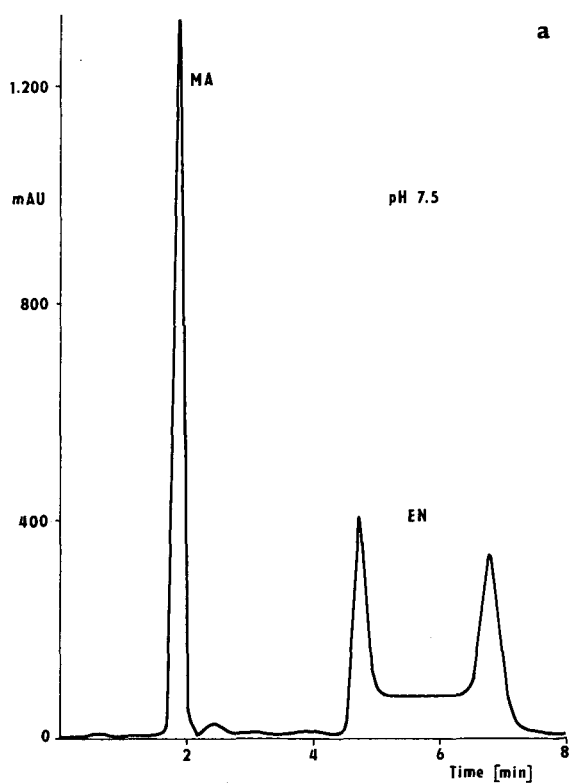


Fig. 8.

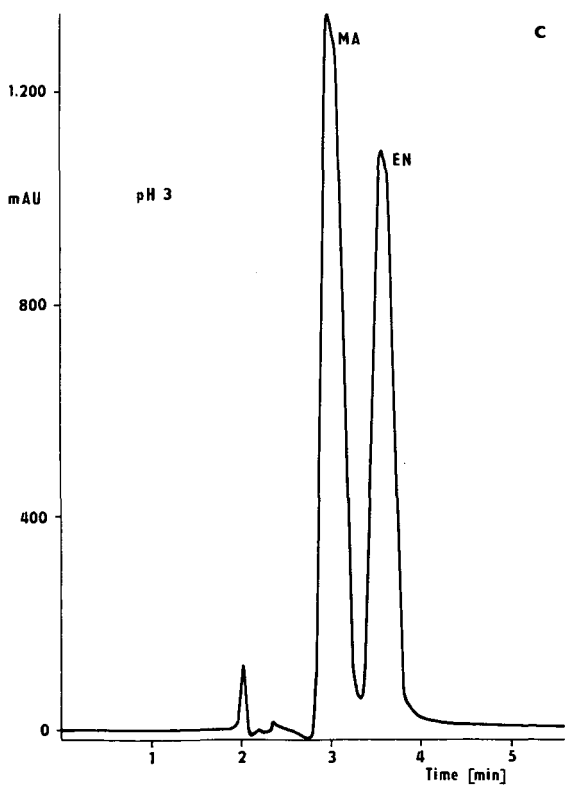
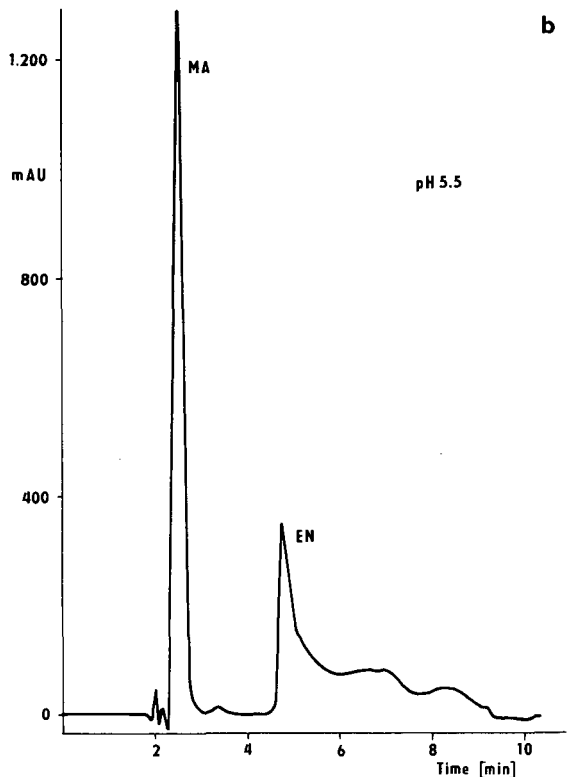


Fig. 8. Effect of pH in the presence of SDS and CTAB on the elution of MA and EN. Mobile phase, 0.05 M phosphate buffer (pH 7, 5.5 and 3)-methanol (4:6 at pH 7, otherwise 3:7, v/v) with 0.1 mM SDS and 0.1 mM CTAB. Column packing, Spherisorb ODS; temperature ambient; flow-rate, 0.5 ml/min; injection volume, 10  $\mu$ l; other conditions as in Fig. 3.

charged sites of the silica matrix of the reversed-phase sorbent and the retention of EN also increases. The retention of EN may increase to such an extent that the order of elution of EN and DKP may change at a concentration of phosphate buffer below 0.02 M. With the increase in ionic strength of the mobile phase, the ion-exchange interaction decreases. On the other hand, the retention of negatively charged molecules of DIAC and DKP is only slightly influenced by interactions with anionic adsorption sites in the chromatographic system used.

In this way, both pH and ionic strength are significant parameters for control of the retention and selectivity of the separation of the examined compounds. A chromatogram of a mixture of all the compounds studied under the optimum conditions, *i.e.*, 60°C, pH 3 and a 40% content of acetonitrile and 0.05 M phosphate buffer, is shown in Fig. 7. All the compounds are well separated in 5 min.

*Influence of SDS and CTAB.* The rotational changes in the molecule of EN in comparison with non-rotating DKP result in a great difference in their peak shapes and widths at lower temperature (Fig. 3). This difference can be decreased significantly by the addition of SDS and CTAB to the mobile phase (Fig. 8). The reduction of the EN peak splitting in the presence of both CTAB and SDS in the mobile phase can be explained by the existence of ionic multilayers of CTAB and SDS in the stationary phase. The high concentration of ionic groups in the stationary phase decreases the electrostatic interactions within the EN molecule in the adsorbed state, which can speed up the transition between the two EN isomers. In this way the use of both CTAB and SDS in the mobile phase at concentrations close to saturation acts in the same direction as the increase in the separation temperature.

The pH of the mobile phase containing CTAB and SDS had a dramatic influence on the elution profile, as shown in Fig. 8. A single, symmetrical peak of EN can be obtained at low pH even at the laboratory temperature (25°C).

## CONCLUSIONS

A decrease in the pH of the mobile phase, an increase in the column temperature and/or the addition of ion-pairing agents can eliminate peak splitting and significantly improve peak shape. The optimum peak shape is achieved at a lower pH (3) of the mobile phase and either at a higher temperature (60°C) or with the addition of both CTAB and SDS to the mobile phase. The resolution and retention of all the compounds studied can be influenced by, in addition to the organic modifier, the pH and ionic strength as the additional ion-exchange mechanism plays a significant role in the chromatographic system used. All these observations can help in the further development of chromatographic separations of proline-containing peptides.

## ACKNOWLEDGEMENTS

We thank Dr. J. Běluša for advice and A. Doubravová for assistance.

## REFERENCES

- 1 D. P. Ip and G. S. Brener, *Anal. Profiles Drug Subst.*, 16 (1987) 207.
- 2 J. D. Rawn, *Biochemistry*, Carolina Biological Supply, Burlington, NC, U.S.A., 1988, pp. 75-77.
- 3 W. R. Melander, J. Jacobson and C. Horvath, *J. Chromatogr.*, 234 (1982) 269.

- 4 J. C. Gesquire, E. Diesis, M. T. Cung and A. Tartar, *J. Chromatogr.*, 478 (1989) 121.
- 5 S. H. Hansen, P. Helboe and U. Lund, *J. Chromatogr.*, 270 (1983) 77.
- 6 S. O. Jansson, I. Andersson and M. L. Johansson, *J. Chromatogr.*, 245 (1982) 45.
- 7 B. A. Persson, S. O. Jansson, M. L. Johansson and P. Lagerström, *J. Chromatogr.*, 316 (1984) 291.
- 8 H. Morawetz, *Macromolecules in Solution*, Wiley, New York, 1965.
- 9 S. Takahashi, K. Inoue, Y. Yanagida, T. Ohashi and K. Watanabe, *Eur. Pat. Appl.*, 0 215 335 A2, 1987.
- 10 S. G. Weber and G. Tramposch, *Anal. Chem.*, 55 (1983) 1771.



## **Analysis of $^{55}\text{Fe}$ -labeled hydroxamate siderophores by high-performance liquid chromatography**

ROBERT J. SPEIRS and GREGORY L. BOYER\*

*Faculty of Chemistry, State University of New York, College of Environmental Science and Forestry, Syracuse, NY 13210-2786 (U.S.A.)*

(First received May 4th, 1990; revised manuscript received October 2nd, 1990)

---

### ABSTRACT

The radiolabeled iron(III) chelates of four different hydroxamate siderophores (desferrioxamine B, rhodotorulic acid, desferriferrichrome and desferriferrichrome A) were analyzed by high-performance liquid chromatography using an absorbance or radioactivity detector. Optimal conditions consisted of a polymeric PRP-1 column and a water to acidified acetonitrile gradient as mobile phase. Silica based columns gave similar resolution, but adsorption of unchelated iron-55 to the silica support limited the desirability of this approach. Detection limits based on radioactivity of the labeled compounds were consistently two to three orders of magnitude greater than that observed using visible absorbance at 436 nm. This method provides a generalized approach for the detection of high affinity iron(III) chelators (*e.g.* siderophores), regardless of their structural type.

---

### INTRODUCTION

Iron, an essential trace metal for the growth of microorganisms, is an element of low biological availability. To overcome this problem, blue-green algae, bacteria, and fungi secrete high affinity iron chelators termed siderophores [1–3]. These compounds play a dual role in microbial ecology. First, they solubilize needed ferric iron which is then absorbed by the cell through specific uptake receptors [4]. Second, they may tie up iron in a form that is unavailable to competing species [5,6]. An understanding of the biochemical ecology of these compounds is essential for our understanding the biochemical ecology of natural systems.

Siderophores exist in a wide variety of structural types [3]. They are usually divided into two groups depending on the nature of their iron-binding ligand: the catechol siderophores (*e.g.* enterobactin), and the hydroxamate siderophores (*e.g.* desferriferrichrome, rhodotorulic acid and desferrioxamine B). These ligands also serve as the basis for the common chemical tests for the detection of siderophores; the Arnow test for catechols and phenolics [7] and the Csaky test for hydroxamates [8]. Recently, several important siderophores have been elucidated that do not fall into either of these structural categories. These include phytosiderophores (*e.g.* mugineic acid [9]) produced by graminaceous plants and rhizobactin produced by the nitrogen

fixing bacterium, *Rhizobium meliloti* [10,11]. Lacking either a hydroxamate or phenolic ligand, these compounds are not detected using the classical chemical assays. Thus there is considerable interest in developing a general procedure for the detection of strong iron-binding compounds.

High-performance liquid chromatography (HPLC) has been used for the separation and analysis of hydroxamate [12,13] siderophores. These compounds are best detected by monitoring the rose-colored ferric complex at approximately 425–440 nm [14]. Detection of the iron complexes at lower wavelengths, such as 220 nm, works well with purified compounds, but may be too non-specific for use in natural samples [15]. Fewer reports have appeared on the use of HPLC for the detection of phenolic-based or mugineic acid-like siderophores. Lacking a distinctly colored iron complex, the phytosiderophores are more difficult to distinguish from interfering compounds.

We report here an HPLC-based assay for the general analysis of siderophores. A common feature of these compounds is their ability to strongly bind iron, hence detection in this procedure is by liquid scintillation counting of the  $^{55}\text{Fe}$ -labeled iron complex. While this work focuses on its use for the analysis of hydroxamate siderophores, the technique provides a general approach for the analysis of all siderophores and strong iron-binding compounds, regardless of their structural type.

## EXPERIMENTAL

### Materials

Rhodotorulic acid (RA) was isolated from iron-limited cultures of *Rhodotorula pilimanae* [16]. Ferrichrome (FC) and ferrichrome A (FCA) were isolated from iron-limited cultures of *Ustilago sphaerogena* [17] using published procedures and identified on the basis of their spectroscopic and thin-layer chromatographic behavior. Desferrioxamine B mesylate salt (Desferal, DES) was a gift from Ciba-Geigy (Suffern, NY, U.S.A.). [ $^{55}\text{Fe}$ ]iron(III) chloride in 0.1 M hydrochloric acid (80 MBq/mg Fe) was purchased from Amersham (Arlington Heights, IL, U.S.A.). Methanol was glass distilled prior to use. Acetonitrile, Scintiverse LC, and other chemicals were HPLC grade or better and purchased from Fisher Scientific (Rochester, NY, U.S.A.).

### Equipment

Our HPLC system consisted of two Waters Assoc. (Milford, MA, U.S.A.) M6000A pumps and a Model 660 gradient controller. The system was equipped with a Rheodyne 7125 injector and a Waters Assoc. Model 440 fixed-wavelength detector using a 436-nm filter. No effort was made to use a metal-free system or components. For the determination of radioactivity, 1-min samples were collected using a Gilson F-80 fraction collector (Gilson, Madison, WI, U.S.A.) connected to the outlet of the UV-VIS detector. These fractions were subsampled, mixed with Scintiverse LC counting cocktail, and then counted in a Packard Tricarb Model 4400 liquid scintillation counter using the preset  $^3\text{H}$  channel. In some applications, continuous detection of the  $^{55}\text{Fe}$  complexes was done using a Radiomatic A-120 HPLC-liquid scintillation counter (Radiomatic Instrument and Chemical Co., Tampa, FL, U.S.A.) equipped with a 0.5-ml flow cell. The column eluent was mixed 1:3 with scintillation fluid prior to the flow cell and total counts recorded at 6 s intervals.



### HPLC conditions

The following reversed-phase columns were used; a silica-based  $\mu\text{Bondapak C}_{18}$  column (Waters Assoc.; 10  $\mu\text{m}$ ; 300  $\times$  3.9 mm), a polymeric polystyrene divinyl benzene-based PRP-1 column (Hamilton, Reno, NV, U.S.A.; 10  $\mu\text{m}$ ; 150  $\times$  4.1 mm), and a polymeric fluorocarbon-based Poly F column (DuPont, Boston, MA, U.S.A.; 20  $\mu\text{m}$ ; 80  $\times$  6.2 mm]. The mobile phase consisted of a 20-min linear gradient from distilled water to either acetonitrile or methanol containing 1% (v/v) glacial acetic acid. Injection volumes were routinely 20  $\mu\text{l}$ . Flow-rates were systematically investigated at 0.5, 1.0 and 2.0 ml/min and 1.0 ml/min was selected as optimal for most applications.

### Methods

$^{55}\text{Fe}$  complexes of desferal and rhodotorulic acid were formed by adding the iron to the deferrated siderophore. Ferrichrome and ferrichrome A were isolated as their  $^{56}\text{Fe}$  complexes and radiolabeled by  $^{55}\text{Fe}$  exchange. A 50- $\mu\text{l}$  volume of 1 M sodium hydroxide solution was added to 200  $\mu\text{l}$  of a ferrichrome or ferrichrome A solution to dissociate the iron complex. This was followed by 2  $\mu\text{l}$  of  $^{55}\text{Fe}$  standard (containing *ca.* 3 kBq  $^{55}\text{Fe}$ ) and the pH was adjusted back to neutral with 50  $\mu\text{l}$  1.0 M hydrochloric acid. Samples were allowed to stand for 1 h prior to analysis by HPLC.

To determine total recoveries of radioactive iron, 86 pmol total iron (containing 385 Bq  $^{55}\text{Fe}$ ) with or without excess chelator were injected on the HPLC system and the entire 20-min gradient collected in a round-bottom flask. The eluent was then concentrated by rotary evaporation to 6 ml and counted via liquid scintillation counting. To correct for possible effects on counting efficiency, the control for this experiment consisted of collecting a blank gradient (no injection) and adding  $^{55}\text{Fe}$  directly to the flask prior to concentration.

For the determination of standard curves, the  $^{55}\text{Fe}$  standard was diluted 1:1000 with 0.1 M hydrochloric acid. This solution was mixed with an equal volume of deferrated siderophore solution (final concentration of Fe = 4.3  $\mu\text{M}$ ) and 20  $\mu\text{l}$  injected on the HPLC system. Peaks corresponding to the radiolabeled siderophore were collected and counted by liquid scintillation counting. All points on the standard curves were run in triplicate.

## RESULTS

The separation of four different hydroxamate siderophores was investigated using three different columns. Only minor differences were observed between their chromatography on the silica-based  $\mu\text{Bondapak C}_{18}$  column and the polymeric Hamilton PRP-1 column (Table I). Either a 0–50% acidified methanol or 0–30% acidified acetonitrile gradient was suitable to cleanly separate the four iron chelates. Detection could be accomplished by monitoring the absorbance of the colored ferric complex at 436 nm (Fig. 1 top). Use of the smaller Poly F column resulted in earlier elution of the larger siderophore complexes (DES, FC, FCA), however, the rhodotorulic acid iron complex was not retained by the column using these mobile phases.

Siderophores are characterized by having a very high affinity for ferric iron (log of the formation constants for their iron complexes are between 29 and 32, depending

TABLE I

## RETENTION TIMES OF FOUR SIDEROPHORES ON THREE DIFFERENT COLUMNS

HPLC conditions: 20-min linear gradient from water to methanol or acetonitrile containing 1% (v/v) glacial acetic acid, 2 ml/min flow-rate. Detection was at 436 nm.

Gradient	Retention time (min)			
	RA	DES	FC	FCA
$\mu$ Bondapak C <sub>18</sub> (Waters Assoc.)				
0-50% acidified methanol	7.2	16.4	13.6	19.4
0-30% acidified acetonitrile	7.4	15.2	13.4	17.6
PRP-1 (Hamilton)				
0-50% acidified methanol	3.2	12.0	17.0	22.8
0-30% acidified acetonitrile	3.8	8.8	10.4	15.8
Poly-F (DuPont)				
0-50% acidified methanol	1.0	5.2	4.4	9.2
0-15% acidified acetonitrile	1.0	6.4	4.6	13.0

on the individual siderophores [18]). <sup>55</sup>Fe is a weak electron-capture radionuclide and can be counted by liquid scintillation counting using techniques similar to those used for tritium. Unlike the  $\gamma$  emitter <sup>59</sup>Fe, <sup>55</sup>Fe requires only minimal shielding and has a long (2.6 year) half life. While the addition of chelators is sometimes used to improve its counting efficiency [19], this was not necessary in our experiments. Addition of the chelators DES or RA at concentrations between 0 and 100  $\mu$ g per vial (1000  $\times$  molar excess) did not affect the counting efficiency nor was quenching of the <sup>55</sup>Fe observed in these experiments (data not shown). Observed counting efficiencies (*ca.* 50%) were close to what we commonly observe for tritium under similar conditions. Thus <sup>55</sup>Fe could be used to provide a second method for the detection of the ferric siderophores. The radiochromatogram for these compounds is shown in Fig. 1 (bottom panel).

Recoveries of both chelated and unchelated iron from the three different columns are shown in Table II. The polymeric columns (PRP-1 or Poly F) showed an excellent recovery for both chelated and unchelated iron. In contrast, the silica-based column gave high though inconsistent recoveries for chelated iron but a very low recovery (44%) for the unchelated iron. This missing iron was apparently adsorbed to the silica since it was possible to strip varying amounts of <sup>55</sup>Fe off the silica by injecting iron-free EDTA through the column (data not shown).

Standard curves were prepared for each of the four siderophores (RA, DES, FC and FCA) between concentrations of 0 and 100 nmol per 20- $\mu$ l injection. In each case, the total iron concentration was held constant at 86 pmol per 20- $\mu$ l injection. A representative plot of the observed radioactivity in the chelator peak versus total chelator concentration for FCA is shown in Fig. 2. At chelator concentration much higher than the fixed iron concentration ( $Fe_T = 4.3 \mu M$ ), the curve resembled a saturable curve. At chelator concentrations equal to or less than the iron concentration, observed counts in the chelator peak were linearly dependent on the chelator concentration. For a chelator-to-iron ratio of 1 or less, the correlation

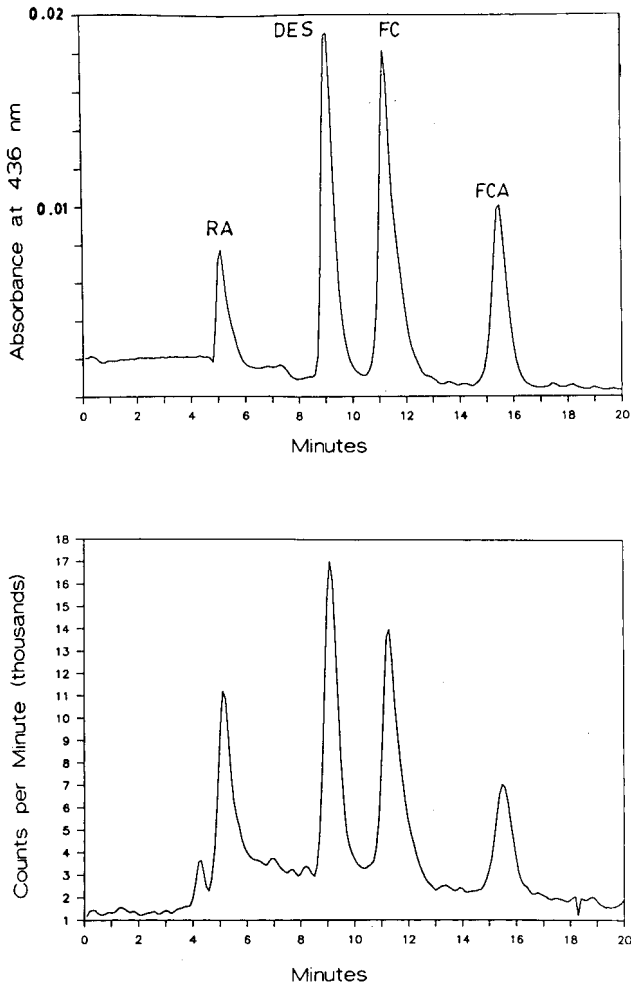


Fig. 1. Chromatograms obtained from a concentrated mixture of  $^{55}\text{Fe}$ -labeled siderophores as determined by monitoring absorbance at 436 nm (top) or counts per min (bottom). HPLC conditions consisted of a PRP-1 column and a 20 min 0–50% acidified acetonitrile in water gradient. Flow-rate was 2 ml/min. To simultaneously observe absorbance and radioactivity on the same run, a mixed siderophore standard containing 0.25 mM FCA, 0.4 mM FC, 0.4 mM DES and 0.7 mM RA was labeled with  $^{55}\text{Fe}$  (385 kBq) and then saturated with excess  $^{56}\text{Fe}$ . The ordinate in the top panel is in arbitrary units but represents approximately 0.02 a.u. full scale.

coefficient for FCA was 0.995. This general pattern was true for both DES and FC as long as the total iron concentration was greater than the total chelator concentration (correlation coefficients for DES and FC were 0.985 and 0.994, respectively). At this iron concentration, the detection limit for the three chelators was 10 pmol per 20- $\mu\text{l}$  injection. This limit was well below that observable by absorbance detection. Only at the higher siderophore concentrations (> 10 nmol per 20- $\mu\text{l}$  injection) was there a measurable peak at 436 nm. Determination of RA concentrations at these low

TABLE II

RECOVERY OF CHELATED AND UNCHELATED  $^{55}\text{Fe}$  FROM THE THREE DIFFERENT COLUMNS AT 1 AND 2 mg/ml CHELATOR CONCENTRATION ( $\pm$  S.D)

Recoveries were determined by counting the entire gradient as described in the *Methods* section. HPLC conditions consisted of a 20-min water-to-acidified acetonitrile gradient at 1 ml/min flow-rate. Molar concentrations: EDTA: 1 mg/ml = 2.7 mM; 2 mg/ml = 5.4 mM; DES: 1 mg/ml = 1.6 mM; 2 mg/ml = 3.3 mM; RA: 1 mg/ml = 2.9 mM; 2 mg/ml = 5.8 mM. Total iron concentration: 4.3  $\mu\text{M}$ .

Column	Unchelated $^{55}\text{Fe}$	Recovery (%)					
		RA (mg)		EDTA (mg)		DES (mg)	
		1	2	1	2	1	2
PRP-1	85% $\pm 12\%$	104% $\pm 4\%$	105% $\pm 5\%$	91% $\pm 8\%$	100% $\pm 5\%$	102% $\pm 11\%$	101% $\pm 1\%$
$\mu\text{Bondapak}$ $\text{C}_{18}$	44% $\pm 5\%$	n.d.	n.d.	87% $\pm 7\%$	116% $\pm 36\%$	97% $\pm 2\%$	115% $\pm 7\%$
Poly F	103% $\pm 21\%$	101% $\pm 1\%$	96% $\pm 5\%$	98% $\pm 3\%$	92% $\pm 8\%$	97% $\pm 2\%$	96% $\pm 7\%$

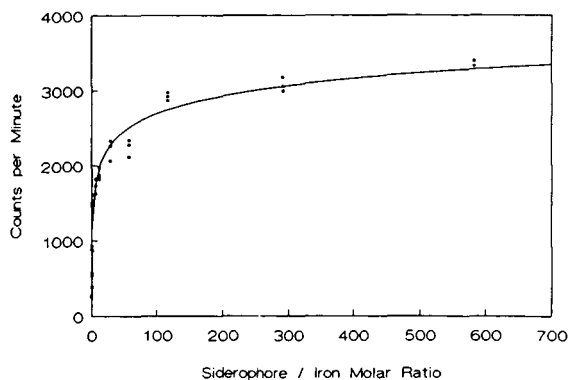
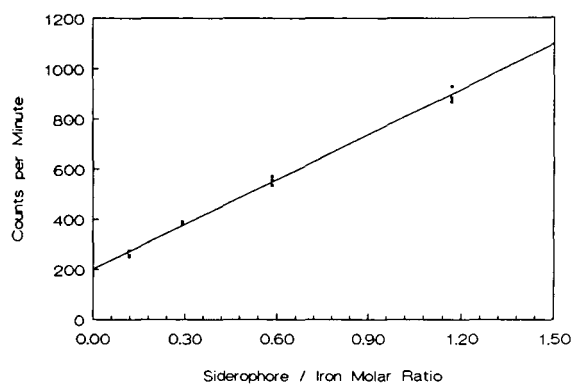


Fig. 2. Counts per min in the ferrichrome A peak as plotted against the siderophore/iron ratio. The total iron concentration was held constant at 4.3  $\mu\text{M}$ . HPLC conditions as in Fig. 1.

concentrations was more difficult due to overlap of the free iron peak with the ferric-RA peak and the fact that RA forms a 2:3 iron-siderophore complex. Its detection limit was generally 10-fold higher than that observed for ferrichrome A. The detection limit of the HPLC assay could be increased by labeling the siderophores with  $^{55}\text{Fe}$  of a higher specific activity. In contrast, the linear range of the standard curve could be increased by the addition of cold ( $^{56}\text{Fe}$ ) ferric iron (*e.g.* Fig. 1). This did, however, result in a corresponding loss in sensitivity at low siderophore concentrations.

## DISCUSSION

Siderophores may play an important role in microbial ecology. They exist in a wide variety of structural types, thus new methods are needed to detect these compounds in natural systems. Recently HPLC has been applied to the study of these compounds. Jalal *et al.* [12] studied nineteen different hydroxamate siderophores of the ferrichrome type and successfully separated them using a reversed-phase column. This approach was used to study siderophore formation in culture filtrates from four different fungi known to produce hydroxamate siderophores. These complexes all have very strong absorption maxima in the 420–450 nm range and can readily be detected using photodiode array detection. This approach would be less successful for the detection of siderophores such as rhizobactin, mugineic acid and possible unknown siderophores which do not form highly colored complexes. For this reason, the ability to detect the siderophore complex based on their affinity for iron rather than on the spectroscopic properties of the iron complex is desirable. The use of radiolabeled siderophores described here is several orders of magnitude more sensitive than the spectroscopic approach and provides for the quantitative determination of siderophore concentrations provided sufficient iron is present to saturate all chelators. As such, it provides a very general method for the quantitative and qualitative analysis of siderophores.

In a similar approach, Glennon *et al.* [20] used a metal-free system and amperometric detection for the direct analysis of siderophoric iron. This technique has both advantages and disadvantages compared to radiolabeling. For the detection of siderophoric iron, an applied potential of 1.0 V was optimal. This high potential greatly shortens electrode life and required that the electrode be polished after every 70 plus injections. This high potential also limits the chromatographic system to isocratic mobile phases, decreasing the diversity of compounds that can be analyzed in a single run. When applied to their *Pseudomonas fluorescens* cultures, problems of background oxidation of EDTA in the culture media forced Glennon *et al.* to use 0.5 V to work with culture supernatants. In contrast, radiolabeling the siderophores using  $^{55}\text{Fe}$  suffers few of these problems. Gradient mobile phases can easily be used to separate complex mixtures of chemically distinct iron complexes. Since detection is of the iron-siderophore complexes, and these complexes are stable on the HPLC time frame, exchange of  $^{55}\text{Fe}$  with cold iron that may be present in the chromatographic system was not a problem. This minimizes need for metal-free systems that have been used by other workers [21,22]. Silica-based  $\text{C}_{18}$  columns and polymeric-based columns (PRP-1) gave comparable resolution. However, there was a marked difference in the recovery of radioactive iron from the two column types. Adsorption of iron to the silica-based columns did occur and could be a potential source of interference, even in the presence

of 1000-fold excess chelator. This was not a problem when polymeric-based columns were used. Others [23] have also reported the use of polymeric columns for the separation of iron and aluminum complexes of desferrioxamine B. While the larger PRP-1 column was generally the preferred of the two polymeric columns, the smaller Poly F based column may be advantageous under limited circumstances. This column would be especially suitable for the quick analysis of ferrichrome analogs due to its short retention times. It may also be useful for the early screening of unknown siderophores due to its high and consistent recoveries of  $^{55}\text{Fe}$ .

In summary, HPLC and radiochemical detection after labeling with  $^{55}\text{Fe}$  provides a rapid and general assay for the quantitative and qualitative analysis of siderophores based only on their ability to bind iron. Unlike other general assays for siderophore detection [20,24], this approach does not appear to be affected by the presence of other weak metal chelators such as citric acid or EDTA commonly present in culture supernatants [25]. While only its use with hydroxamate siderophores is reported here, it provides a rapid and general method for the detection of a wide variety of different strong iron-binding compounds.

#### ACKNOWLEDGEMENTS

We would like to thank Ciba-Geigy for the gift of Desferal and E.I. du Pont de Nemours for the use of the Poly F column. This work is supported by the NOAA Office of Sea Grant, U.S. Department of Commerce, under Grant NA86AA-D-SG045 to the New York Sea Grant Institute.

#### REFERENCES

- 1 G. Winkelmann, D. van der Helm and J. B. Neilands, *Iron Transport in Microbes, Plants and Animals*, VCH, New York, 1989, p. 533.
- 2 G. L. Boyer, A. Gillam and C. G. Trick, in P. Fay and C. van Baalen (Editors), *Cyanobacteria*, Elsevier, Amsterdam, 1987, p. 415.
- 3 R. C. Hider, *Struct. Bonding*, 58 (1984) 25.
- 4 J. B. Neilands, *Ann. Rev. Nutr.*, 1 (1981) 27.
- 5 T. P. Murphy, D. R. S. Lean and C. Nalewajko, *Science (Washington, D.C.)*, 192 (1976) 900.
- 6 L. A. De Weger, B. Schippers and B. Lugtenberg, in G. Winkelmann, D. van der Helm and J. B. Neilands (Editors), *Iron Transport in Microbes, Plants, and Animals*, VCH, New York, 1987, p. 387.
- 7 L. E. Arnow, *J. Biol. Chem.*, 118 (1937) 531.
- 8 T. Z. Csaky, *Acta Chem. Scand.*, 2 (1948) 450.
- 9 Y. Sugiura and K. Nomoto, *Struct. Bonding*, 58 (1984) 107.
- 10 M. J. Smith, J. N. Shoolery, B. Schwyn, I. Holden and J. B. Neilands, *J. Am. Chem. Soc.*, 107 (1985) 1739.
- 11 B. Schwyn and J. B. Neilands, *Comments Agric. Food Chem.*, 1 (1987) 95.
- 12 M. A. F. Jalal, R. Mocharla and D. van der Helm, *J. Chromatogr.*, 301 (1984) 247.
- 13 S. Konetschny-Rapp, H. G. Huschka, G. Winkelmann and G. Jung, *Biol. Met.*, 1 (1988) 9.
- 14 J. B. Neilands, *Struct. Bonding*, 58 (1984) 1.
- 15 A. van der Horst, P. N. F. C. de Goede, H. J. J. Willems and A. C. van Loenen, *J. Chromatogr.*, 381 (1986) 185.
- 16 C. L. Atkin and J. B. Neilands, *Biochemistry*, 7 (1968) 3734.
- 17 J. A. Garibaldi and J. B. Neilands, *J. Am. Chem. Soc.*, 77 (1955) 2429.
- 18 J. B. Neilands, *Ann. Rev. Biochem.*, 50 (1981) 715.
- 19 A. H. Haydon, W. B. Davis, J. L. Arceneaux, G. A. Gentry and B. R. Byers, *Biochim. Biophys. Acta*, 273 (1972) 1.
- 20 J. D. Glennon, M. R. Wolfe, A. T. Senior and N. NiChoileain, *Anal. Chem.*, 61 (1989) 1474.

- 21 S. Venkataram and Y. E. Rahman, *J. Chromatogr.*, 411 (1987) 494.
- 22 S. M. Cramer, B. Nathanael and Cs. Horváth, *J. Chromatogr.*, 295 (1984) 405.
- 23 H. B. Jenny and H. H. Peter, *J. Chromatogr.*, 438 (1988) 433.
- 24 B. Schwyn and J. B. Neilands, *Anal. Biochem.*, 160 (1987) 47.
- 25 R. J. Speirs, P. D. Morse and G. L. Boyer, *Anal. Biochem.*, in preparation.





CHROM. 22 838

## **Simultaneous determination of arsenite, arsenate, selenite and selenate in waters using suppressed ion chromatography with ultraviolet absorbance detection**

S. S. GOYAL\*, A. HAFEZ and D. W. RAINS

*Department of Agronomy and Range Science, University of California, Davis, Davis, CA 95616 (U.S.A.)*

(Received May 30th, 1990)

---

### ABSTRACT

Using Dionex AS4A anion-exchange column, with micromembrane suppressor and UV detector at 195 nm, arsenite, arsenate, selenite and selenate can be determined simultaneously in water samples. The mole fraction of sodium carbonate in the eluent as well as eluent concentration affected the retention times especially for the divalent anions. An eluent of 2.25 mM Na<sub>2</sub>CO<sub>3</sub> and 0.75 mM NaHCO<sub>3</sub> was found to be the most suitable for sample analysis. The responses for all ions tested was linear in 0–5 mg l<sup>-1</sup> range. The system can tolerate up to 1600 mg l<sup>-1</sup> of SO<sub>4</sub><sup>2-</sup>, before affecting arsenate peaks. Selenate peak area was not affected due to SO<sub>4</sub><sup>2-</sup> concentration up to 2000 mg l<sup>-1</sup>. The detection limits using 100-μl loop were 0.1 mg l<sup>-1</sup> for AsO<sub>2</sub><sup>-</sup> and SeO<sub>3</sub><sup>2-</sup> and 0.25 mg l<sup>-1</sup> AsO<sub>4</sub><sup>3-</sup> and SeO<sub>4</sub><sup>2-</sup>.

---

### INTRODUCTION

Metalloids especially selenium and arsenic and their derivatives can widely spread throughout the environment as a result of fuel consumption, industrial, agricultural and natural processes [1]. Although deficiencies of selenium results in selenium-responsive diseases in various animal species, the differences between essential and the toxic concentration is rather narrow [2]. Arsenic compounds represent a carcinogenic hazard in the environment. The continuing interest in tracing the fate of selenium and arsenic, led to the development of several methods for their analysis. The most common methods are: atomic fluorescence spectrometry [3,4], atomic absorption spectroscopy with hydride generator [5,6], inductively coupled plasma [7] (ICP-AES) and electrothermal graphite furnace [8], or spectrophotometry [9–11].

Because the inorganic form of these two elements exists mostly in natural waters in two oxidation states, *i.e.* Se(IV), Se(VI), As(III) and As(V), speciation becomes of particular importance. The ecological fate is also determined by the chemical form. In the afore-mentioned methods, two determinations are required. One before and the other after reduction, to measure both oxidation states. The difference between these two determinations yields the amount existed at higher oxidation states [12,13].

During the last decade the application of high-performance liquid chromato-

graphy (HPLC) for the analysis of inorganic anions (usually referred to as ion chromatography, IC) has provided a reliable, fast, convenient and sensitive alternative to many complex analytical problems. Five different low-capacity anion-exchange columns for non-suppressed ion chromatography [14] (also called single column ion chromatography, SCIC) were evaluated for inorganic anion assay [15]. SCIC was used for the assay of selenite [16], selenate [17] and arsenate [18]. However,  $\text{Cl}^-$  above  $10 \text{ mg l}^{-1}$ ,  $\text{SO}_4^{2-}$  above  $40 \text{ mg l}^{-1}$  and  $\text{PO}_4^{3-}$  above  $30 \text{ mg l}^{-1}$  masked the selenite, selenate and arsenate peaks, respectively [16–18]. The use of suppressed ion chromatography [19] (SIC) offers two advantages for such applications: (1) with high pH eluents, it becomes possible to elute monovalent, divalent and even trivalent anions in a single run and reasonable time and (2) increased sensitivity due to lower background conductivity.

Conventionally, nearly all ion chromatography for inorganic anions has been done using electrical conductivity detection. However, it has been shown that many inorganic anions have suitable chromophores and their detection by an ultraviolet (UV) absorbance detector is possible [20]. The use of UV absorbance detection could provide selectivity against unwanted ionic species specially in cases where sample matrix problems exist. Since the SIC system reduced both the background conductivity as well as the UV absorbance of effluent ( $2.4 \text{ mM Na}_2\text{CO}_3 + 3.0 \text{ mM NaHCO}_3$ ), it was possible to use the system with a UV detector [20]. Ions of fluoride, phosphate, and sulfate did not show UV absorbance whereas arsenite, arsenate, selenite, selenate and many other ions showed absorbance in this region [20].

A method for simultaneous determination of arsenite, arsenate, selenite, selenate ions has not been available. Since arsenite can not be detected by conductivity detection, an ion chromatographic method for its determination is not possible. The objective of this research was to develop a method for simultaneous determination of arsenite, arsenate, selenite and selenate using UV absorbance detection.

## EXPERIMENTAL

All chemicals used in the study were of ACS reagent grade and were used as received from the suppliers.

The SIC system consisted of two HPLC pumps (Model LC-6A), a systems controller (SCL-6A), a UV-VIS detector (Model SPD-6AV), a data system (Model C-R3A, all Shimadzu Scientific Instruments (Columbia, MD), a conductivity detector (Waters Assoc., Milford, MA) and a HPLC injector (Model 7126, Rheodyne, Cotati, CA). The analytical column IonPac AS4A and a guard column AG5 were used with an Anion Micro Membrane Suppressor, AMMS (all columns, Dionex, Sunnyvale, CA). For the purpose of this study the system was used in a binary gradient mode to mix  $3.0 \text{ mM Na}_2\text{CO}_3$  and  $3.0 \text{ mM NaHCO}_3$  to obtain the desired  $\text{Na}_2\text{CO}_3$  molar ratio or to mix ( $2.25 \text{ mM Na}_2\text{CO}_3 + 0.75 \text{ mM NaHCO}_3$ ) and deionized water in desired proportions. However, the actual chromatography was isocratic. The eluents were maintained under nitrogen in order to avoid atmospheric carbon dioxide. The eluent flow-rate was kept constant at  $1.7 \text{ ml min}^{-1}$  throughout the study. The flow-rate of regenerant for AMMS ( $12.5 \text{ mM H}_2\text{SO}_4$ ) was about  $4 \text{ ml min}^{-1}$ . The void volume of the system was  $1.56 \text{ ml}$  (or  $0.92 \text{ min}$  at  $1.7 \text{ ml min}^{-1}$ ).

UV absorbance spectra were generated using a scanning spectrophotometer (Model: Lambda 6, Perkin Elmer Corp., Norwalk, CT).

## RESULTS AND DISCUSSION

The absorption spectra of arsenite, arsenate, selenite and selenate in 190–230 nm range are shown in Fig. 1. It is noteworthy that the lower oxidation states of these ions exhibit relatively greater absorbance. The shortest wavelength on our detector of 195 nm was used for the detection. Other ions commonly encountered in waters, *e.g.*, nitrate and nitrite also absorb in this region but with a different absorption maxima. Fluoride, phosphate and sulfate do not show absorbance in this range [20].

A comparison of UV absorbance *vs.* electrical conductivity chromatograms of these ions in the presence of other commonly present inorganic anions (fluoride, chloride, nitrate and sulfate) is shown in Fig. 2. With UV absorbance, fluoride was not detected and sulfate appeared as a split negative peak. As expected, arsenite was not detected by electrical conductivity. Apparently, the UV absorbance not only provided a means of arsenite detection but also provided selectivity against fluoride. This was important as both the ions co-eluted very close to the void volume on this system. Consequently, UV absorption detection was used in all further work.

*Optimization of chromatographic conditions*

In general, increasing mole fraction of  $\text{Na}_2\text{CO}_3$  in a 3.0 mM  $\text{Na}_2\text{CO}_3 + \text{NaHCO}_3$  eluent decreased the retention times of all ions tested (Fig. 3). The effect seemed to be proportional to the retention times. In other words, the retention of strongly held ions was affected relatively more than the loosely held ions. For example, increasing  $\text{Na}_2\text{CO}_3$  fraction from 0.25 to 1.00 decreased the retention time of  $\text{SeO}_4^{2-}$  from 17.42 min to 6.15 min (a 65% decrease), whereas that of  $\text{NO}_3^-$  from 4.04 min to 2.78 min (a 31% decrease). The retention of arsenite was not affected by the eluent composition suggesting it eluted close to the void volume. Arsenate was an exception in that its retention time decreased until  $\text{Na}_2\text{CO}_3$  mole fraction increased upto 0.50 but the retention increased again as the  $\text{Na}_2\text{CO}_3$  mole fraction increased further beyond 0.75. This probably represents a pH effect of the eluent on the dissociation of arsenate.

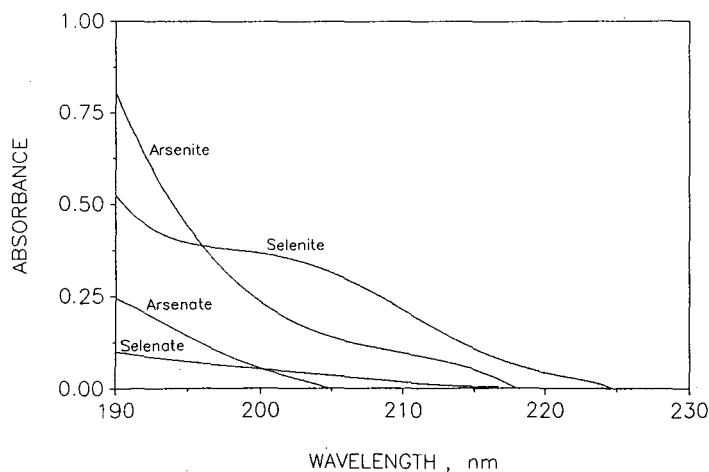


Fig. 1. Absorbance spectra of arsenite, arsenate, selenite, and selenate in 190–250 nm range ( $20 \text{ mg l}^{-1}$ ).

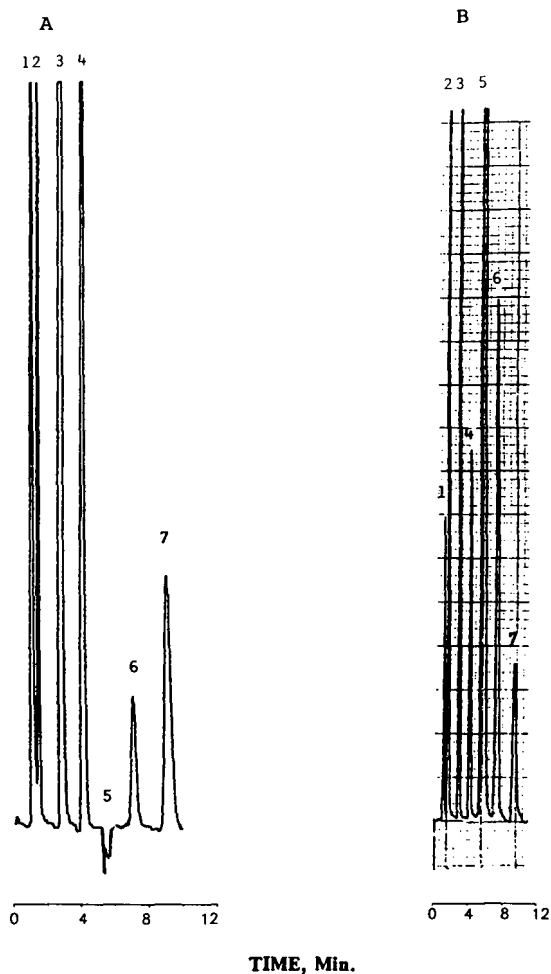


Fig. 2. Comparison between UV absorbance (A) and electrical conductivity detection (B). Peak identification: 1 = arsenite in A and fluoride in B; 2 = chloride; 3 = nitrate; 4 = selenite; 5 = sulfate; 6 = selenate; 7 = arsenate.

An increase in the  $\text{Na}_2\text{CO}_3$  mole fraction from 0.75 to 1.00, increased the eluent pH from 10.2 to 10.6. This would increase the mole fraction of trivalent  $\text{AsO}_4^{3-}$  from 0.05 to 0.18 [21] and thus resulting in a stronger retention. Based on the information shown in Fig. 3, a  $\text{Na}_2\text{CO}_3$  mole fraction of 0.75 was chosen for further work.

A decrease in the eluent strength ( $\text{Na}_2\text{CO}_3 + \text{NaHCO}_3$  concentration), at a  $\text{Na}_2\text{CO}_3$  mole fraction of 0.75, increased the retention times of all ions (Fig. 4). However, the slight improvement in resolution due to increased retention times was negated by longer analysis time. Therefore, an eluent concentration of 3.0 mM was chosen. Under these conditions the total analysis time was about 12.0 min.

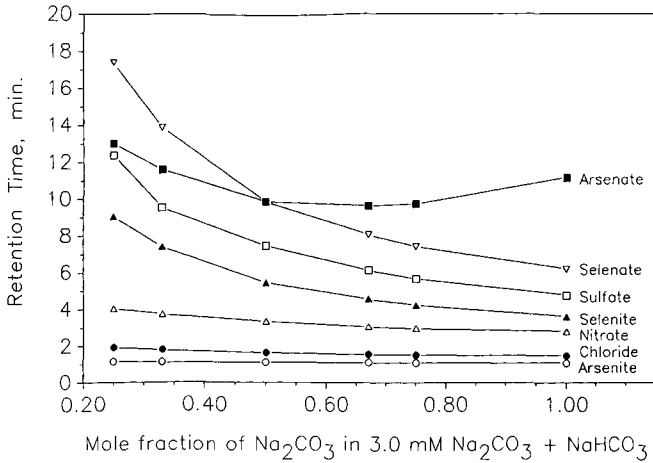


Fig. 3. Effect of eluent composition on the retention times of anions.

*Response linearity and detection limits*

The UV absorbance response, of all four ions over the concentration range (0-5 mg l<sup>-1</sup>, 100-μl injections) tested, was linear (Fig. 5). The detection limits (signal-to-noise ratio of 3.0) using 100-μl injections were measured as: arsenite, 0.1 mg l<sup>-1</sup>; selenite, 0.1 mg l<sup>-1</sup>; selenate, 0.25 mg l<sup>-1</sup>; arsenate, 0.25 mg l<sup>-1</sup>. Lower detection limits should be possible with the use of larger injection volumes and/or a concentrator column. Concentrator columns have been used to lower detection limits by enabling the researcher to load as much as 20-ml sample [16].

*Effect of sample matrix*

A sample concentration of SO<sub>4</sub><sup>2-</sup> greater than 50 mg l<sup>-1</sup> has been a major problem during selenate assay with SCIC [17] and SIC [22]. Selenate signal was

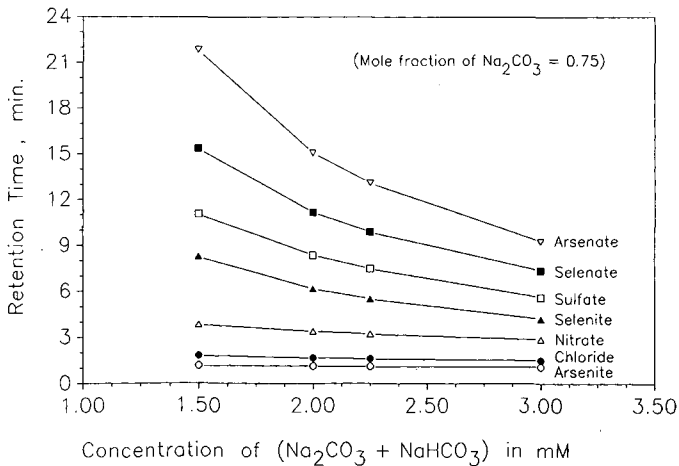


Fig. 4. Effect of eluent concentration on the retention times of anions.

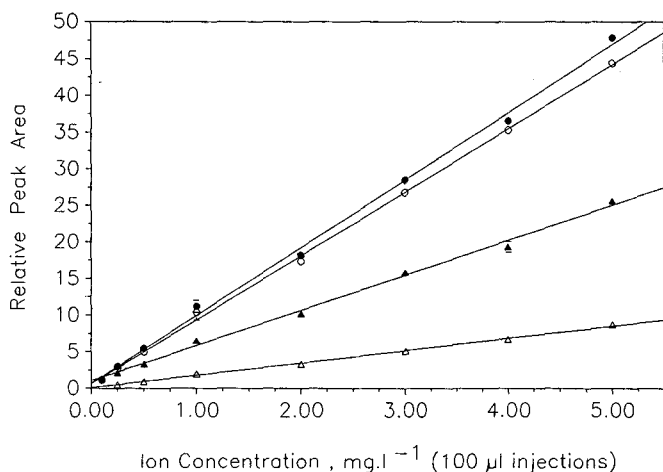


Fig. 5. Linearity of UV absorbance response for selenite, arsenite, selenate, and arsenate. ● = Selenite ( $y = 0.7023 + 9.244x, r = 0.9988$ ); ○ = arsenite ( $y = 0.6265 + 8.741x, r = 0.9995$ ); ▲ = arsenate ( $y = 1.0453 + 4.804x, r = 0.9978$ ); △ = selenate ( $y = 0.8693 + 1.689x, r = 0.9989$ ).

reduced by 5% and 19% in the presence of  $0.3 \text{ mg l}^{-1}$  with SIC [23] and  $60 \text{ mg l}^{-1}$   $\text{SO}_4^{2-}$  with SCIC [17], respectively, using conductivity detection. Removal of  $\text{SO}_4^{2-}$  ions from sample to reduce its concentration, prior to assay, has also been tested with little success. For example, cation-exchange resin in barium form [17] and chemical treatment of sample with barium formate [17] and barium hydroxide [22] has been tried to reduce the  $\text{SO}_4^{2-}$  concentration. Such sample treatment resulted in slight

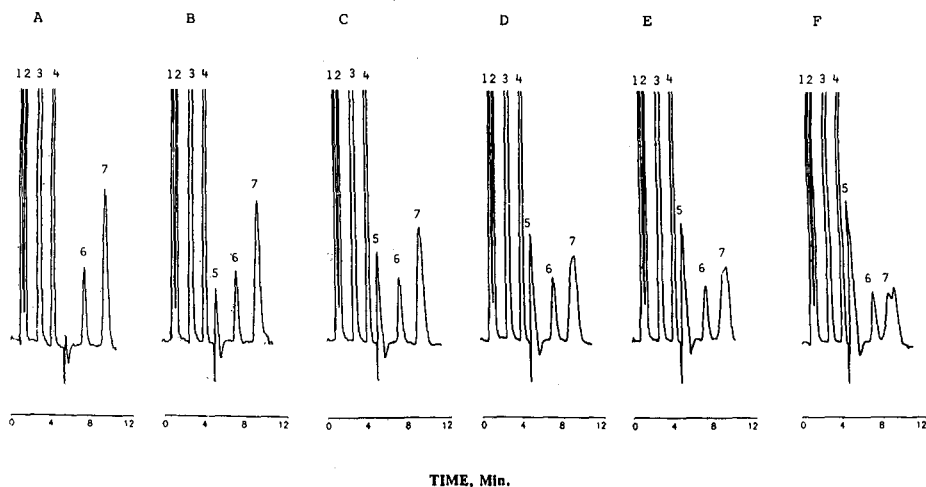


Fig. 6. Effect of high sulfate concentration on the separation and detection of arsenite (1), selenite (4), selenate (6), and arsenate (7) in the presence of chloride (2), nitrate (3), and sulfate (5). Sample composition ( $\text{mg l}^{-1}$ ): chloride, 100; nitrate, 10; arsenite, 20; selenite, 20; selenate, 20; arsenate, 20. Sulfate concentration ( $\text{mg l}^{-1}$ ): A, 400; B, 800; C, 1200; D, 1400; E, 1600; F, 2000.

TABLE I

RELATIVE PEAK AREAS AND RETENTION TIMES FOR ARSENATE AND SELENATE (BOTH AT 20 mg l<sup>-1</sup>) IN THE PRESENCE OF DIFFERENT SO<sub>4</sub><sup>2-</sup> CONCENTRATIONS (20 μl INJECTIONS)

Sulfate (mg l <sup>-1</sup> )	Selenate <sup>a</sup>		Arsenate <sup>b</sup>	
	Time (min)	Peak area (%)	Time (min)	Peak area (%)
400	7.33	100	9.36	100
800	7.28	103	9.33	98
1200	7.27	100	9.32	100
1400	7.27	102	9.34	97
1600	7.24	102	9.33	96
2000	7.23	100	8.78, 9.42	(50 + 45) = 95

<sup>a</sup> Peak number 6 in Fig. 6.

<sup>b</sup> Peak number 7 in Fig. 6.

improvement in resolution but the selenate signal was reduced. In our system, increasing concentration of SO<sub>4</sub><sup>2-</sup> in samples did not affect the peaks of ions with retention times shorter than SO<sub>4</sub><sup>2-</sup> (AsO<sub>2</sub><sup>-</sup>, Cl<sup>-</sup>, NO<sub>3</sub><sup>-</sup>, SeO<sub>3</sub><sup>2-</sup>). The peak heights of ions that eluted after SO<sub>4</sub><sup>2-</sup>, i.e., AsO<sub>4</sub><sup>3-</sup> and SeO<sub>4</sub><sup>2-</sup>, were decreased; however, the retention times and peak areas were not effected significantly (Fig. 6 and Table I). When SO<sub>4</sub><sup>2-</sup> concentration was increased beyond 1400 mg l<sup>-1</sup>, a distortion of arsenate peak was observed. The effect was so pronounced that at 2000 mg l<sup>-1</sup> SO<sub>4</sub><sup>2-</sup>, the arsenate peak appeared forked and two separate peaks were detected (Fig. 6). Interestingly, the peak area (sum of both peaks) was affected only slightly (Table I). The peak for selenate was normal even at 2000 mg l<sup>-1</sup> SO<sub>4</sub><sup>2-</sup>. The high SO<sub>4</sub><sup>2-</sup> mass injected probably saturated the column and disturbed the column equilibrium such that the peaks following were distorted. The use of a diluter (weaker strength) eluent would probably reduce the peak distortion simply by allowing more time for stationary phase re-equilibration in between the peaks. These data show that the ions in question can be effectively quantitated in the presence of 1400 mg l<sup>-1</sup> and perhaps up to 2000 mg l<sup>-1</sup> SO<sub>4</sub><sup>2-</sup>. The increasing concentrations of SO<sub>4</sub><sup>2-</sup> reduced the apparent resolution between AsO<sub>4</sub><sup>3-</sup> and SeO<sub>4</sub><sup>2-</sup>. However, baseline separation (100% practical resolution) was achieved even at the highest SO<sub>4</sub><sup>2-</sup> level tested (Fig. 6). The interference due to high concentration of Cl<sup>-</sup> was not tested but it can be effectively removed by the use of cation-exchange resin in silver form [16].

#### REFERENCES

- 1 L. Fishbein, *Int. J. Environ. Anal. Chem.*, 17 (1984) 113.
- 2 H. Robberecht and R. van Grieken, *Talanta*, 29 (1982) 823.
- 3 R. J. Hall and P. L. Gupta, *Analyst (London)*, 94 (1969) 292.
- 4 A. B. Grant, *N. Z. J. Sci.*, 24 (1981) 65.
- 5 P. O'Neil, K. C. C. Bancroft, *Talanta*, 32 (1985) 69.
- 6 S. M. Workman and P. N. Soltanpour, *Soil Sci. Soc. Am. J.*, 44 (1980) 1331.
- 7 B. Pahlavanpour, M. Thompson and L. Thorne, *Analyst (London)*, 105 (1980) 756.

- 8 S. Xiao-quan, J. Long-Zhu and N. Zhe-ming, *At. Spectrosc.*, 3 (1982) 41.
- 9 W. Qian-Feng, L. Peng-Fel, *Talanta*, 30 (1983) 275.
- 10 W. A. Maher, *Analyst (London)*, 108 (1983) 939.
- 11 K. M. Holtzclaw, R. H. Neal, G. Sposito and S. J. Traina, *Soil Sci. Soc. Am. J.*, 51 (1987) 75.
- 12 T. Kamada, *Talanta*, 23 (1976) 835.
- 13 T. Kamada, T. Shiraishi and Y. Yamamoto, *Talanta*, 25 (1978) 15.
- 14 D. T. Gjerde, J. S. Fritz and G. Schmuckler, *J. Chromatogr.*, 186 (1979) 509.
- 15 P. R. Haddad, P. E. Jackson and A. L. Heckenberg, *J. Chromatogr.*, 346 (1985) 139.
- 16 U. Karlson and W. T. Frankenberger, Jr., *Anal. Chem.*, 58 (1986) 2704.
- 17 U. Karlson and W. T. Frankenberger, Jr., *J. Chromatogr.*, 386 (1986) 153.
- 18 H. C. Mehra and W. T. Frankenberger, Jr., *Soil. Sci. Soc. Am. J.*, 52 (1988) 1603.
- 19 H. Small, T. S. Stevens and W. C. Bauman, *Anal. Chem.*, 17 (1975) 1801.
- 20 R. J. Williams, *Anal. Chem.*, 55 (1983) 851.
- 21 M. Sadiq, T. H. Zaidi and A. A. Mian, *Water, Air Soil Pollut.*, 20 (1983) 369.
- 22 J. A. Oppenheimer, A. D. Eaton and P. H. Krefl, *Report EPA/600/2-84-190*, U.S. Environmental Protection Agency, Cincinnati, OH, 1984.
- 23 D. Chakraborti, D. C. Hillman, K. J. Irgolic and R. A. Zingoro, *J. Chromatogr.*, 249 (1982) 81.



## Separation of lanthanides and yttrium as anionic complexes by isocratic ion-interaction chromatography

ELAINE A. JONES\* and HESTER S. BEZUIDENHOUT

*Mintek, Private Bag X3015, Randburg 2125 (South Africa)*

and

JACOBUS F. VAN STADEN

*Department of Chemistry, University of Pretoria, Pretoria 0002 (South Africa)*

(First received February 22nd, 1990; revised manuscript received July 24th, 1990)

---

### ABSTRACT

Rare earth elements in nitric acid solution can be individually separated by ion-interaction chromatography. The separation is achieved by isocratic elution with oxalic acid as the complexing agent in the eluent and tetra-*n*-butylammonium hydroxide as the ion-pairing reagent. The separated rare earth elements are measured spectrophotometrically after post-column reaction with Arsenazo III, and can be determined at levels  $\geq 0.5$  mg/l with a relative standard deviation of 0.01% for the individual rare earth elements at the 10 mg/l level. The order of elution is from lanthanum to lutetium, yttrium being eluted immediately after terbium.

---

### INTRODUCTION

The determination of rare earth elements (REEs) is important in several industries such as in the nuclear power industry for the lanthanide fission products of irradiated fuels and in the mining industry for the determination of REEs in rock samples. The determination of REEs, particularly the individual members of the group, is a difficult and complex problem. Mintek has been involved for many years in the evaluation of analytical procedures, and in the development of sensitive and reliable methods such as the recently developed atomic emission spectrometric determination of REEs in minerals using a scanning monochromator system.

High-performance liquid chromatography (HPLC) followed by a post-column reaction was used for the separation and determination of REEs as early as 1972. In 1986, Cassidy *et al.* [1] and Barkley *et al.* [2] demonstrated that reversed-phase ion-interaction chromatography is a rapid and accurate method for the separation and determination of lanthanum in nuclear fuels and REEs in refining process streams. They employed a silica-based C<sub>18</sub> reversed-phase column with hydroxyisobutyric acid (HIBA) as the complexing agent and octanesulphonate (C<sub>8</sub>SO<sub>3</sub><sup>-</sup>) as the ion-pairing reagent.

Because REEs have a positively charged trivalent state, they exist in a strongly hydrated state in solution. Organic chelating agents can replace part of the water of

hydration, forming complexes that exhibit wide spreads between the formation constants. When complexes are formed with the positively charged trivalent REEs, the result is a net decrease in the charge of the REEs as the complex, with the largest decrease for the strongest complex [3]. The heavy REEs form strong complexes with a reduction in the positive charge. In ion-interaction chromatography, these complexes will be eluted first. Therefore, with HIBA and  $C_8SO_3^-$ , the order of elution was from lutetium to lanthanum. The separated REEs were measured spectrophotometrically after post-column reaction with Arsenazo III. A similar separation was achieved by Heberling *et al.* [3] with a pellicular latex-agglomerated resin-based ion exchanger, HIBA as the eluent and 4-(2-pyridylazo)resorcinol (PAR) as the chromogenic reagent in the post-column reaction. In this cation-exchange chromatographic separation, not only did the sensitivities of the lighter REEs, which were eluted last, decrease, but also these REEs were not completely resolved. In subsequent work that was based on the work of Cassidy *et al.* [1], the separation of the individual REEs, including the separation of yttrium from dysprosium, was achieved by ion-interaction chromatography [4]. The sensitivities for the REEs in that separation increased during the elution of lutetium to lanthanum, and the individual REEs were completely resolved.

When this order of elution is used to separate and determine trace amounts of REEs in the presence of large amounts of an individual REE, only the REEs heavier than the matrix REE can be separated and determined. All the REEs lighter than the matrix REE will be "swamped" by the relatively large amounts of the matrix REE. In order to separate and determine traces of REE on either side of an individual REE, the order of elution must be reversed, *i.e.*, lanthanum must be eluted first followed by the other REEs, with lutetium being eluted last. This can be achieved by the formation of anionic complexes of the REEs with suitable complexing agents such as citrates, tartrates and oxalates. Anionic complexes formed with the REEs and organic chelating agents exhibit a wide spread in the range of their formation constants. These anionic complexes of the individual REEs can be separated by anion exchange with an elution order from lanthanum to lutetium, a separation that was achieved by Heberling *et al.* [3] with a pellicular latex-agglomerated ion exchanger and gradient elution, using an eluent consisting of various amounts of oxalic and diglycolic acids. However, Heberling *et al.* did not achieve the resolution between ytterbium and lutetium. In addition, the sensitivity for the REEs increased from the minimum for the first REE eluted, lanthanum, to a maximum for dysprosium before decreasing again for ytterbium.

The investigation described in this paper concentrated on the possible use of a silica-based  $C_{18}$  reversed-phase column for the anionic separation of individual REEs by ion-interaction chromatography with an elution order from lanthanum to lutetium so that better sensitivity could be obtained than that achieved by other investigations. Complete resolution between the fourteen individual REEs plus yttrium was also investigated.

## EXPERIMENTAL

### *Apparatus and reagents*

The chromatograph, which was assembled from Spectra-Physics components,

consisted of a pump (SP 8700 XR extended-range LC pump) and an injector fitted with a 50- $\mu$ l sample loop. A photometric detector (SP 8773 XR) was fitted between the column and the computing integrator and was set at a wavelength of 658 nm and an absorbance range of 0.080. The chart speed and attenuation of the computing integrator (SP 4200) were set at 2.5 mm and 32, respectively. The column was a Supelcosil LC-18 (150  $\times$  4.6 mm I.D., 5- $\mu$ m particle size). An in-line filter containing a carbon-frit filter (0.5  $\mu$ m) was placed immediately in front of the column to protect the column from particulate matter. The post-column reactor (PCR) was a modification of that used by Cassidy *et al.* [1]. It was made by the insertion of square-cut Teflon tubing (0.5 and 1.5 mm I.D. and O.D., respectively) into a bored-out Omnifit Teflon tee. A small plug of glass-wool was placed between the eluent inlet tube and the outlet tube to the detector. The PCR reagent reservoir was under a constant helium pressure, and this pressure forced the PCR reagent solution (Arsenazo III) into the PCR. The pressure was maintained with a regulator of 0–2 bar. The PCR solution passed along the outside of the eluent inlet tube, and then entered and mixed with the eluent within the plug of glass-wool. After mixing, the resulting solution flowed into the outlet tube to the detector.

All the solutions were prepared using freshly distilled water, and all the reagents were of analytical-reagent grade. Stock solutions (1 g/l) of the individual REEs were prepared by dissolution of their respective Specpure oxides. The oxides were ignited at 950°C for 3 h and then cooled in a desiccator. The appropriate amount of each oxide was dissolved in nitric acid (1:1). The dissolution of cerium was completed by the addition of small amounts of sulphuric acid and hydrogen peroxide during the reaction. The acid concentration after the dissolution was controlled so that the concentration of nitric acid in each stock solution was 1%. Standard solutions of REEs in the concentration range 1–10 mg/l, either as the REE group or as the cerium and yttrium subgroups, were prepared by suitable dilution and mixing of the stock solutions.

The complexing reagent was oxalic acid. The ion-interaction reagent was a 0.1 *M* solution of tetra-*n*-butylammonium hydroxide (TBAOH), obtained from Merck (Darmstadt, F.R.G.). An aqueous solution containing the appropriate concentrations of oxalic acid and TBAOH was prepared, and the pH of the solution was adjusted to 4.6 with ammonia solution. The solution was then filtered through a Millipore Type HA filter with a pore size of 0.45  $\mu$ m. After filtration, the pH value was checked and adjusted if necessary.

The post-column reagent was Arsenazo III ( $1.5 \cdot 10^{-4}$  *M* solution in 1 *M* acetic acid), obtained from Fluka (Buchs, Switzerland). The reagent solution was also filtered through a 0.45- $\mu$ m filter.

#### *Chromatographic procedure*

Flow-rates of 1.0 ml/min were selected for both the eluent and the Arsenazo III solutions, and the Supelcosil LC-18 column was equilibrated with an aqueous solution containing the required concentration of oxalic acid and TBAOH at pH 4.6 until a stable baseline was obtained. The sample was injected, and the individual REEs were separated by isocratic elution. The eluted REEs were monitored at 658 nm after they had undergone post-column reaction with Arsenazo III. A range of calibration standards for the required concentration levels were analysed, and calibration graphs

of peak height *versus* concentration were prepared for each of the separated REEs. The REEs in the sample were identified by their retention times, and their peak heights were compared with the calibration graphs. A detailed description of the procedure can be obtained from the authors.

## RESULTS AND DISCUSSION

From preliminary work with citric, tartaric and oxalic acids, it appeared that oxalic acid was the most suitable complexing agent for the formation of anionic complexes with the REEs.

The concentration and the stability of an aqueous solution of Arsenazo III in 1 *M* acetic acid that was required for post-column reaction with the REEs was established in earlier work [4], and these conditions were used in this investigation. As stated previously [4], careful control of the purity of the reagents and eluents was found to be necessary to ensure good chromatograms and to reduce baseline noise to a minimum. To eliminate degradation of the column performance by bacterial action, all the water used was freshly distilled and reagents were freshly prepared and filtered through 0.45- $\mu\text{m}$  carbon frit filters. In addition, an in-line filter containing a carbon frit (0.5  $\mu\text{m}$ ) was placed immediately before the column.

### *Separation by isocratic elution*

In this investigation, the univariant method of optimization was used, each variable being optimized while the others were kept constant.

The concentrations of oxalic acid and the ion-interaction agent, TBAOH, in the eluent were varied until the amounts required for the separation of the individual REEs were found. Eluents containing small amounts of oxalic acid resulted in an incomplete formation of the anionic complexes, whereas eluents of relatively concentrated oxalic acid solutions reduced the retention times of the individual anionic complexes of the REEs. In both instances the REEs were not completely separated. The optimum concentration for both the oxalic acid and the TBAOH for the separation of the fourteen REEs was found to be 0.002 *M* (Fig. 1).

The pH of the eluent was varied between 3.5 and 6.0. The peak heights of the REEs were not affected by the pH of the eluent in this range and a pH value of 4.6 was chosen for further work.

Yttrium, which accompanies the REEs, is eluted under these conditions with the same retention time as terbium. It was found that concentrations of 0.0005 and 0.0025 *M* for oxalic acid and TBAOH, respectively, increased the retention times of all the REEs sufficiently to allow the determination of both yttrium and terbium. The time for elution of the REEs increased and the peaks became broader but, when an integrator was used to obtain either the peak height or the peak area for REE determination, the accuracy was not affected. Small variations in the concentration of TBAOH are critical in the separation of terbium and yttrium, and the required concentration for this separation must be strictly controlled. Fig. 2 shows the chromatogram obtained.

During the optimization of the physical parameters, maximum peak heights for all the REEs were obtained with flow-rates of 1.0 ml/min for both the eluent containing oxalic acid and TBAOH and the reagent solution of Arsenazo III (using a sample size of 100  $\mu\text{l}$ ).

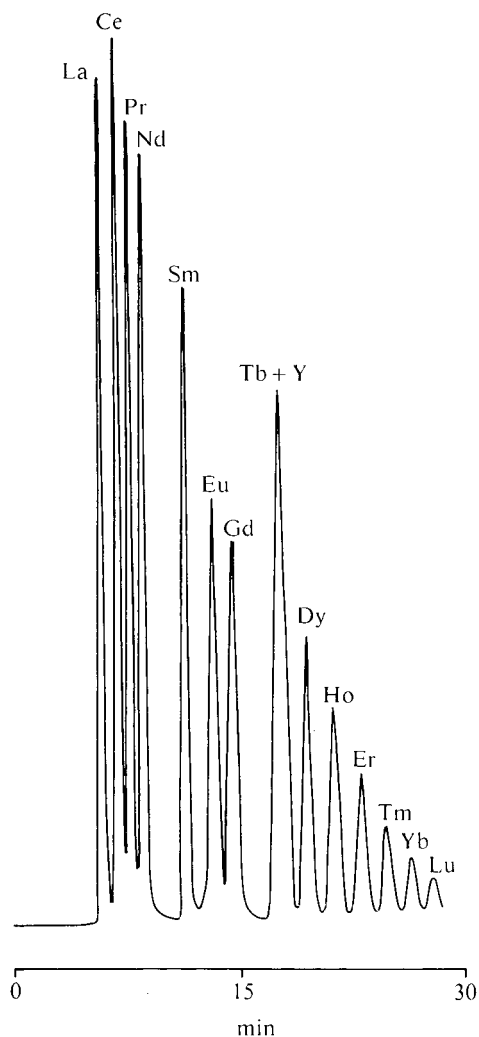


Fig. 1. Chromatogram showing the separation of the REEs. Conditions: oxalic acid, 0.002 *M*; pairing reagent, 0.002 *M* TBAOH; flow-rate of eluent and post-column reagent, 1 ml/min; pH of eluent, 4.6; sample volume, 50  $\mu$ l; concentration of individual REEs, 10 mg/l; post-column reagent,  $1.5 \cdot 10^{-4}$  *M* Arsenazo III plus 1 *M* acetic acid; spectrophotometer wavelength, 658 nm.

#### *Order of elution*

“Dynamic” ion exchangers are formed when hydrophobic ions (TBAOH), which are present in the mobile phase, are adsorbed on the hydrophobic surface of a reversed-phase column to produce a charged layer at the surface, where ion exchange can occur. The smallest ions, *i.e.*, the last and heaviest REEs in the series, form the strongest and most negatively charged complexes with oxalic acid. Therefore, when the REEs are separated by anion exchange, the elution order is from lanthanum to lutetium.

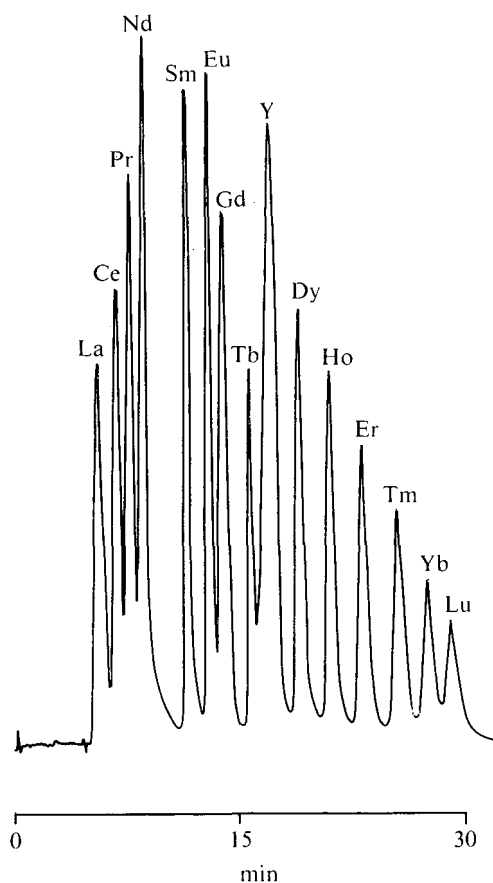


Fig. 2. Chromatogram showing the separation of yttrium from terbium. Conditions: oxalic acid, 0.0005 *M*; pairing reagent, 0.0025 *M* TBAOH; other conditions as in Fig. 1.

The separation of the REEs with this elution order from lanthanum to lutetium is applicable to the determination of trace amounts of REE impurities in a purified REE. The REEs lighter than the purified REE, particularly those adjacent to the individual purified REE, can be detected, identified and quantified. However, the REEs heavier than the individual purified REE could not be determined.

### *Interferences*

Arsenazo III is specific for REEs, uranium and thorium [1]. Any transition metals that are present are not complexed by Arsenazo III under the conditions of the separation. As a result, they are eluted with, or just after, the void peak (about 2 min after injection) and do not interfere with the separation and determination of the REEs.

As most of the samples were in the form of dilute nitric acid solutions and traces of sulphuric acid were present in the standards from the dissolution of cerium, the effects of both nitric and sulphuric acids on the separation were investigated. It was

found that, as the acid concentrations increased, the retention times and the peak heights of the REEs decreased (Fig. 3). Solution of the REEs containing more than 0.05% acid resulted in a lack of resolution between the individual REEs and a reduction in their retention times. When the REE solutions containing 0.09 *M* sulphuric acid were neutralized with sodium hydroxide to pH 6, the retention times and peak heights of the REEs were not affected. Hence the acidity of the sample altered the formation constants of the anionic complexes and influenced the degree of complexation of the REEs. The acid anion had no effect on the separation at this level. To determine the possible effect of the acid anion at higher sulphate molarities, sodium sulphate was added to the REE solutions in the range 0.09–0.35 *M* with respect to the sulphate ion. Above 0.09 *M* of sulphate ion the peak heights decreased, whilst the retention times remained the same, indicating that above this level the sulphate anion acted as a competing ion causing displacement of the anionic complexes of REEs from the cationic sites of the ion-interaction reagent. Therefore, for optimum separation of the REEs the acidity and the acid anions must be controlled.

The small amounts of different hydroxides (lithium and sodium) and ammonia solution that were used for the adjustment of the pH of the eluent to the required level

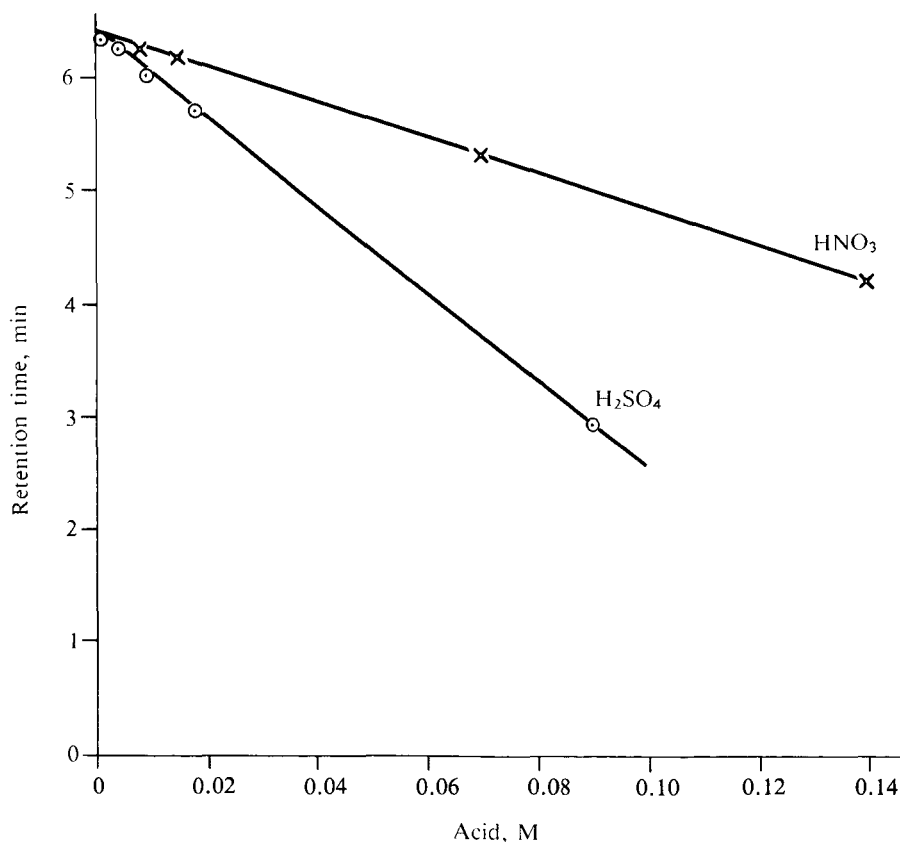


Fig. 3. Effect of acids on retention times. Conditions as in Fig. 1.

had no effect on the retention times or the peak heights. However, when large amounts of alkaline earth elements were present, the peaks obtained were broad, and there was a reduction in both the retention times and the resolution, indicating the effect of the reaction of alkaline earth cations with oxalate on the REE separation.

#### *Sensitivity, precision and accuracy*

The exact value of the detection limit of the REEs depends on the individual REEs, flow-rates of eluent and reagent, sample size and attenuation used. Any of these factors can be varied so that a particular analysis can be optimized. In the chromatograms for the separation of the REEs excluding yttrium (Fig. 1) and the separation of terbium from yttrium (Fig. 2), the attenuation remained constant throughout the elution of the REEs and the increasing insensitivity in the detection of the heavier REEs (terbium, dysprosium, holmium, erbium, thulium, ytterbium and lutetium) is shown by the decreasing peak heights for these particular REEs. However, when the attenuation of the integrator was reduced between the elution of dysprosium and holmium, the sensitivity of the heavier REEs was increased. This increase in sensitivity depended on the attenuation that was used. Other factors that can affect the sensitivity are the background noise from pump pulsations and the purity of both oxalic acid and Arsenazo III. When necessary, the oxalic acid can be recrystallized. As stated previously, an important parameter is the quality of the water used in the preparation of the eluent and the reagent.

With careful control of the above factors individual REEs can be detected at a level of 0.01 mg/l with a limit of determination of 0.5 mg/l and higher. Table I gives the precision of the chromatographic separation and the subsequent detection with Arsenazo III at 658 nm.

TABLE I  
PRECISION OF THE METHOD

Conditions as in Fig. 2.

Element	Relative standard deviation ( $n=10$ )	
	10 mg/l REE	1 mg/l REE
La	0.0120	0.0816
Ce	0.0104	0.0698
Pr	0.0108	0.0509
Nd	0.0126	0.0549
Sm	0.0050	0.0628
Eu	0.0156	0.0333
Gd	0.0176	0.0634
Tb	0.0136	0.0513
Dy	0.0167	0.0478
Ho	0.0138	0.0523
Er	0.0184	0.0369
Tm	0.0174	0.0532
Yb	0.0165	0.0610
Lu	0.0120	0.0447
Y	0.0108	0.0654



TABLE II  
COMPARATIVE DETERMINATIONS OF REE IN NITRIC ACID

All results are expressed as mg/l.

Element	Sample								
	FH 7701			FH 7702			FH 7703		
	C <sub>1</sub> <sup>a</sup>	C <sub>2</sub> <sup>a</sup>	AES <sup>b</sup>	C <sub>1</sub> <sup>a</sup>	C <sub>2</sub> <sup>a</sup>	AES <sup>b</sup>	C <sub>1</sub> <sup>a</sup>	C <sub>2</sub> <sup>a</sup>	AES <sup>b</sup>
La	<1	<0.5	<1	1.0	1.2	1.1	1.9	1.65	1.6
Ce	3190	3110	3270	975	951	1010	88	92	90
Nd	2.4	2.3	2.1	12	10	9.5	12	13	11
Sm	1.2	1.0	0.9	4.2	4.0	4.7	5.1	5.0	4.5
Eu	<1	<0.5	0.20	<1	0.6	0.79	1.4	1.3	1.1
Gd	<1	<0.5	<1	2.0	2.1	1.8	3.2	3.0	3.5

<sup>a</sup> C<sub>1</sub> and C<sub>2</sub> = chromatography.

<sup>b</sup> AES = atomic emission spectrometry.

TABLE III  
COMPARATIVE DETERMINATIONS OF REE IN MINTEK REFERENCE MATERIALS

All results are expressed in mg/kg unless stated otherwise.

Element	Sample									
	66/69		50/71		30/70		18/69		49/71	
	C <sup>a</sup>	AES <sup>b</sup>	C <sup>a</sup>	AES <sup>b</sup>	C <sup>a</sup>	AES <sup>b</sup>	C <sup>a</sup>	AES <sup>b</sup>	C <sup>a</sup>	AES <sup>b</sup>
Y	n.a. <sup>c</sup>	1.38%	n.a.	0.67	n.a.	0.24%	n.a.	184	n.a.	39
La	9.90%	7.82%	3.72%	3.44%	1.38%	1.22%	0.31%	0.22%	495	515
Ce	16.06	16.2%	6.40%	7.09%	2.66%	2.54%	0.42%	0.37%	795	856
Pr	1.53%	1.62%	0.80%	0.77%	0.38%	0.27%	450	436	98	84
Nd	7.4%	6.52%	3.12%	2.97%	1.30%	1.11%	0.12%	0.11%	275	235
Sm	0.95%	1.02%	0.42%	0.38%	0.14%	0.16%	157	168	42	39
Eu	230	222	110	94	32	36	45	42	8	10
Gd	0.78%	0.82%	0.30%	0.32%	0.10%	0.13%	99	113	25	23
Tb	n.a.	702	n.a.	321	n.a.	146	n.a.	12	n.a.	4
Dy	0.30%	0.34%	0.14%	0.17%	702	686	35	51	n.d. <sup>d</sup>	10
Ho	423	445	240	244	72	78	n.d.	5	n.d.	3
Er	895	975	570	633	160	178	n.d.	9	n.d.	4
Tm	140	162	85	94	50	54	n.d.	3	n.d.	2
Yb	385	396	160	182	64	62	n.d.	9	n.d.	2
Lu	44	48	n.d.	11	n.d.	8	n.d.	1	n.d.	2

<sup>a</sup> C = chromatography.

<sup>b</sup> AES = atomic emission spectrometry.

<sup>c</sup> n.a. = Not analysed by chromatography.

<sup>d</sup> n.d. = Not detected.

The accuracy of the chromatographic separation and the subsequent determination of the individual REEs after post-column reaction with Arsenazo III was ascertained by a comparison of the results obtained by chromatography with those obtained by atomic emission spectrometry (AES). The samples included diluted nitric acid solutions obtained during the purification of individual REEs (Table II) and Mintek REE reference materials (Table III). The agreement between the two methods was generally good. However, lanthanum in sample 66/69 and some of the results in the milligrams per kilogram range in the other reference materials, such as erbium and thulium, were more scattered.

#### ACKNOWLEDGEMENT

This paper is published by permission of Mintek.

#### REFERENCES

- 1 R. M. Cassidy, S. Elchuk, N. L. Elliot, L. W. Green, C. H. Knight and B. M. Recoskie, *Anal. Chem.*, 58 (1986) 1181.
- 2 D. J. Barkley, M. Blanchette, R. M. Cassidy and S. Elchuk, *Anal. Chem.*, 58 (1986) 2222.
- 3 S. S. Heberling, J. M. Riviello, M. Shifen and A. W. Ip, *Res. Dev.*, 29 (1987) 74.
- 4 E. A. Jones and M. J. Hemmings, *S. Afr. J. Chem.*, 43 (1990) 51.

## **Preseparation of uranium by reversed-phase partition chromatography**

### **Application to the determination of trace elements in nuclear-grade uranium compounds by inductively coupled plasma atomic emission spectrometry**

ASSAD S. AL-AMMAR\*, H. A. HAMID, B. H. RASHID and H. M. BASHEER

*Chemistry Department, Nuclear Research Centre, Iraqi Atomic Energy Commission, P.O. Box 765, Baghdad (Iraq)*

(First received March 9th, 1990; revised manuscript received May 15th, 1990)

---

#### ABSTRACT

The chromatographic behaviour of a tri-*n*-butyl phosphate (TBP)-impregnated macroporous Amberlite XAD-4 column was investigated for the separation of uranium from impurity elements in nuclear-grade uranium compounds prior to analysis by inductively coupled plasma atomic emission spectrometry (ICP-AES). The parameters affecting separation with this column were optimized. The proposed separation method proved to be rapid and efficient. High recovery factors for all the impurity elements were obtained. The procedure is suitable for routine application to the determination of the impurity elements Mo, Zr, Cd, Co, Ni, Ba, B, Mg, Mn, Fe, Cr, Al, V, Be, Cu, Ti, Se, Zr, Sr, Ca and As.

---

#### INTRODUCTION

Nuclear-grade uranium compounds, such as yellow cake and UO<sub>2</sub> powder, must have certain specifications in order to be suitable for the industrial production of nuclear reactor fuel.

The determination of impurity elements in uranium compounds represents a major part of the quality control programme used to determine the chemical specifications. The impurity elements contents are responsible for corrosion of the nuclear fuel and some act as nuclear poisons, as they have high neutron cross-sections.

Several techniques have been used to determine impurity elements, including spectrochemical analysis [1], atomic absorption spectrometry and inductively coupled plasma atomic emission spectrometry (ICP-AES) [2,3]. The last technique is very convenient owing to its high sensitivity, reproducibility, wide dynamic range, relative freedom from matrix interferences and multi-element measurement capability. However, if ICP-AES is to be used, the uranium must be separated prior to the determination of the impurities because the dense uranium spectrum will severely interfere with

the spectral lines of the analytes. Therefore, several workers have used liquid–liquid extraction methods to separate uranium from the impurities [4–7].

Recently, ion-exchange chromatography [8] and reversed-phase partition chromatography (RPPC) [9] were introduced to separate the impurities from uranium prior to their determination. The RPPC method has nearly the same precision and recovery factors as the liquid–liquid extraction method. However, the RPPC method has the advantages that it is faster and requires less manipulation as the number of samples become large.

One of the most successful applications of the RPPC method is that by Pan and Wang [9]; they determined 40 trace elements in uranium compounds simultaneously by end-on viewed ICP-AES after separation from uranium by RPPC using tris(2-ethylhexyl) phosphate as a uranium extractant supported on Kel-F (polychlorotrifluoroethylene). In the end-on viewed method, the plasma flame is bent from its vertical position so that the spectrometer slit will receive a higher intensity from the emitted spectrum, which increases the sensitivity. However, the method is not suitable for routine use because of the complicated arrangement required. Accordingly, the aim of this work was to modify the experimental design of the method developed by Pan and Wang [9] to make it applicable on a routine basis to the determination of the impurity elements in uranium compounds.

The modification required the use of another type of extractant–support combination, such that the resulting separation column would have a higher capacity for uranium extraction. Therefore, a larger amount of sample could be used to obtain a final solution containing higher concentrations of impurity elements, so that it could be analysed by a normal ICP-AES technique. Accordingly, it was decided to investigate the use of tri-*n*-butyl phosphate (TBP) as a uranium extractant, supported on the macroporous styrene–divinylbenzene polymer Amberlite XAD-4.

The reasons are that TBP is the most commonly used extractant for the purification of uranium on an industrial scale, extracting uranium selectively into the organic phase and leaving the impurities totally in the aqueous phase. TBP is also very stable in highly acidic media where the extraction of uranium usually takes place. Amberlite XAD-4 is often used as a support for different extractants for the separation and preconcentration of trace metal ions by reversed-phase adsorption chromatography [10] and has been used as a support for TBP for the separation of some fission products [11,12] using RPPC. It is used as a support because of its high surface area [750 m<sup>2</sup>/g, according to the manufacturer's data (Aldrich)], and high affinity for organic extractants; this allows it to absorb strongly more than its own weight of the organic extractant. Accordingly, the prepared column will have high efficiency and a long life.

## EXPERIMENTAL

### *Instrumentation and operating parameters*

A Hilger Model E974 MK.1 Polyvac direct-reading spectrometer with a Hilger 2.5-kW ICP lightsource equipped with a Meinhard Model TR-30 concentric glass nebulizer was used. The argon flow-rates were 11, 0.8 and 0.4 l min<sup>-1</sup> for the plasma, auxiliary and nebulizer, respectively.

A Hilger E92B argon humidifier was used. The incident power was 1.7 kW for

the extraction method and 1.25 kW for the RPPC method.

The nebulizer pressure was 35 p.s.i.g. The observation height was 16 mm above the induction coil. The emission intensity was integrated for 15 s.

The following analytical lines were used: Mo 2020.3, Ti 3372.8, Ni 2316.0, Zr 3438.2, Ba 2335.3, Se 1960.3, B 2497.7, Bi<sup>a</sup> 2230.1, Sc<sup>b</sup> 2552.3, Zn 2138.6, Fe 2599.4, Be 3130.4, Mn 2576.1, Cd 2266.0, Mg 2795.5, Co 2286.2, Cr 2835.6, As 1972.6, Al 3082.2, Sr 4077.7, V 3110.7, Ca 3968.5 and Cu 3247.5 Å.

### *Reagents*

Amberlite XAD-4 was purchased from Aldrich with 20–50 mesh size, average particle size 0.5 mm and surface area 750 m<sup>2</sup>/g. It was washed with 10% (v/v) hydrochloric acid in methanol, water, methanol, dichloromethane and finally diethyl ether, then dried overnight at 80–90°C under 1.0–0.5 mmHg pressure.

TBP was purified [13] by equilibration with 5% sodium carbonate solution. High-purity acids and deionized water were used throughout. The argon used was of 99.999% nominal purity. All other reagents were of analytical-reagent grade. Standard solutions were prepared from Merck Titrisol standards.

### *Preparation of the separation column*

A 10-g amount of the washed Amberlite XAD-4 was impregnated with 12 g of TBP by adding the TBP dropwise and with continuous mixing to ensure its uniform distribution over the XAD-4. The mixture was allowed to stand for at least 2 h to ensure good diffusion of the TBP inside the polymeric material. The loading of TBP on XAD-4 was 120% (w/w).

The slurry packing technique was adopted for packing the impregnated Amberlite XAD-4 inside a PTFE column (50 cm × 0.8 cm I.D.). The column was conditioned before use with 10 ml of 4 M nitric acid<sup>c</sup> at a flow-rate of 2 ml/min.

### *Sample treatment*

A sample of uranium oxide or yellow cake containing 1.25 g of uranium was dissolved by heating it gently with 5 ml of 8 M nitric acid. After complete dissolution, 5 ml of water were added and the resulting solution was transferred to the column for uranium separation. The separation was performed at a flow-rate of 0.5 ml/min. The column was then washed with about 12 ml of 4 M nitric acid at a flow-rate of 1.5 ml/min. The wash solution was combined with the sample solution in a 25-ml volumetric flask. A 1-ml volume of a solution containing 500 ppm of scandium and 500 ppm of bismuth (internal standards) was added and the mixture was diluted to volume with 4 M nitric acid.

The sample solution was analysed for impurity elements by measuring it together with standard solutions by ICP-AES. The concentrations of the analytes in the

---

<sup>a</sup> Bi was used as internal standard for the elements Mo, Ba, Al, Cu, Ca, Se, Zn, Cd, As and Sr.

<sup>b</sup> Sc was used as internal standard for the elements Fe, Co, Cr, Ni, V, Ti, Zr, Mg, Be, Mn and B.

<sup>c</sup> The solutions used for column conditioning, washing, regeneration and sample dissolution must be previously saturated with TBP to minimize the loss of TBP from the impregnated Amberlite XAD-4, thus extending the life of the column.

sample were obtained by using the standard curves, which were constructed from the measurements of the standard solutions by ICP-AES. The standard solutions were prepared by mixing the required volumes of stock standard solutions of the elements to be determined and making the final solution 4 M in nitric acid. The final standard solutions contained scandium and bismuth as internal standards. The results of the measurements were corrected using recovery factors previously determined as described in the next section. The concentrations of the impurity elements in the standard solution were taken in accordance with the specifications for nuclear-grade UO<sub>2</sub> powder and nuclear-grade uranium ore concentrate [14,15].

#### *Determination of impurity element recovery factors*

The recovery factors were measured by preparing a standard solution containing 300 µg of each analyte and 1.25 g of uranium per 10 ml of the solution (except for B and Cd, for which the solution contained 2 µg of B and 2 µg of Cd per 10 ml; this solution is a simulation of a solution obtained by dissolving UO<sub>2</sub> powder containing the maximum allowable concentrations of the impurity elements according to the specifications for nuclear-grade UO<sub>2</sub> powder [14]. This standard solution is 4 M in nitric acid. A 10-ml portion of this solution was passed through the column to separate uranium from the impurity elements. The concentrations of the impurity elements in the resulting solution were determined using the same procedure as used for the sample.

#### *Column regeneration*

The used column was freed from absorbed uranium by passing 30 ml of 30% (w/w) ammonium acetate solution through the column at a flow-rate of 1 ml/min, followed by washing with 10 ml of water at a flow-rate of 2 ml/min. The TBP-impregnated Amberlite XAD-4 of the column was stored in water for further use.

## RESULTS AND DISCUSSION

The chromatographic behaviour of uranium on a column prepared as described above was examined quantitatively by separating the uranium from 10 ml of 4 M nitric acid containing 1.25 g of uranium. It was found that the yellow uranium band occupies about one third of the total length of the TPB-impregnated XAD-4 column charge. This band spread to two thirds of the column when washed with 12 ml of 4 M nitric acid.

The eluate was collected and analysed for uranium. The uranium concentration in the eluate was found to be 4 ppm for a freshly prepared column and 4–10 ppm for a regenerated column. This low concentration of uranium will not interfere with the determination of the impurity elements.

The validity of the proposed method with respect to the accuracy, precision and recovery was tested by applying it together with the liquid-liquid extraction method [16], involving extraction of the impurity elements from a 6 M nitric acid solution with 30% (v/v) TBP in carbon tetrachloride, to the analysis of a synthetic standard solution containing the impurity elements and uranium. The accuracy of the proposed method can therefore be determined by comparing the results obtained by the two methods, given in Table I. The agreement between the results obtained indicates

TABLE I

COMPARISON OF LIQUID-LIQUID EXTRACTION AND RPPC METHODS FOR THE DETERMINATION OF IMPURITY ELEMENTS IN A SYNTHETIC URANIUM SOLUTION

Element	Concentration present (ppm)	Concentration determined (ppm)	
		Extraction method <sup>a</sup>	RPPC method <sup>a</sup>
Mo	10	9.5	9.7
Zn	5	5.2	4.9
Cd	2	1.8	1.9
Co	5	4.8	4.7
Ni	10	9.7	10.1
Ba	5	4.9	4.9
B	5	5.2	4.9
Mg	5	4.8	5.0
Mn	5	5.1	4.9
Fe	10	9.8	9.8
Cr	2.5	2.3	2.6
Al	5	5.1	5.0
V	2	2.1	2.1
Be	2	1.8	2.0
Cu	10	9.8	10.1
Ti	5	4.9	4.8
Se	10	9.8	9.7
Zr	2	1.7	1.9
Sr	2	1.8	1.8
Ca	5	5.1	4.9
As	10	9.7	9.7

<sup>a</sup> Average values of two determinations.

the applicability of the proposed method to the determination of impurity elements in nuclear-grade uranium compounds.

Table II shows a comparison between the proposed method and the liquid-liquid extraction method [16] with respect to recovery and precision. The recovery was determined using the procedure given above for recovery factors.

The good recovery and high precision of the present method support its use for the proposed application. The detection limits for the elements determined are given in Table III, and are well below the specification values for impurities in nuclear-grade UO<sub>2</sub> powder [14].

It should be mentioned that the factors taken into consideration in preparing the TBP-impregnated XAD-4 separation column and those in performing the separation process were selected by optimizing the TBP loading, particle size, amount of TBP-impregnated Amberlite XAD-4 and solution composition.

Regarding TBP loading, when separating uranium from impurities it is very important to have a column with the highest possible capacity for uranium extraction in order to make the separation process practical, which can be achieved by using a column with the highest possible percentage loading of the extractant on the support. TBP loadings from 70% to 190% were investigated and it was found that the efficiency of the column for uranium extraction increases linearly with loading. However

TABLE II

COMPARISON OF RECOVERY FACTORS DETERMINED BY RPPC AND LIQUID-LIQUID EXTRACTION METHODS AND OF RELATIVE STANDARD DEVIATIONS

	Recovery factor (%)		Precision as relative standard deviation (%) <sup>a</sup>	
	Extraction method	RPPC method	Extraction method	RPPC method
Mo <sup>6+</sup>	93	91	6	5
Zn <sup>2+</sup>	98	97	3	4
Mg <sup>2+</sup>	99	100	3	3
Mn <sup>2+</sup>	97	98	4	3
Fe <sup>3+</sup>	100	99	3	2
B <sup>3+</sup>	98	97	3	2
Ni <sup>2+</sup>	99	97	5	4
Cd <sup>2+</sup>	96	95	4	3
Co <sup>2+</sup>	99	100	5	6
Ba <sup>2+</sup>	98	99	4	2
Cr <sup>3+</sup>	92	90	5	3
Al <sup>3+</sup>	99	100	4	4
V <sup>4+</sup>	100	99	3	2
Be <sup>2+</sup>	98	99	4	3
Cu <sup>2+</sup>	99	98	3	3
Ti <sup>4+</sup>	96	97	3	2
Zr <sup>4+</sup>	74	70	5	3
As <sup>5+</sup>	98	95	5	4
Se <sup>4+</sup>	94	95	6	4
Sr <sup>2+</sup>	99	97	5	3
Ca <sup>2+</sup>	97	98	4	3

<sup>a</sup>  $n = 5$ .

at loadings higher than 120% the impregnated particles were exceedingly hydrophobic and badly agglomerated, causing poor column packing. This type of agglomeration at high TBP loadings was attributed to the presence of the extractant on the outer surface of the beads [11,17]. Therefore, it was decided to use a column with a 120% TBP loading as the optimum choice.

Regarding particle size, it is well known that a better column performance is generally achieved as the particle size decreases. We investigated the performance of 150–200-mesh Amberlite XAD-4, obtained from the purchased 20–50-mesh material by mechanical crushing followed by sieving. It was found that the separation process using columns prepared as described earlier could not achieve a practical flow-rate (*i.e.*, 0.5 ml/min) without the aid of a pumping mechanism that delivers a pressure higher than atmospheric. However, to simplify the proposed method, this pumping mechanism should be avoided and the separation should be performed by gravity-induced flow under atmospheric pressure. Hence the Amberlite used should have a mesh size smaller than 150. Nevertheless, the column used in this work contained the purchased well defined, nearly round 20–50-mesh Amberlite XAD-4 and no investigation of the performance of a column loaded with 50–150-mesh material was made. It is believed that no improvement in column performance would be achieved as the 50–150-mesh Amberlite has fractured particles due to the mechanical crushing and



TABLE III

DETECTION LIMITS FOR IMPURITY ELEMENTS DETERMINED BY RPPC SEPARATION WITH TBP-IMPREGNATED AMBERLITE XAD-4 FOLLOWED BY ICP-AES MEASUREMENT

Element	Detection limit ( $\mu\text{g/g U}$ )	Element	Detection limit ( $\mu\text{g/g U}$ )
Mo	1.3	Al	3.2
Zn	0.16	V	0.8
Cd	0.11	Be	2.4
Co	0.61	Cu	0.4
Ni	0.57	Ti	0.51
Ba	0.63	Se	4.1
B	0.13	Zr	0.58
Mg	0.02	Sr	0.05
Mn	0.12	Ca	0.12
Fe	0.36	As	4.3
Cr	0.55		

therefore the prepared column will have an irregular packing and irregular flow (channelling). This is supported by the work Louis and of Duyckaerts [11], who investigated the performance of a TBP-impregnated Amberlite XAD-4 column for the separation of americium(111). They found that the experimental results, when used to calculate the  $A$  term in the Van Deemter equation give values that are within a factor of 11–25 of the particle size of the Amberlite used. They attributed this discrepancy to the use of fractured particles obtained by the mechanical crushing of 20–50-mesh XAD-4.

The amount of TBP-impregnated Amberlite XAD-4 used was chosen as a compromise between the following effects: the efficiency of the separation of uranium from impurities increases with increasing amount of packing, and the time required for washing and column regeneration increases with increasing amount of packing.

It was found that the repeated use of the same TBP-impregnated Amberlite XAD-4 column for uranium separation led to a gradual loss of absorbed TBP and a consequent decrease in column capacity. To prevent this effect, throughout the separation procedure solutions that had been previously saturated with TBP were used. This was found to extend the life of the column to more than 80 separations.

It is worth-mentioning that the acidity of solutions passed through the column was chosen according to previous studies by Hamlin *et al.* [18] and Walker and Vita [19].

## CONCLUSION

Reversed-phase partition chromatography with TBP-impregnated macroporous Amberlite XAD-4 column was found, after optimizing the parameters affecting the separation process, to be rapid and highly efficient for the separation of uranium from impurity elements prior to analysis by ICP-AES. The overall method is accurate, precise, free from interferences from the uranium matrix and could be applied on a routine basis to determine impurity elements in nuclear-grade uranium compounds.

## REFERENCES

- 1 *1988 Annual Book of ASTM Standards*, Vol. 12.01, Nuclear Energy (1), American Society for Testing and Materials, Philadelphia, PA, 1988, method ASTM C 696.
- 2 P. M. Santoliquido, *J. Res. Natl. Bur. Stand.*, (1988) 452.
- 3 K. Kato, *At. Spectrosc.*, 7 (1986) 129.
- 4 M. A. Floyd and R. W. Morrow, *Spectrochim. Acta, Part B*, 38 (1983) 303.
- 5 T. J. Seshagiri and Y. Babu, *Talanta*, 31 (1984) 773.
- 6 R. Ko, *Appl. Spectrosc.*, 38 (1984) 909.
- 7 H. J. Wachtendonk and R. Baurmann, *ICP Inf. Newsl.*, 10 (1984) 277, Abstract No. 111.
- 8 P. Burba and P. G. Willmer *Fresenius' Z. Anal. Chem.*, 323 (1986) 811.
- 9 F. Pan and X. Wang, *Fenxi Huaxue*, 15 (1987) 322.
- 10 J. N. King, *Report No. IS-T-1198*, Ames Laboratory, Ames, IA, 1986.
- 11 R. E. Louis and G. Duyckaerts, *J. Radioanal. Nucl. Chem.*, 81 (1984) 305.
- 12 R. E. Louis and G. Duyckaerts, *J. Radioanal. Nucl. Chem.*, 90 (1985) 105.
- 13 Z. Marzenko, *Separation and Spectrophotometric Determination of Elements*, Ellis Horwood, Chichester, 2nd ed., 1987, p. 611.
- 14 *1988 Annual Book of ASTM Standards*, Vol. 12.01, Nuclear Energy (1), American Society for Testing and Materials, Philadelphia, PA, 1988, method ASTM C 753-81, p. 194.
- 15 *1988 Annual Book of ASTM Standards*, Volume 1201, Nuclear Energy (1), American Society for Testing and Materials, Philadelphia, PA, 1988, method ASTM C 967-87, p. 396.
- 16 G. P. Larson and R. E. Slagle, *Report, Y/DK-357*, Contribution to ASTM C-26-05 Task Group (1983), prepared for submission to ASTM Meeting, Quebec City, July 13, 1983.
- 17 E. Herrmann, *J. Chromatogr.*, 38 (1968) 498.
- 18 A. G. Hamlin, B. J. Roberts, W. Loughlin and S. G. Walker, *Anal. Chem.*, 33 (1961) 1547.
- 19 C. R. Walker and O. A. Vita, *Anal. Chim. Acta*, 43 (1968) 27.

CHROM. 22 764

## Determination of contributions of different types of solute–sorberent interactions in gas-adsorption chromatography by linear regression of adsorption energies

OLEG G. LARIONOV\*, VICTOR V. PETRENKO and NATALIA P. PLATONOVA

*Institute of Physical Chemistry, U.S.S.R. Academy of Sciences, Leninskiy Prospect 31, 117915 Moscow (U.S.S.R.)*

(First received December 29th, 1989; revised manuscript received July 24th, 1990)

---

### ABSTRACT

The gas chromatographic adsorption energies of 30 sorbates were processed by using descriptors which define dispersion, orientation and donor–acceptor interactions. Hydrogen treated, thermally graphitized carbon black, barium sulphate and a porous polymer of medium polarity were used as sorbents. A four-variable regression equation for all sorbents with  $R \approx 0.97$  and a relative standard deviation of *ca.* 5% was developed. The importance of the different solute–sorberent interactions (SSI) for each sorberent studied is discussed. The contributions of the SSI to the total adsorption energy of Rohrschneider's substances for the sorbents were calculated.

---

### INTRODUCTION

The concept of polarity is widely used for both the classification and the selection of sorbents for gas chromatographic (GC) analyses. This concept expresses the ability of a sorberent to show predominant retention of polar molecules in comparison with non-polar *n*-alkanes. Rohrschneider's method of polarity determination based on the differences in Kováts retention indices (RI) of the set of solutes on two stationary phases is widely used [1]. A method taking into account the energetic inequivalence of RI units on different stationary phase has also been described [2]. Various publications has been devoted to RI simulation [3–7] and to establishing their dependence on adsorbent and adsorbate parameters [8]. As any differences in the polarities and selectivities of sorbents are primarily associated with changes in the nature of solute–sorberent interactions (SSI), the quantitative relationship of the contributions of various types of SSI may be considered as a measure of a sorberent's polarity and selectivity.

We have attempted to obtain a quantitative description of the GC properties of adsorbents by dividing the adsorption energies and RI into components describing different types of SSI. This paper deals with a description of adsorption energies. In a subsequent paper the possibility determining the polarity and selectivity of adsorbents by using the same method for RI will be considered.

## THEORY

Adsorption energy may be represented as follows (if no charge-transfer complexes form):

$$\Delta U_{\text{ads.}} = \Delta U_{\text{disp.}} + \Delta U_{\text{ind.}} + \Delta U_{\text{or.}} + \Delta U_{\text{hydr.}} \quad (1)$$

The expressions for the first three terms are well known [9,10].

The energy of hydrogen bond formation may be represented by

$$\Delta U_{\text{hydr.}} = Wd_a Wa_s + Wa_a Wd_s \quad (2)$$

where  $Wa_s$  and  $Wd_s$  are electron-acceptor and electron-donor energetic constants of a sorbate molecule and  $Wd_a$  and  $Wa_a$  are the same constants of a counterpart (in our case an adsorbent surface) [11]. It is worth noting that the hydrogen bond constants  $Wa$  and  $Wd$  are related to similar constants for charge-transfer complexes [11]. We assumed that eqn. 2 can be inserted in eqn. 1 to describe in some way donor-acceptor SSI in general.

Substituting the well known expressions for  $\Delta U_{\text{disp.}}$ ,  $\Delta U_{\text{ind.}}$  and  $\Delta U_{\text{or.}}$  [9,10] and eqn. 2 into eqn. 1 and performing some simplifications, the following equation was obtained:

$$\Delta U = K_1\alpha + K_2(2\mu^2/3kT + \alpha) + K_3Wa + K_4Wd + K_5 \quad (3)$$

where  $\alpha$  is the polarizability of a sorbate molecule,  $\mu$  its dipole moment and  $Wa$  and  $Wd$  its electron-acceptor and -donor constants. The coefficients  $K_1$ – $K_4$  are proportional to the physico-chemical adsorbent characteristics involved in the expressions for each type of SSI. The term  $K_5$  was included in eqn. 3 to account for neglected SSI. Accordingly, a knowledge of the coefficient values would allow us to establish the ability of an adsorbent to effect certain SSI quantitatively.

Eqn. 3 is applicable to multiple linear regression, in which case desired values of the coefficients for a sorbent may be obtained by using molecular parameters of a set of sorbates and their adsorption energies on the sorbent.

The physico-chemical and topological parameters of sorbate molecules were obtained by the following way. Polarizability was calculated from the Lorentz-Lorenz equation:

$$\alpha = \frac{3}{4\pi L} \cdot V_m \cdot \frac{(n^2 - 1)}{(n^2 + 2)} \quad (4)$$

where  $V_m$  is the molar volume and  $n$  is the refractive index. Dipole moments were taken from ref. 12 and the constants  $Wd$  and  $Wa$  for the gas phase were calculated from the data in ref. 11. To take into account steric effects, some topological descriptors were also involved. The molecular connectivity indices (MCI) of the first order were calculated from the expression

$${}^1\chi = \sum^n (\delta_i \delta_j)^{-1/2} \quad (5)$$

where  $n$  is the number of valence bonds in a molecule and  $\delta_i$  and  $\delta_j$  are the number of atomic valences directed to the adjoining non-hydrogen (e.g., C, O, N) atoms. For cyclic molecules the allowance for a ring of 0.5 was subtracted from the values of  ${}^1\chi$ . MCI of the second order were calculated from the expression

$${}^2\chi = \sum^k (\delta_i \delta_j \delta_m)^{-1/2} \quad (6)$$

where  $k$  is the number of all three atom chains in a molecule (with multiple bonds taken into account). Further details of the theory of MCI can be found elsewhere [13].

## EXPERIMENTAL

The method proposed above was used to process literature data on the adsorption energies ( $\Delta U$ ) for the non-polar adsorbent hydrogen treated thermally graphitized carbon black (HT GTCB) (adsorbent I [14]) and for polar BaSO<sub>4</sub> modified with NaCl (adsorbent III [15]). Our experimental data for a porous polymer of medium polarity (adsorbent II) were also processed. This adsorbent is a copolymer of ethylene dimethacrylate (EDMA) with epithiopropyl methacrylate (ETPMA) with a specific surface area of 66 m<sup>2</sup>/g and containing 11% of sulphur [16].

The determination of adsorption energies was performed with a Tswett-165 chromatograph with flame ionization detection. Glass columns (50 cm × 1.2 and 3 mm I.D.) were used. The flow-rate of the carrier gas (helium) was 4–8 cm/s. Before measurements the sorbent was warmed for 6 h in a helium flow at 190°C. The heats of adsorption were measured in the range 135–175°C. Kováts retention indices at 150°C were calculated.

A set of 30 substances was used for regression analyses on the adsorbents studied. It included *n*-alkanes, *n*-alkenes, aromatic hydrocarbons, alcohols, ethers, alkylacetates, ketones, nitroalkanes, chloro-substituted compounds and pyridine. Because of the different polarities of the adsorbents, the compositions of the sets of compounds on each adsorbent were slightly different.

We used ref. 17 as the mathematical basis for the multiple linear regression. BASIC programs with matrix operators were performed on an Iskra 226 personal computer.

The correlation coefficient  $r$  and standard error  $s$  were used to evaluate the regression fits.

## RESULTS AND DISCUSSION

### *Discussion of eqn. 3*

First the regression analyses were performed in accordance with eqn. 3. The results for each substance on HT GTCB are shown in the first column of Table I, and the integrated results for all adsorbents in the first column of Table II. As HT GTCB is a non-polar adsorbent, all deviations of the calculated  $\Delta U$  values from the experimental values seem to be connected only with the rough description of dispersion SSI by the  $K_1\alpha$  term in eqn. 3. These deviations are probably associated with

TABLE I

REFERENCE VALUES  $-\Delta U$  ON HT GTCB [14] AND THEIR DEVIATIONS AGAINST THOSE CALCULATED WITH EQN. 8 WITH DIFFERENT  $G$

All values in kJ/mol.

No.	Solute	$-\Delta U$ [14]	Deviation without $G$	$G_1$	Deviation with $G_1$	$G_2$	Deviation with $G_2$
1	Hexane	39.4	+0.5	0.78	-1.0	0.67	-2.1
2	Heptane	44.0	+0.4	0.82	-1.2	0.70	-2.2
3	Octane	49.4	+0.4	0.86	-0.8	0.73	-2.0
4	Nonane	55.6	-0.3	0.90	-0.8	0.75	-2.7
5	Benzene	36.2	-1.0	0.85	+0.2	0.85	+2.9
6	Toluene	44.4	-3.3	0.93	-0.8	0.81	-1.3
7	Ethylbenzene	47.9	-1.2	0.94	+0.8	0.85	+1.8
8	Fluorobenzene	38.1	-2.1	0.93	+0.5	0.89	+2.6
9	Chlorobenzene	43.8	-1.6	0.93	+0.1	0.85	+1.4
10	Bromobenzene	45.0	+0.3	0.93	+1.5	0.82	+1.9
11	<i>n</i> -Propanol	28.6	-1.5	0.71	-1.1	0.77	+0.1
12	Isopropanol	28.0	-0.8	0.79	+1.0	0.68	-1.3
13	<i>n</i> -Butanol	34.7	-2.2	0.75	-2.8	0.80	-0.6
14	Isobutanol	31.4	+1.2	0.80	+1.7	0.74	+1.2
15	<i>sec.</i> -Butanol	31.6	+0.7	0.80	+1.3	0.75	+0.8
16	<i>tert.</i> -Butanol	30.2	+2.7	0.65	-0.4	0.64	-0.4
17	Diethyl ether	31.6	+1.1	0.75	-0.6	0.70	-0.9
18	Di- <i>n</i> -propyl ether	41.6	+2.6	0.82	0.0	0.74	-0.1
19	Di- <i>n</i> -butyl ether	53.3	+1.1	0.90	-0.5	0.79	-0.8
20	Acetone	26.9	+0.9	0.81	+0.7	0.70	-1.1
21	Methyl ethyl ketone	32.9	+0.2	0.81	-1.3	0.76	-1.1
22	Methyl <i>n</i> -propyl ketone	37.7	+0.5	0.85	-0.9	0.78	-0.7
23	Methyl <i>n</i> -butyl ketone	42.9	+0.7	0.89	-0.6	0.80	-0.5
24	Ethyl acetate	34.8	-2.1	0.92	+0.2	0.86	+0.4
25	<i>n</i> -Propyl acetate	39.9	-1.7	0.96	+0.9	0.86	+0.7
26	<i>n</i> -Butyl acetate	44.9	-1.1	1.00	+2.1	0.86	+1.3
27	Dichloromethane	23.9	0.0	0.67	+0.3	0.67	+0.6
28	Chloroform	28.9	+0.6	0.79	+1.9	0.65	-0.4
29	Carbon tetrachloride	30.3	+4.5	0.65	+0.3	0.63	+1.2
30	1,2-Dichloroethane	29.3	+0.5	0.71	-0.6	0.73	+1.4

TABLE II

CORRELATION COEFFICIENTS  $r$  AND RELATIVE STANDARD DEVIATIONS  $s$  FOR  $-\Delta U$  ANALYSES ON THREE SORBENTS WITH EQN. 8 WITH DIFFERENT  $G$

Sorbent	with $G=1$		with $G_1$		with $G_2$	
	$r$	$s$ (%)	$r$	$s$ (%)	$r$	$s$ (%)
HT GTCB	0.980	4.7	0.991	3.2	0.984	4.2
EDMA-ETPMA	0.905	5.5	0.952	4.0	0.971	3.1
BaSO <sub>4</sub>	0.960	9.2	0.970	8.0	0.971	7.8

the fact that large molecules do not contact a surface with all of their atoms. This phenomenon may be taken into account by including in the term  $K_1\alpha$  some steric factor ( $G \leq 1$ ) for each molecule. Hence the product  $K_1G\alpha$  should have the meaning of the effective polarizability of a molecule for adsorption on a surface.

The steric factor was generated by means of spatial characteristics of a molecule (molar volume and MCI of various orders) in two ways, as follows. Modelling a relatively simple expression for  $G$ , providing minimum deviations of  $\Delta U$  on HT GTCB and further using of  $G$  values obtained for adsorption on all other surfaces, we obtained the following expression:

$$G_1 = {}^2\chi/9 - 0.56 {}^4\chi_c + 0.6 \quad (0.65 \leq G \leq 1) \quad (7)$$

(2) It was noted that ratio  $Z = {}^1\chi/V_m$  was high for planar or small molecules (carbon dioxide, benzene, pyridine, dioxane, nitromethane) whereas small  $Z$  values are characteristic of long-chain molecules with mobile segments ( $n$ -alkane,  $n$ -alkenes, ethers) or highly branched molecules (*tert.*-butanol, neopentane,). Assuming that the molecules with maximum  $Z$  value have the best contact with a surface, one can assume that relationship  $G_2 = Z/Z_{\max}$  reflects the degree of engagement of a molecule with a surface. Values of  $G$  obtained in such a way were  $0.63 \leq G_2 \leq 1.00$ . Both values,  $G_1$  (obtained by the first method) and  $G_2$  (by the second) are given in Table I.

Inclusion of any of these steric factors in eqn. 3 decreases the standard error and increases the correlation coefficient of regression analyses while the number of adjustable terms was invariant (see Table II). However, the use of the steric factor  $G_2$  is preferable because it has a physical meaning and its value has a better correlation with the stereochemistry of molecules (*e.g.*,  $n$ -butanol 0.80, isobutanol 0.74, *tert.*-butanol 0.64). Therefore, the final form of the eqn. 3 for all adsorbents is

$$\Delta U = K_1G\alpha + K_2(2\mu^2/3kT + G\alpha) + K_3Wa + K_4Wd + K_5 \quad (8)$$

Although eqn. 8 is fairly simple, it involves all kinds of SSI which are of importance in GC [18].

The parameters of sorbate molecules in eqn. 8 are uncorrelated with each other. The correlation matrix is given in Table III.

#### *Results of data processing*

The results of the three adsorbent analyses using eqn. 8 are shown in Table IV and in Figs. 1-3. All regression coefficients are given with their standard errors. The significance of every regression coefficient (in this instance it is the significance of a certain type of SSI for adsorption on the adsorbent) may be obtained from Student's  $t$ -test as ratio of the coefficient to its standard error ( $t = K_i/s_i$ );  $t$  values are given in Table IV.

The  $t$  values show that for HT GTCB such sorbent characteristics as dipole moment on the surface and electron-donor and electron-acceptor ability of the surface have negligible deviations from zero. This is in accordance with HT GTCB being a non-polar sorbent and with the absence of any functional groups being able to undergo specific SSI on its surface.

On polymer sorbent II, dispersion SSI are also of most importance. In addition,

TABLE III  
CORRELATION MATRIX FOR DESCRIPTORS USED IN EQN. 8

Descriptor	$\alpha G$	$\mu^2$	$Wa$	$Wd$
$\alpha G$	1.00	-0.435	-0.587	-0.465
$\mu^2$		1.000	-0.062	0.164
$Wa$			1.000	0.386
$Wd$				1.000

TABLE IV  
REGRESSION COEFFICIENTS  $K_i$  WITH THEIR STANDARD ERROR AND STUDENT'S  $t$ -TEST ON THREE SORBENTS OBTAINED WITH EQN. 8 WITH  $G_2$ .

Coefficient	HT GTCB		EDMA-ETPMA		BaSO <sub>4</sub>	
	$K_i$	$t$	$K_i$	$t$	$K_i$	$t$
$K_1$	33.1 ± 1.4	23.1	30.9 ± 1.5	20.1	18.1 ± 4.3	4.2
$K_2$	1.5 ± 1.1	1.0	8.1 ± 0.9	9.3	41.4 ± 3.4	12.3
$K_3$	1.0 ± 1.4	0.7	13.2 ± 1.2	11.0	35.2 ± 4.1	8.6
$K_4$	0.1 ± 0.8	0.1	5.2 ± 0.6	8.2	14.2 ± 1.7	8.3
$K_5$	9.6 ± 1.5	6.5	13.1 ± 1.8	7.2	10.2 ± 5.1	2.0
$s$ (%)		4.2		3.1		7.8
$r$		0.984		0.971		0.971

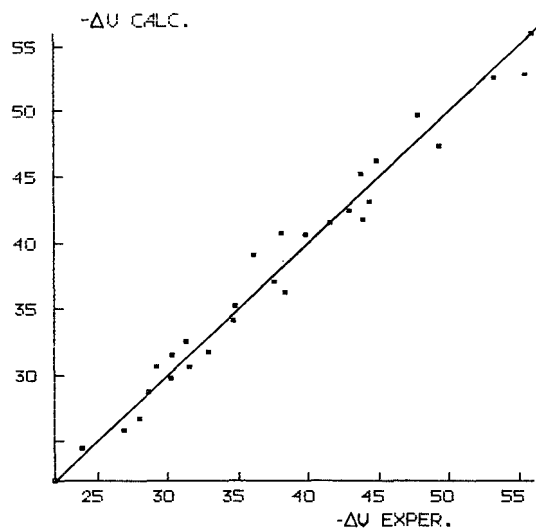


Fig. 1. Experimental and calculated values of  $-\Delta U$  (kJ/mol) on HT GTCB.



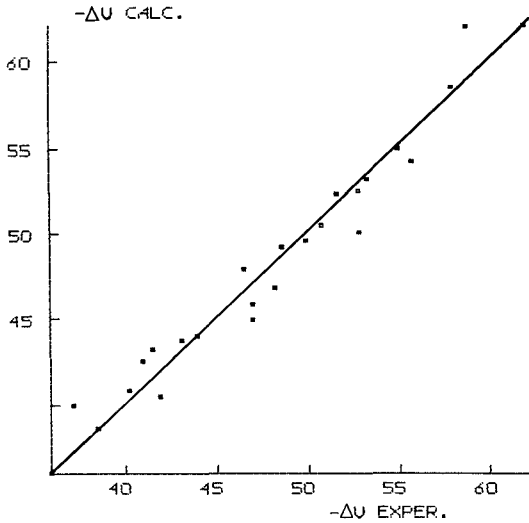


Fig. 2. Experimental and calculated values of  $-\Delta U$  (kJ/mol) on EDMA-ETPMA.

the specific SSI induced by carboxy and epithio groups are significant. Some electron-acceptor capability of the surface ( $K_4$ ) apparently may account for the partial positive charge of the carbon atom in the carboxy group.

As expected, on ionic  $\text{BaSO}_4$  the orientation SSI caused by the spatial separation of charges on the surface is most significant. The electron-donor capability of  $\text{SO}_4^{2-}$  and the electron-acceptor capability of  $\text{Ba}^{2+}$  are also of importance for adsorption. The significance of dispersion SSI on this adsorbent is minimal in comparison with specific SSI.

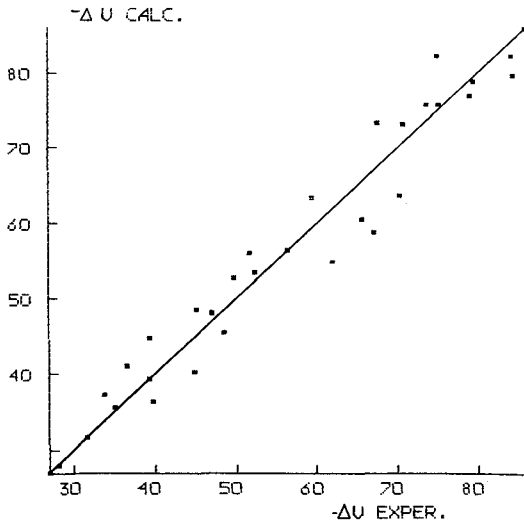


Fig. 3. Experimental and calculated values of  $-\Delta U$  (kJ/mol) on  $\text{BaSO}_4$ .

TABLE V  
CONTRIBUTIONS OF DIFFERENT KINDS OF SSI TO TOTAL ADSORPTION ENERGY  $\Delta U$  (%)

Sorbate	Adsorbent	Dispersion	Orientation and induction	Electron acceptor	Electron donor
Benzene	I	100	0	0	0
	II	93	2	0	5
	III	72	0	0	18
<i>n</i> -Propanol	I	96	2	2	0
	II	61	6	20	13
	III	25	20	34	21
Methyl ethyl ketone	I	96	4	0	0
	II	71	17	0	12
	III	28	52	0	20
Nitromethane	I	—	—	—	—
	II	66	27	0	7
	III	—	—	—	—
Pyridine	I	—	—	—	—
	II	—	—	—	—
	III	32	32	0	36

Consideration of the coefficient values for three adsorbents leads to following conclusions. The pronounced decrease in  $K_1$  for transfer from HT GTCB and the porous polymer to  $\text{BaSO}_4$  represents the change to a surface consisting of hardly polarizable ions instead of molecular structures. The appreciable increasing in  $K_2$  from 8.1 to 41.1 for the pair II–III seems to be connected with the ionic character of the  $\text{BaSO}_4$  surface. The changes in  $K_3$  and  $K_4$  from zero to certain values indicate the occurrence of electron-donor and electron-acceptor centres on the surfaces.

The polarity of adsorbents calculated on the basis of the "specific" coefficients  $K_2$ – $K_4$  increases considerably in the sequence HT GTCB < EDMA–ETPMA <  $\text{BaSO}_4$ , as expected.

The coefficients  $K_1$ – $K_5$  obtained allow us to calculate different SSI contributions to the total adsorption energy. The contributions correspond to the summands of eqn. 8. As the free term  $K_5$  on all adsorbents was highly correlated with coefficient  $K_1$ ,  $K_5$  can be assigned to dispersion SSI. All other coefficients were uncorrelated. The correlation matrix is given in Table VI.

TABLE VI  
CORRELATION BETWEEN THE REGRESSION COEFFICIENTS

Coefficient	$K_1$	$K_2$	$K_3$	$K_4$	$K_5$
$K_1$	1.00	0.559	0.615	0.253	–0.947
$K_2$		1.000	0.433	–0.022	–0.627
$K_3$			1.000	–0.152	–0.581
$K_4$				1.000	–0.447
$K_5$					1.000

Contributions calculated in such a manner are given in Table V. The contribution of dispersion SSI is about 100% on HT GTCB for all substances and decreases for polar molecules on polar adsorbents; it is only 25% for *n*-propanol on BaSO<sub>4</sub>. The orientation contribution on the polymer adsorbent is rather small. On ionic BaSO<sub>4</sub> it is predominant for molecules with high dipole moments (e.g., 52% for methyl ethyl ketone). The electron-donor ability of the surface of EDMA-ETPMA or BaSO<sub>4</sub> takes effect for the adsorption of alcohols only. With BaSO<sub>4</sub> this contribution is predominant (34%). The electron-acceptor capability of the adsorbents surfaces of II and III takes effect for all substances of Rohrschneider's series and reach a maximum for pyridine.

The method developed seems to be of some interest for the determination of adsorbent capability for different kinds of SSI in GC.

#### REFERENCES

- 1 L. Rohrschneider, *J. Chromatogr.*, 22 (1966) 6.
- 2 R. V. Golovnya and T. A. Misharina, *Izv. Akad. Nauk SSSR, Ser. Khim.*, (1979) 787.
- 3 O. Papp, Gy. Szász, M. Farkas, G. Simon and I. Hermech, *J. Chromatogr.*, 403 (1987) 19.
- 4 A. N. Korol', *Usp. Khim.*, 51 (1982) 1225.
- 5 W. Ecking, *Z. Chem.*, 25 (1985) 240.
- 6 D. N. Grigoryeva and R. V. Golovnya, *Zh. Anal. Khim.*, 40 (1985) 1730.
- 7 F. Patte, M. Etcheto and P. Laffort, *Anal. Chem.*, 54 (1982) 2239.
- 8 J. Hradil, F. Švec, N. M. Gogitidze and T. T. Andronikashvili, *J. Chromatogr.*, 291 (1984) 103; 324 (1985) 277.
- 9 P. Claverie, in B. Pullman (Editor), *Intermolecular Interactions: From Diatomics to Biopolymers*, Wiley, New York, 1978, p. 99.
- 10 H. Lamparczyk and A. Radecky, *Chromatographia*, 18 (1984) 715.
- 11 V. A. Terentyev, *Thermodynamics of Donor-Acceptor Bonds*, Saratov University Publishing House, Saratov, 1981, p. 36.
- 12 O. A. Osipov, V. J. Minkin and A. D. Garnovsky, *Reference Book on Dipole Moments*, Vysshaya Shkola, Moscow, 1976, p. 54.
- 13 L. B. Kier and L. H. Hall, *Molecular Connectivity in Chemistry and Drug Research*, Academic Press, New York, 1976, p. 54.
- 14 A. V. Kiselev and Ya. Yashin, *Gas and Liquid Adsorption Chromatography*, Khimiya, Moscow, 1979, p. 42.
- 15 L. D. Belyakova, O. G. Larionov and L. M. Strokina, *Izv. Akad. Nauk SSSR, Ser. Khim.*, (1988) 1491 and 2454.
- 16 J. Hradil, F. Švec, N. P. Platonova, L. D. Belyakova and V. Maroušek, *J. Chromatogr.*, 469 (1989) 143.
- 17 N. Draper and G. Smith, *Applied Regression Analysis*, Finansy i Statistika, Moscow, 1986, p. 340.
- 18 T. Takagi, Ya. Shindo, H. Fujiwara and Yo. Sasaki, *Chem. Pharm. Bull.*, 37 (1989) 1556.



## Gas chromatographic identification of complex mixtures of halomethanes and haloethanes by using the correlation between their retention and vapour pressure

TOMASO C. GERBINO<sup>a</sup> and GIANRICO CASTELLO\*

*Istituto di Chimica Industriale, Università di Genova, Corso Europa 30, 16132 Genova (Italy)*

(First received April 12th, 1990; revised manuscript received July 31st, 1990)

---

### ABSTRACT

The linear correlation between relative retention values of halogenated hydrocarbons (methanes, ethanes and ethenes) having one or more identical or different halogen atoms in the molecule and their vapour pressures was used for identification purposes in gas chromatography. Absolute and relative retention values were measured at various temperatures on non-polar (OV-1) and polar (SP-1000) packed columns, and some correlations were found that permit peak identification. The calculation of retention times when the vapour pressures of the substances are known or, on the contrary, the calculation of this parameter on the basis of gas chromatographic analysis are possible.

---

### INTRODUCTION

When very complex mixtures of halogenated compounds have to be analysed, *e.g.*, in the polluted environment, the identification of different compounds on the basis of their retention times on columns of different polarities is very useful and can avoid the use of more complex and expensive techniques that are often not suitable for routine field analysis. When standard samples are not available for the identification of less common compounds, the use of correlations between retention behaviour, physical properties and structure of these compounds can assist in tentative identification [1–8].

In a previously published paper [9], the correlation between the relative retention values,  $r$ , the retention index values,  $I$ , the retention volumes,  $V_R$ , and the vapour pressure,  $p^\circ$ , of many halogenated hydrocarbons was investigated. For the non-polar stationary phase used, OV-1, a good linear correlation between vapour pressure and  $I$  was found, which permits the separation of a complex mixture of compounds to be predicted at any temperature of the column. Further, the linear dependence of  $I$  values on temperature can be used to confirm the qualitative identification of a substance, being correlated with its structure [10–12]. On the polar stationary phase SP-1000, the

---

<sup>a</sup> Present address: CASTALIA, Società Italiana per l'Ambiente, Via dei Pescatori 35, 16129 Genova, Italy.

correlation was found to be non-linear and unsuitable for the calculation of retention values at different temperatures.

On the other hand, the use of an Antoine-type equation [13,14], the constants of which were calculated starting from experimental values, permitted the calculation of  $I$  values at any temperature on both polar and non-polar stationary phases. The determination of  $I$  values, however, by using the classical Kováts equation [15] with respect to linear alkanes, requires accurate measurements of the retention times of the compounds mixed with several linear alkane homologues. When electron capture detection (ECD) is used, the negligible response to alkanes requires the use of different homologous series of electron-absorbing compounds, *e.g.*, linear iodoalkanes [16], and the determination of the correlation between their retention times and that of linear alkanes. The identification by means of retention index values is therefore unsuitable or very complex.

In contrast, the measurement of relative retention values,  $r$ , with respect to a reference compound present in the sample or added to it is much easier and does not require a complete series of reference substances. When the analyses are made on the same column and under reproducible temperature conditions, the validity of the  $r$  values for identification purposes can be equivalent to the use of other retention values (the Kováts retention index or the specific retention volume,  $V_g$ ) that are independent of many analytical parameters but whose determination is more difficult.

Of course, it is necessary to verify that the  $r$  values show regular behaviour as a function of the structure, boiling point and vapour pressure of the analyte substances, similar to that shown by the  $I$  and  $V_g$  values, and to investigate the effect of the column polarity on the elution of the analyte compounds.

## EXPERIMENTAL

Two columns of different polarity were used: non-polar OV-1 and polar SP-1000, both 10% (w/w) on Chromosorb W DMCS (80–100 mesh), with length 3 m and I.D. 2 mm. A Varian (Palo Alto, CA, U.S.A.) Model 3760 gas chromatograph was used with thermal conductivity detection (TCD), in order to permit the injection of samples with the same concentration of each component, owing to the small difference in the TCD responses to substances belonging to various homologous series (alkanes, alcohols, halogenated compounds with a different number of halogen atoms in the molecule). In fact, the use of specific detectors, which are insensitive to certain compounds, may require different amounts of each substance to be injected in order to obtain peaks of comparable area. The width and shape of some peaks may therefore change owing to column saturation and the resolution between adjacent peaks or the determination of some parameters (*e.g.*, column efficiency) may be influenced. Obviously, the analysis of low-concentration authentic samples in the environment must be made with sensitive ECD, taking into account the possible effect of the different sensitivities of various compounds.

The samples used included chloro-, bromo- and iodo-methanes, -ethanes and -ethenes with one or more different halogen atoms in the molecule. The choice of these components permitted many different "homologous series" to be investigated, by changing the substituent halogen or increasing the number of halogen atoms in the molecule. Helium was used as the carrier gas at a flow-rate of  $30 \text{ cm}^3 \text{ min}^{-1}$ . All the

samples were analysed at 50, 75, 100 and 125°C on both columns. The discussion below is based on the values at 100°C, but the results can also be applied to the retention values found at different temperatures.

#### THEORY

For many homologous series of compounds the following relationships were found [17,18]:

$$\log p^\circ = K_3 + K_4 n \quad (1)$$

$$\log \gamma = K_5 + K_6 n \quad (2)$$

where  $n$  is the number of structural units in the molecule (*i.e.* carbon atoms, methylene groups, chlorine atoms, etc.) and  $K_3$ ,  $K_4$ ,  $K_5$  and  $K_6$  are constants for each homologous series at a given temperature. For such compounds  $\log \gamma$  and  $\log p^\circ$  are related:

$$\log \gamma = a + b \log p^\circ \quad (3)$$

where

$$a = K_5 - (K_3 K_6 / K_4) \quad (4)$$

$$b = K_6 / K_4 \quad (5)$$

Taking into account the general equation for retention volume,  $V_R$ :

$$V_R = \frac{N_1 RT}{\gamma p^\circ} \quad (6)$$

where  $N_1$  is the number of moles of stationary phase in the column, the following equation is derived:

$$\log V_R = \log(N_1 RT) - a - (b + 1) \log p^\circ \quad (7)$$

Further, as for homologous series the boiling points,  $B_p$ , are linearly correlated with the  $p^\circ$  values [13]:

$$\log p^\circ = K_1 + K_2 B_p \quad (8)$$

the following relationship is obtained:

$$\log V_R = \log(N_1 RT) - a - (b + 1)(K_1 + K_2 B_p) \quad (9)$$

showing that, on a given column at a constant temperature,  $V_R$  depends linearly on the boiling point, a readily available parameter, whereas tabulated  $p^\circ$  values are often difficult to obtain. As the  $V_g$  (specific retention) values are obtained from the adjusted

retention volumes,  $V'_R$ , by taking into account the amount of liquid phase in the column, and therefore differ from  $V'_R$  by a constant ratio, the correlation shown above is also true when  $V'_g$  or  $I$  values are considered.

Similar results can be obtained for  $r$  values [19], by starting from the equation

$$\log r_{s,q} = \log(p_q^\circ/p_s^\circ) + \log(\gamma_q/\gamma_s) \quad (10)$$

where  $r_{s,q}$  is the relative retention of substance  $s$  with respect to a reference compound  $q$ . Eqn. 8 is suitable for application with very dilute solutions such as occur in gas-liquid chromatography.

By taking into account eqns. 1, 2 and 8, the following relationship is obtained:

$$\log r_{s,q} = A_1 - a_1 \log p_s^\circ = A_2 - a_2 B_p \quad (11)$$

where

$$A_1 = \log(p_q^\circ \gamma_q) - K_5 + (K_3 K_6 / K_4) \quad (12)$$

$$A_2 = A_1 - a_1 K_1 \quad (13)$$

$$a_1 = 1 + (K_6 / K_4) \quad (14)$$

$$a_2 = -a_1 K_2 \quad (15)$$

showing that for homologous series the behaviour of  $r$  values is as linear as that of  $V'_R$  values as a function both of  $p^\circ$  and of  $B_p$ .

Fig. 1A and B show the linear dependence of  $r$  and  $V'_R$  values of a homologous series on  $p^\circ$  and  $B_p$ , respectively. Further, when neither  $p^\circ$  nor  $B_p$  values for a given compound are available, but it belongs to a homologous series and its number of

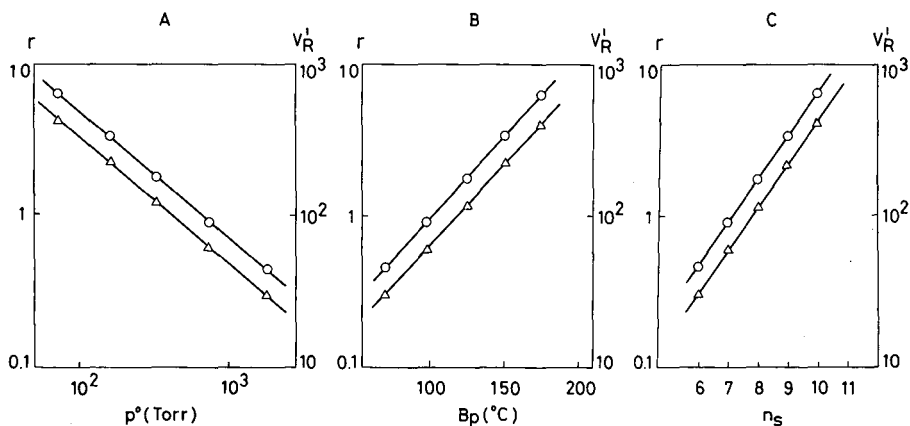


Fig. 1. Regular behaviour of (O) relative retention  $r$  and ( $\Delta$ ) adjusted retention volume  $V'_R$  of  $C_6$ - $C_{10}$   $n$ -alkanes on non-polar OV-1 column at  $100^\circ\text{C}$ . Values are shown as a function of (A) vapour pressure at  $100^\circ\text{C}$ ,  $p^\circ$ , (B) boiling point at 760 Torr,  $B_p$  and (C) number of structural units in the molecule,  $n_s$ .



TABLE I

HALOGENATED COMPOUNDS ANALYSED, GROUPED BY STRUCTURE, THEIR RETENTION RELATIVE TO 1-CHLORO-2-BROMOETHANE,  $r$ , ON NON-POLAR AND POLAR COLUMNS AT 100°C AND, WHEN AVAILABLE, BOILING POINTS AT 760 TORR,  $B_p$ , AND VAPOUR PRESSURE AT 100°C,  $p^\circ$ .

Adjusted retention,  $t'_R$ , of reference compound: 4.28 min on OV-1, 17.33 min on SP-1000.

No.	Compound	OV-1		SP-1000		$B_p$ (°C)	$p^\circ$ at 100°C (Torr)
		$t'_R$ (min)	$r$	$t'_R$ (min)	$r$		
1	CH <sub>3</sub> CHCl <sub>2</sub>	0.81	0.373	1.34	0.195	57.28	2303
2	CH <sub>2</sub> =CCl <sub>2</sub>	0.56	0.258	0.52	0.076	37	
3	ClCH=CCl <sub>2</sub>	1.91	0.884	2.54	0.369	87	
4	Cl <sub>2</sub> C=CCl <sub>2</sub>	4.12	1.898	3.18	0.462	121	412
5	CCl <sub>4</sub>	1.58	0.728	1.35	0.196	76.5	1315
6	ClCH <sub>2</sub> CH <sub>2</sub> Cl	1.30	0.599	3.86	0.561	83.5	1129
7	CHCl <sub>3</sub>	1.04	0.479	2.84	0.413	61.7	2203
8	CHBr <sub>2</sub> Cl	3.40	1.567	14.57	2.120	119.5	
9	CHBrCl <sub>2</sub>	1.90	0.875	6.48	0.943	90	
10	CHBr <sub>3</sub>	6.02	2.774	32.55	4.730	149.5	162
11	CH <sub>3</sub> CCl <sub>3</sub>	1.37	0.630	1.37	0.199	74.1	
12	CH <sub>2</sub> Cl <sub>2</sub>	0.50	0.230	1.65	0.240	40	
13	CH <sub>3</sub> CH <sub>2</sub> I	1.12	0.516	1.34	0.195	72.3	
14 <sub>c</sub>	BrCH=CHBr ( <i>cis</i> )	3.06	1.410	10.83	1.576	112.5	
14 <sub>t</sub>	BrCH=CHBr ( <i>trans</i> )	2.53	1.165	5.58	0.812	108	
15	BrCH <sub>2</sub> CH <sub>2</sub> Br	3.69	1.700	12.13	1.765	131.4	339
16	Cl <sub>3</sub> CCHCl <sub>2</sub>	11.15	5.138	30.02	4.369	162	124
17	CH <sub>3</sub> I	0.60	0.276	0.77	0.112	42.4	3378
18	Cl <sub>3</sub> CCH <sub>2</sub> Cl	4.95	2.281	11.60	1.688	130.5	312
19	ClCH=CHCl ( <i>trans</i> )	0.76	0.350	1.10	0.160	47.5	3214
20	ClCH=CHCl ( <i>cis</i> )	1.00	0.461	2.41	0.350	60.3	2187
21	ClCH <sub>2</sub> CH <sub>2</sub> Br	2.17	1	6.87	1	107	682
22	CH <sub>2</sub> I <sub>2</sub>	7.22	3.327	44.58	6.489	182	
23	CBrCl <sub>3</sub>	2.97	1.369	3.92	0.570	104	
24	C <sub>2</sub> H <sub>3</sub> Br	0.60	0.276	0.70	0.102	38.4	4248
25	Cl <sub>2</sub> CHCHCl <sub>2</sub>	6.76	3.115	43.35	6.601	146	184
26	Br <sub>2</sub> CHCHBr <sub>2</sub>	60.4	27.834	—	—	243.5	6
27	CH <sub>2</sub> BrCl	1.05	0.484	3.44	0.500	68.1	
28	CH <sub>2</sub> ClI	2.12	0.977	8.55	1.244	109	
29	CH <sub>2</sub> Br <sub>2</sub>	1.84	0.848	7.00	1.018	97	833
30	Cl <sub>3</sub> CCCl <sub>3</sub>	21.64	9.972	30.12	4.384	186	38
31	CBr <sub>4</sub>	18.79	8.659	112.80	16.419	190	47
32	CHI <sub>3</sub>	49.50	22.811	—	—	218	
33	ICH <sub>2</sub> CH <sub>2</sub> I	14.20	6.543	—	—	200	
34	CH <sub>3</sub> CH <sub>2</sub> Cl	0.33	0.152	0.33	0.048	12.3	9225

structural units,  $n_s$ , is known, the  $B_p$  value being linearly correlated with  $n_s$  [13], a linear relationship between  $r$ ,  $V'_R$  and  $n_s$  is observed (Fig. 1C):

$$\log r_{s,q} = \log(p_q^\circ \gamma_q) - (K_3 + K_5) - (K_4 + K_6)n_s \quad (16)$$

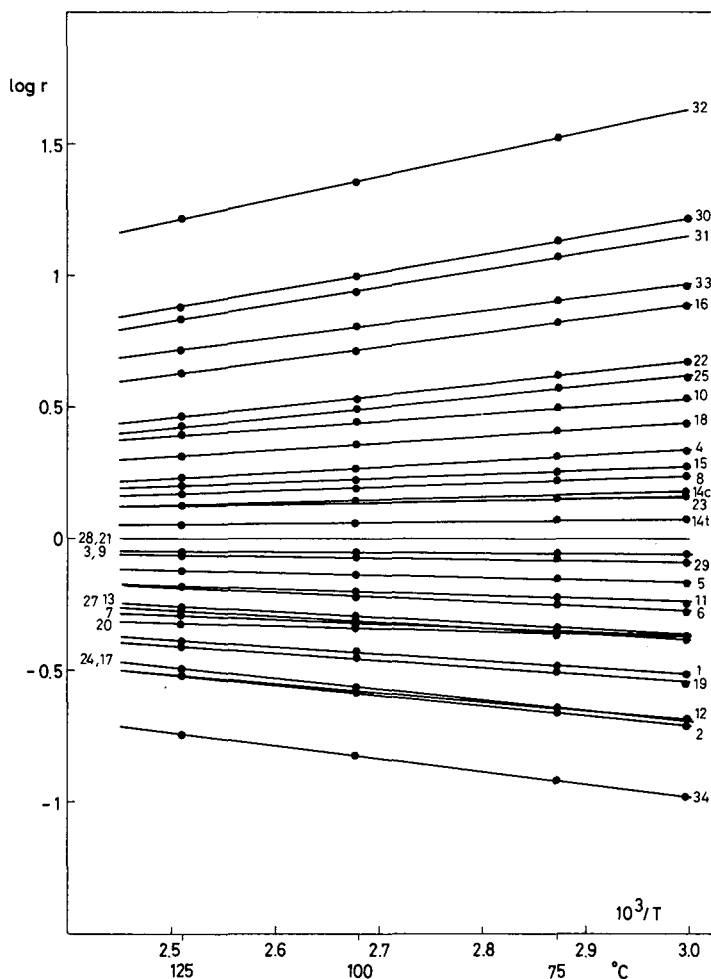


Fig. 2. Retention times relative to 1-chloro-2-bromoethane of halogenated compounds listed in Table I, analysed on non-polar OV-1 column, as a function of the reciprocal of absolute temperature of the column.

The linear behaviour expressed by eqns. 11 and 16 is also found when the structural units of the molecule considered are different from methylenic groups or carbon atoms, but are halogen atoms, substituent groups, etc. [13,20].

#### RESULTS AND DISCUSSION

Table I lists the analytes, their adjusted retention times,  $t_R$ , measured at 100°C and the  $r$  values measured with respect of 1-chloro-2-bromoethane. This substance was selected as the reference compound instead of trichloroethylene, generally used as the reference in the analysis of haloalkanes in the environment [9], because its peak showed no interference with the analyte compounds under any analytical conditions and

because its presence was never observed in authentic environmental samples, making this compound a good choice as a reference for internal standard quantitative calibration. Boiling points obtained from the literature and vapour pressures calculated by using the Antoine equation are also shown. Figs. 2 and 3 show the linear change of  $r$  values with respect of 1-chloro-2-bromoethane as a function of the reciprocal of the absolute temperature of the column.

The correlation between  $\log r$  on the non-polar OV-1 column and  $\log p^\circ$  (both at  $100^\circ\text{C}$ ) is shown for many haloalkanes and for  $\text{C}_6\text{-C}_{10}$   $n$ -alkanes in Fig. 4. On completely non-polar columns the retention should depend only on vapour pressure and therefore all compounds should lie on the same straight line. The experimental points are on three near-parallel lines, whose correlation coefficients are very high ( $>0.999$ ); for each straight line the gas chromatographic behaviour depends only on

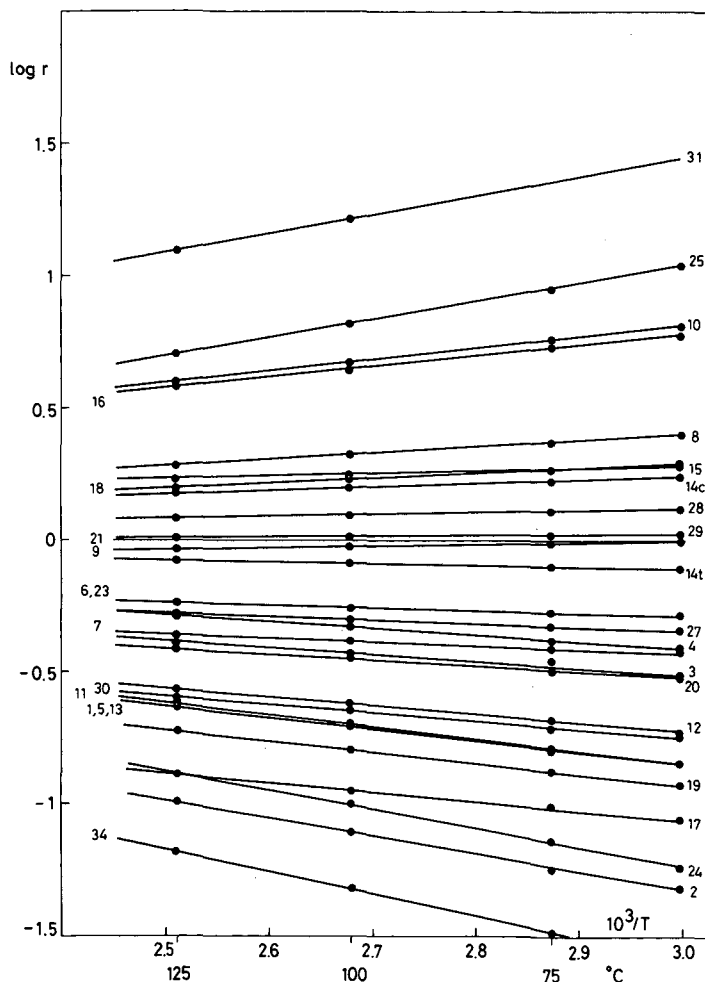


Fig. 3. Retention times relative to 1-chloro-2-bromoethane of halogenated compounds listed in Table I, analysed on polar SP-1000 column, as a function of the reciprocal of absolute temperature of the column.

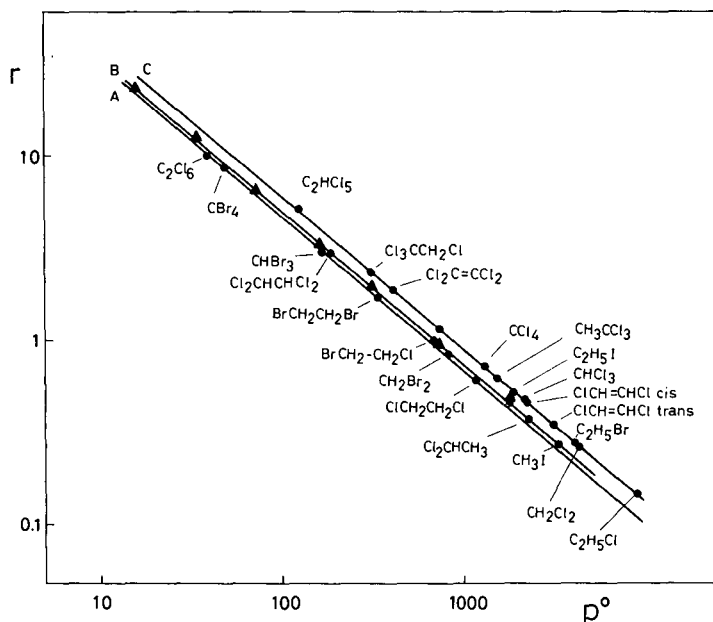


Fig. 4. Linear correlation between  $r$  and  $p^\circ$  values of various halogenated compounds (●) and  $C_6$ – $C_{10}$   $n$ -alkanes (▲) on non-polar OV-1 column. Temperature,  $100^\circ\text{C}$ .

the vapour pressure of the solute, the activity coefficient,  $\gamma$ , being constant. The lines are closely spaced, showing that the difference between  $\gamma$  values for the various series of compounds is small but not negligible. On the polar SP-1000 column the interaction due to dipole moments or to hydrogen bonding can be much greater than the structural effects (*e.g.*, symmetry or steric hindrance). Therefore, in Fig. 5 the network of straight lines connecting the compounds belonging to the same homologous series shows a fine structure.

The same behaviour, although less evident, is also shown by the  $\log r$  vs.  $\log p^\circ$  plot on the non-polar column. It is possible to draw in Fig. 4 some straight lines that connect compounds containing the same number of hydrogen atoms or an increasing number of atoms of the same halogen.

Fig. 6 shows on an arbitrary enlarged scale this fine structure: closed circles represent the compounds, also plotted in Fig. 4, whose  $r$  and  $p^\circ$  values are experimentally known. Open circles show the halomethanes whose  $r$  values were measured (Table I) while  $p^\circ$  values are not available. By starting from the experimental data, the equations of the straight lines shown in Fig. 6 and the  $p^\circ$  values for other compounds can be calculated.

Table II shows the coefficients (slope and intercept) of the equation (simplified form of eqn. 11)

$$\log p^\circ = s \log r + i \quad (17)$$

calculated by using experimental  $r$  values.

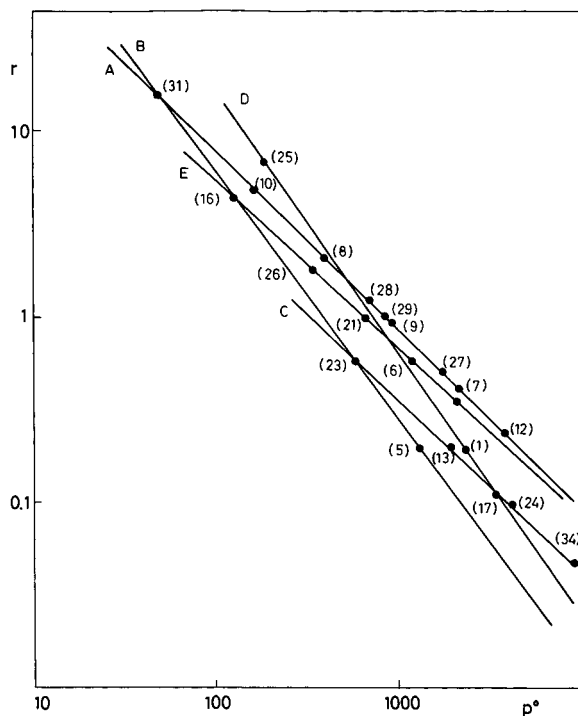


Fig. 5. Linear correlation between  $r$  and  $p^\circ$  values of various halogenated compounds on polar SP-1000 column. Temperature,  $100^\circ\text{C}$ .

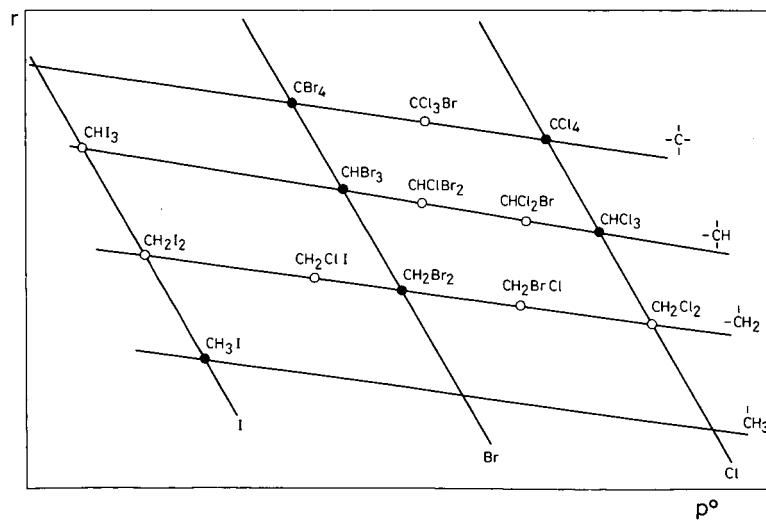


Fig. 6. Arbitrary scale enlargement of a section of Fig. 4 (OV-1,  $100^\circ\text{C}$ ), showing the fine structure of lines where halomethanes belonging to different homologous serie lie. ●, Experimental values; ○, calculated values (see text).

TABLE II

SLOPE  $s$  AND INTERCEPT  $i$  OF EQN. 17 CALCULATED FROM EXPERIMENTAL VALUES ON OV-1 AND ON SP-1000 COLUMNS

Identification of lines refers to Figs. 6 and 7. Correlation coefficient for all lines  $>0.99$ .

Column	Line	$s$	$i$
OV-1 (Fig. 6)	C	-1.34	2.93
	CH	-1.48	2.86
	CH <sub>2</sub>	-1.47	2.81
	I	-1.36	2.75
	Br	-1.37	2.82
	Cl	-1.23	2.94
SP-1000 (Fig. 7)	A	-1.04	2.93
	B	-0.75	2.58
	C	-0.83	2.77
	D	-0.92	2.98
	E	-0.82	2.74

Table III shows the  $p^\circ$  values calculated with eqn. 17 by using experimental  $r$  values and the coefficients reported in Table II.

The same procedure can be applied to obtain the  $r$  values when  $p^\circ$  is known. Moreover, by taking into account eqns. 11 and 16, similar fine structure plots could be obtained that permit the retention of any halomethane whose  $B_p$  or  $n$  values are known to be calculated by plotting  $\log r$  as a function of these variables.

Another method for calculating the  $r$  value of a given compound follows from the constant difference,  $\Delta = \log r_1 - \log r_2$ , observed when a halogen atom is replaced with another halogen (Table IV). By using the  $r$  values obtained from the  $\Delta$  values in Table IV and the parameters of eqn. 17 shown in Table II, the  $r$  and  $p^\circ$  values for some halomethanes can be predicted (Table V). The described procedure can be followed for any stationary phase. Fig. 7 shows with arbitrarily enlarged scale

TABLE III

VAPOUR PRESSURES,  $p^\circ$ , AT 100°C CALCULATED WITH EQN. 17 BY USING THE COEFFICIENTS IN TABLE II AND EXPERIMENTAL  $r$  VALUES IN TABLE I FOR COMPOUNDS SHOWN WITH OPEN CIRCLES IN FIGS. 6 (OV-1) AND 7 (SP-1000)

Compound	$p^\circ$ (Torr)	
	OV-1	SP-1000
CH <sub>2</sub> Cl <sub>2</sub>	4276	3824
CH <sub>2</sub> ClBr	1905	1771
CH <sub>2</sub> ClI	676	681
CH <sub>2</sub> I <sub>2</sub>	111	120
CHCl <sub>2</sub> Br	901	911
CHClBr <sub>2</sub>	379	389
CCl <sub>3</sub> Br	563	588
CHI <sub>3</sub>	7	

TABLE IV

EXPERIMENTAL  $\Delta$  VALUES (SEE TEXT) WITH DIFFERENT HALOGEN ATOMS (X) AS SUBSTITUENTS IN THE MOLECULE

Column	Structure	Substitution		$\Delta$	
		of	with		
OV-1	CX <sub>4</sub>	Cl	Br	0.268	
		Cl	Br	0.254	
	CX <sub>3</sub>	Br	I	0.305	
		Cl	I	0.559	
	CH <sub>2</sub> X <sub>2</sub>	Cl	Br	0.240	
		Br	I	0.296	
		Cl	I	0.537	
		XCH <sub>2</sub> -CH <sub>2</sub> X	Cl	Br	0.227
	Br		I	0.292	
	Cl		I	0.518	
	SP-1000		CX <sub>4</sub>	Cl	Br
		Cl		Br	0.354
CHX <sub>3</sub>		Br	I	0.543	
		Cl	I	0.896	
CH <sub>2</sub> X <sub>2</sub>		Cl	Br	0.306	
		Br	I	0.402	
	Cl	I	0.710		

plots A and B in Fig. 5. Closed circles represent experimental data and open circles the compounds whose  $r$  values are known and that are assumed to lie on a straight line on the basis of structural characteristics.

Tetrahalomethanes belong to line B whereas tri- and dihalomethanes lie on line A (a hyperfine structure with different lines for di- and trihalo compounds is possible,

TABLE V

$r$  VALUES FOR VARIOUS COMPOUNDS CALCULATED BY USING  $\Delta$  VALUES IN TABLE IV AND  $p^\circ$  VALUES OBTAINED FROM EQN. 17 WITH THE PARAMETERS IN TABLE II

Compound	OV-1		SP-1000	
	$r$	$p^\circ$ (Torr)	$r$	$p^\circ$ (Torr)
CHCl <sub>2</sub> I	1.73	327	3.25	326
CHClI <sub>2</sub>	6.29	48	25.58	48
CHBr <sub>2</sub> I	5.59	57	16.51	57
CHBrI <sub>2</sub>	11.30	20	57.65	20
CH <sub>2</sub> BrI	1.64	315	2.56	320
CCl <sub>2</sub> Br <sub>2</sub>	2.52	248	1.77	252
CClBr <sub>3</sub>	4.69	108	5.32	110
CHI <sub>3</sub> <sup>a</sup>		7	202	

<sup>a</sup> See text.

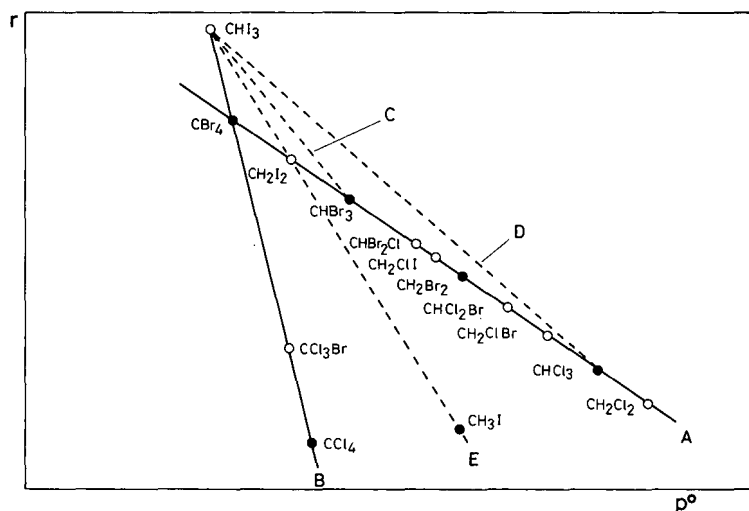


Fig. 7. Arbitrary scale enlargement of a section of Fig. 5 (SP-1000, 100°C) showing the fine structure of lines where halomethanes belonging to different homologous series lie. ●, Experimental values; ○, calculated values that lie on a straight line (see text).

but not evident at this scale and with the obtained accuracy of retention data). Parameters of eqn. 17 for lines A and B (Table II) can be used to calculate  $p^\circ$  values shown in Table III, and  $\Delta$  values (Table IV) to calculate  $p^\circ$  and  $r$  values shown in Table V. The final  $p^\circ$  values obtained by following this method and using experimental data measured on polar and non-polar stationary phases are very similar, notwithstanding the great difference in retention values on the two columns.

When a compound lies on two or more straight lines, *i.e.*, belongs to different "homologous" series, its  $r$  and  $p^\circ$  values can be calculated in several ways. As an example,  $\text{CH}_3\text{I}$  lies on line E (Fig. 7) (increasing number of iodine atoms in the methane molecule) and by using data in Tables II and III its calculated  $r$  value on SP-1000 is 203. Fig. 7 also shows that  $\text{CH}_3\text{I}$  lies on line B and by following the procedure described above the calculated  $r$  value on SP-1000 is 202, in good agreement with that calculated by interpolating line E.

Mixed Br and I trihalomethanes ( $\text{CHBr}_2\text{I}$ ,  $\text{CHBrI}_2$ ) belong to line C and mixed Cl and I trihalomethanes ( $\text{CHCl}_2\text{I}$ ,  $\text{CHClI}_2$ ) to line D (Fig. 7). Parameters of eqn. 17 for lines C and D (Table II) and  $\Delta$  values (Table IV) can be used to calculate both  $r$  and  $p^\circ$  values shown in Table V. The  $p^\circ$  values obtained by using the experimental data measured on polar and non-polar stationary phases are very similar, although many values were calculated by starting from the  $r$  value for  $\text{CH}_3\text{I}$ , available only on the non-polar stationary phase.

The fine structure of the  $\log r$  vs.  $\log p^\circ$  plots is also shown by haloethanes and -ethenes (Fig. 8). Closed circles represent compounds whose  $r$  and  $p^\circ$  values are experimentally known, and open circles compounds whose  $r$  values were measured on a non-polar OV-1 column. The straight line M relates to the haloethenes and the non-symmetrical haloethanes, and line N to the symmetrical haloethanes. Lines P, Q and R connect the compounds obtained by symmetrical or non-symmetrical



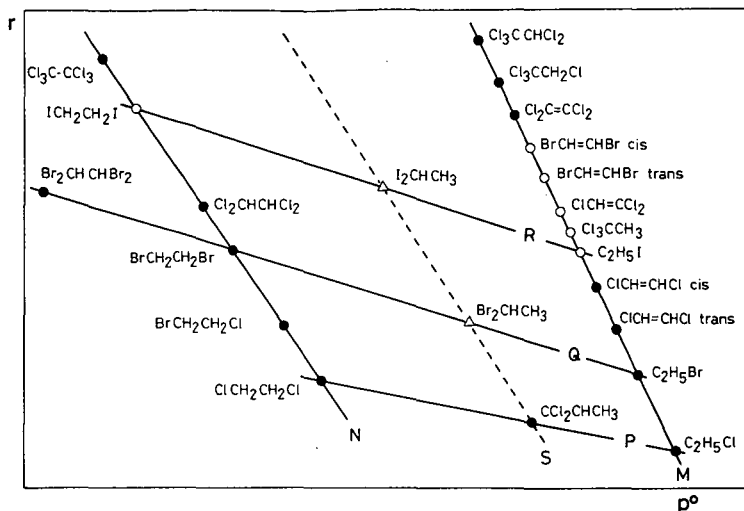


Fig. 8. Arbitrary scale enlargement of a section of Fig. 4 (OV-1, 100°C), showing the fine structure of lines where haloethanes and ethenes belonging to different homologous serie lie. ●, Experimental values; ○, calculated values.  $\Delta$  (Dashed line), probable position of non-symmetrical dihaloethanes (see text).

substitution of an increasing number of halogen atoms on the ethane molecule. Parameters of the straight-line equations for lines M, N, P, Q and R are shown in Table VI, and permit  $p^\circ$  values to be calculated for the compounds as listed in Table VII.

Hyperfine structure that cannot be appreciated with the experimental accuracy of  $r$  values is probably present in this instance also. The empirical attribution of a compound to a given straight line on the basis of experimental data can permit the calculation of its  $p^\circ$  value. As an example, the calculation of  $p^\circ$  for  $\text{Br}_2\text{CHCHBr}_2$  by using the parameters of line Q (Table VI) and experimental  $r$  value (Table I) gives a value of 6.9, similar to the value of 6.3 found in the literature [21]. Other regular behaviour (e.g., the dashed line S in Fig. 8 that connects the non-symmetrical dihaloethanes) can probably be used for the calculation of  $p^\circ$  and  $r$  values, but experimental data so far available do not permit this hypothesis to be verified.

TABLE VI

SLOPE  $s$  AND INTERCEPT  $i$  OF EQN. 17 CALCULATED FROM RETENTION DATA MEASURED ON NON-POLAR OV-1 COLUMN

Data refer to the line shown in Fig. 8. Correlation coefficients for all lines  $>0.99$ .

Line	$s$	$i$
M	-1.23	2.94
N	-1.20	2.81
P	-1.54	2.69
Q	-1.39	2.85
R	-1.33	2.91

TABLE VII

$p^\circ$  VALUES CALCULATED WITH PARAMETERS IN TABLE VI FOR VARIOUS COMPOUNDS SHOWN IN FIG. 6, AND  $p^\circ$  AND  $r$  VALUES CALCULATED BY USING  $\Delta$  VALUES IN TABLE IV

Compound	$p^\circ$ (Torr)	$r$
C <sub>2</sub> H <sub>5</sub> I	1987	
ClCH=CHCl	1021	
BrCH=CHBr ( <i>trans</i> )	726	
BrCH=CHBr ( <i>cis</i> )	573	
ICH <sub>2</sub> CH <sub>2</sub> I	66	
BrCH <sub>2</sub> CH <sub>2</sub> I	152	3.33
ClCH <sub>2</sub> CH <sub>2</sub> I	288	1.97

### CONCLUSIONS

The suggested method permits the relative retention of a given compound not available as a standard to be predicted with an acceptable accuracy and the choice of possible identification in a complex chromatogram to be restricted to a few compounds.

When two or more compounds have very close retention times, this permits the elution order to be calculated to predict if the column efficiency is high enough for the separation of the peaks or to calculate the number of theoretical plates necessary to obtain the minimum resolution [22].

### ACKNOWLEDGEMENTS

This work was supported by the Ministero della Pubblica Istruzione, Italy. The authors gratefully acknowledge the cooperation of Mrs. Graziella Bitossi in the preparation of this paper.

### REFERENCES

- 1 K. C. Swallow, N. S. Shifrin and P. J. Doherty, *Environ. Sci. Technol.*, 22 (1988) 13.
- 2 M. N. Hasan and P. C. Jurs, *Anal. Chem.*, 60 (1988) 978.
- 3 A. Robbat, G. Xyrafas and D. Marshall, *Anal. Chem.*, 60 (1988) 982.
- 4 W. P. Eckel, *Hazardous Waste Hazardous Mater.*, 6 (1989) 43.
- 5 F. Morishita, Y. Terashima, M. Ichise and T. Kojima, *J. Chromatogr. Sci.*, 21 (1983) 209.
- 6 C. H. Collins, C. A. Bertran, A. L. Pires Valente, P. A. de Leone, A. L. Murta and K. E. Milina, *Chromatographia*, 26 (1988) 168.
- 7 N. Dimov and R. Milina, *J. Chromatogr.*, 463 (1989) 159.
- 8 A. Sabljic, *J. Chromatogr.*, 314 (1984) 1.
- 9 G. Castello and T. C. Gerbino, *J. Chromatogr.*, 437 (1988) 33.
- 10 L. Soják and J. Janák, *Anal. Chem.*, 45 (1973) 293.
- 11 L. Soják, J. Krupčík and J. Janák, *J. Chromatogr.*, 195 (1980) 43.
- 12 G. Castello, M. Berg and M. Lunardelli, *J. Chromatogr.*, 79 (1973) 23.
- 13 H. Purnell, *Gas Chromatography*, Wiley, Chichester, 1962.
- 14 J. Tackács, P. Raycsányi, L. Káplár and I. Olácsi, *J. Chromatogr.*, 41 (1969) 438.
- 15 E. Kováts, *Helv. Chim. Acta*, 41 (1958) 1915.
- 16 G. Castello and G. D'Amato, *J. Chromatogr.*, 58 (1971) 127.

- 17 G. J. Pierotti, C. H. Deal, E. L. Derr and P. E. Porter, *J. Am. Chem. Soc.*, 78 (1956) 2989.
- 18 D. A. Leathard and B. C. Shurlock, in J. H. Purnell (Editor), *Progress in Gas Chromatography*, Wiley, New York, 1968, p. 1.
- 19 E. F. G. Herington, in P. H. Desty (Editor), *Vapour Phase Chromatography*, Butterworths, London, 1957, p. 5.
- 20 C. S. G. Phillips and P. L. Timms, *Anal. Chem.*, 35 (1963) 505.
- 21 R. C. Weast (Editor), *CRC Handbook of Chemistry and Physics*, Chemical Rubber, Cleveland, OH, 51st ed., 1970.
- 22 J. H. Purnell, in F. Bruner (Editor), *The Science of Chromatography*, Elsevier, Amsterdam, 1985, p. 362.



## Adsorption/thermal desorption for the determination of volatile organic compounds in water

MICHAEL E. ROSEN and JAMES F. PANKOW\*

*Department of Environmental Science and Engineering, Oregon Graduate Institute, 19600 NW Von Neumann Drive, Beaverton, OR 97006 (U.S.A.)*

(Received May 16th, 1990)

---

### ABSTRACT

An adsorption/thermal desorption (ATD) method for volatile organic compounds is developed using small bed volume (0.68 cm<sup>3</sup>) cartridges of the sorbent Tenax-TA. The method allows an ATD cartridge to be desorbed and analyzed with *ca.* 30  $\mu$ l of residual water still on the cartridge. The method employs a water trap between the ATD thermal desorber and the capillary column. Results obtained indicate that (1) column plugging by ice can be avoided completely, (2) the water trap has a high transmission efficiency, (3) excellent chromatography can be obtained and (4) good comparability of results is obtainable between purge and trap and ATD for many volatile organic compounds at concentrations ranging for fractions of  $\mu$ g/l to hundreds of  $\mu$ g/l.

---

### INTRODUCTION

Adsorption/thermal desorption (ATD) is a method that can be used for the determination of organic compounds in both air and water [1,2]. During the adsorption (sampling) step, the sample is passed at a controlled flow-rate through a cartridge containing the sorbent Tenax. If the sorption takes place efficiently, the cartridge effluent will be essentially free of analytes. Following aqueous sampling, most of the water in the sorbent bed is removed, the cartridge is thermally desorbed, and the analytes are focussed on a capillary gas chromatography (GC) column using whole column cryotrapping (WCC).

The advantages of ATD are its sensitivity and wide range of compound applicability. With aqueous samples containing 1,1,1-trichloroethane (1,1,1-TCA), ATD can be used with sample volumes of the order of 50 ml; for polycyclic aromatic hydrocarbons (PAHs), sample volumes of many liters can be used. Detection limits are in the low  $\mu$ g/l range for 1,1,1-TCA, and in the low ng/l range for PAHs. Prior work in our laboratory with aqueous ATD has emphasized compounds of volatility equal to or less than that of 1,1,1-TCA. Therefore, up to now, many important volatile organic compounds (VOCs) have not been considered in the context of ATD.

As a class, VOCs in water can be determined by purge and trap (P&T), or by the very simple method of purge with whole column cryotrapping [3,4] (P/WCC). However, since dissolved VOCs can be lost during sampling, the availability of an

ATD-based method applicable to the full range of VOCs will be advantageous. For example, ATD allows direct *in situ* sampling in groundwater wells and in surface waters in a manner that avoids volatilization losses [5]. Following sampling, the small ATD cartridge can be returned to the laboratory for analysis.

In order to develop ATD for VOCs, a technique was needed that would separate the residual water on a sample cartridge from the VOCs without also losing large portions of the analytes. Indeed,  $\mu\text{l}$  quantities of water can plug a capillary GC column under WCC conditions. The repeated injection of 2  $\mu\text{l}$  of water can also cause a loss in reproducibility when detection is by mass spectrometry [4]. The centrifugation/vacuum desiccation procedure for ATD cartridges developed by Pankow and Isabelle [6] for semi-volatile compounds cannot be used for VOCs due to unacceptable losses during the vacuum step [2]<sup>a</sup>. Losses will also occur with the desiccation methods of Bertsch *et al.* [7] and Versino *et al.* [8]. However, the water trap technique described by Pankow [4] can remove large amounts of water from a gas stream while still allowing volatile analytes to pass quantitatively onto a GC column.

Use of the Pankow [4] water trap to desiccate a hot, moist gas stream provides for the condensation of water in a short trap packed with glass beads. Condensation will occur whenever the temperature of the trap is below the dewpoint of the original gas stream; if the trap is cooled to a low, subambient temperature, a high desiccation efficiency can be obtained. (Even when some cooling is used, very volatile analytes will pass directly onto the column. Less volatile analytes may be partially condensed in a cold water trap; once the transfer of analytes is nearly ended, the trap can be returned to ambient temperature for a short period to transfer condensed analytes to the column.) In general, the overall transfer efficiency of the water trap will be very high for VOCs since the volume of condensed water will be small.

The water trap is ideally suited for use in an ATD-based method for VOCs. Such a trap can be placed between an ATD desorber and the column. A cartridge from which only the bulk of the water has been removed by centrifugation can then be desorbed. This paper describes the development of that application; cooling of the water trap was not employed.

## EXPERIMENTAL

### *Basic methodologies*

Cartridges were prepared according to methods described by Pankow and co-workers [2,5]. Briefly, each sorbent cartridge was constructed of Pyrex glass. Each 0.68 cm<sup>3</sup> bed volume was packed with *ca.* 0.13 g of 60/80 mesh Tenax-TA (Alltech Assoc., Deerfield, IL, U.S.A.). Small plugs of silanized glass wool held the Tenax in place. Cartridges were cleaned by a combined solvent extraction/thermal desorption procedure. Prior to introduction of sample water to a cartridge, a mild vacuum was pulled on the cartridge to maximize wetting when the water flow was initiated. After sampling, each cartridge was centrifuged at 3500 rpm for 10 min, leaving *ca.* 30  $\mu\text{l}$  of water on the cartridge. The thermal desorption apparatus used has been described by

---

<sup>a</sup> A 20-min vacuum desiccation of a cartridge from which the bulk of the water has been removed by centrifugation causes unacceptable losses for compounds with Henry's gas law constants of  $2 \cdot 10^{-3}$  atm m<sup>3</sup>/mol, or greater [9].

Pankow *et al.* [2]. The Hewlett-Packard 5790 GC used was interfaced to a Finnigan 4000 mass spectrometer/data system (MS/DS) as described by Pankow and Isabelle [10].

### Water trap

Fig. 1 is a schematic diagram illustrating the water trap and its position between the desorber and the GC. An 8 cm long piece of 0.32 cm O.D.  $\times$  0.22 cm I.D. stainless-steel (SS) tubing filled with 0.5 mm diameter glass beads served as the water trap. The beads were held in place using small plugs of glass wool. A small aluminum block which could be heated with a 150-W cartridge heater surrounded the trap. The temperature in the block was measured using a thermocouple.

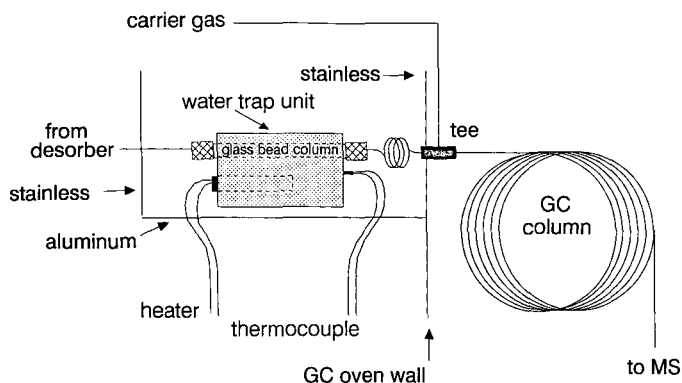


Fig. 1. Schematic diagram showing GC location of water trap unit between ATD desorber and GC column. Gas line connected to tee inside of GC oven supplied carrier gas for backflushing the water trap and for the GC run.

The water trap system was housed in an open aluminium box measuring  $6.4 \times 6.4 \times 15.2$  cm. One end of the box was mounted on the front of the GC. The other end served as a mounting plate for the desorber. Six 0.64 cm diameter holes were drilled in the floor of the box to permit air circulation through the box. The ends of the box were of SS to help insulate the box from the GC and from the desorber.

The water trap was connected to the desorber and the column using 1/16 in. O.D. SS tubing and Swagelok reducing unions. The 8-cm long piece of tubing for the trap/column connection was coiled and was connected to a SS union tee mounted on the endplate of the box. This coil provided additional thermal isolation from the GC oven. The fused-silica capillary GC column used was 30 m long with a "megabore" I.D. of 0.53 mm. The phase was DB-624 with a  $3.0 \mu\text{m}$  film thickness (J&W Scientific, Folsom, CA, U.S.A.). The column was inserted into the GC end of the tee, and to the midpoint of the tee. The connection was made with a Vespel/graphite ferrule. The middle arm of the tee was connected to an auxiliary source of carrier gas that was used after the desorption and during the actual GC run. A 0.64 cm O.D. SS tube connected to a small carbon vane air pump was inserted through one of the holes in the floor of the box and served to keep the water trap system at ambient temperature during the

desorption. Of special interest in this regard was avoiding the formation of any cold zones in the line leading from the trap into the GC.

#### *Desorption procedure*

Each cartridge was desorbed for 5 min at 250°C (column head pressure, 10 p.s.i.; column flow-rate, 9 ml/min). The WCC temperature used during the desorption was -30°C. The use of a megabore column helped prevent the column from plugging with ice during the desorption. The trap remained at ambient temperature during the desorption. After the desorption, a valve was switched and flow was diverted from the desorber to the lower carrier line (LCL) leading to the SS tee. At the same time, the GC oven temperature was first raised ballistically to 10°C, then upwards at 5°C/min. For the GC run, the LCL provided carrier gas at 10 p.s.i. and 9 ml/min with the "sweep" line of the desorber in the open position. After beginning the GC run, the cartridge heater in the aluminum block was activated for 5 min. This heated the water trap to 150°C to backflush water and any residual analytes out of the trap and then out of the sweep line of the desorber. In preparation for the next run, the temperature of the desorber was then brought back to ambient temperature with coolant water, and the water trap was brought back to ambient with the compressed air.

#### *"Dry" vs. wet standards comparison*

A series of analyses were performed to compare the response of the system when desorbing cartridges containing just 2  $\mu$ l of a methanol standard solution, vs. cartridges containing the same amount of standard plus 30  $\mu$ l of water. The methanol standard contained ca. 50 ng/ $\mu$ l of a series of VOCs and internal standard compounds. The raw MS area for the main quantitation ion of each compound was determined for each analysis. The mean areas were compared for the two different types of analyses.

#### *Analysis of actual groundwater samples*

Groundwater samples were collected on 6/20/86 from a well located in Repauno, NJ, U.S.A. Using procedures described by Rosen [9], eight replicate samples were collected at the surface for analysis by ATD, and eight were collected for analysis by capillary P&T using WCC as described by Pankow and Rosen [11].

## RESULTS AND DISCUSSION

#### *Prevention of column plugging*

The water trap was found to remove enough water from the cartridge desorption analysis stream to consistently prevent the column from plugging with ice during the WCC trapping step. In fact, during the analysis of over 60 samples (see also Rosen [9]), the column never plugged. Tests showed that even 70  $\mu$ l of water could be desorbed from a cartridge without plugging the column. Indeed, the amount of water transferred to the column will be independent of the amount of water desorbed from the cartridge to the trap. The factors affecting the efficiency of the trap are discussed in detail by Pankow [4].

#### *"Dry" vs. wet standards comparison*

Table I presents average responses for the analyses of the wet and "dry"



TABLE I

AVERAGE GC-MS AREA COUNTS  $\pm$ S.D. FOR 100 ng EACH OF SELECTED COMPOUNDS DESORBED FROM DRY AND WET ATD CARTRIDGES (THREE REPLICATES EACH)

30  $\mu$ l of water on each wet cartridge

Compound	Dry cartridge	Wet cartridge
1,1-Dichloroethane	73 300 $\pm$ 692	60 900 $\pm$ 9320
Bromochloromethane	35 300 $\pm$ 607	31 800 $\pm$ 479
Trichloromethane	55 000 $\pm$ 894	52 900 $\pm$ 269
Benzene	162 000 $\pm$ 3160	148 000 $\pm$ 1200
Trichloroethene	38 000 $\pm$ 809	30 100 $\pm$ 255
1-Chloro-2-bromopropane	41 600 $\pm$ 137	39 300 $\pm$ 548
Tetrachloroethene	21 200 $\pm$ 184	19 100 $\pm$ 275
1,4-Dichlorobutane	192 000 $\pm$ 1910	213 000 $\pm$ 6340
1,1,2,2-Tetrachloroethane	68 200 $\pm$ 2440	87 300 $\pm$ 2830

standards for VOCs with a range of volatilities. The reproducibilities for both sets of standards were very good. In some cases, the responses for compounds desorbed from wet cartridges were slightly higher than the responses obtained from dry cartridges, and *vice versa*. Though relatively small, in some cases, the differences were statistically significant at the 95% confidence level. As discussed below, incomplete transmission through the trap due to analyte retention in the 30  $\mu$ l of condensed water could not have been responsible for significant losses. The differences were most likely due to the fact that water transferred to the column during the cartridge desorption affected: (1) the column flow-rate and therefore the analyte concentrations in the MS source; and (2) the MS source ionization characteristics. Though not used here, Pankow [4] has recommended using the water trap at a subambient temperature so as to minimize such effects by condensing as much water as possible in the trap. In any event, the amount of water placed on the standard cartridges should always be similar to the amount on the sample cartridges.

#### *Transmission efficiency of the water trap*

A lower limit for the transmission efficiency of the water trap for a given analyte will be given by [4]

$$E \approx \{1 - \exp[-(H/RT)(V_g/V_s)]\} \cdot 100\% \quad (1)$$

where  $H$  is the Henry's gas law constant of the analyte (atm m<sup>3</sup>/mol),  $R$  is the gas constant (8.2  $\cdot$  10<sup>-5</sup> m<sup>3</sup> atm/mol K),  $T$  is temperature (K),  $V_g$  is the volume of gas that flows past the water condensed in the trap, and  $V_s$  is the volume of condensed water. The value of  $E$  will decrease as  $H$  decreases. Most VOCs have  $H$  values significantly greater than 1  $\cdot$  10<sup>-4</sup> atm m<sup>3</sup>/mol. For a desorption carrier gas flow-rate of 9 ml/min, a transfer time of 5 min will give  $V_g = 45$  ml. Thus, under the conditions of this work, for  $V_s = 0.030$  ml, at  $T = 293$  K, we obtain  $E \approx 100\%$  for all VOCs. This theoretical result was verified experimentally by: (1) analyzing a wet standard cartridge without back-flushing the trap; then (2) re-analyzing it. The re-analysis allowed analytes

a second chance to move onto the column: just trace amounts of a few less volatile compounds were found in the resulting chromatogram.

### Chromatography

Fig. 2 presents a typical total ion chromatogram for the analysis of a wet standard cartridge. The analyte peaks were very sharp, and most were baseline resolved. All analytes in the chromatogram exhibited peak widths of no more than 10 s, *i.e.*, peak widths as sharp as can be obtained on a column of this bore. Background contamination obscured the first peak. However, the extracted mass chromatogram for the primary quantitation ion for that compound was clean and sharp.

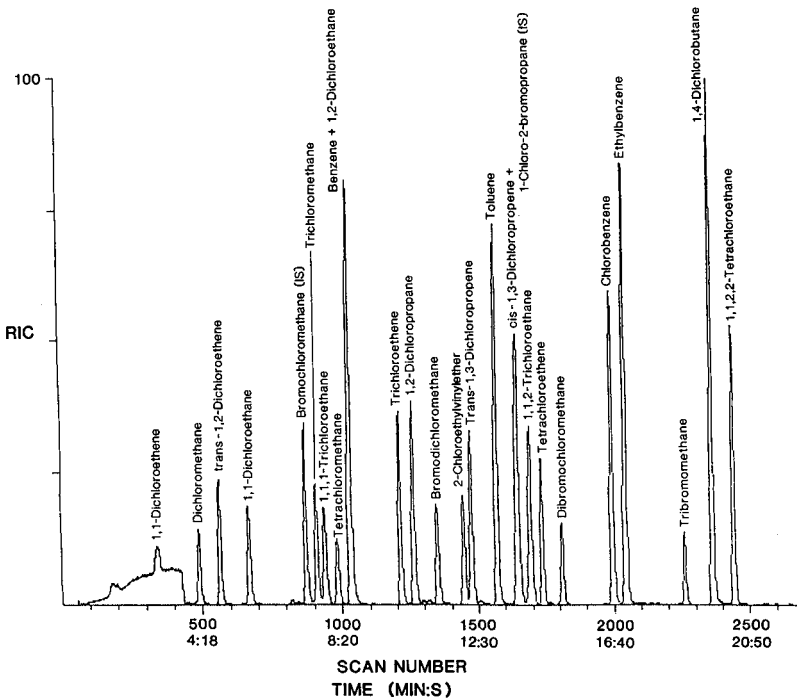


Fig. 2. Chromatogram obtained analyzing a wet cartridge for a range of VOCs. Each peak represents 100 ng.

### Comparison of ATD with results obtained by P&T

The results of the analyses of the groundwater samples collected at a well in Repauno, NJ, U.S.A. are presented in Table II. The ATD and P&T results are quite comparable for a wide range of compounds and concentrations.

TABLE II  
COMPARISON OF ATD AND P&T/WCC RESULTS FOR SAMPLES FROM REPAUNO, NJ, U.S.A.  
[9]

Compound	Method	Mean conc. <sup>a</sup> ( $\mu\text{g/l}$ )	S.D. ( $\mu\text{g/l}$ )	C.V. <sup>b</sup> (%)
Dichloromethane	ATD	0.24	0.037	15.0
	P&T/WCC	ND <sup>c</sup>	—	—
<i>cis</i> -1,2-Dichloroethene	ATD	1.9	0.035	1.8
	P&T/WCC	2.7	0.37	14.0
Trichloromethane	ATD	29.0	0.53	1.8
	P&T/WCC	32.0	0.64	2.0
1,2-Dichloroethane	ATD	1.4	0.083	5.9
	P&T/WCC	1.1	0.095	8.6
Tetrachloromethane	ATD	1.8	0.12	6.7
	P&T/WCC	1.4	0.035	2.5
Benzene	ATD	18.0	0.53	2.9
	P&T/WCC	20.0	0.83	4.2
Trichloroethane	ATD	35.0	0.52	1.5
	P&T/WCC	35.0	1.3	3.7
Toluene	ATD	0.15	0.010	6.7
	P&T/WCC	NQ <sup>d</sup>	—	—
Tetrachloroethene	ATD	340.0	20.0	5.9
	P&T/WCC	370.0	17.0	4.6
Chlorobenzene	ATD	36.0	2.6	7.2
	P&T/WCC	48.0	1.8	3.8
<i>o</i> -Xylene	ATD	0.34	0.012	3.5
	P&T/WCC	NQ	—	—
Nitrobenzene	ATD	210.0	15.0	7.1
	P&T/WCC	250.0	14.0	5.6

<sup>a</sup> Mean of eight replicates.

<sup>b</sup> C.V. = (S.D./mean conc.) · 100%.

<sup>c</sup> ND = not detected.

<sup>d</sup> NQ = detected, but too low to be quantitated.

#### ACKNOWLEDGEMENTS

This work was financed in part with federal funds from the United States Geological Survey under an Intergovernmental Personnel Agreement dated June 10, 1985. The authors also gratefully acknowledge the assistance of Lorne M. Isabelle in a portion of this work.

#### REFERENCES

- 1 M. P. Ligocki and J. F. Pankow, *Anal. Chem.*, 57 (1985) 1138.
- 2 J. F. Pankow, M. P. Ligocki, M. E. Rosen, L. M. Isabelle and K. M. Hart, *Anal. Chem.*, 60 (1988) 40.
- 3 J. F. Pankow and M. E. Rosen, *Env. Sci. Technol.*, 22 (1988) 398.
- 4 J. F. Pankow, *Env. Sci. Technol.*, 25 (1991) in press.
- 5 J. F. Pankow, L. M. Isabelle, J. P. Hewetson and J. A. Cherry, *Ground Water*, 23 (1985) 775.
- 6 J. F. Pankow and L. M. Isabelle, *J. Chromatogr.*, 237 (1982) 25.
- 7 W. Bertsch, M. E. Anderson and G. Holzer, *J. Chromatogr.*, 112 (1975) 701.

- 8 B. Versino, H. Knoppel, M. DeGroot, A. Peil, J. Poelman, H. Schauenberg, H. Vissens and F. Geiss, *J. Chromatogr.*, 122 (1976) 373.
- 9 M. E. Rosen, *Ph.D. Thesis*, Oregon Graduate Institute, Beaverton, OR, 1988.
- 10 J. F. Pankow and L. M. Isabelle, *Anal. Chem.*, 56 (1984) 2997.
- 11 J. F. Pankow and M. E. Rosen, *J. High Resol. Chromatogr. Chromatogr. Commun.*, 7 (1984) 504.

## Isomer identification and gas chromatographic retention studies of monomeric cyclic fatty acid methyl esters

JOSÉ A. ROJO<sup>a</sup> and EDWARD G. PERKINS\*

*Department of Food Science, Burnside Research Laboratory, University of Illinois, 1208 West Pennsylvania Avenue, Urbana, IL 61801 (U.S.A.)*

(First received April 18th, 1990; revised manuscript received September 7th, 1990)

---

### ABSTRACT

The structural isomers of saturated C<sub>18</sub> cyclic fatty acid methyl esters were identified in a purified heated oil fraction by gas chromatography–mass spectrometry using high resolution capillary columns and selected ions abundance. Empirical mathematical models were developed based on the sequential pattern of elution of *trans*- and *cis*-1,2-disubstituted cyclohexyl fatty acid esters, in order to be able to predict their chromatographic retention characteristics. These models are proposed as an auxiliary technique for the fast identification of the different cyclic fatty acid isomers present in a used fat. The experimental design and the statistical significance of the results are discussed.

---

### INTRODUCTION

The non-urea adducting fraction (NUA-fraction) isolated from heated fats and oils contains the most important toxic substances formed during thermal treatments [1,2]. Among these substances, monomeric C<sub>18</sub> cyclic fatty acids (CFAs) deserve special consideration because of their proven digestive absorbability, hepatic toxicity and biological effects [3–5].

Several analytical approaches have been proposed to determine the amount of CFAs formed in fats and oils. Most are based on quantitative gas chromatography (GC) of the CFA as the corresponding hydrogenated methyl ester derivatives, which are then isolated and concentrated in the NUA fraction [6–9,10]. Concentration of CFA as low as 0.01% can be easily detected in fats and oils using this approach. So far, all the proposed analytical methods for CFA, face a number of limitations such as: uncertainty in CFA identification, lack of resolution of CFA from interfering substances, unavailability of standards (pure CFA), ambiguities in the analytical conditions used and long analysis time per sample. Furthermore, the statistical reliability of these methods has not been properly evaluated.

---

<sup>a</sup> Present address: Proctor & Gamble de Venezuela C.A., M-108, P.O. Box 020010, Miami, FL 33102, U.S.A.

Recently, there has been renewed interest in research on cyclic fatty acids. Several studies on heated fats and oils proved the formation of  $C_{18}$  CFA isomers with a disubstituted cyclopentyl nucleus in addition to the most widely known disubstituted cyclohexyl isomers [6,8,9,11–14]. Next, the chemical synthesis of the former isomers confirmed their proposed structures [15,16]. Concurrently, more selective and efficient analytical methods were developed by applying novel techniques [8,9,10–13]. Sebedio [12] reported a method based on the application of methoxy-bromomercuric acid fractionation for the simpler isolation and characterization of CFA in heated oils. GC coupled with a Fourier transform infrared spectrometer (FT-IR) was used to characterize the geometry of the ethylenic bonds of CFA fractions [13] prepared by a multi-step procedure including high-performance liquid chromatography (HPLC) [9]. GC–mass spectrometry (MS) using high-resolution capillary columns has been shown to be the best alternative for the analysis and structure characterization of CFA [8–12]. This technique offers the unique possibility of identifying and quantifying individual cyclohexyl and cyclopentyl  $C_{18}$  CFA isomers contained in NUA fractions. Although many improvements have been achieved [10], auxiliary techniques to facilitate isomer identification, when GC–MS facilities are not available, have not received much attention.

In this study we describe the use of empirical mathematical models to predict and/or confirm the chromatographic retention characteristics of individual isomeric  $C_{18}$  hydrogenated cyclic fatty acid methyl esters (HCFAM). The models were developed based on the sequential pattern of elution of the different cyclic isomers at several isothermal conditions. GC–MS was used for initial isomer identification. The statistical evaluation and significance of the final models are discussed.

## EXPERIMENTAL

### *Materials*

GC reference fatty acid methyl ester (FAME) mixture containing equal amounts of saturated esters for equivalent chain length (ECL) calculation were purchased from Nu-Check Prep. (Elysian, MN, U.S.A.). All solvents used were nongrade quality.

### *Isomeric mixtures of $C_{18}$ cyclic fatty acids*

Methyl esters of  $C_{18}$  HCFAM prepared by alkaline isomerization of linseed oil according to Eisenhower *et al.* [17] and Friedrich *et al.* [18], were further purified by urea fractionation as described by Rojo and Perkins [10]. Purity of the isomeric mixtures determined by GC–MS was over 95%.

### *Capillary gas chromatography*

The system used was a Hewlett-Packard 5790A capillary gas chromatograph (Avondale, PA, U.S.A.) equipped with an inlet splitter system fitted with a Jennings glass liner, flame ionization detector and electronic integrator (HP 3390A). Three fused-silica wall-coated open tubular capillary columns (Supelco, Bellefonte, PA, U.S.A.) of different relative 'polarity' were used with this system. In order of increasing polarity they are: column A: 30 m  $\times$  0.25 mm I.D. coated with SPB®-1 (dimethylpolysiloxane bonded phase), 0.25  $\mu$ m film thickness; column B: 30 m  $\times$  0.25

mm I.D. coated with Supelcowax®-10 (polyethylene oxides bonded phase), 0.25  $\mu\text{m}$  film thickness; and column C: 100 m  $\times$  0.25 mm I.D. coated with SP-2560 (blend of cyanoalkylpolysiloxanes), 0.20  $\mu\text{m}$  film thickness. The columns were operated at isothermal and/or programmed temperature conditions in the range 140 to 250°C as specified. The carrier gas was hydrogen at a split ratio 1:100 and average linear velocities in the range 32–50 cm/s were set by adjusting accordingly the column head pressure for each column. The injector port and detector temperatures were 250°C and 270°C, respectively.

#### GC-MS

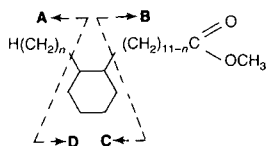
A Hewlett-Packard 5985B GC-MS system was used with the chemical ionization-electron impact (CI-EI) source set at 70 eV and 200°C. The capillary columns specified above were also used with this system. Each column was interfaced directly to the mass spectrometer and operated at the specified temperature, using helium as the carrier gas, with a split ratio of 1:20 using column pressures below 10 p.s.i. in order to compensate for the vacuum existent at the column end connected to the mass spectrometer system. The injector port temperature was 250°C. For CI mode, methane was used as the reactant gas.

#### Model fitting methodology for retention data of HCFAM

The isomeric mixture of HCFAMs was used to obtain retention data at selected temperatures of individual  $\text{C}_{18}$  methyl  $\omega$ -(2-*n*-alkylcyclohexyl) alkanooate structural isomers (mol.wt. 296). The isomers were identified by their individual mass fragmentation pattern as previously described [8,14]. A series of seven structural isomers ( $1 \leq n \leq 7$ ), each one separated as a pair of *trans*- and *cis*-ring isomer peaks, were detected during GC-MS. The retention data were obtained in an experiment designed to evaluate the effect of temperature on the retention profile of each group of isomeric HCFAM (either *cis* or *trans*). The effect was measured at two levels of constant column head pressure, 10 and 15 p.s.i. and every 10°C in the range of 160 to 210°C. The capillary column selected for this experiment was a new fused-silica Supelcowax®-10 with the specifications outlined above and operated under split conditions using hydrogen as a carrier gas. The data expressed as ECL [19] were fitted by the linear least squares method into polynomial equations with two independent variables, namely, the structural parameter *n* in the general formula and temperature. Several linear combinations of the independent variables were tested for statistical significance in order to build up the model. Statgraphics® software for microcomputers (STSC, Rockville, MD, U.S.A.) was used for this purpose.

#### RESULTS AND DISCUSSION

A combination of GC-MS and high-resolution gas chromatography (HRGC) was used to study the GC-retention profile of individual  $\text{C}_{18}$  HCFAMs. EI GC-MS of compounds eluted from capillary columns of different selectivity and "polarities", was carried out to identify all the HCFAM structural isomers present in the mixture. The procedure used for the identification is illustrated in Fig. 1. The expected MS fragmentation pattern of the cyclohexyl isomers has been already described in the literature [6] and is characterized by the formation of four important ions:



The presence of molecular ion at  $m/e$  296 (confirmed by CI GC-MS) combined with relatively selected ion abundance of the most characteristic ion fragment of each isomer enables its conclusive identification in the mixture. For each structural isomer, characterized by the parameter  $n$ , one pair of two ring isomers, *cis* and *trans*, was detected as shown in Fig. 1.

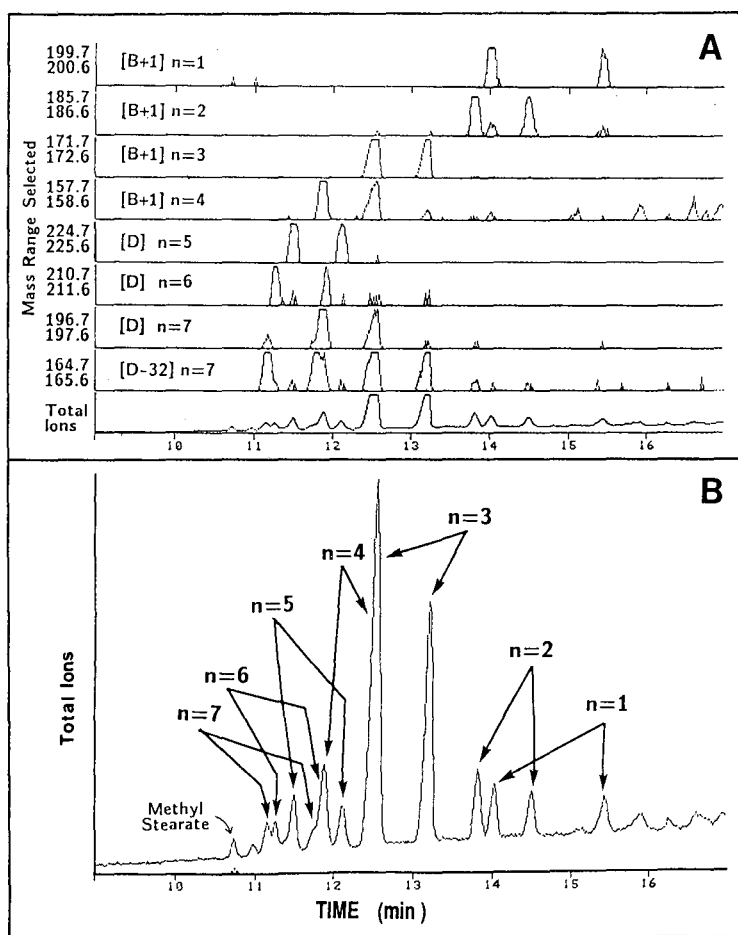


Fig. 1. GC-MS identification of HCFAM isomers in NUA-fractions prepared from linseed oil. (A) Relatively selected ion abundance of most specific ion fragments of HCFAM isomers. (B) Total ion chromatogram showing final peak identification. Conditions: initial temperature  $190^\circ\text{C}$ , raised up to  $210^\circ\text{C}$  at  $1.5^\circ\text{C}/\text{min}$ ; column B (Supelcowax-10); carrier gas helium. EI GC-MS, source at 70 eV and  $200^\circ\text{C}$ .



The ion fragment  $B + 1$ , which results after the rearrangement and addition of a hydrogen atom, was found to be very specific for the identification of the first four isomers of the series. As the size of the lateral alkyl chain,  $H(CH_2)_n$ , increases ( $n > 4$ ), fragment  $D$ , produced by  $\alpha$ -cleavage next to the ring, and the ion  $D - 32$  resulting from loss of methanol from  $D$ , both become more specific for the identification of the other members of the series. The identification of isomers with  $n > 7$ , is more difficult because of lack of resolution from other isomers and due to their relatively small concentration in the isomeric mixture.

It has been generally assumed that, under GC conditions for separation of FAME in polar capillary columns, the retention region for HCFAM lies between methyl stearate (18:0) and methyl arachidate (20:0). However, the possibility that some cyclic monomers may have retention times shorter or equal to methyl stearate with certain phases has been suggested [20], but no conclusive evidence was shown.

The polarity of the stationary phase is the most important parameter in determining the range of HCFAM elution (Fig. 2). The curves shown in Fig. 2 were obtained by connecting the ECL of all the HCFAM isomers identified by GC-MS for each column. Separate curves for *trans*- and *cis*-isomers are shown. In the least polar column (column A, dimethyl polysiloxane) it was clearly demonstrated that many of the cyclohexyl isomers eluted before 18:0 at 190°C. In addition, the resolution of many cyclic isomers is impaired in these conditions, as shown by the relatively smaller slope of the *cis* and *trans* ECL vs.  $n$  curves for column A in Fig. 2. On the other hand, for the most polar column (column C), two of the *cis*-isomers have ECL greater than 20. Similarly, the relatively greater separation between the *cis*- and *trans*-curves for column C illustrates the improved *cis*-/*trans*-isomer separation possible with this column.

Using column C, it was possible to obtain base-line separation, even under isothermal conditions, of the generally co-eluting pair of methyl *trans*-9-(2'- $n$ -propylcyclohexyl) nonanoate ( $n = 3$ ) and methyl *cis*-8-(2'- $n$ -butylcyclohexyl) octanoate ( $n =$

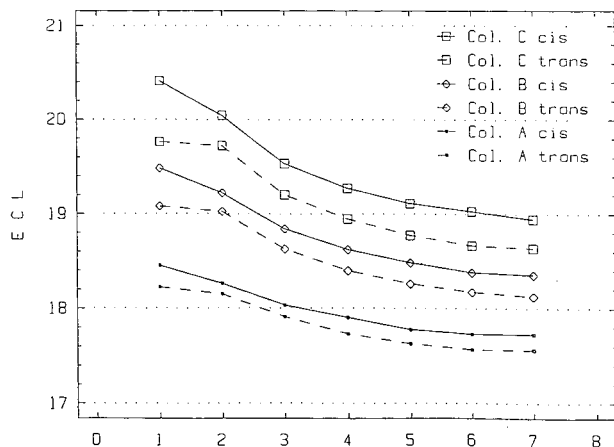


Fig. 2. Equivalent chain length (ECL) of HCFAM isomers in various capillary columns. Oven temperature constant = 190°C; column A: 30 m  $\times$  0.25 mm; SPB-1; column B: 30 m  $\times$  0.25 mm, Supelcowax-10; column C: 100 m  $\times$  0.25 mm, SP-2560.

4). The improved resolution observed for column C, however, should be attributed to the combined effect of stationary phase polarity and column length, when compared to columns A and B. Therefore, better isomer resolution may be achieved by increasing column length in non-polar columns. Finally, the trends observed (Fig. 2) suggest that an interesting alternative to improve HCFAM resolution should be obtained by coupling in series two capillary columns of different selectivity in increasing

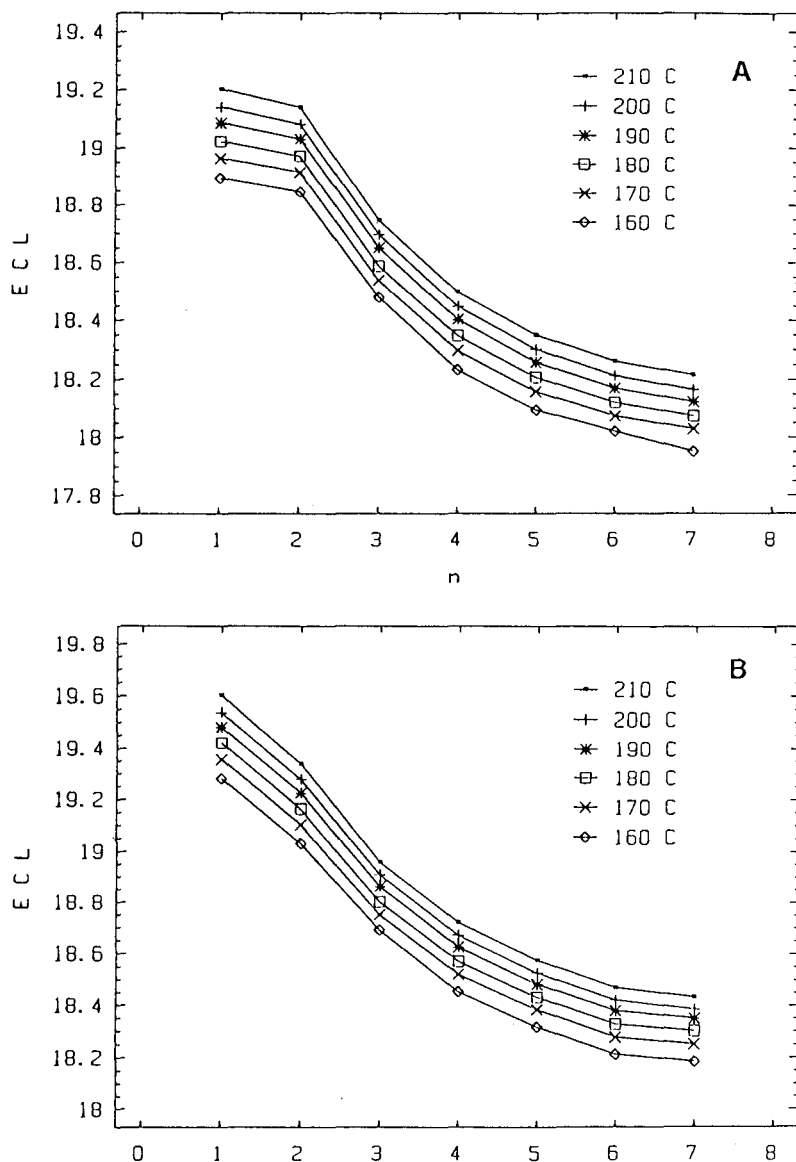


Fig. 3. Equivalent chain length of HCFAM at different temperature levels. (Column pressure 15 p.s.i.). (A) *Trans*-isomers. (B) *Cis*-isomers.

order of polarity. The expected effect is a higher slope and wider separation gap between the ECL *vs.* *n* curves.

For routine purposes, the capillary column B (polyethylene oxides bonded phase) offers good resolution in reasonable time for the most important isomers of HCFAM. Therefore, this column was selected to develop empirical mathematical models to predict the GC retention characteristics, expressed as ECL, of cyclic isomers under different oven temperature conditions.

The initial interest in developing retention models for HCFAM was to address the individual quantification of cyclopentyl as well as cyclohexyl isomers in fresh and heated oils. Furthermore, a more practical interest on these models lies in their application as an auxiliary technique to facilitate the identification of chromatographic peaks in complex mixtures when the availability of pure standards is limited. They become particularly useful in an industrial environment and in laboratories where GC-MS facilities are not readily available.

The results of the experiment performed at 15 p.s.i. constant column head pressure are shown in Fig. 3A and B for *trans*- and *cis*-isomers, respectively. The almost constant separation between ECL *vs.* *n* curves at different temperatures is equivalent to the change in ECL for each particular isomer. This constant change clearly shows the linear effect of oven temperature (*T*) on ECL increase (*n* = constant):

$$\text{ECL} = a + bT$$

TABLE I

DIFFERENCES IN EQUIVALENT CHAIN LENGTH OF HCFAMs AT 15 AND 10 p.s.i. FOR TWO OVEN TEMPERATURES

Average carrier gas linear velocities (cm/s): column pressure 15 p.s.i.: 47.8 (170°C) 45.3 (210°C); column pressure 10 p.s.i.: 32.2 (170°C) 30.5 (210°C).

Oven temperature (°C)	<i>n</i>	<i>trans</i> -HCFAMs			<i>cis</i> -HCFAMs		
		A, 15 p.s.i.	B, 10 p.s.i.	A - B	A, 15 p.s.i.	B, 10 p.s.i.	A - B
170°C	1	18.962	18.964	0.002	19.355	19.361	0.006
	2	18.912	18.914	0.002	19.101	19.106	0.005
	3	18.537	18.526	0.011	18.749	18.743	0.006
	4	18.296	18.299	0.003	18.519	18.523	0.004
	5	18.156	18.163	0.007	18.382	18.388	0.006
	6	18.072	18.079	0.007	18.276	18.283	0.007
	7	18.028	18.032	0.004	18.249	18.262	0.013
		Average:		0.0051	Average:		0.0067
210°C	1	19.200	19.205	0.005	19.602	19.613	0.011
	2	19.138	19.142	0.004	19.337	19.345	0.008
	3	18.744	18.725	0.019	18.956	18.943	0.013
	4	18.497	18.499	0.002	18.719	18.722	0.003
	5	18.348	18.354	0.006	18.574	18.578	0.004
	6	18.260	18.269	0.009	18.469	18.476	0.007
	7	18.214	18.222	0.008	18.431	18.445	0.014
		Average:		0.0076	Average:		0.0086

The same experiment was conducted at 10 p.s.i. column pressure and very similar results were obtained (Table I). When, paired observations for the two pressure levels studied at two selected temperatures were compared, the deviations are smaller than 0.02 in all cases and may be attributed to the change in column efficiency with the change in gas linear velocity between pressure levels.

To broaden the scope of the model inference, the ECL values for each isomer obtained at both column pressure levels were used as independent replicates for statistical analysis and estimation of model parameters. In other words, the deviations were pooled with the overall experimental error and the ECL at both pressure levels were considered as estimates of the same means.

The pooled experimental data for 10 and 15 p.s.i. were used to fit a second degree polynomial illustrated by the equation:

$$y_i = b_0 + b_1x_{1i} + b_2x_{2i} + b_{11}x_{1i}^2 + b_{22}x_{2i}^2 + b_{12}x_{1i}x_{2i}$$

in which  $y_i$  represent the ECL,  $x_{1i}$ , the oven temperature in °C, and  $x_{2i}$  is the reciprocal of the isomer structural parameter  $n$  ( $1/n$ ) in the general formula of HCFAM given above. Other predictor variable and data transformations were attempted, but their coefficients of determination ( $R^2$ ) were generally much lower than those for the former combination. The estimated regression coefficients and their 95% confidence interval were shown in Table II for *cis*- and *trans*-HCFAM.

The statistical analysis of the model was carried out as described by Deming [21]. These results are included in Table III. The overall  $F$ -ratio associated with the complete second degree equation, that is  $F = MS_{\text{factors}}/MS_{\text{residual}}$ , is a measure of the goodness of fit of the model. For *trans*- and *cis*-HCFAM ECL models, the corresponding  $F$ -values are respectively 700 and 1400 times larger than the tabulated critical values at  $p = 0.001$  significance level, implying that the fitted surface of the models is worthy of interpretation.

TABLE II  
MODEL FITTING RESULTS

Regression coefficients and their 95% confidence intervals.

Model	Regression coefficient	Estimate	Standard error	95% Confidence interval	
				Lower limit	Upper limit
<i>trans</i> -HCFAM	$b_0$	16.512077	0.399654	15.716250	17.307904
	$b_1$	0.006020	0.004328	- 0.002599	0.014638
	$b_2$	4.033373	0.124699	3.785061	4.281685
	$b_{11}$	- 0.000004	0.000012	- 0.000028	0.000020
	$b_{22}$	- 2.744220	0.046186	- 2.836189	- 2.652250
	$b_{12}$	0.001445	0.000607	0.000236	0.002654
<i>cis</i> -HCFAM	$b_0$	16.761162	0.306607	16.150618	17.371705
	$b_1$	0.006363	0.003320	- 0.000248	0.012974
	$b_2$	3.578681	0.095667	3.388181	3.769182
	$b_{11}$	- 0.000005	0.000009	- 0.000023	0.000013
	$b_{22}$	- 2.238535	0.035433	- 2.309092	- 2.167977
	$b_{12}$	0.001837	0.000466	0.000909	0.002765

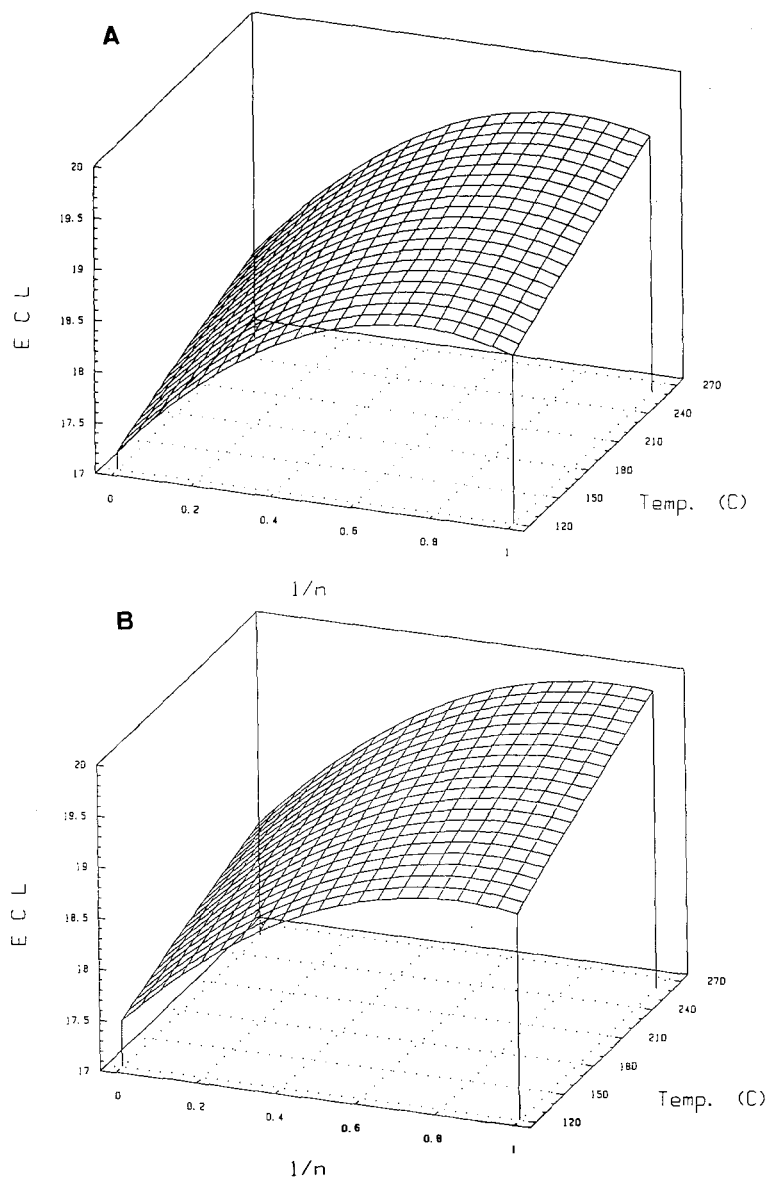


Fig. 4. Fitted polynomial response surfaces. (A) *Trans*-HCFAM isomers; (B) *cis*-HCFAM isomers.

The fitted polynomial response surfaces are illustrated in Fig. 4A and B. Superimposing the surfaces demonstrates that the ECL separation gap between *cis*- and *trans*-isomers, (*i.e.* the space between surfaces) remains practically constant within the temperature range covered by the experiment. This means that isomer separation, in the particular GC column used, cannot be substantially improved by independent manipulation of the oven temperature within the range of column pressure used. In

TABLE III  
ANALYSIS OF VARIANCE (ANOVA) OF LINEAR MODELS FOR ECL OF *trans*- AND *cis*-HCFAM

Source	d.f. <sup>a</sup>	ECL Models		<i>trans</i> -HCFAM		<i>cis</i> -HCFAM		<i>F</i> -ratio
		<i>SS</i> <sup>b</sup>	<i>MS</i>	<i>SS</i>	<i>MS</i>	<i>SS</i>	<i>MS</i>	
Total	84	28760.53	342.387			29516.56	351.388	
Due to the mean	1	28748.56	28748.556			29502.15	29502.150	
Correlation for the mean	83	11.9738	0.1443			14.4096	0.1736	
Due to the factors	5	11.9182	2.3836	3347.38***		14.3769	2.8754	6860.60**
Residuals	78	0.055543	0.0007			0.032691	0.0004	
Lack of fit	36	0.053128	0.0015	25.68**		0.029186	0.0008	9.72**
Pure experimental uncertainty	42	0.002414	0.0001			0.003504	0.0001	
<i>R</i> <sup>2</sup>			0.9954				0.9977	
<i>R</i> <sup>2</sup> (adjusted for d.f.)			0.9951				0.9976	
Standard error of estimate			0.0267				0.0205	

<sup>a</sup> Degrees of freedom.

<sup>b</sup> Sum of squares.

<sup>c</sup> Mean squares.

<sup>d</sup>  $MS_{\text{factors}}/MS_{\text{residual}}$ .

\*\*\* = Significance at  $p = 0.001$  level.

addition, the linear effect of temperature on ECL is shown by the constant slope and lack of curvature of the surfaces in the direction of temperature increase. This is also demonstrated by the extremely small and non-significant value of the regression coefficient for the quadratic temperature term ( $b_{11}$ ) in Table II.

In addition, other conclusions arise by extrapolating the response surfaces to temperature regions not covered by the experiment and normally not used for the particular separation under study with Supelcowax-10 capillary columns. First, many *trans*-HCFAM isomers with high  $n$  values (small  $1/n$ ) elute before methyl stearate (ECL = 18.0) at oven temperatures less than 160°C (Fig. 4A). The same was true for some *cis*-HCFAM isomers (Fig. 4B). Similarly, all of the HCFAM isomers elute before methyl arachidate (ECL = 20) even at temperatures as high as 270°C, close to the upper limit temperature for the stationary phase used. Finally, a word of caution should be outlined here as clearly stated by Cochran and Cox [22]: "The polynomial surface should be regarded only as an approximation to the true function within the region covered by the experiment". Therefore the above outlined predictions outside the region should be experimentally verified before putting reliance on them.

The lowest and highest oven temperature for GC analysis of HCFAM are limited by several analytical considerations. From a practical point of view, temperatures lower than 150°C require extremely high column head pressure to achieve acceptable peak efficiencies for  $C_{18}$  HCFAM in a reasonable elution time. Furthermore, there is a theoretical lowest limit related with the relative volatility of the compounds of interest. The upper temperature limit, however is mainly related with the thermal stability of the analytes and the stationary phase as well.

In order to check the models predictive ability, three chromatographic runs were performed at two isothermal oven temperatures not commonly used for this analysis. In Table IV the predicted and observed ECL values for *trans*- and *cis*-isomers are compared at the two selected temperatures (140 and 240°C) outside the experimental region under study. The relatively small differences, from a practical point of view, prove an acceptable extrapolation ability for the models presented here. Furthermore, the elution of two  $C_{18}$  *trans*-cyclohexyl isomers before ECL = 18 (methyl stearate), as postulated by the models, was confirmed experimentally. Again, the warning concerning extrapolation should be stressed here since the models represented by the regression surfaces are only an approximation to the true situations.

To make assertions about the adequacy of the function estimation, in a statistical sense, the  $F$ -test for lack of fit should be considered, that is  $F = MS_{1of}/MS_{pe}$ . In addition, the assumption that the residuals are normally distributed with constant variance needs also to be confirmed. In Table III, the  $F$ -ratios for lack of fit, calculated as described by Deming [21], exhibit highly significant values for both models. This observation obviously seems to be in conflict with the also highly significant goodness of fit previously outlined. This situation, however, often arises if we use a highly precise measurement process like those used in the area of instrumental analysis. In this case, the  $F$ -test for lack of fit was statistically significant because the estimated variance due to pure experimental uncertainty was relatively very small. Finally, in a practical sense, the residuals were small enough for our particular application and can be considered acceptable when using the described models as auxiliary techniques in the identification of HCFAM isomers.

When examining the distribution of residuals against the predicted values (Fig.

TABLE IV  
COMPARISON BETWEEN PREDICTED AND OBSERVED ECL VALUES OUTSIDE THE TEMPERATURE REGION COVERED BY THE EXPERIMENT

Model	<i>n</i>	240		140		240			
		Observed	Predicted	Difference	Observed	Predicted	Difference	Observed	Predicted
<i>trans</i> - HCFAM	1	19.379	19.382	0.004	18.777	18.775	19.380	19.382	0.003
	2	19.305	19.250	-0.055	18.734	18.715	19.305	19.250	-0.054
	3	18.862	18.901	0.039	18.371	18.390	18.862	18.901	0.039
	4	18.635	18.670	0.035	18.135	18.171	18.636	18.670	0.033
	5	18.488	18.512	0.024	18.000	18.021	18.491	18.512	0.021
	6	18.381	18.400	0.019	17.912	17.913	18.376	18.400	0.024
	7	18.381	18.316	-0.065	17.865	17.832	18.376	18.316	-0.060
<i>cis</i> - HCFAM	1	19.795	19.793	-0.002	19.162	19.155	19.795	19.793	-0.002
	2	19.514	19.462	-0.052	18.917	18.916	19.514	19.462	-0.052
	3	19.083	19.103	0.021	18.583	18.588	19.083	19.103	0.020
	4	18.858	18.877	0.019	18.357	18.377	18.860	18.877	0.017
	5	18.709	18.726	0.017	18.222	18.236	18.712	18.726	0.015
	6	18.588	18.620	0.032	18.103	18.135	18.595	18.620	0.025
	7	18.525	18.541	0.016	18.060	18.060	18.538	18.541	0.002



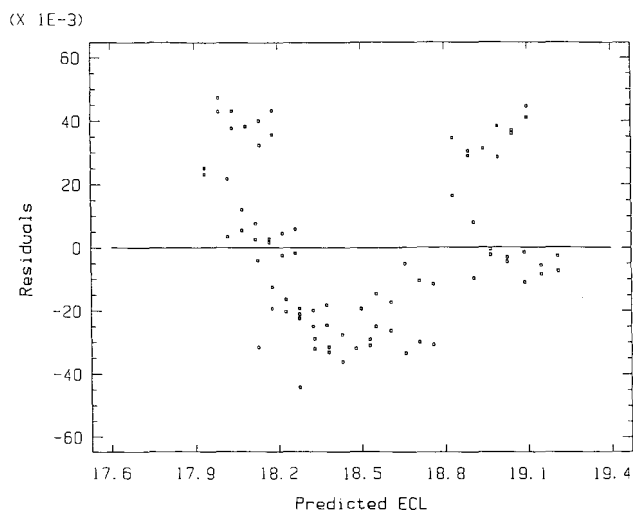


Fig. 5. Residual plot for predicted ECL of *trans*-HCFAM isomers using polynomial equation. (Regression coefficients in Table II; ANOVA in Table III).

5) it becomes apparent that the largest residuals are associated with small and/or large values for ECL (U-shaped distribution). In other words, this indicates that there was some kind of dependence of residuals from the data and the assumption of normal distribution of the error was not supported by the results.

This concern was addressed through examination of the data illustrated by Fig. 3A and B which demonstrate that the ECL values for isomers with  $n = 1$  (*cis* or *trans*) are those that unexpectedly do not follow the apparent uniform exponential decrease trend in ECL observed by the other isomers (with  $n > 1$ ). This suggests that the exclusion of the observations of ECL with  $n = 1$  from the data should drastically

TABLE V

MODEL FITTING RESULTS USING REDUCED DATA (ISOMERS WITH  $2 \leq n \leq 7$ )

Regression coefficients and their 95% confidence intervals

Model	Regression coefficients	Estimate	Standard error	95% Confidence interval	
				Lower limit	Upper limit
<i>trans</i> -HCFAM	$b_0$	16.8422576	0.037506	16.767697	16.917456
	$b_1$	0.004436	0.000195	- 0.004047	0.004826
	$b_2$	2.600720	0.143695	2.313839	2.887601
	$b_{22}$	- 0.7388755	0.112359	- 0.963075	- 0.514435
	$b_{12}$	0.002386	0.000668	0.001052	0.003720
<i>cis</i> -HCFAM	$b_0$	17.083701	0.048204	16.987463	17.179938
	$b_1$	0.004252	0.000251	- 0.003751	0.004753
	$b_2$	2.575192	0.184682	2.206482	2.943902
	$b_{22}$	- 1.043228	0.144408	- 1.331532	- 0.754923
	$b_{12}$	0.003206	0.000858	0.001493	0.004919

TABLE VI  
ANALYSIS OF VARIANCE (ANOVA) OF LINEAR MODELS FOR ECL OF *trans*- AND *cis*-HCFAM USING REDUCED DATA  
Isomers with  $2 \leq n \leq 7$ .

Source	d.f. <sup>a</sup>	ECL Models					
		<i>trans</i> -HCFAM			<i>cis</i> -HCFAM		
		SS <sup>b</sup>	MS <sup>c</sup>	F-ratio <sup>d</sup>	SS	MS	F-ratio
Total	72	24404.74	338.955		24976.68	346.898	
Due to the mean	1	24397.16	24397.158		24969.46	24969.455	
Corr. for the mean	71	7.5824	0.1068		7.2247	0.1018	
Due to the factors	4	7.5731	1.8933	13632.95**e	7.2093	1.8023	7856.71**
Residuals	67	0.009305	0.0001		0.015370	0.0002	
Lack of fit	31	0.007112	0.0002	3.76**	0.012309	0.0004	4.67**
Pure experimental uncertainty	36	0.002193	0.0001		0.003061	0.0001	
R <sup>2</sup>			0.9988			0.9979	
R <sup>2</sup> (Adjusted for d.f.)			0.9987			0.9977	
Standard error of estimate			0.0118			0.0151	

<sup>a</sup> Degrees of freedom.

<sup>b</sup> Sum of squares.

<sup>c</sup> Mean squares.

<sup>d</sup>  $MS_{\text{factors}}/MS_{\text{residual}}$ .

<sup>e</sup> \*\* = Significance at  $p = 0.01$  level.

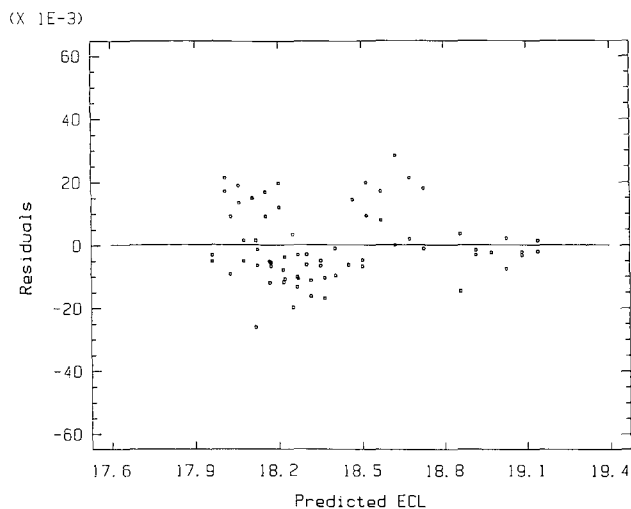


Fig. 6. Residual plot for predicted ECL for *trans*-HCFAM isomers using polynomial equation fitted with reduced data. (Regression coefficients in Table V; ANOVA in Table VI).

reduce the lack of fit and contribute to a more homogeneous distribution of residuals of the new "restricted" model.

The regression coefficients and the statistical analysis of the fitted models for the reduced experimental data ( $2 \leq n \leq 7$ ) are shown in Tables V and VI, respectively. In Table V the quadratic term for oven temperature has not been included at 0.01% probability level for *trans*- and *cis*-HCFAM models. The results of the analysis of variance in Table VI show that the lack of fit for the new restricted models, even though still highly significant, has been substantially reduced when compared with the previous models. In addition, the residual plot for *trans*-HCFAM of the new restricted model, illustrated in Fig. 6, clearly shows a more homogeneous distribution of the errors which supports the validity of the statistical assumptions. A similar plot was obtained for the *cis*-HCFAM new model estimated with the reduced data.

Finally, this apparently arbitrary selection of data can be substantiated with two facts which support the exclusion of the HCFAM isomers with  $n = 1$  from the data. First, these particular isomers have a unique MS fragmentation pattern when compared with the other isomers of the series, since they do not show the fragments D, D-32 and D-32-18 during EI mass spectrometry [6]. Secondly, these isomers do not occur at significant levels in fresh and heated edible fat and oils. Therefore, it seems that an additional unknown parameter is associated with cyclic isomers with  $n = 1$ . This parameter should account for the observed differences that justify an special treatment for the  $n = 1$  cyclic isomers.

#### ACKNOWLEDGEMENT

Partial support from the University of Illinois Agricultural Experimental Station is greatly acknowledged.

## REFERENCES

- 1 E. G. Perkins, *Rev. Fr. Corps Gras*, 23 (1976) 312.
- 2 B. Potteau and J. Causeret, *Rev. Fr. Corps Gras*, 18 (1971) 591.
- 3 N. Combe, M. J. Constantin and B. Entressangles, *Lipids*, 16 (1981) 8.
- 4 W. T. Iwaoka and E. G. Perkins, *Lipids*, 11 (1976) 349.
- 5 W. T. Iwaoka and E. G. Perkins, *J. Am. Oil Chem. Soc.*, 55 (1978) 734.
- 6 B. Potteau, P. Dubois and J. Rigaud, *Ann. Technol. Agric.*, 27 (1978) 655.
- 7 A. Gere, C. Gertz and O. Morin, *Rev. Fr. Corps Gras*, 31 (1984) 341.
- 8 J. A. Rojo and E. G. Perkins, *J. Am. Oil Chem. Soc.*, 64 (1987) 414.
- 9 J. L. Sebedio, J. Prevost and A. Grandgirard, *J. Am. Oil Chem. Soc.*, 54 (1987) 1026.
- 10 J. A. Rojo and E. G. Perkins, *J. Am. Oil Chem. Soc.*, 66 (1989) 1593.
- 11 J. L. Sebedio, J. L. Le Quere, O. Morin, J. M. Vatele and A. Grandgirard, *J. Am. Oil Chem. Soc.*, 66 (1989) 704.
- 12 J. L. Sebedio, *Fette, Seifen, Anstrichm.*, 57 (1985) 267.
- 13 J. L. Sebedio, J. L. Le Quere, E. Semon, O. Morin, J. Prevost and A. Grandgirard, *J. Am. Oil Chem. Soc.*, 64 (1987) 1324.
- 14 J. A. Rojo, *MS Thesis*, University of Illinois, Urbana-Champaign, IL, 1985.
- 15 J. M. Vatele, J. L. Sebedio and J. L. Le Quere, *Chem. Phys. Lipids*, 48 (1988) 119.
- 16 J. A. Rojo and E. G. Perkins, *Lipids*, 24 (1989) 467.
- 17 R. A. Eisenhauer, R. E. Beal and E. L. Griffin, *J. Am. Oil Chem. Soc.*, 40 (1963) 129.
- 18 J. P. Friedrich, E. W. Bell and L. E. Gast, *J. Am. Oil Chem. Soc.*, 42 (1965) 643.
- 19 T. K. Miwa, K. L. Mikolajczak, F. R. Earle and I. A. Wolff, *Anal. Chem.*, 32 (1960) 1739.
- 20 A. Grandgirard and F. Julliard, *Rev. Fr. Corps Gras*, 30 (1983) 123.
- 21 S. N. Deming, in B. R. Kowalski (Editor), *Chemometrics: Mathematics and Statistics in Chemistry (NATO ASI Series C, Vol. 138)*, Reidel, Dordrecht, 1984, p. 267.
- 22 W. G. Cochran and G. M. Cox, *Experimental Designs*, Wiley, New York, 2nd ed., 1957, pp. 244–291.

## Capillary gas chromatographic behavior of stereoisomeric bile acids with a *vicinal* glycol structure by their "mixed" alkylboronate derivatives

TAKASHI IIDA\* and ICHIRO KOMATSUBARA

College of Engineering, Nihon University, Koriyama, Fukushima-ken, 963 (Japan)

FREDERIC C. CHANG

Department of Chemistry, Harvey Mudd College, Claremont, CA 91711 (U.S.A.)

and

JUNICHI GOTO and TOSHIO NAMBARA

Pharmaceutical Institute, Tohoku University, Aobayama, Sendai, 980 (Japan)

(First received May 2nd, 1990; revised manuscript received August 14th, 1990)

---

### ABSTRACT

The capillary gas chromatographic (GC) behavior of 25 bile acids with a *vicinal* 6,7- or 3,4-glycol structure, differing from one another in the stereochemical configuration [diaxial *trans*, diequatorial *trans* and axial-equatorial (or *vice versa*) *cis*], was studied. Methylene unit (MU) values were determined for each of the bile acids as their nine classes of hydroxyl derivatives: complete methyl ester (Me)-trimethylsilyl (TMS) and Me-dimethylethylsilyl (DMES) ether and Me-acetate (Ac) derivatives, and their so-called "mixed" cyclic alkylboronate derivatives, Me-methylboronate (MB)-TMS, Me-MB-DMES, Me-MB-Ac, Me-*n*-butylboronate (*n*BB)-TMS, Me-*n*BB-DMES and Me-*n*BB-Ac. Changes in the MU values of each bile acid due to the different derivatizations were used for the determination of the number of hydroxyl groups and the stereochemical relationship of 1,2-diol groups in the molecules. The *cis*-glycol type of compound, regardless of its  $\alpha,\alpha$ - or  $\beta,\beta$ -configuration, formed the corresponding mixed cyclic alkylboronate derivatives. On the other hand, both the diaxial and diequatorial *trans*-glycols yielded a GC peak corresponding to the persilylated or peracetylated derivatives, although the latter compounds were occasionally accompanied by a second peak corresponding to the mixed alkylboronate-silyl ether derivative. The retention data would be useful for analysing bile acid mixtures extracted from biological samples.

---

### INTRODUCTION

Numerous studies have been reported on the gas chromatographic (GC) separation, identification and quantification of various bile acids related to 5 $\alpha$ - and 5 $\beta$ -cholanoic acids [1-4]. However, they were almost exclusively concerned with bile acids with isolated hydroxyl groups. Similar studies on 4- or 6-hydroxylation products of common bile acids, *i.e.*, lithocholic (3 $\alpha$ -OH), deoxycholic [3 $\alpha$ ,12 $\alpha$ -(OH)<sub>2</sub>], chenodeoxycholic [3 $\alpha$ ,7 $\alpha$ -(OH)<sub>2</sub>], ursodeoxycholic [3 $\alpha$ ,7 $\beta$ -(OH)<sub>2</sub>] and cholic [3 $\alpha$ ,7 $\alpha$ ,12 $\alpha$ -(OH)<sub>3</sub>] acids, which possess a *vicinal* 1,2-diol function in the molecules

[5–7], have been limited to a few exceptions, probably owing to their restricted availability or non-existence.

A number of unusual bile acids with a 1,2-glycol structure at the 6,7- or 3,4-positions have recently been found in significant amounts in biological samples from patients with liver diseases and in newborn infants and fetuses [5–7]. These compounds are of great current interest in biological and metabolic studies. The qualitative and quantitative analyses of such bile acids have usually been performed by GC and GC–mass spectrometry (MS), after suitable GC derivatization.

Among various derivatization procedures, cyclic alkyl- or arylboronate derivatives (*e.g.*, methyl- [8–12] and *n*-butylboronates [9,13,14]) or cyclic dialkylsilylene derivatives (*e.g.*, di-*tert*-butyl- [15,16] and diethylsilylenes [17]) as protecting groups of diols have been shown to be suitable for the GC and GC–MS of 1,2-, 1,3- or 1,4-dihydroxylated compounds such as steroids and prostaglandins. In particular, the so-called “mixed” cyclic alkylboronate–silyl ether or alkylboronate–ester derivatives, introduced by Brooks and co-workers [8,9], have been widely used for the characterization of various bifunctional steroids having both a 1,2- or 1,3-diol system and isolated hydroxyl groups in the molecules [8–13], although the technique requires further derivatization for the isolated hydroxyl groups that are unable to form the cyclic boronate. Cyclic boronate formation with an unknown compound yields specific structural information, and the derivatives generally are better resolved by chromatographic separation of a mixture. In addition, the cyclization product obtained provided a mass spectrum containing characteristic ions with prominent intensity.

As a result of work on a programme of synthesizing potential bile acid metabolites, a series of di-, tri- and tetrahydroxylated bile acids with a *vicinal* 3,4- or 6,7-glycol structure, which differ from one another in the stereochemical configuration of the 1,2-diol system [*i.e.*, diaxial *trans*-, diequatorial *trans*- and axial–equatorial (or *vice versa*) *cis*-glycols], are now available. In this paper, we describe the capillary GC behavior of 25 sterically different bile acids as their mixed methyl- and *n*-butylboronate derivatives and their complete methyl ester–trimethylsilyl (Me–TMS) and methyl ester–dimethylethylsilyl (Me–DMES) ether and methyl ester–acetate (Me–Ac) derivatives. Although the GC behavior of some 3,6,7-trihydroxy bile acids with a *cis*-glycol structure as their mixed methylboronate–TMS ether derivatives is known [9], analogous *trans*-glycols have not been reported hitherto.

## EXPERIMENTAL

### *Samples and reagents*

All the stereoisomeric 5 $\alpha$ - and 5 $\beta$ -cholanoic acids having a *vicinal* 3,4- or 6,7-glycol structure were from collections in our laboratory, which include new and natural bile acids recently synthesized by us [18–20].

The silylating reagents, TMS–HT (hexamethyldisilazane and trimethylchlorosilane in anhydrous pyridine) and N,N-dimethylethylsilylimidazole (DMESI), were obtained from Tokyo Kasei Kogyo (Tokyo, Japan). Methylboronic acid was purchased from Aldrich (Milwaukee, WI, U.S.A.). *n*-Butylboronic acid and 4-dimethylaminopyridine were available from Tokyo Kasei Kogyo. All solvents were of analytical-reagent grade and used without further purification.

*GC instrument and column*

A Shimadzu GC-14A gas chromatograph equipped with a flame ionization detector and data-processing system (Chromatopac C-R6A) was used isothermally. It was fitted with an aluminum-clad flexible fused-silica capillary column (25 m × 0.25 mm I.D.) with a thin film (0.1 μm) of bonded and cross-linked methylpolysiloxane (equivalent to OV-101) and operated under the following conditions: carrier gas (helium) flow-rate, 1.5 ml/min; splitting ratio, 1:50; and column temperature, 270°C. The column, HiCap CBPM1, was purchased from Shimadzu (Kyoto, Japan).

*Derivatization procedures*

Bile acid samples were first converted into the C-24 methyl esters by the usual diazomethane method [1]. Each of the bile acid methyl esters was then subjected to the nine classes of hydroxyl derivatizations prior to GC, and their structures are depicted in Fig. 1, as exemplified by a 5β-3,6,7-triol. The mixed alkylboronate deriv-

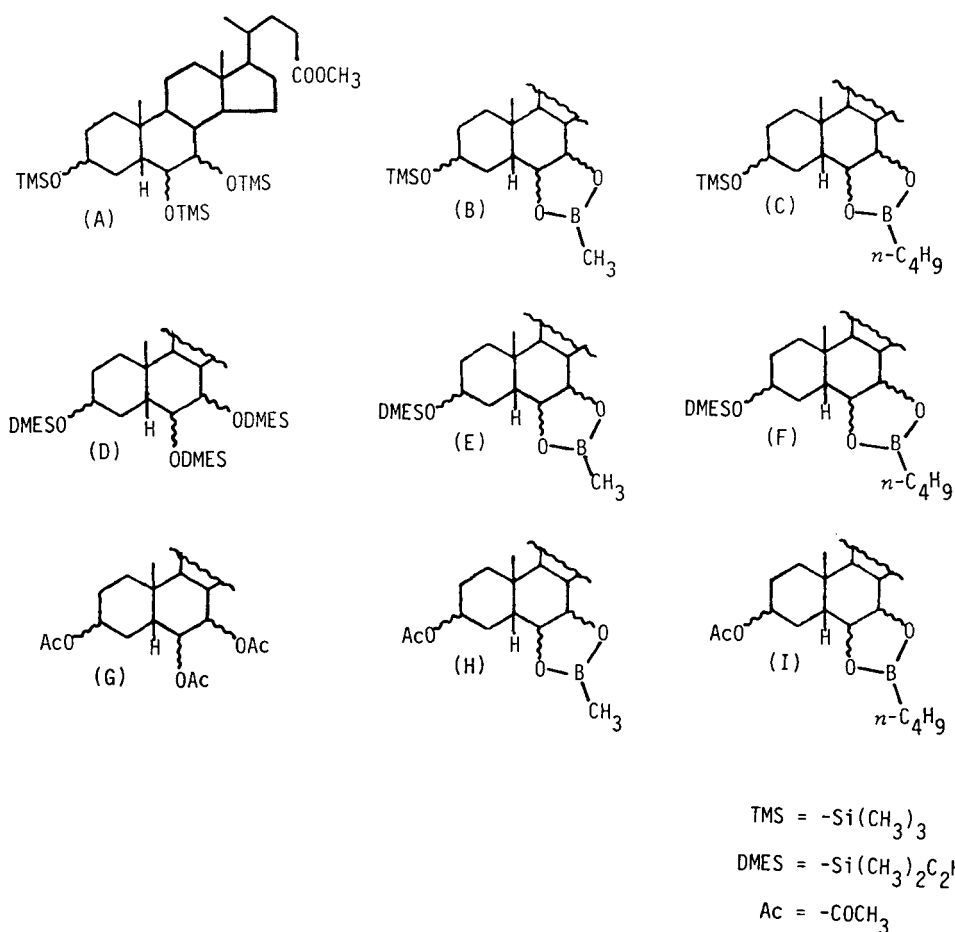


Fig. 1. Derivatizations examined.

TABLE I

MU VALUES OF THE Me-TMS (A), Me-MB-TMS (B), Me-nBB-TMS (C), Me-DMES (D), Me-MB-DMES (E), Me-nBB-DMES (F), Me-MB-DMES (G), Me-nBB-Ac (H) AND Me-nBB-Ac (I) DERIVATIVES OF BILE ACIDS

Position and configuration of hydroxyls	Me-TMS (A)	Me-MB-TMS (B)	Me-nBB-TMS (C)	Me-DMES (D)	Me-MB-DMES (E)	Me-nBB-DMES (F)	Me-MB-DMES (G)	Me-MB-Ac (H)	Me-nBB-Ac (I)
3 $\alpha$	31.26			32.67			32.47		
3 $\alpha$ ,6 $\alpha$	32.30			34.62			34.76		
3 $\alpha$ ,7 $\alpha$	32.12			34.44			33.99		
3 $\alpha$ ,7 $\beta$	32.53			34.78			34.92		
3 $\alpha$ ,12 $\alpha$	31.88			34.13			33.35		
3 $\alpha$ ,7 $\alpha$ ,12 $\alpha$	32.24			35.64			34.35		
3 $\alpha$ ,7 $\beta$ ,12 $\alpha$	32.87			35.77			35.65		
3 $\alpha$ ,6 $\alpha$ ,7 $\alpha$	33.15	33.15	35.15	36.12	34.30	36.45	35.54	34.05	36.15
3 $\alpha$ ,6 $\alpha$ ,7 $\beta$	34.33	33.61	35.75	37.13			36.43		
3 $\alpha$ ,6 $\beta$ ,7 $\alpha$	32.26			35.30			35.71		
3 $\alpha$ ,6 $\beta$ ,7 $\beta$	33.30	32.98	35.41	36.31	34.18	36.64	36.78	34.05	36.57
3 $\beta$ ,6 $\alpha$ ,7 $\alpha$	33.05	32.76	34.83	36.12	34.18	36.22	35.38	33.89	35.82
3 $\beta$ ,6 $\alpha$ ,7 $\beta$	34.62	33.35	35.64	37.28			36.09		
3 $\beta$ ,6 $\beta$ ,7 $\alpha$	31.88			35.09			35.38		
3 $\beta$ ,6 $\beta$ ,7 $\beta$	33.84	33.33	35.67	36.62	34.59	36.94	36.43	34.13	36.74
3 $\alpha$ ,6 $\alpha$ ,7 $\beta$ (5 $\alpha$ )	34.88	33.21	35.65	37.93			36.78		
3 $\alpha$ ,6 $\beta$ ,7 $\beta$ (5 $\alpha$ )	33.46	32.98	35.34	36.44	34.18	36.56	36.99	34.30	36.66
3 $\alpha$ ,6 $\alpha$ ,7 $\alpha$ ,12 $\alpha$	33.33	33.39	35.29	37.28	35.33	37.37	35.72	34.48	36.62
3 $\alpha$ ,6 $\alpha$ ,7 $\beta$ ,12 $\alpha$	34.26	33.89	36.21	37.84			37.00		
3 $\alpha$ ,6 $\beta$ ,7 $\alpha$ ,12 $\alpha$	32.42			36.48			36.01		
3 $\alpha$ ,6 $\beta$ ,7 $\beta$ ,12 $\alpha$	32.93	33.30	35.68	36.72	35.33	37.78	37.26	34.78	37.37
3 $\alpha$ ,6 $\alpha$ ,7 $\beta$ ,12 $\alpha$ (5 $\alpha$ )	34.69	33.53	34.65	38.60			37.36		
3 $\alpha$ ,4 $\beta$	33.58	31.79		35.55			34.39		
3 $\beta$ ,4 $\alpha$	31.76			33.89			33.92		
3 $\beta$ ,4 $\beta$	33.02	31.84	34.84	35.19	31.88	34.82	34.16	31.84	34.88
3 $\alpha$ ,4 $\beta$ ,7 $\alpha$	33.96		35.41	36.78		36.30	35.46		
3 $\beta$ ,4 $\beta$ ,7 $\alpha$	34.23	32.00	34.84	36.91	33.02	35.74	35.54	33.15	35.96
3 $\alpha$ ,4 $\beta$ ,12 $\alpha$	34.11			37.06			34.94		
3 $\beta$ ,4 $\alpha$ ,12 $\alpha$	32.84			35.87			34.81		
3 $\beta$ ,4 $\beta$ ,12 $\alpha$	33.18	32.48	35.43	36.15	33.45	36.33	34.94	32.89	35.89
3 $\alpha$ ,4 $\beta$ ,7 $\alpha$ ,12 $\alpha$	34.68	32.39	35.06	38.39		37.56	35.58		
3 $\beta$ ,4 $\beta$ ,7 $\alpha$ ,12 $\alpha$	34.42		35.05	37.98	34.44	37.12	35.95	33.72	36.46



atives (B, C, E, F, H and I) were prepared in two steps by a combination of boronic cyclization followed by silylation or acetylation [8,9].

*Complete methyl ester-trimethylsilyl (Me-TMS; A) and methyl ester-dimethylethylsilyl (Me-DMES; D) ether derivatives*

To each bile acid methyl ester (50–100  $\mu\text{g}$ ), silylating reagent (TMS-HT or DMESI, 50  $\mu\text{l}$ ) was added and the mixture was allowed to stand for 30 min at room temperature [4].

*Complete methyl ester-acetate (Me-Ac; G) derivatives*

To each bile acid methyl ester (50–100  $\mu\text{g}$ ), acetic anhydride (20  $\mu\text{l}$ ), dry pyridine (30  $\mu\text{l}$ ) and 4-dimethylaminopyridine (10  $\mu\text{g}$ ) were added and the mixture was heated at 60°C for 30 min [9]; for 3,4-glycols, acetylation was carried out at 120°C for 2 h.

*Methyl ester-cyclic alkylboronate derivatives*

To each bile acid methyl ester (50–100  $\mu\text{g}$ ), methylboronic (or *n*-butylboronic) acid (50  $\mu\text{g}$ ) and dry pyridine (50  $\mu\text{l}$ ) were added and the mixture was heated at 60°C for 30 min.

*Methyl ester-methylboronate-trimethylsilyl (Me-MB-TMS; B), methyl ester-*n*-butylboronate-trimethylsilyl (Me-*n*BB-TMS; C), methyl ester-methylboronate-dimethylethylsilyl (Me-MB-DMES; E), and methyl ester-*n*-butylboronate-dimethylethylsilyl (Me-*n*BB-DMES; F) ether derivatives*

Mixed cyclic boronate-silyl ether derivatives were prepared by a slight modification of the procedure of Brooks and co-workers [8,9]. After methylation and alkylboronation, the resulting derivative, prepared as above was treated with silylating reagent (TMS-HT or DMESI, 50  $\mu\text{l}$ ) and the mixture was allowed to stand for 30 min at room temperature.

*Methyl ester-methylboronate-acetate (Me-MB-Ac; H) and methyl ester-*n*-butylboronate-acetate (Me-*n*BB-Ac; I) derivatives*

After methylation and alkylboronation, the resulting derivative, prepared as above, was treated with acetic anhydride (20  $\mu\text{l}$ ), dry pyridine (30  $\mu\text{l}$ ) and 4-dimethylaminopyridine (10  $\mu\text{g}$ ) and the mixture was heated at 60°C for 30 min (or at 120°C for 2 h for 3,4-glycols).

After the reactions, an aliquot of the sample solutions was injected directly into the GC system without clean-up [21] simultaneously with an internal reference standard.

## RESULTS AND DISCUSSION

Twenty-five bile acids possessing a *vicinal* 6,7- or 3,4-glycol structure differing in stereochemical configuration were used to study the GC behavior accompanying various hydroxyl derivatizations. Table I shows the 25 compounds examined plus seven common bile acids and the retention data observed for the nine classes of derivatives: Me-TMS (A), Me-MB-TMS (B), Me-*n*BB-TMS (C), Me-DMES (D),

ME-MB-DMES (E), Me-*n*BB-DMES (F), Me-Ac (G), Me-MB-Ac (H) and Me-*n*BB-Ac (I). The reaction products usually afforded a sharp and symmetrical peak that facilitates the separation of isomers when analyzed using a non-selective fused-silica capillary column (HiCap CBPM1). Retention data were expressed as methylene unit (MU) values. In order to minimize the discrepancies in the MU values [7], the same column was used throughout the determination of the retention data for all the compounds.

#### *GC behaviors of complete silyl ether and acetate derivatives*

As bile acids have conventionally been analyzed as their complete Me-TMS, Me-DMES or Me-Ac derivatives [1,2], we initially examined the GC behavior of the 25 acids. The ten stereoisomers of 3,6,7-triols including two 5 $\alpha$ - (*allo*) series of compounds were well resolved as their Me-TMS ether derivatives on this column, emerging in the order  $3\beta,6\beta,7\alpha < 3\alpha,6\beta,7\alpha < 3\beta,6\alpha,7\alpha < 3\alpha,6\alpha,7\alpha < 3\alpha,6\beta,7\beta < 3\alpha,6\beta,7\beta$  (5 $\alpha$ )  $< 3\beta,6\beta,7\beta < 3\alpha,6\alpha,7\beta < 3\beta,6\alpha,7\beta < 3\alpha,6\alpha,7\beta$  (5 $\alpha$ ). Their Me-DMES ether derivatives followed essentially the same elution order, as shown in Fig. 2a. The 3,6,7,12-tetrahydroxy stereoisomers likewise resemble the 3,6,7-trihydroxy compounds in that the relative mobilities of analogous derivatives follow a similar order,

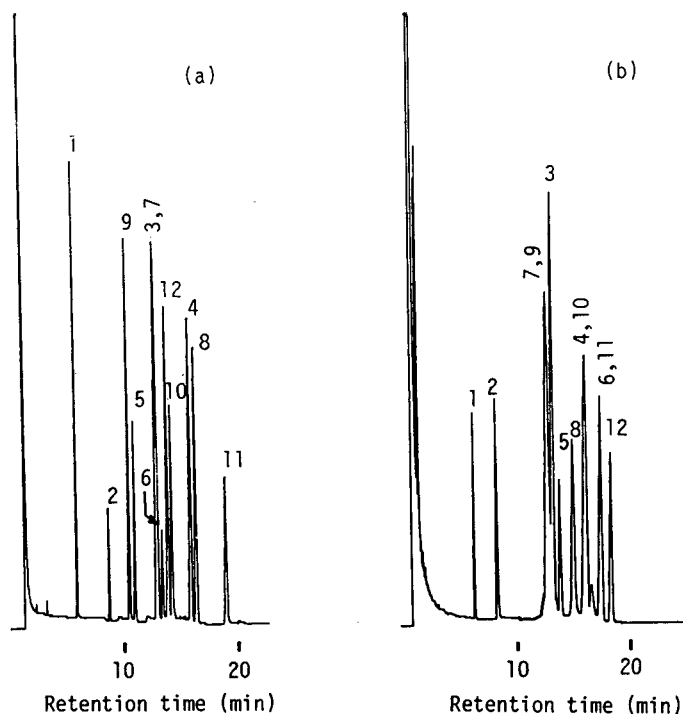


Fig. 2. Capillary GC of a mixture of the 3,6,7-trihydroxy stereoisomers as their (a) Me-DMES and (b) Me-Ac derivatives. Peaks: 1 = C<sub>32</sub>; 2 = deoxycholic acid; 3 = 3 $\alpha,6\alpha,7\alpha$ ; 4 = 3 $\alpha,6\alpha,7\beta$ ; 5 = 3 $\alpha,6\beta,7\alpha$ ; 6 = 3 $\alpha,6\beta,7\beta$ ; 7 = 3 $\beta,6\alpha,7\alpha$ ; 8 = 3 $\beta,6\alpha,7\beta$ ; 9 = 3 $\beta,6\beta,7\alpha$ ; 10 = 3 $\beta,6\beta,7\beta$ ; 11 = 3 $\alpha,6\alpha,7\beta$  (5 $\alpha$ ); 12 = 3 $\alpha,6\beta,7\beta$  (5 $\alpha$ ).

*i.e.*,  $3\alpha,6\beta,7\alpha,12\alpha < 3\alpha,6\beta,7\beta,12\alpha < 3\alpha,6\alpha,7\alpha,12\alpha < 3\alpha,6\alpha,7\beta,12\alpha < 3\alpha,6\alpha,7\beta,12\alpha$  (5a).

It is evident from the above observations that, for each silyl ether derivative, 6 $\beta$ ,7 $\alpha$ -diaxial *trans*-glycols are eluted much faster than the corresponding 6 $\alpha$ , 7 $\beta$ -diequatorial *trans*-analogs; compounds with a 6 $\alpha$ ,7 $\alpha$ - or 6 $\beta$ ,7 $\beta$ -axial-equatorial (or *vice versa*) *cis*-glycol structure appear between the two *trans*-epimers. A similar elution order was also observed with the silyl ether derivatives of the stereoisomeric 3,4-glycols (diaxial 3 $\beta$ ,4 $\alpha$  < axial-equatorial 3 $\beta$ ,4 $\beta$  < diequatorial 3 $\alpha$ , 4 $\beta$ ), except for the 3,4,7-trihydroxy isomers, in which the 3 $\alpha$ ,4 $\beta$ ,7 $\alpha$ -triol shows a smaller retention time than the 3 $\beta$ ,4 $\beta$ ,7 $\alpha$ -counterpart.

As expected [4,22,23], the trend of the differences in the retention times was in good agreement with earlier observations. Thus, the Me-DMES ethers have longer retention times than the corresponding Me-TMS ethers owing to the heavier ethyl group, and the MU values obtained for the Me-DMES ethers were increased nearly consistently by *ca.* 1 unit per one hydroxyl group in comparison with those of the corresponding Me-TMS ethers. Average differences in the MU values between the two silyl ether derivatives were 2.20 ( $n=7$ ) for di-, 2.95 ( $n=17$ ) for tri- and 3.79 ( $n=7$ ) for tetrahydroxylated bile acids.

The elution order of the Me-Ac derivatives (G) of the bile acids differed from that found for the corresponding silyl ethers mentioned above [24,25], and the following general elution order of 6,7-glycols was observed: equatorial-axial *cis*- < diaxial *trans*- < diequatorial *trans*- < axial-equatorial *cis*-glycols. However, the peaks of derivatives of several isomeric pairs of the 3,6,7-triols were found to overlap (Fig. 2b). In addition, under mild acetylation conditions at 60°C for 30 min, the Me-Ac derivative of the 3,4-glycol type of compounds often gave two well resolved peaks, probably owing to steric hindrance. These compounds were therefore acetylated by more drastic conditions at 120°C for 2 h and, as expected, afforded essentially a single peak. These observations suggest that this derivative is not suitable for the profile analysis of the type of compound [26].

#### *GC behaviors of mixed alkylboronate-silyl ether and alkylboronate-acetate derivatives*

The mixed alkylboronate derivatives were prepared in two steps by a slight modification of the method published by Brooks and co-workers [8,9]. The method involves alkylboronic cyclization combined with silylation or acetylation. Fig. 3 shows representative chromatograms of mixtures of the nine classes of derivatives [six mixed cyclic alkylboronates (B,C,E,F,H,I) and three unmixed (A,D,G)] of each of 3 $\beta$ ,4 $\beta$ ,12 $\alpha$ - and 3 $\alpha$ ,6 $\beta$ ,7 $\alpha$ -trihydroxy-5 $\beta$ -cholanoic acid. Fig. 3a, for the derivatives of the axial-equatorial *cis*-glycol 3 $\beta$ ,4 $\beta$ ,12 $\alpha$ -triol acid, shows a distinct separation of the components with single well shaped peaks, whereas Fig. 3b, for the corresponding mixture of derivatives of the diaxial *trans*-glycol 3 $\alpha$ ,6 $\beta$ ,7 $\alpha$ -stereoisomer shows only three poorly resolved peaks.

Essentially identical retention GC behaviours were found for all of the other *cis*- and *trans*-glycol types of compounds. The results indicate that under the derivatization conditions used, the *cis*-glycols (6 $\alpha$ ,7 $\alpha$ -, 6 $\beta$ ,7 $\beta$ - and 3 $\beta$ ,4 $\beta$ -), regardless of  $\alpha$ , $\alpha$ - or  $\beta$ , $\beta$ -configuration, form "mixed" alkylboronate derivatives [9], whereas the *trans*-glycols (6 $\alpha$ ,7 $\beta$ -, 6 $\beta$ ,7 $\alpha$ -, 3 $\alpha$ ,4 $\beta$ - and 3 $\beta$ ,4 $\alpha$ -), not being able to form cyclic esters, are derivatized to one of the persilyl or peracetate forms.

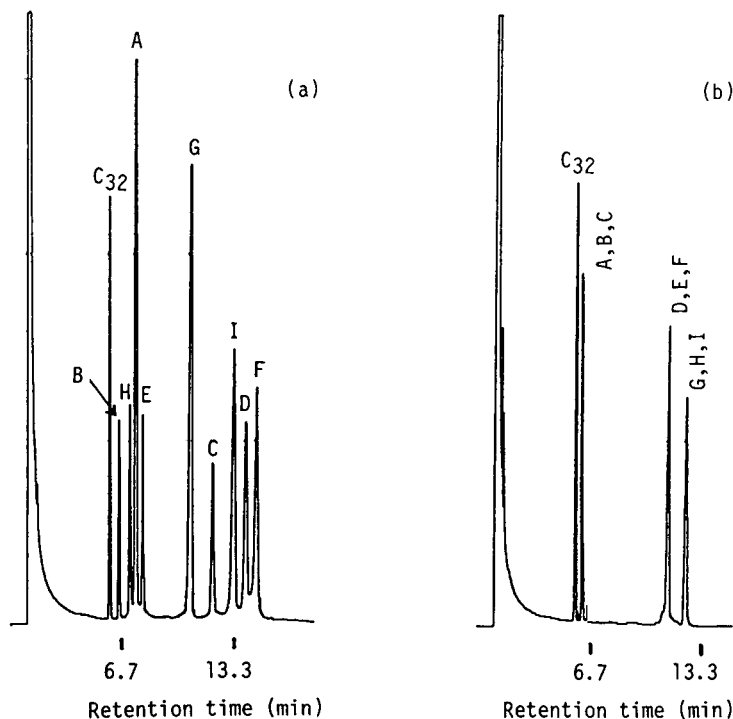


Fig. 3. Capillary GC of a mixture of the hydroxyl derivatization products of (a)  $3\beta,4\beta,12\alpha$ - and (b)  $3\alpha,6\beta,7\alpha$ -trihydroxy- $5\beta$ -cholanoic acids. Peaks: A = Me-TMS; B = Me-MB-TMS; C = Me-*n*BB-TMS; D = Me-DMES; E = Me-MB-DMES; F = Me-*n*BB-DMES; G = Me-Ac; H = Me-MB-Ac; I = Me-*n*BB-Ac.

However, with the diequatorial *trans*-glycols ( $6\alpha,7\beta$ - or  $3\alpha,4\beta$ -), although in most instances they resemble their diaxial *trans*-analogs in not forming mixed boronate derivatives, in some instances they do give two well separated peaks, particularly when the two-step derivatization process is used to form the Me-MB-TMS and Me-*n*BB-TMS derivatives (see Table I). In these instances one peak corresponds to the mixed alkylboronate-silyl ether and the other the persilyl ether, indicating that partial formation of the cyclic derivative had taken place. Although the former is usually much smaller than the latter (Fig. 4), the ratio of the two peaks is hardly influenced by the boronation conditions examined [reaction time (30, 60 and 120 min) and reaction temperature (60, 80 and  $100^\circ\text{C}$ )], as exemplified by  $5\beta$ - $3\alpha,6\alpha,7\beta$ -triol. Peak identification must therefore be carried out cautiously when interpreting the GC results for naturally occurring diequatorially hydroxylated bile acids as the mixed alkylboronate-silyl ether derivatives.

From the above findings, the changes in the MU values due to cyclic alkylboronate formation were calculated. The results are given in Table II, where the  $\Delta[\text{Um}]_{\text{B-S}}$  and  $\Delta[\text{Um}]_{\text{B-A}}$  are the MU increments [22] based on the Me-TMS (B-A and C-A) and Me-DMES (E-D and F-D) ethers and Me-Ac (H-G and I-G), respectively, for the same compound which forms the alkylboronate ester; a negative

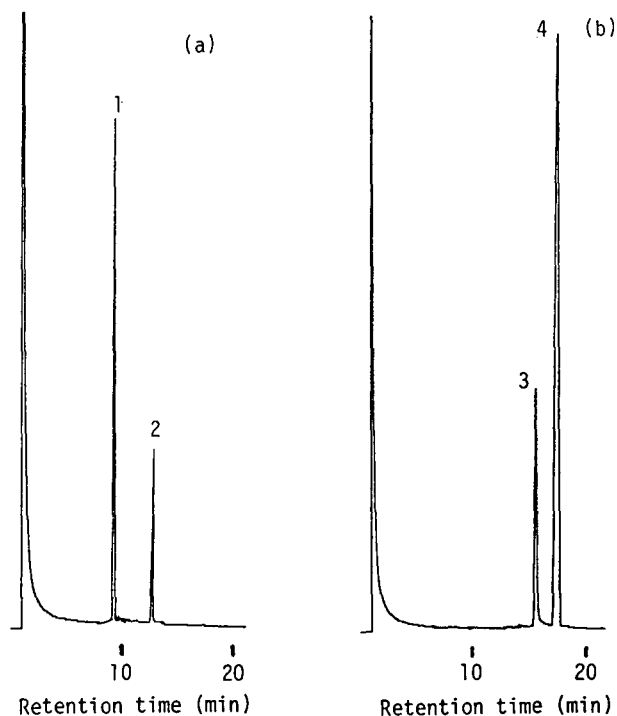


Fig. 4. Capillary GC of the products of diequatorial *trans*-glycols, (a)  $3\alpha,6\alpha,7\beta$ - and (b)  $3\alpha,4\beta,7\alpha$ -tri-hydroxy- $5\beta$ -cholanoic acids, derivatized to their Me-*n*BB-TMS and Me-*n*BB-DMES ethers, respectively. Peaks: 1 = Me-TMS; 2 = Me-*n*BB-TMS; 3 = Me-*n*BB-DMES; 4 = Me-DMES.

value denotes that the retention time of the mixed alkylboronate derivatives is shorter than that of the corresponding persilylated or peracetylated compounds. The  $\Delta[\text{Um}]_{\text{B-S}}$  and  $\Delta[\text{Um}]_{\text{B-A}}$  values observed were in the ranges  $-2.23$  to  $0.37$  (B-A) for Me-MB-TMS,  $0.38$  to  $2.75$  (C-A) for Me-*n*BB-TMS,  $-3.89$  to  $-1.39$  (E-D) for Me-MB-DMES,  $-1.17$  to  $1.06$  (F-D) for Me-*n*BB-DMES,  $-2.73$  to  $-1.24$  (H-G) for Me-MB-Ac and  $-0.33$  to  $0.95$  (I-G) for Me-*n*BB-Ac. The Me-*n*BB-TMS ethers always give large positive  $\Delta[\text{Um}]_{\text{B-S}}$  values, whereas the Me-MB-DMES ether and Me-MB-Ac derivatives gave large negative values. Further, with regard to these derivatives,  $6\beta,7\beta$ -glycols usually show a larger value than the corresponding  $6\alpha,7\alpha$ -isomers, with a few exceptions, thus permitting a facile determination of the stereochemical relationship. The other derivatives showed positive or negative values depending on the structure of substrates.

In order to clarify further the general features of cyclic alkylboronations, the MU and  $\Delta[\text{Um}]_{\text{D-T}}$  values were expressed graphically, where  $\Delta[\text{Um}]_{\text{D-T}}$  is the difference in the MU values between the analogous DMES and TMS ether derivatives (e.g., Me-*n*BB-DMES vs. Me-*n*BB-TMS) for the same compound on this column [22]. Fig. 5 shows the interrelationship between the  $\Delta[\text{Um}]_{\text{D-T}}$  values and the number of hydroxyl groups in a molecule. As mentioned above, a plot of the  $\Delta[\text{Um}]_{\text{D-T}}$  value vs. number of hydroxyl groups for the Me-DMES and Me-TMS ethers [22] showed

TABLE II  
 $\Delta[\text{Um}]_{\text{B}-\text{S}}$  AND  $\Delta[\text{Um}]_{\text{B}-\text{A}}$  VALUES OBSERVED FOR AXIAL-EQUATORIAL (OR VICE VERSA) CIS- AND DIEQUATORIAL TRANS-GLYCOLS

Position and configuration of hydroxyls	$\Delta[\text{Um}]_{\text{B}-\text{S}}$ <sup>a</sup>					$\Delta[\text{Um}]_{\text{B}-\text{A}}$ <sup>b</sup>				
	B-A (Me-MB-TMS -Me-TMS)	C-A (Me-nBB-TMS -Me-TMS)	E-D (Me-MB-DMES -Me-DMES)	F-D (Me-nBB-DMES -Me-DMES)	H-G (Me-MB-Ac -Me-Ac)	I-G (Me-nBB-Ac -Me-Ac)				
3 $\alpha$ ,6 $\alpha$ ,7 $\alpha$	0	2.00	-1.82	0.33	-1.49	0.61				
3 $\alpha$ ,6 $\alpha$ ,7 $\beta$	-0.72	1.42	-2.13	0.33	-2.73	-0.21				
3 $\alpha$ ,6 $\beta$ ,7 $\beta$	-0.32	2.11	-1.94	0.10	-1.49	0.44				
3 $\beta$ ,6 $\alpha$ ,7 $\beta$	-1.27	1.02	-2.03	0.32	-2.30	0.31				
3 $\beta$ ,6 $\alpha$ ,7 $\alpha$	-0.29	1.78	-2.26	0.12	-2.69	-0.33				
3 $\beta$ ,6 $\beta$ ,7 $\alpha$	-0.51	1.83	-1.95	0.09	-1.24	0.90				
3 $\beta$ ,6 $\beta$ ,7 $\beta$	-1.67	0.77	-1.39	1.06	-2.48	0.11				
3 $\alpha$ ,6 $\alpha$ ,7 $\beta$ (5 $\alpha$ )	-0.48	1.88	-3.31	-0.37	-2.32	0.72				
3 $\alpha$ ,6 $\beta$ ,7 $\beta$ (5 $\alpha$ )	0.06	1.96	-3.89	-0.48	-2.39	0.42				
3 $\alpha$ ,6 $\alpha$ ,7 $\alpha$ ,12 $\alpha$	0.06	1.96	-2.70	0.18	-2.05	0.95				
3 $\alpha$ ,6 $\alpha$ ,7 $\beta$ ,12 $\alpha$	-0.37	1.95	-3.54	-0.83	-2.23	0.51				
3 $\alpha$ ,6 $\beta$ ,7 $\beta$ ,12 $\alpha$	0.37	2.75								
3 $\alpha$ ,6 $\alpha$ ,7 $\beta$ ,12 $\alpha$ (5 $\alpha$ )	-1.16									
3 $\alpha$ ,4 $\beta$	-1.79	1.07								
3 $\beta$ ,4 $\beta$	-1.18	1.82								
3 $\alpha$ ,4 $\beta$ ,7 $\alpha$		1.45								
3 $\beta$ ,4 $\beta$ ,7 $\alpha$	-2.23	0.61								
3 $\beta$ ,4 $\beta$ ,12 $\alpha$	-0.70	2.25								
3 $\alpha$ ,4 $\beta$ ,7 $\alpha$ ,12 $\alpha$		0.38								
3 $\beta$ ,4 $\beta$ ,7 $\alpha$ ,12 $\alpha$	-2.03	0.63								

<sup>a</sup> Differences in the MU values [22] between the persilyl and the corresponding "mixed" alkyboronate-silyl ether derivatives.

<sup>b</sup> Differences in the MU values [22] between the peracetate and the corresponding "mixed" alkyboronate-acetate derivatives.

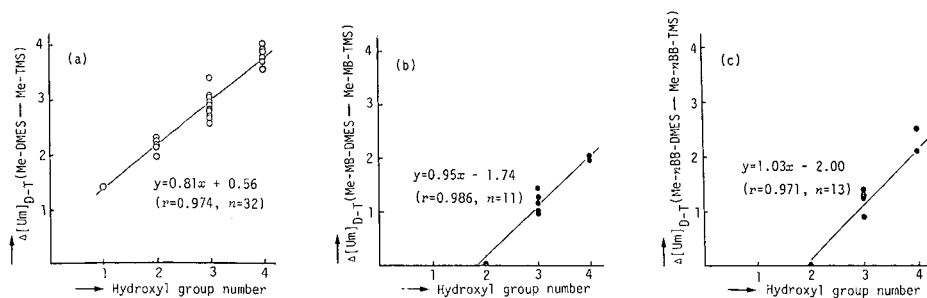


Fig. 5. Relationship of hydroxyl group number to  $\Delta[\text{Um}]_{\text{D-T}}$  value of (a) Me-DMES vs. Me-TMS; (b) Me-MB-DMES vs. Me-MB-TMS; and (c) Me-MB-DMES vs. Me-nBB-TMS. (○) Persilyl and (●) alkylboronate-silyl ether peaks.

good linearity (Fig. 5a), defined as  $y = 0.81x + 0.56$  ( $r = 0.974$ ,  $n = 32$ ), indicating that the addition of hydroxyl groups produces nearly consistent increases (*ca.* 1 unit per hydroxyl group) in the  $\Delta[\text{Um}]_{\text{D-T}}$  values. On the other hand, plots of the  $\Delta[\text{Um}]_{\text{D-T}}$  value vs. number of hydroxyl groups for Me-MB-DMES and Me-MB-TMS ethers afforded the regression line expressed as  $y = 0.95x - 1.74$  ( $r = 0.986$ ,  $n = 11$ ) (Fig. 5b) with a much smaller intercept (*ca.* -2 units in the  $\Delta[\text{Um}]_{\text{D-T}}$  value) and with a similar slope. The line consisted of values of the derivatives of axial-equatorial (or *vice versa*) *cis*-glycols and those of one of the two peaks arising from some diequatorial *trans*-glycols mentioned above. The  $\Delta[\text{Um}]_{\text{D-T}}$  value of -2 units reflects the greater reduction in retention time achieved by replacing two *vicinal* DMES groups (rather than two TMS groups) with a cyclic boronate. The value of 2 thus arises from the mass difference of 28 (2DMES-2TMS), and would be similar for the other types of cyclic boronate derivatives (Me-nBB-DMES and Me-nBB-TMS) (Fig. 5c).

There were also close correlations between the MU values of the mixed *n*-butylboronates with those of the corresponding methylboronate derivatives (Fig. 6), and a statistically significant correlation was found for each of the three graphs. For example, the regression line with a large intercept and with a smaller slope of less than

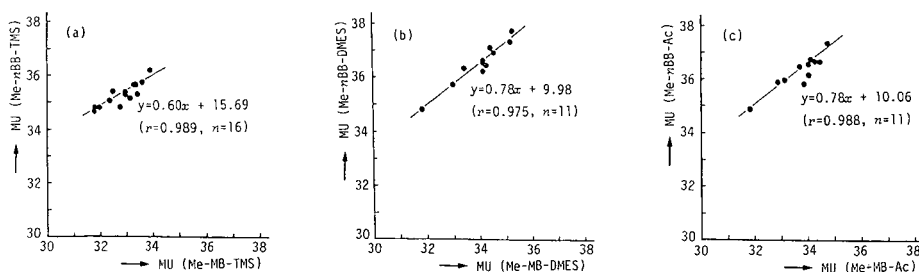


Fig. 6. Relationship between the MU values of (a) Me-nBB-TMS and Me-MB-TMS, (b) Me-nBB-DMES and Me-MB-DMES and (c) Me-nBB-Ac and Me-MB-Ac.

1.0, expressed as  $y = 0.60x + 15.69$  ( $r = 0.989$ ,  $n = 16$ ) (Fig. 6a), was obtained from the data for the Me-*n*BB-TMS *vs.* Me-MB-TMS ethers. Analogously, regression lines with a similar intercept and slope to the line in Fig. 6a were also observed for the MU values for the other two combinations [Me-*n*BB-DMES *vs.* Me-MB-DMES (Fig. 6b) and Me-*n*BB-Ac *vs.* Me-MB-Ac (Fig. 6c)] by changing the boronate esters from methyl to the heavier *n*-butyl group.

The above high correlations suggest that if either the  $\Delta[\text{Um}]_{\text{D-T}}$  value or the MU value for the mixed methyl (or the corresponding *n*-butyl) boronation product of an unknown bile acid is known, the number of hydroxyl groups and the presence or absence and the stereochemical relationship (*cis* and *trans*) of a *vicinal* glycol structure can be characterized mathematically by applying the regression equations.

In conclusion, the capillary GC behavior of bile acids with a *vicinal* glycol structure, as their mixed cyclic alkylboronate derivatives, on a non-polar capillary column provided important information concerning the presence or absence and/or the stereochemical configuration of the 1,2-diol groups. Of the several derivatives examined, Me-MB-DMES or Me-*n*BB-TMS seems to be most suitable. The retention data would be helpful for identifying an unknown bile acid of the types examined in this study, or for establishing its structure.

#### REFERENCES

- 1 P. Eneroth and J. Sjövall, in P. P. Nair and K. Kritchevsky (Editors), *The Bile Acids*, Vol.1, Plenum Press, New York, 1971, p. 121.
- 2 J. M. Street and K. D. R. Setchell, *Biomed. Chromatogr.*, 2 (1988) 229.
- 3 W. H. Elliott, R. L. B. Walsh, C. M., M. M. Mui, M. A. Thorne and C. M. Siegfried, *J. Chromatogr.*, 44 (1969) 452.
- 4 T. Iida, T. Momose, T. Tamura, T. Matsumoto, J. Goto, T. Nambara and F. C. Chang, *J. Chromatogr.*, 389 (1987) 155.
- 5 W. H. Elliott, in H. Danielsson and J. Sjövall (Editors), *Sterols and Bile Acids*, Elsevier, Amsterdam, 1985, p. 303.
- 6 K. D. R. Setchell, P. P. Nair and D. Kritchevsky (Editors), *The Bile Acids*, Vol.4, Plenum Press, New York, 1988.
- 7 R. Dumaswala, K. D. R. Setchell, L. Zimmer-Nechemias, T. Iida, J. Goto and T. Nambara, *J. Lipid Res.*, 30 (1989) 847.
- 8 C. J. W. Brooks, W. J. Cole, H. B. McIntyre and A. G. Smith, *Lipids* 15 (1980) 745.
- 9 C. J. W. Brooks, G. M. Barrett and W. J. Cole, *J. Chromatogr.*, 289 (1984) 231.
- 10 S. Takatsuto, B. Ying, M. Morisaki and N. Ikekawa, *J. Chromatogr.*, 239 (1982) 233.
- 11 N. Ikekawa, S. Takatsuto, T. Kitsuwu, H. Saito, T. Morishita and H. Abe, *J. Chromatogr.*, 290 (1984) 289.
- 12 S. Takatsuto and N. Ikekawa, *Chem. Pharm. Bull.*, 34 (1986) 3435.
- 13 K. Ichimura, H. Yamanaka, K. Chiba, T. Shinozuka, Y. Shiki, K. Saito, S. Kusano, S. Ameniya, K. Oyama, Y. Nozaki and K. Kato, *J. Chromatogr.*, 375 (1986) 5.
- 14 B. Johansson and I. Fromark, *J. Chromatogr.*, 341 (1985) 462.
- 15 C. J. W. Brooks, W. J. Cole and G. M. Barrett, *J. Chromatogr.*, 315 (1984) 119.
- 16 C. J. W. Brooks and W. J. Cole, *Analyst (London)*, 110 (1985) 587.
- 17 H. Miyazaki, M. Ishibashi, M. Itoh and K. Yamashita, *Biomed. Mass Spectrom.*, 11 (1984) 377.
- 18 T. Iida, T. Momose, T. Tamura, T. Matsumoto, F. C. Chang, J. Goto and T. Nambara, *J. Lipid Res.*, 30 (1989) 1267.
- 19 T. Iida, T. Momose, F. C. Chang, J. Goto and T. Nambara, *Chem. Pharm. Bull.*, 37 (1989) 3323.
- 20 T. Iida, I. Komatsubara, S. Yoda, J. Goto, T. Nambara and F. C. Chang, *Steroids*, in press.
- 21 T. Iida, T. Itoh, K. Hagiwara, F. C. Chang, J. Goto and T. Nambara, *Lipids*, 24 (1989) 1053.
- 22 H. Miyazaki, M. Ishibashi, M. Itoh and T. Nambara, *Biomed. Mass Spectrom.*, 4 (1977) 23.
- 23 A. Fukunaga, Y. Hatta, M. Ishibashi and H. Miyazaki, *J. Chromatogr.*, 190 (1980) 339.
- 24 P. A. Szczepanik, D. L. Hachey and P. D. Klein, *J. Lipid Res.*, 17 (1976) 314.
- 25 P. A. Szczepanik, D. L. Hachey and P. D. Klein, *J. Lipid Res.*, 19 (1978) 280.
- 26 G. Janssen, S. Toppet, F. Compennolle and G. Parmentier, *Steroids*, 53 (1989) 677.



CHROM. 22 837

## Indirect determination of isocyanates by gas chromatography

CINDY B. FANSKA\* and THOMAS J. BYERLEY

*Midwest Research Institute, 425 Volker, Kansas City, MO 64110 (U.S.A.)*

and

J. DAVID EICK

*Department of Oral Biology, School of Dentistry, University of Missouri at Kansas City, 650 East 25th Street, Kansas City, MO 64104 (U.S.A.)*

(Received July 10th, 1990)

---

### ABSTRACT

A gas chromatographic method was developed to determine the purity of synthesized isocyanate monomers, specifically isocyanatoacrylates, and to determine the isocyanate content of synthesized polymers and prepolymers. The method is a modification of an ASTM procedure in which an isocyanate is allowed to react with excess di-*n*-butylamine. In the ASTM method, the amount of isocyanate present is calculated indirectly from the amount of unreacted di-*n*-butylamine, determined by back titration with standard hydrochloric acid. Determination of the excess di-*n*-butylamine by the gas chromatographic method developed has the advantages of providing better precision and requiring less sample than the titrimetric method. The two methods were compared using phenyl isocyanate as a model test compound. A synthesized monomer, methyl  $\alpha$ -isocyanatoacrylate, was also analyzed, for comparison by both methods.

---

### INTRODUCTION

Several isocyanatoacrylate monomers are being synthesized and evaluated under an NIDR grant: "Development of new multifunctional dental adhesive, DE08223". These include the  $\alpha$  and  $\beta$  isomers of methyl, ethyl, and hexyl isocyanatoacrylate. Prepolymers and copolymers of these monomers contain active isocyanate groups which will react with the hydroxyl and amino functional groups in tooth and composite materials to form covalent chemical bonds. Accurate information on the isocyanate content of the synthesized monomers and polymers is required for this work.

Current analytical methods are limited by high sample consumption requirements and/or by specificity of the methods, requiring modifications for each different compound of interest. These methods can be classified as direct or indirect. Direct methods measure isocyanate content from detector response to the isocyanate compound or its derivative. Indirect methods generally react the isocyanate with excess di-*n*-butylamine (*n*-DBA). The isocyanate content is calculated after quantitating the detector response to the unreacted *n*-DBA. The work reported here involves development of an indirect gas chromatographic method which provides precise

quantitation for isocyanate content while not requiring large sample consumption or compound-specific parameters.

The literature on isocyanates and their reactions spans many years. Various analytical techniques have been utilized for quantitation. In addition to the ASTM method [1] cited, these techniques include spectroscopic methods such as IR [2–4] and UV [5], and chromatographic methods such as gas chromatography (GC) and high-performance liquid chromatography (HPLC). Although a few reported GC methods involve direct injection and detection of isocyanates [6,7], most involve some form of derivatization. After hydrolysis of isocyanates to amines and subsequent derivatization, usually with perfluoro fatty acid anhydrides [8–12], the corresponding amides can be detected. Other methods involve detection of the corresponding amines after hydrolysis [13] or detection of the corresponding urethanes after reaction with ethanol [14,15]. Various detection modes have been utilized. These include flame ionization (FID), nitrogen-specific (NPD) and electron-capture (ECD) detection.

Some reported HPLC methods involve derivatization of isocyanates with amines for detection of the resulting ureas with UV [16,17], fluorescence [18,19], or electrochemical [20] detectors. Aromatic isocyanates can be reacted with ethanol prior to HPLC analysis and detected as the corresponding urethanes either by UV or electrochemically [21–23]. Wong and Frisch [24] determined concentrations of unreacted phenyl isocyanate during kinetic studies of the reaction between phenyl isocyanate and *n*-butanol, by allowing the excess to react with *n*-DBA. Sample aliquots were quenched with *n*-DBA solutions and the amount of phenyl isocyanate calculated indirectly from the amount of unreacted *n*-DBA determined by back titration. Wong and Frisch also performed HPLC analyses to detect the reaction product, di-*n*-phenyl-butyl urea, as well as initial and intermediate products.

## EXPERIMENTAL

### *Reagents*

Phenyl isocyanate and dodecane were obtained from Aldrich (Milwaukee, WI, U.S.A.). *n*-DBA was obtained from Eastman Kodak (Rochester, NY, U.S.A.). Toluene was obtained from Burdick and Jackson (Muskegon, MI, U.S.A.) and was certified to contain not more than 0.005% water. Isopropanol was obtained from Fisher Scientific (Fair Lawn, NJ, U.S.A.). Bromphenol blue indicator was prepared by mixing 0.100 g of bromphenol blue, obtained from Fisher Scientific, with 1.5 ml of 0.1 *M* sodium hydroxide solution and diluting to 100 ml with deionized water. Hydrochloric acid solution, 0.1 *M*, was obtained as Dilut-IT from Baker (Phillipsburg, NJ, U.S.A.) and was prepared with deionized water as per package directions. Methyl  $\alpha$ -isocyanatoacrylate was synthesized at Midwest Research Institute.

### *Titration procedure*

The ASTM method [1] was utilized. This method covers the determination of the isocyanate group content of a urethane intermediate or prepolymer. Possible interferences include phosgene, the carbamyl chloride of isocyanate, hydrogen chloride, or any other acidic or basic impurities of sufficient strength.

Replicate samples (at least five) of phenyl isocyanate or synthesized methyl  $\alpha$ -isocyanatoacrylate (Fig. 1), 1.1 mequiv., were accurately weighed into 250-ml

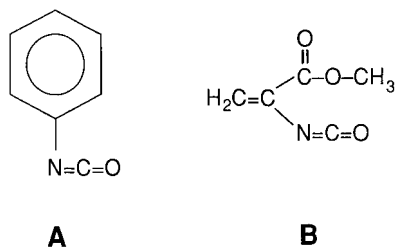


Fig. 1. Structures of (A) phenyl isocyanate and (B) methyl  $\alpha$ -isocyanatoacrylate.

erlenmeyer flasks. Toluene, 25 ml, was added to each flask, which was then stoppered and swirled to mix. Using a pipet, 25 ml of a 0.1 *M* di-*n*-butylamine solution in toluene was added to each flask. The solutions were magnetically stirred for 30 min with stoppers in place. Isopropanol, 100 ml, was added to each. Five drops of the bromphenol blue indicator was added, and each sample was titrated with the 0.1 *N* hydrochloric acid to a yellow end point. Blank titrations were run including all reagents but omitting the isocyanate sample compound.

The isocyanate (NCO) content was calculated as follows:

$$\text{NCO, \%} = \{(B - V) \cdot M \cdot 0.0420\} / W \cdot 100$$

where *B* = milliliters of HCl required to titrate the blank, *V* = milliliters of HCl required to titrate the sample, *M* = molarity of HCl (0.1000), 0.0420 = milliequivalent weight of the NCO group, *W* = weight of sample in grams.

#### *Gas chromatography procedure*

The GC method developed is a modification of the ASTM procedure in that the isocyanate compound is allowed to react with excess *n*-DBA, but the amount of unreacted *n*-DBA is determined by GC analysis rather than by titration. An internal standard was added to correct for any volumetric and injection errors.

#### *GC apparatus and operating conditions*

A Varian Model 3700 gas chromatograph (Varian Instruments, Sunnyvale, CA, U.S.A.) equipped with a flame ionization detector and Model 8000 autosampler was used. The injector temperature was 300°C and the detector temperature was 320°C; the nitrogen carrier gas flow-rate was 70 ml/min.

A glass column (2 m  $\times$  4 mm I.D.) packed with 10% SP-2401 on Supelcoport (100–120 mesh) (Supelco, Bellefonte, PA, U.S.A.) was programmed with an oven temperature ramp of 65 to 100°C at 10°C/min and a final hold of 2 min. The sample injection volume was 1  $\mu$ l. The attenuation was 256 at a range of  $10^{-10}$ . The retention times, peak areas, and internal standard quantitations were determined with a Nelson Analytical Model 4400 chromatography data system (Perkin-Elmer Nelson Systems, Cupertino, CA, U.S.A.). The retention times for *n*-DBA and for the dodecane internal standard were 2.3 min and 4.4 min, respectively.

### *Preparation of standard solutions for GC analyses*

Standards at four concentration levels ranging from 400 to 1600  $\mu\text{mol}$  *n*-DBA per 25 ml toluene were prepared from stock solutions of *n*-DBA and dodecane internal standard.

### *Sample preparation for GC analyses*

Replicate samples (at least five) of phenyl isocyanate or synthesized methyl  $\alpha$ -isocyanatoacrylate (Fig. 1), 900–1100  $\mu\text{mol}$ , were weighed accurately into 25-ml volumetric flasks. A stock solution containing 41.36 mg/ml *n*-DBA and 40.0 mg/ml dodecane, internal standard, was prepared. Five milliliters of this stock solution was pipetted into each volumetric flask. The flasks were filled to volume with toluene and the solutions mixed well. A small stirring bar was introduced into each flask, and the solutions were magnetically stirred for at least 30 min prior to injection into the GC system. Unreacted stock blanks were prepared using all reagents above except the isocyanate sample compound.

### *GC analysis and calculations*

Samples were analyzed concurrently with multilevel standards, unreacted di-*n*-butylamine stock blanks, and internal standard blanks. Three replicate injections of each sample were made and five to nine replicate injections of each standard were made using an autosampler.

Areas for the *n*-DBA and internal standard peaks were integrated by the Nelson Analytical data system, and normal internal standard calculations and linear calibration curves were used to quantitate the amount of *n*-DBA detected. The difference in the amount of *n*-DBA detected, in  $\mu\text{mol}$ , between the unreacted stock blank and the reacted isocyanate sample solution also represents the molar amount of isocyanate detected.

### *Range and precision study*

Triplicate samples of phenyl isocyanate at each of six levels were analyzed by both the GC and titration methods. The sample amounts, ranging from 25 to 1000  $\mu\text{mol}$ , were obtained from serially diluted stock solutions. The data were analyzed to determine the precision of the methods at each sample amount level.

## RESULTS

### *Comparison of GC and titration results*

The percent isocyanate (NCO) contents determined for phenyl isocyanate by the GC and titration methods were:

Method	NCO (%)
GC	$34.47 \pm 0.31\%$ C.V. (coefficient of variation)
Titration	$34.42 \pm 1.6\%$ C.V.

The theoretical NCO content for a pure sample of phenyl isocyanate is 35.27%. The results above, expressed as sample purity are 97.73 and 97.58%, respectively. The label purity was 98 + %.

The percent NCO contents determined for the synthesized methyl  $\alpha$ -isocyanatoacrylate by the two methods are:

Method	NCO (%)
GC	$30.50 \pm 0.17\%$ C.V.
Titration	$30.55 \pm 0.37\%$ C.V.

The theoretical NCO content for a pure sample of methyl  $\alpha$ -isocyanatoacrylate is 33.06%.

Statistical calculations utilizing the *t*-test at the 95% confidence level indicate no significant differences between the results obtained from the GC method and those from the titration method.

A typical GC chromatogram obtained from the reaction of phenyl isocyanate and *n*-DBA by the described method is shown in Fig. 2.

#### Linearity of GC method

Linear regression analysis (concentration vs. response defined as the peak area ratio of *n*-DBA to internal standard) was performed. The correlation coefficients for standard curves were  $> 0.9999$ .

#### Range and precision study

Comparison of the precision for the GC and titration methods at six different sample amounts is shown in Fig. 3. The levels of precision for the two methods at the 1000- and 500- $\mu$ mol levels are quite comparable. However, below 500  $\mu$ mol, the precision of the GC method was significantly better than that of the titration method. Preliminary results indicate the applicability of the GC method to a ten-fold lower

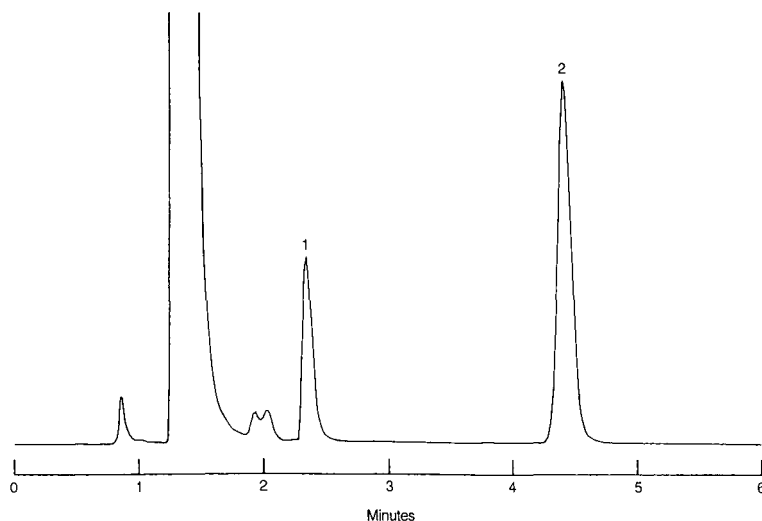


Fig. 2. Typical chromatogram obtained from the reaction of phenyl isocyanate and *n*-DBA using the reported method. Peaks: 1 = unreacted di-*n*-butylamine; 2 = dodecane, internal standard.

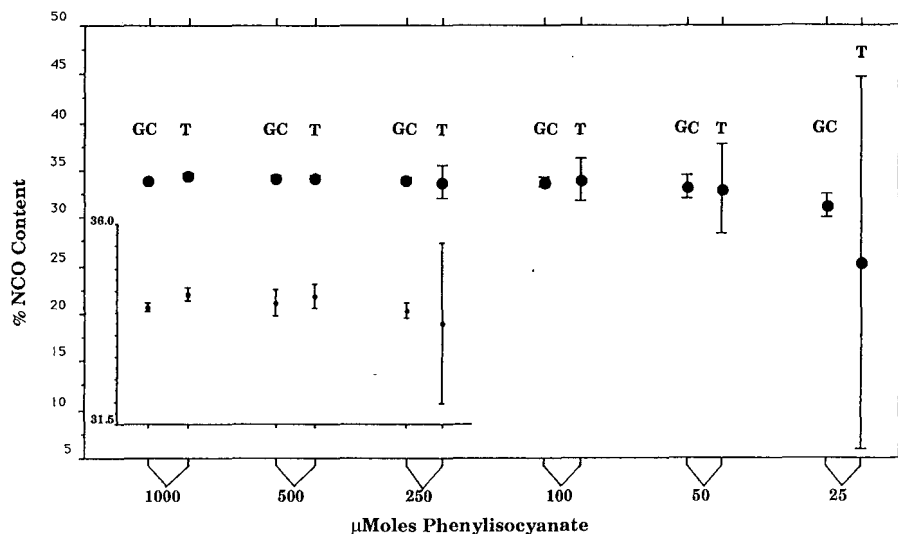


Fig. 3. Comparison of the precision of the GC and titration (T) results from triplicate samples at six sample levels. The mean results of triplicate determinations are indicated by the dots. The bracketed bars represent the confidence intervals for each set of analyses at the 95% confidence level. The inset is a scale expansion of the confidence intervals above it.

sample range. However, utilization of a GC column optimized for amine analyses may be required for the lower range application.

## DISCUSSION

### Method development

Several aspects of the reaction and the GC method were investigated. The completeness of the reaction was considered. Initial investigations were made to determine if a catalyst (di-*n*-butyltin dilaurate), heat (45°C), or additional reaction time would improve the *n*-DBA-isocyanate reaction. Results indicated that none of these factors had a significant effect on the extent of the reaction.

Some detection response differences were observed with different GC conditions, particularly with the injector temperature. One factor in this effect is the presence of the non-eluted urea reaction product on the column. During the GC analysis of phenyl isocyanate, the reaction product, di-*n*-butylphenyl urea (phenyl dibutyl urea), remains on the column and can cause a reduction in the amount of *n*-DBA detected in subsequent injections. The column oven temperature must be increased significantly in order to elute the urea.

No information on the boiling point of di-*n*-butylphenyl urea was found in the literature. The melting point is reported to be 85–86°C [25]. To determine the boiling point of the reaction product, a small amount was synthesized in toluene and recrystallized from ethanol. Differential scanning calorimetry (DSC) analysis of the resulting product indicated a melting point of 83.7°C (purity of 99.90 mol% [26]) and a boiling point of 267.1°C with no residue.

An injector temperature higher than the boiling point of di-*n*-butylphenyl urea was chosen (300°C) to minimize the retention of *n*-DBA during subsequent injections. Di-*n*-butylphenyl urea will elute from the column at oven temperatures of 250–270°C but does not yield a well shaped peak. Care must be taken to bake the ureas off the column periodically.

#### *Comparison of indirect vs. direct methods*

The indirect method of determining isocyanate content by reaction with *n*-DBA and subsequent quantitation of the unreacted *n*-DBA by GC has several advantages over direct GC analysis. With direct injection and detection of isocyanates, sample collection and stability are concerns because isocyanates will react readily with moisture and amines. In the indirect methods, reaction with *n*-DBA “fixes” the isocyanate concentration at that point. Direct analysis is limited to those isocyanate compounds which are volatile enough for GC and which are not thermally labile. With indirect analysis, volatility and stability are not concerns since the compound being quantitated in the GC system is the unreacted *n*-DBA, not the isocyanate.

Additionally, basing the GC method on quantitation of *n*-DBA, regardless of what isocyanate compound is being analyzed, means that the method can be applied to any isocyanate without modification of the GC parameters or column. In contrast, direct injection and detection of isocyanates or their derivatives (amines, amides, or urethanes) require that the analytical parameters be adapted to each compound of interest. With this GC analysis for *n*-DBA, however, one must determine that other compounds, such as impurities or starting materials in a synthesis reaction mixture, do not coelute with *n*-DBA or the internal standard.

A significant advantage of the indirect methods over direct methods is that no isocyanate compound is needed to generate standard solutions for calibration. This greatly reduces the amount of sample required for analysis. In fact, for the indirect methods, the isocyanate sample identity is not required.

#### *Comparison of indirect methods —GC vs. titration*

Quantitation of the GC analyses, by means of electronic integration, is inherently less subjective than quantitation of titration analyses. Also, multiple injections of each weighed sample and standard can be made with the GC method whereas only one titration can be performed per weighing. This additional data, the use of an internal standard, the ability to automate sample injection, and objective quantitation yields analytical results which are more precise.

The GC method can provide data on isocyanate content using much less sample than for a titration analysis with comparable precision.

Additionally, for isocyanate synthesis, the indirect GC method may provide more information than titrations since it may be possible to quantitate the starting materials and the *n*-DBA content concurrently, if these starting materials elute at appropriate retention times. This would provide dual confirmation of the reaction status.

#### CONCLUSION

The analysis method reported here appears, from data obtained on the two

sample compounds, to be a valid, precise and objective alternative to titration for the determination of isocyanate content of compounds. The method is capable of quantifying samples containing 100–1200  $\mu\text{mol}$  of isocyanate. Preliminary results indicate the applicability to a 10–120- $\mu\text{mol}$  range. The ability to use reduced amounts of sample, obtain higher precision, include an internal standard, and to automate the analyses are significant analytical advantages.

#### ACKNOWLEDGEMENTS

This work was funded in part by the National Institute for Dental Research, National Institutes of Health, Grant No. DE08223, Development of New Multi-functional Dental Adhesive.

#### REFERENCES

- 1 *Method D2572-87: Standard Test Method for Isocyanate Groups in Urethane Materials or Prepolymers, Vol. 06.02, Paint-Pigments, Resins and Polymers; Cellulose*, American Society for Testing and Materials, Philadelphia, PA, 1990, p. 374.
- 2 K. G. Flynn and D. R. Nenortas, *J. Org. Chem.*, 28 (1963) 3527.
- 3 F. W. Abbate and H. Ulrich, *J. Appl. Polym. Sci.*, 13 (1969) 1929.
- 4 I. C. Kogon, *J. Org. Chem.*, 24 (1959) 438.
- 5 F. W. VanderWeij, *J. Polym. Sci. Polym. Chem. Ed.*, 19 (1981) 381, 3063.
- 6 G. Skarping, B. E. F. Smith and M. Dalene, *J. Chromatogr.*, 331 (1985) 331.
- 7 B. B. Wheals and J. Thomson, *Chem. Ind. (London)*, (1967) 753.
- 8 G. Skarping, C. Sango and B. E. F. Smith, *J. Chromatogr.*, 208 (1981) 313.
- 9 G. Skarping, L. Renman and M. Dalene, *J. Chromatogr.*, 270 (1983) 207.
- 10 G. G. Esposito and T. W. Dolzine, *Anal. Chem.*, 54 (1982) 1572.
- 11 G. Skarping, L. Renman and B. E. F. Smith, *J. Chromatogr.*, 267 (1983) 315.
- 12 G. Skarping, B. E. F. Smith and M. Dalene, *J. Chromatogr.*, 303 (1984) 89.
- 13 G. Audunsson and L. Mathiasson, *J. Chromatogr.*, 261 (1983) 253.
- 14 G. Skarping, M. Dalene and L. Mathiasson, *J. Chromatogr.*, 435 (1988) 453.
- 15 G. Skarping, L. Renman, C. Sango, L. Mathiasson and M. Dalene, *J. Chromatogr.*, 346 (1985) 191.
- 16 K. L. Dunlap, R. L. Sandridge and J. Keller, *Anal. Chem.*, 48 (1976) 497.
- 17 D. C. Hakes, G. D. Johnson and J. S. Marhevka, *Am. Ind. Hyg. Assoc. J.*, 47 (1986) 181.
- 18 S. P. Levine, J. H. Hoggatt, E. Chladek, G. Jungclaus and J. L. Gerlock, *Anal. Chem.*, 51 (1979) 1106.
- 19 L. H. Kormos, R. L. Sandridge and J. Keller, *Anal. Chem.*, 53 (1981) 1122.
- 20 S. D. Meyer and D. E. Tallman, *Anal. Chim. Acta*, 146 (1983) 227.
- 21 M. Dalene, L. Mathiasson, G. Skarping, C. Sango and J. F. Sandstrom, *J. Chromatogr.*, 435 (1988) 469.
- 22 E. H. Nieminen, L. H. Saarinen and J. T. Laakso, *J. Liq. Chromatogr.*, 6 (1983) 453.
- 23 D. A. Bagon and C. J. Purnell, *J. Chromatogr.*, 190 (1980) 175.
- 24 S. W. Wong and K. C. Frisch, *J. Polym. Sci. Polym. Chem. Ed.*, 24 (1986) 2867.
- 25 *Beilsteins Handbuch der Organischen Chemie*, Vol. 12, Supplement 3, Part 2, Springer, Berlin, Heidelberg, 1972, p. 763, System No. 1627/H 349.
- 26 *Method E928-85 (Reapproved 1989): Standard Test Method for Mol Percent Impurity by Differential Scanning Calorimetry, Vol. 14.02, General Test Methods, Nonmetal; Laboratory Apparatus; Statistical Methods; Appearance of Materials; Durability of Nonmetallic Materials*, American Society for Testing and Materials, Philadelphia, PA, 1990, p. 585.



# Correlation between structure and gas chromatographic behaviour of nitrogen-containing heterocyclic compounds

## I. Methyl substitution of pyridopyrimidine derivatives

O. PAPP, Gy. SZÁSZ\* and J. KÖKÖSI

*Institute of Pharmaceutical Chemistry, Semmelweis Medical University, Hőyes E. ú. 9. H-1092 Budapest (Hungary)*

and

I. HERMECZ

*Chinoin Pharmaceutical Works, Budapest (Hungary)*

(First received March 29th, 1990; revised manuscript received August 21st, 1990)

---

### ABSTRACT

The methyl isomers of 4-oxopyridopyrimidine and tetrahydro-4-oxopyridopyrimidine and their 2,3-polymethylene derivatives were investigated. The compounds were characterized by their gas chromatographic retention indices measured on apolar and medium-polarity stationary phases. On the basis of the retention index increments, numerical values are given to characterize the shielding effects exerted on the polar centres of the molecule by methyl groups substituted at different positions. The steric and electronic effects are also characterized by retention index values.

---

### INTRODUCTION

Investigations on the relationships between chemical structure and physico-chemical data have already led to many valuable results [1,2]. Some investigations have revealed a correlation between the retention data and other physico-chemical parameters [3–6]. Retention data can be processed by mathematical methods, *e.g.*, by factor analysis [7], graphical evaluation [8] or pattern recognition [9]. As surveyed by Ettre [10], the Kováts retention index and its derivatives can be used to characterize retention.

The behaviour of C<sub>9</sub>–C<sub>14</sub> alkylbenzene was described by Engewald and Wernich [11] using  $H^S$ ,  $dI_{CH_2}$  and  $\Delta I$  values determined on four stationary phases with different polarities on the basis of the retention index additivity.

The structure–retention index relationship for aliphatic fatty acid esters was examined in detail by Haken and Srisukh [12]. For about 70 benzene and naphthalene derivatives, Macák *et al.* [13] found a correlation between the retention index and the type and position of the functional group [13]. The structure–retention index

relationship for cyclic alcohols was described by Heintz *et al.* [14]. Nakazawa *et al.* [15] examined 37 methyl derivatives of carbazole and found a relationship between the sites and number of the substituents and their  $t'_R$  values. Morishita *et al.* [16] determined the shielding effect of certain carbon atoms of the alkyl chain with respect to the sulfhydryl group attached to it.

In previous investigations on the physico-chemical properties of nitrogen-containing pyrido[1,2-*a*]pyrimidines and condensed quinazolines, we reported the determination of some parameters that play important roles in the pharmacokinetic phase (solubility [17,18],  $\log P$  [19,20],  $pK_a$  [21], molar refraction [22]), and also structural relationships. In this series of papers, we demonstrate how the site of alkyl substitution, the number of carbon atoms in the substituent and variations in the number of atoms in the ring system are manifested in the retention data. This paper presents gas chromatographic results that provide information about the manner and extent to which methyl groups substituted at different points on the skeleton influence the retention behaviour and associated physico-chemical properties. In the evaluation of the retention index increments, we accepted that  $dI_{Me}^{apol} = 100$  index units (i.u.) (Me = methyl) only for those alkyl side-chains where the increment relates to a carbon atom following after a carbon chain with  $Z > 5$ . Accordingly, for methyl groups on heterocyclic rings a considerable difference from 100 i.u. is to be expected, and this can give information on the position-dependent interaction of the stationary phase and the chromatographed compound, and hence on the electronic and steric properties of the molecules in a systematically constructed series of positional isomers.

## EXPERIMENTAL

Thirty-four nitrogen-containing heterocyclic compounds were synthesized by a method described elsewhere [23]. The purity of the compounds was controlled by spectroscopic and chromatographic methods. In three of the compounds (**1**, 4*H*-pyrido[1,2-*a*]pyrimidin-4-one; **3**, 4*H*-cyclopenteno[2,3-*e*]pyrido[1,2-*a*]pyrimidin-4-one; **5**, 1,2,3,4-tetrahydro-11*H*-pyrido[2,1-*b*]quinazolin-11-one), ring A is aromatic; the other three (**2**, 6,7,8,9-tetrahydro-4*H*-pyrido[1,2-*a*]pyrimidin-4-one; **4**, 6,7,8,9-tetrahydro-4*H*-cyclopenteno[2,3-*e*]pyrido[1,2-*a*]pyrimidin-4-one; **6**, 1,2,3,4,6,7,8,9-octahydro-11*H*-pyrido[2,1-*b*]quinazolin-11-one) are tetrahydro derivatives.

The positions of the substituents and the retention data are shown in Tables I and II.

For compounds **1** and **2** there are methyl substituents at all possible positions. Compounds **3–6** were regarded as 2,3-polymethylene derivatives of **1** and **2**, and hence substituted only at positions 6–9.

### Instruments and conditions

A Hewlett-Packard Model 5710A gas chromatograph provided with a flame

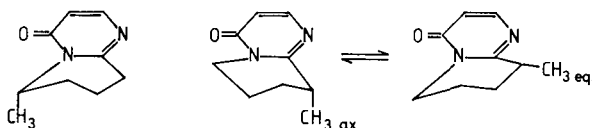


Fig. 1. 6-Methyl- (left) and 9-methyltetrahydropyridopyrimidine (right) conformers.

ionization detector was used. The retention times and the retention index values were determined from seven parallel measurements with a standard deviation of 2 i.u., using a Digint 80 integrator (Chinoin, Nagylétény, Hungary). The column temperature was 220 and 240°C and the injector port and detector temperatures were 250°C. The carrier gas was nitrogen at a flow-rate of 25 ml/min. The column (1.8 m × 2 mm I.D.) contained 5% OV-1, 5% OV-25 and 5% OV-225 (Macherey, Nagel & Co., Düren, F.R.G.) on Chromosorb W AW DMCS (80–100 mesh). The retention index values were calculated as means of seven measurements. The standard deviation was found to be less than 2 i.u.

## RESULTS AND DISCUSSION

The chromatographic behaviour of the compounds was analysed by systematic comparison of the retention indices and their derivative values were calculated as follows:  $dI_{\text{Me}}^{\text{OV-1}} = I_{\text{toluene}}^{\text{OV-1}} - I_{\text{benzene}}^{\text{OV-1}}$  and  $\Delta dI_{\text{Me}} = dI_{\text{Me}}^{\text{pol}} - dI_{\text{Me}}^{\text{apoli}}$ , both at the same temperature. The numerical values for compounds **1–6** are given in Tables I and II.

The data for compound **1** reveal that, on the basis of the increments for the methyl groups, three regions can be characterized in the molecules: the environment of nitrogen N-1 (C-2 and C-9), the cyclic acid amide (C-3 and C-6) and the part of ring A distant from the polar groups (C-7 and C-8). The ability of N-1 to interact is decreased by the C-2 and C-9 substituents to almost the same extent as the C-3 and C-6 substituents decrease that of the carbonyl group. The C-7 and C-8 substituents not exerting a steric effect do not reduce the interaction ability of polar groups; indeed, they may even increase it slightly through a hyperconjugation effect. A comparison of the data on the aromatic system **1** with those on the tetrahydro derivative **2** demonstrates that the effects on ring B are almost the same, but those on ring A differ.

TABLE I

RETENTION INDEXES OF METHYL ISOMERS **1** AND **2** ON OV-1 AND OV-25 STATIONARY PHASES

Compound	Site of methyl substitution	Retention indices		Increments	
		$I_{220^\circ\text{C}}^{\text{OV-1}}$	$I_{220^\circ\text{C}}^{\text{OV-25}}$	$dI_{\text{Me}}^{\text{OV-1}}$	$d\Delta I_{\text{Me}}^{\text{OV-25-OV-1}}$
<b>1</b>	—	1580	2124	—	—
<b>1a</b>	2	1648	2189	68	–3
<b>1b</b>	3	1638	2168	58	–21
<b>1c</b>	6	1636	2150	56	–20
<b>1d</b>	7	1696	2234	116	–6
<b>1e</b>	8	1703	2239	123	–8
<b>1f</b>	9	1647	2159	67	–32
<b>2</b>	—	1581	2128	—	—
<b>2a</b>	2	1657	2203	76	–1
<b>2b</b>	3	1637	2170	56	–14
<b>2c</b>	6	1578	2081	–3	–50
<b>2d</b>	7	1654	—	73	—
<b>2e</b>	8	1638	—	102	—
<b>2f</b>	9	1615	2114	34	–48

TABLE II

RETENTION INDICES OF COMPOUNDS **3**, **4**, **5** AND **6** ON OV-1 AND OV-225 STATIONARY PHASES

Compound	Site of methyl substitution	Retention indices		Increments	
		$I_{220^{\circ}\text{C}}^{\text{OV-1}}$	$I_{220^{\circ}\text{C}}^{\text{OV-25}}$	$dI_{\text{Me}}^{\text{OV-1}}$	$d\Delta I_{\text{Me}}^{\text{OV-25-OV-1}}$
<b>3</b>	—	1968	2890	—	—
<b>3a</b>	6	2020	2865	52	-77
<b>3b</b>	7	2084	3017	116	11
<b>3c</b>	8	2089	3034	121	23
<b>3d</b>	9	2023	2880	55	-65
<b>4</b>	—	1961	2917	—	—
<b>4a</b>	6	1942	1820	-8	-59
<b>4b</b>	7	1998	2929	37	-25
<b>4c</b>	8	2000	2929	39	-27
<b>4d</b>	9	1978	2843	17	59
<b>5</b>	—	2064	2972	—	—
<b>5a</b>	6	2120	2947	56	-81
<b>5b</b>	7	2189	3098	125	-10
<b>5c</b>	8	2190	3125	126	-27
<b>5d</b>	9	2123	2951	59	-80
<b>6</b>	—	2059	2995	—	—
<b>6a</b>	6	2045	2902	-14	-79
<b>6b</b>	7	2095	3009	36	-22
<b>6c</b>	8	2097	3011	38	-22
<b>6d</b>	9	2071	2924	12	-83

The reason for this is presumably that the saturation of ring A eliminates the planar character of the system and the substituents may cause conformational changes in the multiplanar flexible ring.

NMR investigations by Tóth [24] indicated that the 6- and 9-methyl substituents are in pseudo-axial positions on the half-chair conformer (Fig. 1). In accordance with this, they hinder the solvent-solute interaction more effectively. On the other hand, the 7- and 8-methyl substituents are in equatorial positions [24] and hence they influence the molecule-stationary phase interaction only by modifying the ring conformation. For compounds **1-6**, the various polar and apolar solvent-solute interactions can be distinguished by comparing the  $dI_{\text{Me}}$  and  $d\Delta I_{\text{Me}}$  values relating to the same positions. The difference of about 50 i.u. between the two series originates from the interaction of the aromatic system.

Subsequently, methyl-substituted tricyclics saturated or unsaturated in ring A were investigated. The  $dI_{\text{Me}}$  values for 6,7,8,9-methyl-substituted compounds **3** and **5** (planar because of aromatic ring A) correspond well with the data for **1**, but the  $dI_{\text{Me}}$  values for saturated **4** and **6** differ from those for **2** measured at the same position. In these instances, the polar groups are already shielded (2,3-polymethylenepyridopyrimidines) and the introduction of the second substituent probably causes a larger difference because of the resulting double shielding. However, the  $dI_{\text{Me}}$  values can be divided into two groups here too, according to the extent of the difference: positions 6 and 9 close to the polar centres, and positions 7 and 8 distant from them. In the latter

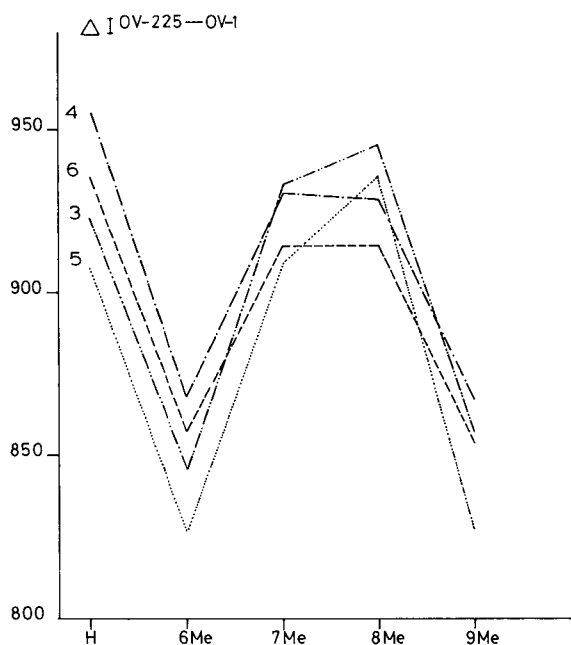


Fig. 2.  $\Delta I$  values of methyl (Me) isomers 3-6 as a function of the substitution site.

instance the validity of the rule  $dI_{\text{Me}}^{\text{OV-1}} = 100$  i.u. is presumed, and the surplus of 22 i.u. for the 7- and 8-methyl derivatives of **3** and **5** can be interpreted in terms of hyperconjugation, while the deficit of 62 i.u. for the similar derivatives of **4** and **6** can be explained by the increased steric influence. In contrast with the  $dI_{\text{Me}}$  values, which express several kinds of interactions, the steric effect does not participate in the  $d\Delta I_{\text{Me}}$  values. This can also be seen on comparison of the  $dI$  and  $I$  values for **5** and **6**. The almost identical increment values in the same positions show that the planar or multiplanar character of the ring system can be characterized by different  $dI_{\text{Me}}$  values, but by similar  $\Delta I_{\text{Me}}$  values.

The combined effect of the substituent and the skeleton is shown in Fig. 2, which presents the  $\Delta I^{(\text{OV-225})-(\text{OV-1})}$  values for **3-6** and their methyl isomers as a function of the substitution site. The shapes of the curves indicate that the polarity sequence is influenced both by the saturated-unsaturated character of ring A and by the number of atoms in ring C. Thus, the polarity sequence for the ring size is  $4 > 6 > 3 > 5$  for both the non-substituted compounds and the majority of the methyl derivatives. The 7- and 8-methyl isomers of **3** and **5** differ from this sequence, because in these compounds the methyl substituent is involved in hyperconjugation interaction with the aromatic system, and this interaction causes a considerable retention index surplus on the polar stationary phase.

## REFERENCES

- 1 J. K. Seydel and K.-J. Schaper, *Chemische Struktur und Biologischen Aktivität von Wirkstoffen*, Verlag Chemie, Weinheim, New York, 1979.
- 2 S. H. Yalkowsky, A. A. Sinkula and S. C. Valvani, *Physical Chemical Properties of Drugs*, Marcel Dekker, New York, 1980.
- 3 K. D. Bartle and M. L. Lee, *Chromatographia*, 14 (1981) 71.
- 4 F. Saura-Calixto and A. Garcia-Raso, *Chromatographia*, 14 (1981) 143.
- 5 G. Dahlmann, H. J. K. Köser and H. H. Oelert, *Chromatographia*, 12 (1979) 665.
- 6 V. M. Nabivach and A. V. Kirilenko, *Chromatographia*, 13 (1980) 93.
- 7 Z. Buydens and D. L. Massart, *Anal. Chem.*, 53 (1981) 1990.
- 8 A. Váradi and T. Tóth, *Magy. Kém. Foly.*, 80 (1974) 41.
- 9 J. K. F. Huber and G. Reich, *Anal. Chim. Acta*, 122 (1980) 139.
- 10 L. S. Ettre, *Chromatographia*, 7 (1974) 141.
- 11 W. Engewald and L. Wernrich, *Chromatographia*, 9 (1976) 540.
- 12 J. K. Haken and D. Srisukh, *J. Chromatogr.*, 219 (1981) 45.
- 13 J. Macák, V. Nabivach, P. Buryan and S. Sindler, *J. Chromatogr.*, 234 (1982) 285.
- 14 M. Heintz, M. Gruselle, A. Druilhe and D. Lefort, *Chromatographia*, 9 (1976) 367.
- 15 T. Nakazawa, M. Kuroki and Y. Tsunashima, *J. Chromatogr.*, 211 (1981) 388.
- 16 F. Morishita, H. Murakita, Y. Takemura and T. Kojima, *J. Chromatogr.*, 239 (1982) 483.
- 17 Zs. Halász-Ignáth, Gy. Szász, J. Kökösi and I. Hermecz, *Acta Pharm. Hung.*, 53 (1983) 203.
- 18 Zs. Halász-Ignáth, Gy. Szász and I. Hermecz, *Acta Pharm. Hung.*, 56 (1986) 34.
- 19 O. Papp, K. Valkó, Gy. Szász, I. Hermecz, J. Vámos, K. Hankó-Novák and Zs. Halász-Ignáth, *J. Chromatogr.*, 252 (1982) 67.
- 20 K. Hankó-Novák, Gy. Szász, O. Papp, J. Vámos and I. Hermecz, *Acta Pharm. Hung.*, 53 (1983) 208.
- 21 K. Hankó-Novák, M. Józán, Gy. Szász, J. Kökösi and I. Hermecz, *Acta Pharm. Hung.*, 54 (1984) 280.
- 22 O. Papp, M. Józán, Gy. Szász and I. Hermecz, *J. Chromatogr.*, 403 (1987) 11.
- 23 I. Hermecz and Z. Mészáros, *Adv. Heterocycl. Chem.*, 33 (1983) 241.
- 24 G. Tóth, *Dissertation*, Hung. Acad. Sci., Budapest, 1983.

# Correlation between structure and gas chromatographic behaviour of nitrogen-containing heterocyclic compounds

## II. Alkyl substitution of quinazolone derivatives

O. PAPP, Gy. SZÁSZ\* and L. ÖRFI

*Institute of Pharmaceutical Chemistry, Semmelweis Medical University, Hőgyes E. ú. 9, H-1092 Budapest (Hungary)*

and

I. HERMECZ

*Chinoin Pharmaceutical Works, Budapest (Hungary)*

(First received March 29th, 1990; revised manuscript received August 21st, 1990)

---

### ABSTRACT

Mono- and dialkyl-substituted quinazolones were synthesized by literature or its modifications. Six homologous series were prepared, varying in the substituent introduced and its position. The retention indices of the compounds were determined on OV-1 and OV-25 stationary phases. The influence of the number of carbon atoms in the homologues alkyl chain on the *I* and  $\Delta I$  values could be characterized well. The behaviour of the alkylquinazolones and the ring-closed tricyclic with the same number of carbon atoms could also be characterized numerically. A dominant effect was exerted by the substituent in the neighbouring position to the alkyl chain.

---

### INTRODUCTION

2,3-Substituted quinazolone derivatives include many compounds with valuable pharmacological effects [1], *e.g.*, a theophylline-like antiasthmatic effect [2,3]. The bronchodilator effect varies considerably as a function of the substitution. It is maximum for the condensed ring and the corresponding disubstitution [4]. During an analysis of the physico-chemical parameters of pyrido[1,2-*a*]pyrimidines and quinazolones with an antiasthmatic effect, we characterized the structural features connected with the action of many nitrogen-containing tricyclics [5,6]. This paper describes a gas chromatographic investigation and the quantitative relationship between the structure and physico-chemical properties of 2,3-substituted quinazolones.

### EXPERIMENTAL

The apparatus and chromatographic conditions were as described in Part I [7].

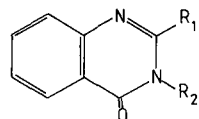
The 2,3-substituted quinazolones were synthesized by appropriate modification of the original literature methods [8].

## RESULTS AND DISCUSSION

Six homologous series of alkyl-substituted 4-oxoquinazoline derivatives were prepared with various substituents  $R_1$  and  $R_2$  (Table I). The homologous series

TABLE I

SERIES OF COMPOUNDS AND RETENTION INDEX VALUES



No. of series	$R_1$	$R_2$	$I_{220}^{OV-1}$ <sup>a</sup>	$I_{220}^{OV-2.5}$ <sup>b</sup>	$\Delta I$
1	H	H	1733	2360	627
	CH <sub>3</sub>	H	1736	2337	601
	C <sub>2</sub> H <sub>5</sub>	H	1788	2365	577
	C <sub>3</sub> H <sub>7</sub>	H	1853	2418	565
	C <sub>4</sub> H <sub>9</sub>	H	1955	2509	554
	C <sub>5</sub> H <sub>11</sub>	H	2050	2604	554
2	CH <sub>3</sub>	CH <sub>3</sub>	1733	2293	560
	C <sub>2</sub> H <sub>5</sub>	CH <sub>3</sub>	1800	2333	533
	C <sub>3</sub> H <sub>7</sub>	CH <sub>3</sub>	1865	2380	515
	C <sub>4</sub> H <sub>9</sub>	CH <sub>3</sub>	1957	2467	510
	C <sub>5</sub> H <sub>11</sub>	CH <sub>3</sub>	2050	2551	501
	3	CH <sub>3</sub>	C <sub>2</sub> H <sub>5</sub>	1749	2276
C <sub>2</sub> H <sub>5</sub>		C <sub>2</sub> H <sub>5</sub>	1805	2302	497
C <sub>3</sub> H <sub>7</sub>		C <sub>2</sub> H <sub>5</sub>	1869	2349	480
C <sub>4</sub> H <sub>9</sub>		C <sub>2</sub> H <sub>5</sub>	1962	2430	468
C <sub>5</sub> H <sub>11</sub>		C <sub>2</sub> H <sub>5</sub>	2050	2515	465
4		H	H	1733	2360
	H	CH <sub>3</sub>	1639	2201	562
	H	C <sub>2</sub> H <sub>5</sub>	1664	2199	535
	H	C <sub>3</sub> H <sub>7</sub>	1740	2265	525
	H	C <sub>4</sub> H <sub>9</sub>	1835	2349	514
	H	C <sub>5</sub> H <sub>11</sub>	1926	2442	516
5	CH <sub>3</sub>	H	1736	2337	601
	CH <sub>3</sub>	CH <sub>3</sub>	1733	2293	560
	CH <sub>3</sub>	C <sub>2</sub> H <sub>5</sub>	1749	2276	527
	CH <sub>3</sub>	C <sub>3</sub> H <sub>7</sub>	1826	2330	504
	CH <sub>3</sub>	C <sub>4</sub> H <sub>9</sub>	1915	2416	501
	CH <sub>3</sub>	C <sub>5</sub> H <sub>11</sub>	2003	2507	504
6	C <sub>2</sub> H <sub>5</sub>	H	1788	2365	577
	C <sub>2</sub> H <sub>5</sub>	CH <sub>3</sub>	1800	2333	533
	C <sub>2</sub> H <sub>5</sub>	C <sub>2</sub> H <sub>5</sub>	1805	2302	497
	C <sub>2</sub> H <sub>5</sub>	C <sub>3</sub> H <sub>7</sub>	1873	2350	477
	C <sub>2</sub> H <sub>5</sub>	C <sub>4</sub> H <sub>9</sub>	1961	2430	469
	C <sub>2</sub> H <sub>5</sub>	C <sub>5</sub> H <sub>11</sub>	2050	2520	470



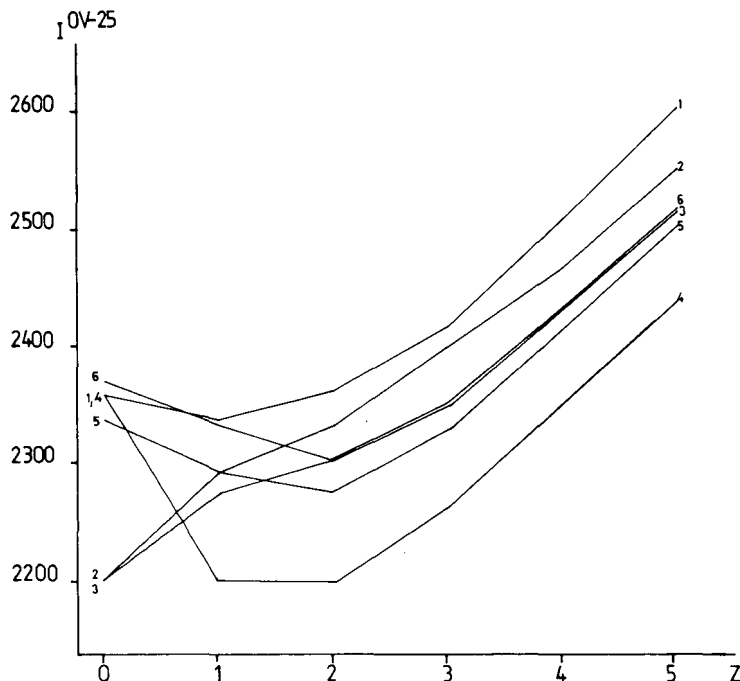


Fig. 1. Relationship between number of carbon atoms ( $z$ ) and retention index of compounds in homologous series. Series 1-6 as in Table I.

contain  $C_1$ - $C_5$  substituents with the differences that the homologous series are connected to C-2 or N-3 with hydrogen, methyl or ethyl on the other atom. The retention index values measured on stationary phase OV-1 are represented as a function of the number of carbon atoms in Fig. 1. The initial parts of the curves verify the relationship formulated by Kováts: for an alkyl group connected to a polar functional group,  $dI_{(CH_2)_{z+1}}^{apol} - dI_{(CH_2)_z}^{apol} \approx 100$  index units (i.u.) only if  $z > 5$ .

The different courses of the six curves also demonstrate that the retention index and  $dI_{CH_2}$  increment values obtained do not depend only on whether the alkyl chain is connected to C-2 or N-3; their values are additionally influenced by the constant substituents of the individual series (H,  $CH_3$ ,  $C_2H_5$ ). The influence of the  $R_1$  and  $R_2$  substituents on the retention properties of the molecule can be studied better if the  $\Delta I$  values are depicted as a function of the number of carbon atoms (Fig. 2). The resulting exponential curves are described by the equation

$$\Delta I = a \cdot 10^{-bz} + c$$

where  $a$ ,  $b$  and  $c$  are empirical constants and  $z$  is the number of carbon atoms. The values of the constants were determined by the method of least squares by iteration. The optimum values were indicated by the correlation coefficient. The mean of the difference between the measured and calculated values was less than 1.5 i.u. The

graphical representation reveals that for the different disubstituted derivatives the polarity curves of the homologous series follow almost the same course, which means that an increase in the length of the alkyl groups at positions 2 and 3 of the quinazolone skeleton causes essentially the same change in polarity. There is an important difference in the retention behaviour of the two monosubstituted series. This difference can be attributed to the free NH group, which can interact specifically with the polar stationary phase and may form a hydrogen bridge.

From a comparison of the two series, the extent of this interaction can be expressed numerically for the given pair of stationary phases as  $39 \pm 2$  i.u. The extent of the change in polarity can be followed better via the derivatives of the polarity curves. Differentiation of eqn. 1 with respect to  $z$  gives

$$\frac{d\Delta I}{dz} = ab \cdot \ln 10 \cdot 10^{-bz} \quad (2)$$

which expresses the polarity change per carbon atom change. By representing the results for the six series graphically, we obtain the curves shown in Fig. 3.

The changes in the degree of polarity in the four homologous series with alkyl disubstitution are nearly the same; they decrease exponentially with an increase in the number of carbon atoms, and for  $z > 5$  tend to zero. The 2-alkylquinazolone homologues display the smallest decrease in polarity and the 3-alkylquinazolones the steepest. On the above basis it appears that the relationship between the number of carbon atoms for  $z = 0-5$  and the  $\Delta I$  values representing the polarity of the compound can be applied generally for homologous series containing a polar functional group.

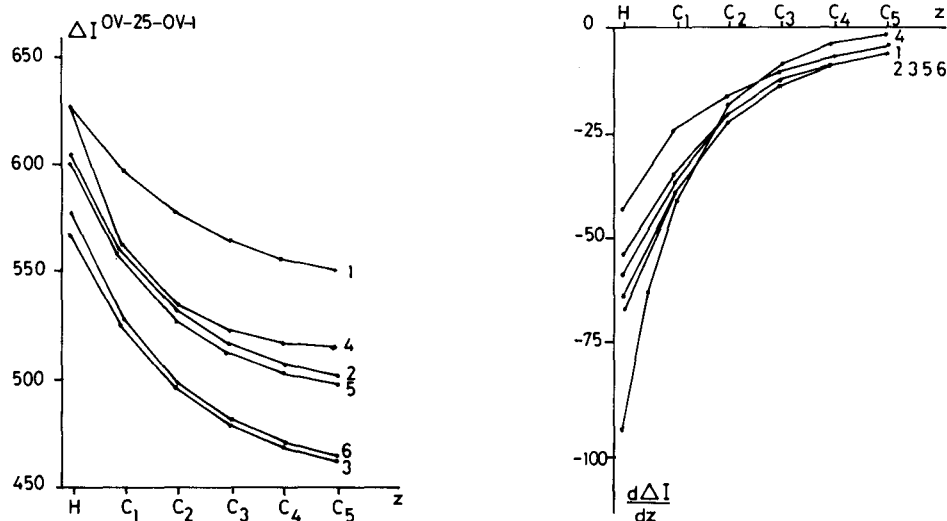
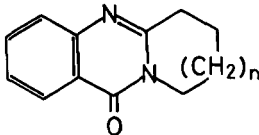
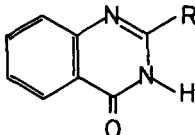


Fig. 2. Relationship between number of carbon atoms ( $z$ ) and polarity of compounds in homologous series. Series 1-6 as in Table I.

Fig. 3. Derived curves of correlation between number of carbon atoms and polarity.

TABLE II

DIFFERENCE IN POLARITY OF NITROGEN-CONTAINING TRICYCLIC AND ALKYL-SUBSTITUTED QUINAZOLONES WITH THE SAME NUMBER OF CARBON ATOMS

				
<i>n</i>	$\Delta I^{OV-1-OV-25}$	R	$\Delta I^{OV-1-OV-25}$	<i>d</i> $\Delta I$
0	670	Propyl	565	105
1	658	Butyl	554	104
2	638	Pentyl	554	84
3	629	Hexyl	544	85

For example, we obtained curves with a similar course to the retention index values for the alkyl homologues of benzoic acid published by Pias and Gasco [9] or those of the N-alkylaniline derivatives investigated by Váradi and Tóth [10].

Subsequently, the data on the aliphatic and cycloaliphatic 2,3-substituted compounds (*I*,  $\Delta I$ ,  $dI/dz$ ) were compared in a search for a relationship between the retention properties and the polarity of aliphatic and cyclic compounds with the same number of carbon atoms (Table II).

For the same number of carbon atoms, it can be assumed that the extents of the inductive effect towards the quinazolone ring are nearly the same, and any difference is an expression of the difference in the steric effects of the freely rotating aliphatic methylene groups relative to the rigid or flexible ring. From a comparison of the tricyclic and the corresponding disubstituted aliphatic quinazolones, this "ring effect" cause a difference of *ca* 100–150 i.u., *i.e.*, for the same number of carbon atoms the ring closure causes a polarity change equivalent to that of about one methylene group. The correlations found are well supported by the previously published  $pK_s$  and  $\log P$  values for the compounds [5,6]. The  $pK_s$  values, which change in parallel with the electronic changes, agree well, whereas the partition coefficient values, which express the steric and polarity changes, exhibit a difference corresponding to one methylene group, as expressed numerically by the gas chromatographic method.

## REFERENCES

- 1 S. Johne, *Prog. Drug Res.*, 26 (1982) 259.
- 2 A. H. Amin, D. R. Mehta and S. S. Samarth, *Prog. Drug Res.*, 14 (1970) 218.
- 3 I. Hermezc, L. Vasvári-Debreczy, Á. Horváth, S. Virágh, T. Breining and J. Kökösi, *Ger. Pat.*, 3 339 635; *C.A.*, 101 (1984) 130 705.
- 4 I. Hermezc, L. Vasvári-Debreczy, Á. Horváth, M. Balogh, J. Kökösi, C. De Vos and L. Rodriguez, *J. Med. Chem.*, 30 (1987) 1543.

- 5 K. Hankó-Novák, M. Józán, Gy. Szász, J. Kőkösi and I. Hermecz, *Acta Pharm. Hung.*, 54 (1984) 280.
- 6 K. Hankó-Novák, Gy. Szász, O. Papp, J. Vámos and I. Hermecz, *Acta Pharm. Hung.*, 53 (1983) 208.
- 7 O. Papp, G. Szász, J. Kőkösi and I. Hermecz, *J. Chromatogr.*, 537 (1991) 365.
- 8 W. L. F. Armarego, *Adv. Heterocycl. Chem.*, 1 (1963) 93.
- 9 B. Pias and L. Gasco, *J. Chromatogr.*, 104 (1975) D14.
- 10 A. Váradi and T. Tóth, *Magy. Kém. Foly.*, 80 (1974) 41.

## Correlation between structure and gas chromatographic behaviour of nitrogen-containing heterocyclic compounds

### III. Variation of ring size

O. PAPP, Gy. SZÁSZ\* and J. KÖKÖSI

*Institute of Pharmaceutical Chemistry, Semmelweis Medical University, Hőgyes E. ú. 9, H-1092 Budapest (Hungary)*

and

I. HERMECZ

*Chinoin Pharmaceutical Works, Budapest (Hungary)*

(First received March 29th, 1990; revised manuscript received August 21st, 1990)

---

#### ABSTRACT

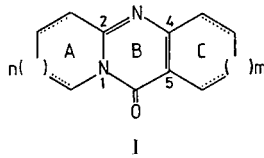
Ring homologues of the desoxyvasicinone type, which exert an antiasthmatic effect, were investigated. The retention indices and the solvent–solute interactions (expressed by the  $dI$  and  $\Delta I$  values) revealed that an increase in ring size led to a decrease in the polar character in the investigated heterocyclic rings, but not in the homocyclics. The  $dI_{Me}$  values of methyl groups introduced at the same position in the ring homologues demonstrated that an increase in the number of ring atoms ensures conformational freedom in ring A that can be expressed by numerical data. The structural and conformational differences influencing the retention data were confirmed by NMR investigations.

---

#### INTRODUCTION

The tricyclic pyrrolo [2,1-*b*] quinazolone alkaloid desoxyvasicinone is a drug [1,2] with a theophylline-like antiasthmatic effect. Wide-ranging research work was started to develop a favourable effect profile, as a result of which effective derivatives were found among aromatic analogues with different ring sizes [3,4]. Following extensive synthetic investigations by Hermecz *et al.* [5], homologues varying in ring size were available, on the basis of which the physico-chemical changes and characteristics could be analysed.

The methyl isomers of nitrogen-containing heterocyclic compounds and their alkyl homologues were earlier characterized by means of the Kováts retention index and derivative data. This paper describes gas chromatographic investigations of tricyclic ring-homologue derivatives condensed in the 1,2- and 4,5-positions containing a central pyrimidone ring (I).



$$n = 0, 1, 2, 3; \quad m = 0, 1, 2, 3$$

TABLE I  
CLASSIFICATION OF INVESTIGATED COMPOUNDS

Series	Group				
	1	2	3	4	5
(a) $m = 0, 1, 2, 3$	$n = 0$	$n = 1$	$n = 2$	$n = 3$	$n = 1$
(b) $n = 0, 1, 2, 3$	$m = 0$	$m = 1$	$m = 2$	$m = 3$	$m = 1$

TABLE II  
RETENTION INDICES OF COMPOUNDS OF TYPE I ON OV-1 AND OV-225 STATIONARY PHASES

Compound	Ring size		Aromatic ring	$f_{240^\circ\text{C}}^{\text{OV-1}}$	$f_{240^\circ\text{C}}^{\text{OV-225}}$	$f_{240^\circ\text{C}}^{\text{OV-225-OV-1}}$
	$n$	$m$				
1	0	0	—	1870	2875	1005
2	0	1	—	1973	2969	996
3	0	2	—	2050	3057	1007
4	0	3	—	2117	3091	974
5	1	0	—	1961	2917	965
6	1	1	—	2059	2995	936
7	1	2	—	2144	3064	920
8	1	3	—	2200	3110	910
9	2	0	—	2003	2891	888
10	2	1	—	2102	2984	882
11	2	2	—	2162	3045	883
12	2	3	—	2226	3100	874
13	3	0	—	2081	2969	888
14	3	1	—	2165	3049	884
15	3	2	—	2243	3110	867
16	3	3	—	2300	3166	866
17	1	0	A	1968	2890	922
18	1	1	A	2064	2972	908
19	1	2	A	2158	3059	901
20	1	3	A	2216	3104	888
21	0	1	C	1958	3005	1047
22	1	1	C	2058	3048	910
23	2	1	C	2101	3030	929
24	3	1	C	2181	3086	905

## EXPERIMENTAL

The apparatus and chromatographic conditions were as described in Part I [6].

*Materials*

Ten series were prepared from 24 tricyclic compounds with the general formula I. Two series contain aromatic rings A and C (**5a**, **5b**), and eight series contain saturated rings A and C. The ring size was changed between 5 and 8. The series investigated are listed in Table I.

Under the above conditions, the retention indices of the 24 compounds in ten four-membered series, involving systematic changes in ring size, were determined on OV-1 and OV-225 stationary phases. The structures and the measured data are given in Table II.

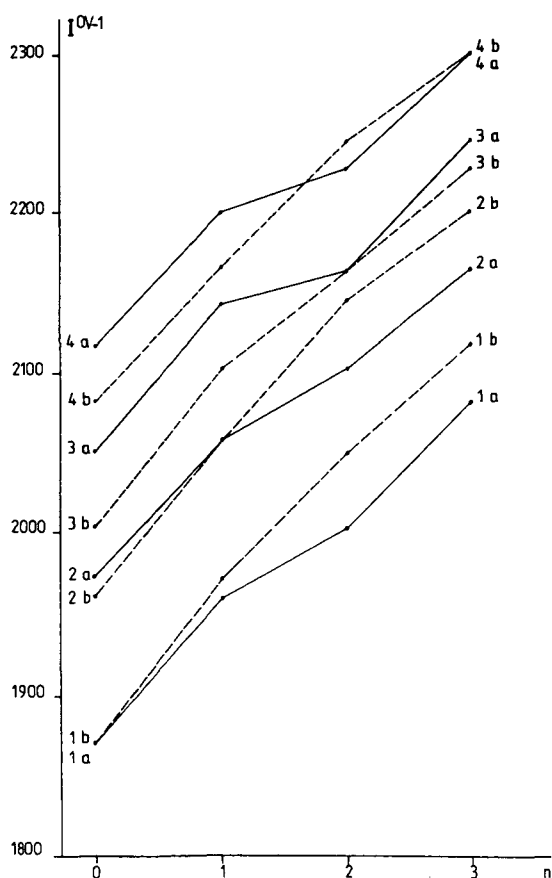


Fig. 1.  $I^{OV-1}$  values of tricyclic ring homologous series. Solid lines, heterocyclic homologues; dashed lines, carbocyclic homologues.

## RESULTS AND DISCUSSION

The series of curves depicting the retention index values of the ring homologues as a function of the ring size reveal that there is no appreciable difference in retention index in response to a change in the size of rings A and C on OV-1 apolar stationary phase (Fig. 1). However, it is striking that the retention index increases uniformly with an increase in the number of carbon atoms in the carbocycle, whereas in the heterocyclic series  $dI_{CH_2}$  varies as a function of the ring size.

The same correlation is manifested more strikingly on the more polar stationary phase OV-225 (Fig. 2). As a consequence, the retention index for compound **9**, which is longer than **5** by a  $CH_2$  group, is not larger, but smaller, by 26 index units (i.u.). At the same time the change in the size of ring C of the carbocycle leads to a change of nearly 100 i.u., which corresponds to the concept of Kováts [7] ( $dI_{CH_2} = 100$  i.u.).

The correlation  $dI_{CH_2} = 100$  i.u. demonstrates that the hydrophobic effect of the change in the size of ring C nearly corresponds to that for the *n*-alkane homologous series, but the behaviour of the heterocyclic system is essentially different. If the difference between the retention index values measured on the two stationary phases,  $\Delta I$ , is plotted as a function of the change in ring size (Fig. 3), there is little variation for ring C, whereas there is a steep decrease and then an approach to a limiting value for

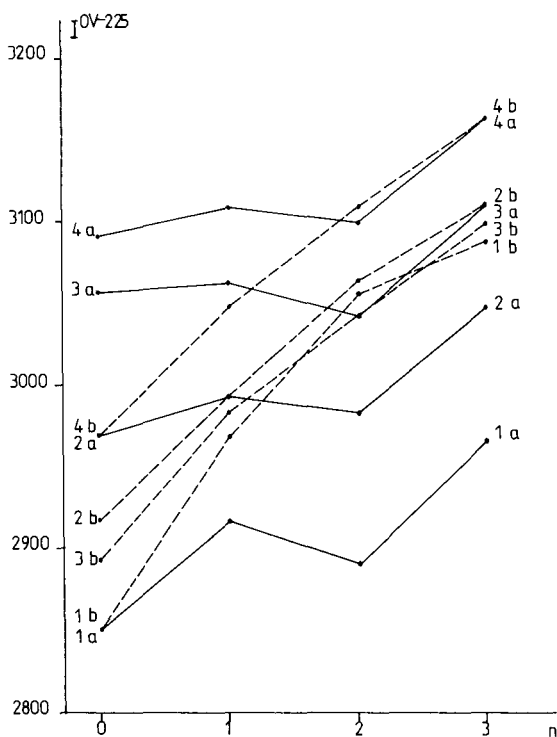


Fig. 2.  $I^{OV-225}$  values of tricyclic ring homologues series. Lines as in Fig. 1 and groups of compounds as in Table I.



ring A. The  $\Delta I$  values, which express the polar interaction of the compounds, indicate that the polarity changes to larger extent in response to a change in ring size for rings containing heteroatoms than for homocyclic rings.

In tricyclics containing a pyrimidine ring, the polarity of the system is determined by N-1 and the C-4 carbonyl group as structural elements. This effect is shown in Fig. 4 as a function of the variation in ring size.

Thus, the retention index values can be correlated with the difference originating from the positions of the rings and their freedom of conformational motion. Ring C, which is condensed to the unsaturated C-2-C-3 bond, contains four sterically rigidified cyclic carbon atoms, and the connected methylene groups cause changes with the same tendency. In the nitrogen-bridgehead condensed heterocycle, a more fundamental change occur as a consequence of the freer conformational motion due to the change in the ring size.

This can be explained in part by the structural arrangement of the rings, and in part by the conjugational interaction of the isolated electron pair on N-5 with the C-4 carbonyl group and by the deformation of the ring system. The similar courses of the curves of the individual series express the general tendency of the correlation.

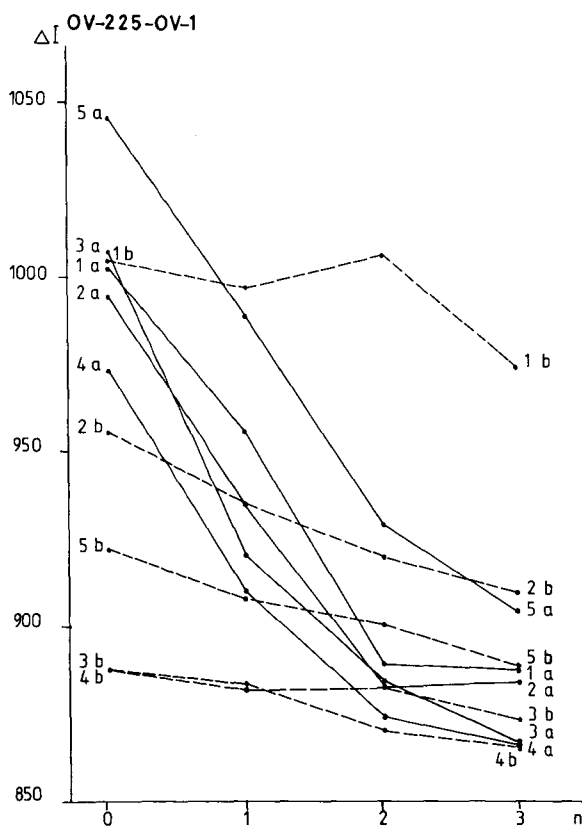


Fig. 3.  $\Delta I^{OV-225-OV-1}$  values of tricyclic ring homologues series. Lines as in Fig. 1 and groups of compounds as in Table I.

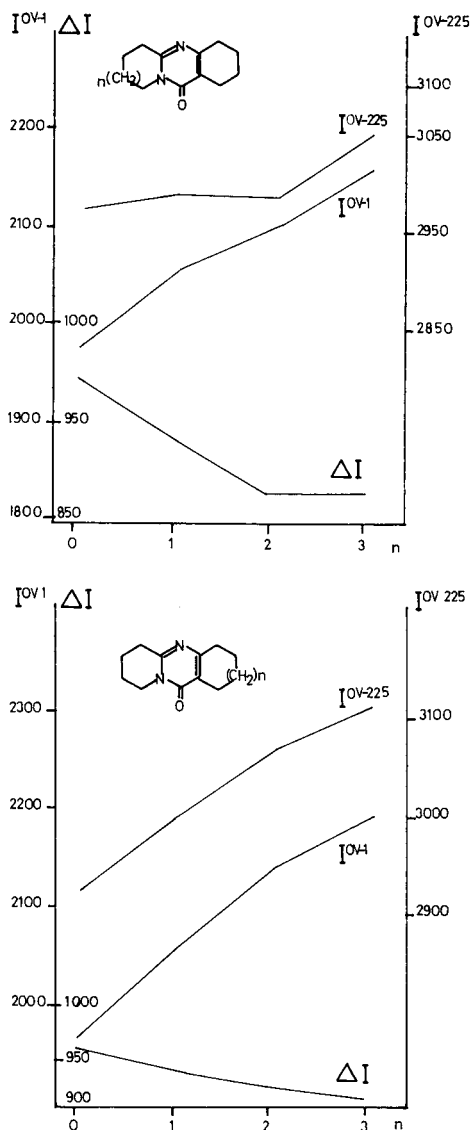
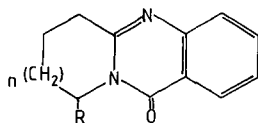


Fig. 4. Influence of changes in the size of rings A and C on retention indices.

To confirm that the change in polarity is influenced by the differences originating from the conformational motion of ring A, a gas chromatographic investigation was performed on a series in which there was a methyl substituent on the methylene group near the nitrogen bridgehead. The retention index values relating to the methyl group were determined by taking the difference between the retention indices for the two series (on OV-1 stationary phase).

The values obtained as a function of the change in ring size are given in Table III. The variation in the  $dI$  value of the 6-methyl substituents of the ring homologue

TABLE III

 $dI_{Me}^{OV-1}$  VALUES AND CHEMICAL SHIFTS AS A FUNCTION OF RING SIZE

Ring A size	$J_{240}^{OV-1}$		$dI_{Me}$	Chemical shift, CH-CH <sub>3</sub> (ppm)	Coupling constant (Hz)
	R = CH <sub>3</sub>	R = H			
$n = 0$	1942	1973	-31	4.84 m	3.4
$n = 1$	2045	2059	-14	5.06 m	3.1
$n = 2$	2123	2101	22	5.84 m	3.0

derivatives can be explained predominantly by steric reasons. The  $^1H$  NMR data indicate that the investigated methyl groups are all quasi-axial, which can be explained by the 1,3-allyl strain between the methyl groups and the neighbouring carbonyl groups. The chemical shift of the quasi-equatorial methylene proton connected to the methyl group changes significantly with variation in the ring size and reveals the difference in the ring strain and configuration. The steric positions of the methyl groups also differ on the rings of different size, as a consequence of the change in conformation. This difference, originating from the changes in conformational and steric structure, is expressed by the difference in the  $\Delta I$  values obtained in the course of the gas chromatographic investigations.

## REFERENCES

- 1 D. R. Mehta, J. S. Naravan and R. M. Desai, *J. Org. Chem.*, 28 (1963) 445.
- 2 H. L. Bhalla and A. Y. Nimbkar, *Drug Dev. Ind. Pharm.*, 8 (1982) 883.
- 3 C. K. Atal, *Chemistry and Pharmacology of Vasicine: a New Oxytocic and Abortifacient*, Regional Research Laboratory, Jammu, 1980.
- 4 M. P. Jain, V. N. Gupta and C. K. Atal, *Indian J. Chem.*, 24B (1985) 336.
- 5 I. Hermech, L. Vasvári-Debreczy, Á. Horváth, S. Virág, T. Breining and J. Kökösi, *Ger. Pat.*, 3 339 635; *C.A.*, 101 (1984) 130 705.
- 6 O. Papp, G. Szász, J. Kökösi and I. Hermech, *J. Chromatogr.*, 537 (1991) 365.
- 7 E. Kováts, *Helv. Chim. Acta*, 41 (1959) 132.



## Determination of nine acidic herbicides in water and soil by gas chromatography using an electron-capture detector

FUNG NGAN\*<sup>a</sup> and THOMAS IKESAKI

*Anlab, 1914 S Street, Sacramento, CA 95814 (U.S.A.)*

(First received May 1st, 1990; revised manuscript received August 14th, 1990)

---

### ABSTRACT

Two simple and convenient methods are described for the extraction, analysis and clean-up of nine acidic herbicides in water and soil samples. The extracted acidic herbicides were converted into their methyl esters by a modified method using diazomethane. The methylated herbicides were analyzed by gas chromatography with electron-capture detection using a Restek Rt<sub>x</sub>-35 0.53 mm I.D. capillary column and simultaneously confirmed using an Rt<sub>x</sub>-5 capillary column. A simple clean-up procedure using a micro disposable Florisil column is also described. The mean recoveries for all herbicides from water were >95% and from soils >86%. The recoveries of herbicides after Florisil column clean-up were greater than 89%. Each sample run required about 25 min, including confirmation. The methods described are suitable as an initial screening procedure in the rapid simultaneous determination of nine acidic herbicides in large numbers of environmental samples at reasonable cost.

---

### INTRODUCTION

Chlorophenoxy acid herbicides and related compounds (Table I) are widely used to control broad-leaved weeds and other vegetation. They are inexpensive and very potent even at low concentrations. These herbicides are formulated in the form of esters, alkaline salts and acids. After application, they may pass into streams, rivers or lakes with the possibility of environmental contamination. Several reports [1–5] have described the effects of ingestion of these herbicides by humans. Generally they cause pyrexia, nausea, hypotonia, confusion, coma, metabolic acidosis, convulsions, cytoskeletal perturbation and renal damage.

Many methods for the determination of different herbicides have been described [6–11]. At present, there are two Environmental Protection Agency (EPA) methods (615, 8150) [12,13] that have been standardized and are recommended for the determination of these types of herbicides in water and soil, respectively. However, the procedures in these two methods are cumbersome and time consuming. It is impossible to analyse large numbers of samples within a reasonable time and cost by using the current procedures. Recently, new methods [14,15] have been described that

---

<sup>a</sup> Present address: 1075 Olive Dr. 38, Davis, CA 95616, U.S.A.

TABLE I  
HERBICIDES USED

Systematic name (common name)	Structure
3,6-Dichloro-2-methoxybenzoic acid (dicamba)	
4-Chloro-2-methylphenoxyacetic acid (MCPA)	
2-(2,4-Dichlorophenoxy)propionic acid (dichlorprop)	
2-(4-Chloro-2-methylphenoxy)propionic acid (mecoprop)	
2,4-Dichlorophenoxyacetic acid (2,4-D)	
2-(2,4,5-Trichlorophenoxy)propionic acid (fenoprop)	
2,4,5-Trichlorophenoxyacetic acid (2,4,5-T)	
2-sec-Butyl-4,6-dinitrophenol (dinoseb)	
4-(2,4-Dichlorophenoxy)butyric acid (2,4-DB)	

will replace EPA method 8150 [13]. However, the procedures are still long and time consuming. In addition, no clean-up procedures were suggested [15]. Currently there is no alternative efficient method to replace EPA method 615 for the analysis of water samples.

The purpose of this work was to develop a simple, rapid procedure for the determination of these herbicides in environmental soil and water samples. The methods proposed are suitable as an initial screening procedure in the rapid analysis of large numbers of samples.

Generally, the identification of a herbicide in one chromatographic column is not sufficient and should be confirmed by a secondary analysis. The methods described elsewhere [12,13] required three or four chromatographic columns for confirmation, with inconvenient column changes. Gas chromatography-mass spectrometry GC-MS has been suggested [15] for confirmation. However, the price of the instrumentation is high and sample analysis becomes expensive. In this paper, we suggest a dual-column approach for initial confirmation. Herbicides found in one column can be confirmed simultaneously using a different column.

Herbicides present in the environment might be in salt form or as esters such as butyl, isooctyl or butoxyethyl. These different esters show different retention times in gas chromatography (GC) and therefore they must be hydrolysed before any analysis. After hydrolysis, the herbicide salts are acidified. However, the resulting acid forms of the herbicides are insufficiently volatile and sensitive for analysis by gas chromatography (GC), hence they must be converted into a more volatile form. Esterification silylation, alkylation and other derivatization procedures have been used to convert stable compounds into more volatile derivatives before analysis [6,14,16-18]. We have developed a new methyl esterification procedure by modifying previously described methods [12,19,20]. The modified methyl esterification procedure has proved to be safe, rapid and easy to operate without any hazard of explosion.

Some of the clean-up procedures involved lengthy liquid-liquid partition steps. However, loss of analytes might occur during the transfer processes. Increased contamination due to transfer of solvent between glassware might also interfere with sample analysis. However, some samples are clean enough for the clean-up procedure to be eliminated to save time. Here we present a simple procedure using a micro disposable Florisil column to clean up the extracted samples if the background interference is high. Florisil (synthetic magnesium silicate) has been widely used for the clean-up of pesticide extracts [21-23]. However, the choice of an appropriate solvent is critical. The ideal solvent will elute the extracted herbicides without co-elution of the extraneous material.

## EXPERIMENTAL

### *Reagents*

The solvents diethyl ether (peroxide-free), hexane and methylene chloride, all of pesticide quality, were obtained from American Burdick and Jackson (Muskegon, MI, U.S.A.). Sodium sulfate (anhydrous), granular, neutral, analytical-reagent grade (also from American Burdick and Jackson), was washed with methylene chloride and diethyl ether and then heated in an oven at 130°C for 13 h.

Florisil (60-100 mesh) (Fisher Scientific, Pittsburgh, PA, U.S.A.; Lot No.

897135) was activated at 130°C for at least 16 h. Silicic acid, 100-mesh powder (analytical-reagent grade) (Aldrich, Milwaukee, WI, U.S.A.) was used.

N-Methyl-N-nitroso-*p*-toluenesulfonamide (Diazald) of high purity and carbitol (diethylene glycol monoethyl ether) were purchased from Aldrich.

All herbicides in the acid form (1000 mg/l) were purchased as certified high-purity solutions from Nanogens (Watsonville, CA, U.S.A.). Each herbicide was converted into the methyl ester by the esterification procedure described below, and stock standard solutions were prepared. Working calibration standard solutions were prepared in *n*-hexane by serial dilution of the stock standard solutions and compared frequently with check standards for signs of degradation and evaporation. The stock standard solutions were stored at 40°C and protected from light.

#### *Apparatus and materials*

The apparatus used included an MNNG (1-methyl-3-nitro-1-nitrosoguanidine) diazomethane generation apparatus (Aldrich, Cat. No. Z10,100-1), a Buchi Rotovapor equipped with a temperature-controlled water-bath and a syringe with a narrow gauge (No. 22) needle.

Silane-treated glass-wool was obtained from Alltech (Deerfield, IL, U.S.A.). Boiling chips were high-purity, plain amphoteric alundum granules (Hengar, Philadelphia, PA, U.S.A.), washed with acetone and diethyl ether and stored in an oven at 200°C for at least 2 h before use.

The GC system consisted of a Varian Model 3400 gas chromatograph equipped with <sup>63</sup>Ni electron-capture detectors (dual channels), a Varian Model 8040 autosampler and a Spectra-Physics SP4290 integrator with a memory module installed. The operating conditions were as follows: a 5-mm deactivated glass Uniliner inside a Uniliner sleeve adapter (Restek, Bellefonte, PA, U.S.A.) were installed in the injection port at 210°C; detector temperature, 310°C; carrier gas (helium) flow-rate, 7 ml/min in both columns; nitrogen make-up gas flow-rate, 20 ml/min in both detectors; direct injection mode [24]; column temperature program, from 140 to 180°C at 3°C/min and then to 184°C at 0.5°C/min.

The following GC columns were used: (1) a 0.3–0.5 m × 0.53 mm I.D. capillary guard column (J & W Scientific, Rancho Cordova, CA, U.S.A.) was connected to the injector Uniliner and the other end was connected with a Chromfit low-dead-volume Y-splitter (Western Scientific, Danville, CA, U.S.A.); (2) an Rt<sub>x</sub>-35 capillary column with 30 m × 0.53 mm I.D., film thickness 0.5 μm (Restek), or with DB-608 (J & W Scientific), was connected at one end with the Y-splitter and at the other end with detector A; (3) an Rt<sub>x</sub>-5 capillary column (30 m × 0.53 mm I.D.), film thickness 1.5 μm (Restek), or with DB-5 (J & W Scientific), was installed in the same way as the Rt<sub>x</sub>-35 column, but connected to detector B.

#### *Analysis of water samples*

A reagent water sample (500 ml) was poured into a 1-l round-bottomed flask and NaOH pellets (40 g) were added with a few boiling chips. A reflux condenser was installed immediately on the flask. The water sample was then heated to reflux for *ca.* 25–30 min and then cooled in an ice-bath. The aqueous solution contained salts of free acid herbicides. While the basic aqueous solution was still in the ice-bath, it was acidified with *ca.* 85 ml of concentrated HCl to pH < 1.0. When the acidified solution



has been cooled to room temperature, it was transferred into a 1-l separating funnel and extracted with diethyl ether ( $4 \times 100$  ml). Diethyl ether was used to rinse the 1-l round-bottomed flask before performing each extraction. The ether layers were collected, dried by passage through anhydrous sodium sulfate in a stemless funnel plugged with a small amount of glass-wool and evaporated to 1 ml using a rotary evaporator set at  $40^{\circ}\text{C}$ . The concentrated ether solution contained the acid form of the herbicides. The sample was then ready for methylation with diazomethane. For recovery studies, 500 ml of herbicide-free water sample were spiked with herbicide methyl esters (Table II) prepared in *n*-hexane and shaken vigorously to obtain homogeneity before extraction began.

#### Soil sample analysis

A soil sample (50 g) was thoroughly mixed with *ca.* 10–15 ml of 50% (v/v) HCl in a 500-ml erlenmeyer flask. The pH was  $< 1$ . Diethyl ether (100 ml) was added to the acidified soil sample, sealed with a stopcock valve attached to a stopper and shaken manually for 1 min.

After settling, the stopcock was opened slowly and the ether layer was decanted and filtered through Whatman No. 41 (18.5-cm) filter-paper. The above extraction procedure was repeated a further three times. At this point the ether solution contained both the acid and ester parts of the herbicides. The ether layers were collected in a 1-l round-bottomed flask and evaporated to 3–4 ml using a rotary evaporator at  $40^{\circ}\text{C}$ . Distilled water (400 ml) was added to the flask with 40 g of NaOH pellets and the mixture was subjected to base hydrolysis as described above. After hydrolysis, some brown precipitate had formed. It was allowed to settle, cooled in an ice-bath and then passed through filter-paper into a 1-l separating funnel. The filtered basic solution was then acidified with *ca.* 85 ml of concentrated HCl to pH  $< 1$ . After cooling to room temperature in an ice-bath, it was extracted with four portions of 100 ml of

TABLE II  
SPIKE CONCENTRATION RANGES AND RECOVERIES OF HERBICIDES FROM WATER

Analyte	Spike concentration range ( $\mu\text{g/l}$ ) <sup>a</sup>	Mean recovery (%) <sup>b</sup>	
		Low concentration	High concentration
Dicamba	0.1–5	101 $\pm$ 5.2	109 $\pm$ 4.5
MCPA	10–500	98 $\pm$ 5.6	118 $\pm$ 5.5
Dichlorprop	0.06–3	100 $\pm$ 5.2	106 $\pm$ 4.8
Mecoprop	1.4–70	97 $\pm$ 4.9	117 $\pm$ 3.9
2,4-D	0.1–5	96 $\pm$ 6.0	99 $\pm$ 5.8
Fenoprop	0.05–0.5	101 $\pm$ 6.1	105 $\pm$ 5.3
2,4,5-T	0.1–5	102 $\pm$ 7.2	116 $\pm$ 8.5
Dinoseb	0.1–5	95 $\pm$ 5.4	111 $\pm$ 7.0
2,4-DB	0.1–5	98 $\pm$ 4.9	104 $\pm$ 5.4
Av. R.S.D. <sup>c</sup>		5.6	5.6

<sup>a</sup> Herbicide methyl ester was used as spike in a 500-ml water sample.

<sup>b</sup> Mean recovery was calculated based on an  $R_{\text{t}}$ -35 capillary column and five replicate analyses.

<sup>c</sup> Average relative standard deviation (%).

TABLE III  
SPIKE CONCENTRATION RANGES AND RECOVERIES OF HERBICIDES FROM SOIL

Analyte	Spike concentration range ( $\mu\text{g}/\text{kg}$ ) <sup>a</sup>	Mean recovery (%) <sup>b</sup>	
		Low concentration	High concentration
Dicamba	0.2-10	90 $\pm$ 5.1	98 $\pm$ 5.9
MCPA	20-1000	88 $\pm$ 5.9	94 $\pm$ 6.9
Dichlorprop	1.2-60	91 $\pm$ 6.5	101 $\pm$ 7.5
Mecoprop	20-1000	89 $\pm$ 6.7	99 $\pm$ 7.5
2,4-D	2-100	88 $\pm$ 5.8	92 $\pm$ 6.4
Fenoprop	0.2-10	91 $\pm$ 7.9	93 $\pm$ 8.3
2,4,5-T	0.4-20	87 $\pm$ 5.4	99 $\pm$ 6.2
Dinoseb	0.4-20	86 $\pm$ 8.8	96 $\pm$ 9.6
2,4-DB	2-100	89 $\pm$ 7.0	97 $\pm$ 8.0
Av. R.S.D. <sup>c</sup>		6.6	7.4

<sup>a</sup> Herbicide methyl ester was used as spike in a 50 g of herbicide-free soil sample.

<sup>b</sup> Mean recovery was calculated based on an Rt<sub>x</sub>-35 capillary column and five replicate analyses.

<sup>c</sup> Average relative standard deviation (%).

diethyl ether as described for the analysis of water samples. For recovery studies, 50 g of herbicide-free soil sample were sprayed with herbicide methyl esters prepared in *n*-hexane and homogenized with a glass rod (Table III).

#### Esterification

The procedure and precautions for using the Aldrich MNNG diazomethane apparatus are described in detail elsewhere [19,25]. A concentrated 1-ml ether sample was transferred from the volumetric flask to the outside tube of the apparatus. The volumetric flask was rinsed with *ca.* 2 ml of diethyl and combined with the diethyl ether in the outside tube of the apparatus. Diethyl ether (1 ml) was added to the inside tube through its screw-cap opening, together with 1 ml of carbitol. Approximately 0.3-0.4 g of Diazald was placed in the inside tube, and then the two parts were assembled with a butyl O-ring and held with a pinch-type clamp. The lower part was immersed in an ice-water bath and about 1.5 ml of 37% KOH was injected dropwise through the silicone-rubber septum via a syringe with a narrow-gauge (No. 22) needle.

The apparatus was shaken gently by hand every 10 min for about 40 min to ensure completion of the reaction. At the beginning, the Diazald might settle at the bottom of the inside tube, so it was necessary to shake well to allow the Diazald to react with the carbitol and the base. After *ca.* 5 minutes, the yellow color of diazomethane should persist in the outside tube of the diethyl ether solution. An additional 0.1-0.2 g of Diazald can be added if the yellow color of the diazomethane-diethyl ether solution does not appear. When the reaction was complete, the yellow diethyl ether solution in the outside tube was evaporated to dryness by shaking in a warm water-bath (60°C) inside a well circulated hood. The diazomethane gas and the diethyl ether should evaporate easily. A gentle stream of nitrogen might also be used to dry the ether solution. *n*-Hexane (5 ml) was added to the tube for water samples. The whole esterification procedure should be carried out inside a fume-hood. The sample

was readily analyzed by GC. For soil samples, 10 ml of *n*-hexane should be added. Any unreacted diazomethane in the inside tube was destroyed by adding 0.1–0.2 g of silicic acid.

#### *Florisol clean-up*

Some dirty samples with a lot of background interferences required clean-up. A micro disposable Florisol column was prepared by adding a layer of *ca.* 1 cm of anhydrous sodium sulfate to a 5.75-in. long disposable pipet plugged with a small amount of glass-wool. On top of the sodium sulfate, a layer of 6–7 cm of heat-activated Florisol was added. The micro Florisol column was then rinsed with *n*-hexane to remove any impurities. The esterified sample (1 ml) was pipetted slowly through the Florisol column and the column was then washed with about 5 ml of *n*-hexane. The *n*-hexane layer was discarded. The column was washed with 15 ml of methylene chloride. The herbicide esters were contained in the methylene chloride, which was collected and dried with a gentle stream of nitrogen. *n*-Hexane (1 ml) was added and the sample was ready for GC analysis.

#### *Calibration standards*

A minimum of five calibration points for each standard should be prepared by dilution of the stock standard solutions with *n*-hexane. The stock standard solutions were prepared by esterification of 10 ml of the certified pure herbicide acids (1000 mg/l) by the esterification procedure described above. The standards should be checked frequently with the commercially available certified pure herbicide methyl esters for signs of degradation or evaporation. A 1- $\mu$ l volume of each standard was injected and analysed by gas chromatography.

## RESULTS AND DISCUSSION

As shown in Table IV, nine herbicides are well separated in both capillary columns. The run time was about 15 min in channel A and 20 min in channel B. The total run time for both channels to be completed would be about 25 min. With the Y-splitter installed in the gas chromatograph plus a memory module in the integrator, it is easy to confirm the herbicides from the different columns simultaneously. The dual-column approach has two advantages. First, it provides secondary confirmation without the necessity to change columns in the gas chromatograph. Second, the cost of using this approach is much cheaper than GC–MS and yet provides high accuracy. It can initially screen out large amounts of undetected compounds. However, if the concentrations of the herbicides in the sample are high, a GC–MS method should be used for final confirmation. The reproducibility of the dual column system is good and consistent. Both the  $R_{t_x}$ -35 and  $R_{t_x}$ -5 capillary columns gave good resolutions of all nine herbicides. In another experiment, we tested DB-608 and DB-5 capillary columns from J & W Scientific and obtained similar results. Detection limits for nine herbicides in both capillary columns are presented in Table V. They are comparable to or even lower than those for the EPA methods.

A reagent water sample was spiked with nine herbicide methyl esters and extracted with diethyl ether. The spike levels and mean recoveries are given in Table II. The mean recoveries were >95% for all the herbicides with an average relative stan-

TABLE IV

RETENTION TIMES OF NINE METHYL ESTER HERBICIDES SEPARATED ON  $R_{t_x}$ -35 AND  $R_{t_x}$ -5 CAPILLARY COLUMNS

Conditions: 1- $\mu$ l injection; helium carrier gas, 7 ml/min; nitrogen make-up gas, 20 ml/min; columns temperature programmed from 140 to 180°C at 3°C/min and then to 184°C at 0.5°C/min; direct injection mode.

Analyte	Retention time (min)	
	$R_{t_x}$ -35	$R_{t_x}$ -5
Dicamba	6.38	8.87
MCPA	7.26	9.90
Dichlorprop	8.06	11.18
Mecoprop	8.91	12.59
2,4-D	9.14	11.75
Fenoprop	11.39	15.36
2,4,5-T	12.87	16.37
Dinoseb	13.8	19.16
2,4-DB	14.49	18.96

dard deviation of 5.6%. In another experiment, we used different esters of 2,4-D (e.g., butyl, isooctyl or butoxyethyl ester). The mean recoveries were also >95%. The use of a large amount of NaOH (1 mol) is necessary in order to carry out the hydrolysis step efficiently. Also, because it is not clear how high the herbicide concentration will be in the samples, it is safer to use an excess amount of base. When acidified with *ca.* 85 ml of concentrated HCl, a large amount of sodium chloride is formed in the aqueous solution. This salt facilitates the recovery of the herbicides, as the solubility of the acidic herbicides was decreased in the aqueous solution by the salt. Ground-water samples were also tested and similar results were obtained. In addition, similar result to those obtained before (Table II) were obtained when the acid forms of the herbicides were used to spike the samples.

The water extraction and the hydrolysis take about 1 h. The procedure is short

TABLE V

DETECTION LIMITS ON  $R_{t_x}$ -35 AND  $R_{t_x}$ -5 GC COLUMNS

Conditions as in Table IV.

Analyte	Detection limit ( $\mu$ g/l)	
	$R_{t_x}$ -35	$R_{t_x}$ -5
Dicamba	0.05	0.03
MCPA	15.0	12.0
Dichlorprop	0.10	0.07
Mecoprop	5.00	3.00
2,4-D	0.20	0.15
Fenoprop	0.06	0.04
2,4,5-T	0.08	0.06
Dinoseb	0.04	0.02
2,4-DB	0.80	0.50

and simple and hence minimizes the chance of loss of analytes and contamination between glassware. Most of time, the water samples are clean enough to be analyzed by GC. If there is a lot of background interference, they can be cleaned by the Florisil clean-up procedure described above.

The spike levels and mean recoveries for soil samples are presented in Table III. The mean recoveries of nine herbicides were  $> 86\%$  with an average relative standard deviation of  $7\%$ . After the hydrolysis, some brown precipitate was formed because some organic material was extracted into the concentrated diethyl ether and became insoluble in the basic solution. The precipitate might be basic or neutral organic compounds. This procedure is a major clean-up step that eliminates many interferences in soil samples. Indeed, it helps to clean the samples as soil usually contains a lot of organic material. This proposed method for soil samples is short, simple and yet accurate in comparison with the current EPA procedures.

These methods do not distinguish between salt, acid or ester forms of the herbicides because after hydrolysis and methylation all the herbicides will be converted to the methyl esters.

The methyl esterification reagent, diazomethane, can be generated from several different precursors by the action of alkali on N-methyl-N-nitrosourea [26], N-methyl-N-nitroso-N'-nitroguanidine [27] or N-methyl-N-nitroso-*p*-toluenesulfonamide (Diazald) [28] in the presence of diethyl ether. Currently, the bubbler method and the Diazald kit method are recommended in EPA methods [12,13,15]. The bubbler method is suggested for samples that have low concentrations of herbicides. However, the method requires a source of nitrogen, test-tubes and several glass delivery tubes, and hence becomes cumbersome when there are many samples that need esterification. The Diazald kit method requires the assembly of a set of distillation glassware for the safe preparation of diazomethane. However, if the temperature is raised above  $90^{\circ}\text{C}$ , it might cause an explosion. In addition, solutions of diazomethane decompose rapidly in the presence of solid materials such as calcium chloride, copper powder and boiling chips. Instead of using the above two methods, we used the MNNG diazomethane generation apparatus [19,25]. However, MNNG is not used in our test because it is toxic, carcinogenic and a potent mutagen and generates only 1 mmol or less of diazomethane [25,29]. Diazald is the preferred reagent because of its large-scale production of diazomethane [29,30] and stability. The time required for the whole reaction is *ca.* 40 min. Diazomethane is a carcinogen and unstable under certain conditions. The precautions required to prepare diazomethane are described in detail in the literature [19,26].

Our modified esterification process is very convenient to operate and we have been using this method for 1 year without any difficulty or accident. However, care should be taken when transferring reagents into the inside tube, as some reagents could leak out of the small hole in the inside tube and thus contaminate the sample in the outside tube. Diazomethane reacts with both carboxylic acids and phenols and also with other compounds that have active hydrogens. Hence it is suitable to convert dinoseb into its methyl ether derivative for analysis. The precursor of diazomethane, Diazald, gave consistent and nearly maximum yields of esters when compared with MNNG. The derivatization yields are  $100\%$  when compared to the commercially available esters standard. The diazomethane gas generated from the reaction tube is sufficient to convert all the acidic herbicides to the ester forms, as the concentrations

TABLE VI  
MEAN RECOVERIES OF HERBICIDES FROM FLORISIL COLUMN

Analyte	Mean recovery (%) <sup>a</sup>	Analyte	Mean recovery (%) <sup>a</sup>
Dicamba	93	Fenoprop	100
MCPA	89	2,4,5-T	92
Dichlorprop	90	Dinoseb	98
Mecoprop	95	2,4-DB	90
2,4-D	100		

<sup>a</sup> Calculation was based on an Rt<sub>x</sub>-35 capillary column and five replicate analyses.

of the herbicides in the environment are usually low. The modified esterification procedure provides several advantages. First, there is no need to distil the diazomethane from its precursors, which might cause an explosion. Second, fresh diazomethane is supplied each time directly from the reaction flask to the samples. Third, the procedure is easy to manage and is rapid, so it can save a lot of work and time. Fourth, Diazald is a safer and more stable compound than MNNG. Fifth, it can generate diazomethane in amounts greater than 1 mmol.

The disposable micro Florisil column is economical and easy to prepare and use. The recovery of the herbicides after the clean-up procedure was >89% (Table VI).

One of the acidic herbicides, dalapon (2,2-dichloropropionic acid), was also tested. However, we found that Dalapon (b.p. 98–99°C) was volatile enough to be analysed by GC without esterification. If it is included in our experiment, losses might occur because dalapon ester is very volatile. Dalapon occurs mainly as the sodium or magnesium salt in the environment. Thus, after acidification, it was ready for analysis by GC.

The proposed methods here are simple and rapid and large numbers of environmental samples can be analyzed within a reasonable time and at reasonable cost in the laboratory.

#### ACKNOWLEDGEMENT

The authors thank Dr. Dave Cooper of the University of California, Davis, CA, for reviewing the manuscript.

#### REFERENCES

- 1 P. Berwick, *J. Am. Med. Assoc.*, 214 (1970) 1114.
- 2 L. F. Prescott, J. Park and I. Darrien, *Br. J. Clin. Pharmacol.*, 7 (1979) 111.
- 3 W. D. E. Wells, N. Wright and W. B. Yeoman, *Clin. Toxicol.*, 18 (1981) 273.
- 4 Y. Li, W. Zhao and I. N. Chou, *J. Toxicol. Environ. Health*, 20 (1987) 11.
- 5 P. H. Casey and W. R. Collie, *J. Pediatr.*, 104 (1984) 313.
- 6 G. Yip, *J. Assoc. Off. Agric. Chem.*, 45 (1962) 367.
- 7 D. C. Abbott, H. Egan, E. W. Hammond and J. Thomson, *Analyst (London)*, 89 (1964) 480.
- 8 D. F. Goerlitz and W. L. Lamar, *U.S. Geol. Surv. Water Supply Pap.*, (1967) 1817-C.
- 9 W. P. Cochrane and R. Purkayastha, *Toxicol. Environ. Chem. Rev.*, 1 (1973) 137.
- 10 A. W. Ahmed, V. N. Mallet and M. J. Bertrand, *J. Assoc. Off. Anal. Chem.*, 72 (1989) 365.

- 11 T. Tsukioka and T. Murakami, *J. Chromatogr.*, 469 (1989) 351.
- 12 *Test Methods: Methods for Nonconventional Pesticides. Chemical Analysis of Industrial and Municipal Wastewater, EPA 440/1-83/079C, No. 615*, U.S. Environmental Protection Agency, Washington, DC, 1983.
- 13 *Test Methods for Evaluating Solid Waste, SW-846*, U.S. Environmental Protection Agency, Washington, DC, 2nd ed., 1982.
- 14 D. F. Gurka, F. L. Shore and S. T. Pan, *J. Assoc. Off. Anal. Chem.*, 70 (1987) 889.
- 15 D. F. Gurka, F. L. Shore and S. T. Pan, *J. Assoc. Off. Anal. Chem.*, 69 (1986) 970.
- 16 C. W. Stanley, *J. Agric. Food Chem.*, 14 (1966) 321.
- 17 M. J. Bertrand, A. W. Ahmed, B. Sarrasin and V. N. Mallet, *Anal. Chem.*, 59 (1987) 1302.
- 18 W. P. Cochrane, *J. Chromatogr. Sci.*, 17 (1979) 124.
- 19 H. M. Fales, T. M. Jaouni and J. F. Babashak, *Anal. Chem.*, 45 (1973) 2302.
- 20 *Mini Diazald Apparatus (Technical Information Bulletin, No. AL-121)*, Aldrich, Milwaukee, WI, 1982.
- 21 P. A. Mills, B. A. Bong, L. R. Kamps and J. A. Burke, *J. Assoc. Off. Anal. Chem.*, 55 (1972) 39.
- 22 V. Lopez-Avila, N. S. Dodhiwala, J. Milanese and W. F. Beckert, *J. Assoc. Off. Anal. Chem.*, 72 (1989) 93.
- 23 G. Yip, *J. Assoc. Off. Anal. Chem.*, 54 (1971) 966.
- 24 *HALFMIL Capillary Columns (0.530 mm ID)*, Restek, Bellefonte, PA, 2nd ed., 1989, p. 38.
- 25 *MMNG Diazomethane-Generation Apparatus (Technical Information Bulletin, No. AL-132)*, Aldrich, Milwaukee, WI, 1982.
- 26 F. Arndt, in A. H. Blatt (Editor), *Organic Syntheses*, Coll. Vol. 2, Wiley, New York, 1950, p. 165.
- 27 A. F. McKay, *J. Am. Chem. Soc.*, 70 (1948) 1974.
- 28 Th. J. de Boer and H. J. Backer, in N. Rabjohn (Editor), *Organic Syntheses*, Coll. Vol. 4, Wiley, New York, 1963, p. 250.
- 29 *Diazald, MMNG and Diazomethane Generator (Technical Information Bulletin, No. AL-180)*, Aldrich, Milwaukee, WI, 1990.
- 30 M. Hudlicky, *J. Org. Chem.*, 45 (1980) 5377.





## Determination of selenium in organic compounds on a silica gel sintered thin-layer chromatographic plate with 2,3-diaminonaphthalene after direct digestion

RYOICHI HASUNUMA\* and TADAO OGAWA

*Department of Chemistry, Kitasato University, 1-15-1, Kitasato, Sagamihara, Kanagawa, 228 (Japan)*

JUKICHI ISHII

*Iatron Laboratories Inc., 1-11-4 Higashi-Kanda, Chiyoda-ku, Tokyo 101 (Japan)*

and

YASUHIRO KAWANISHI

*Department of Chemistry, Kitasato University, 1-15-1, Kitasato, Sagamihara, Kanagawa, 228 (Japan)*

(First received January 4th, 1990; revised manuscript received August 7th, 1990)

---

### ABSTRACT

Biologically interesting selenium compounds such as selenomethionine, selenocystine and trimethylselenonium were digested directly on a silica gel sintered thin-layer chromatographic (TLC) plate. Digestion was performed with nitric acid–perchloric acid (2:1, v/v) by heating at 210°C for 15 min. Selenite formed on the plate was revealed with 2,3-diaminonaphthalene reagent and determined using a TLC scanner. The recoveries of selenomethionine, selenocystine and trimethylselenonium were  $94 \pm 7$ ,  $99 \pm 9$  and  $97 \pm 10\%$ , respectively, with a detection limit of 0.4 ng of selenium. Linearity between fluorescence intensity and selenium content was found in the range 3–250 ng of selenium.

---

### INTRODUCTION

Selenium is an essential trace element for animals [1], and the metabolism of selenium compounds has become of interest in connection with its role in human health and diseases. It is important to know what chemical species are present and how they are distributed in tissues.

Concentrations of selenium compounds in biological materials are usually very low. For example, the concentration of selenium in tissues and urine from healthy humans is less than 1  $\mu\text{g/g}$  [2] and 100  $\mu\text{g/l}$  [3], respectively. The mean daily intake of selenium estimated for the Japanese population is about 100  $\mu\text{g}$  [4].

Selenoamino acids are readily separated by paper chromatography [5] or thin-layer chromatography (TLC) [6] using conventional solvent systems for the separation of amino acids. Fluorimetry [7] is a suitable method for the determination of trace amounts of selenium. However, when fluorimetry is applied directly to the TLC plate, the usual precoated layer is destroyed by the hot acid treatment. Extraction of

samples from cut sections scraped off the plate is another approach for fluorimetry, but is very tedious.

To overcome this drawback, we used a silica gel sintered TLC plate [8]. The purpose of this study was to establish standard procedures for the direct digestion and determination of separated selenium compounds on the silica gel sintered TLC plate.

It has been reported that the complete digestion of trimethylselenonium (TMSe) ion requires drastic conditions (210°C, 30 min) [9]. We found, however, that the time was shortened to 10 min when the reaction occurred on a silica gel thin layer.

A linear relationship between the fluorescence intensity and the selenium content in the separated compounds was found in the range 3–250 ng of selenium.

## EXPERIMENTAL

### *TLC plates*

Silica gel sintered TLC plates (10 × 10 cm), prepared with uniform-sized silica gel (15 μm) by Iatron Labs. (Tokyo, Japan) were used. Similar plates, now available commercially from Gasukuro Kogyo (Tokyo, Japan), were also used.

Before use, the plates were dipped in fuming nitric acid overnight at room temperature, washed and rinsed with distilled water and heated at 400°C for 2 h in an electric furnace.

Precoated silica gel TLC plates (Kieselgel 60; Merck, Darmstadt, F.R.G.), were used for examination of the purity of authentic samples. The plates were developed in normal glass chambers (26 × 26 × 13 cm) saturated with the solvent system used.

### *Reagents*

A mixture of 60% nitric acid (for determination of harmful metals; Wako, Osaka, Japan) and 60% perchloric acid (for determination of harmful metals; Wako) (2:1, v/v) was used for digestion.

2,3-Diaminonaphthalene (DAN) reagent was prepared by dissolving 1 g of DAN (Wako) in 100 ml of 0.3 M hydrochloric acid at 50°C for 20 min. The solution was washed with 10 ml of cyclohexane (for HPLC; Wako) four times to remove impurities [10] and filtered off. The filtrate was mixed with 20 ml of 1 M glycine-HCl buffer (pH 1.5) and adjusted to 100 ml with distilled water. The solution was stored in a freezer and thawed before use.

Other chemicals were of analytical-reagent grade.

### *Authentic samples*

Seleno-DL-methionine (SeMet) (>99.9%) and seleno-DL-cystine [(SeCys)<sub>2</sub>] (>90%) were purchased from Sigma (St. Louis, MO, U.S.A.). TMSe iodide (>99.999%) was obtained from TRI Chemical Lab. (Kanagawa, Japan). Selenium standard solution (1000 ppm, as selenious acid, for atomic absorption spectrometry) and other selenium-containing compounds were purchased from Wako. Their purities were checked on a precoated silica gel plate and on a silica gel sintered TLC plate. Detection was performed with ninhydrin and by the present method, respectively. All the compounds were found to be chromatographically pure.

### *Authentic sample solutions*

Authentic samples were dissolved in distilled water. Their concentrations were evaluated by the method reported previously [7] and adjusted to 3000  $\mu\text{g}/\text{ml}$  of selenium for the stock solutions of SeMet and TMsE iodide and to 300  $\mu\text{g}/\text{ml}$  of selenium for that of  $(\text{SeCys})_2$  owing to the poor solubility in the latter instance [11]. Authentic sample solutions were used after dilution to a concentration of 100  $\mu\text{g}/\text{ml}$  of selenium.

An "authentic mixture" of SeMet,  $(\text{SeCys})_2$  and TMsE was prepared so as to contain 200  $\mu\text{g}/\text{ml}$  of selenium for each constituent.

### *Solvent systems*

The following solvent systems were used all proportions by volume: (A) *n*-propanol–28% ammonia–water (8:1:1); (B) chloroform–methanol–28% ammonia–water (60:35:4:4); (C) *n*-butanol–acetic acid–water (4:1:1); (D) *n*-propanol–1 *M* acetic acid (7:3); (E) isopropanol–formic acid–water (20:1:5); and (F) phenol–water (5:1, ammonia vapour saturated).

### *Procedure*

To establish the standard procedures for digestion, aliquots (0.5  $\mu\text{l}$ ) of authentic sample solutions were spotted separately on a TLC plate and digested at 150, 180, 210 or 250°C for various times. Recoveries of selenium were calculated from the ratios of the fluorescence intensities of the spots to that of the selenium standard solution on the same plate. Fluorescence intensities were measured according to the following procedures.

"Authentic mixture" was applied to a silica gel sintered TLC plate together with the selenium standard solution in a volume of 0.5  $\mu\text{l}$  with a Microcaps (Drummond Scientific, Broomall, PA, U.S.A.). After development, the solvents were removed in an air oven. The TLC plate was sprayed with the digestion reagent, covered with a clean glass plate to keep it wet with the reagent, placed upside down on a hot-plate and heated at 210°C. After 15 min, the glass cover-plate was removed to evaporate the digestion reagent. After about 30 s, the TLC plate was cooled and sprayed with 6 *M* hydrochloric acid and heated again at 100°C for 5 min to convert selenate to selenite. The plate was cooled, spotted in one corner with 0.1% cresol red as an indicator and neutralized in a vessel saturated with ammonia vapour until the colour became yellow. The plate was sprayed with DAN reagent and heated at 60°C for 10 min to form a fluorophore, 4,5-benzopiazselenol [7], and sprayed a solution of Triton X-100–chloroform (1:4, v/v) to enhance the fluorescence intensity [12,13]. The fluorescence intensity of spots on the TLC plate was scanned with a Shimadzu CS-910 dual-wavelength TLC scanner (fluorescence mode, 540-nm cut filter, excitation at 388 nm) and recorded with a Hewlett-Packard 3390A integrator.

## RESULTS AND DISCUSSION

To evaluate the purities of the authentic samples, the selenium contents were determined by the method reported previously [7]. Table I gives the analytical results for authentic samples. The purities from selenium contents of SeMet,  $(\text{SeCys})_2$  and TMsE iodide were  $98 \pm 2$ ,  $90 \pm 2$  and  $101 \pm 2\%$  (mean  $\pm$  standard deviation) from five runs, respectively, and agreed with the manufacturers' data.

TABLE I  
ANALYTICAL RESULTS FOR AUTHENTIC SAMPLES

An aliquot of each authentic sample was weighed and dissolved in distilled water. The concentrations were determined by the method reported previously [7]. The values are means  $\pm$  standard deviations from five runs.

Authentic sample	Selenium content ( $\mu\text{g/ml}$ )		Purity (%) (mean $\pm$ S.D.)
	Calculated	Found (mean $\pm$ S.D.)	
SeMet (> 99.9%) <sup>a</sup>	246	240 $\pm$ 6	98 $\pm$ 2
(SeCys) <sub>2</sub> (> 90%) <sup>a</sup>	219	198 $\pm$ 5	90 $\pm$ 2
TMSe (> 99.999%) <sup>a</sup>	174	176 $\pm$ 3	101 $\pm$ 2

<sup>a</sup> Manufacturers' data.

Table II gives the  $R_F$  values of the selenium compounds with each solvent system. In general, good separations were obtained. Fig. 1 shows a thin-layer chromatogram of the authentic mixture which contained 200 ng of selenium in one spot (1  $\mu\text{l}$ ).

Selenoamino acids could be easily digested on the TLC plate at 150°C. TMSe is a metabolite of selenium that has been identified in the urine of mammals [14,15], and it has been reported that the compound is resistant against digestion [16]. To complete digestion of the compound, the reaction temperature had to be raised above 150°C. The relationship between digestion temperature and recoveries of the authentic sample [SeMet, (SeCys)<sub>2</sub> and TMSe] is shown in Fig. 2. (SeCys)<sub>2</sub> was most easily digested in 10 min at 150°C. The digestion of TMSe was difficult at 150 or 180°C.

Table III shows the recoveries of the authentic sample [SeMet, (SeCys)<sub>2</sub> and TMSe] at 210°C. The digestion for the selenium compounds almost complete in 10 min at 210°C.

TABLE II  
 $R_F$  VALUES OF SELENIUM COMPOUNDS ON SILICA GEL SINTERED PLATES DEVELOPED WITH VARIOUS SOLVENT SYSTEMS

Systems A–F as specified under *Solvent systems* were used. Detection was performed both with ninhydrin and by the present method.

Selenium compound	Solvent system					
	A	B	C	D	E	F
Selenomethionine	0.68	0.67	0.62	0.73	0.78	0.80
Selenocystine	0.41	0.19	0.34	0.58	0.44	0.34
TMSe iodide	0	0	0.14	0.33	0.21	0.94
Selenotaurine	0.70	0.68	0.66	0.76	0.71	0.62
Selenious acid	0.26	0.26	0.48	0.70	0.71	0.35
Selenic acid	0.21	0.10	0.51	0.64	0.47	0.21

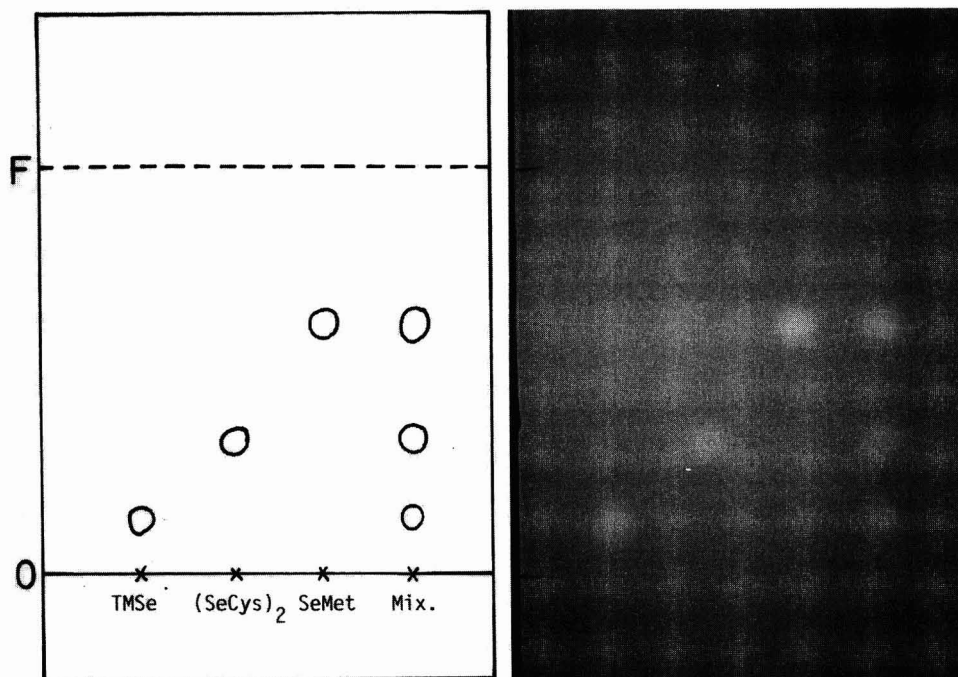


Fig. 1. Separation of selenium compounds on a silica gel sintered TLC plate. The authentic samples [SeMet, (SeCys)<sub>2</sub> and TMSe] and the authentic mixture were spotted (1  $\mu$ l) and developed with *n*-butanol-acetic acid-water (4:1:1, v/v/v) followed by digestion and UV detection (365 nm). Each spot contained about 200 ng of selenium.

After the colour development with DAN reagent, the TLC plate was sprayed with a solution of Triton X-100-chloroform (1:4, v/v) [12] and the fluorescence intensity was enhanced [13] by a factor of 100. If a solution of either paraffin oil-*n*-hexane (2:1, v/v) [17], glycerol-ethanol (1:1, v/v) [17] or 1.8% cycloheptaamylose [18] was sprayed, the fluorescence intensity was enhanced by a factor of only 30, 3 or 3, respectively. The standard procedures for the digestion were adopted as described under *Procedure*.

Fig. 3 shows the calibration graph for selenium standard solution in the range 12.5–300 ng of selenium. A linear relationship exists up to 100 ng selenium. Lower responses at selenium levels > 100 ng may be attributed to self-quenching due to the high concentration. If the plate was untreated with the solution for fluorescence enhancement, the linearity was extended up to 250 ng of selenium.

Fig. 4 shows the calibration graphs for SeMet, (SeCys)<sub>2</sub> and TMSe ion in the range 3–100 ng of selenium. It is noteworthy that each selenium compound gave the same calibration graph. This result strongly suggests that these organic selenium compounds were digested completely and reacted stoichiometrically with DAN without any interfering effect. The detection limit was 0.4 ng of selenium with a signal-to-noise ratio of 3.

Using the proposed method, it became possible to identify selenium-containing

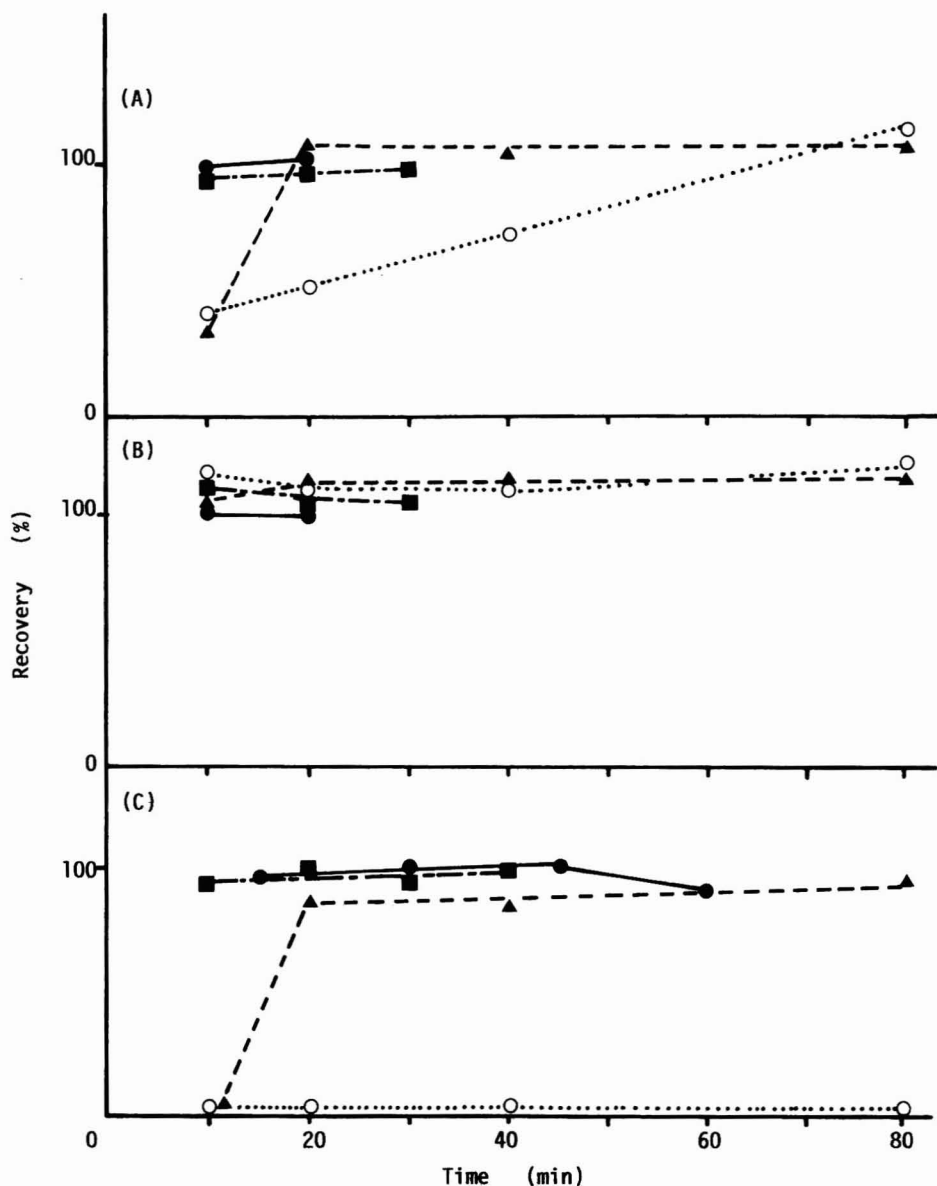


Fig. 2. Temperature and recoveries of selenium compounds. Aliquots ( $0.5 \mu\text{l}$ ) of authentic sample [(A) SeMet; (B) (SeCys)<sub>2</sub>; (C) TMSe] solutions which contained  $100 \mu\text{g/ml}$  of selenium were spotted separately on a TLC plate and digested at (○) 150, (▲) 180, (●) 210 or (■) 250°C for various times. Recoveries of selenium were calculated from the ratios of the fluorescence intensities of the spots to that of the selenium standard solution on the same plate. The values are means of three runs.

compounds directly and to determine selenium in them on a TLC plate on which biological materials have been separated. Although organic selenium compounds so far known as constituents of biological materials are confined broadly to those used

TABLE III

## RECOVERIES OF SELENIUM COMPOUNDS AFTER DIGESTION AT 210°C

Aliquots (0.5  $\mu$ l) of authentic sample [SeMet, (SeCys)<sub>2</sub> and TMSe] solutions containing 100  $\mu$ g/ml of selenium were spotted separately on a TLC plate, digested at 210°C and determined by fluorimetry using a TLC scanner. Recoveries of selenium were calculated from the ratios of the fluorescence intensities of the spots to that of the selenium standard solution on the same plate. The values were means  $\pm$  standard deviations for three runs.

Time (min)	Recovery (%) (Mean $\pm$ S.D.)		
	SeMet	(SeCys) <sub>2</sub>	TMSe
5	96 $\pm$ 7	92 $\pm$ 6	88 $\pm$ 4
10	103 $\pm$ 2	99 $\pm$ 3	96 $\pm$ 5
15	94 $\pm$ 7	99 $\pm$ 9	97 $\pm$ 10
20	99 $\pm$ 5	101 $\pm$ 7	103 $\pm$ 3

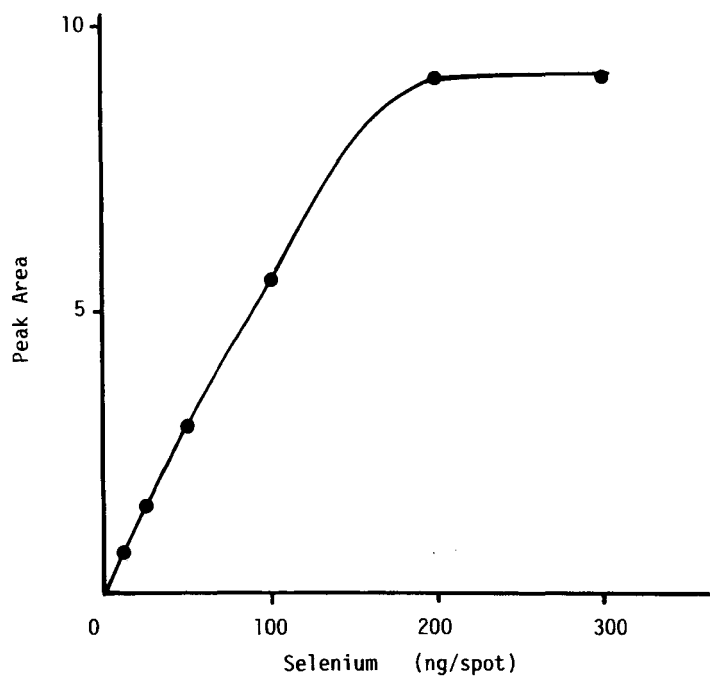


Fig. 3. Linear relationship between fluorescence intensities and selenium concentration. The selenium compound in the range 12.5–300 ng of selenium was developed with *n*-butanol–acetic acid–water (4:1:1, v/v/v) and determined by fluorimetry using a TLC scanner.

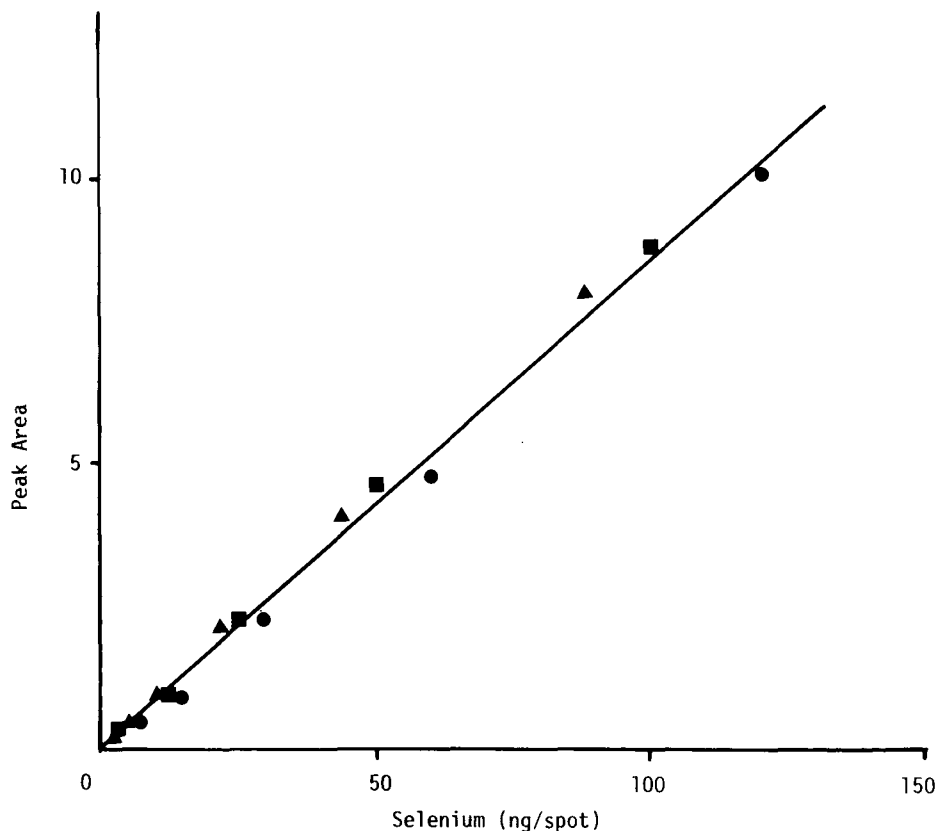


Fig. 4. Calibration graphs for (●) SeMet, (■) (SeCys)<sub>2</sub> and (▲) TMSe in the range from 3–100 ng of selenium. The authentic mixture [SeMet, (SeCys)<sub>2</sub> and TMSe] was developed with *n*-butanol–acetic acid–water (4:1:1, v/v/v) followed by digestion and determination by fluorimetry using a TLC scanner.

in this study, the proposed method showed open up a new approach to acquiring a better understanding of selenium metabolism.

#### ACKNOWLEDGEMENTS

We thank Dr. Makoto Murakami (Institute of Physical and Chemical Research) for valuable discussions and Mr. Kenji Shimura (Kitasato University) for technical assistance. We are indebted to Gasukuro Kogyo for their generous supply of sintered TLC plates.

#### REFERENCES

- 1 K. Schwarz and C. M. Foltz, *J. Am. Chem. Soc.*, 79 (1957) 3292.
- 2 H. A. Schroeder, D. V. Frost and J. J. Balassa, *J. Chron. Dis.*, 23 (1970) 227.
- 3 H. J. Robberecht and H. A. Deelstra, *Talanta*, 31 (1984) 497.
- 4 H. Sakurai and K. Tsuchiya, *Environ. Physiol. Biochem.*, 5 (1975) 107.



- 5 P. J. Peterson and G. W. Butler, *J. Chromatogr.*, 8 (1962) 70.
- 6 K. R. Millar, *J. Chromatogr.*, 21 (1966) 344.
- 7 R. Hasunuma, T. Ogawa and Y. Kawanishi, *Anal. Biochem.*, 126 (1982) 242.
- 8 T. Okumura, T. Kadono and M. Nakatani, *J. Chromatogr.*, 74 (1972) 73.
- 9 H. J. Robberecht, R. E. Van Grieken, P. A. Van Den Bosch, H. Deelstra and D. Vanden Berghe, *Talanta*, 29 (1982) 1025.
- 10 Y. Shibata, M. Morita and K. Fuwa, *Anal. Chem.*, 56 (1984) 1527.
- 11 R. E. Huber and R. S. Criddle, *Arch. Biochem. Biophys.*, 122 (1967) 164.
- 12 S. Uchiyama and M. Uchiyama, *J. Liq. Chromatogr.*, 3 (1980) 681.
- 13 W. Funk, V. Dammann, T. Couturier, J. Schiller and L. Volker, *J. High Resolut. Chromatogr. Chromatogr. Commun.*, 9 (1986) 224.
- 14 J. L. Byard, *Arch. Biochem. Biophys.*, 130 (1969) 556.
- 15 I. S. Palmer, D. D. Fischer, A. W. Halverson and O. E. Olson, *Biochim. Biophys. Acta*, 177 (1969) 336.
- 16 J. Neve, M. Hanocq, L. Molle and G. Lefebvre, *Analyst (London)*, 107 (1982) 934.
- 17 S. Uchiyama and M. Uchiyama, *J. Chromatogr.*, 153 (1978) 135.
- 18 T. Kinoshita, F. Iinuma, K. Atsumi and A. Tsuji, *Anal. Biochem.*, 77 (1977) 471.



CHROM. 22 753

## Determination of absolute mobilities, p*K* values and separation numbers by capillary zone electrophoresis

### Effective mobility as a parameter for screening

J. L. BECKERS\*, F. M. EVERAERTS and M. T. ACKERMANS

*Laboratory of Instrumental Analysis, Eindhoven University of Technology, P.O. Box 513, 5600 MB Eindhoven (The Netherlands)*

(First received May 15th, 1990; revised manuscript received August 7th, 1990)

---

#### ABSTRACT

Migration times or apparent mobilities can never be used for the identification of ionic species in capillary zone electrophoresis if an electroosmotic flow (EOF) is present, because the velocity of this flow varies considerably with the "state" of the capillary. From the migration times of the EOF and the ionic species, the effective mobilities can be calculated. These effective mobilities are nearly independent of the concentrations of the sample ionic species. Although a large excess of one of the sample components can cause different values of the calculated effective mobility, they are reproducible if the matrix has a constant composition and in this way effective mobilities can be used for screening purposes. In the determination of effective mobilities the use of a "true" EOF marker is extremely important.

If effective mobilities are measured in two different electrolyte systems at different pH values, at which the degrees of dissociation differ sufficiently, the absolute ionic mobilities and p*K* values of ionic species can be calculated. Values obtained in this way, for mobility and p*K* were compared with data obtained isotachophoretically, showing good agreement.

Theoretically, the separation number in zone electrophoresis, defined as the number of components that can be separated within a unit of mobility, varies widely with the mobilities of the ionic species and the EOF. Experimentally obtained values of the separation number are significantly lower than the calculated values owing to the method of injection, temperature effects during analysis and amount of sample. For low-molecular-weight ionic species separations are possible if the effective mobilities differ by about one unit for cations and 0.2–0.3 for anions. A negative wall charge (at higher pHs) diminishes the separation number of cations considerably, especially on applying small diameter capillaries, owing to attractive forces between the wall and analytes.

---

#### INTRODUCTION

Since the availability of commercial apparatus, capillary zone electrophoresis (CZE) has been the subject of rapid development and is now applied in many areas, especially in the biological and biochemical fields.

For screening possibilities, the most important questions are as follows: (1) does the component migrate in a chosen electrolyte system and what parameter can be used to recognize it?; (2) is the separation capacity of the method sufficient to separate the

component adequately from other components of a complex matrix and can it be identified in a simple way?; and (3) at what level can the component be detected?

In this paper we discuss the possibility of open capillary zone electrophoresis for screening purposes on a qualitative basis. When using open capillary zone electrophoresis, the electroosmotic flow (EOF) is a very important parameter, in addition to the effective mobility<sup>a</sup>, determining the migration behaviour of components. As the EOF velocity strongly varies with the "state" of the capillary, the migration time (or apparent mobility<sup>a</sup>) can never be used in a proper way for screening purposes. The effective mobilities of components can be calculated from the experimentally obtained apparent mobilities and the mobility of the EOF. From the effective mobilities also the *pK* values and absolute mobilities<sup>a</sup> of the components can be calculated. These data are also important in the choice of a suitable electrolyte system for the separation of various components in complex matrices.

Until now, mobilities and *pK* values have often been determined by isotachopheresis (ITP) [1–8]. The calculation of mobilities and *pK* values in ITP is laborious, however, as in ITP all zones have different parameters such as *pH*, concentration and temperature, through which the data have to be calculated in an iterative way. The correction for the concentration dependence of mobilities and for activities is often troublesome for mixtures of ionic species with different charges. Further, in ITP the choice of the *pH* of the electrolyte systems is limited to about 3–11. Low *pH*s cannot be applied in the separation of cations owing to the great influence of hydrogen ions on the zone conductivity and high *pH*s can hardly be used in the separation of anions owing to the disturbance by carbonate. Especially at low *pH*s major problems can be expected in finding an appropriate slow terminator in the separation of cations because hydrogen ions can act as a terminator with relatively high effective mobilities [9,10]. Generally, the determination of the mobilities of weak acids and bases with low mobility and also those of the subspecies from multivalent acids and bases is difficult.

In CZE, on the other hand, many of these limitations are not present. Background electrolytes at low and high *pH*s can be used easily, there is no need for a terminator and corrections for several effects are relative easy because all parameters in the background electrolyte can be considered to be nearly constant, such as ionic strength, *pH*, temperature and electric field strength.

Effective mobilities for low-molecular-weight ionic species determined in CZE and, from these values, calculated *pK* values and absolute ionic mobilities are presented, and compared with ITP data. In the CZE experiments special attention was paid to the reproducibility and the effect of the EOF, taking into account the influence of the composition of the samples, such as the concentrations of the sample ions and the effect of the presence of background electrolyte in the sample solution.

Using CZE as a screening method, the effective mobility ("yes or no", in combination with, *e.g.*, the use of UV absorbance ratios at different wavelengths) can be the only way to identify substances, stressing the importance of the determination of mobilities from electropherograms.

For the experiments, representatives of several classes of compounds were

---

<sup>a</sup> Note that the apparent mobility refers to the net migration behaviour, including the velocity of the EOF, and the effective and absolute mobility refer to the pure electrophoretic migration behaviour.

chosen, such as procaine (an anaesthetic) and some antibiotics used in cattle-breeding. Antibiotics are often administered on a large scale to food-producing animals in order to guarantee safe products such as milk, meat and eggs. Their presence in food is forbidden, however, and for this reason there is a need for screening facilities for all these components. The  $\beta_2$ -agonists clenbuterol and fenoterol were studied. In addition to the use of  $\beta_2$ -agonists for the treatment of asthmatic diseases, they have a positive effect on the fat/meat ratio in cattle, which explains their improper use. We also measured the effective mobility of levamisol, an anthelmintic or vermicide used against maggots. As an example of coccidiostats, used to treat parasitic diseases especially in the intestines of cattle, sheep, goats, dogs, cats, rabbits and poultry, amprolium was studied. In Fig. 1 some characteristic structural formulae are given.

## THEORETICAL

### *Determination of mobilities and $pK$ values*

If in CZE the applied voltage  $V$  and the length of the capillary  $L_c$  are known, the electric field strength is

$$E = V/L_c \text{ (V/m)} \quad (1)$$

If the distance from the injection point to the detector,  $L_d$ , and the migration time  $t$  of

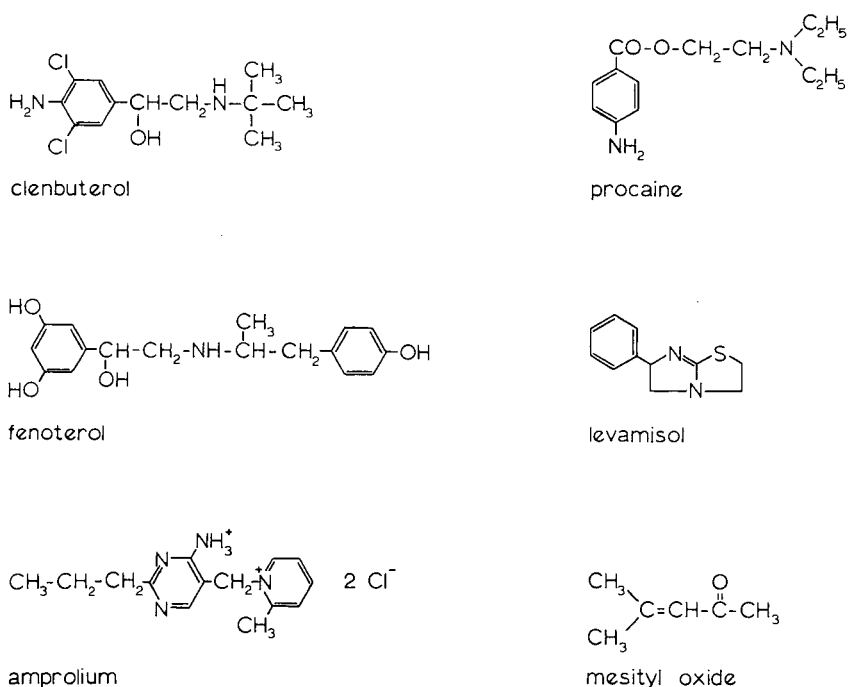


Fig. 1. Some characteristic structural formulae.

a component are known, the velocity  $v$  and the apparent mobility  $m_{\text{app}}$  can be calculated using

$$m_{\text{app}} = v/E = L_d/tE \text{ (m}^2/\text{V} \cdot \text{s)} \quad (2)$$

In CZE, a high EOF can generally act in the direction of the cathode using silica capillaries. The velocity of the EOF can be determined using the “migration” time,  $t_{\text{EOF}}$ , of an uncharged substance and, because this velocity shows a linear relationship with  $E$ , the  $m_{\text{EOF}}$  can be defined as

$$m_{\text{EOF}} = L_d/t_{\text{EOF}}E \text{ (m}^2/\text{V} \cdot \text{s)} \quad (3)$$

and the effective mobility of a component can be obtained from

$$m_{\text{eff}} = m_{\text{app}} - m_{\text{EOF}} \quad (4)$$

If the absolute values of the effective mobilities of anionic species are smaller than  $m_{\text{EOF}}$ , they can be determined in the upstream mode (UM) simultaneously with cations migrating in the downstream mode (DM). From the effective mobility, the absolute ionic mobility can be calculated, correcting for activities, dissociation and concentration dependence of the mobility.

If the effective mobility of a component is known for two different electrolyte systems at different pHs, at which the component shows a different degree of dissociation, both its pK value and its absolute mobility can be calculated. For a monovalent acid the calculation is as follows. The thermodynamic equilibrium constant for the equilibrium



is defined as

$$K_{\text{th}} = \gamma_{\text{Z}^-} \gamma_{\text{H}^+} \frac{[\text{H}^+][\text{Z}^-]}{[\text{HZ}]} \quad (6)$$

with the assumption that for HZ the activity coefficient  $\gamma = 1$ . Hence,

$$\text{p}K_{\text{th}} = -\log \gamma_{\text{Z}^-} - \log \gamma_{\text{H}^+} + \text{pH} - \log \frac{[\text{Z}^-]}{[\text{HZ}]} \quad (7)$$

Because the effective mobility  $m_{\text{eff}} = \alpha m_c$ , where  $m_c$  is the ionic mobility at a specific equivalent concentration  $c$ , it follows that

$$\frac{[\text{Z}^-]}{[\text{HZ}]} = \frac{\alpha}{1 - \alpha} = \frac{m_{\text{eff}}}{m_c - m_{\text{eff}}} \quad (8)$$

The value of  $m_c$  can be calculated from the ionic equivalent conductance  $\lambda_c$  using Faraday's constant,  $F$ . For the ionic equivalent conductance in mixed solutions we

used the expression according to Bennewitz, Wagner and Kuchler as described by Falkenhagen [11]:

$$\lambda_c = \lambda_0 - (0.229\lambda_0 + 30.1)\sqrt{c} \quad (9)$$

where  $\lambda_c$  and  $\lambda_0$  are the ionic equivalent conductances at an equivalent concentration  $c$  and infinite dilution, respectively. This relationship can be used for very dilute solutions of a particle in a bulk of the background electrolyte.

If the effective mobilities are known in two different electrolyte systems, we have

$$\begin{aligned} -\log \gamma_{Z,1}^- - \log \gamma_{H,1}^+ + \text{pH}_1 - \log \left( \frac{m_{\text{eff},1}}{m_{c,1} - m_{\text{eff},1}} \right) = \\ -\log \gamma_{Z,2}^- - \log \gamma_{H,2}^+ + \text{pH}_2 - \log \left( \frac{m_{\text{eff},2}}{m_{c,2} - m_{\text{eff},2}} \right) \end{aligned} \quad (10)$$

The activity coefficients  $\gamma$  can be calculated by

$$-\log \gamma = \frac{0.5085 z^2 \sqrt{\mu}}{1 + 0.3281 a \sqrt{\mu}} \quad (11)$$

where  $z$  is the valency of the component,  $\mu$  is the ionic strength of the solution as determined by the background electrolyte and  $a$  is the effective hydrated diameter of the ion in Å. If the effective hydrated diameter was unknown, 5 Å is assumed.

If the ionic strengths and the equivalent concentrations of two electrolyte systems are known, all activity coefficients can be calculated with eqn. 11. Using Faraday's constant and eqn. 9,  $m_{c,1}$  and  $m_{c,2}$  can be replaced by the absolute ionic mobility and thus the only unknown parameter in eqn. 10 is the absolute ionic mobility, which can be calculated. With eqn. 7,  $pK_{\text{th}}$  can be obtained. Analogous derivations can be given for multivalent anions and cations.

#### *Effect of the electroosmotic flow*

From eqn. 4, it can be concluded that the effect of the EOF is extremely important in the determination of effective mobilities. In Fig. 2 the calculated relationship between migration time and effective mobility for an  $E$  gradient of 25 kV/m and  $L_c$  and  $L_d$  of 1 m is given for several values of  $m_{\text{EOF}}$ . It can be clearly seen that at low EOF only cations can be determined whereas at high EOF simultaneously anions in the UM can be determined with  $|m| < m_{\text{EOF}}$ . A disadvantage at high EOF is, however, that the separation power for cations diminishes.

#### *Separation number*

In gas chromatography the separation number ( $SN$ ) [12]

$$SN = \frac{t_{R(z+1)} - t_{R(z)}}{w_{h(z)} + w_{h(z+1)}} - 1 \quad (12)$$

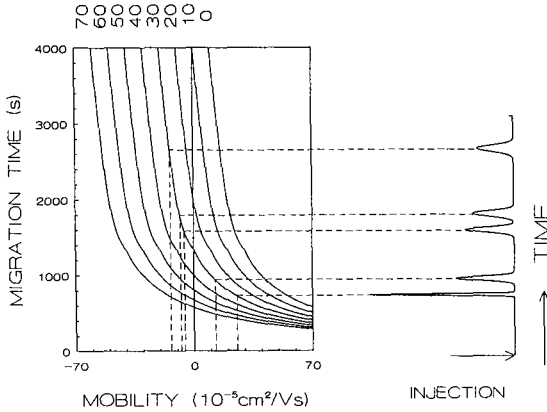


Fig. 2. Calculated relationship between migration time and effective mobility applying an  $E$  gradient of 25 kV/m. The different lines are marked with numbers representing the mobility ( $\times 10^5$ ) of the EOF ( $\text{cm}^2/\text{V} \cdot \text{s}$ ). At large EOF velocities negative ions can be analysed in the upstream mode. From this relationship electropherograms can be deduced, as shown for an  $m_{\text{EOF}}$  of  $30 \cdot 10^{-5} \text{ cm}^2/\text{V} \cdot \text{s}$ .

where  $t_R$  is the retention time and  $w_h$  the peak width at half-height, is used in order to calculate the number of component peaks which can be placed between peaks of two consecutive homologous standards with  $z$  and  $z + 1$  carbon atoms with a resolution of  $R_s = 1.177$ .

In CZE, an analogous expression can be used as a parameter for the separation power. We can define the separation number  $SN_m$  as

$$SN_m = \left| \frac{t_{m-0.5} - t_{m+0.5}}{2(\sigma_{m+0.5} + \sigma_{m-0.5})} \right| \quad (13)$$

This number indicates how many components can be separated at an effective mobility  $m$  within a unit of effective mobility. Using the absolute value, this equation can be used for both cations and anions, independent of the direction of the EOF.

Using eqns. 2 and 4, the migration time can be calculated from the effective mobility and  $m_{\text{EOF}}$  and, using for  $\sigma$  the expression

$$\sigma^2 = 2Dt \text{ (m}^2\text{) or } \sigma^2 = 2Dt/v^2 \text{ (s}^2\text{)} \quad (14)$$

$SN_m$  can be calculated. In the calculations other effects of zone broadening, such as  $\sigma_{\text{inj}}$ , are neglected.

In Fig. 3 the calculated relationship between  $SN_m$  values and effective mobilities is given for several values of EOF ( $L_c$  and  $L_d = 1 \text{ m}$ ,  $E = 25 \text{ kV/m}$ ). For the diffusion constant  $D$  we used in the calculations the Einstein expression

$$D = mkT/ez \quad (15)$$

It can be seen from Fig. 3 that if the mobility is tending to zero  $SN_m$  is strongly increasing because  $D$  is decreasing to zero. Very low diffusion constants will only act



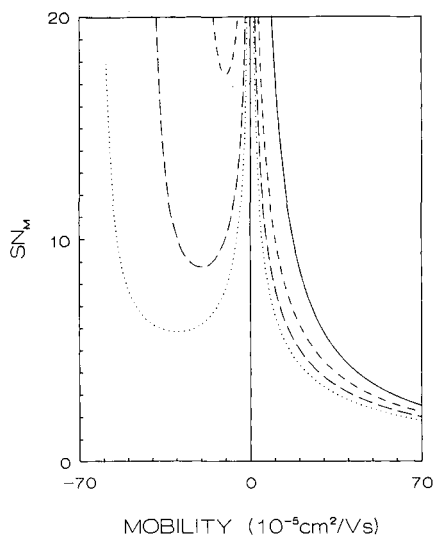


Fig. 3. Calculated relationship between  $SN_m$  values and effective mobilities for  $m_{EOF} \cdot 10^5$  ( $\text{cm}^2/\text{V} \cdot \text{s}$ ) of 0 (—), 20 (-----), 40 (- - -) and 60 (···). For further explanation, see text.

for very large molecules such as DNA fragments, causing a high peak capacity. For small molecules this will be not true as, generally, a very low mobility means that an ionic species for the greater part will be present as a neutral molecule with a large diffusion constant. Therefore, we recalculated  $SN_m$  as a function of the effective mobility, under the assumption that  $D$  is determined by the Stokes–Einstein relationship:

$$D = kT/6\pi\eta a \quad (16)$$

taking arbitrarily an average value for  $D$  of  $5 \cdot 10^{-10} \text{ m}^2/\text{s}$ .

This relationship is shown in Fig. 4 ( $L_c$  and  $L_d = 1 \text{ m}$ ,  $E = 25 \text{ kV/m}$ ). It can be clearly seen that the separation number increases at lower effective mobilities because the difference in migration time is increasing at an equal diffusion constant.

In Fig. 5, the relationship between the separation number  $SN_{20}$  (at an effective mobility of  $2 \cdot 10^{-4} \text{ cm}^2/\text{V} \cdot \text{s}$ ,  $L_c$  and  $L_d = 1 \text{ m}$ ) as a function of the applied voltage is given, showing that an increasing separation power is obtained by applying higher voltages.

## EXPERIMENTAL

For all CZE experiments the P/ACE™ System 2000 HPCE (Beckman, Palo Alto, CA, U.S.A.) was used. All experiments were carried out at  $25^\circ\text{C}$  in the constant-voltage mode at  $25 \text{ kV}$ , unless mentioned otherwise. Several different capillaries were applied. Further information concerning the apparatus is given elsewhere [13]. For all ITP experiments the apparatus described previously [14] was used.

Table I gives the compositions of all the electrolyte systems used.

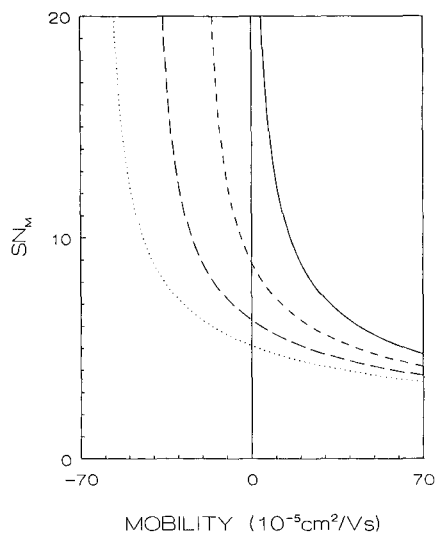


Fig. 4. Calculated relationship between  $SN_m$  values and effective mobilities for  $m_{\text{EOF}} \cdot 10^5$  ( $\text{cm}^2/\text{V} \cdot \text{s}$ ) of 0 (—), 20 (-----), 40 (- - - -) and 60 (· · ·), assuming a diffusion constant of  $5 \cdot 10^{-10}$   $\text{m}^2/\text{s}$ .

## RESULTS AND DISCUSSION

### *Choice of the EOF marker*

For the calculation of effective mobilities from the apparent mobility and the EOF, the velocity of the EOF has to be precisely known. There are several ways to

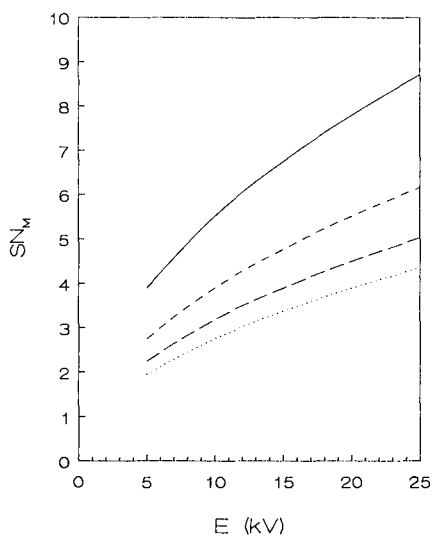


Fig. 5. Calculated relationship between  $SN_m$  values and  $E$  gradient for  $m_{\text{EOF}} \cdot 10^5$  ( $\text{cm}^2/\text{V} \cdot \text{s}$ ) of 0 (—), 20 (-----), 40 (- - - -) and 60 (· · ·) at an effective mobility of  $2 \cdot 10^{-4}$   $\text{cm}^2/\text{V} \cdot \text{s}$ .

TABLE I

## COMPOSITIONS OF BACKGROUND ELECTROLYTES AT DIFFERENT pH VALUES

All buffer solutions were prepared by adding the buffering counter ion to the cations until the desired pH was reached. All phosphate buffers were prepared by adding orthophosphoric acid to 0.01  $M$  KOH until the desired pH was reached.

Cation <sup>a</sup>	Buffering counter ion <sup>a</sup>	pH
0.02 $M$ $\beta$ -Alanine	Formic acid	3.5
0.02 $M$ $\beta$ -Alanine	Formic acid	3.8
0.02 $M$ $\beta$ -Alanine	Acetic acid	3.9
0.02 $M$ EAC	Formic acid	4.0
0.02 $M$ EAC	Acetic acid	4.4
0.02 $M$ $\beta$ -Alanine	Acetic acid	4.7
0.02 $M$ EAC	Acetic acid	5.0
0.02 $M$ HIST	MES	6.1
0.02 $M$ HIST	MES	6.2
0.01 $M$ KOH	MES	6.2
0.02 $M$ TEA	MOPS	7.0
0.04 $M$ Imidazole	MOPS	7.5
0.02 $M$ TRIS	MOPS	7.9
0.02 $M$ TRIS	MOPS	8.2
0.02 $M$ DEA	BICINE	9.0

<sup>a</sup> BICINE = N,N-Bis(2-hydroxyethyl)glycine; DEA = diethanolamine; EAC =  $\epsilon$ -aminocaproic acid; HIST = histidine; MES = 2-(N-morpholino)ethanesulphonic acid; MOPS = morpholinopropanesulphonic acid; TEA = triethanolamine; TRIS = tris(hydroxymethyl)aminomethane.

measure the EOF. In Fig. 6 some possibilities are shown schematically. The real EOF displacement is indicated with an arrow. Using a neutral EOF marker, it is possible that this marker indicates the EOF displacement (2). If the marker, however, meets

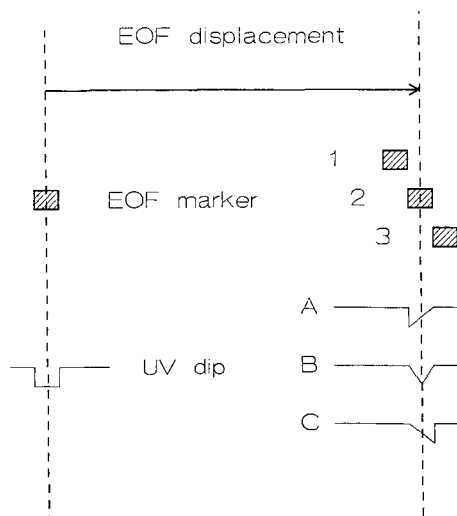


Fig. 6. Several possibilities of measuring EOF. For further explanation, see text.

a power of attraction from the capillary or if it is partially negatively charged by complexation with negative ions of the background electrolyte it will be too slow (1), or it will be too quick if it is positively charged by complexation (3).

Because many electrolyte systems (*e.g.*, the system HIST–MES at pH 6.2; see Table I) absorb UV light at a wavelength of 214 nm, sample solutions with a lower buffer concentration than the background electrolyte show a dip in the UV signal, because the local concentration of the buffer is lower. If an aqueous sample solution is introduced, the original concentration (UV) dip can indicate the correct EOF displacement (B), but because the shape of the concentration dip can change owing to diffusion effects, the shape can become asymmetric [15,16] to one of the sides (A or C), depending on the mobilities of the background ionic species, indicating the wrong EOF.

In the first instance we compared (UV detection at 214 and 254 nm) as EOF markers acetone, benzene, crotonaldehyde, mesityl oxide (MO) and paracetamol in a background electrolyte at pH 8.2. The best results (high absorbance and symmetrical peaks) were obtained using MO as EOF marker. In all further experiments we always measured at a wavelength of 214 nm. In Fig. 7 the measured UV signal for a sample solution of (a) 0.0001 *M* MO in 100% buffer and mixtures of (b) 1% water and 99% buffer and (c) 50% water and 50% buffer are shown. In Table II the measured migration times and calculated  $m_{\text{EOF}}$  are given for the 0.0001 *M* MO solution in 100% buffer and the mixture of 1% water in 99% buffer. In the latter instance the observed UV dip is used for the determination of the EOF. The background electrolyte was HIST–MES at pH 6.2. It can be concluded that the reproducibility of the experimental values is good and MO can be used as a true EOF marker in this system.

In Fig. 8, (a) the UV dip on injecting water as a sample and (b) the UV signal on injecting an aqueous solution of 0.0005 *M* MO are shown for the system KOH–MES at

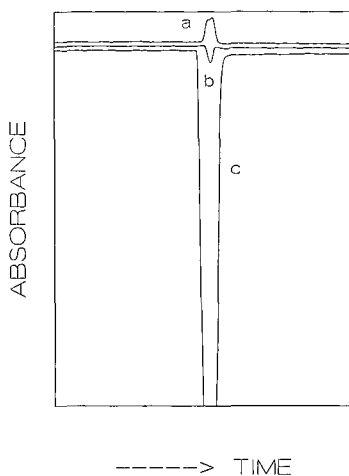


Fig. 7. Measured UV signal for a sample solution of (a) 0.0001 *M* MO in 100% buffer, (b) a mixture of 1% water and 99% buffer solution and (c) 50% water and 50% buffer solution. Background electrolyte, HIST–MES at pH 6.2. Capillary from Scientific Glass Engineering, I.D. 72  $\mu\text{m}$ ,  $L_c = 56.55$  cm and  $L_d = 49.60$  cm. Pressure injection time, 5 s.

TABLE II

MEASURED MIGRATION TIME  $t$  (min) AND  $m_{\text{EOF}} \cdot 10^5$  ( $\text{cm}^2/\text{V} \cdot \text{s}$ ) USING A HIST-MES BACKGROUND ELECTROLYTE AT pH 6.2

Capillary from Scientific Glass Engineering, I.D.  $72 \mu\text{m}$ ,  $L_c = 56.55 \text{ cm}$  and  $L_d = 49.60 \text{ cm}$ . Pressure injection time, 5 s. Applied voltage, 25 kV.

No.	0.0001 M MO in 100% background electrolyte		1% water and 99% background electrolyte	
	$t$	$m_{\text{EOF}}$	$t$	$m_{\text{EOF}}$
1	3.55	52.67	3.55	52.67
2	3.54	52.82	3.55	52.67
3	3.56	52.53	3.56	52.53
4	3.56	52.53	3.55	52.67
5	3.56	52.53	3.55	52.67

pH 6.2. In this instance the EOF marker lies behind the water dip. In Table III the  $m_{\text{EOF}}$  and effective mobilities of clenbuterol and benzoic acid are given, using for the calculation of the  $m_{\text{EOF}}$  (1) the beginning of the UV dip, (2) the lowest point of the UV dip (with MO present), (3) the middle of the UV dip (without MO) and (4) the UV peak of MO. The importance of the use of a "true" EOF marker will be clear considering the differences in the effective mobilities. The experiments with the system KOH-MES were carried out applying 10 kV, in order to avoid temperature effects, as this system shows much higher electric currents than HIST-MES owing to the higher con-

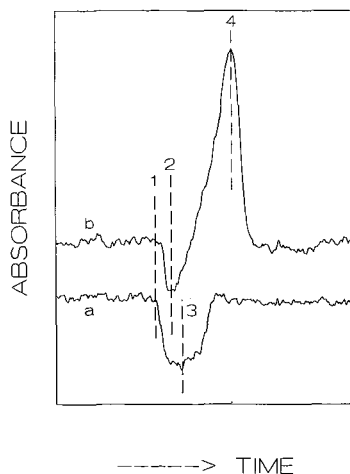


Fig. 8. Measured UV signal for a background electrolyte of 0.01 M KOH at pH 6.2 adjusted by adding MES, for a sample consisting of (a) 100% water and (b) 0.0005 M MO in water. (1) Beginning and (3) middle of the UV signal for 100% water and (2) lowest point and (4) top of the UV signal for 0.0005 M MO in water. Capillary from Scientific Glass Engineering, I.D.  $72 \mu\text{m}$ ,  $L_c = 56.43 \text{ cm}$  and  $L_d = 49.83 \text{ cm}$ . Pressure injection time, 1 s.

TABLE III

MEASURED MIGRATION TIME  $t$  (min) AND  $m \cdot 10^5$  ( $\text{cm}^2/\text{V} \cdot \text{s}$ ) USING A KOH-MES BACKGROUND ELECTROLYTE AT pH 6.2

Capillary from Scientific Glass Engineering, I.D.  $72 \mu\text{m}$ ,  $L_c = 56.43$  and  $L_d = 49.83$  cm. Pressure injection time, 5 s. Applied voltage, 10 kV.

EOF marker point	EOF		Clenbuterol		Benzoic acid	
	$t$	$m$	$t$	$m$	$t$	$m$
1	8.167	57.38	6.274	17.31	18.172	-31.59
2	8.240	56.88	6.274	17.82	18.172	-31.09
3	8.368	56.01	6.274	18.69	18.172	-30.22
4	8.406	55.75	6.274	18.95	18.172	-29.96

ductivity of the system. If an EOF marker was used, it was carefully checked whether the migration times of the water dip and EOF marker were identical.

#### *Electroosmotic flow*

In Fig. 9 the measured velocity of the EOF,  $v_{\text{EOF}}$ , as a function of the applied voltage is given for the apparatus used at two different times. As expected, a linear relationship is obtained, although the values differ in time. The background electrolyte was the TRIS-MOPS system at pH 8.2. In both instances the EOF marker was dissolved in both water and buffer and identical values were obtained in each case.

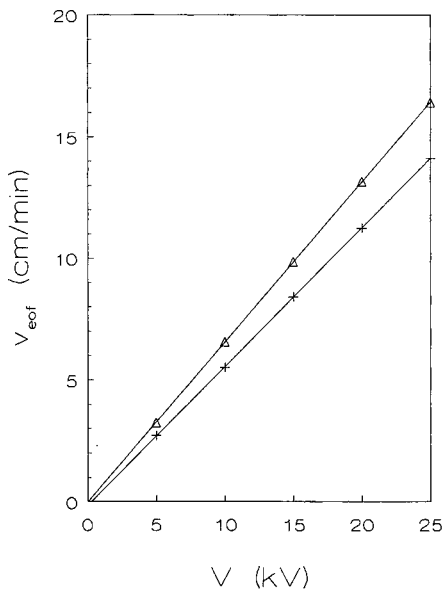


Fig. 9. Measured relationship between the velocity of the EOF and applied voltage at two different times. Background electrolyte, TRIS-MOPS at pH 8.2. Capillary from Scientific Glass Engineering, I.D.  $72 \mu\text{m}$ ,  $L_c = 56.95$  cm and  $L_d = 50.05$  cm. Pressure injection time, 5 s.

TABLE IV

$m_{\text{EOF}} \cdot 10^5$  ( $\text{cm}^2/\text{V} \cdot \text{s}$ ) AS A FUNCTION OF pH FOR THE ORIGINAL BECKMAN CAPILLARY (I) AND A SCIENTIFIC GLASS ENGINEERING CAPILLARY (II-V) AT DIFFERENT TIMES

For composition of background electrolytes, see Table I. V: Phosphate buffers.

pH	I			IV		V	
	$m_{\text{EOF}}$	$m_{\text{EOF}}$	$m_{\text{EOF}}$	pH	$m_{\text{EOF}}$	pH	$m_{\text{EOF}}$
3.8	33.8	30.2	28.0	3.8	27.8	2.5	15.1
4.4	36.2	37.1	35.0	5.0	52.4	3.0	26.8
5.0	47.5	—	—	6.1	45.3	4.0	36.1
6.2	55.6	56.2	53.1	7.0	44.5	5.0	47.1
7.5	61.7	61.8	60.4	7.9	62.4	6.0	56.9
8.2	69.9	72.1	73.1	9.0	59.4	7.0	65.0
						8.0	70.6
						9.0	73.1

In order to measure the effect of the pH on the EOF, measurements were carried out in several background electrolytes. In Table IV the  $m_{\text{EOF}}$  values for some electrolytes are given for the original Beckman capillary cartridge (I). Series II and III and series IV and V were measured with two different Scientific Glass Engineering (SGE) capillaries.

On running ultracentrifuged serum samples, a dramatic change in the EOF resulted. For a pH of 3.8, the migration time of the EOF changed from about 5.6 to 21.2 min for an SGE capillary. In order to examine what happens with time we measured the migration times of a mixture of amprolium, levamisol, clenbuterol (all

TABLE V

MEASURED MIGRATION TIMES  $t$  (min) AND EFFECTIVE MOBILITIES  $m \cdot 10^5$  ( $\text{cm}^2/\text{V} \cdot \text{s}$ ) FOR A SAMPLE OF AMPROLIUM, LEVAMISOL, CLENBUTEROL, MESITYL OXIDE AND BENZOIC ACID WITH  $\beta$ -ALANINE-FORMIC ACID BACKGROUND ELECTROLYTE AT pH 3.8.

Capillary from Scientific Glass Engineering, I.D.  $72 \mu\text{m}$ ,  $L_c = 57 \text{ cm}$  and  $L_d = 50 \text{ cm}$ . Pressure injection time, 5 s. Applied voltage, 25 kV.

No.	Amprolium		Levamisol		Clenbuterol		EOF (MO)		Benzoic acid	
	$t$	$m$	$t$	$m$	$t$	$m$	$t$	$m$	$t$	$m$
1	4.206	36.22	5.444	25.95	6.780	19.07	21.229	8.95		
2	4.012	36.56	5.126	26.27	6.299	19.36	17.589	10.80		
3	3.855	36.80	4.881	26.45	5.938	19.52	15.231	12.47		
4	3.791	36.79	4.771	26.50	5.777	19.56	14.257	13.33		
5	3.740	36.84	4.692	26.55	5.666	19.59	13.624	13.96		
6	3.598	36.92	4.451	26.76	5.316	19.81	11.927	15.93		
7	3.498	36.89	4.306	26.69	5.110	19.75	10.900	17.43	23.139	-9.22
8	3.433	36.84	4.211	26.61	4.975	19.68	10.265	18.51	20.570	-9.27
9	3.390	36.75	4.140	26.59	4.875	19.67	9.844	19.30	18.917	-9.26
10	3.336	36.77	4.063	26.58	4.768	19.67	9.414	20.18	17.394	-9.26

TABLE VI

EFFECTIVE MOBILITIES  $m \cdot 10^5$  ( $\text{cm}^2/\text{V} \cdot \text{s}$ ) FOR SEVERAL IONIC SPECIES IN A HIST-MES BACKGROUND ELECTROLYTE AT pH 6.2

The sample components were dissolved in water (W) and background electrolyte (B). If the capillaries were rinsed with 0.1 M KOH the measurements are indicated as WR and BR. Capillary from Scientific Glass Engineering, I.D. 72  $\mu\text{m}$ ,  $L_c = 56.55$  cm and  $L_d = 49.60$  cm. Pressure injection time, 5 s. Applied voltage, 25 kV. Variances are given in parentheses.

Compound	Concentration (M)	W (5 expts.)	B (25 expts.)	WR (5 expts.)	BR (5 expts.)	Average
Procaine	0.0001	20.87 (0.07)	20.68 (0.02)	20.74 (0.06)	20.82 (0.09)	20.72 (0.17)
	0.00005	20.96 (0.00)	20.82 (0.11)	20.87 (0.06)	20.86 (0.05)	20.84 (0.10)
	0.00001	20.82 (0.00)	20.80 (0.19)	20.94 (0.05)	20.86 (0.27)	20.83 (0.18)
Clenbuterol	0.0001	18.13 (0.07)	18.30 (0.17)	18.15 (0.04)	18.10 (0.09)	18.06 (0.15)
	0.00005	18.21 (0.00)	18.10 (0.09)	18.12 (0.08)	18.11 (0.06)	18.12 (0.11)
	0.00001	18.09 (0.00)	18.10 (0.14)	17.93 (0.43)	18.07 (0.07)	18.07 (0.20)
Fenoterol	0.0001	16.12 (0.10)	16.03 (0.14)	16.06 (0.03)	16.06 (0.08)	16.05 (0.13)
	0.00005	15.91 (0.35)	16.08 (0.10)	16.14 (0.08)	16.10 (0.06)	16.08 (0.17)
	0.00001	16.05 (0.00)	16.09 (0.16)	16.19 (0.09)	15.92 (0.45)	16.07 (0.15)
Mesityl oxide	0.0001	52.17 (0.07)	51.04 (0.92)	48.83 (0.49)	51.89 (0.19)	51.01 (1.17)
	0.00005	52.09 (0.00)	50.64 (0.95)	47.68 (0.18)	51.40 (0.06)	50.33 (1.38)
	0.00001	51.94 (0.00)	50.55 (0.96)	47.36 (0.05)	51.34 (0.16)	50.43 (1.47)
Uric acid	0.0001	-22.40 (0.06)	-22.53 (0.10)	-22.35 (0.03)	-22.53 (0.06)	-22.49 (0.11)
	0.00005	-22.48 (0.02)	-22.58 (0.10)	-22.43 (0.03)	-22.52 (0.04)	-22.54 (0.09)
	0.00001	-22.58 (0.02)	-22.70 (0.11)	-22.62 (0.04)	-	-22.66 (0.10)
<i>p</i> -Hydroxyphenylacetic acid	0.0001	-26.41 (0.60)	-26.89 (0.54)	-26.57 (0.04)	-26.55 (0.27)	-26.73 (0.15)
	0.00005	-26.81 (0.02)	-26.88 (0.10)	-26.70 (0.04)	-26.82 (0.03)	-26.84 (0.10)
	0.00001	-26.95 (0.02)	-27.02 (0.09)	-26.94 (0.05)	-	-26.99 (0.08)
Benzoic acid	0.0001	-29.28 (0.05)	-29.41 (0.10)	-29.13 (0.04)	-29.31 (0.04)	-29.35 (0.13)
	0.00005	-29.41 (0.01)	-29.53 (0.12)	-	-	-29.51 (0.11)
	0.00001	-29.59 (0.03)	-29.69 (0.11)	-	-	-29.66 (0.11)



positive ions), MO (EOF marker) and benzoic acid (negative ion) ten times. After each run we rinsed the capillary repeatedly: 10 min with 0.1 M KOH, 10 min with water and 10 min with the background electrolyte. The result of the measurements are given in Table V. Although there appears to be a dramatic course of EOF with time, all the effective mobilities of the sample components were nearly constant.

It can be concluded from Table V that migration times (or apparent mobilities) can never be used for the identification of sample components without problems. Although in the above experiments severe changes in EOF occurred and hence also in the apparent mobilities of sample ionic species, we noticed that the effective mobilities were fairly constant.

#### *Effective mobility*

To investigate the reproducibility with time of the effective mobility, several experiments were carried out with a sample consisting of the positive ions procaine, clenbuterol and fenoterol and the negative ions of uric, *p*-hydroxyphenylacetic and benzoic acid. As EOF marker we always used MO. All measurements were always carried out several times on different days and the variance is given in parentheses (see Table VI). In order to study the effect of the sample concentrations we measured at three concentrations, *viz.*,  $1 \cdot 10^{-4}$ ,  $5 \cdot 10^{-5}$  and  $1 \cdot 10^{-5}$  M. Further, we measured the sample components dissolved both in water and in background electrolyte. Between all measurements we only rinsed the capillary with background electrolyte for 5 min, except where the columns are headed WR and BR. In that case there was an extra rinsing step with 0.1 M KOH for 5 min and with water for 5 min. In Table VI all effective mobilities, calculated from the apparent mobilities, are given. Although sometimes the EOF differs, the effective mobilities are remarkably constant.

In Table VII all effective mobilities (in duplicate, calculated from the measured apparent mobilities) for the same components as in Table VI are given for several background electrolytes at different pHs (note that all electrolyte systems have a different ionic strength and equivalent concentration). The negative ions show smaller effective mobilities at low pHs (not fully ionized) and so do the positive ions at high pHs. Fenoterol is even negative, possibly owing to the ionization of phenolic groups at high pH.

#### *Calculation of $pK$ values and absolute mobilities*

If effective mobilities are known in two different electrolyte systems, the absolute ionic mobility and the  $pK$  value of a component can be calculated using eqns. 9, 10 and 11.

In Table VIII the results of the calculations of  $pK$  values and absolute mobilities for several acids are given using the effective mobilities of the systems at pH 4 and 6.2 (HIST–MES) using CZE. The results are compared with data given by Hirokawa *et al.* [3] and with data obtained isotachophoretically using the concept of the isoconductor and specific zone resistance [17]. The CZE experiments were carried out using 50- $\mu$ m capillaries. Compared with 75- $\mu$ m capillaries, the peaks obtained for negative ions were much more gaussian, owing to the repulsive forces between anions and the negative wall charge. For cations, smaller diameters led to strongly tailing peaks. The ITP experiments were carried out with a leading electrolyte of 0.01 M HCl with EAC at pH 4 in combination with a terminator of 0.01 M pivalic acid, whereas for the system of

TABLE VII

EFFECTIVE MOBILITIES  $m \cdot 10^5$  ( $\text{cm}^2/\text{V} \cdot \text{s}$ ) FOR SEVERAL IONIC SPECIES IN SEVERAL BACKGROUND ELECTROLYTES AT DIFFERENT pH VALUES

Capillary from Scientific Glass Engineering, I.D.  $72 \mu\text{m}$ ,  $L_c = 56.55 \text{ cm}$  and  $L_d = 49.60 \text{ cm}$ . Pressure injection time, 5 s. Applied voltage, 25 kV. For the composition of the background electrolytes see Table I. 1 = Procaine; 2 = clenbuterol; 3 = fenoterol; 4 = mesityl oxide; 5 = uric acid; 6 = *p*-hydroxyphenylacetic acid; 7 = benzoic acid.

pH	1	2	3	4	5	6	7
3.9	22.49	19.25	17.42	29.45	- 0.81	-23.24	-11.35
	22.04	19.01	17.13	26.15	- 0.85		-11.07
5.0	21.39	18.87	17.02	52.23	- 7.60	-27.17	-26.93
	21.09	18.57	16.99	52.53	- 7.79	-27.29	-27.05
6.1	20.57	17.90	16.03	45.28	-20.48	-26.46	-29.06
	20.69	18.00	15.92	45.39	-20.55	-26.59	-29.25
7.0	19.96	17.19	14.28	44.52	-24.96	-26.42	-29.17
	19.84	17.30	14.39	44.42	-24.75	-26.30	-29.08
7.9	18.62	17.24	9.87	62.33	-25.30	-26.09	-28.94
	18.41	17.03	9.66	62.54	-25.44	-26.23	-29.03
9.0	11.20	14.55	- 1.11	59.36	-26.15	-26.38	-29.20
	11.20	15.43	- 1.11	59.36	-26.09	-26.33	-29.20

TABLE VIII

CALCULATED  $pK$  VALUES AND ABSOLUTE MOBILITIES  $m \cdot 10^5$  ( $\text{cm}^2/\text{V} \cdot \text{s}$ ) FOR SEVERAL ACIDS USING EXPERIMENTAL DATA FOR TWO DIFFERENT ELECTROLYTE SYSTEMS WITH (I) ISOTACHOPHORESIS AND (II) OPEN CAPILLARY ZONE ELECTROPHORESIS AND (III) LITERATURE VALUES

Capillary from Siemens, I.D.  $50 \mu\text{m}$ ,  $L_c = 77.33 \text{ cm}$  and  $L_d = 70.53 \text{ cm}$ . Pressure injection time, 1 s. Applied voltage, 25 kV.

Compound	(I) ITP		(II) CZE		(II) Ref. 3	
	$pK$	$m$	$pK$	$m^a$	$pK$	$m$
<i>m</i> -Aminobenzoic acid	4.79	-31.49	4.74	-31.64 <sup>b</sup>	-	-
Benzoic acid	4.18	-33.26	4.16	-33.40	4.19	-32.9
Hippuric acid	3.63	-27.50	3.60	-27.77	2.70	-25.3
<i>p</i> -Methoxyphenylacetic acid	4.37	-28.75	4.37	-29.03	4.36	-29.7
Nicotinic acid	4.85	-33.71	4.82	-33.44	4.82	-34.6
<i>p</i> -Nitrobenzoic acid	3.38	-31.92	3.49	-31.94 <sup>c</sup>	3.52	-32.3
$\alpha$ -Dinitrophenol	4.01	-32.33	4.04	-32.39	4.02	-31.3
2,6-Dinitrophenol	3.65	-33.96	3.73	-33.99 <sup>c</sup>	3.71	-31.3
Phenylacetic acid	4.29	-30.84	4.28	-31.10	4.41	-31.7
Propionic acid	4.89	-37.41	-	-	4.87	-37.1
Sulfanilic acid	3.12	-33.81	3.27	-33.93 <sup>c</sup>	3.23	-33.7
Uric acid	5.55	-31.08	5.41	-29.99 <sup>d</sup>	-	-

<sup>a</sup> Marked values were determined using electrolyte systems at pH values of <sup>b</sup> 4.7 and 6.2, <sup>c</sup> 3.5 and 6.2 and <sup>d</sup> 5.0 and 6.2.

pH 6 a leading electrolyte of 0.01  $M$  HCl with HIST and 0.01  $M$  MES as terminator was used.

From Table VIII, it can be concluded that absolute mobilities and  $pK$  values can be obtained in this way, provided that a good set of effective mobilities is available. Note that for this reason, for some ionic species (see Table VIII) pHs other than 4 were chosen in order to obtain larger differences between the degrees of dissociation (effective mobilities) for these components in the two electrolyte systems. For  $m$ -aminobenzoic acid a pH of 4.7 was chosen as the lowest pH in order to avoid the possibility that this component partially dissociates to a positive ionic form. For uric acid a pH of 5 was chosen as the lowest pH in order to obtain a real electrophoretic migration.

#### *Zone electrophoresis for screening purposes*

For qualitative screening, the most important question is whether the component of interest can be recognized from the matrix. As already shown, the effective mobility, which can be calculated from absolute mobility,  $pK$  value and EOF, can be used as a parameter. A complicating factor in the analysis of complex matrices is often the presence of an excess of one of the components such as sodium chloride in urine or serum. Beckers and Everaerts [15,16] showed that this can lead to different migration behaviour during the analysis. Schoots *et al.* [18] showed that if the composition of the sample (uraemic serum samples) is nearly constant, reproducible migration times are found, although the migration times differ considerably compared with those of the pure components.

To investigate the effect of the presence of a sample component in excess, we determined the effective mobilities of the mixture in Tables VI and VII (all components were  $10^{-4}$   $M$ , either in water or dissolved in buffer) and added increasing amounts of sodium chloride. In Table IX all effective mobilities, calculated from the measured apparent mobilities, are given. It can be concluded that up to about 0.01  $M$  NaCl the effective mobilities are nearly constant, except for potassium and sodium, as they are not migrating in a proper CZE way. At higher concentrations of NaCl the effective mobilities decrease, although these values are reproducible. Using higher background concentrations this effect will, of course, diminish.

An interesting point in these experiments was that on adding larger amounts of NaCl to the sample, in the first instance a UV dip was obtained, but at a certain NaCl concentration the UV signal of the EOF marker increased rapidly. The explanation is that if a high concentration of NaCl is present, at the point of the sample injection (note: the EOF position) the local ionic strength is very high, and according to Kohlrausch an adaptation to this original concentration always takes place. This means that at the point of the EOF later in the analysis a higher background concentration will be found, giving a high UV signal if the background electrolyte shows UV absorption.

In Fig. 10 this effect is shown for samples of aqueous NaCl solutions (without EOF marker). For higher concentrations of NaCl there is an increasing UV signal at the point of the EOF. The consequence of this effect for complex matrices can be that uncharged components migrating at the EOF position are covered by this effect. The choice of a non-UV-absorbing background electrolyte will be important.

As an example of screening possibilities, we added the same components (0.0001

TABLE IX

EFFECTIVE MOBILITIES  $m \cdot 10^5$  ( $\text{cm}^2/\text{V} \cdot \text{s}$ ) DETERMINED IN AN INCREASING AMOUNT OF SODIUM CHLORIDE DISSOLVED IN WATER AND BUFFER SOLUTION WITH HIST-MES AS BACKGROUND ELECTROLYTE AT pH 6.2

Capillary from Scientific Glass Engineering, I.D.  $72 \mu\text{m}$ ,  $L_c = 56.43 \text{ cm}$  and  $L_d = 49.83 \text{ cm}$ . Pressure injection time, 5 s. Applied voltage, 25 kV. 1 = Procaine; 2 = clenbuterol; 3 = fenoterol; 4 = mesityl oxide; 5 = uric acid; 6 = *p*-hydroxyacetic acid; 7 = benzoic acid.

Solution	NaCl (M)	K	Na	1	2	3	4	5	6	7
Water	0	66.97	47.52	20.96	18.27	16.18	45.28	-21.70	-26.96	-29.53
	0.0001	68.00	47.65	20.86	18.15	16.26	45.61	-21.82	-27.11	-29.74
	0.0005	67.54	46.50	20.85	18.16	16.27	45.39	-21.78	-27.08	-29.69
	0.001	67.32	48.12	20.86	18.15	16.26	45.61	-21.76	-27.09	-29.68
	0.005	67.32	48.12	20.86	18.15	16.26	45.61	-21.70	-27.03	-29.62
	0.01		47.19	20.63	17.94	16.05	45.61	-21.64	-26.94	-29.53
	0.05		50.74	19.48	17.10	15.47	45.39	-21.33	-26.53	-29.09
	0.1		52.36	18.92	16.79	15.19	45.28	-21.22	-26.38	-28.92
Buffer	0	68.44	47.17	20.84	18.16	16.09	45.17	-21.77	-27.02	-29.63
	0.0001	70.44	47.52	20.96	18.27	16.18	45.28	-21.79	-27.06	-29.68
	0.0005	71.99	47.63	20.84	18.16	16.29	45.17	-21.71	-27.01	-29.58
	0.001	69.02	48.45	20.96	18.27	16.38	45.38	-21.70	-26.97	-29.55
	0.005		47.87	20.85	18.16	16.07	45.39	-21.75	-27.03	-29.62
	0.01		48.81	20.62	17.94	16.07	45.39	-21.63	-26.94	-29.50
	0.05		51.24	19.48	17.10	15.28	45.39	-21.42	-26.57	-29.15
	0.1		53.38	18.92	16.79	15.00	45.28	-21.31	-26.46	-28.98
10-Fold diluted urine spiked with components 1-7	—	69.99	47.08	20.29	17.82	15.94	45.72	-21.34	-26.71	-29.25

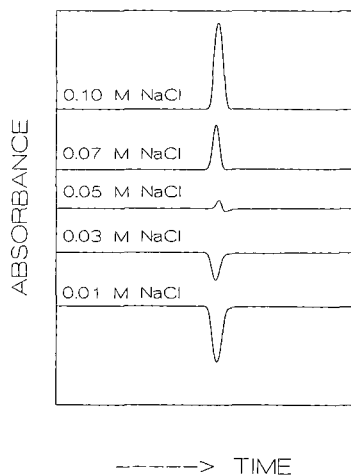


Fig. 10. Measured UV signal for the background electrolyte HIST-MES at pH 6.2 for different aqueous solutions of NaCl without EOF marker. For further explanation, see text. Capillary from Siemens, I.D.  $50 \mu\text{m}$ ,  $L_c = 77.33 \text{ cm}$  and  $L_d = 70.53 \text{ cm}$ . Pressure injection time, 1 s.

$M$ ) to 10-fold diluted ultrafiltered human urine (with about 0.015  $M$  NaCl) and determined the effective mobilities of the components. These values are also given in Table IX, and it can be seen that the components can be easily recognized from the effective mobilities. Potassium and sodium are indicated by negative UV dips in the electropherogram. Using capillaries with small diameters (50  $\mu\text{m}$ ), cations showed increasing tailing peaks owing to wall attraction forces.

### Separation number

An important aspect in screening is the separation number. This number indicates how many peaks can be distinguished within a unit of effective mobility. As already indicated under Theoretical, this number can theoretically be about 4–8 for cations with mobilities of 20–30 and different EOF. In practice, this number will be much smaller because the total variance will be affected by the variances of the injection and detection and by several other effects causing zone broadening. To obtain an impression of the order of magnitude in practice we measured an electropherogram of a mixture of nineteen ionic species in a HIST–MES electrolyte system at pH 6.2 and calculated the separation number for the effective mobilities by

$$SN_m = \left| \frac{t_{m-0.5} - t_{m+0.5}}{4\sigma_m} \right| \quad (17)$$

In Fig. 11 the electropherogram for this separation is given and in Table X all data are presented.

In Fig. 12 the relationship between the separation numbers (both those according to eqn. 17 and the theoretical values, assuming a diffusion constant of  $5 \cdot 10^{-10} \text{ m}^2/\text{s}$ ) and the effective mobilities is given for an  $m_{\text{EOF}}$  of  $47.97 \cdot 10^{-5} \text{ cm}^2/\text{V} \cdot \text{s}$ .

From Fig. 12 it can be concluded that the experimentally obtained separation numbers are smaller than the theoretical values owing to several zone broadening

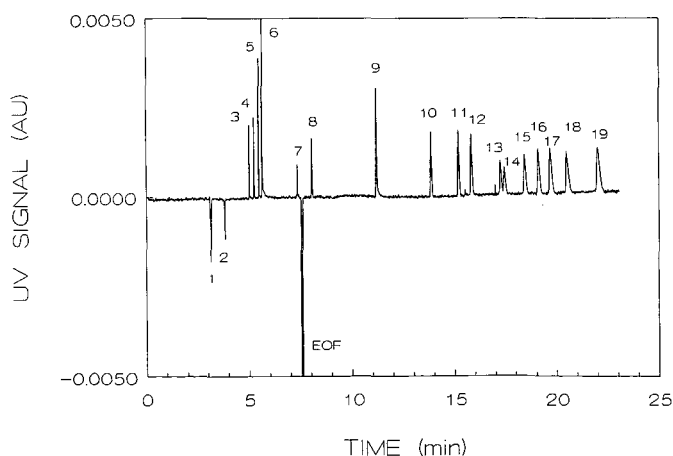


Fig. 11. Electropherogram of a mixture of nineteen components in a HIST–MES background electrolyte at pH 6.2. See Table X for the composition of the sample. Capillary from Siemens, I.D. 50  $\mu\text{m}$ ,  $L_c = 77.33 \text{ cm}$  and  $L_d = 70.53 \text{ cm}$ . Pressure injection time, 5 s.

TABLE X

MIGRATION TIMES  $t$  (min), EFFECTIVE MOBILITIES  $m \cdot 10^5$  ( $\text{cm}^2/\text{V} \cdot \text{s}$ ), PEAK WIDTH AT HALF-HEIGHT  $w$  (min), SEPARATION NUMBER  $SN$  AND THEORETICAL PLATE NUMBERS  $N$  FOR SEVERAL COMPONENTS IN A HIST-MES BACKGROUND ELECTROLYTE AT pH 6.2 AND MIGRATION TIMES  $t$  (min) AND EFFECTIVE MOBILITIES  $m \cdot 10^5$  ( $\text{cm}^2/\text{V} \cdot \text{s}$ ) OF THE COMPONENTS IN SPIKED HUMAN URINE

A and B: peak numbers of the components in Figs. 11 and 13, respectively. Peaks 8, 11 and 12 in Fig. 13 are unknown. Capillary from Siemens, I.D. 50  $\mu\text{m}$ ,  $L_c = 77.33$  cm and  $L_d = 70.53$  cm. Applied voltage, 25 kV.

Component	A	B	Sample mixture					Human urine	
			$t$	$m$	$w$	$SN$	$N (\times 10^{-5})$	$t$	$m$
Potassium	1	1	3.19	66.01	0.045	0.37	0.278	3.16	65.26
Sodium	2	2	3.85	46.47	0.024	1.00	1.42	3.86	44.39
Levamisol	3	3	5.02	24.46	0.019	2.15	3.86	4.91	24.25
Procaine	4	4	5.27	21.03	0.018	2.49	4.74	5.14	20.93
Clenbuterol	5	5	5.49	18.26	0.017	2.87	5.77	5.35	18.15
Fenoterol	6	6	5.66	16.27	0.020	2.59	4.43	5.51	16.18
Creatinine	7	7	7.36	1.43	0.030	2.92	3.33	7.09	1.48
EOF			7.58	47.97	0.050	—	—	7.30	49.81
<i>o</i> -Nitrophenol	8		8.07	—	2.91	0.034	3.10	3.12	
Bromothymol blue	9		11.21	—	15.53	0.043	4.73	3.76	
Uric acid	10	9	13.87	—	21.75	0.065	4.79	2.52	12.94
Hippuric acid	11	10	15.21	—	24.06	0.074	5.06	2.34	14.09
<i>p</i> -Methoxyphenylacetic acid	12		15.84	—	25.01	0.081	5.02	2.11	
<i>p</i> -Hydroxyphenylacetic acid	13		17.26	—	26.90	0.089	5.42	2.08	
Phenylacetic acid	14		17.45	—	27.13	0.092	5.36	1.99	
<i>p</i> -Nitrobenzoic acid	15		18.44	—	28.25	0.094	5.86	2.13	
Orotic acid	16		19.12	—	28.95	0.110	5.38	1.67	
Benzoic acid	17		19.69	—	29.50	0.123	5.11	1.42	
Sulphanilic acid	18		20.50	—	30.23	0.129	5.28	1.40	
Aspirin	19		22.02	—	31.46	0.150	5.24	1.19	

effects, especially for cations. In Fig. 13 the electropherogram of 10-fold diluted human urine spiked with levamisol, procaine, clenbuterol and fenoterol is shown. The migration times and calculated effective mobilities are given in Table X. Using the effective mobilities, the components (1) potassium, (2) sodium, (3) levamisol, (4) procaine, (5) clenbuterol, (6) fenoterol, (7) creatinine, (9) uric acid and (10) hippuric acid can easily be recognized.

#### CONCLUSION

It can be concluded from the foregoing experiments that in open capillary zone electrophoresis with EOF for low-molecular-weight substances, migration times or apparent mobilities can never be used for identification of the components. The effective mobility, however, which can be calculated from the migration time and the EOF velocity, can be used as a parameter for identification. The choice of a "true" EOF marker is extremely important.

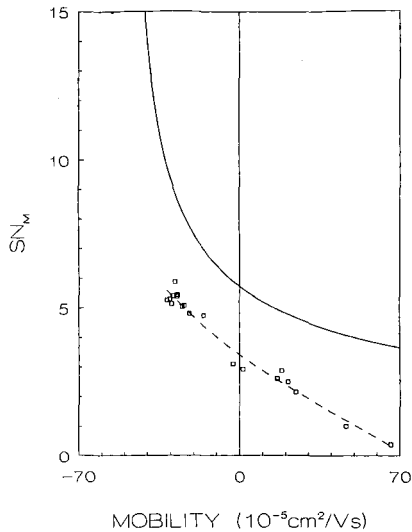


Fig. 12. Relationship between theoretical separation numbers (solid line) and experimentally determined separation numbers (dashed line) and effective mobility. The experimentally determined numbers were calculated from the electropherogram in Fig. 11.

If the ionic strength of the matrix is high compared with that of the background electrolyte, differences in effective mobilities can be expected, although they are reproducible if the matrix is of constant composition. Hence effective mobilities can be used for screening purposes.

From effective mobilities, measured in two different electrolyte systems at pH values where the degrees of dissociation of a component differ sufficiently, the absolute mobility and  $pK$  value can be calculated. The separation number, indicating how many components can be separated within a unit of mobility, is, however, much smaller than the theoretical values.

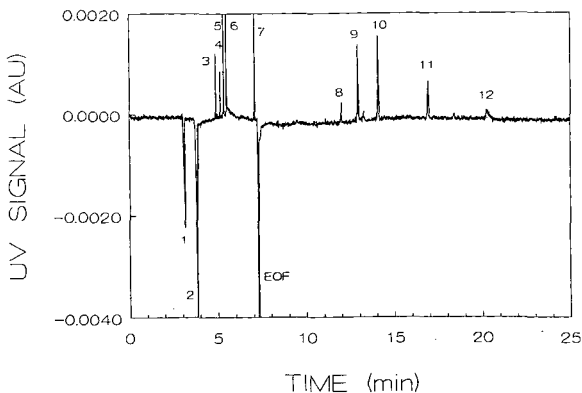


Fig. 13. Electropherogram of 10-fold diluted human urine, spiked with levamisol, procaine, clenbuterol and fenoterol ( $0.0001 M$ ) in a HIST-MES background electrolyte at pH 6.2. See Table X for the composition of the sample. Capillary from Siemens, I.D.  $50 \mu m$ ,  $L_c = 77.33$  cm and  $L_d = 70.53$  cm. Pressure injection time, 1 s.

## ACKNOWLEDGEMENTS

The authors express their gratitude to the State Institute for Quality Control of Agricultural Products (RIKILT, The Netherlands) for financial support of this investigation and gifts of several chemicals.

## REFERENCES

- 1 T. Hirokawa and Y. Kiso, *J. Chromatogr.*, 252 (1982) 33.
- 2 T. Hirokawa, M. Nishino and Y. Kiso, *J. Chromatogr.*, 252 (1982) 49.
- 3 T. Hirokawa, M. Nishino, N. Aoki, Y. Kiso, I. Sawamoto, T. Yagi and J.-I. Akiyama, *J. Chromatogr.*, 271 (1983) D1-D106.
- 4 J. Pospichal, M. Deml, Z. Zemlova and P. Bocek, *J. Chromatogr.*, 320 (1985) 139.
- 5 J. Pospichal, M. Deml and P. Bocek, *J. Chromatogr.*, 390 (1987) 17.
- 6 I. Hoffmann, R. Muenze, I. Dreyer and R. Dreyer, *J. Radioanal. Chem.*, 74 (1982) 53.
- 7 J. L. Beckers, *J. Chromatogr.*, 320 (1985) 147.
- 8 T. Hirokawa, T. Tsuyoshi and Y. Kiso, *J. Chromatogr.*, 408 (1987) 27.
- 9 P. Bocek, P. Gebauer and M. Deml, *J. Chromatogr.*, 217 (1981) 209.
- 10 P. Bocek, P. Gebauer and M. Deml, *J. Chromatogr.*, 219 (1981) 21.
- 11 H. Falkenhagen, *Elektrolyte*, Hirzel, Leipzig, 1932.
- 12 C. F. Poole and S. A. Schuette, *Contemporary Practice of Chromatography*, Elsevier, Amsterdam, 1984.
- 13 V. P. Burolla, S. L. Pentoney and R. Zare, *Am. Biotechnol. Lab.*, 7, No. 10 (1989) 20.
- 14 Th. P. E. M. Verheggen, J. L. Beckers and F. M. Everaerts, *J. Chromatogr.*, 452 (1988) 615.
- 15 J. L. Beckers and F. M. Everaerts, *J. Chromatogr.*, 508 (1990) 3.
- 16 J. L. Beckers and F. M. Everaerts, *J. Chromatogr.*, 508 (1990) 19.
- 17 J. L. Beckers and F. M. Everaerts, *J. Chromatogr.*, 470 (1989) 277.
- 18 A. C. Schoots, Th. P. E. M. Verheggen, P. M. J. M. de Vries and F. M. Everaerts, *Clin. Chem.*, 36 (1990) 435.



## Isotachopheresis with electroosmotic flow: open *versus* closed systems

J. L. BECKERS\*, F. M. EVERAERTS and M. T. ACKERMANS

*Laboratory of Instrumental Analysis, Eindhoven University of Technology, P.O. Box 513, 5600 MB Eindhoven (The Netherlands)*

(First received June 7th, 1990; revised manuscript received August 8th, 1990)

---

### ABSTRACT

If isotachopheretic (ITP) experiments are carried out in open systems, an electroosmotic flow (EOF) will act on the ITP system. In ITP experiments with EOF in open systems four modes can be distinguished, *viz.*, anionic, cationic, reversed anionic and reversed cationic modes. The applicability of these modes depends strongly on the velocity of the EOF. Examples of separations are given showing some typical features of these modes. Detailed consideration of a mathematical model for ITP with EOF showed that this model is identical with that of ITP without EOF.

---

### INTRODUCTION

Generally, electrophoretic equipment consists of five modules, *viz.*, (1) an anode and (2) a cathode compartment, connected to each other by (3) a separation unit, (4) a high-voltage supply and (5) a detector.

Such equipment can be used for all electrophoretic modes, *viz.*, for isotachopheresis (ITP), zone electrophoresis (ZE), moving boundary (MB) and isoelectric focusing (IEF). The choice of the electrolytes in the separation unit and electrode compartments determines which electrophoretic mode operates. For example, for the ZE mode the whole equipment will generally be filled with the same background electrolyte, whereas for ITP a leading and terminating electrolyte will be used.

So far, ITP has been carried out in laboratory-made or commercial apparatus with closed systems, *i.e.*, no electroosmotic flow (EOF) occurs. At present, commercial apparatus for CZE is available generally with open capillaries. Because this equipment must be suitable for ITP it is of interest to check the possibilities for ITP in open systems, especially with regard to reproducibility and qualitative and quantitative aspects.

In this paper, a mathematical model for ITP with EOF in open systems is given, the different ITP modes are considered and some typical isotachopherograms are discussed.

## THEORETICAL

If ITP experiments are performed in open capillaries, an EOF will act on the ITP system and four different modes can be distinguished. In Fig. 1a, the situation is given for the cationic ITP mode (CM). In this instance the capillary will be filled with the leading electrolyte L, while the terminator solution T will be present on the inlet side of the apparatus. The sample solution S will be introduced between L and T. The detector is placed at the outlet side. The EOF will generally act (using silica capillaries) in the direction from inlet to outlet through which the cationic ITP system will be pushed forwards with an extra velocity of the EOF compared with cationic ITP experiments in closed systems.

In Fig. 1b the situation is given for the anionic ITP mode (AM). Here the cathode must be placed at the inlet side and the anode at the outlet. The capillary will be filled with the leading electrolyte L and the terminator T must be present at the inlet. This procedure can be compared with ITP with a counterflow [1] and is only useful if the velocity of the leading ions is greater than that of the EOF during the whole experiment. Remember that in this instance anionic species with mobilities lower than that of the EOF must also migrate to the anode according to the isotachophoretic condition.

If the velocity of the EOF is greater than that of the anionic ITP system, there is a net migration in the direction of the cathode. The only way to carry out the

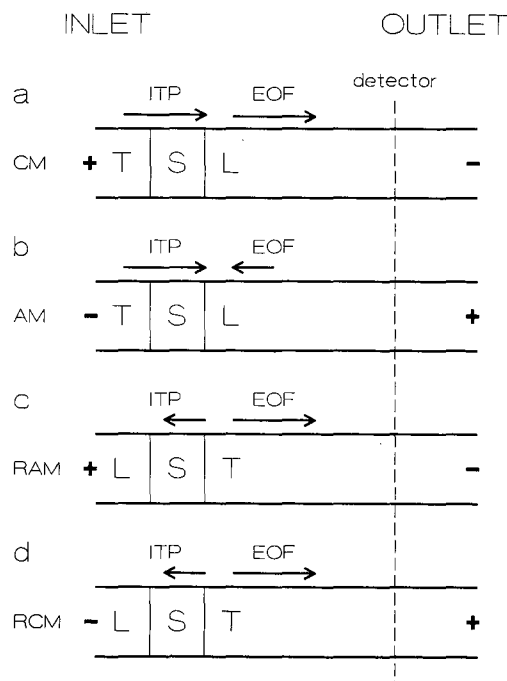


Fig. 1. Schematic representation of the four modes in ITP experiments with EOF. (a) CM represents the cationic, (b) AM the anionic, (c) RAM the reversed anionic and (d) RCM the reversed cationic mode. For further explanation, see text.

experiments is to place the anode at the inlet side and the cathode at the outlet side (see Fig. 1c). The capillary must be filled with the terminating electrolyte T and the leading electrolyte L must be present at the inlet. Although the ITP separation takes place in the direction of the anode, there will be a net velocity of the ITP system in the direction of the outlet (detector side) and the components will be detected in a reversed order compared with a normal anionic ITP system, *viz.*, first the terminator, then all sample components with increasing mobilities and finally the leading ions. We shall call this the reversed anionic ITP mode (RAM). If the velocity of the leading ions is greater than that of the EOF, the ITP system will move to the anode and the components cannot be detected at the outlet.

Analogously to the RAM, we can consider the reversed cationic mode (RCM), which can be applied if there is a reversed EOF (*e.g.*, using coated capillaries and/or additives to the electrolyte system) from the cathode to the anode, with a velocity greater than that of the cationic ITP system (see Fig. 1d). Here the cathode must be placed at the inlet and the anode at the outlet. The capillary must be filled with the terminator solution and the inlet vessel with the leading electrolyte. As in the RAM, the components will be detected in the reverse order. We shall not consider the RCM as this mode will generally not be useful in practice.

It will be clear that the velocity of the EOF is extremely important in the migration behaviour of ITP systems. A complicating factor is, moreover, the fact that in ITP experiments the velocity of the EOF will continuously change. At the beginning of the experiments the EOF will be determined by the composition of the electrolyte in the capillary, *i.e.*, the leading electrolyte for a normal ITP system. During the analysis the capillary will be filled more and more with terminator solution, with a concentration and pH different from those of the leading electrolyte and hence with a different zeta potential and with an  $E$  gradient much larger than that of the leading electrolyte according to the isotachophoretic condition. Generally, this will lead to a higher velocity of the EOF.

For non-compressible solutions it can be assumed, however, that at a certain time the velocity over the whole capillary will be constant, and thus the EOF displacement in a time span will be constant over the whole capillary. This is used in the mathematical model for ITP with EOF.

#### *The isotachophoretic model*

For the calculation of parameters of the different zones in ITP with EOF, we modified an ITP model, already published elsewhere [2,3].

In this model the reduced number of parameters is always four in all zones, *viz.*,  $[L]_i$  or  $[A]_i$ ,  $[B]_i$ ,  $E$  and pH. For all zones always four known parameters and/or equations are necessary, by means of which all parameters can be calculated. For the leading zone the known parameters are generally  $[L]_i$  and  $[B]_i$  and the equations are Ohm's law and the electroneutrality (EN). For all other zones the four available equations are the EN, Ohm's law, the buffer equation and the isotachophoretic condition (IC).

Tiselius [4] pointed out that a substance that consists of several forms with different mobilities in equilibrium with each other will generally migrate as a uniform substance with an effective mobility given by

$$\bar{m} = \frac{\sum_{i=1}^n m_{z-i} \frac{\prod_{j=1}^i K_j}{[\text{H}_3\text{O}^+]^i} + m_z}{1 + \sum_{i=1}^n \frac{\prod_{j=1}^i K_j}{[\text{H}_3\text{O}^+]^i}} \quad (1)$$

For simplicity, the effect of the ionic strength is not considered in this equation. In the computer programs, however, this effect is corrected for using the Debye–Hückel–Onsager relationship.

Although in the general descriptions of equilibria and effective mobility of a substance, no differences exist between the leading, sample, terminating and buffer ionic species, we shall distinguish between them using the symbols L, A, T and B. For the description of the “steady state” in ITP with EOF, we further need the mass balance of the buffer, the principle of electroneutrality, the modified Ohm’s law and the isotachophoretic condition.

*Mass balance of the buffer*

With the mass balance of the buffer (Ohm’s law and the EN must also be obeyed), the leading zone determines the conditions of the proceeding zones. The mass balance of the buffer can be derived as follows for a cationic ITP system (see Fig. 2a).

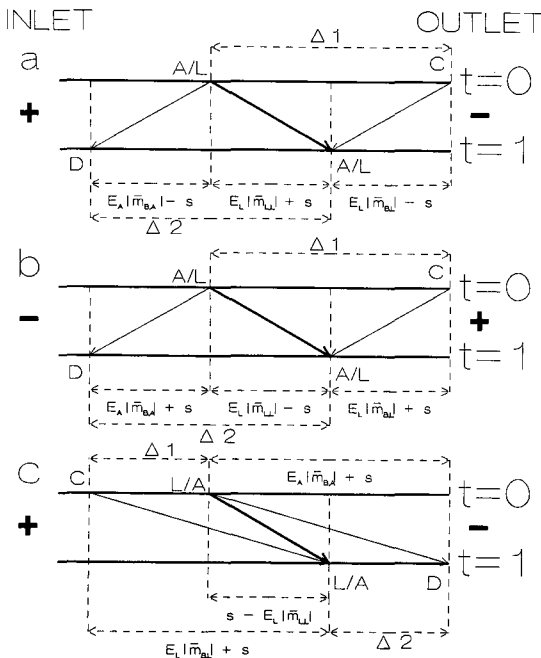


Fig. 2. Migration paths of the buffering counter ionic species over a zone boundary between a leading zone and a sample zone (L/A), for the (a) cationic, (b) anionic and (c) reversed anionic modes. For further explanation, see text.

The zone boundary L/A moves in a unit of time over a distance of  $E_L|\bar{m}_{L,L}| + s$  or  $E_A|\bar{m}_{A,A}| + s$ , assuming that the contribution of displacement by the EOF is  $s$  at a certain moment. For cationic species the displacement is increased with  $s$ , whereas for anions, moving in the opposite direction, the net displacement will be decreased with  $s$ . The anionic buffering counter ions at time  $t = 0$  present at the zone boundary L/A will reach point D at  $t = 1$ . The distance from L/A to D then will be  $E_A|\bar{m}_{B,A}| - s$ . The buffer ionic species at  $t = 0$  present in point C, will just reach the boundary L/A at  $t = 1$ . The distance from C to L/A is then  $E_L|\bar{m}_{B,L}| - s$ .

This means that all buffer ionic particles present in the leading zone between L/A and C with a concentration of  $[B]_{t,L}$  at time  $t = 0$  ( $\Delta 1$ ) will be present in the zone A with a concentration of  $[B]_{t,A}$  between L/A and D at  $t = 1$  ( $\Delta 2$ ). Therefore, the buffer mass balance will be as follows:

$$[B]_{t,A}(E_A|\bar{m}_{B,A}| - s + E_L|\bar{m}_{L,L}| + s) = [B]_{t,L}(E_L|\bar{m}_{B,L}| - s + E_L|\bar{m}_{L,L}| + s) \quad (2)$$

or

$$[B]_{t,A}(E_A|\bar{m}_{B,A}|/E_L + |\bar{m}_{L,L}|) = [B]_{t,L}(|\bar{m}_{B,L}| + |\bar{m}_{L,L}|) \quad (2a)$$

or

$$[B]_{t,A}(|\bar{m}_{L,L}||\bar{m}_{B,A}|/\bar{m}_{A,A}| + |\bar{m}_{L,L}|) = [B]_{t,L}(|\bar{m}_{B,L}| + |\bar{m}_{L,L}|) \quad (2b)^a$$

or

$$[B]_{t,A}(|\bar{m}_{B,A}|/\bar{m}_{A,A}| + 1) = [B]_{t,L}(|\bar{m}_{B,L}|/|\bar{m}_{L,L}| + 1) \quad (2c)$$

The buffer balance in ITP with EOF is identical with that in closed systems, because the contributions of the EOF for anions and cations cancel each other. Following this procedure for anionic separations with an ITP velocity greater than that of the EOF (see Fig. 2b) and for a reversed anionic ITP system (see Fig. 2c), the same equation is always obtained.

### *The principle of electroneutrality*

In accordance with the principle of electroneutrality (EN), the arithmetic sum of all products of the concentration of all forms for all ionic species and the corresponding valences, present in each zone, must be zero. For the electroneutrality of a zone we can write

$$[H_3O^+] - [OH^-] + \sum_{i=0}^{n_A} (z - i)[A^{z-i}] + \sum_{i=0}^{n_B} (z - i)[B^{z-i}] = 0 \quad (3)$$

### *Modified Ohm's law*

Working at a constant current density:

$$E_L\sigma_L = E_A\sigma_A \quad (4)$$

<sup>a</sup> After applying the isotachophoretic condition (see eqn. 7).

or the function

$$RFQ = E_L \sigma_L / E_A \sigma_A - 1 \quad (5)$$

must be zero.

The overall electric conductivity,  $\sigma$ , of a zone is the sum of the values  $c(E\bar{m} + s)zF/E$  and consequently for a cationic separation

$$[\text{H}_3\text{O}^+](E\bar{m}_\text{H} + s) - [\text{OH}^-](E\bar{m}_\text{OH} + s) + \sum_{i=0}^{n_A} [\text{A}^{z-i}][E\bar{m}_{z-i}(z-i) + s(z-i)] + \sum_{i=0}^{n_B} [\text{B}_{z-i}][E\bar{m}_{z-i}(z-i) + s(z-i)] \quad (6)$$

in all zones is constant, under the condition that mobilities for negative ions are indicated with a negative sign.

Elaboration shows that for all cases the effects of the displacement of the EOF cancel each other. The consequence of this is that for electrolyte systems with an equal zone conductance, equal electric currents must be measured on applying the same electric field gradient, for different velocities of the EOF. To check this, the electric current and  $m_{\text{EOF}}$  were measured by applying 25 kV, filling the capillary with solutions of nearly equal conductivity at different pH. For the latter we mixed 99 ml of a solution of 0.010 M sodium chloroacetate with 1 ml of a buffer (ionic strength also 0.01) and measured the pH of the mixture. The results are given in Table I.

Although the  $m_{\text{EOF}}$  varies from about  $25 \cdot 10^{-5}$  to  $70 \cdot 10^{-5}$   $\text{cm}^2/\text{V} \cdot \text{s}$ , the measured electric current is nearly constant, indicating that the conductivity of a zone is independent of the EOF.

#### Isotachophoretic condition

In the steady state all zones move with a velocity equal to that of the leading zone, therefore:

$$E_L \bar{m}_{\text{L,L}} + s = E_A \bar{m}_{\text{A,A}} + s \quad (7)$$

TABLE I

MEASURED ELECTRIC CURRENT  $I$ ,  $t_{\text{EOF}}$  AND  $m_{\text{EOF}}$  FOR SEVERAL ELECTROLYTE SYSTEMS WITH EQUAL CONDUCTIVITY AT DIFFERENT pH APPLYING 25 kV

Pressure injection 5 s of the EOF marker 0.001 M mesityl oxide; UV detection at 254 nm.

Buffer solution	pH of the mixed solution	Measured $I$ ( $\mu\text{A}$ )	$t_{\text{EOF}}$ (min)	$m_{\text{EOF}} \times 10^5$ ( $\text{cm}^2/\text{V} \cdot \text{s}$ )
0.01 M HCl + EAC	4.70	18.7	7.26	26.17
0.01 M HCl + EAC	5.25	18.7	5.74	33.10
0.01 M HCl + HIST	6.05	18.8	4.72	40.25
0.01 M HCl + IMID	6.89	18.8	3.74	50.80
0.01 M HCl + TRIS	7.81	18.8	3.06	62.09
0.01 M HCl + DEA	8.80	18.7	2.69	70.63

The contributions in the displacement by the EOF cancel each other.

### *Calculation procedure*

As the effect of the displacement of the EOF is cancelled in all equations, the mathematical model of ITP without EOF can also be used for ITP with EOF. The calculation procedure is described completely in refs. 2 and 3.

## EXPERIMENTAL

For all CZE experiments the Beckman (Palo Alto, CA, U.S.A.) P/ACE™ System 2000 HPCE was used. All experiments were carried out at 25°C. An original Beckman capillary was used in all experiments. The capillary length was 57 cm and the distance between injection and the detector was 50 cm; I.D. was 75  $\mu\text{m}$ .

## RESULTS AND DISCUSSION

### *Electroosmotic flow in ITP in open systems*

The most important parameter that determines whether an ITP system can migrate in the desired mode is the velocity of the EOF,  $v_{\text{EOF}}$ .

In ITP experiments, the EOF will be determined in the first instance by the electrolyte solution in the capillary, generally the leading electrolyte. Later, the capillary will be filled more and more with terminator solution. Because in ITP experiments the concentration of this terminator zone is lower than that of the leading electrolyte and there is a higher  $E$  gradient, this will lead to a higher  $v_{\text{EOF}}$ .

The  $v_{\text{EOF}}$  can be measured by weighing the mass of buffer transferred from the anode to cathode (or *vice versa*) over a time period using a Mettler Model AE160 digital balance [5,6] or placing a UV-absorbing species in the high-voltage reservoir and monitoring the UV absorption of the earth reservoir [7].

To obtain a qualitative impression of the  $v_{\text{EOF}}$  we used two different approaches. One was to inject alternately leading electrolyte and a mixture of a UV-absorbing EOF marker and leading electrolyte until the whole capillary was filled. Monitoring the absorbance of the equidistant EOF marker bands in the leading electrolyte during the electrophoretic experiments gives an idea of changes in the EOF velocity. The other method was to record the voltage drop over the capillary tube at a constant electric current. For a constant EOF, the relationship between voltage drop and time should be linear.

As an example to demonstrate the changes in the  $v_{\text{EOF}}$  during ITP experiments, we shall consider the separation of a cationic leading and terminating electrolyte system. For ITP in closed systems for the cationic mode we can detect the leading zone L and the terminating zone T', adapted to the conditions of the leading zone. The concentration boundary between the original terminator solution T and the adapted terminating zone T' does not move in ITP without EOF and will not be detected (see Fig. 3a). For ITP in open systems an extra velocity of the EOF will act on the system, independent of the electrophoretic movement. This means that the concentration boundary between the original terminator solution T and the adapted T' zone will migrate into the capillary. If this original solution is a dilute solution of acetic acid with a high  $E$  gradient and a large contribution to the EOF, the EOF increases rapidly until

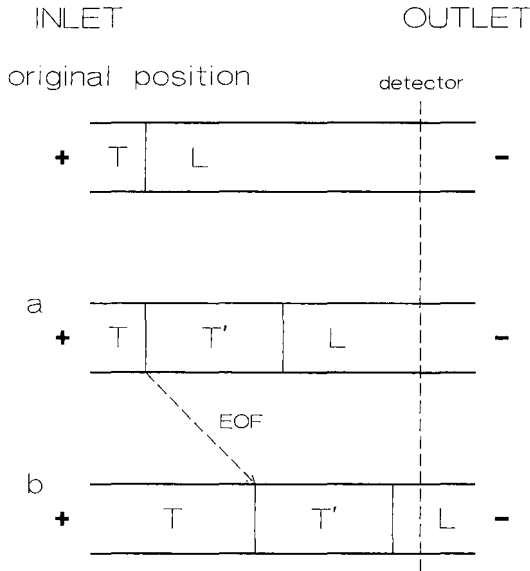


Fig. 3. Original position of leading and terminating electrolytes for the cationic mode for ITP. The zones formed during the experiment are shown for ITP (a) without and (b) with EOF. Note that the concentration boundary T/T' does not move without EOF, but will pass the detector by the velocity of the EOF.

the capillary is completely filled with the original terminator solution T.

The isotachopherogram for this separation is given in Fig. 4. The capillary was alternately filled with the leading electrolyte, 0.01 *M* potassium hydroxide solution at pH 5, adjusted by adding acetic acid (pressure injection 22 s) and leading electrolyte mixed with 0.002 *M* mesityl oxide (pressure injection 3 s). The terminating solution was

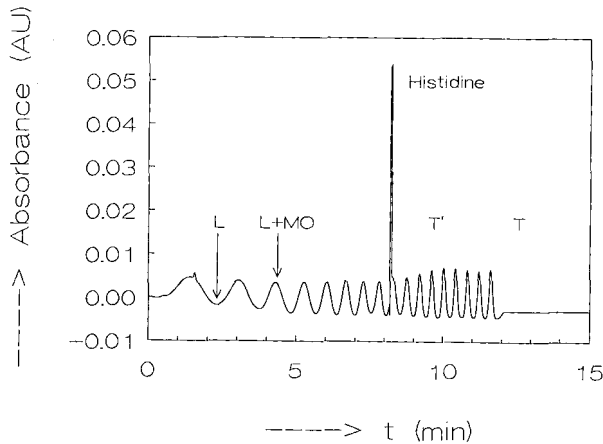


Fig. 4. Isotachopherogram for the cationic mode with a leading electrolyte L of potassium acetate at pH<sub>L</sub> 5 and a terminator T of acetic acid at pH 3.5. The leading electrolyte was alternately mixed up with 0.002 *M* mesityl oxide (L + MO bands). The sample zone histidine indicates the transition between leading L and adapted terminating zone T'. UV detection at 254 nm. Electric current, 4  $\mu$ A.



acetic acid at pH 3.5. The sample histidine was added to mark the transition between the leading and adapted terminating zones. Note that the time intervals between the MO peaks are decreasing, indicating that the  $v_{\text{EOF}}$  increases strongly during the experiment. In Fig. 5 the calculated  $v_{\text{EOF}}$  as a function of time is given. From the number of MO peaks over the separation length from the inlet to the detector, the distance between the equidistant peaks can be calculated and using the differences in time between the adjacent peaks the velocity at that time can be calculated.

It can be concluded that the EOF varies considerably during ITP experiments if no special precautions are taken to prevent the EOF.

### Cationic mode

As an example of the cationic mode, Fig. 6 shows the isotachopherogram for the separation of sodium and lithium in a system with the leading electrolyte 0.01 *M* potassium hydroxide solution at pH<sub>L</sub> 5, adjusted by adding nicotinic acid. The terminator was 0.01 *M* histidine at pH 5.5, adjusted by adding nicotinic acid. Using a UV-absorbing counter ion, nicotinic acid, the different zones show different UV absorbances because the concentrations in the sample zones are different. The leading zone L, the sample zones of (1) sodium and (2) lithium, the (T') adapted terminating zone of histidine and (T) the original histidine solution can be clearly seen. The UV dip (3) indicates the original sampling spot and determines the concentration boundary.

Cationic ITP experiments can easily be carried out, although the separation power is diminished compared with ITP in closed systems.

### Reversed anionic mode

The requirement in order to obtain a RAM is that  $E_{\text{T}}|m_{\text{EOF,T}}| > E_{\text{T}}|\bar{m}_{\text{T}}|$ . In that case the net migration velocity will be  $E_{\text{T}}|m_{\text{EOF,T}}| - E_{\text{T}}|\bar{m}_{\text{T}}|$ , in the first instance. Finally, the net velocity will be  $E_{\text{L}}|m_{\text{EOF,L}}| - E_{\text{L}}|\bar{m}_{\text{L}}|$  and if this net velocity is greater

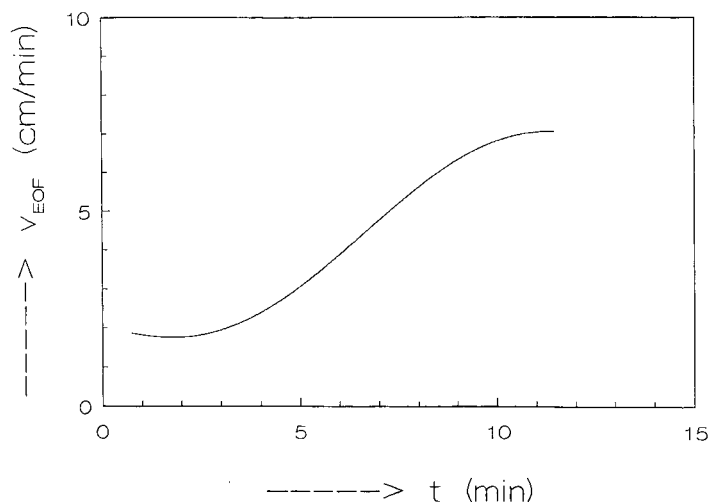


Fig. 5. Calculated  $v_{\text{EOF}}$  as a function of time for the experiment as described in Fig. 4. For further explanation, see text.

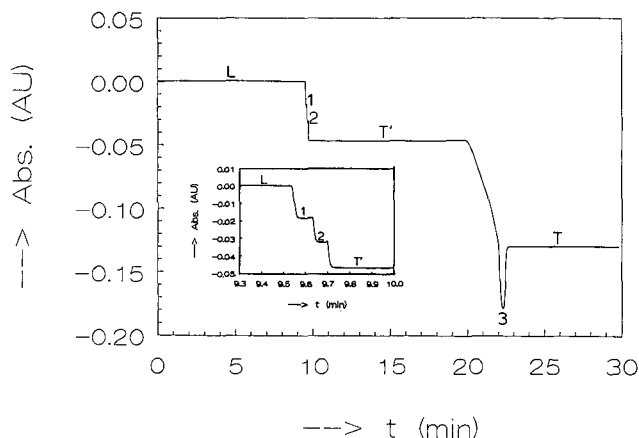


Fig. 6. Isotachopherogram for the separation of (1) sodium and (2) lithium (pressure injection 5 s; concentrations of the sample ions 0.005 *M*) using a leading electrolyte L of potassium nicotinate at pH 5 and terminator histidine nicotinate at pH 5.5. Position (3) indicates the concentration boundary between (T') adapted and (T) original terminator solution, which moves under the influence of the EOF. Electric current, 4  $\mu$ A. UV detection at 254 nm. The sample zones can be clearly seen in the enlarged inset.

than zero this mode can be used for separations. As an example of the reversed anionic mode, in Fig. 7 the isotachopherogram is given using as the leading electrolyte 0.0025 *M* acetic acid at pH<sub>L</sub> 6.4, adjusted by adding histidine, and the terminator 0.0025 *M* MES at pH 6, adjusted by adding histidine. As the sample we introduced a solution of 0.0025 *M* sodium propanoate (pressure injection 10 s). Fig. 8 shows the original position and (a) the zones formed after some time in a closed system and (b) the situation expected in open systems. The zones will further be detected in the reverse order. This situation can be recognized in Fig. 7, where the order of detection is the sodium dip of the sample solution in the original T zone, the transported concentration

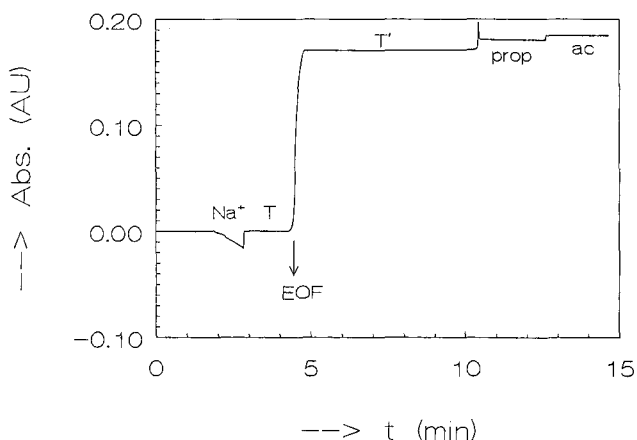


Fig. 7. Isotachopherogram for separation in the reversed anionic mode. Leading electrolyte, 0.0025 *M* histidine acetate at pH 6.4. Terminator, MES at pH 6, adjusted by adding histidine. Pressure injection 10 s of 0.0025 *M* sodium propanoate. Electric current, 4  $\mu$ A. UV detection at 214 nm.

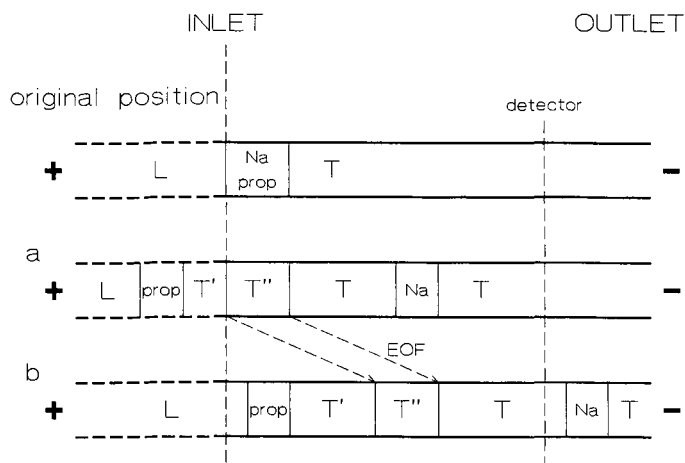


Fig. 8. Original position of the different electrolytes for the reversed anionic mode for ITP. The zones formed during the experiment are shown for ITP (a) without and (b) with EOF. Note that the separation proceeds in the direction of the anode. Without EOF the concentration boundaries T'/T'' and T''/T can never be detected, but as a result of the EOF they can reach the detector.

boundary between original terminator solution and adapted T' zone (this transition can be marked with an EOF marker) and finally the propanoate zone and leading acetate zone. In practice, the T'' zone, adapted to the original sample solution, will generally be short and masked by, *e.g.*, the UV water dip or EOF marker.

#### Anionic mode

The greatest problems arise in finding a good ITP system for the anionic mode. In most instances the voltage drop increased until a certain value far below that expected theoretically, indicating that the ITP system moved in the anionic mode but after a certain moment no longer moved. At a pH of 4 (low  $v_{\text{EOF}}$ ) a migrating anionic mode could be carried out, using as the terminating ion formate with a high mobility. How can this be explained?

In Table II the calculated pH,  $SZR_{25}$  and concentrations are given for MES as terminator using the leading electrolyte 0.01 M HCl at pH<sub>L</sub> 6 adjusted by adding

TABLE II

CALCULATED pH AND  $SZR_{25}$  AND CONCENTRATIONS FOR SOME TERMINATING ZONES IN ELECTROLYTE SYSTEMS AT pH<sub>L</sub> 6 AND 4 AND MEASURED  $m_{\text{EOF}}$  AND VOLTAGE DROP AT 15  $\mu\text{A}$  FOR THESE SOLUTIONS

Electrolyte	pH	$SZR_{25}$ ( $\Omega$ m)	$m_{\text{EOF}} \times 10^5$ ( $\text{cm}^2/\text{V} \cdot \text{s}$ )	Voltage drop at 15 $\mu\text{A}$ (kV)
0.01 M HCl + histidine	6.00	10.33	39.6	17.86
0.00654 M MES	6.43	42.99	50.94	73.53
0.025 M HCl + EAC	4.00	4.33	18.54	7.75
0.0225 M formate	4.29	7.62	24.4	12.6
0.0200 M acetate	4.69	16.47	35.85	25.33

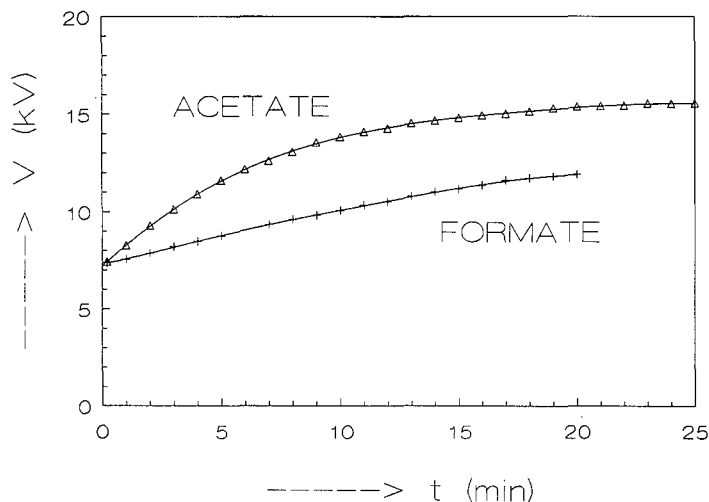


Fig. 9. Measured voltage drop as a function of time during ITP experiments with EOF in the anionic mode using a leading of 0.025 *M* HCl at pH<sub>L</sub> 4, adjusted by adding EAC and terminator solutions of 0.01 *M* sodium formate and 0.01 *M* sodium acetate. Electric current 15  $\mu$ A.

histidine and for formate and acetate zones for the leading electrolyte 0.025 *M* HCl at pH<sub>L</sub> 4 adjusted by adding EAC. All these solutions were carefully prepared and the  $m_{\text{EOF}}$  and voltage drop for these solutions were measured and recalculated to an electric current of 15  $\mu$ A. The results are given in Table II.

In Fig. 9 the measured voltage drop as a function of time is given for acetate and formate as terminating solution in the system 0.025 *M* HCl–EAC at pH<sub>L</sub> 4. It can be seen that for formate the expected voltage drop of 12.6 kV is fairly reached and we could see the formate step in the isotachopherogram. For acetate the expected voltage drop of about 25.33 kV was not reached, but the voltage drop stopped at about 15 kV, which means that the ITP system came to a standstill.

The explanation is as follows. In first instance the net velocity of the ITP system is determined by  $E_L|\bar{m}_L| - E_L|m_{\text{EOF,L}}|$ . Finally, the net velocity is  $E_T|\bar{m}_T| - E_T|m_{\text{EOF,T}}|$ . According to the ITP condition,  $E_L\bar{m}_L = E_T\bar{m}_T$ . Generally  $E_T|m_{\text{EOF,T}}|$  will be much larger than  $E_L|m_{\text{EOF,L}}|$  because of the higher *E* gradient and generally larger  $m_{\text{EOF}}$  (see Table II). This means that the net velocity of the ITP system will become zero during the experiment and the system will not migrate from that time.

## CONCLUSIONS

The mathematical model for ITP without EOF (closed systems) is also valid for ITP with EOF (open systems). Four modes can be distinguished for ITP with EOF. The cationic mode can be applied without problems, although the available separation length is not used optimally, compared with closed systems, owing to the extra velocity of the EOF. Some precautions must be taken in the choice of the terminator to avoid strong fluctuations in the net migration velocity of the ITP system. The reversed cationic mode is of almost no value and can only be applied using additives or coated

capillaries in order to obtain a strong reversed EOF. The reversed anionic mode can be used at high pH (with a high  $v_{\text{EOF}}$ ) and with the “counter current” of the EOF this mode can be of interest in some instances. The anionic mode is only of interest if the  $v_{\text{EOF}}$  is low, such as in the use of non-aqueous solvents. Otherwise, problems can be expected concerning the choice of the terminator solution. Too high  $E$  gradients in the terminator solution can lead to a standstill of the ITP system during the experiments.

A first comparison between ITP in open and closed systems shows that ITP in closed systems is preferable, because no special precautions have to be taken in the choice of the electrolyte systems concerning the EOF. Unless the EOF can be strongly reduced, problems can be expected when applying ITP in open systems. The presence of an EOF, however, facilitates the use of “hyphenated” techniques, making the use of a “make-up” stream superfluous.

Experiments are currently being carried out on quantitative aspects of ITP with EOF.

#### SYMBOLS AND ABBREVIATIONS

A	sample ionic species A
B	buffering counter ionic species B
$E$	electric field strength (V/m)
$F$	Faraday constant (C/equiv.)
$K$	concentration equilibrium constant
L	leading ionic species L
$m$	mobility at infinite dilution ( $\text{m}^2/\text{V} \cdot \text{s}$ )
$\bar{m}$	effective mobility ( $\text{m}^2/\text{V} \cdot \text{s}$ )
$n$	number of protolysis steps
$s$	displacement by the EOF in a unit of time (m/s)
$SZR_{25}$	specific zone resistance at 25°C ( $\Omega \text{ m}$ )
T	terminating ionic species
T', T''	adapted terminating zones
$v_{\text{EOF}}$	velocity of the EOF (m/s)
$z$	charge of an ionic species (equiv./mol)
$\sigma$	zone conductivity ( $\Omega^{-1} \text{ m}^{-1}$ )

#### *First subscript*

A, B, T and L	according to substance A, B, T and L
t	total

#### *Second subscript*

A, B, T and L	in the zone of substance A, B, T and L
---------------	--

#### *Superscript*

$z$	maximum charge of an ionic species
( ) <sup><math>i</math></sup>	to the $i$ th degree

#### *Examples*

$[\text{B}]_{\text{L,A}}$	total concentration of substance B in zone A
$ \bar{m}_{\text{B,A}} $	absolute value of the effective mobility of substance B in the zone of substance

*Abbreviations*

DEA	diethanolamine
EAC	$\epsilon$ -aminocaproic acid
HIST	histidine
IMID	imidazole
MES	2-(N-morpholino)ethanesulphonic acid
MO	mesityl oxide
TRIS	tris(hydroxymethyl)aminomethane

## ACKNOWLEDGEMENT

The authors express their gratitude to the State Institute for Quality Control of Agricultural Products (RIKILT, The Netherlands) for financial support of this investigation.

## REFERENCES

- 1 F. M. Everaerts, J. L. Beckers and Th. P. E. M. Verheggen, *Isotachophoresis, Theory, Instrumentation and Applications*, Elsevier, Amsterdam, 1976.
- 2 J. L. Beckers and F. M. Everaerts, *J. Chromatogr.*, 480 (1989) 69.
- 3 J. L. Beckers and F. M. Everaerts, *J. Chromatogr.*, 508 (1990) 3.
- 4 A. Tiselius, *Nova Acta Reg. Soc. Sci. Ups., Ser. 4*, (1930) 4.
- 5 K. D. Altria and C. F. Simpson, *Chromatographia*, 24 (1987) 527.
- 6 A. A. M. van de Goor, B. J. Wanders and F. M. Everaerts, *J. Chromatogr.*, 470 (1989) 95.
- 7 T. Tsuda, K. Nomura and G. Nagakawa, *J. Chromatogr.*, 385 (1983) 264.

## Note

---

# Post-column oligosaccharide dehydrogenase reactor for coulometric detection of malto-oligosaccharides in a liquid chromatographic system

NOBUTOSHI KIBA\*, KAZUYOSHI SHITARA and MOTOHISA FURUSAWA

*Department of Applied Chemistry and Biotechnology, Faculty of Engineering, Yamanashi University, Kofu 400 (Japan)*

and

YOSHINORI TAKATA

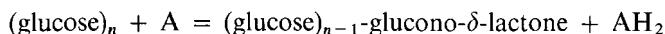
*Naka Works, Hitachi Ltd., Katsuta 312 (Japan)*

(First received May 29th, 1990; revised manuscript received August 2nd, 1990)

Malto-oligosaccharides (MOSs) can be separated successfully on cation- [1–3] and anion-exchange [4] resins and chemically bonded stationary phases with amino [5] or carbamoyl [6] groups. MOSs, which bear a free formyl group, can be detected with high sensitivity and selectivity with the aid of electrochemical detectors [3–5].

An immobilized enzyme reactor is suitable for use in the post-column reaction system because of its high selectivity [7]. By coupling liquid chromatography (LC) with electrochemical detection to the immobilized enzyme reactor, further selectivity can be achieved. An immobilized glucoamylase reactor has been used in a post-column reaction system for the determination of MOSs with pulsed amperometric detection [8].

Oligosaccharide dehydrogenase (ODH) catalyses the oxidation of the glucose unit of MOSs, producing a glucono-lactone end [9]. The reaction catalysed by the enzyme is [10]



where  $n \geq 1$ , A is a hydrogen acceptor such as phenazine methosulphate, 1-methoxyphenazine methosulphate, 1-acetamidophenazine methosulphate, Meldola blue, phenylindophenol or 2,6-dichlorophenylindophenol and  $\text{AH}_2$  is the reduced form of the acceptor.

This paper describes a post-column immobilized ODH reactor system coupled to anion-exchange chromatography and coulometric detection for the determination of MOSs up to maltoheptaose. The MOSs from the separation column are mixed with 1-methoxyphenazine methosulphate (MPS) solution and oxidized in an immobilized

ODH reactor. MPS is reduced to  $\text{MPSH}_2$  according to the amount of MOSs present in the solution. The  $\text{MPSH}_2$  is monitored by coulometric detection.

## EXPERIMENTAL

### Reagents

D-Glucose ( $G_1$ ), D-maltose ( $G_2$ ), maltotriose ( $G_3$ ), maltotetraose ( $G_4$ ), maltopentaose ( $G_5$ ), maltohexaose ( $G_6$ ) and maltoheptaose ( $G_7$ ) were obtained from Nakalai Tesque (Kyoto, Japan), 1-methoxyphenazine methosulphate (MPS) from Dojindo (Kumamoto, Japan) and oligosaccharide dehydrogenase (ODH, from *Staphylococcus* sp., 130 U/mg protein) from Toyo Jozo (Tokyo, Japan). Poly(vinyl alcohol) beads (9  $\mu\text{m}$ , GS-520) were purchased from Asahi Kasei (Tokyo, Japan). TSK gel SAX (5  $\mu\text{m}$ ) (Tosoh, Tokyo, Japan) was packed into a stainless-steel column (30 cm  $\times$  5.8 mm I.D.). The counter electrode electrolyte was potassium hexacyanoferrate(II)–potassium hexacyanoferrate(III)–potassium nitrate–potassium hydroxide solution with a concentration of 0.1 M of each component.

The mobile phases were 0.2 M sodium acetate–0.1 M sodium hydroxide solution and 0.3 M sodium acetate–0.1 M sodium hydroxide solution. The mobile phases were deaerated. All other reagents were of analytical-reagent grade.

### Immobilization of ODH

The method for the preparation of the aminated poly(vinyl alcohol) beads was similar to that of Matsumoto *et al.* [11]. The beads were packed into a stainless-steel column (5 cm  $\times$  4 mm I.D.) by the slurry-packing method. Glutaraldehyde solution (4.0%) in 0.1 M sodium hydrogencarbonate was pumped through the column for 2 h at 0.3 ml/min and then the column was washed with deaerated water for 30 min at 0.5 ml/min. The enzyme solution [5 mg in 10 ml of 0.05 M phosphate buffer (pH 7.0)] was circulated through the column at 0.3 ml/min for 4 h at room temperature. The enzyme solution was kept at about 4°C throughout the procedure.

### LC system

The liquid chromatographic system is shown in Fig. 1. It consisted of a mobile phase pump (Model 655; Hitachi, Tokyo, Japan), a pulse damper (Model LOD-1; Gasukuro Kogyo, Tokyo, Japan), an injector with a 50- $\mu\text{l}$  loop (Model SVI-5U7;

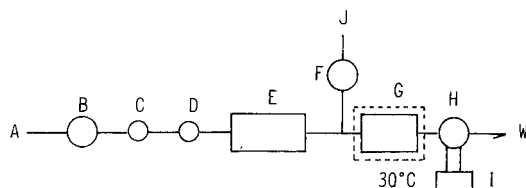


Fig. 1. Flow diagram of liquid chromatographic system for coulometric detection of malto-oligosaccharides with an immobilized enzyme column reactor. A = Mobile phase (0.1 M sodium hydroxide–0.2 M sodium acetate or 0.1 M sodium hydroxide–0.3 M sodium acetate, 0.8 ml/min); B = LC pump; C = damper; D = injector with 50- $\mu\text{l}$  loop; E = analytical column (30 cm  $\times$  5.8 mm I.D., TSK gel SAX, 5  $\mu\text{m}$ ); F = reagent pump; G = reactor (5 cm  $\times$  4 mm I.D.); H = coulometric monitor; I = data processor; J = reagent solution (25 mM MPS in 0.5 M acetic acid, 0.2 ml/min); W = waste.



Sanuki Kogyo, Tokyo, Japan), a separation column containing TSK gel SAX ( $5\ \mu\text{m}$ ) ( $30\ \text{cm} \times 5.8\ \text{mm I.D.}$ ), a double plunger reagent pump (Model DMX-2200; Sanuki Kogyo), the column reactor ( $5\ \text{cm} \times 4\ \text{mm I.D.}$ ) packed with the immobilized enzyme, a coulometric monitor (Model 655A-26; Hitachi) and a data processor (Chromatocorder II; System Instruments, Tokyo, Japan). The column reactor was kept at  $30^\circ\text{C}$ .

The mobile phase and deaerated reagent solution consisting of  $0.5\ \text{M}$  acetic acid containing  $25\ \text{mM}$  MPS were pumped at  $0.8$  and  $0.2\ \text{ml/min}$ , respectively, and mixed before the column reactor. Enzymatic reaction proceeded in the reactor and the  $\text{MPSH}_2$  produced was monitored coulometrically at an electrolytic potential of  $0.6\ \text{V vs. Fe(CN)}_6^{3-}/\text{Fe(CN)}_6^{4-}$ . At the electrolytic potential, the electrolytic efficiency for  $\text{MPSH}_2$  reached 100% and the background current was moderately small ( $0.5\ \mu\text{A}$ ).

## RESULTS AND DISCUSSION

### *Properties of immobilized ODH column reactor*

To evaluate the immobilized enzyme reactor,  $\text{G}_5$  was selected as a model substrate and the experiments were carried out in the flow-injection mode by omitting the separation column.

The influence of pH on the enzyme activity was studied over the range 7.0–9.0 using sodium acetate ( $0.3\ \text{M}$ ) and acetic acid. As shown in Fig. 2, the optimum pH was about 8.0. The electrolytic efficiency for  $\text{MPSH}_2$  was 100% in the pH range 7.0–9.0.

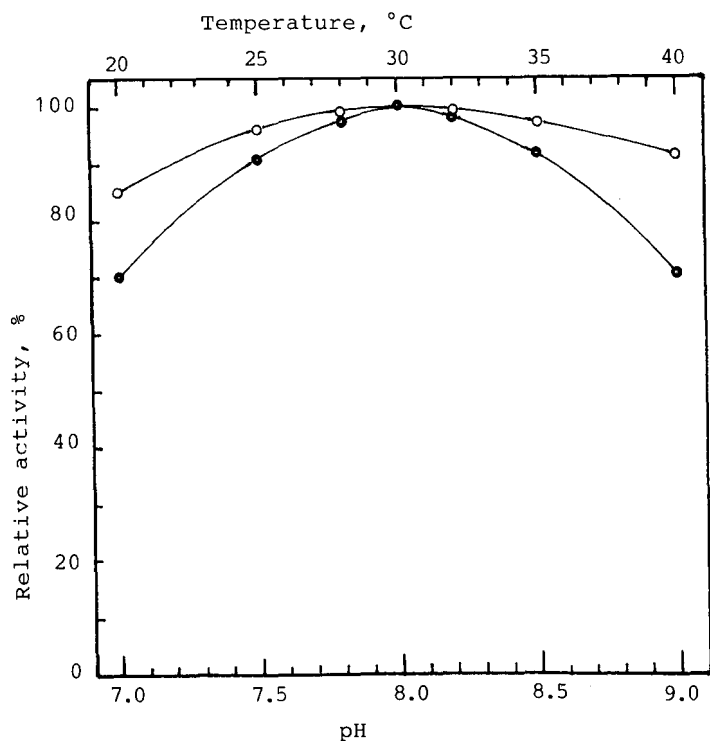


Fig. 2. Effects of (○) pH and (●) temperature on the activity of the immobilized enzyme.

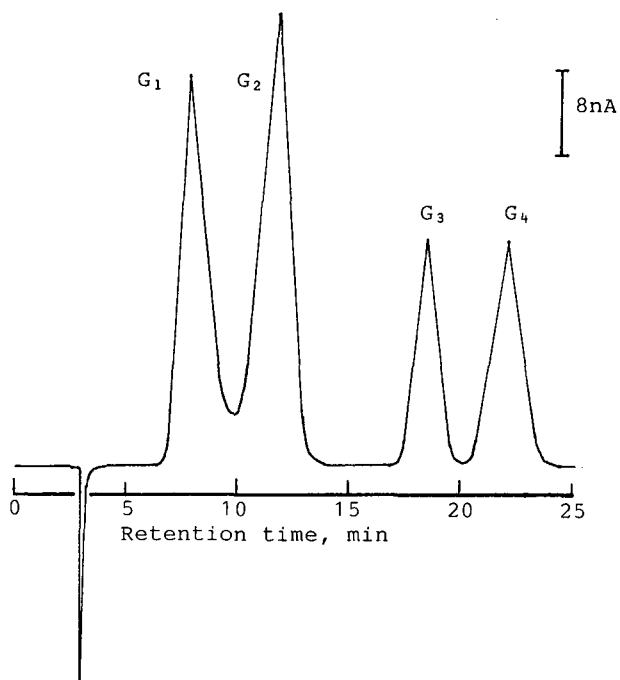


Fig. 3. Chromatogram of a standard mixture of glucose (G<sub>1</sub>), maltose (G<sub>2</sub>), maltotriose (G<sub>3</sub>) and maltotetraose (G<sub>4</sub>) (each 500 pmol). A TSK gel SAX column (30 cm × 5.8 mm I.D.) was used at room temperature with 0.1 M sodium hydroxide–0.2 M sodium acetate as the mobile phase at a flow-rate of 0.8 ml/min.

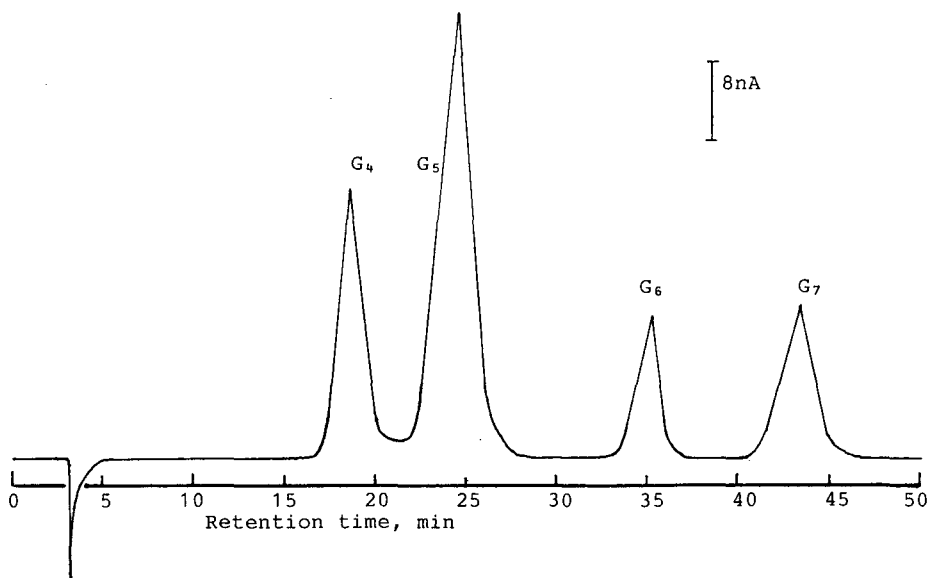


Fig. 4. Chromatogram of a standard mixture of maltotetraose (G<sub>4</sub>), maltopentaose (G<sub>5</sub>), maltohexaose (G<sub>6</sub>) and maltoheptaose (G<sub>7</sub>) (each 500 pmol). Mobile phase, 0.1 M sodium hydroxide–0.3 M sodium acetate at a flow-rate of 0.8 ml/min.

The activity in buffer solutions such as Tris-HCl, tricine-NaOH, bicine-NaOH and phosphate at pH 8.0 was identical with that in sodium acetate-acetic acid. In the buffers containing borate the activity was about one tenth of that in sodium acetate-acetic acid. The activity of the immobilized enzyme at various temperatures was examined. The maximum activity was observed at 30°C, as shown in Fig. 2.

The optimum concentration of MPS was investigated. The response increased linearly with increasing concentration of MPS and became constant at above 5 mM for 1 mM G<sub>5</sub> at a flow-rate of 1.0 ml/min. Considering the stoichiometry between MOSs and MPS (1:1), it will be safe to use five times the level of the MOS concentration. The response decreased linearly as the flow-rate increased from 0.5 to 2.0 ml/min. To confirm the operational stability of the reactor, it was used for 10 h in a day and stored at 4°C in 0.1 M phosphate buffer (pH 7.0) when not in use. The reactor retained more than 80% of its original activity after 1 month. Storage stability was also examined. The enzyme was lyophilized and stored at -20°C in the presence of glycine (0.1 g/g of the immobilized enzyme). The activity was 95% of the initial value after 2 months.

ODH catalyses the oxidation of MOSs, other oligosaccharides and monosaccharides. The substrate specificity toward saccharides was examined. The immobilized enzyme was active towards G<sub>1</sub> (relative activity 100), G<sub>2</sub> (112), G<sub>3</sub> (70), G<sub>4</sub> (71), G<sub>5</sub> (59), G<sub>6</sub> (65), G<sub>7</sub> (53), xylose (39), galactose (93), mannose (34) and lactose (105). With 0.3 M sodium acetate-acetic acid (pH 8.0) and 5 mM MPS at a flow-rate of 1.0 ml/min at 30°C, 1 mM D-glucose (50 μl) was oxidized to a lactone in 24% yield.

#### *Separation of MOSs by LC*

As the immobilized ODH was deactivated in aqueous acetonitrile (30%, v/v) or methanol (3%, v/v) and borate was undesirable for the enzymatic reaction, an anion-exchange column with sodium acetate solution as mobile phase was used in an attempt to separate the MOSs at room temperature. Separation of mixtures of G<sub>1</sub>, G<sub>2</sub>, G<sub>3</sub> and G<sub>4</sub> and of G<sub>4</sub>, G<sub>5</sub>, G<sub>6</sub> and G<sub>7</sub> was effected on a TSK gel SAX column with 0.2 M sodium acetate-0.1 M sodium hydroxide and 0.3 M sodium acetate-0.1 M sodium hydroxide, respectively, as mobile phase as shown in Figs. 3 and 4. An effective separation of individual members from G<sub>1</sub> to G<sub>7</sub> was achieved using gradient elution, accomplished by maintaining the sodium hydroxide concentration at 0.1 M and increasing the sodium acetate concentration from 0.01 to 0.6 M in 20 min. Gradient elution caused serious problems with regard to the operational stability of the immobilized enzyme. The immobilized enzyme was almost completely deactivated after repeating the gradient ten times. The separation parameters for the MOSs are listed in Tables I and II. The flow-rate of the mobile phase was kept constant at 0.8

TABLE I

SEPARATION PARAMETERS FOR GLUCOSE, MALTOSE, MALTOTRIOSE AND MALTO-TETRAOSE

Saccharide	Abbreviation	Capacity factor	Resolution	Separation factor
Glucose	G <sub>1</sub>	1.66		
Maltose	G <sub>2</sub>	3.00	1.36	1.81
Maltotriose	G <sub>3</sub>	5.16	2.47	1.72
Maltotetraose	G <sub>4</sub>	6.38	1.37	1.24

TABLE II

SEPARATION PARAMETERS FOR MALTOTETRAOSE, MALTOPENTAOSE, MALTOHEXA-  
OSE AND MALTOHEPTAOSE

Saccharide	Abbreviation	Capacity factor	Resolution	Separation factor
Maltotetraose	G <sub>4</sub>	4.85	1.62	1.39
Maltopentaose	G <sub>5</sub>	6.72	3.08	1.50
Maltohexaose	G <sub>6</sub>	10.08	2.37	1.26
Maltoheptaose	G <sub>7</sub>	12.67		

ml/min. The flow-rate of the reagent solution influenced the band broadening and the conversion efficiencies. An increase in the flow-rate of the reagent solution from 0.2 to 0.5 ml/min resulted in a decreased response due to a lower residence time in the column reactor and hence in a lower conversion efficiency. At lower flow-rates, from 0.05 to 0.1 ml/min, serious problems arose with respect to reproducibility because of incomplete mixing of the reagent solution with the mobile phase. The flow-rate of the reagent solution was set to 0.2 ml/min. At this flow-rate, the contribution of the post-column reactor system to band broadening was less than 25% of the peak width. Concentrations of 25 mM MPS and 0.5 M acetic acid in the reagent solution were chosen, resulting in an MPS concentration of 5 mM and pH 8 in the column reactor.

The peak areas were plotted against the concentration of the MOSs. Calibration graphs were prepared for G<sub>1</sub>, G<sub>2</sub>, G<sub>3</sub>, G<sub>4</sub>, G<sub>5</sub>, G<sub>6</sub> and G<sub>7</sub>, covering the range 0.01–1 mM. The ratio of peak areas for G<sub>1</sub>, G<sub>2</sub>, G<sub>3</sub>, G<sub>4</sub>, G<sub>5</sub>, G<sub>6</sub> and G<sub>7</sub> was 100:127:50:87:163:40:49. Detection limits (signal-to-noise ratio = 3) for G<sub>1</sub>, G<sub>2</sub>, G<sub>3</sub>, G<sub>4</sub>, G<sub>5</sub>, G<sub>6</sub> and G<sub>7</sub> were 0.5 (4.5), 0.5 (8.6), 0.7 (18), 0.7 (23), 0.4 (17), 2.0 (99) and 3.0 μM (173 ng per 50-μl injection), respectively. The detection limit (0.5 μM) for G<sub>1</sub> by this method is equal to that reported previously for glucose using anion-exchange chromatography with pulsed amperometric detection [12].

The immobilized ODH column reactor is concluded to be useful for the coulometric detection of trace amount of MOSs. MOSs have been determined amperometrically by anion-exchange chromatography using immobilized glucoamylase post-column [8]. The detection limit for G<sub>7</sub> was 6.8 μM. This method is more sensitive (3.0 μM).

## REFERENCES

- 1 F. W. Scott and G. Hatina, *J. Food Sci.*, 53 (1988) 264.
- 2 H. Derler, H. F. Hormeyer and G. Bonn, *J. Chromatogr.*, 440 (1988) 281.
- 3 K. B. Hicks and A. T. Hotchkiss, Jr., *J. Chromatogr.*, 441 (1988) 382.
- 4 K. Koizumi, Y. Kubota, T. Tanimoto and Y. Okada, *J. Chromatogr.*, 464 (1989) 365.
- 5 S. Tabata and T. Ide, *Carbohydr. Res.*, 176 (1988) 245.
- 6 K. Koizumi, T. Utamura and Y. Kubota, *J. Chromatogr.*, 409 (1987) 396.
- 7 H. Jansen and R. W. Frei, in K. Zech and R. W. Frei (Editors), *Selective Sample Handling and Detection in High-Performance Liquid Chromatography, Part B*, Elsevier, Amsterdam, 1989, Ch. 5, p. 216.
- 8 L. A. Larew and D. C. Johnson, *Anal. Chem.*, 60 (1988) 1867.
- 9 T. Ikeda, T. Shibata, S. Todoroki and M. Senda, *Anal. Chim. Acta*, 230 (1990) 75.
- 10 *Catalog of Toyo Jozo Enzymes*, Toyo Jozo, Tokyo, 1986, p. 71.
- 11 I. Matsumoto, Y. Ito and N. Seno, *J. Chromatogr.*, 239 (1982) 747.
- 12 L. E. Welch, D. A. Mead, Jr., and D. C. Johnson, *Anal. Chim. Acta*, 204 (1988) 323.

## Note

# High-performance liquid chromatographic determination of flavonoid glucosides from *Helichrysum italicum*

PIERGIORGIO PIETTA\*, PIERLUIGI MAURI and CLAUDIO GARDANA

Dipartimento di Scienze e Tecnologie Biomediche, Sezione Chimica Organica, Via Celoria 2, 20133 Milan (Italy)

and

ROBERTO MAFFEI FACINO and MARINA CARINI

Istituto Chimica Farmaceutica Tossicologica, Viale Abruzzi 42, 20131 Milan (Italy)

(First received May 14th, 1990; revised manuscript received September 3rd, 1990)

*Helichrysum italicum* G. Don (*H. angustifolium* D.C.) is a plant widely distributed in the Mediterranean area, and its flowering tops are used in folk medicine for their anti-inflammatory and anti-allergic properties [1]. The constituents of the drugs are terpenes, sterols [2] and flavonoids [3,4]. Thin-layer chromatography was recently utilized to isolate and identify flavonoid derivatives from the species *H. graveolens* [5]. However, high-performance liquid chromatography (HPLC) is the method of choice for the separation and quantification of complex natural mixtures of flavonoids [6]. Recently we reported that eluents containing C<sub>3</sub> alcohols yield better separations than those obtained with the customary acetonitrile (methanol)–water–acetic acid system [7]. According to this approach, an isocratic reversed-phase HPLC method for the separation of the main flavonoid glucosides of *H. italicum* has been developed, and the results are described in this paper.

## EXPERIMENTAL

### Materials

Naringenin-4'-glucoside, kaempferol-3-glucoside and 4,2',4',6'-tetrahydroxy-chalcone-2'-glucoside were isolated from *H. italicum* according to the literature [4]. The flowering tops of *H. italicum* were collected from the Ligurian mountains and authenticated at the Department of Botany (University of Milan). 2-Propanol was of HPLC grade (Baker, Deventer, The Netherlands).

### Apparatus

The HPLC analyses were performed on a Waters Assoc. (Milford, MA, U.S.A.) liquid chromatograph equipped with a Model U6K universal injector and a Model 510 pump connected to a Model HP 1040A photodiode-array detector (Hewlett-Packard,

Waldbronn, F.R.G.). The column was C<sub>8</sub> Aquapore RP 300 (7 μm spherical) (250 × 4.6 mm I.D.) (Brownlee Labs., Santa Clara, CA, U.S.A.). The eluent was 2-propanol-water (20:80) at a flow-rate of 1.5 ml/min.

The acquisition of UV spectra was automatic at the apex, both inflection points and the base of all peaks (200–500 nm, 2-nm steps).

#### Purity of chromatographic peaks

The UV spectra acquired for each peak, after subtraction of the corresponding UV base spectrum, were computer normalized and the plots were superimposed. Peaks were considered to be chromatographically pure when there was exact coincidence among their corresponding UV spectra.

#### Sample preparation

The flowers of *H. italicum* (6 g) were extracted by percolation with 70% ethanol, the solvent was evaporated under vacuum and the residue dissolved in methanol (10 ml). After centrifugation, the methanol was evaporated to dryness under vacuum to give a brownish yellow crude extract (0.5 g). This was suspended in water (20 ml) and, after filtration, the aqueous solution was evaporated to yield the flavonoid glucosides fraction (ca. 130 mg).

For HPLC analysis, a methanolic solution (6.5 mg/ml) was prepared; 5-μl aliquots were injected.

#### Calibration graphs

Naringenin-4'-glucoside, kaempferol-3-glucoside and 4,2',4',6'-tetrahydroxychalcone-2'-glucoside were dissolved in methanol (0.5 mg/ml). Replicate injections of these solutions (2.5–15 μl) were made. UV detection was at 254 nm.

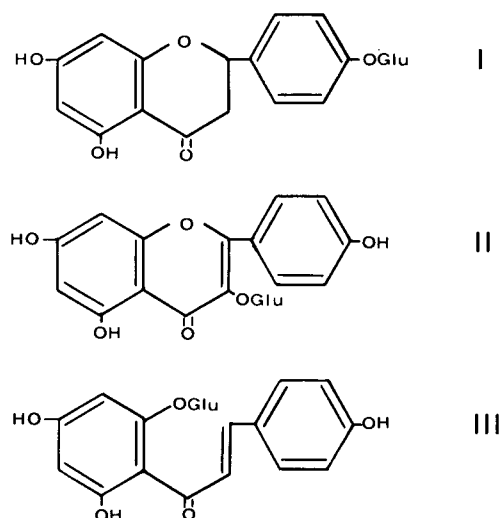


Fig. 1. Structures of main *Helichrysum italicum* flavonoid glucosides: naringenin-4'-glucoside (I), kaempferol-3-glucoside (II) and 4,2',4',6'-tetrahydroxychalcone-2'-glucoside (III).

## RESULTS AND DISCUSSION

Naringenin-4'-glucoside (I), kaempferol-3-glucoside (II) and 4,2',4',6'-tetrahydroxychalcone-2'-glucoside (III) are the main flavonoids of *H. italicum* (Fig. 1). These compounds were isolated from *H. italicum* and their structures were confirmed by mass and NMR spectrometry [4]. For the separation of these flavonoids, a simple 20% isopropanol solvent as an alternative to the acetonitrile (methanol)-acetic acid-water system yielded very satisfactory results (Fig. 2).

A typical chromatogram obtained from the flavonoid fraction of *H. italicum* is shown in Fig. 3. The UV spectra acquired for each peak were computer normalized and the plots were superimposed, obtaining exact coincidence among the curves. Consequently, the peaks were assumed to be pure. Moreover, the UV spectra of the peaks of interest and those of their corresponding standards were identical, which confirmed the previous identification through the retention times.

Rectilinear responses between peak areas and amounts injected were obtained when replicate injections ( $n = 6$ ) of I-III reference solutions (1-7.5  $\mu\text{g}$ ) were made. The relationships were as follows:

$$\begin{array}{lll} y = 178x + 47 & r = 0.999 & \text{(naringenin-4'-glucoside)} \\ y = 900x + 56 & r = 0.995 & \text{(kaempferol-3-glucoside)} \\ y = 627x - 59 & r = 0.998 & \text{(4,2',4',6'-tetrahydroxychalcone-2'-glucoside)} \end{array}$$

where  $y$  = peak area and  $x$  = amount injected ( $\mu\text{g}$ ).

Quantification in the flavonoid fraction was achieved by external standardization and the contents of naringenin-4'-glucoside, kaempferol-3-glucoside and 4,2',4',6'-tetrahydroxychalcone-2'-glucoside were 9.2, 3.1 and 1.6%, respectively.

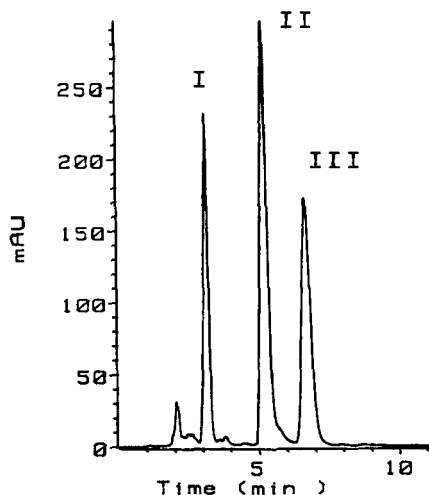


Fig. 2. High-performance liquid chromatogram of naringenin-4'-glucoside (I, 5  $\mu\text{g}$ ), kaempferol-3-glucoside (II, 3  $\mu\text{g}$ ) and 4,2',4',6'-tetrahydroxychalcone-2'-glucoside (III, 2  $\mu\text{g}$ ) standards. Column, 7- $\mu\text{m}$  C<sub>8</sub> Aquapore RP 300; eluent, 2-propanol-water (20:80); flow-rate, 1.5 ml/min; detection, 254 nm.

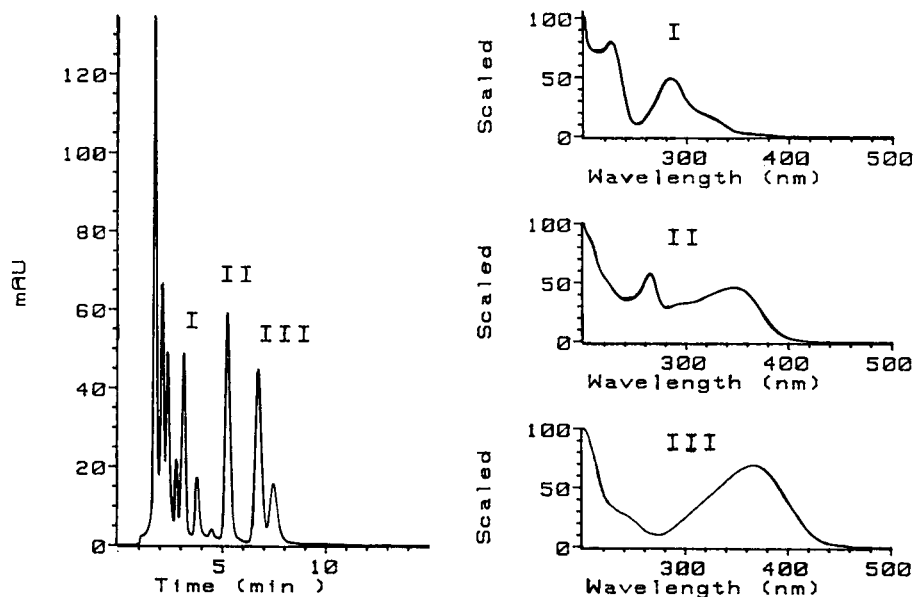


Fig. 3. Typical chromatogram of an *H. italicum* extract. See Fig. 2 for chromatographic conditions.

The reproducibility of the method was  $98.0 \pm 1.9\%$  and recovery tests on known amounts of standards added to the extract gave  $97.2 \pm 2.5\%$ . Intra-day and inter-day assay variations were 3.1% and 2.9%, respectively.

In conclusion, the described procedure provides further support for the validity of using eluents based on  $C_3$  alcohols for the isocratic reversed-phase determination of flavonoids in medicinal plants.

#### REFERENCES

- 1 B. Cubukcu and S. Bingol, *Plant. Med. Phytother.*, 18 (1984) 28.
- 2 P. Manitto, D. Monti and E. Colombo, *Phytochemistry*, 11 (1972) 2112.
- 3 L. Opitz, D. Ohlendorf and R. Hansel, *Phytochemistry*, 10 (1971) 1948.
- 4 R. Maffei Facino, M. Carini, M. Mariani and C. Cipriani, *Acta Ther.*, 14 (1988) 323.
- 5 B. Cubukcu and B. Damadyan, *Fitoterapia*, 47 (1986) 124.
- 6 D. J. Daigle and E. J. Conkerton, *J. Liq. Chromatogr.*, 11 (1988) 309.
- 7 P. G. Pietta, P. L. Mauri, E. Manera, P. L. Ceva and A. Rava, *Chromatographia*, 27 (1989) 509.



## Note

# Isocratic column liquid chromatographic separation of a complex mixture of epicuticular flavonoid aglycones and intracellular flavonol glycosides from *Cistus laurifolius* L.

THOMAS VOGT and PAUL-GERHARD GÜLZ\*

Botanisches Institut, Universität Köln, Gyrhofstraße 15, 5000 Köln 41 (F.R.G.)

(First received November 28th, 1989; revised manuscript received August 7th, 1990)

Reversed-phase high-performance liquid chromatography (RP-HPLC) is the method of choice for the separation flavonoid compounds [1]. HPLC protocols have been developed for the identification of methylated flavonoid aglycones [2], but the separation of different isomeric 3-O-methylflavonol derivatives is still difficult [3]. Thin-layer chromatography (TLC) on polyamide is able in some instances to separate closely related 3-O-methylflavonol or flavone isomers [4]. The very complex mixture of epicuticular flavonoids from *Cistus laurifolius* [5–7] is mainly composed of closely related isomeric quercetin mono- and dimethyl ethers. To study this material we developed a simple isocratic RP-HPLC system that allows a good resolution of these isomeric methyl ethers. In contrast to most other eluents, which utilize methanol or acetonitrile, the isocratic separation takes advantage of the dipole–dipole interactions of tetrahydrofuran with the flavonoids. The eluent system developed for analytical RP-HPLC also gave good results in preparative isolation even of the minor flavonol aglycones by reversed-phase low-pressure liquid chromatography (RP-LPLC).

## EXPERIMENTAL

### *Methylated flavonoid aglycones (Fig. 1)*

Leaves of *C. laurifolius* were washed with chloroform to extract the epicuticular resin–wax mixture from their surface. Waxes were separated from the resin by dilution of the mixture in hot methanol (50–60°C) (1 g of extract in 50 ml of methanol) and cooling for 12 h in a freezer (–20°C). This resulted in the precipitation of the waxes, leaving about 95% of the crude resin in the supernatant.

Terpenoids were separated from the flavonoid aglycones by column chromatography (CC) on a Sephadex LH-20 (Pharmacia, Freiburg, F.R.G.) column (100 cm × 3.0 cm I.D.) with methanol as eluent. Terpenoids were eluted first and identified by TLC on silica gel 60 (Merck, Darmstadt, F.R.G.) [solvent, toluene–ethyl acetate

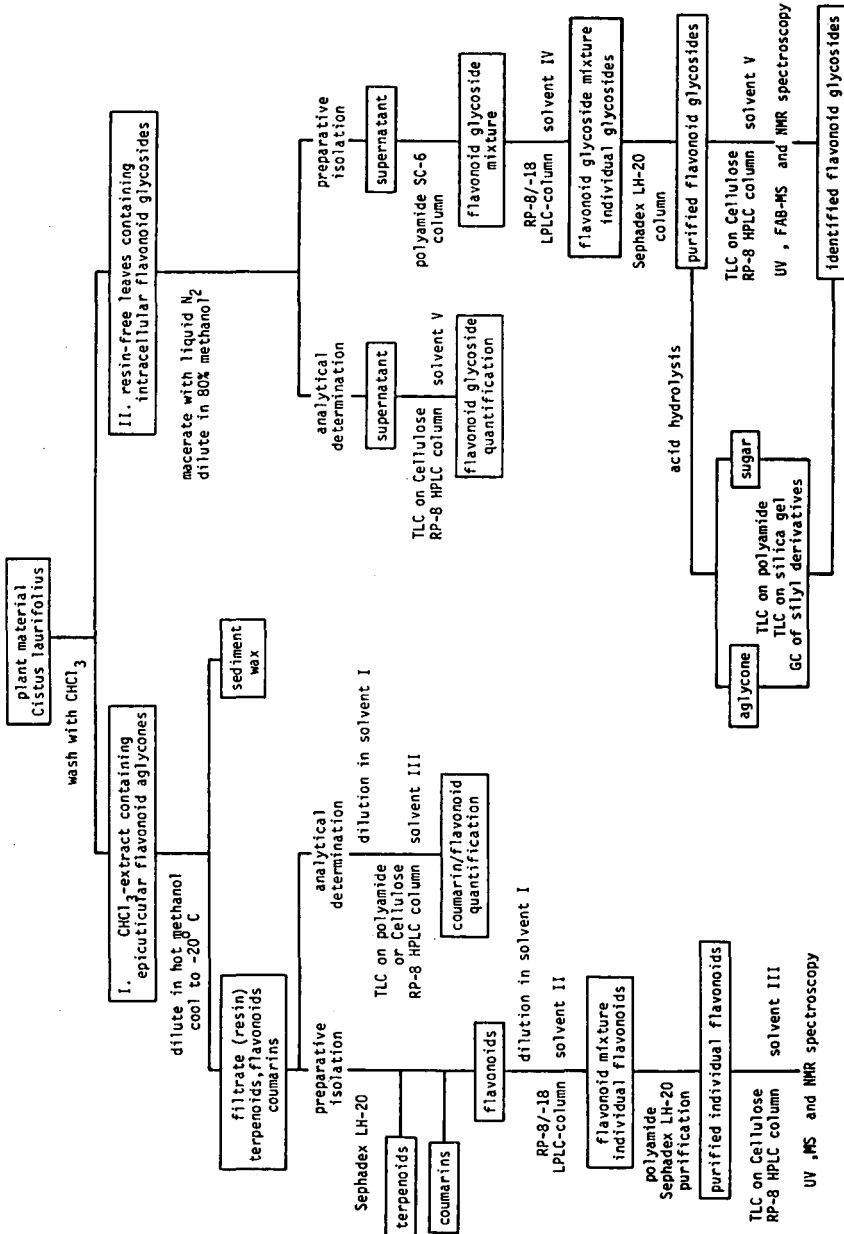


Fig. 1. Extraction, isolation and identification of epicuticular and intracellular flavonoids of *C. laurifolius*.

(9:1)], sprayed with concentrated sulphuric acid and heated at 100°C for 10 min. Then the coumarins (scopoletin and ayapin) were eluted, followed by flavonoid bands. Coumarins and flavonoids were detected at 350 nm with a hand UV lamp. For analytical HPLC of single leaf extract, the removal of terpenoids was not necessary.

For preparative separations, the flavonoid fraction were taken up in 3 ml of solvent I [water-methanol-acetonitrile-tetrahydrofuran (65:10:5:25)] and injected directly onto an RP-18 (alternatively RP-8) LPLC column (40 cm × 3 cm I.D.), particle size 40–60 μm, prepared in the laboratories [8] according to a method described by Glatz [9]. A Duramat D-80 pump with pulsation suppression (Chemic und Filter Verfahrenstechnik, Heidelberg, F.R.G.) was used. Flavonoids were eluted by a step-wise gradient of water (containing 0.5% trifluoroacetic acid)-methanol-acetonitrile-tetrahydrofuran from 75:5:5:18 to 70:8:5:18 to 65:10:5:20 (solvents IIa, b and c) at a flow-rate of 8 ml/min and a pressure of 3–4 bar. The column was equilibrated before use with 200 ml of solvent IIa. Fractions were collected and monitored by detection with a hand UV lamp at 350 nm. If necessary, the separation was repeated to enrich individual flavonoids.

Further purification of individual flavonoids was achieved by chromatography on a Sephadex LH-20 column (100 cm × 2 cm I.D.) with methanol as eluent. Purified flavonoids were identified by comparison with authentic samples [5–7] according to their relative retention times in HPLC, co-chromatography by TLC using polyamide DC-6 and DC-11 [mobile phase, toluene-methyl ethyl ketone-methanol (65:25:15 or 8:1:1)] and microcrystalline cellulose [mobile phase, water-acetic acid (6:4)] (Macherey-Nagel, Düren, F.R.G.) and UV spectrometry. The 5-O-methylflavonols were also characterized by mass and <sup>1</sup>H NMR spectrometry [7].

For analytical HPLC analysis, the resin samples, after precipitation of the waxes, were dried under nitrogen, weighed and dissolved in 1 ml of methanol per 10 mg of resin. Aliquots of 50 μl were dried under nitrogen and diluted again in about 200–300 μl of solvent I. Samples of 30 μl were then injected onto a Hypersil MOS-RP-8 HPLC column (125 mm × 4.6 mm I.D.) (particle size 5 μm) (Chromatographie Service, Eschweiler, F.R.G.). A Spectra-Physics (Santa Barbara, CA, U.S.A.) HPLC system was used with a Rheodyne 20-μl loop and a Shimadzu C-R6A UV detector (Shimadzu Europa, Duisburg, F.R.G.). Isocratic elution was performed with solvent system III: water (containing 0.5% phosphoric acid)-methanol-acetonitrile-tetrahydrofuran (68:6:6:20) at a flow-rate of 1.2 ml/min. Preparatively isolated flavonoid mixtures were dried under nitrogen and an aliquot was diluted in solvent I and injected onto the HPLC column.

External standards were prepared from crystalline samples of quercetin-3-O-methyl ether (que-3-OMe), que-3,3'-diOMe, que-3,7-diOMe, que-5,3'-diOMe, que-7,3'-diOMe and the coumarin scopoletin. Quercetin, que-3,7,3',4'-tetraOMe, kampferol (kae), kae-3,7,4'-triOMe, apigenin (ap) and ap-4'-OMe were purchased from Roth (Karlsruhe, F.R.G.).

#### *Flavonol glycosides (Fig. 1)*

The chloroform-washed leaves were macerated in liquid nitrogen and extracted twice in 80% methanol (300 ml per 100 g of leaves) for glycoside analysis. The combined supernatants were carefully evaporated and fractionated by CC on 200 g of polyamide SC-6 (Macherey, Nagel & Co.) in a 40 cm × 7.5 cm I.D. column with

consecutive elution with 2 l of water, 8 l of water-methanol (1:1) and 3 l of methanol as eluents. Fractions were dried, taken up in 3 ml of solvent system I and applied to the equilibrated column with stepwise gradient elution with water (containing 0.5% trifluoroacetic acid)-methanol-acetonitrile-tetrahydrofuran from 85:4:4:7 to 82:5:5:8 to 80:6:6:9 (solvents IVa, b and c). Individual bands were recovered after UV detection at 350 nm with a hand UV lamp.

Sugars were identified by hydrolysis of 1 mg of flavonoid glycoside with 2 ml of 2 M trifluoroacetic acid for 30 min, evaporation of the acid and extraction of the aglycone with diethyl ether. Aglycones were detected by TLC on polyamide DC-6 with toluene-methanol-methyl ethyl ketone-acetylacetone (3:3:2:1). The water soluble sugars were identified by TLC [10] on silica gel plates (Merck). About 0.5-1 mg of the dried sugar was silylated with 20  $\mu$ l of N-methyl-N-trimethylsilyltrifluoroacetamide (MSTFA) (Macherey, Nagel & Co.) in 50  $\mu$ l of pyridine for 1 h at room temperature and subsequently analysed by gas chromatography on a 10-m OV-1 column [11] using a Hewlett-Packard Model 5710 gas chromatograph with a flame ionization detector and a Hewlett-Packard Model 3380 integrator (Hewlett-Packard, Boeblingen, F.R.G.) with temperature programming from 110°C (2 min isothermal) to 240°C at 6°C/min and a carrier gas (nitrogen) flow-rate of 2 ml/min. Individual sugar standards were obtained from Roth or Merck.

For analytical HPLC studies of flavonoids, one leaf (500 mg fresh weight) was macerated in liquid nitrogen taken up in 5 ml of 80% methanol in a glass vial and stored for 12 h at 4°C. A 100- $\mu$ l volume of the supernatant was evaporated to dryness under nitrogen and the residue was dissolved in solvent I, injected directly on to a Hypersil MOS-RP-8 (5  $\mu$ m) column and eluted with water (containing 0.5% phosphoric acid)-methanol-acetonitrile-tetrahydrofuran (81:6.5:5.5:7) (solvent system V) at a flow-rate of 1.2 ml/min (Fig. 1).

In some instances the flavonoid pattern was checked by TLC on microcrystalline cellulose [mobile phase, water-acetic acid (8:2)].

Crystalline standards (kae-3-rhamnosidoglucoside or que-3-rhamnosidoglucoside) were available from Roth or obtained by preparative RP-LPLC (myr-3-galactoside, myr-3-rhamnoside, que-3-galactoside). Kae-3-rham-glc was added as an external standard to the macerated leaves to determine the total recovery of flavonoid glycosides from the leaves (recovery = 90-100% of the flavonoids). After every preparative run the RP-LPLC column was cleaned by elution in the opposite direction with 200 ml of water (containing 2% phosphoric acid)-acetonitrile-tetrahydrofuran (10:45:45) under the prevailing optimum elution conditions.

## RESULTS AND DISCUSSION

The resin of *C. laurifolius* consists of 31 phenolic aglycones (29 different flavonoids and two coumarins). Some of these aglycones were present only in negligible amounts and did not appear in the HPLC profile of the aglycone mixture (Fig. 2). The isocratic HPLC system was able to separate the 5-O-methyl derivatives well from the rest of the flavonol aglycones. This result is not especially dependent on the use of tetrahydrofuran in the solvent. Short retention times for 5-O-methyl flavonoids have been reported with other columns and eluent systems [12,13]. 5-Hydroxy groups form strong intramolecular hydrogen bonds with the 4-keto group of the heterocyclic ring,

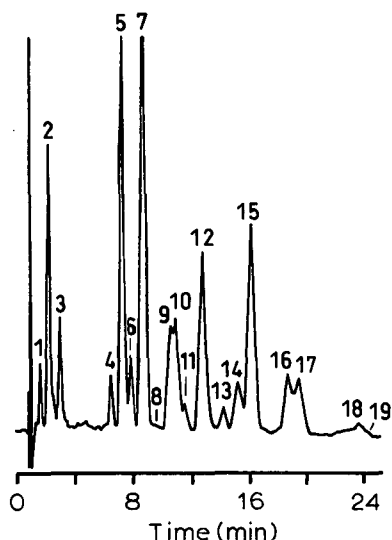


Fig. 2. HPLC of the crude resin of *C. laurifolius* after precipitation of the waxes. Hypersil MOS-RP-8, 5  $\mu\text{m}$ ; column, 125 mm  $\times$  4.6 mm I.D.; solvent system, III; flow-rate, 1.2 ml/min; UV detection at 350 nm. Peaks: 1 = scopoletin (coumarin); 2 = que-3,5,3'-triOMe (traces of the coumarin ayapin); 3 = que-5,3'-diOMe; 4 = luteolin; 5 = que-3-OMe (traces of lut-3'-OMe); 6 = que-3,4'-diOMe; 7 = que-3,3'-diOMe (traces of quercetin and apigenin); 8 = naringenin; 9 = que-3'-OMe; 10 = kae-3-OMe; 11 = lut-7-OMe; 12 = que-3,7'-diOMe; 13 = que-7-OMe (traces of que-3,7,3',4'-tetraOMe); 14 = que-3,7,3'-triOMe (traces of ap-4'-OMe); 15 = ap-7-OMe; 16 = que-7,3'-diOMe; 17 = kae-3,7-diOMe; 18 = ap-7,4'-diOMe; 19 = kae-7-OMe.

reducing its polarity and increasing the interaction with the hydrocarbon chains of the column matrix. If the protons are replaced with methyl groups, the polarity of the 4-keto group is enhanced, which leads to shorter retention times for the 5-O-methyl flavonoids. The use of tetrahydrofuran in the solvent is important for the separation of isomeric 3-O-methylflavonols. Previously, que-3,4'-diOMe could be separated from its 3,3'-isomer only by TLC on polyamide-11 [4]. Now it is possible to separate these closely related isomers by RP-HPLC. The separation and determination of the 3,7- and 3,4'-diOMe and the 3,7,3'- and 3,7,4'-triOMe flavonol isomers was completely successful. This system can also be applied to the separation of flavone isomers, as shown for ap-7-OMe and ap-4'-OMe.

As the complex flavonoid pattern of *C. laurifolius* results in only slightly different retention times for individual flavonoids, even the solvent composition of the sample before injection is very crucial. Dissolving the sample in methanol prevents the separation of the two 5-O-methyl derivatives and leads to co-elution of luteolin (lut), que-3-OMe and que-3,4'-diOMe and que-7-OMe, que-3,7,3'-triOMe and ap-7-OMe, respectively.

The conditions for analytical HPLC were directly transferred to the preparative RP-LPLC for the isolation and identification of several flavonoid aglycones after pre-fractionation of the pure resin on a Sephadex LH-20 column. As shown in the one-step purification of the 5-O-methyl derivatives from the other flavonoids [7], this

method leads to the isolation of que-3,4'-diOMe, a minor resin compound. A 20-fold concentration was achieved by chromatographing the Sephadex fraction twice on an RP-18 LPLC column using solvent system I. After a final Sephadex step the mixture contained 71% of que-3,4'-diOMe, 24% of que-3,3'-OMe and 5% of que-3-OMe, compared with 3% of que-3,4'-diOMe in the crude flavonoid mixture. The concentrated 4'-O-methyl isomer was identified by UV spectrometry and HPLC and TLC

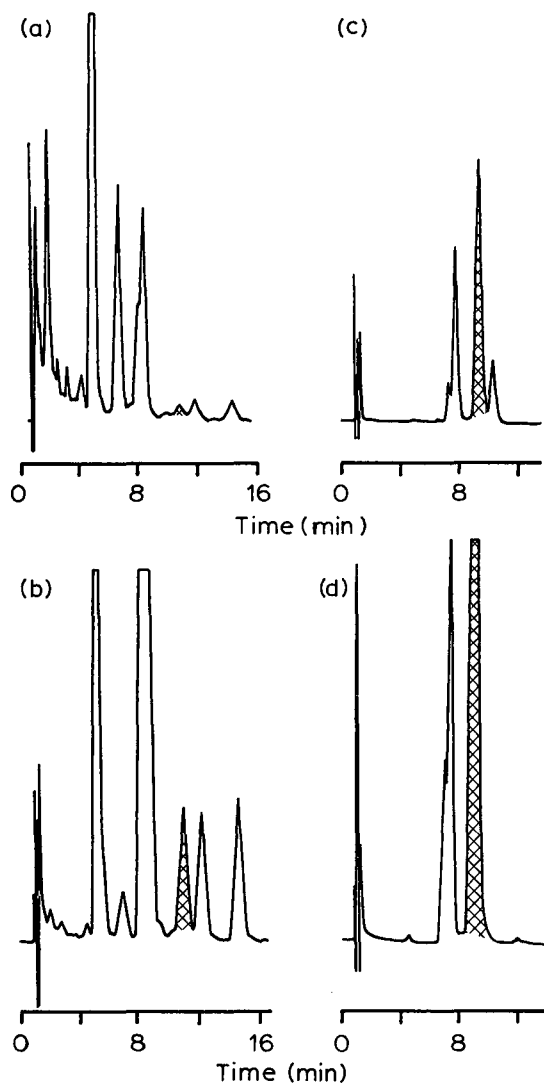


Fig. 3. Stepwise purification and preparative isolation of quercetin-3-O- $\beta$ -arabinoside (shaded). Hypersil MOS RP-8, 5  $\mu$ m; column, 125 mm  $\times$  4.6 mm I.D.; solvent system, V; flow-rate 1.2 ml/min; UV detection at 350 nm. (a) Crude intracellular flavonoid extract; (b) after polyamide SC-6 column, eluent 50% methanol; (c) after one RP-18 LPLC passage, solvent system V; (d) after purification by column chromatography on Sephadex LH-20, eluent methanol.

co-chromatography with an original standard. The following components were purified to 95% que-3-OMe, 97% apigenin and 92% kae-3-OMe by injecting the flavonoid mixture twice onto the LPLC column with subsequent purification by CC on Sephadex LH-20. In the same manner it was possible to identify some minor flavonoids from the complex resin mixture not detected previously [6], e.g., luteolin, lut-7-OMe and que-7-OMe.

In addition to the aglycone isolations, the purification of intracellular flavonol glycosides was also substantially improved by using the RP-LPLC technique by modifying the HPLC solvent. The purification of minor components including que-3-arabinoside (que-3-ara) on an RP-18 LPLC column is illustrated in Fig. 3. After elution of the crude extract from a polyamide SC-6 column, the fraction that contained the main amount of que-3-ara was subsequently chromatographed using the RP-18 LPLC system (solvent V). The desired component was concentrated 10-fold in one step. After purification by Sephadex LH-20, the substance was suitable for submission to  $^1\text{H}$  NMR analysis. In the same way, other glycosides were purified with the aid of RP-LPLC and crystallized from methanol-water solutions.

When closely related or isomeric flavonoids are present, the application of RP-HPLC or RP-LPLC mainly based on tetrahydrofuran as eluent may be the method of choice for preparative isolation and identification. Even complex mixtures of flavonoids are well separated with the LPLC technique with only slight modifications of the solvent system used for HPLC. The choice of RP-8 instead of RP-18 did not influence the separation significantly.

#### ACKNOWLEDGEMENTS

We thank V. Wray (Braunschweig, F.R.G.) for NMR analysis of myr-3-gal, myr-3-ara, myr-3-rham-glc and que-3-ara-glc, E. Wollenweber (Darmstadt, F.R.G.) for samples of que-7-OMe, que-3,4'-diOMe and of que-3,7,4'-triOMe, G. Weissenboeck (Köln, F.R.G.) for a sample of que-3-glc, D. Strack (Braunschweig, F.R.G.) for a sample of kae-3-glc and B. Ellis (Vancouver, Canada) for his help with the preparation of the manuscript.

#### REFERENCES

- 1 D. J. Daigle and E. J. Conkerton, *J. Liq. Chromatogr.*, 11 (1988) 309.
- 2 L. R. Snyder, *J. Chromatogr. Sci.*, 16 (1978) 223.
- 3 W. Wollenweber, in J. B. Harborne (Editor), *The Flavonoids*, Academic Press, New York, 1988, p. 233.
- 4 E. Wollenweber, *Supplement Chromatographie 1982*, GIT-Verlag, Darmstadt, 1982, pp. 50-54.
- 5 E. Wollenweber and K. Mann, *Z. Naturforsch., Teil C*, 37 (1984) 303.
- 6 T. Vogt, P. Proksch and P.-G. Gülz, *J. Plant Physiol.*, 131 (1988) 25.
- 7 T. Vogt, P.-G. Gülz and V. Wray, *Phytochemistry*, 27 (1988) 3712.
- 8 H. Hemmers, P.-G. Gülz, F. J. Marner and V. Wray, *Z. Naturforsch., Teil C*, 44 (1989) 193.
- 9 B. Glatz, *Dissertation*, Stuttgart, 1979.
- 10 S. A. Hansen, *J. Chromatogr.*, 107 (1975) 224.
- 11 K. R. Markham, *Techniques for Flavonoid Identification*, Academic Press, London, 1982.
- 12 K. van de Castele, H. Geiger and C. F. van Sumere, *J. Chromatogr.*, 240 (1982) 81.
- 13 F. A. T. Barberan, F. Tomas, L. Hernandez and F. Ferreres, *J. Chromatogr.*, 347 (1985) 443.

## Note

---

# Behaviour of concanavalin A on DEAE-Sephadex and CM-Sephadex<sup>a</sup>

CYNTHIA ELIAS

*Chemical Engineering Division, National Chemical Laboratory, Pashan, Pune 411 008 (India)*  
and

A. M. DIWAN\*

*Department of Zoology, University of Poona, Ganeshkhind, Pune 411 007 (India)*

(First received December 5th, 1989; revised manuscript received April 20th, 1990)

Concanavalin A (Con A) is a lectin isolated from jack bean. It is composed of four subunits each having a molecular weight of 26 500 and containing one  $\text{Ca}^{2+}$  and one  $\text{Mg}^{2+}$  per subunit. It is conventionally purified either by ion-exchange chromatography on CM-cellulose [1] or by affinity chromatography on Sephadex [2]. The Sephadex ion exchangers are composed of an ion-exchange group and dextran. The individual roles of these two moieties in the adsorption and desorption of dextran binding proteins are not well defined, but it has been generally assumed that the ion-exchange group is responsible for retention. The present investigation was undertaken to test this hypothesis. Con A has the ability to interact with both the ion-exchange group and dextran. Hence the adsorption and elution behaviour of this protein on DEAE-Sephadex and CM-Sephadex under different conditions was studied.

## EXPERIMENTAL

Concanavalin A (CSIR Centre for Biochemicals, New Delhi, India), CM-Sephadex C-50 and DEAE-Sephadex A-50 (Pharmacia, Uppsala, Sweden) were used. All other chemicals were of analytical-reagent grade. The purity of Con A was ascertained by polyacrylamide gel electrophoresis (PAGE) under native and denaturing conditions [3]. The bands were revealed by staining the gels after electrophoresis with Coomassie Brilliant Blue G-250.

The influent protein solution was prepared by dissolving Con A in 50 mM Tris-HCl buffer (pH 8.3) or 50 mM acetate buffer (pH 5.0), depending on the pH required for the binding. The adsorption of protein on DEAE-Sephadex was carried

---

<sup>a</sup> NCL Communication No. 4798.



out under different conditions, *viz.*, low salt (0.01 *M* NaCl), low salt with glucose (0.01 *M* NaCl, 0.1 *M* glucose) and high salt (1 *M* NaCl).

The resin was washed with the loading buffer until the absorbance of the effluent at 280 nm was negligible (<0.1). Elution of the protein was carried out with different eluting agents such as low salt with glucose, high salt and high salt with glucose (1 *M* NaCl, 0.1 *M* glucose). The solutions were prepared in 50 mM Tris-HCl buffer (pH 8.3) or 50 mM acetate buffer (pH 5.0). The retention and elution of Con A (in 5-ml fractions) were determined by measuring the absorbance at 280 nm.

## RESULTS AND DISCUSSION

The Con A preparation showed a single band in native PAGE and multiple bands in sodium dodecyl sulphate PAGE, as reported by Wang *et al.* [3]. The protein was therefore considered to be electrophoretically pure. Retention of Con A on DEAE-Sephadex was almost identical under conditions of low salt and low salt with glucose. However, 1 *M* NaCl could elute 50% of the protein retained in the presence of low salt and only 20% in low salt with glucose (Table I). The results further show that elution with 1 *M* NaCl-0.1 *M* glucose leads to a better and faster desorption of protein (Fig. 1). Moreover, no protein was seen in the effluent when the elution was effected with low salt with glucose. It was also observed that Con A was retained on DEAE-Sephadex under high-salt conditions, and the protein could not be eluted with high salt with glucose.

Con A desorbed by a high salt concentration may bind to Sephadex and hence elution is faster in the presence of glucose. In addition, as the sugar-Con A complex is more basic than free Con A [4], it is not expected to be retained on anion exchangers. The firm retention of Con A on DEAE-Sephadex under high-salt conditions may be attributed to affinity interactions which are stronger, probably owing to the dissociation of the tetrameric protein.

The results of experiments carried out using CM-Sephadex show that the amount of protein retained per gram of resin was higher for CM-Sephadex than

TABLE I

ELUTION OF CONCAVALIN A FROM DEAE-SEPHADEX AND CM-SEPHADEX WITH DIFFERENT ELUENTS

Parameter	DEAE-Sephadex (pH 8.3)			CM-Sephadex (pH 5.0)			CM-Sephadex (pH 8.3)	
	Low salt <sup>a</sup>	Low salt-glucose <sup>a</sup>	High salt <sup>a</sup>	Low salt <sup>a</sup>	Low salt-glucose <sup>a</sup>	High salt <sup>a</sup>	Low salt <sup>a</sup>	Low salt-glucose <sup>a</sup>
Protein retained (mg/g resin)	84	85	63	145	143	58	8.0	27.0
Recovery (%)								
Low salt-glucose <sup>a</sup>	0	—	—	13.0	—	—	0.0	5.0
High salt <sup>a</sup>	48.0	20	—	47.0	42.0	—	62.0	—
High salt-glucose <sup>a</sup>	63	—	9.0	58.0	—	24.0	—	—

<sup>a</sup> Low salt = 0.01 *M* sodium chloride; low salt-glucose = 0.01 *M* sodium chloride-0.1 *M* glucose; high salt = 1 *M* sodium chloride; high salt-glucose = 1 *M* sodium chloride-0.1 *M* glucose.

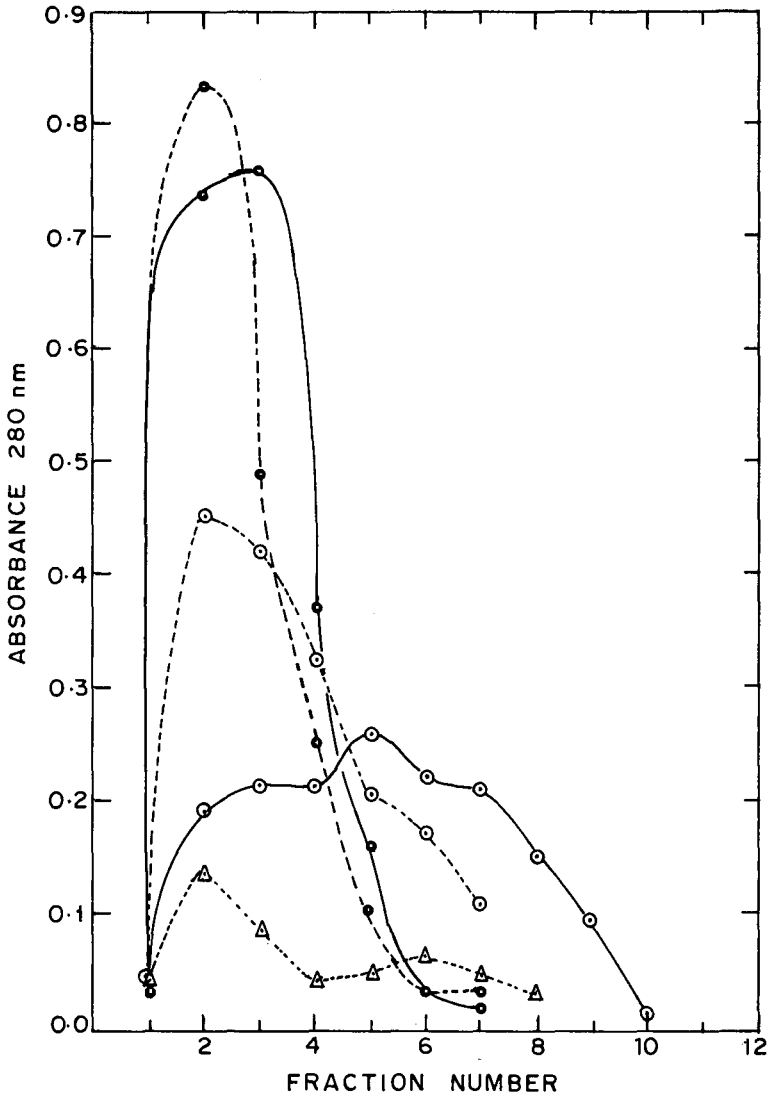


Fig. 1. Chromatographic elution profiles of Con A on (solid line) DEAE-Sephadex (pH 8.3) and (dashed line) CM-Sephadex (pH 5.0). (●) 1 *M* sodium chloride and 0.1 *M* glucose; (○) 1 *M* sodium chloride; (△) 0.01 *M* sodium chloride and 0.1 *M* glucose.

DEAE-Sephadex (Table I). However, as with DEAE-Sephadex, the amount of protein retained on the matrix under low-salt binding conditions was the same in the presence or absence of glucose. About 12% of the protein retained could be eluted by low salt with glucose. Similarly, Con A was desorbed faster when high salt with glucose was the eluent. The protein could also be retained on CM-Sephadex under high-salt conditions, and an appreciable amount of Con A thus retained could be eluted using

high salt with glucose. At pH 5.0, Con A exists in its dimeric form [5], which would explain the adsorption–elution behaviour observed above.

These results indicate that Sephadex may participate in the retention of Con A on CM-Sephadex. It is evident that as the protein can be eluted with glucose alone, the sugar-binding sites are not involved in the ionic coupling. The fraction of Con A eluted by low salt with glucose is bound only to the dextran moiety of the matrix. The protein so eluted is also not due to the microheterogeneity of Con A, if any. It can therefore be concluded that the retention of Con A on CM-Sephadex is due to both charge- and sugar-specific interactions. However, the protein seems to bind preferentially to the ion-exchange group, which may be due to the capacity of the ion exchanger.

Further experiments with CM-Sephadex showed that Con A was retained on the matrix at pH 8.3, although the retention was relatively less (Table I). This retention could be improved by the presence of glucose, probably owing to the increased basicity of the protein. We expected that at pH 8.3 Con A would be retained mainly by affinity interactions. However, it was found that low salt with glucose was unable to bring about significant elution of the protein, whereas high salt provided a better eluent. This may be a result of the weaker affinity interactions and ionic forces at pH 8.3 in comparison with those existing at pH 5.0. The observation that the protein loaded in the presence of glucose could not be desorbed by high salt cannot be explained satisfactorily. It should also be mentioned that in all the experiments 100% recovery of the protein was not observed, which may be due to the poor sensitivity of the method used.

In the above study, Con A was used as a model representing those proteins which bind to dextran. It can be concluded that in such cases glucose–sodium chloride would be a good eluting agent.

#### ACKNOWLEDGEMENT

One of the authors (C.E.) thanks the Council of Scientific and Industrial Research (CSIR), New Delhi, for financial assistance.

#### REFERENCES

- 1 F. Obata, R. Sakai and H. Shiokawa, *J. Biochem.*, 84 (1978) 103.
- 2 B. B. L. Agarwal and I. J. Goldstein, *Biochim. Biophys. Acta*, 133 (1967) 376.
- 3 J. L. Wang, B. A. Cunningham and G. M. Edelman, *Proc. Natl. Acad. Sci. U.S.A.*, 68 (1971) 1130.
- 4 H. Akedo, Y. Mori and M. Kabayashi, *Biochem. Biophys. Res. Commun.*, 79 (1972) 106.
- 5 I. J. Goldstein and R. D. Poretz, in I. E. Liener, N. Sharon and I. J. Goldstein (Editors), *The Lectins*, Academic Press, London, 1986, p. 52.

## Note

---

### Large-scale isolation and purification of human apolipoproteins A-I and A-II<sup>a</sup>

ALEXANDER SIGALOV\*, OLGA ALEXANDROVICH and ELENA STRIZEVSKAYA  
*U.S.S.R. Research Centre for Preventive Medicine, Petroverigsky Street 10, 101953 Moscow (U.S.S.R.)*  
(First received April 25th, 1990; revised manuscript received June 24th, 1990)

Plasma high-density lipoprotein (HDL) is a complex of lipids (largely phosphatidylcholine and cholesteryl esters) and proteins. The major proteins associated with HDL are designated apo A-I and apo A-II [1]. Isolation of apo A-I and apo A-II generally includes ultracentrifugation to isolate HDL, delipidation to obtain apo HDL proteins free of lipids and chromatographic separation of apo A-I and apo A-II from other HDL proteins [2]. An alternative approach for isolation of apo A-I and apo A-II with scale-up potential far beyond the practical application of ultracentrifugation became available when a chromatographic procedure utilizing phenyl-Sepharose to adsorb lipoproteins from plasma was described [3,4]. Immunological and electrophoretic characterization in addition to amino acid determination appeared sufficient to determine the quality of these proteins.

Purified apo A-I and apo A-II proteins are most often used as tracers, standards and immunogens in conjunction with apo A-I and apo A-II immunoassays.

This paper describes a modified large-scale method for the isolation of purified apo A-I and apo A-II from human serum.

#### EXPERIMENTAL

##### *Materials and standards*

Ammonium hydrogencarbonate, sodium chloride, urea, Coomassie Brilliant Blue R-250, sodium dodecyl sulphate (SDS), ammonium peroxodisulphate, N,N-methylenebisacrylamide, acrylamide and N,N,N',N'-tetramethylethylenediamine were obtained from Serva (Heidelberg, F.R.G.). Protein molecular mass standards were purchased from Pharmacia (Uppsala, Sweden).

---

<sup>a</sup> Presented at the *11th International Symposium on Biomedical Applications of Chromatography and Electrophoresis, Tallin, April 24–28th, 1990.*

### *Isolation and delipidation of HDL from human serum*

HDL of density 1.063–1.210 g/ml was isolated from fasting serum of normolipidaemic donors by sequential ultracentrifugation [5] in a Beckman (Berkeley, CA, U.S.A.) Model L8-70 ultracentrifuge using a 45.Ti rotor. The isolated HDL fraction was extensively dialysed against 50 mM ammonium hydrogencarbonate buffer (pH 8.2), lyophilized and delipidated by an original procedure using a chloroform–methanol–diethyl ether solvent system [6].

### *Gel permeation and anion-exchange chromatography*

The proteins were solubilized in 10 mM Tris–HCl buffer (pH 8.6) containing 8 M urea (Tris–urea buffer) and applied to a Toyopearl HW-55F (Toyo Soda, Tokyo, Japan) column (90.0 × 3.5 cm I.D.). Elution was carried out with the same buffer at a flow-rate of 40 ml/h and 8-ml fractions were collected. Following analysis by polyacrylamide gel electrophoresis (PAGE) [7], fractions containing apo A-I and apo A-II were pooled. The apolipoprotein pool was applied to a DEAE-Toyopearl 650M (Toyo Soda) column (40.0 × 3.2 cm I.D.), equilibrated with Tris–urea buffer. Elution was effected with a linear gradient of sodium chloride from 0.02 to 0.15 M in Tris–urea buffer (1000 ml total gradient volume) at a flow-rate of 60 ml/h. Fractions of 6 ml each were collected. Those containing apo A-I and apo A-II were pooled separately and extensively dialysed against 50 mM ammonium hydrogencarbonate buffer (pH 8.2). After dialysis, the samples were desalted by gel permeation chromatography using a Toyopearl HW-40F (Toyo Soda) column (70.0 × 2.2 cm I.D.) with the same buffer at a flow-rate of 80 ml/h and finally lyophilized.

### *Characterization of proteins*

Proteins were quantified according to Lowry *et al.* [8] and spectrophotometrically at 280 nm using extinction coefficients of 1.22 and 1.82 AU/mg protein · ml for apo A-I and apo A-II, respectively [9]. Lipid phosphorus analysis was performed utilizing the method of Bartlett [10]. Homogeneity was confirmed by SDS-PAGE on 15% polyacrylamide gels under both reducing and non-reducing conditions [7] and by urea-PAGE [11]. Identification of apo A-I and apo A-II was confirmed by electrophoretic mobility and immunoelectrophoresis [12]. Amino acid analyses of purified apo A-I and apo A-II were made in a Beckman 6300 amino acid analyser after 72 h of acid hydrolysis.

## RESULTS AND DISCUSSION

A modified scheme for the preparative isolation and purification of apolipoproteins A-I and A-II, the major HDL proteins [1], from the 1.063–1.210 g/ml HDL material has been developed. The main aim of this work was to increase the efficiency of the method and to obtain apo A-I and apo A-II with the highest degree of purity. For this reason, we modified the conditions of the HDL delipidation (the total time of the modified procedure was 1 h) [6] and, as reported here, used Toyopearl HW-55F and DEAE-Toyopearl 650M for gel permeation and anion-exchange chromatography, respectively. The use of these packings allowed increased speed of elution without worsening the separation. Typical elution profiles are shown in Fig. 1. After the anion-exchange chromatography and dialysis steps, apo A-I and apo A-II proteins

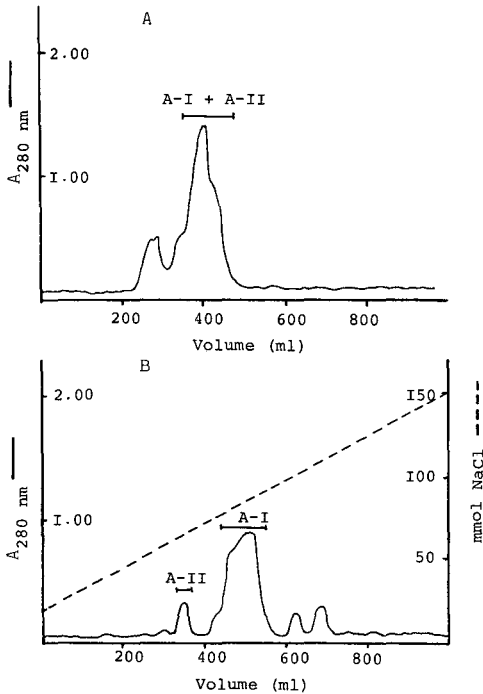


Fig. 1. (A) Toyopearl HW-55F chromatography of delipidated 1.063–1.210 g/ml HDL. Elution buffer, 10 mM Tris-HCl (pH 8.6)–8 M urea; (B) DEAE-Toyopearl 650M chromatography of pooled A-I + A-II-containing fractions. Starting buffer, 10 mM Tris-HCl (pH 8.6)–8 M urea–0.02 M sodium chloride; linear gradient of NaCl from 0.02 to 0.15 M in the same buffer, total gradient volume 1000 ml; flow-rate, 60 ml/h.

proved to be homogeneous according to the SDS-PAGE and urea-PAGE data (not shown).

The apo A-I and apo A-II proteins were desalted using a Toyopearl HW-40F column (both proteins were eluted with the void volume) for the complete removal of urea and inorganic salts.

The homogeneity apo A-I and apo A-II proteins purified by this procedure was confirmed by SDS-PAGE (see Fig. 2, lanes 2, 4, 5 and 7) and urea-PAGE (not shown). Densitometric scanning of these gels gave a single symmetrical peak as an indication of homogeneity. The molecular mass of apo A-I was determined electrophoretically to be near 28 000 and was unaffected by reduction (see Fig. 2, lane 3). The molecular mass of apo A-II was estimated in the same way to be near 17 000, but after reduction gave an estimated molecular mass of about 8600 (see Fig. 2, lanes 5 and 6). These characteristics were appropriate for apo A-I [13] and for apo A-II [14]. No phospholipid was detected in either the isolated apo A-I or apo A-II.

The identity of the isolated proteins with apo A-I and apo A-II was confirmed by immunoelectrophoresis with monospecific antibodies to human apo A-I and apo A-II, respectively [12]. Furthermore, amino acid analyses of the purified apo A-I and apo

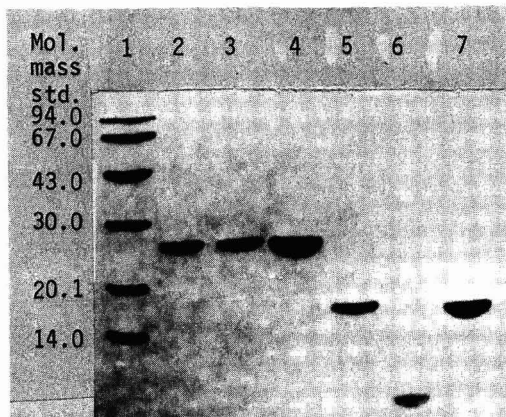


Fig. 2. SDS-PAGE in 15% polyacrylamide gel of purified apo A-I and apo A-II. Lanes: 1 = low-molecular-mass standards from Pharmacia (molecular masses of the standards are those provided by Pharmacia ( $\times 10^{-3}$ )); 2, 3, 4 = 10  $\mu$ g, 10  $\mu$ g (with 2% of 2-mercaptoethanol) and 30  $\mu$ g of purified apo A-I, respectively; 5, 6, 7 = 10  $\mu$ g, 10  $\mu$ g (with 2% of 2-mercaptoethanol) and 30  $\mu$ g of purified apo A-II, respectively. Apo A-I and apo A-II were identified by comparison with known standards.

A-II proteins were compatible with the compositions derived from published sequences (data not shown) [14,15].

Isolated apo A-I and apo A-II proteins were successfully used as immunogens and as standards for assigning values to sera for use as secondary standards.

The efficiency of the described procedure was determined by the real yield of the lyophilized apo A-I and apo A-II proteins. A full cycle of isolation of these proteins from human serum lasted 10–14 days, including the preparation of 1.063–1.210 g/ml HDL. The average amount of the recovered lyophilized protein was about 300 mg per cycle for apo A-I and 60 mg per cycle for apo A-II. The average concentrations of apo A-I and apo A-II in pooled unextracted human serum were 1.5 and 0.4 mg/ml, respectively, according an immunoturbidimetric assay. Hence, the real yields of purified proteins were about 50% and 40% for apo A-I and apo A-II, respectively, taking into account the volume of the initial human serum (about 400 ml).

Unfortunately, in many papers [2,16–18] no data are given that allow the calculation of the real yield of purified apo A-I and apo A-II proteins, which is particularly important when procedures alternative to ultracentrifugation are used [3,4]. The lack of such data makes it impossible to compare these methods with our technique with respect to efficiency.

In conclusion, we have described a method suitable for the large-scale preparation of lyophilized apo A-I and apo A-II from human serum with real yields of purified proteins of about 50% and 40%, respectively. The high degree of purity makes it possible to use the recovered proteins as primary standards for apo A-I and apo A-II immunoassays.

#### ACKNOWLEDGEMENTS

We thank Svetlana Bezruchkina and Natalya Isaeva for excellent technical assistance.

## REFERENCES

- 1 R. B. Gennis and A. Jonas, *Annu. Rev. Biophys. Bioeng.*, 6 (1977) 195.
- 2 G. L. Mills, P. A. Lane and P. K. Weech, in R. H. Burdon and P. H. Van Knippenberg (Editors), *A Guide Book to Lipoprotein Technique*, Elsevier, Amsterdam, 1984, p. 384.
- 3 S. D. Carson, *Biochim. Biophys. Acta*, 750 (1982) 317.
- 4 S. E. Ross and S. D. Carson, *Anal. Biochem.*, 149 (1985) 166.
- 5 R. J. Havel, H. A. Eder and J. H. Bragdon, *J. Clin. Invest.*, 34 (1955) 1345.
- 6 A. B. Sigalov, in preparation.
- 7 U. K. Laemmli, *Nature (London)*, 227 (1970) 680.
- 8 O. H. Lowry, N. J. Rosebrough, A. L. Farr and R. J. Randall, *J. Biol. Chem.*, 133 (1951) 265.
- 9 C. Edelstein, C. T. Lim and A. Scanu, *J. Biol. Chem.*, 247 (1972) 5842.
- 10 G. R. Bartlett, *J. Biol. Chem.*, 234 (1959) 466.
- 11 B. J. Davis, *Ann. N.Y. Acad. Sci.*, 121 (1964) 404.
- 12 H. G. M. Clarke and T. Freeman, *Clin. Sci.*, 35 (1968) 403.
- 13 N. H. Baker, T. Delahunty, A. M. Gotto and R. L. Jacson, *Proc. Natl. Acad. Sci. U.S.A.*, 71 (1974) 3631.
- 14 H. B. Brewer, S. E. Lux, R. Ronan and K. M. John, *Proc. Natl. Acad. Sci. U.S.A.*, 69 (1972) 1304.
- 15 H. B. Brewer, T. Fairwell, A. Larue, R. Ronan, A. Houser and T. J. Bronzert, *Biochem. Biophys. Res. Commun.*, 80 (1978) 623.
- 16 S. E. Lux and K. M. John, *Biochim. Biophys. Acta*, 278 (1972) 266.
- 17 R. L. Jacson and A. M. Gotto, *Biochim. Biophys. Acta*, 285 (1972) 36.
- 18 L. B. Vitello and A. Scanu, *J. Biol. Chem.*, 251 (1976) 1131.



## Note

---

# Preparative high-performance liquid chromatography on chemically modified porous glass

## Isolation of acidic saponins from ginseng

HIDEKO KANAZAWA, YOSHIKO NAGATA, YOSHIKAZU MATSUSHIMA\* and MASASHI TOMODA

*Kyoritsu College of Pharmacy, Shibakoen 1-5-30, Minato-ku, Tokyo 105 (Japan)*

and

NOBUHARU TAKAI

*Institute of Industrial Science, University of Tokyo, Roppongi 7-22-1, Minato-ku, Tokyo 106 (Japan)*

(First received June 5th, 1990; revised manuscript received August 14th, 1990)

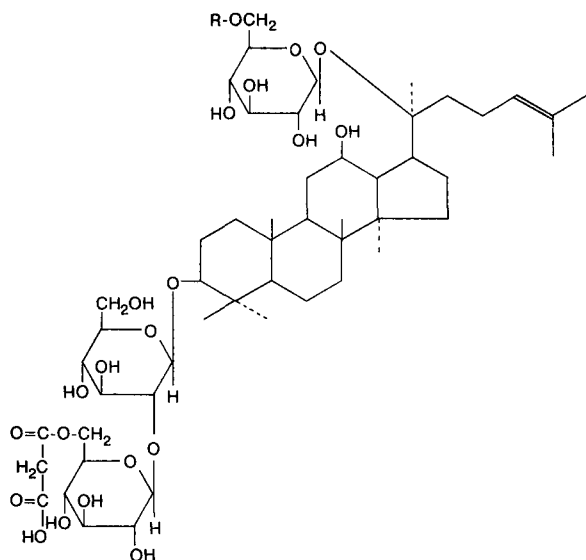
Octadecylsilylated porous glass (MPG-ODS) has been demonstrated to be a useful packing material for reversed-phase high-performance liquid chromatography (HPLC) [1]. It is especially suitable for the determination of saponins of ginseng and bupleum root [2-5]. We recently reported a successful application of a large-scale column of MPG-ODS for the preparative high-performance liquid chromatography (HPLC) of ginsenoside-Rb<sub>1</sub>, -Rc, -Rb<sub>2</sub>, -Rd, -Rg<sub>1</sub> and -Re [6].

Kitagawa *et al.* [7] found that white ginseng contained a considerable amount of acidic malonate of the dammarane saponins malonyl ginsenoside-Rb<sub>1</sub>, -Rb<sub>2</sub>, -Rc and -Rd (Fig. 1). The malonyl ginsenosides are reported to be unstable and readily demalonylated on heating and hence are not present in red ginseng. We have shown that the malonyl ginsenosides could also be determined rapidly and accurately by HPLC on MPG-ODS [4]. These results prompted us to investigate the preparative HPLC of the malonyl ginsenosides, and the results are presented in this paper.

### EXPERIMENTAL

#### *Materials*

Octadecylsilylated porous glass (MPG-ODS) was supplied by Ise Chemical Industries [packed columns of MPG-ODS are now commercially available from Wako (IPG-55-ODS-10H) and Hitachi (Hitachi Gel 3161)]. The particle size of the packing material was 10  $\mu\text{m}$  for the analytical and 20  $\mu\text{m}$  for the preparative columns. Acetonitrile used as the mobile phase in analytical HPLC was of HPLC grade (Wako, Tokyo, Japan). Water was deionized and distilled. Other chemicals were of analytical-reagent grade.



malonyl ginsenoside-Rb<sub>1</sub> : R=  $\beta$ -D-glucopyranosyl

malonyl ginsenoside-Rb<sub>2</sub> : R=  $\alpha$ -L-arabinopyranosyl

malonyl ginsenoside-Rc : R=  $\alpha$ -L-arabinofuranosyl

malonyl ginsenoside-Rd : R=H

Fig. 1. Structure of malonyl ginsenosides.

### Analytical HPLC

The analytical HPLC system was composed of a Tosoh Model CCPM multi-pump, a Rheodyne Model 7125 valve, a Tosoh Model UV-8000 monitor and a Hitachi Model 833A data processor. The system was operated at room temperature. A stainless-steel column (150  $\times$  4 mm I.D.) packed with MPG-ODS was used. The mobile phases were mixtures of acetonitrile and 50 mM KH<sub>2</sub>PO<sub>4</sub> solution at a flow-rate of 1 ml/min. The peaks were monitored at 203 nm unless stated otherwise. A Hitachi Model L-3000 system was used for multi-channel spectrophotometric detection.

### Preparative HPLC

The preparative HPLC system consisted of a Tosoh Model CCPM prep pump, a Model UV-8010 monitor, a Model SC-8010 system controller and data processor, a Model FC-8000 fraction collector and a Model PP-8010 recorder. MPG-ODS was packed into stainless-steel tubing of 500  $\times$  20 mm I.D. and 500  $\times$  50 mm I.D. The peaks were monitored at 203 nm and the system was operated at room temperature.

### Sample preparation from the crude drug

Roots of *Panax ginseng* were pulverized and extracted with 70% methanol at room temperature. The extract was evaporated and dissolved in water. The aqueous solution was passed through a solid phase, Mega Bond Elute (Analytichem International), pretreated with water and methanol. After the solid phase had been washed with water and 30% methanol, the sample was eluted with methanol and the eluate was evaporated to dryness under reduced pressure. The residue was dissolved in the eluent and injected into the preparative HPLC system.

### Purification procedure

The chromatographic fractions were evaporated *in vacuo* to remove acetonitrile or in some instances diluted with water. The aqueous solutions were passed through a Sep-Pak C<sub>18</sub> cartridge (Waters Assoc., Milford, MA, U.S.A.) pretreated with methanol and the cartridge was washed with water and 30% methanol. The saponins were eluted with methanol and the eluate was evaporated to dryness under reduced pressure. The residue was dissolved in water and freeze-dried.

### RESULTS

The determination of neutral ginsenosides by HPLC on an MPG-ODS column was successful with the use of mixtures of acetonitrile and water as the mobile phase [2,3,5]. For the determination of acidic saponins of ginseng, bupleum root and glycyrrhiza by the method, addition of inorganic phosphate to the mobile phases was required [4]. The mobile phases used in preparative HPLC were mixtures of acetonitrile and 50 mM KH<sub>2</sub>PO<sub>4</sub> solution. A mobile phase containing 25% acetonitrile was used for the separation of the malonyl ginsenosides on the 500 × 20 mm I.D. column. The flow-rate was 15 ml/min and the pressure was 55 kg/cm<sup>2</sup>. In a run, an extract from 0.5 g of ginseng root was injected in the HPLC system. The chromatogram is shown in Fig. 2.

The three malonyl ginsenosides were separated within 45 min and the average yields were 2.0 mg of purified malonyl ginsenoside-Rb<sub>1</sub>, 1.1 mg of malonyl ginsenoside-Rc and 0.9 mg of malonyl ginsenoside-Rb<sub>2</sub> per gram of ginseng root.

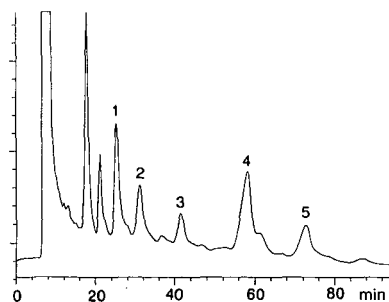


Fig. 2. Preparative chromatogram of a ginseng extract. Peaks: 1 = malonyl ginsenoside-Rb<sub>1</sub>; 2 = malonyl ginsenoside-Rb<sub>2</sub>; 3 = malonyl ginsenoside-Rc; 4 = ginsenoside-Rb<sub>1</sub>; 5 = ginsenoside-Rc. Column, MPG-ODS (500 × 20 mm I.D., particle size 20 μm); an extract from 0.5 g of ginseng was injected; eluent, acetonitrile-50 mM KH<sub>2</sub>PO<sub>4</sub> (25:75); flow-rate, 15.0 ml/min; detection, 203 nm.

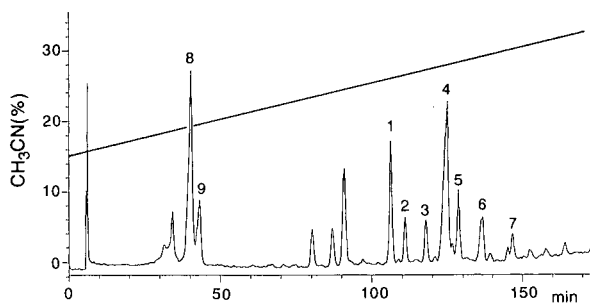


Fig. 3. Preparative chromatogram of a ginseng extract. Peaks: 1 = malonyl ginsenoside-Rb<sub>1</sub>; 2 = malonyl ginsenoside-Rc; 3 = malonyl ginsenoside-Rb<sub>2</sub>; 4 = ginsenoside-Rb<sub>1</sub>; 5 = ginsenoside-Rc; 6 = ginsenoside-Rb<sub>2</sub>; 7 = ginsenoside-Rd; 8 = ginsenoside-Rg<sub>1</sub>; 9 = ginsenoside-Re. Column, MPG-ODS (500 × 20 mm I.D., particle size 20 μm); an extract from 0.4 g of ginseng was injected; eluent, acetonitrile-50 mM KH<sub>2</sub>PO<sub>4</sub> with acetonitrile concentrations as plotted on the ordinate; flow-rate, 20.0 ml/min; detection, 203 nm.

The isolation of both the major acidic and neutral ginsenosides in a single run on the 500 × 20 mm I.D. column was achieved by linear gradient elution from 15% to 50% acetonitrile in 180 min at a flow-rate of 20 ml/min. As shown in Fig. 3, the peaks of six neutral saponins (peaks 4–9) and three acidic saponins (peaks 1–3) were well resolved. Under the conditions applied, ginsenoside-Rg<sub>1</sub>, -Re, -Rb<sub>1</sub>, -Rc, -Rb<sub>2</sub> and -Rd and malonyl ginsenoside-Rb<sub>1</sub>, -Rb<sub>2</sub> and -Rc were isolated within 180 min.

Preparative HPLC on the 500 × 50 mm I.D. column was carried out using step gradient elution. The mobile phase compositions were acetonitrile 20% at 0–100 min and 25% at 100–220 min with a flow-rate of 39.9 ml/min and a pressure of 40 kg/cm<sup>2</sup>. The chromatogram is shown Fig. 4. In a single run, 5.5 mg of pure malonyl ginsenoside-Rb<sub>1</sub>, 3.5 mg of malonyl ginsenoside-Rb<sub>2</sub> and 2.9 mg of malonyl ginsenoside-Rc were separated from 8 g of ginseng roots.

The purity of the collected fractions was monitored by analytical HPLC. A multi-channel spectrophotometer was also employed for the detection of UV-absorbing impurities. Each fraction gave a single chromatographic peak and did not

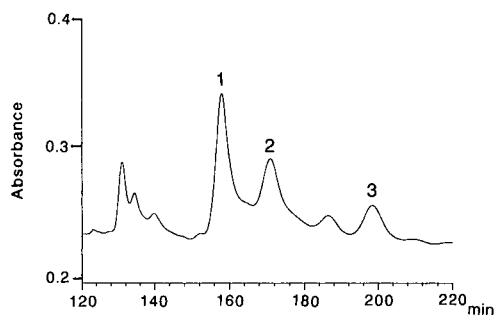


Fig. 4. Preparative chromatogram of a ginseng extract. Peaks: 1 = malonyl ginsenoside-Rb<sub>1</sub>; 2 = malonyl ginsenoside-Rc; 3 = malonyl ginsenoside-Rb<sub>2</sub>. Column, MPG-ODS (500 × 50 mm I.D., particle size 20 μm); an extract from 8.0 g of ginseng was injected; eluent, 0–100 min, acetonitrile-50 mM KH<sub>2</sub>PO<sub>4</sub> (20:80), and 100–220 min, acetonitrile-50 mM KH<sub>2</sub>PO<sub>4</sub> (25:75); flow-rate, 39.9 ml/min; detection, 203 nm.

contain any detectable UV-absorbing impurities. The retention times and UV spectra were the same as those for authentic samples of the assigned peaks. The fractions were also analysed by the thin-layer chromatography (TLC) with the lower layer of chloroform-methanol-water (13:7:2) as the solvent. A single TLC spot with the same  $R_F$  value as that for an authentic sample was observed for each fraction. The fractions were evaporated and freeze-dried as described under Experimental. White crystalline products were obtained.

#### DISCUSSION

There have been several reports [8-12] on the preparative-scale HPLC of neutral saponins from *Panax ginseng*. In a previous paper, we reported the preparative HPLC of neutral ginsenosides on MPG-ODS columns [6]. However, no report on the preparative HPLC of malonyl ginsenosides has appeared previously.

Malonyl ginsenosides were successfully separated by preparative HPLC on a reversed-phase column of MPG-ODS chemically modified porous glass as described above. The MPG-ODS column achieved the rapid analysis of neutral and acidic ginsenosides [2,4]. Retention times for the panaxatriol ginsenosides were almost half those on silica-ODS columns [13]. The rapid separation renders savings of time and solvent in the HPLC procedure. The proportion of organic solvent in the mobile phase was much smaller in HPLC with MPG-ODS than with silica-ODS columns. As we use large volumes of solvents in the preparative-scale HPLC, the savings in organic solvent are advantageous from both economical and environmental points of view.

A pore size of 550 Å seems to be favourable for the separations of ginsenosides and related saponins. The sharp separation of the peaks may be due to the narrow distribution range of the pore size [1,6]. The column was not suitable for the compounds of smaller molecular size [14].

As the ginsenosides and malonyl ginsenosides were well resolved on the preparative scale at room temperature, the method was suitable for the preparative separation of heat-unstable acidic saponins. The mobile phase for preparative HPLC contained inorganic phosphate, which must be removed from the separated fractions. It was easily removed by the solid-phase extraction technique.

In conclusion, the method is simple, rapid and convenient and is suitable for the purification of heat-unstable malonyl ginsenosides. It should be applicable to the isolation of other saponins of crude drugs. The MPG-ODS column has a number of advantages over conventional normal- and reversed-phase columns for the chromatography of saponins.

#### ACKNOWLEDGEMENTS

This work was supported in part by the Science Research Promotion Fund of the Japan Private School Promotion Foundation and by Ise Chemical Industries. Technical assistance by Emi Kurosaki, Fumiko Ishii and Tomomi Yoshinaga is gratefully acknowledged.

## REFERENCES

- 1 Y. Matsushima, Y. Nagata, K. Takakusagi, M. Niyomura and N. Takai, *J. Chromatogr.*, 332 (1985) 265.
- 2 H. Kanazawa, Y. Nagata, Y. Matsushima, M. Tomoda and N. Takai, *Chromatographia*, 24 (1987) 517.
- 3 H. Kanazawa, Y. Nagata, Y. Matsushima, M. Tomoda and N. Takai, *Shoyakugaku Zasshi*, 43 (1989) 121.
- 4 N. Takai, H. Kanazawa, Y. Nagata, Y. Matsushima and M. Tomoda, *Seisan Kenkyu*, 41 (1989) 773.
- 5 H. Kanazawa, Y. Nagata, Y. Matsushima, M. Tomoda and N. Takai, *J. Chromatogr.*, 507 (1990) 327.
- 6 H. Kanazawa, Y. Nagata, Y. Matsushima, M. Tomoda and N. Takai, *Chem. Pharm. Bull.*, 38 (1990) 1630.
- 7 I. Kitagawa, T. Taniyama, T. Hayashi and M. Yosikawa, *Chem. Pharm. Bull.*, 31 (1983) 3353.
- 8 T. Nagasawa, T. Yokozawa, Y. Nishino and H. Oura, *Chem. Pharm. Bull.*, 28 (1980) 2059.
- 9 T. Nagasawa, T. Yokozawa, Y. Nishino and H. Oura, *Chem. Pharm. Bull.*, 28 (1980) 3701.
- 10 J. Zhou, M. Z. Wu, S. Taniyasu, H. Besso, O. Tanaka, Y. Saruwatari and T. Fuwa, *Chem. Pharm. Bull.*, 29 (1981) 2844.
- 11 H. Kaizuka and K. Takahashi, *J. Chromatogr.*, 258 (1983) 235.
- 12 H. Yamaguchi, H. Matsuura, R. Kasai, K. Mizutai, H. Fujino, K. Ohtani, T. Fuwa and O. Tanaka, *Chem. Pharm. Bull.*, 34 (1986) 2856.
- 13 T. G. Petersen and B. Palmqvist, *J. Chromatogr.*, 504 (1990) 139.
- 14 Y. Nagata, Y. Kim, Y. Nakamichi, Y. Matsushima and N. Takai, *Annu. Rep. Kyoritsu Coll. Pharm.*, 34 (1989) 39.

## Note

# High-performance liquid chromatography of substituted trinuclear osmium carbonyl clusters, $\text{Os}_3(\text{CO})_{12-n}[\text{P}(\text{C}_6\text{F}_5)_3]_n$ ( $n = 0, 1, 2$ )

H. G. ANG\*, W. L. KWIK and W. K. LEONG

*Department of Chemistry, National University of Singapore, Lower Kent Ridge Road, Singapore 0511 (Singapore)*

(First received March 27th, 1990; revised manuscript received August 20th, 1990)

The advantages of high-performance liquid chromatography (HPLC) over thin-layer chromatography (TLC) and column chromatography (CC) for the separation and purification of organometallic compounds and metal clusters have been well recognized [1]. These include better resolution, inert separation conditions, quantitative recovery and the relatively small sample sizes required. In particular, as an osmium carbonyl cluster reaction often yields a host of closely related products it has become desirable to establish a HPLC method that offers not only quantitative separation but also unequivocal identification of the chromatographic peaks. The latter would be especially useful in instances of incompletely resolved chromatographic peaks. Efforts towards these ends have led to two recent reports [2,3] on the HPLC study of various osmium carbonyl clusters.

In our laboratory, a systematic study is currently being carried out to elucidate the retention mechanism and hence identify the relevant parameters that are crucial to a satisfactory separation of substituted osmium carbonyl clusters. This paper presents the findings of a study of the normal- and reversed-phase chromatographic behaviour of several substituted phosphine clusters and compares them with those for the acetonitrile complexes of osmium reported earlier.

## EXPERIMENTAL

### *Preparation and stabilities of samples*

The preparation of  $\text{Os}_3(\text{CO})_{11}[\text{P}(\text{C}_6\text{F}_5)_3]$  (I) has been reported elsewhere [4].  $\text{Os}_3(\text{CO})_{10}[\text{P}(\text{C}_6\text{F}_5)_2]$  (II) was prepared by heating the bisacetonitrile complex  $\text{Os}_3(\text{CO})_{10}(\text{CH}_3\text{CN})_2$  and  $(\text{C}_6\text{F}_5)_3\text{P}$  (2 equiv.) in *n*-hexane at 70°C for 1 h, and purified by TLC on silica using hexane-dichloromethane (90:10) as eluent. Its m.p. is 179–181°C. It was characterized by IR, NMR and elemental analyses. Elemental analysis (calculated values in parentheses):  $\text{Os}_3(\text{CO})_{10}[\text{P}(\text{C}_6\text{F}_5)_2]$  (II), C 29.4 (28.8), P 3.37 (3.24), F 30.0 (29.8)%.  $^{19}\text{F}$  NMR ( $\text{CD}_3\text{Cl}$ ):  $\delta$  -51.4(s), -69.3(q) and -81.6(t)

ppm (reference: trifluoroacetic acid).  $^{31}\text{P}$  NMR ( $\text{CD}_3\text{Cl}$ ):  $\delta -90.7$  ppm. IR ( $\text{CH}_2\text{Cl}_2$ ):  $\nu$  (CO) 2107s, 2056vs, 2042vs, 2024vs, 1992s and 1983s. The clusters  $\text{Os}_3(\text{CO})_{12}$  (III),  $\text{Os}_3(\text{CO})_{11}(\text{CH}_3\text{CN})$  (IV) and  $\text{Os}_3(\text{CO})_{10}(\text{CH}_3\text{CN})_2$  (V) were prepared according to literature methods [5–7].

The chromatogram of each compound was determined in order to establish that the sample contained only a single component in each instance. Further, the stabilities of I–V in methanol, acetonitrile, *n*-hexane and dichloromethane were checked by monitoring the solution UV spectra of these compounds in the respective solvents. No apparent decomposition was detected up to 8 h. All chromatographic runs were made using freshly prepared solutions, however.

#### Instrumental method

HPLC separations were done on a Hewlett-Packard HP 1090 liquid chromatograph equipped with a Model 1040A diode-array detector, an HP 85B personal computer and a Model 3392A integrator.

The columns used were HP-100, 10  $\mu\text{m}$  (250  $\times$  4.6 mm I.D.) for normal-phase analysis and LiChrosorb 100 CH-18/2, 5  $\mu\text{m}$  (250  $\times$  4 mm I.D.) for reversed-phase analysis. The mobile phases were dichloromethane–*n*-hexane (5:95) at a flow-rate of 1.0 ml/min and acetonitrile–methanol (55:45) at a flow-rate of 0.5 ml/min for normal- and reversed-phase separations respectively. The temperature in all the runs was 35°C.

All solvents were of HPLC grade and were filtered and degassed in helium prior to use. Samples were dissolved in premixed mobile phases filtered through a 0.45- $\mu\text{m}$  pore filter and injected in 5- $\mu\text{l}$  volumes with a Rheodyne Model 7010 injector.

The column dead volume was determined using *n*-hexane for the silica column with dichloromethane as mobile phase. For the  $\text{C}_{18}$  column, this was determined with reference to the first baseline peak which appeared on injection [8].

All retention times and volumes were corrected for dead volumes due to connecting tubings.

#### RESULTS AND DISCUSSION

Figs. 1 and 2 show chromatograms of the osmium clusters. Good baseline

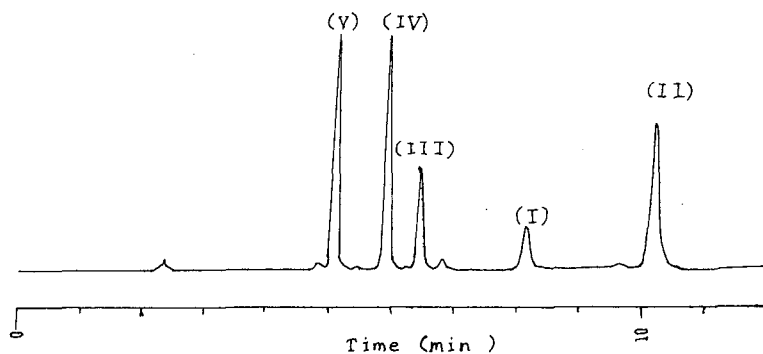


Fig. 1. Separation of  $\text{Os}_3(\text{CO})_{11}[\text{P}(\text{C}_6\text{F}_5)_3]$  (I),  $\text{Os}_3(\text{CO})_{10}[\text{P}(\text{C}_6\text{F}_5)_3]_2$  (II),  $\text{Os}_3(\text{CO})_{12}$  (III),  $\text{Os}(\text{CO})_{11}(\text{CH}_3\text{CN})$  (IV) and  $\text{Os}_3(\text{CO})_{10}(\text{CH}_3\text{CN})_2$  (V) on a LiChrosorb 100 CH-18/2 column. Mobile phase, acetonitrile–methanol (55:45); detection, UV (254 nm).



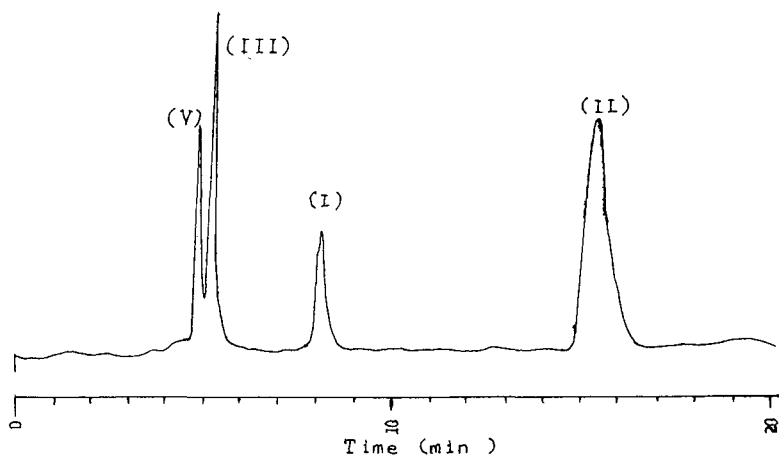


Fig. 2. Separation of  $\text{Os}_3(\text{CO})_{11}[\text{P}(\text{C}_6\text{F}_5)_3]$  (I),  $\text{Os}_3(\text{CO})_{10}[\text{P}(\text{C}_6\text{F}_5)_3]_2$  (II),  $\text{Os}_3(\text{CO})_{12}$  (III) and  $\text{Os}_3(\text{CO})_{10}(\text{CH}_3\text{CN})_2$  (V) on an HP silica-100 column. Mobile phase, dichloromethane-*n*-hexane (5:95); flow-rate,  $1.0 \text{ cm}^3 \text{ min}^{-1}$ ; detection, UV (230 nm).

separation was observed for all five compounds I–V on the  $\text{C}_{18}$  column with the mobile phase employed. For the normal-phase separation, chromatographic peaks due to I, II, V, III (or IV) are well resolved. Over a range of mobile phases with various proportions of dichloromethane in *n*-hexane, III and IV eluted at nearly the same time in each instance.

The capacity factor  $k'$  and the theoretical plate number  $N$  were evaluated for all chromatographic peaks in reversed- and normal-phase separations (Table I) [9]. The  $k'$  values fall into the optimum range of  $0.5 < k' < 5$ .

The  $N$  values of 58 000–76 000 in the reversed-phase separation are comparable to the expected value of 80 000 for a column of the given specifications. Those in the normal-phase separation, in the range 11 000–13 000 are low in comparison with the values evaluated using standard equations for a well packed column of the given specifications [9]. However, for most practical applications these values are acceptable [10].

The elution order of I, II and III on the reversed-phase column is such that the retention volumes increase with increasing number of phenyl groups resulting in III being eluted first followed by I and then II. The retardation of clusters containing triarylphosphine ligands has been reported for both reversed- and normal-phase separations of a series of derivatives of the tetranuclear clusters  $(\text{Cp})\text{NiOs}_3(\mu\text{-H})_3(\text{CO})_8\text{L}$  [11–13] [ $\text{Cp}$  = cyclopentadienyl;  $\text{L}$  = CO,  $\text{PPh}_2\text{H}$ ,  $\text{Ph}_3$  and  $\text{P}(o\text{-tolyl})_3$ ]. The differences in retention volumes of that series of compounds were correlated with the different degrees of steric hindrance with the derivative containing the largest aryl group (tris-tolyl) being eluted last. For the clusters III, IV and V, their relative solubilities in the mobile phase appear to be the dominant factor. Thus V has the highest solubility and is eluted first, followed by IV and finally III. Current theories on the retention mechanism of chemically bonded phases [14–16] are in support of these correlations.

TABLE I  
CAPACITY FACTORS ( $k'$ ) AND NUMBER OF THEORETICAL PLATES ( $N$ ) UNDER (A) REVERSED-PHASE AND (B) NORMAL-PHASE CONDITIONS

Parameter	$Os_3(CO)_{1,0}(CH_3CN)_2$		$Os_3(CO)_{1,1}(CH_3CN)$		$Os_3(CO)_{1,2}$		$Os_3(CO)_{1,1}P(C_6F_5)_3$		$Os_3(CO)_{1,0}P(C_6F_5)_3$	
	A <sup>a</sup>	B <sup>b</sup>	A	B	A	B	A	B	A	B
$k'$	1.48	0.78	1.89	0.92	2.16	2.01	3.00	2.01	4.03	4.70
$N$ ( $m^{-1}$ )	58 190	11 500	68 060	13 000	72 010	12 670	75 390	12 670	76 740	12 640

<sup>a</sup>  $t_0 = 2.00$ .

<sup>b</sup>  $t_0 = 2.68$ .

Polar interactions between the silica surface and the ligands apparently determine the order of elution for the normal-phase separation. Thus the retention volumes increase with the number of substituted phosphines  $[P(C_6F_5)_3]$  for I, II and III, and with the number of carbonyls for III and V. The larger differences in retention volumes among I, II and III than between III and IV are consistent with the more polar character of the  $P(C_6F_5)_3$  group relative to the carbonyl which, on the other hand, is more similar to acetonitrile.

In most chromatographic studies, it has often been assumed that the relative retention time of each compound remains unchanged on going from a pure sample to a mixture. Moreover, two closely overlapped peaks may be mistaken as being due to a single component. In an effort to establish unequivocally the identity and purity of the observed chromatographic peaks, the absorption spectra of the eluates at the specified time corresponding to the peak maxima were determined using a photo-diode-array detector and an evaluation program of the Data Evaluation Pack software

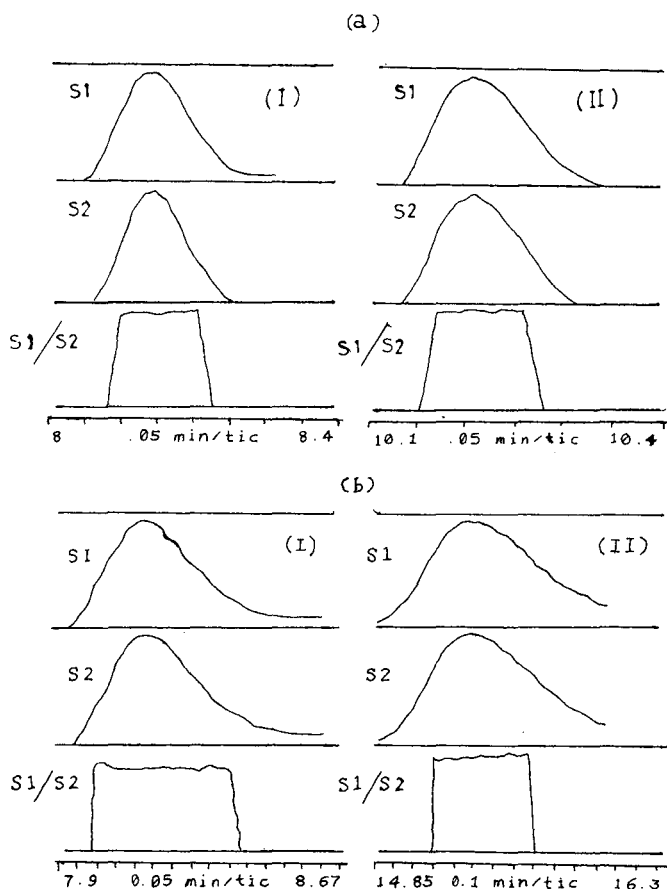


Fig. 3. Signal plots at 230 nm (S1), 254 nm (S2) and ratio plots (S1/S2) for  $Os_3(CO)_{11}[P(C_6F_5)_3]$  (I) and  $Os_3(CO)_{10}[P(C_6F_5)_3]_2$  (II) under (a) reversed-phase and (b) normal-phase conditions.

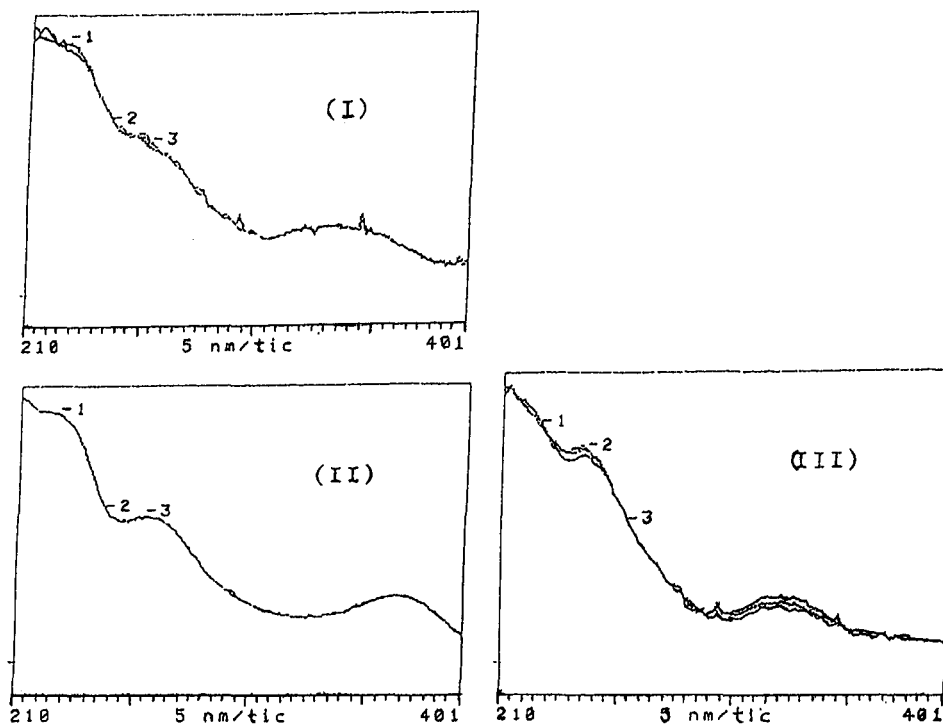


Fig. 4. Overlays of spectra at (1) upslope, (2) apex and (3) downslope for reversed-phase separation of  $\text{Os}_3(\text{CO})_{11}[\text{P}(\text{C}_6\text{F}_5)_3]$  (I)  $\text{Os}_3(\text{CO})_{10}[\text{P}(\text{C}_6\text{F}_5)_3]_2$  (II) and  $\text{Os}_3(\text{CO})_{12}$  (III).

of the HP 85B computer. Comparisons of the spectra thus obtained with the individual spectra of the five compounds which were determined separately on a Perkin-Elmer Lambda-9 spectrophotometer established unequivocally the identities of the observed chromatographic peaks as given in Figs. 1 and 2.

Further, the purity of each of the chromatographic peaks was verified through determinations of (a) the ratios of the heights of a chromatographic peak monitored at two or more wavelengths and (b) the overlay of the absorption spectra at three different points (upslope, apex and downslope) of each peak. For a pure chromatographic peak, the ratio of two signals across a peak elution profile should remain fairly constant. Some typical ratio plots and plots of spectral overlays of selected chromatographic peaks are given in Figs. 3 and 4. Using these methods, each of the chromatographic peaks in the reversed-phase separation was found to correspond to a single osmium cluster. For the normal-phase separation, peaks corresponding to I, II and V are pure whereas the peak due to the overlap of III and IV is characterized by a varying ratio plot and also an ill-matched spectral overlay.

## REFERENCES

- 1 A. Casoli, A. Mangia and G. Predieri, *Chem. Rev.*, 89 (1989) 407.
- 2 R. Khattar, B. F. G. Johnson and J. Lewis, *J. Organomet. Chem.*, 334 (1988) 221.
- 3 H. G. Ang, W. L. Kwik and W. K. Leong, *J. Organomet. Chem.*, 379 (1989) 325.
- 4 H. G. Ang, W. L. Kwik and W. K. Leong, *Acta Crystallogr.*, Sect. C, 45 (1989) 1713.
- 5 B. F. G. Johnson, J. Lewis and P. A. Kilty, *J. Chem. Soc. A*, (1968) 2859.
- 6 B. F. G. Johnson, J. Lewis and D. Pippard, *J. Organomet. Chem.*, 145 (1978) C4.
- 7 M. Tachikawa and J. R. Shapley, *J. Organomet. Chem.*, 124 (1977) C19.
- 8 W. L. Hine, T. E. Riene, D. W. Armstrong, DeMond, A. Ala and T. Ward, *Anal. Chem.*, 57 (1985) 237.
- 9 L. R. Snyder, in C. Horváth (Editor), *J. High Performance Liquid Chromatography: Advances and Perspectives*, Vol. 3, Academic Press, New York, 1983, Ch. 5.
- 10 V. R. Meyer, *J. Chromatogr.*, 334 (1985) 197.
- 11 A. Casoli, A. Mangia, G. Predieri and E. Sapa, *J. Chromatogr.*, 447 (1988) 187.
- 12 A. Casoli, A. Mangia and G. Predieri, *Anal. Chim. Acta*, 176 (1985) 259.
- 13 A. Casoli, A. Mangia, G. Predieri and G. Sappa, *Anal. Chim. Acta*, 152 (1984) 289.
- 14 K. A. Dill, *J. Phys. Chem.*, 91 (1987) 1980.
- 15 D. E. Martire and R. E. Boehm, *J. Phys. Chem.*, 87 (1983) 1045.
- 16 P. T. Ying, J. G. Dorsey and K. A. Dill, *Anal. Chem.*, 61 (1989) 2540.

## Note

---

# Liquid crystals for the gas chromatographic determination of the stereochemistry of insect sex pheromones<sup>a</sup>

I. NESTEROVA\*, B. REKHTER and G. ROSHKA

*All-Union Institute for Biological Control, Prospekt Mira 58, Kishinev 277072 (U.S.S.R.)*

and

Z. WITKIEWICZ

*Institute of Chemistry, Military Technic Academy, 01-489 Warsaw 49 (Poland)*

(First received April 25th, 1990; revised manuscript received June 19th, 1990)

Many of the insect sex pheromones that have been identified are linear aliphatic alcohols, aldehydes or acetates, with a chain length of 12–18 carbon atoms and one or two olefinic linkages. If synthetic pheromones are to be used in pest management, a precise knowledge of their isomeric purity is required because their biological activity depends on the stereochemistry of the product synthesized.

Various techniques may be used for the determination of the geometric isomers of insect sex pheromones. The analytical and semi-preparative separations were performed on silver nitrate-coated silica gel on thin-layer plates or in columns [1]. However, none of these methods was convenient or accurate enough for the detection of isomeric impurity.

There have been several reports on the use of high-performance liquid chromatographic (HPLC) columns with silver nitrate-coated silica. HPLC of the olefinic pheromones on silver nitrate-coated silica gel with benzene as mobile phase has been described [2]. Another approach was the use of silver nitrate-containing isopropanol as the mobile phase and LiChrosorb RP-8 reversed stationary phase for the HPLC separation of aliphatic unsaturated pheromones [3]. Houx and Voerman [4] reported the HPLC of acetates of olefinic long-chain alcohols at moderate pressures on a silicagel-based, strongly acidic ion exchanger loaded with silver ions and using methanol as mobile phase. A practical, reproducible procedure developed to prepare analytical and preparative silver nitrate-coated silica columns for the separation of geometric isomers of pheromones with one and two double bonds was described by Heath *et al.* [5]. Heath and Sonnet [6] developed a method for the *in situ* coating of silver nitrate onto silica gel in HPLC columns, and effectively separated a series of

---

<sup>a</sup> Presented at the 11th International Symposium on Biomedical Applications of Chromatography and Electrophoresis, Tallin, April 24–28th 1990.

geometric isomers. However, HPLC currently suffers from a lack of detection sensitivity, which precludes its use to submicrogram levels for the identification of natural pheromones.

The development of high-polarity stationary phases has made possible the analysis of isomeric pheromones on packed gas chromatographic (GC) columns [7]. However, the resolution of the isomers of conjugated dienes on packed columns is not good. Many investigators have made use of capillary columns with diethylene glycol succinate [8–12], 1,2,3-tris( $\beta$ -cyanethoxy)propane [13] or cyanopropylsiloxane [14] for the determination of the geometric and positional isomers of mono- and diunsaturated alcohols and their derivatives. However, it is difficult to obtain high-efficiency capillary columns with polar stationary phases, which are necessary to obtain satisfactory resolution of the geometric isomers of many known pheromones.

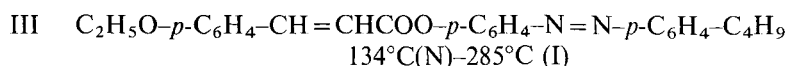
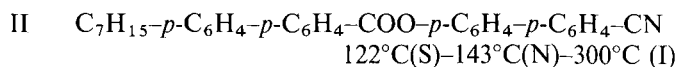
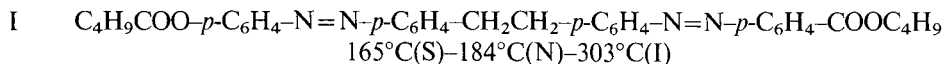
Recently many workers have used liquid crystals as GC stationary phases which exhibit unique selectivity towards geometric isomers. A smectic liquid crystal, diethyl 4,4'-azoxydicinnamate, was reported [15] as a GC stationary phase for the rapid and efficient analysis of mono- and diunsaturated conjugated long-chain acetates and aldehydes, which have previously only been separated on capillary GC columns, and also some pheromone isomers which have not yet been separated even by this method. A packed GC column was used. However, this liquid crystalline phase was unsuitable for the direct determination of the corresponding alcohols. The nematic liquid crystal 4-(*p*-methoxycinnamyloxy)-4'-methoxyazobenzene has been found [16] to exhibit similar chromatographic properties to the above smectic liquid crystal, but it allowed the direct chromatography of alcohols.

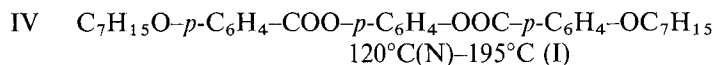
Several reports have been published [12,17,18] concerning the use of cholesteric liquid crystals that showed potential as stationary phases in the separation of aliphatic insect pheromone geometric isomers by capillary GC. The unique resolving power of the liquid crystalline stationary phase was coupled with the high efficiency of the capillary column.

Interest in liquid crystals is increasing because of their unique abilities in the separation and analysis of many mixtures. In this work, an attempt was made to apply liquid crystals containing benzene rings as stationary phases for the separation of *trans* and *cis* isomers of aliphatic acetates with 10–13 carbon atoms and one and two unsaturated bonds and to establish their chromatographic properties in detail.

## EXPERIMENTAL

The liquid crystalline stationary phases tested have the following formulae:





The liquid crystals I, II and III were obtained from the Institute of Chemistry, Military Technical Academy (Warsaw, Poland) and IV from Reakhim (U.S.S.R.). Stationary phase I melts at 165°C and is converted into the smectic phase; the transition to the nematic phase takes place at 184°C and to the isotropic liquid at 303°C. Liquid crystals III and IV have only a nematic mesophase, ranging from 134 to 285°C and from 120 to 195°C, respectively.

The liquid crystalline stationary phases I, II and III were deposited on Chromosorb W AW DMCS (80–100 mesh) (Applied Science Labs., State College, PA, U.S.A.) and IV on Chromaton N-Super (0.125–0.16 mm) (Chemapol, Prague, Czechoslovakia) from chloroform solution by evaporation of the solvent in a rotary vacuum evaporator. The packings were then dried and screened. Glass columns of 3 mm I.D. filled with packings prepared in this way were placed in the thermostat of a Tswet Model 100 gas chromatograph (U.S.S.R.) equipped with a flame ionization detector. The temperature of the column was increased at 2°C/min and the carrier gas (nitrogen) flow-rate was 20 ml/min. The columns were conditioned at 200°C for 7 h. The characteristics of the prepared columns are given in Table I.

The stationary phases were tested at temperatures ranging from 200 to 100°C during cooling of the columns. The highest temperature was limited by the thermal stability of the liquid crystals.

Efficiency, selectivity and retention data tests were carried out using a mixture of *trans,cis*- and *cis,cis*-7,9-dodecadienyl acetate. The retention times of the *n*-alkanes were used for calculating the dead time and the retention indices of the geometric isomers. The Kováts retention indices and efficiencies were calculated from generally known equations.

The selectivities (*r*) of the liquid crystalline stationary phases were determined from the dependence of the relative retention time and the Kováts retention indices of *trans,cis*- and *cis,cis*-7,9-dodecadienyl acetate on temperature. The selectivity is equal to the ratio of the adjusted retention time of *cis,cis*-7,9-dodecadienyl acetate to that of *trans,cis*-7,9-dodecadienyl acetate ( $r = t'_{ZZ}/t'_{EZ}$ ).

The efficiency of the column was expressed in terms of the height equivalent to a real plate (HERP).

TABLE I  
CHARACTERISTICS OF THE COLUMNS

Column	Stationary phase	Amount of phase on the support (%)	Column length (m)
1	I	10.0	3
2	II	7.5	3
3	III	7.5	2
4	IV	7.5	3



## RESULTS AND DISCUSSION

Fig. 1. shows the dependence of the efficiency on temperature for columns 1–4. Higher efficiencies are obtained for columns containing stationary phases IV, II and III (0.51, 1.1 and 1.6 mm, respectively). It can be seen that the efficiencies are greatest at the crystallization points of the liquid crystals and in the range of their transitions from the mesophase to the solid state. The lowest efficiency is shown by the column 1, and is distinctly lower than those of the other columns. Its efficiency is optimum over the temperature range 190–200°C, which corresponds to the nematic phase of the liquid crystal I.

The dependence of the Kováts retention indices for *trans,cis*- and *cis,cis*-7,9-dodecadienyl acetate on temperature for stationary phases I–IV is shown in Fig. 2. These dependences for stationary phases I and IV are linear, corresponding to the equation  $I = at + b$ . In these instances all the phase transitions are seen distinctly and affect the values of the coefficients in the equation. The Kováts retention indices of *trans,cis* and *cis,cis* isomers increase with increasing temperature and the difference between the retention indices reached a maximum value of 33 units at 200°C for liquid crystal I. The Kováts retention indices of *trans,cis*- and *cis,cis*-7,9-dodecadienyl acetate decrease with decreasing temperature in the nematic state of liquid crystal IV and rise distinctly after its crystallization (120°C). The difference between the retention indices of isomers is 19 units on supercooling and transition of the stationary phase to the solid state. The Kováts retention indices of the isomers decrease insignificantly with a decrease in temperature from 200 to 120°C in the nematic and smectic ranges of liquid crystal II and decrease distinctly when the stationary phase adopts the solid state. The maximum difference between the Kováts retention indices of *cis,cis*- and *trans,cis*-7,9-dodecadienyl acetate (38 units) is observed with stationary phase III. In this instance the transition from the nematic phase to the solid state is not observed. However, the greatest difference between the Kováts retention indices of the *cis,cis* and *trans,cis* isomers (59 units) is achieved for this stationary phase at 200°C.

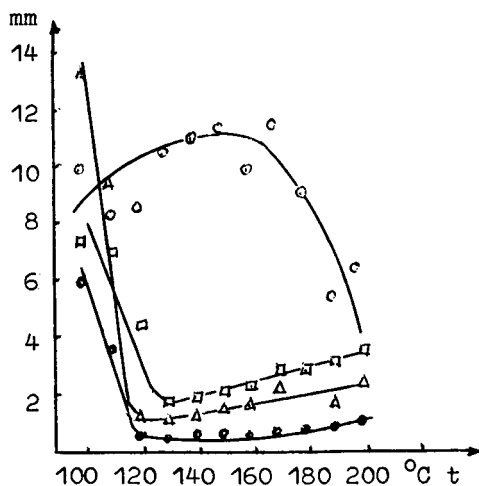


Fig. 1. Temperature dependence of the real plate height for phases (○) I, (△) II, (□) III and (●) IV.

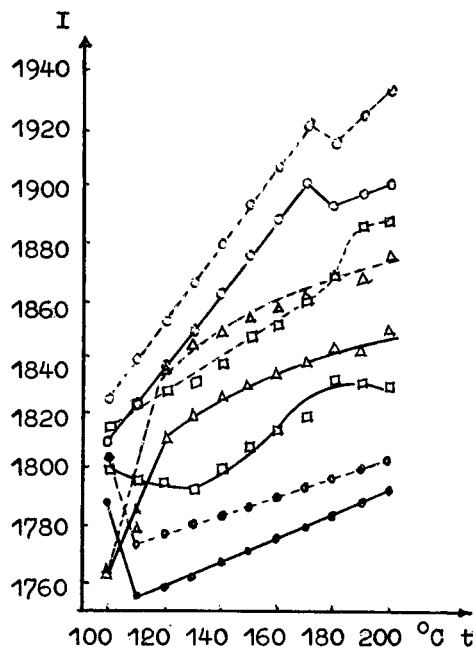


Fig. 2. Temperature dependence of the Kováts retention indices of *trans,cis*- (solid lines) and *cis,cis*-7,9-dodecadienyl acetate (dashed lines) on phases (○) I, (△) II, (□) III and (●) IV.

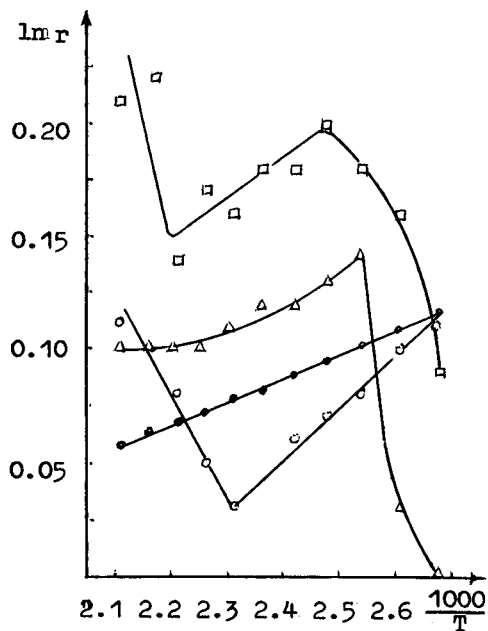


Fig. 3. Temperature dependence of the relative retention times of *cis,cis*- and *trans,cis*-7,9-dodecadienyl acetate on phases (○) I, (△) II, (□) III and (●) IV.

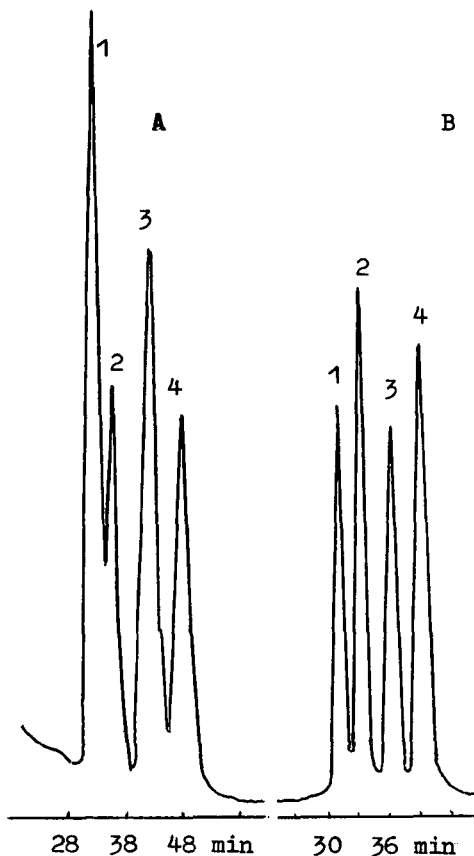


Fig. 4. Separation of the geometric isomers of the European grape vine moth pheromone on the liquid crystalline stationary phases: (1) *cis,trans*-, (2) *trans,cis*-, (3) *cis,cis*- and (4) *trans,trans*-7,9-dodecadienyl acetate. (A) Column III, temperature 130°C; (B) column IV, temperature 160°C.

Fig. 3. shows variation of selectivity expressed as the logarithm of the relative retention times of *cis,cis*- and *trans,cis*-7,9-dodecadienyl acetate with temperature. The highest selectivity is obtained for the liquid crystalline stationary phase III. Phases I, II and IV have lower selectivities than III. The plots differ considerably. The transition is not observed for the liquid crystals III and IV.

The knowledge of the temperature dependence of the selectivity and efficiency gave the possibility of establishing the optimum temperature conditions where the column has the best separating properties with respect to the geometric isomers of the compounds studied. Fig. 4 shows examples of such separations.

#### CONCLUSIONS

The results of these investigations show that the phases tested may find practical application for the separation of the geometric isomers of aliphatic diunsaturated conjugated acetates. Liquid crystal IV exhibits the best separation properties because

a column containing this stationary phase has the highest efficiency. Attempts to separate the geometric isomers of acetates with one olefinic bond and with two olefinic bonds separated by methylene groups were made on all the columns, but they failed.

## REFERENCES

- 1 I. P. Nesterova and G. K. Roshka, in N. A. Filippov, *Integrirovannaya Zashchita Ovoshchnykh i Plodovykh Kultur*, Shtiintsa, Kishinev, 1985, p. 59.
- 2 R. R. Heath, J. H. Tumlinson, R. E. Doolittle and A. T. Proveaux, *J. Chromatogr. Sci.*, 13 (1975) 380.
- 3 G. Schomburg and K. Zegarski, *J. Chromatogr.*, 114 (1975) 174.
- 4 N. W. H. Houx and S. Voerman, *J. Chromatogr.*, 129 (1976) 456.
- 5 R. R. Heath, J. H. Tumlinson and R. E. Doolittle, *J. Chromatogr. Sci.*, 15 (1977) 10.
- 6 R. R. Heath and P. E. Sonnet, *J. Liq. Chromatogr.*, 3 (1980) 1129.
- 7 I. V. Kleshnina, A. S. Kovaleva and L. L. Ivanov, in S. U. Chekmenev, *Materialy Soveshchaniya po Progressivnym Metodam Borby s Vrediteliami Selskokhozyaistvennykh Kultur*, Moscow, 1973, p. 121.
- 8 D. Warthen and N. Green, *J. Am. Chem. Soc.*, 46 (1969) 191.
- 9 H. Disselnkötter, K. Eiter, W. Karl and D. Wendisch, *Tetrahedron*, 32 (1976) 1591.
- 10 M. Macdonald and J. Weatherston, *J. Chromatogr.*, 118 (1976) 195.
- 11 J. D. Warthen, Jr., R. M. Waters and D. J. Voaden, *Chromatographia*, 10 (1977) 720.
- 12 I. P. Nesterova, K. V. Belyaeva, G. K. Roshka and V. M. Rastegaeva, in N. A. Filippov, *Novye Methody v Zatshite Rastenii*, Shtiintsa, Kishinev, 1987, p. 66.
- 13 I. P. Nesterova, G. K. Roshka and V. M. Rastegaeva, *Zh. Anal. Khim.*, 37 (1982) 1491.
- 14 R. R. Heath, G. E. Burnsed, J. H. Tumlinson and R. E. Doolittle, *J. Chromatogr.*, 189 (1980) 199.
- 15 R. Lester, *J. Chromatogr.*, 156 (1978) 55.
- 16 R. Lester and D. R. Hall, *J. Chromatogr.*, 190 (1980) 35.
- 17 R. R. Heath, J. R. Jordan, P. E. Sonnet and J. H. Tumlinson, *J. High Resolut. Chromatogr. Chromatogr. Commun.*, 2 (1979) 712.
- 18 R. R. Heath, J. R. Jordan and P. E. Sonnet, *J. High Resolut. Chromatogr. Chromatogr. Commun.*, 4 (1981) 328.

## Note

---

# Simultaneous determination of tributyl phosphate and dibutyl phosphate in spent fuel reprocessing streams by gas chromatography

Y. KUNO\*, T. HINA and T. AKIYAMA

*Power Reactor and Nuclear Fuel Development Corporation, Tokai-mura, Ibaraki (Japan)*  
and

M. MATSUI

*Analytical Application Laboratory, Simadzu Corporation, Azuma, Tukuba-shi, Ibaraki (Japan)*

(First received June 25th, 1990; revised manuscript received September 11th, 1990)

In Purex-type nuclear fuel reprocessing plants, dibutyl phosphate (DBP) is mainly formed as a degradation product resulting from the deterioration of the extractant, tributyl phosphate (TBP), in radiolytic and chemical processes [1–4]. The so-called “red-oil” is known to be formed during evaporation of the solution containing TBP under certain conditions [3,5]. It has been reported, on the other hand, that the concentration of DBP in the aqueous phase is of concern in the reformation of the organic phase [6]. The rapid and sensitive determination of TBP and DBP is therefore required in order to establish their concentrations in the aqueous phase of reprocessing streams.

Gas chromatography (GC) may be most suitable method to determine rapidly trace amounts of organic compounds. Brodda and Merz [7], Ladrielle *et al.* [8] and Lee and Ting [9] have reported the application of GC to the determination of DBP. Their methods, however, require derivatization of DBP by reactions such as esterification or silylation prior to the GC determination because of the poor volatility of DBP. These operations are so tedious and time consuming that they may not be appropriate for rapid determinations.

Recently, it was found that OV-17 stationary phase coated on Tenax GC was suitable for the direct determination of dicarboxylic acids and hydroxycarboxylic acids in their underivatized forms [10,11]. In this work, GC condition including column packing materials such as stationary phase-coated Tenax GC were investigated for the simultaneous determination of TBP and DBP without the derivatization of DBP. The recovery of TBP and DBP from the aqueous phase in reprocessing streams containing fission products (FPs) or plutonium was also examined.

## EXPERIMENTAL

*Reagents*

Standard aqueous solutions of TBP (100 ppm) and DBP (1000 ppm) were prepared by dissolving TBP (>97%) and DBP (>95%) (Tokyo Kasei) in water. Other reagents were of analytical-reagent grade.

*Extraction of TBP and DBP*

A 3-ml volume of sodium hydroxide solution (10%) was added to 5 ml of the aqueous solution containing the FP elements (*ca.* 50 g/l, 2 M nitric acid). After the precipitate had been removed by filtration, the acidity of the supernatant was made 3 M in nitric acid. TBP and DBP contained in the supernatant were extracted by vigorous shaking with chloroform (1:1, v/v) for a few minutes. For the solutions from the aqueous product streams of plutonium, 2 ml of sodium hydroxide solution (30%) were added to 5 ml of the sample solution containing 50–100 mg of plutonium (1 M nitric acid) in order to precipitate the plutonium. The other operations were as already described. All operations were carried out in a glove-box or in a radioactively shielded space (hot cave).

*Gas chromatography*

A Shimadzu Model GC-14A gas chromatograph equipped with a hydrogen flame ionization detector and a flame photometric detector and a Chromatopac C-R4A data processor were used. A 1.0 m × 2.6 mm I.D. glass column was packed with 5% OV-101, 5% OV-17 or 5% OV-25, and 0.5 and 1.0 m × 2.6 mm I.D. columns with 1% PEG-20M. Tenax GC (80–100 mesh) was employed as a solid support. A solution coating technique [10] was used for the preparation of the packing and column conditioning was carried out for 10 h in a stream of nitrogen carrier gas at 260°C for PEG-20M and at 270°C for the other packings. The operating conditions were as follows: column temperature, 220°C, injection port and detector temperatures, 300°C; and carrier gas flow-rate, 50 ml/min. Certain amounts of TBP and DBP dissolved in *n*-hexane or chloroform were injected into the column with a 1- $\mu$ l syringe.

## RESULTS AND DISCUSSION

*Comparison of columns*

Table I gives the numbers of theoretical plates and the separation factors of TBP/DBP in different columns. The separation factors obtained suggest that only OV-17 and PEG-20M are suitable for the simultaneous determination of TBP and DBP. Table I also indicates that the number of theoretical plates for TBP with OV-17 was greater than that with PEG-20M, whereas that for DBP with PEG-20M was greater than that with OV-17. The retention times of TBP and DBP with PEG-20M were 3.61 and 13.44 min, respectively, whereas those with OV-17 were 5.27 and 2.47 min, respectively. This implies a reverse order of elution of TBP and DBP in the two columns. The sensitivities of DBP relative to TBP were 0.035 and 0.128 with OV-17 and PEG-20M, respectively. It can be concluded that the PEG-20M column is the most appropriate for the simultaneous determination of TBP and DBP.

TABLE I  
NUMBERS OF THEORETICAL PLATES AND SEPARATION FACTORS

Column	No. of theoretical plates		Separation factor, TBP/DBP
	TBP	DBP	
OV-101	9.73	9.11	0.01 <sup>a</sup>
OV-17	30.73	7.53	0.73
OV-25	14.66	15.15	0.02 <sup>a</sup>
PEG-20M	16.07	50.00	1.81

<sup>a</sup> TBP and DBP were not separated.

#### Determination of TBP and DBP

The limits of determination of TBP and DBP with flame ionization detection (FID) were 1 and 5 ng, respectively, while those with flame photometric detection (FPD) were 0.2 and 1 ng, respectively. It was found that the FID response was consistently linear over a wide range up to  $10^4$  ng of both TBP and DBP, whereas the FPD response showed linearity within narrower ranges, between 0.2 and  $10^3$  ng for TBP and between 1 and  $10^2$  ng for DBP. The determination of DBP with FPD, however, can give a reproducible quadratic curve with a range of  $10^3$ , which is sufficient for the practical requirements for DBP determinations. The relative standard deviations for seven replicate measurements of TBP and DBP were, respectively, 4.1% at 10 ng and 5.3% at 50 ng when FID was employed, whereas those with FPD were 3.2% at 10 ng and 5.2% at 50 ng. Fig. 1 shows a typical chromatogram obtained with a 1.0-m PEG-20M column.

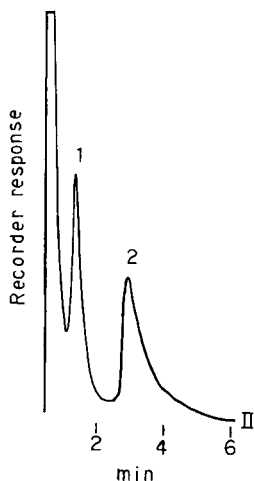


Fig. 1. Separations of TBP and DBP. Column: 1% PEG-20M on Tenax GC (1.0 m  $\times$  2.6 mm I.D.); column temperature, 220°C; injection port temperature, 300°C; detector temperature, 300°C; carrier gas flow-rate, nitrogen 50 ml/min; hydrogen, 0.6 kg/cm<sup>2</sup>; air, 0.5 kg/cm<sup>2</sup>. Peaks: 1 = TBP (10 ng); 2 = DBP (50 ng).

TABLE II

## DETERMINATION OF TBP AND DBP RECOVERED FROM PRACTICAL SAMPLES

Sample	TBP added (ppm)	TBP found (ppm) <sup>a</sup>	DBP added (ppm)	DBP found (ppm) <sup>a</sup>
HALW <sup>b,c</sup> (ca. 50 g FPs/l 2 M HNO <sub>3</sub> )	100	94 ± 5	100	90 ± 5
Plutonium nitrate <sup>c</sup> (30 g/l, 2 M HNO <sub>3</sub> )	100	93 ± 5	100	86 ± 7

<sup>a</sup> Mean ± average deviation for five results.

<sup>b</sup> HALW = highly active liquid waste.

<sup>c</sup> TBP and DBP levels originally present in the solutions were negligible.

### Recovery of TBP and DBP from aqueous solutions

Previous studies suggested that the separation of DBP from TBP with chloroform was satisfactory after DBP had been back-extracted into the aqueous phase [9]. This implies that TBP and DBP dissolved in an aqueous phase may be simultaneously extracted with chloroform with high recovery. The recoveries of TBP and DBP in nitric acid solutions with a wide range of concentrations (1–6 M) were examined by the procedure given. The average recoveries for TBP and DBP within the above range were  $96 \pm 3\%$  and  $92 \pm 6\%$ , respectively. It was observed in the solutions

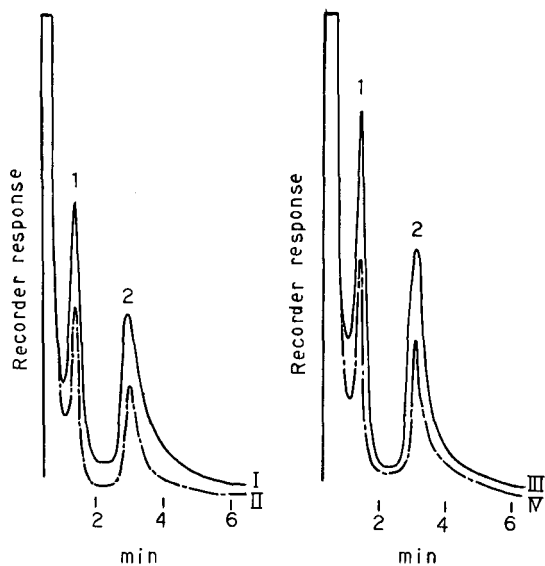


Fig. 2. Gas chromatograms of TBP and DBP recovered from practical samples. TBP and DBP were recovered from standard TBP- and DBP-added samples of HALW (I, II) and plutonium nitrate (III, IV). (I) 1 = TBP (20 ppm), 2 = DBP 100(ppm); (II) 1 = TBP (10 ppm), 2 = DBP (50 ppm); (III) 1 = TBP (30 ppm), 2 = DBP (150 ppm); (IV) 1 = TBP (15 ppm), 2 = DBP (75 ppm). Column, 1% PEG-20M on Tenax GC (1.0 m × 2.6 mm I.D.). Conditions as in Fig. 1.



from the reprocessing streams that a large portion of DBP, mainly generated as a radioactive degradation product or as a hydrolysis product of TBP, was converted into a precipitate of DBP metal complexes. This type of precipitate could also be a source of the third phase [6] during evaporation. Therefore, it is important to determine DBP contained in both the supernatant and the precipitate. The recoveries of TBP and DBP were examined in solutions including FP elements. It was confirmed that more than 95% and 86% of TBP (100 ppm) and DBP (500 ppm), respectively, were recovered from solutions including 500 ppm of Fe, Zr, Ru, Cr, Y, Se, Sr, Mo, Pd, Ag, Cs, La, Ce, Sm, Eu, Gd, Ni, Cd, Rb, Nd and Ba. This implies that good recoveries of not only TBP and DBP freely contained in aqueous solutions but also DBP contained in the precipitate of DBP metal complexes from the solutions containing various metal ions can be achieved using the proposed procedures. The results suggest that DBP present in a precipitate as a complex may be converted into free DBP by making the solutions alkaline.

#### *Determination of TBP and DBP in practical samples*

The accuracy of the method was examined by analysing practical samples to which known amounts of TBP and DBP had been added. The results are given in Table II. The values found agreed well with the amounts added. Fig. 2 shows the chromatograms of TBP and DBP including a precipitate recovered from a practical samples. The times required for one determination of TBP and DBP in aqueous solutions from highly radioactive liquid waste streams and plutonium streams were *ca.* 1 h and 40 min, respectively. It is concluded that TBP and DBP in the aqueous phase of reprocessing streams can be determined by GC without any interferences.

#### REFERENCES

- 1 General Electric Co., *USAEC Report*, HW-31000, Hanford Atomic Products Operation, Richland, WA, 1955.
- 2 L. L. Burger and E. D. McClanahan, Jr., *USAEC Report*, HW-52943, Hanford Atomic Products Operation, Richland, WA, 1957.
- 3 M. Benedict, T. H. Pigford and H. W. Levi, *Nuclear Chemical Engineering*, McGraw-Hill, New York, 1981, Ch. 10, p. 511.
- 4 T. H. Siddall, in J. F. Flagg (Editor), *Solvent Extraction Processes Based on TBP in Chemical Processing of Reactor Fuels*, Academic Press, New York, 1961, Ch. 5.
- 5 R. M. Wagner, *USAEC Report*, HW-27492, Hanford Atomic Products Operation, Richland, WA, 1953.
- 6 R. Becker, L. Stieglitz, H. Bautz and R. Will, *KFK3983*, Kernforschungszentrum, Karlsruhe, 1985.
- 7 B. G. Brodda and E. Merz, *Fresenius' Z. Anal. Chem.*, 273 (1973) 113.
- 8 T. Ladrielle, P. Wannet and D. J. Aspers, *Radiochem. Radioanal. Lett.*, 59 (1983) 355.
- 9 Y. Lee and G. Ting, *Anal. Chim. Acta*, 106 (1979) 373.
- 10 M. Matsui and T. Kitsuwu, *Bunseki Kagaku*, 37 (1988) 63.
- 11 M. Matsui, *J. Food Hyg. Soc. Jpn.*, 27 (1986) 212.

## Note

---

### Localization of amino acids on thin-layer chromatograms with acetylacetone–formaldehyde reagent

M. B. DEVANI\*, C. J. SHISHOO, S. A. SHAH, K. P. SONI and R. S. SHAH

*Department of Pharmaceutical Chemistry, L. M. College of Pharmacy, Ahmedabad-380 009 (India)*

(First received November 16th, 1989; revised manuscript received August 31st, 1990)

Various reagents have been suggested for revealing amino acids on thin-layer chromatogram [1]. Some of these are specific whereas others give coloured spots with most amino acids.

Although ninhydrin comes closest to the ideal detection agent, showing reactivity and sensitivity towards most amino acids, the colour formed is unstable [2,3]. It gives a faint yellow colour with proline and hydroxyproline [1,4]. Only under controlled conditions of pH and temperature and in the presence of organic solvents having maximum water content does the colour intensity approach 100% [5,6]. It was therefore, considered of interest to develop a new reagent for the localization of amino acids on thin-layer chromatographic (TLC) plates.

It was reported earlier that primary amines react with acetylacetone–formaldehyde reagent to produce yellow products in aqueous medium [7]. This observation has been utilized to detect the amino acids on thin-layer chromatograms.

#### EXPERIMENTAL

Glass plates (10 × 20 cm) were coated with an aqueous slurry of silica gel [BDH, Glaxo Laboratories (India)] using a Desaga spreader. The plates were dried in an oven at  $105 \pm 2^\circ\text{C}$  for 30 min.

#### *Reagent*

Formaldehyde [37% (w/v); 15.0 ml] was mixed with freshly distilled acetylacetone (7.8 ml) and diluted to 100 ml with acetate buffer solution (pH 4.7) [8]. A freshly prepared reagent solution was used.

#### *Standard solution of amino acids*

Amino acids (0.1 mmol) were weighed accurately and dissolved in and diluted to 100 ml with water. A freshly prepared solution was used.

TABLE I

DETECTION OF AMINO ACIDS ON A TLC PLATE WITH ACETYLACETONE-FORMALDEHYDE REAGENT

Amino acid	Detection limit ( $10^{-4}$ mmol)		
	Proposed reagent		Ninhydrin reagent [1]
	Visible light	UV light	
Glycine	1.3	0.26	0.13
L-Lysine.HCl	1.6	0.27	0.27
L-Arginine.HCl	2.3	0.47	0.47
L-Tyrosine	5.5	0.55	1.6
L-Leucine	2.2	0.60	0.76
DL-Isoleucine	6.0	0.68	—
DL-Valine	6.8	0.76	0.85
DL-Serine	4.7	0.95	0.76
L-Cystine	2.0	1.2	—
L-Glutamic acid	2.7	1.3	2.7
DL-Methionine	3.3	1.3	0.67
L-Histidine.HCl	3.1	1.5	2.6
DL-Tryptophan	9.7	1.9	2.4
DL-Alanine	6.7	2.2	1.0
DL-Threonine	4.1	2.5	4.1
L-Ornithine.HCl	17.0	2.9	—
Hydroxyproline	7.6	3.0	3.8
L-Aspartic acid	15.0	6.0	7.5
L-Asparagine	22.0	6.0	7.5
L-Proline	26.0	6.9	8.6

*Thin-layer chromatogram*

Appropriately diluted standard amino acid solution ( $10.0 \mu\text{l}$ ) was spotted on the plate. After evaporation of solvent, it was developed with *n*-butanol-acetic acid-water (40:5:7) [9] and dried at room temperature. The plate was sprayed evenly with the reagent solution and heated in an oven at  $100 \pm 2^\circ\text{C}$  for 10 min. The spots were examined under both visible and UV light (UVK-125-254). The results are recorded in Table I.

## RESULTS AND DISCUSSION

The proposed reagent gives well defined, stable, yellow spots with all the amino acids. The spots are more easily detected under UV than visible light. The limit of detection of amino acids was found to be in the range  $0.26 \cdot 10^{-4} - 6.9 \cdot 10^{-4}$  mmol and  $1.3 \cdot 10^{-4} - 26 \cdot 10^{-4}$  mmol amino acid under UV and visible light, respectively.

The sensitivity of the reagent was compared with that of ninhydrin reagent [1] (Table 1). The reactivity of the proposed reagent with tyrosine, leucine, valine, glutamic acid, histidine, tryptophan, threonine, proline, hydroxyproline, asparagine and aspartic acid is distinctly superior to that of ninhydrin.

A study of the effect of pH on reaction showed that the maximum colour yield is obtained at pH 4.7.

The effect of temperature on rate of colour development was studied. The colour intensity increased with increase in temperature. Heating of the TLC plate (after spraying with the reagent) at  $100 \pm 2^\circ\text{C}$  for 10 min was found to be most suitable. The spot was remained stable for more than 24 h.

In the proposed procedure, amino acids seem to react with acetylacetone-formaldehyde reagent to form N-substituted 3,5-diacetyl-1,4-dihydrolutidine, which gives a yellow colour in visible light and fluorescence under UV light.

The reagent is also applicable to the detection of small peptides. The product is suitable for their densitometric determination.

#### ACKNOWLEDGEMENT

The authors thank Cadila Labs., Ahmedabad, India, for the gift of samples of amino acids.

#### REFERENCES

- 1 E. Stahl, *Thin Layer Chromatography, A Laboratory Hand Book*, Springer, Berlin, 1965, pp. 405-406.
- 2 H. W. Adams and H. G. Stuart, *Analyst (London)*, 76 (1951) 553.
- 3 E. Kewerau and T. Wieland, *Nature (London)*, 168 (1951) 77.
- 4 A. Jeanes, C. S. Wise and R. J. Dimler, *Anal. Chem.*, 23 (1951) 415.
- 5 W. H. Fitzpatrick, *Science (Washington, D.C.)*, 109 (1949) 469.
- 6 W. Troll, R. K. Canna, *J. Biol. Chem.*, 200 (1953) 803.
- 7 S. A. Shah, *Ph.D. Thesis*, Gujarat University, Ahmedabad, 1986.
- 8 *Indian Pharmacopoeia*, Vol. II, The Controller of Publications, Dehli, 1985, p. A143.
- 9 N. A. N. Rao and T. K. Wadhvani, *J. Indian Inst. Sci.*, 37A (1955) 130.

## Letter to the Editor

---

### **Pitfalls in the choice of isotherms for the calculation of band profiles in preparative chromatography**

Sir,

The last years have brought significant advances in the theory of non-linear chromatography and, especially, in the prediction of the individual elution band profiles in preparative liquid chromatography by computer simulation [1–9]. With the increasing power of computers, accurate approximations have become possible. Some of the various finite difference algorithms that can be used for the correct simulation of chromatograms have been discussed recently [10]. These algorithms are procedures of propagating the chromatographic signal through a grid of time and space coordinates. Except at very low column efficiencies (number of theoretical plates,  $N < 1000$ ) they all give nearly identical band profiles. The central part of any of these simulation methods is the calculation of the fraction of the sample molecules that has to be propagated, using the proper distribution isotherm (mostly, competitive Langmuir isotherms are chosen for lack of a better equation). Of these methods, the Craig model appears as a particular case that requires that this equilibration be done by iterations at each step along the grid [10]. For this reason, the implementation of a Craig model is bound to consume much longer computing times than other methods that do not require this iterative calculation [11–13].

Attempts have been made at eliminating the time consuming equilibration step of the Craig model [2,14–16]. In a recent publication, an algorithm has been proposed that replaces the two-component competitive Langmuir isotherm with a new numerical approximation [17]. This algorithm is claimed to be “accurate to within  $\pm 10\%$  for a wide range of sample concentrations and sample  $k'$  values” ( $k'$  = capacity factor) [17]. Indeed, many of the peak shapes shown in this work resemble those found in experimental preparative chromatography [18,19] and those obtained in band profile calculations by other groups [3,5–8,10]. Surprisingly, however, at high sample loads, the formation of double peaks is predicted. According to the literature, this should not be possible with a monotonically curved isotherm [20,21], such as the Langmuir isotherm. So far, to the best of our knowledge, it has never been reported to have occurred in any experiment.

Furthermore, the authors report [17,22] that the retention times predicted with their method agree poorly with their experimental data or with the results of calculations we have published [3,6,7,12]. They tried to circumvent this consistent disagreement by using an empirical factor with which they multiply the sample size (or the injection concentration). Agreement is then claimed between experimental results

and the results of the calculations performed with the “corrected” sample load. The value of the correction factor is given as intermediate between 1.5 and 1.8 [17,22].

In our own work, we have always observed an excellent agreement between experimental band profiles and the results of the simulations when they were carried out using the equilibrium isotherms determined on the same column [23–26]. Thus, the unexpected peak profiles presented in ref. 17 deserved some investigation. We have also noticed that the individual elution band profiles are sensitive to minor changes in the isotherms. As we report here, the exact nature of the isotherms used [17] is the cause for the questionable results. Since the published procedure (Appendix, ref. 17) contains some inconsistencies and typographical errors, we give the version we used in Appendix I, with the list of changes made to the published program [17]. Judging by the excellent agreement between our results and those published, the program in Appendix I is a very close match to what the authors of ref. 17 have used.

#### PROCEDURE AND EXPERIMENTAL CONFIGURATION

##### *Langmuir isotherm*

In Craig simulations, the total amount of a sample component in one column plate must be distributed between the stationary and the mobile phases according to its equilibrium isotherm. Then, the fraction in the mobile phase moves forward to the next plate, whereas the fraction in the stationary phase stays behind and is equilibrated with the mobile phase coming from the preceding plate. Thus, it is necessary to calculate both equilibrium concentrations from the total amount of each component contained in the plate.

For the lack of a better model, the most commonly used isotherm in liquid–solid chromatography is the competitive Langmuir isotherm:

$$q_i = \frac{a_i C_i}{1 + \sum_{j=1}^n b_j C_j} \quad (1)$$

where  $q_i$  and  $C_i$  are the local equilibrium concentrations of the compound  $i$  in the stationary and the mobile phases, respectively, and  $a_i$  and  $b_i$  are coefficients the numerical values of which are characteristic of the compound  $i$  and the phase system and determine the saturation capacity of the column.

The Langmuir competitive isotherm is a convenient first order approximation the most serious inconvenient of which is not to satisfy the Gibbs–Duhem equation, unless the column saturation capacities,  $a_i/b_i$ , are the same for the two components. There are some possibilities to correct for this drawback [27]. Experimental results show reasonably good agreement with profiles calculated using a competitive Langmuir isotherm model [25].

For the calculation of chromatographic profiles, it is necessary to keep track of the amounts of each compound, rather than of concentrations. Thus, it is convenient to report both amounts in the same units. The amount in the stationary phase is also divided by the volume of mobile phase in one plate. Instead of the  $a_i$  parameter, we use the limiting retention factor at infinite dilution,  $k'_{0,i}$ :

$$q'_i = \frac{k'_{0,i} C_i}{1 + \sum b_j C_j} \quad (2)$$

This allows us the use of the same numerical values, whether we discuss compound amounts as in ref. 17 ( $w_s$ ,  $w_m$ ) or their concentrations ( $q$ ,  $C$ ).

When there is only one component, eqn. 1 can be rearranged and solved in closed form for  $C$ . For a multi-component mixture, there are no closed form solutions giving the mobile phase concentrations as functions of the total amount of each component. Nevertheless, it is straightforward to calculate the numerical solution by an iterative approximation such as the following one. If the above definition of the stationary phase concentrations is followed, the amounts in either phase are proportional to the quantities  $C$  or  $q'$ , respectively. The total amount of a component in one cell divided by the volume of the mobile phase in this cell then corresponds to the sum of the amounts of the component  $i$  in the two phases contained in this cell:

$$T_i = C_i + q'_i \quad (3)$$

For the two components, X and Y, we have:

$$q'_X = T_X - C_X = \frac{k'_{0,X}C_X}{1 + b_X C_X + b_Y C_Y}$$

and

$$q'_Y = T_Y - C_Y = \frac{k'_{0,Y}C_Y}{1 + b_X C_X + b_Y C_Y} \quad (4)$$

The total amounts,  $T_X$  and  $T_Y$ , of the two components in the cell considered are known. Eqns. 4, then, have to be solved for the two mobile phase concentrations,  $C_X$  and  $C_Y$ . We can consider the denominator in eqn. 4 as a correction factor and solve for  $C_i$  in the numerator (see Appendix II). After each iteration step, the value of the denominator is updated, using the new values of the concentrations  $C_i$ . When the difference between two successive values of the two concentrations drops below  $1 \cdot 10^{-10}$ , the approximation is considered as satisfactory and the resulting concentrations are used in the propagation step. This procedure has proven to be very robust and converges rapidly.

### *Isotherm parameters*

According to the Appendix of ref. 17, "in a Langmuir type system [...] a one-stage equilibrium is assumed, having a mobile phase volume of 1.0 ml and a stationary phase capacity of 0.1 g of sample<sup>2</sup>". For a 400-plate system, the dead volume is 400 ml and the saturation capacity is 40 g. In order to inject an amount of 20% of the column saturation capacity for one of the two components of the mixture, we need a sample solution containing 8 g of each component for 1 ml of mobile phase (the content of one plate). This is quite unrealistic, but the injection had to be carried out during one cycle time in order to duplicate the published results. For a more realistic simulation, the injection should last several cycle times and its profile should mirror the experimental injection profile. In our computations, we have chosen a 10 cm long column and a mobile phase velocity of 0.1 cm/s, which gives a cycle time of  $\Delta t = 0.25$  s. The space increment along the column is  $\Delta z = 0.025$  cm.

The Langmuir parameters,  $b_i$ , can be calculated from the relationship:

$$\frac{k'_{0,i}}{b_i} = 0.1 \quad (5)$$

The values of the various input parameters used are presented in Table I. Note that the values of  $b_i$  are not used in the computation method described in ref. 17.

### Computation times

The execution times for three simulation runs carried out with different loads are given in Table II. They are reported as the times required for the completion of one band propagation step, including the equilibration in one Craig plate. The equilibration according to the procedure described in the previous section needs an average of five iterations to converge to a concentration difference of  $1 \cdot 10^{-10}$ . This may take up to 15 iterations in the vicinity of steep concentration gradients, i.e., for the band fronts. The explicit isotherm from ref. 17 avoids these iterations but requires two exponentiations at low sample loads or one square root at high loads. On the machine language level, both these operations require rather complex manipulations. The end result is that there is no clear computational advantage in using the isotherm of ref. 17. Depending on the computer used (VAX or PC with different processors), it may be either somewhat slower or slightly faster than the iteration procedure.

## RESULTS AND DISCUSSION

The most striking feature of the isotherm of ref. 17 is the concentration discontinuity observed for a sample amount of 0.175 units ( $w_{\max}$  for  $k_x = 1$ ). At low concentrations, the isotherm agrees quite closely with the corresponding competitive Langmuir isotherm (eqn. 1). When the cumulative load of both components in one Craig stage exceeds this threshold amount, the algorithm follows a distribution law that is completely different from the one used at lower total loads. The two branches of

TABLE I  
PARAMETERS USED IN THE COMPUTER SIMULATIONS

---

*Numerical simulation of band propagation in non-linear chromatography*

- (1) Input profiles (for a load of  $2 \times 20\%$  of saturation):  
 Calculation 1: concentration 8.00 during 0.25 s  
 Calculation 2: concentration 8.00 during 0.25 s
- (2) Column: column length 10 cm  
 linear velocity 0.10 cm/s  
 height equivalent to a theoretical plate for  $k' = \infty$  250  $\mu\text{m}$  (400 plates)
- (3) Retention at low load, isotherm data:  
 Calculation 1: 200.0 s  $k' = 1.0$   $b = 10.00$   
 Calculation 2: 270.0 s  $k' = 1.7$   $b = 17.00$
- (4) Craig simulation:  
 grid spacing [10]  $\Delta z = 0.025000$  cm  $\Delta t = 0.250000$  s
- The sample sizes are given as loading factors, i.e. fractional column saturations.
-



TABLE II

EXECUTION TIMES ON DEC VAX 6000-440: TIME NEEDED FOR ONE EQUILIBRATION FOLLOWED BY A PROPAGATION STEP. 400 CRAIG STAGES,  $k' = 1.0$  and 1.7.

Load	Ref. 17	Langmuir	Difference
$2 \times 2.5\%$ of capacity	60 $\mu$ s	42 $\mu$ s	+30%
$2 \times 20\%$ of capacity	60 $\mu$ s	59 $\mu$ s	+2%
$2 \times 30\%$ of capacity	57 $\mu$ s	62 $\mu$ s	-8%

the isotherm do not even link up at this point (Fig. 1). As a result, the concentrations of the two components in both phases change abruptly. As the concentration in one phase increases, the concentration in the other phase decreases by the corresponding amount. This property is illustrated in Fig. 1 which shows, for one component, the amount adsorbed in the stationary phase of one stage *versus* the total amount in both phases. This discontinuity is disconcerting and makes no physical sense.

The objective of introducing the upper part of the isotherm seems to have been to force complete saturation of the stationary phase at all sample loads above the threshold. When only one component is present, the concentration in the stationary phase is set equal to the saturation limit. For a binary mixture (Fig. 1), the numerical value of a complicated function (Appendix I) determines the relative amount supplied by each component to complete stationary phase loading. The amounts in the mobile phase are calculated as the leftovers of this process.

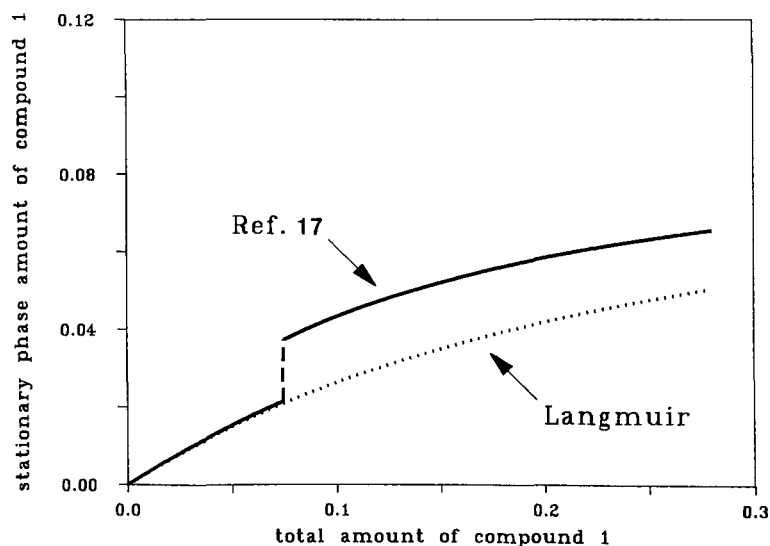


Fig. 1. Distribution isotherm of the first component of a binary system calculated according to the procedure described in ref. 17 and comparison with Langmuir isotherm. Plot of the amount of first component in the stationary phase *versus* the total amount of component 1 in the system (solid line). Langmuir isotherm in dotted lines. Amount of component 2 constant ( $w_2 = 0.10$  g/ml).

This choice of a constant equilibrium concentration at all high mobile phase concentrations is rather unfortunate. According to thermodynamics, when the concentration in one phase is changed, the equilibrium is restored by a proper change in the other phase. This would be impossible if the concentration in one phase were fixed. Therefore a saturation concentration can be only an asymptotic limit.

The effects of the isotherm shape on calculated band profiles are shown by the example in Fig. 2. It compares the chromatograms calculated with isotherms obtained using the algorithms in either Appendix I (solid lines) or Appendix II (true competitive Langmuir isotherm, dotted lines). The "experimental conditions" for this simulation are equivalent to those given in ref. 17 for Fig. 5e, to which the result must be compared.

The chromatogram calculated following the iterative procedure (dotted lines) is in close qualitative agreement with experimental band profiles reported in earlier work [23–26]. It exhibits the typical tag-along effect reported previously [3,6]. Due to the strong blockage of the adsorbent surface by the molecules of the first component, the front of the second component band moves much faster than its tail [28]. This phenomenon leads to the formation of a plateau trailing behind the maximum of the second band and often eroded into a shoulder by the finite kinetics of mass transfer [6,28].

In contrast, the profiles produced by the discontinuous isotherm exhibit a shoulder preceding the band maximum (Fig. 3e in ref. 17) or even a second peak (Fig.

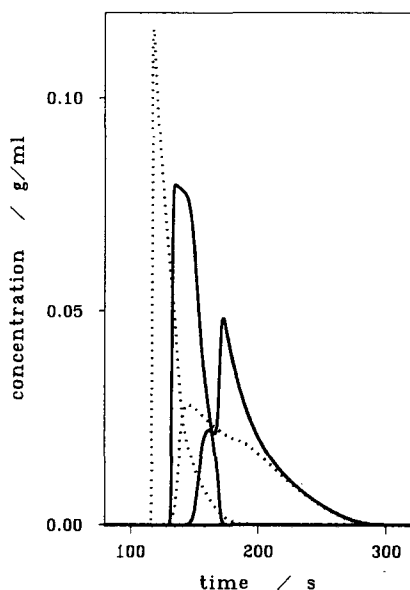


Fig. 2. Chromatograms calculated using the two isotherm calculation procedures described in the present paper. Craig model program. Solid line: individual band profiles obtained with the discontinuous isotherm calculated according to the procedure in ref. 17 (Appendix). Dotted line: individual band profiles obtained with the Langmuir competitive isotherm calculated according to the procedure in Appendix II of this work. Conditions:  $k'_1 = 1$ ,  $\alpha = 1.7$ , loading factors:  $L_{r,1} = L_{r,2} = 0.20$ , 400 plates. Compare to Fig. 5e in ref. 17.

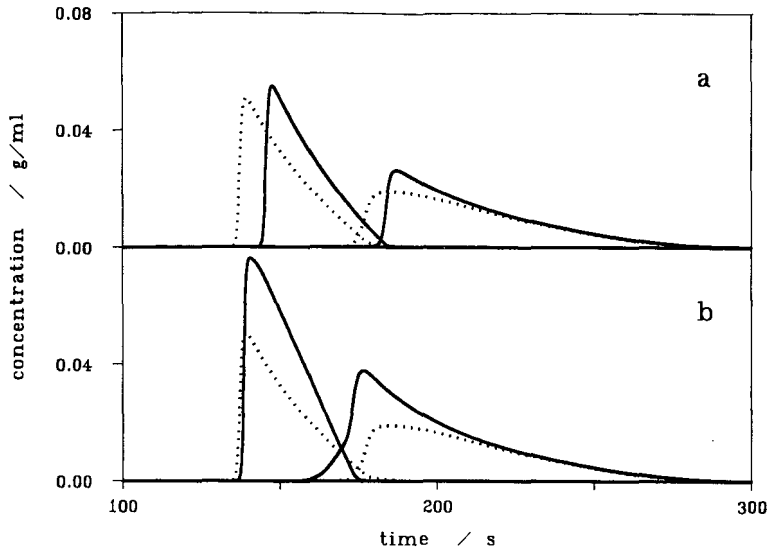


Fig. 3. Chromatograms calculated using the two isotherm calculation procedures described in the present paper. Craig model program. Solid line: individual band profiles obtained with the discontinuous isotherm, calculated according to the procedure in ref. 17 (Appendix I). (a) Calculation made with the true sample amount. (b) Calculation made with an adjusted sample size equal to 1.5 times the true sample amount. Dotted line: individual band profiles obtained with the competitive Langmuir isotherm calculated according to the iterative procedure in Appendix II, for the true sample amount (both in a and b). Conditions:  $k'_1 = 1$ ,  $\alpha = 1.7$ ,  $L_{t,1} = L_{t,2} = 0.10$ ,  $n_c = 400$  plates. Compare to Fig. 5d in ref. 17.

2, loading factor 20% for each component, separation factor,  $\alpha = 1.7$ ). The position of the valley between the two peaks of the second band corresponds to the region at the rear of the first band where the cumulative sample concentration drops suddenly below the threshold level. Concurrently, the amount adsorbed falls from complete saturation down to the values determined by the lower part of the isotherm (see Fig. 1). These band shapes are not consistent with a monotonically curved isotherm.

Fig. 3a compares the chromatograms obtained with the two isotherms under the same conditions as in Fig. 2 but with a lower sample size (loading factors = 10%). Both chromatograms have band profiles that look quite reasonable, with almost touching band separation. There is still a serious difference in the retention times however. Both peaks calculated with the discontinuous isotherm (Fig. 3a, solid lines) appear at higher retention times than expected (dotted lines). The explanation lies in the shape of the isotherm. Whereas its lower part is virtually identical to the Langmuir model, the higher part has a much higher fraction of the sample adsorbed. Accordingly, the band fronts move more slowly than with asymptotic saturation behavior and the retention times are too long.

The procedure selected to correct for this discrepancy tries to remedy the effects of an incorrect isotherm by an adjustment of the sample size [17]. If the loading factor for a given sample size is multiplied by an arbitrary factor, the bands elute faster [28]. Values between 1.5 and 1.8 are suggested for the correction factor [17,22]. As seen in Fig. 3b, this approach is only moderately successful. Although the retention times of

the first component band are about the same for the chromatogram calculated using the true Langmuir isotherm (dotted lines same as in Fig. 3a) and the one calculated with a correction factor of 1.5 using the discontinuous isotherm (solid lines), the band profiles are markedly different. Of special importance is the fact that with the Langmuir isotherm we come close to a touching band separation, whereas the chromatogram simulated with the discontinuous isotherm and an adjusted sample size (increased by 50%) exhibits a much poorer resolution. When a correction factor of 1.8 is used, the agreement between the two procedures is still worse. This shows that the use of a fixed correction factor cannot permit the calculation of consistently correct retention times or peak profiles. It cannot be trusted either in the derivation of the correct sample size that would allow touching band separations (Fig. 3b), as is the aim of the CRAIG4 subprogram and software packages built around it [29].

#### CONCLUSION

In this paper we have shown that it may be both unnecessary and risky to replace an implicit function (the competitive Langmuir isotherm) by an explicit approximation. The approximation proposed in a recent paper [17] does not help to save computation time. Instead, it introduces a discontinuity in the equilibrium concentrations, which renders the isotherm meaningless and leads to incorrect and rather unusual peak shapes. If a Langmuir isotherm has been chosen to represent the experimental results, an iterative solution is to be preferred.

#### ACKNOWLEDGEMENTS

This work has been supported in part by Grant CHE-8901382 of the National Science Foundation and by the cooperative agreement between the University of Tennessee and the Oak Ridge National Laboratory. We acknowledge support of our computational effort by the University of Tennessee Computing Center.

#### APPENDIX I

##### *Procedure to calculate equilibrium concentrations*

*Isotherm of ref. 17 (for symbols see ref. 17):*

Calculate once, outside loop:

$$\alpha = k_y/k_x \rightarrow \sqrt{\alpha}$$

$$A = -(\alpha - 1)$$

$$D_x = 0.5/k_x + 0.7 k_x^{0.37}$$

$$D_y = 0.5/k_y + 0.7 k_y^{0.37}$$

$$C_x = 0.62 10^{D_x} k_x^{-0.4}$$

$$C_y = 0.62 10^{D_y} k_y^{-0.4}$$

$$w_{max} = 0.175 - 0.013 \log k_x$$

Calculate inside loop for every plate at every time: ( $w_x$  and  $w_y$  are the amounts of X and Y in that plate)

$$\begin{aligned}
 w_{\text{tot}} &= w_x + w_y \\
 \text{if } w_{\text{tot}} > w_{\text{max}}: \\
 Q &= w_{\text{tot}} - 0.1 \\
 B &= w_x (\alpha - 1) + 0.1 + \alpha Q \quad (\text{Note 1}) \\
 C &= -w_x \alpha Q
 \end{aligned}$$

$$\begin{aligned}
 w_{\text{xm}} &= [-B + (B^2 - 4AC)^{\frac{1}{2}}]/2A \\
 w_{\text{xs}} &= w_x - w_{\text{xm}} \\
 w_{\text{ys}} &= 0.1 - w_{\text{xs}} \\
 w_{\text{ym}} &= w_y - w_{\text{ys}} \\
 \text{(if only one compound is present, } w_{\text{xs}} \text{ or } w_{\text{ys}} &= 0.1) \quad (\text{Note 2})
 \end{aligned}$$

$$\begin{aligned}
 \text{if } w_{\text{tot}} \leq w_{\text{max}}: \\
 J_x &= w_x + w_y \sqrt{\alpha} \quad (\text{Note 3}) \\
 J_y &= w_y + w_x / \sqrt{\alpha} \quad (\text{Note 3})
 \end{aligned}$$

$$\begin{aligned}
 R_x &= (1/k_x) + C_x J_x^{D_x} \\
 R_y &= (1/k_y) + C_y J_y^{D_y} \\
 w_{\text{ws}} &= w_x / (1 + R_x) \\
 w_{\text{xm}} &= w_x - w_{\text{xs}} \\
 w_{\text{ys}} &= w_y / (1 + R_y) \\
 w_{\text{ym}} &= w_y - w_{\text{ys}}
 \end{aligned}$$

*Changes versus the original version of ref. 17*

*Note 1:* original:  $B = [w_x(\alpha - 1)] + 0.1\alpha Q$

Using the product  $0.1\alpha Q$  can lead the program to take the square root of a negative value.

*Note 2:* original: for  $w_x = 0$ ,  $w_{\text{ys}} = 0.1$ ,  $w_{\text{ym}} = 0.1 - w_y$ ;

for  $w_y = 0$ ,  $w_{\text{xs}} = 0.1$ ,  $w_{\text{xm}} = 0.1 - w_x$ .

These instructions do not conserve mass.

*Note 3:* original:  $J_x = w_x + (\alpha^{\frac{1}{2}} w_y) w_y$

$J_y = w_y + (\alpha^{-\frac{1}{2}} w_x) w_x$

The repetition of  $w_i$  is obviously an editing error.

## APPENDIX II

### *Procedure to calculate equilibrium concentrations*

Langmuir isotherm: for the purpose of this paper, the variables used below can be equated with those from ref. 17 according to:

$$\begin{aligned}
 T_x &= w_x \\
 C_x &= w_{\text{xm}} \\
 q'_x &= w_{\text{xs}}
 \end{aligned}$$

The Langmuir parameter  $b$  is not used in ref. 17.

Calculate inside loop for every plate at every time:

iterative approximation:

$$\text{denominator} = 1 + b_x C_x + b_y C_y$$

$$C_x = T_x / (1 + k_x / \text{denominator})$$

$$C_y = T_y / (1 + k_y / \text{denominator})$$

repeat until convergence (typically five times)

$$q'_x = T_x - C_x$$

$$q'_y = T_y - C_y$$

Department of Chemistry, University of Tennessee,  
Knoxville, TN 37996-1600 and Division of Analytical  
Chemistry, Oak Ridge National Laboratory,  
Oak Ridge, TN 37831-6120 (U.S.A.)

MARTIN CZOK  
GEORGES GUIOCHON\*

- 1 J. H. Knox and M. Pyper, *J. Chromatogr.*, 363 (1986) 1.
- 2 L. R. Snyder, G. B. Cox and P. E. Antle, *Chromatographia*, 24 (1987) 82.
- 3 G. Guiochon and S. Ghodbane, *J. Phys. Chem.*, 92 (1988) 3682.
- 4 M. W. Phillips, G. Subramanian and S. M. Cramer, *J. Chromatogr.*, 454 (1988) 1.
- 5 A. J. Howard, G. Carta and C. H. Byers, *Ind. Eng. Chem. Res.*, 27 (1988) 1873.
- 6 G. Guiochon, S. Ghodbane, S. Golshan-Shirazi, J.-X. Huang, A. M. Katti, B.-C. Lin and Z. Ma, *Talanta*, 36 (1989) 19.
- 7 A. M. Katti and G. Guiochon, *Anal. Chem.*, 61 (1989) 982.
- 8 C. K. Lee, Q. Yu, S. U. Kim and N.-H. L. Wang, *J. Chromatogr.*, 484 (1989) 29.
- 9 S. Golshan-Shirazi and G. Guiochon, *Anal. Chem.*, 61 (1989) 2380.
- 10 M. Czok and G. Guiochon, *Anal. Chem.*, 62 (1990) 189.
- 11 P. Rouchon, M. Schonauer, P. Valentin and G. Guiochon, *Sep. Sci. Technol.*, 22 (1987) 1793.
- 12 G. Guiochon, S. Golshan-Shirazi and A. Jaulmes, *Anal. Chem.*, 60 (1988) 1856.
- 13 B. C. Lin, Z. Ma and G. Guiochon, *Sep. Sci. Technol.*, 25 (1989) 809.
- 14 J. E. Eble, R. L. Grob, P. E. Antle and L. R. Snyder, *J. Chromatogr.*, 384 (1987) 25.
- 15 J. E. Eble, R. L. Grob, P. E. Antle and L. R. Snyder, *J. Chromatogr.*, 384 (1987) 45.
- 16 J. E. Eble, R. L. Grob, P. E. Antle and L. R. Snyder, *J. Chromatogr.*, 405 (1987) 1.
- 17 L. R. Snyder, J. W. Dolan and G. B. Cox, *J. Chromatogr.*, 483 (1989) 63.
- 18 J. Newburger, L. Liebes, H. Colin and G. Guiochon, *Sep. Sci.*, 22 (1987) 1933.
- 19 J. Newburger and G. Guiochon, *J. Chromatogr.*, 484 (1989) 153.
- 20 E. Glueckauf, *Proc. Roy. Soc. (London)*, A186 (1946) 35.
- 21 R. Aris and N. R. Amundson, *Mathematical Methods in Chemical Engineering*, Prentice-Hall, Englewood Cliffs, NY, 1973.
- 22 G. B. Cox, L. R. Snyder and J. W. Dolan, *J. Chromatogr.*, 484 (1989) 409.
- 23 S. Golshan-Shirazi, S. Ghodbane and G. Guiochon, *Anal. Chem.*, 60 (1988) 2630.
- 24 S. Golshan-Shirazi and G. Guiochon, *Anal. Chem.*, 60 (1988) 2634.
- 25 A. M. Katti and G. Guiochon, *J. Chromatogr.*, 499 (1990) 5.
- 26 S. Jacobson, S. Golshan-Shirazi and G. Guiochon, *J. Am. Chem. Soc.*, 112 (1990) 6492.
- 27 S. Golshan-Shirazi and G. Guiochon, *J. Chromatogr.*, submitted for publication.
- 28 S. Golshan-Shirazi and G. Guiochon, *Anal. Chem.*, 62 (1990) 217.
- 29 L. R. Snyder, J. W. Dolan, D. C. Lommen and G. B. Cox, *J. Chromatogr.*, 484 (1989) 425.

(First received February 15th, 1990; revised manuscript received October 17th, 1990)

## Letter to the Editor

---

### **Pitfalls in the choice of isotherms for the calculation of band profiles in preparative chromatography**

#### **A reply**

Sir,

Czok and Guiochon in the preceding paper [1] have called into question our program (CRAIG4) [2] for the computer simulation of separations by preparative high-performance liquid chromatography (HPLC). Since a substantial body of work reported by us is directly [2–5] or indirectly [6,7]<sup>a</sup> based on these computer simulations, the validity of conclusions derived from this work [2–7] is similarly brought into question. Three major points have been raised by Czok and Guiochon:

(1) The approximate isotherm used in CRAIG4 is unnecessary; an exact isotherm can be used with no sacrifice in computation time.

(2) The CRAIG4 isotherm is physically meaningless and yields incorrect predictions of separation.

(3) Conclusions derived from the use of CRAIG4 “... cannot be trusted ...”, specifically for the BIOPREP program described in ref. 8.

In the present paper we will respond to each of these issues.

#### DISCUSSION

##### *(1) Approximate vs. exact isotherms for use in computer simulation*

It is stated in ref. 1 that the Craig (or other) models of preparative HPLC require comparable computation time, regardless of whether an exact or our approximate isotherm is used. This was not obvious (to us) at the time our computer simulation studies began in 1984, but the data of Table II of ref. 1 provides a convincing demonstration that this is in fact true. The comparable computation times for simulations based on either approximate or exact isotherms was recently confirmed by Poppe [9], and we now have no reason to doubt that this is the case.

Therefore we agree with ref. 1 that (in view of our *present* knowledge) there was no advantage to our past use of approximate Langmuir isotherms for the computer simulation of preparative HPLC, in place of exact solutions.

---

<sup>a</sup> The algorithm used for computer simulation in refs. 6, 7 is similar to that criticized in ref. 1 and thus is subject to the same questions.

(2) *Accuracy of computer simulations based on the isotherm of ref. 2*

The authors of ref. 1 have speculated on the rationale for our use of the isotherm of ref. 2, since the only justification<sup>a</sup> given in ref. 2 was that "... our algorithm has been found to be accurate to within about  $\pm 10\%$  ...". In order to better appreciate the reason for the apparent discrepancy between Fig. 1 of ref. 1 and the latter claim, the basis of our approximate isotherm requires a further discussion (which should have been given in ref. 2).

*Origin of the isotherm of ref. 2.* The original reason for the development of CRAIG4 was to simulate preparative HPLC under gradient elution conditions [3–5] (its later application to isocratic systems [2] was an afterthought). Since gradient separations involve mobile phases with a broad range of small-sample capacity factors,  $k'$  ( $k_0$ ), a two-solute isotherm was needed that would be applicable for (roughly)  $1 < k_0 < 1000$  and a wide range of sample compositions (varying amounts of solutes X and Y). The isotherm of ref. 2 was developed empirically to meet these conditions (see discussion of Appendix), and several hundred comparisons were carried out between the predictions of this isotherm and those for the exact Langmuir isotherm for a two-component system. These comparisons indicated that the isotherm of ref. 2 was indeed accurate within "about  $\pm 10\%$ ", but we also observed somewhat larger errors for  $k_0 < 3$ .

Upon seeing ref. 1, we re-examined the agreement between the approximate and exact isotherms and confirmed the observations of Czok and Guiochon. The accuracy of our isotherm may be better appreciated by comparing single-solute isotherms for different values of  $k_0$ , as in Fig. 1. The isotherm discontinuity which is the basis of the criticism presented in ref. 1 is clearly seen in each of these examples. However, this discontinuity becomes progressively smaller for larger values of  $k_0$ . For simulations of preparative HPLC based on gradient elution, it appears to us that the effects of this discontinuity will be small for solutes that are initially well retained ( $k_0 > 10$ ). This is confirmed by the good agreement between experimental and simulated chromatograms for single-solute gradient elution [3].

*Accuracy of CRAIG4 simulations.* We were aware that the isotherm of ref. 2 is only an approximation of the exact Langmuir isotherm<sup>b</sup>. However our goal in the various studies based on the CRAIG4 program has been described [2] as "... to uncover general (if approximate) relationships for application to preparative HPLC, rather than to present equations for predicting preparative HPLC separations exactly". In this connection it should be recalled that the requirements<sup>c</sup> for Langmuir adsorption in reversed-phase HPLC systems (especially for large samples) are unlikely to be met exactly in practice. An apparent failure of the Langmuir model for a representative two-component sample has also been reported by Katti and Guiochon [12].

---

<sup>a</sup> A number of inferential checks on the reliability of this isotherm were also reported; see Table III of ref. 2 and Fig. 2 of ref. 3 as well as related discussion.

<sup>b</sup> Our earlier use of Craig simulations [10,11] employed polynomial equations which fit the Langmuir isotherm more accurately than the isotherm of ref. 2, without any discontinuity.

<sup>c</sup> *I.e.*, 1-for-1 replacement of sorbed solvent molecules by the adsorbing solute molecule, negligible interactions between solute and solvent molecules in the mobile and stationary phases, etc.



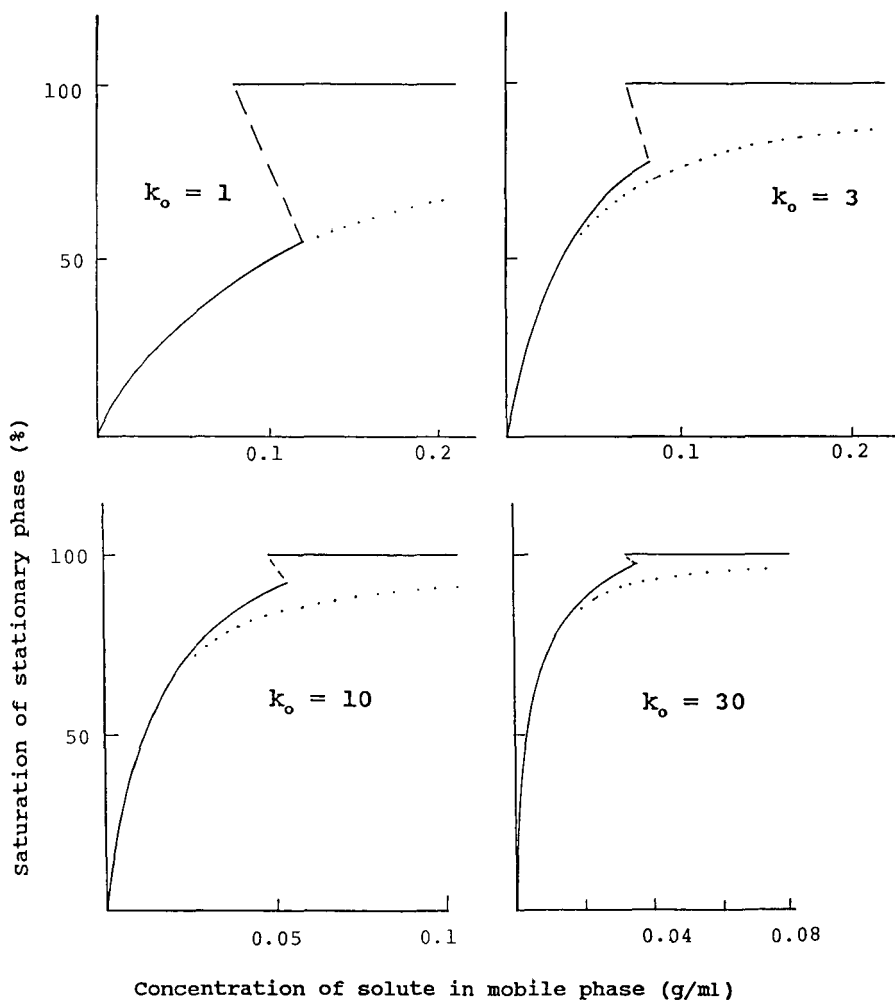


Fig. 1. Approximate (solid lines) vs. exact (dotted lines) Langmuir isotherms for a single solute. Conditions of Fig. 1, ref. 1.

Czok and Guiochon [1] stress the erroneous peak shapes that can be obtained via CRAIG4 simulations. Guiochon and co-workers continue to place considerable emphasis on band shape (“displacement” and “tag-along” effects) [13], whereas our recent studies deal solely with production rate as a function of separation conditions—or the relative overlap of two adjacent bands and their resulting purity. At this stage in the development of the theory of preparative HPLC, we feel that band shape *per se* should be of less concern. In this connection we might cite (a) the comment in ref. 1 that “... individual elution band profiles are sensitive to *minor* changes in the isotherms” (computer simulations), and (b) the diversity of band shapes encountered in experimental preparative HPLC separations [14].

Returning to the question of the accuracy (and use) of our predictions of band overlap in preparative HPLC (based on an empirical adjustment of sample size by a factor of 1.8), the data of ref. 1 fail to show that predictions based on CRAIG4 are inadequate for our intentionally approximate treatment of preparative HPLC. The only quantitative comparisons of *overlap* between CRAIG4 simulations and those of Ghodbane and Guiochon [15] (that we are aware of) indicate agreement of  $\pm 2\%$  absolute, or  $\pm 5\%$  relative—which we judge to be adequate.

Ref. 1 also refers to inaccuracies in the prediction of retention by CRAIG4. Apart from the effect of such retention errors on predictions of band overlap (which from the above discussion appear not to be serious), such discrepancies would not affect any of the conclusions reached by us on the basis of our use of CRAIG4.

Finally, Czok and Guiochon [1] suggest that the BIOPREP program described in ref. 8 "... cannot be trusted ..." because of possible deficiencies in the CRAIG4 program. In fact the BIOPREP program is based on a completely different approach than that used in CRAIG4, as a careful reading of ref. 8 indicates.

### (3) *Conclusions derived from CRAIG4*

It is worthwhile to examine some of the conclusions [2–5] reached on the basis of CRAIG4 simulations, as a further check on their relative reliability and value. That is, are our findings "reasonable" in terms of what was already known concerning preparative HPLC? And, do these conclusions provide further insight into preparative HPLC? The computer simulations of refs. 2–5 represent an extension of prior work [16–19] dealing with lightly loaded preparative HPLC ("touching band" separations in both isocratic and gradient modes) to the case of larger samples and overlapping bands. The major aim of these studies was to define general conditions for the maximum production rate (g/h) of the desired (purified) product, using the general approach of Knox and Pyper [16] for "touching band" separation.

The main conclusions reached by us in refs. 2–5 are as follows.

*First*, there is a marked parallelism between lightly and heavily overloaded preparative HPLC in the dependence of the maximum production rate on the sample characteristics ( $k_0$  and separation factor,  $\alpha$ ) and separation conditions (values of the plate number  $N_0$  and the weight of sample). Relative to the case of an optimized "touching band" separation, production rate can be increased by further increase in sample size and decrease in column plate number—with a corresponding increase in band overlap and decrease in the recovery of pure product.<sup>a</sup>

The optimum choice of the (small-sample) column plate number  $N_0$  can be related to the resolution  $R_s$  observed for a small sample. This should be about  $R_s = 1.7^a$  for the touching band case (100% recovery of pure product),  $R_s = 1.2$  for moderate overlap of the two bands (95% recovery of pure product) and  $R_s = 0.9$  for heavy overlap (50% recovery). The production rate increases for these three cases in the ratio of 1 (100% recovery):4 (95% recovery):20 (50% recovery), showing a marked advantage to the use of heavier column loadings.

Finally, the required plate numbers for *e.g.*, 95% recovery of pure product are

---

<sup>a</sup> Knox and Pyper suggest a value of  $R_s = 2$ , but this ignores the displacement of one solute by the other.

relatively low: about  $N_0 = 200$  for  $\alpha = 2$ , and  $N_0 = 3000$  for  $\alpha = 1.25^a$ . In the latter connection, it is probable that most preparative HPLC separations carried out at the present time use columns and flow-rates that provide excessively large  $N_0$  values, in turn yielding below-optimum production rates.

*Second*, earlier work has shown (for the case of a small sample and closely eluting solute bands) that an isocratic separation can always be duplicated by a gradient run with “corresponding” conditions; *i.e.*, a gradient steepness  $b$  which is equivalent to the mobile phase composition (%B) used in the isocratic separation [21] ( $1/b \approx k'$ ). This conclusion was subsequently shown to be true of lightly loaded (“touching band”) separations as well [19]. Recent studies based on CRAIG4 simulations [3–5] have now extended this generalization to heavily overloaded preparative HPLC. That is, the various conclusions summarized above for overlapping-band isocratic separation have been shown to apply also to gradient elution, for the case of “corresponding” conditions. This further suggests that the more approximate computer simulations used by us for isocratic elution are in fact adequate in terms of our “practical” objectives.

We leave to the reader the question of whether the above conclusions based on CRAIG4 simulations are (a) reasonable and (b) of practical value.

## CONCLUSIONS

In summary, we agree with Czok and Guiochon that our use of an empirical isotherm (in our CRAIG4 program) in place of the exact Langmuir isotherm introduces some error into resulting simulations of preparative HPLC, and there is no compensating advantage in terms of computation time. However this observation must be qualified by several other facts.

*First*, our use of computer simulations based on CRAIG4 has been aimed at deriving approximate, general guidelines that will be helpful to practical workers. Since the Langmuir isotherm is only a crude approximation for most HPLC separations of practical interest, any generalizations based on an isotherm of slightly different shape are not likely to be much different.

*Second*, Czok and Guiochon [1] have emphasized certain differences in separations predicted by CRAIG4 *vs.* the exact Langmuir isotherm; *i.e.*, band shape and retention. Our work has instead focused on separation as measured in terms of band overlap and band purity. Such evidence as has so far been reported suggests that band overlap as predicted by our approach (using CRAIG4) agrees within about  $\pm 2\%$  with band overlap predicted by the exact Langmuir isotherm.

*Finally*, our work based on CRAIG4 is an attempt to extend the conclusions of previous workers on lightly loaded (“touching band”) separations to the case of heavily loaded (overlapping band) preparative HPLC. The CRAIG4 results suggest that lightly and heavily overloaded separations are remarkably similar, despite striking differences in the shapes of the solute bands in the two cases. Well documented generalizations that apply to the “touching band” case can now be extended (with minor modification) to overlapping band separations.

---

<sup>a</sup> Preparative HPLC on a production scale should in most cases involve values of  $\alpha > 1.5$ , as the result of careful selection of separation conditions; see, *e.g.*, ref. 20.

Finally, in our opinion, the Knox–Pyper model of preparative HPLC [16] continues to provide the best available conceptual picture of these separations. Computer simulations based on more detailed and “exact” models will no doubt continue to add to our understanding of preparative HPLC. However such work (including our own) has not yet significantly modified the elegant (if approximate) guidelines set forth in ref. 16.

## APPENDIX

The discontinuity in the isotherms of Fig. 1 (and Fig. 1 of ref. 1) arise from our use of a two-part function to represent the Langmuir isotherm. In an earlier study [10] we showed that the one-solute isotherm can be used as the basis for a reasonable approximation to the two-solute isotherm (thereby simplifying and shortening the calculations needed in computer simulation), if different functions are used for light and heavy loadings of the stationary phase (column). In earlier work (prior to our use of CRAIG4) computer simulation was restricted to rather small samples, allowing use of a single function for the isotherm, with no discontinuity as in Fig. 1. CRAIG4 was intended for application to a wide range of sample sizes, leading to the use of the two-part function illustrated in Fig. 1.

The accuracy of the smaller-sample function that forms part of the CRAIG4 isotherm can be seen in the various comparisons of Fig. 1 and Fig. 1 of ref. 1 (first part of the isotherm). Unfortunately, values of  $\alpha$  (which are of major importance in the accurate description of preparative HPLC) begin to deviate from the chosen (correct) values at higher loadings—just beyond the first segment of these isotherms. The second (large-sample) function that comprises the CRAIG4 isotherm is designed to maintain the value of  $\alpha$  at a constant (correct) value regardless of sample size.

*LC Resources Inc.,  
3182C Old Tunnel Road, Lafayette, CA 94549 (U.S.A.)*

L. R. SNYDER\*

*Prochrom, Indianapolis, IN 46278 (U.S.A.)*

G. B. COX

- 1 M. Czok and G. Guiochon, *J. Chromatogr.*, 537 (1991) 497.
- 2 L. R. Snyder, J. W. Dolan and G. B. Cox, *J. Chromatogr.*, 483 (1989) 63.
- 3 G. B. Cox, L. R. Snyder and J. W. Dolan, *J. Chromatogr.*, 484 (1989) 409.
- 4 L. R. Snyder, J. W. Dolan and G. B. Cox, *J. Chromatogr.*, 484 (1989) 437.
- 5 L. R. Snyder, J. W. Dolan and G. B. Cox, *J. Chromatogr.*, 540 (1991) in press.
- 6 L. R. Snyder, G. B. Cox and P. E. Antle, *J. Chromatogr.*, 444 (1988) 303.
- 7 G. B. Cox, P. E. Antle and L. R. Snyder, *J. Chromatogr.*, 444 (1988) 325.
- 8 L. R. Snyder, J. W. Dolan, D. C. Lommen and G. B. Cox, *J. Chromatogr.*, 484 (1989) 425.
- 9 H. Poppe, personal communication, February 1990.
- 10 J. E. Eble, R. L. Grob, P. E. Antle and L. R. Snyder, *J. Chromatogr.*, 405 (1987) 1.
- 11 J. E. Eble, R. L. Grob, P. E. Antle and L. R. Snyder, *J. Chromatogr.*, 384 (1987) 45.
- 12 A. M. Katti and G. Guiochon, *J. Chromatogr.*, 499 (1990) 21.
- 13 S. Ghodbane and G. Guiochon, *J. Chromatogr.*, 444 (1988) 275.
- 14 M. Verzele and C. Dewaele, *Preparative High-Performance Liquid Chromatography*, TEC, Ghent, 1986, pp. 75–77.
- 15 S. Ghodbane and G. Guiochon, *J. Chromatogr.*, 452 (1988) 209.
- 16 J. H. Knox and H. M. Pyper, *J. Chromatogr.*, 363 (1986) 1.
- 17 L. R. Snyder, G. B. Cox and P. E. Antle, *Chromatographia*, 24 (1987) 82.

- 18 L. R. Snyder and G. B. Cox, *J. Chromatogr.*, 483 (1989) 85.
- 19 J. E. Eble, R. L. Grob, P. E. Antle and L. R. Snyder, *J. Chromatogr.*, 405 (1987) 51.
- 20 L. R. Snyder, J. L. Glajch and J. J. Kirkland, *Practical HPLC Method Development*, Wiley-Interscience, New York, 1988.
- 21 L. R. Snyder, in Cs. Horváth (Editor), *High-Performance Liquid Chromatography — Advances and Perspectives*, Vol. 1, Academic Press, New York, 1980, p. 207.

(Received September 25th, 1990)

CHROM. 22 777

## Letter to the Editor

---

### Detection of choline and acetylcholine by high-performance liquid chromatography

#### Limitations, pitfalls, sample preparation

Sir,

The determination of choline esters [1] has received a new impulse from the introduction of a high-performance liquid chromatographic (HPLC) method with electrochemical detection, first described by Potter and co-workers [2,3]. The two enzymes acetylcholinesterase (AChE) and choline oxidase (ChO) used to generate electrochemically detectable hydrogen peroxide were later immobilized in a short post-column reactor [4–9]. The selectivity of this method is achieved in three ways: (1) by the number of theoretical plates of the cation-exchange separation column, (2) by the selectivity of the immobilized enzymes in the post-column reactor and (3) by the low oxidation potential of the electrochemical detector (+ 500 mV using a platinum electrode and an Ag/AgCl reference electrode) at which only few other substances are also taken up that could possibly interfere.

A major drawback of the originally described methods was the very short lifetime of the usually silica-based cation-exchange separation column under the assay conditions [silica is dissolved at alkaline pH (> 7.2)] [7]. This paper compares the performance of commercially available cation-exchange columns and describes some experience in working with the HPLC method for the detection of choline and acetylcholine.

#### HPLC SYSTEM

The HPLC system consisted of a constant-flow pump (Model 600/200; Gynkotek, Munich, F.R.G.) and as an electrochemical detector either an ELDEC 102 (Chromatofield, Chateauneuf-les-Martigues, France) or a model M 20 (Gynkotek). The platinum electrode, the detection chamber and the enzyme reactor with the immobilized enzymes were manufactured by Biometra (Göttingen, F.R.G.) [9]. The running buffer was 100 mmol/l phosphate buffer (pH 7.6) containing 7 mmol/l tetramethylammonium perchlorate (TMA). The flow-rate was varied between 0.5 and 1.5 ml/min.

## CATION SEPARATION COLUMNS

The cation-exchange separation columns tested are listed in Table I. In the first few days of use the Nucleosil columns provided the highest number of theoretical plates. Four Nucleosil columns were tested: three Nucleosil 5 SA (packed by Macherey-Nagel, Düren, F.R.G.) and one Nucleosil 5 SA (packed by Gynkotek). The best results were obtained with the column packed by Gynkotek. However, the performance of all the columns decreased after a few days, so that the assay became inadequate at a very early stage after starting the system (Fig. 1A). The lifetime never exceeded 10 days, the columns suddenly becoming completely blocked owing to the dissolution of the silica-based Nucleosil at pH 7.6 (see above). This pH of the running buffer was a compromise: a more acidic pH would have prevented dissolution of the silica, but would not have been tolerated by the enzymes in the enzyme reactor; on the other hand, an even more alkaline pH range (8.0–8.5) would have been optimum for the enzymatic reaction [10]. An acceptable retention time of < 10 min for acetylcholine could only be obtained with high flow-rates of 1.2–1.5 ml/min (Table I) at an extremely high back-pressure (> 150 bar). With such flow-rates, the lifetimes of the columns were even shorter.

Excellent results were obtained with Hamilton PRP-X 200 columns [a macroporous poly(styrene–divinylbenzene) copolymer; Hamilton, Reno, NV, U.S.A.]. Both of the columns tested could still be used after 4 weeks. During that time the performance of the columns did not decrease noticeably. The peaks were sharp and the retention times on the short column (No. 6, Table I) were 3.2 min for choline and 8.8 min for acetylcholine at a flow-rate of 0.7 ml/min (Fig. 1B). Under these conditions choline could still be distinguished from the solvent peak. With the long Hamilton PRP X-200 column (No. 5, Table I) the retention times were 3.1 min for choline and 11.3 min for acetylcholine at a flow-rate of 1.5 ml/min. Even under these conditions the back-pressure was very low (33 bar).

No separation of choline and acetylcholine could be achieved with the Bio-Gel TSK-SP-5PW column (No. 7, Table I) or the Microanalyzer MA7C cartridge (No. 8, Table I) (both supplied by Bio-Rad Labs., Munich, F.R.G.). On the Bio-Gel TSK-SP-5PW column only one peak with a retention time of 7.3 min at a flow-rate of 0.5 ml/min appeared for both substances. This peak could be shifted by varying the ionic strength of the running buffer between 10 and 100 mmol/l phosphate or by changing the flow-rate from 0.5 up to 1.5 ml/min. A separation of the two substances could never be achieved, and the peak height and peak area depended on the amount of choline and/or acetylcholine injected. This suggested that acetylcholine was cleaved on the column and detected as choline. With the Microanalyzer MA7C cartridge the choline esters appeared in the solvent peak, indicating that they were not retarded on the column.

## DETECTION LIMIT

The detection limit (three times the signal-to-noise ratio) depended on the sample volume, on the cation separation column and on the age of the enzyme reactor. Increasing the injection volume fivefold (from 10 to 50  $\mu$ l) resulted in only a 3.5-fold decrease in the relative detection limit owing to an increase in the peak width. The

TABLE I  
COLUMN SPECIFICATIONS, RETENTION TIMES AND NUMBER OF THEORETICAL PLATES FOR THE CATION-EXCHANGE SEPARATION COLUMNS TESTED

No. Column	Dimensions (length $\times$ I.D.) (mm)	Lifetime (days)	Flow- rate (ml/min)	Choline		Acetylcholine	
				Retention time (min)	Peak width (mm)	Retention time (min)	Peak width (mm)
						Theoretical plates Per column	Theoretical plates Per column
1	Nucleosil 5 SA (Macherey, Nagel & Co.)	<10					
			After 4 days of use:				
			1.0	4.0	4.3	479	2397
			1.0	8.3	5.5	1256	10045
2	Nucleosil 5 SA (Macherey, Nagel & Co.)	<10					
			1.2	5.4	3.6	1270	10158
3	Nucleosil 5 SA (Macherey, Nagel & Co.)	<10					
			1.5	6.6	3.5	1958	15664
4	Nucleosil 5 SA (Gynkotek)	<10					
			8 days later:				
			1.5	5.7	6.2	468	3746
			0.7	6.7	6.1	670	2683
5	PRP-X 200 (Hamilton)	>28					
			1.5	3.2	3.7	404	1616
6	PRP-X 200 (Hamilton)	>28					
			0.7	3.2	3.8	388	2586
7	Bio-Gel TSK-SP-5PW (Bio-Rad Labs.)	- <sup>a</sup>	0.5	7.3	18.0	263	3509
						No separation between choline and acetylcholine	
8	Microanalyzer MA7C (Bio-Rad Labs.)	- <sup>a</sup>					
						No separation of sample peak from solvent peak	

<sup>a</sup> Lifetimes cannot be given for columns 7 and 8 as they were only used for 2-3 days to test the separation of choline and acetylcholine. By that time no decrease in performance or in the number of theoretical plates was noticed.



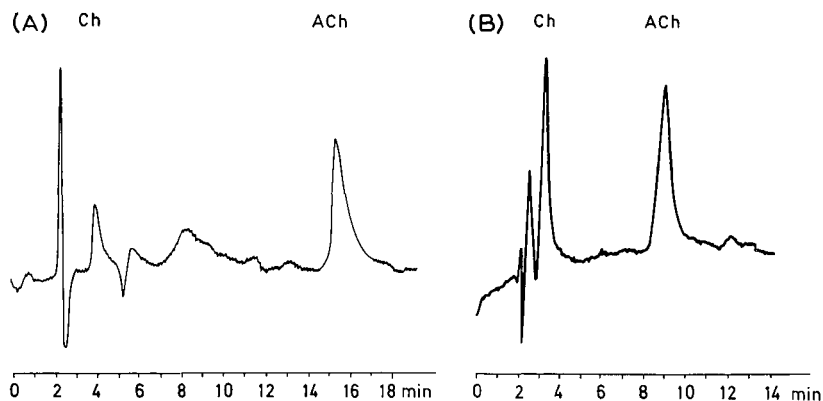


Fig. 1. Separation of choline and acetylcholine on various cation-exchange columns. (A) Nucleosil 5 SA column. 125 pmol of choline and 125 pmol of acetylcholine were injected in a sample volume of 10  $\mu$ l onto a Nucleosil 5 SA column (No. 1, Table I). The column was used for 4 days continuously. Oxidation potential, +500 mV; detector sensitivity, 0.5 nA/V (full-scale); running buffer, 100 mmol phosphate buffer (pH 7.6) containing 7 mmol/l tetramethylammonium perchlorate; flow-rate, 1.0 ml/min. (B) Hamilton PRP-X 200 column. 266 pmol of choline and 414 pmol of acetylcholine were injected in a sample volume of 20  $\mu$ l onto a Hamilton PRP-X 200 column (No. 7, Table I). The column was used for 6 days continuously. Oxidation potential, +500 mV; detector sensitivity, 0.02 nA per 10 mV (full-scale); running buffer, as in (A); flow-rate, 0.7 ml/min.

method was 4–8 times more sensitive for choline than for acetylcholine. With the Nucleosil 5 SA column the absolute detection limit was 9 pmol of choline and 39 pmol of acetylcholine in a 10- $\mu$ l injection volume; with the Hamilton PRP-X 200 column it was 11 pmol of choline and 85 pmol of acetylcholine in a 20- $\mu$ l injection volume. Shortly before the enzyme reactor broke down the detection limit increased.

#### SAMPLE PREPARATION

Deproteinization with perchloric acid is usually sufficient for sample preparation [11]. However, an extraction procedure may be necessary to increase the sample concentration of acetylcholine and/or to remove acetylcholine esterase inhibitors [12]. We modified the ion-pair extraction with dipicrylamine (DPA) as described by Eksborg and Persson [13,14] to obtain free acetylcholine for HPLC with electrochemical detection. The specimens were shaken twice for 8 min in a vertical shaker with 5 ml of  $1.2 \cdot 10^{-3}$  mol/l DPA solution in dichloromethane followed by centrifugation for 10 min at 4°C. The aqueous phase was discarded, the combined organic phases were evaporated to dryness under a stream of nitrogen and the residue was resuspended in 1 ml of Bio-Rex-9 (Bio-Rad Labs.) in methanol. After sedimentation of the anion-exchange resin, the supernatant was transferred to a new tube, in which the methanol was evaporated at 37°C under a stream of nitrogen. The residue was resuspended in 25  $\mu$ l of HPLC running buffer.

Choline and/or acetylcholine dissolved in Krebs–Ringer hydrogencarbonate solution (pH 7.4) used for perfusion of isolated guinea-pig hearts were thus treated. Acetylcholine could be concentrated by factor of 4; with an injection volume of 20  $\mu$ l

the acetylcholine concentration of a 1.1  $\mu\text{mol/l}$  solution could still be detected. Under the conditions described here, choline was extracted to only a very limited extent, resulting in its almost complete loss. The procedure is fast and simple to perform (ten samples within 2 h).

#### CONCLUSIONS

The HPLC method with electrochemical detection for the detection of choline esters is a very suitable quantitative method for routine analyses. It provides the highest selectivity of all currently available methods. The total amount of acetylcholine necessary for detection is in the range of that in other methods, *e.g.*, the radio-enzyme assay of Goldberg and McCaman [15] and McCaman and Stetzler [16] or the isotachophoretic method of Haen *et al.* [17], with the advantage of easier handling and possible automation. Not all cation-exchange separation columns are suitable. Silica-based columns yield optimum separations of choline esters within the first 3–4 days of use, but deteriorate under the assay conditions (pH 7.6), having a lifetime of less than 10 days. Reports in the literature recommend repacking these columns every week [10]. This situation is very unfortunate, as the sensitivity of the electrochemical detector and the stability of its baseline increase over 3–4 days. The detection limit depends on the sample volume, on the age of the enzyme reactor and on the cation separation column. The best results were obtained with Hamilton PRP-X 200 columns. With an HPLC injection volume of 20  $\mu\text{l}$ , the absolute detection limit for acetylcholine is 85 pmol. The method is about 4–8 times more sensitive for choline than for acetylcholine. Enrichment of the acetylcholine concentration is possible by ion-pair extraction using dipicrylamine, with an enrichment by a factor of 4.

#### ACKNOWLEDGEMENT

This study was supported by BMVg grant In San I 2683-V-4886.

*Walther-Straub-Institute of Pharmacology and Toxicology,*  
*University of Munich, Nussbaumstr. 26,*  
*D-8000 Munich 2 (F.R.G.)*

E. HAEN\*

*Institute of Organic Chemistry,*  
*University of Tübingen, Auf der Morgenstelle 18,*  
*D-7400 Tübingen (F.R.G.)*

H. HAGENMAIER

*Walther-Straub-Institute of Pharmacology and Toxicology,*  
*University of Munich, Nussbaumstr. 26,*  
*D-8000 Munich 2 (F.R.G.)*

J. REMIEN

- 1 Y. Maruyama, Y. Ikarashi and L. Blank, *Trends Pharmacol. Sci.*, 8 (1987) 84.
- 2 P. E. Potter, J. L. Meek and N. H. Neff, *J. Neurochem.*, 41 (1983) 188.
- 3 P. E. Potter, M. Hadjiconstantinou, J. L. Meek and N. H. Neff, *J. Neurochem.*, 43 (1984) 288.
- 4 J. L. Meek and C. Eva, *J. Chromatogr.*, 317 (1984) 343.
- 5 C. Eva, M. Hadjiconstantinou, N. H. Neff and J. L. Meek, *Anal. Biochem.*, 143 (1984) 320.

- 6 T. Yao and M. Sato, *Anal. Chim. Acta*, 172 (1985) 371.
- 7 G. Damsma, B. H. C. Westerink and A. S. Horn, *J. Neurochem.*, 45 (1985) 1649.
- 8 M. Asano, T. Miyauchi, T. Kato, K. Fujimori and K. Yamamoto, *J. Liq. Chromatogr.*, 9 (1986) 199.
- 9 H. Stadler and T. Nesselhut, *Neurochem. Int.*, 9 (1986) 127.
- 10 G. Damsma, G. D. Lammerts van Bueren, B. H. C. Westerink and A. S. Horn, *Chromatographia*, 24 (1987) 827.
- 11 K. Koshimura, S. Miwa, K. Lee, Y. Hayashi, H. Hasegawa, K. Hamahata, M. Fujiwara, M. Kimura and Y. Itokawa, *J. Neurochem.*, 54 (1990) 533.
- 12 S. Okuyama and Y. Ikeda, *J. Chromatogr.*, 431 (1988) 389.
- 13 S. Eksborg and B. A. Persson, *Acta Pharm. Suec.*, 8 (1971) 205.
- 14 S. Eksborg and B. A. Persson, in I. Hanin (Editor), *Choline and Acetylcholine: Handbook of Chemical Assay Methods*, Raven Press, New York, 1974, p. 181.
- 15 A. M. Goldberg and R. E. McCaman, *J. Neurochem.*, 20 (1973) 1.
- 16 R. E. McCaman and J. Stetzler, *J. Neurochem.*, 28 (1977) 669.
- 17 E. Haen, I. Fiedler, A. Gerbes and L. Szinicz, *Naunyn-Schmiedeberg's Arch. Pharmacol.*, 322 (1983) R1.

(First received November 14th, 1989; revised manuscript received August 27th, 1990)

## Author Index

- Ackermans, M. T., see Beckers, J. L. 537(1991)407
- Ackermans, M. T., see Beckers, J. L. 537(1991)429
- Akiyama, T., see Kuno, Y. 537(1991)489
- Al-Ammar, A. S., Hamid, H. A., Rashid, B. H. and Basheer, H. M.  
Preseparation of uranium by reversed-phase partition chromatography. Application to the determination of trace elements in nuclear-grade uranium compounds by inductively coupled plasma atomic emission spectrometry 537(1991)287
- Alexandrovich, O., see Sigalov, A. 537(1991)464
- Ang, H. G., Kwik, W. L. and Leong, W. K.  
High-performance liquid chromatography of substituted trinuclear osmium carbonyl clusters,  $\text{Os}_3(\text{CO})_{12-n}[\text{P}(\text{C}_6\text{F}_5)_3]_n$  ( $n=0, 1, 2$ ) 537(1991)475
- Basheer, H. M., see Al-Ammar, A. S. 537(1991)287
- Beckers, J. L., Everaerts, F. M. and Ackermans, M. T.  
Determination of absolute mobilities,  $pK$  values and separation numbers by capillary zone electrophoresis. Effective mobility as a parameter for screening 537(1991)407
- Beckers, J. L., Everaerts, F. M. and Ackermans, M. T.  
Isotachophoresis with electroosmotic flow: open *versus* closed systems 537(1991)429
- Bezuidenhout, H. S., see Jones, E. A. 537(1991)277
- Bourque, A. J. and Krull, I. S.  
Solid-phase reagent containing the 3,5-dinitrophenyl tag for the improved derivatization of chiral and achiral amines, amino alcohols and amino acids in high-performance liquid chromatography with ultraviolet detection 537(1991)123
- Bourrier, M.-J., see Goiffon, J.-P. 537(1991)101
- Boyer, G. L., see Speirs, R. J. 537(1991)259
- Brun, M., see Goiffon, J.-P. 537(1991)101
- Byerley, T. J., see Fanska, C. B. 537(1991)357
- Carini, M., see Pietta, P. 537(1991)449
- Cartoni, G. P., Cocioli, F., Pontelli, L. and Quattrucci, E.  
Separation and identification of free phenolic acids in wines by high-performance liquid chromatography 537(1991)93
- Castello, G., see Gerbino, T. C. 537(1991)305
- Chang, F. C., see Iida, T. 537(1991)345
- Cocioli, F., see Cartoni, G. P. 537(1991)93
- Cox, G. B., see Snyder, L. R. 537(1991)507
- Crimmins, D. L., see Thoma, R. S. 537(1991)153
- Czok, M. and Guiochon, G.  
Pitfalls in the choice of isotherms for the calculation of band profiles in preparative chromatography 537(1991)497
- Devani, M. B., Shishoo, C. J., Shah, S. A., Soni, K. P. and Shah, R. S.  
Localization of amino acids on thin-layer chromatograms with acetylacetone-formaldehyde reagent 537(1991)494
- Diwan, A. M., see Elias, C. 537(1991)460
- Eick, J. D., see Fanska, C. B. 537(1991)357
- Elias, C. and Diwan, A. M.  
Behaviour of concanavalin A on DEAE-Sephadex and CM-Sephadex 537(1991)460
- Ellegren, H., see Kågedal, L. 537(1991)17
- Engström, B., see Kågedal, L. 537(1991)17
- Everaerts, F. M., see Beckers, J. L. 537(1991)407
- Everaerts, F. M., see Beckers, J. L. 537(1991)429
- Facino, R. M., see Pietta, P. 537(1991)449
- Fanska, C. B., Byerley, T. J. and Eick, J. D.  
Indirect determination of isocyanates by gas chromatography 537(1991)357
- Finn, N., see Smith, R. M. 537(1991)51
- Ford, S. H., Gallery, J., Nichols, A. and Shambee, M.  
High-performance liquid chromatographic analysis of the (cyanoaquo) stereoisomers of several putative vitamin  $\text{B}_{12}$  precursors 537(1991)235
- Furusawa, M., see Kiba, N. 537(1991)443
- Gallery, J., see Ford, S. H. 537(1991)235
- Gardana, C., see Pietta, P. 537(1991)449
- Gerbino, T. C. and Castello, G.  
Gas chromatographic identification of complex mixtures of halomethanes and haloethanes by using the correlation between their retention and vapour pressure 537(1991)305
- Goiffon, J.-P., Brun, M. and Bourrier, M.-J.  
High-performance liquid chromatography of red fruit anthocyanins 537(1991)101
- Goto, J., see Iida, T. 537(1991)345
- Goyal, S. S., Hafez, A. and Rains, D. W.  
Simultaneous determination of arsenite, arsenate, selenite and selenate in waters using suppressed ion chromatography with ultraviolet absorbance detection 537(1991)269
- Guiochon, G., see Czok, M. 537(1991)497
- Gülz, P.-G., see Vogt, T. 537(1991)453



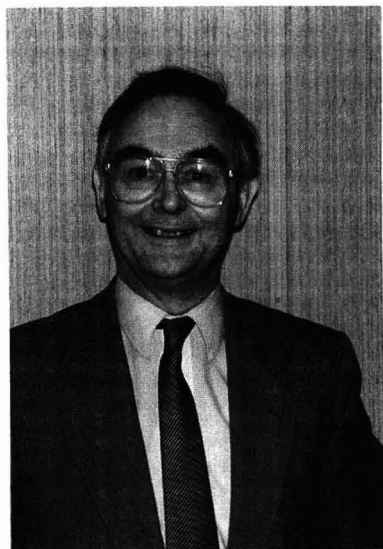
- Haen, E., Hagenmaier, H. and Remien, J.  
Detection of choline and acetylcholine by high-performance liquid chromatography. Limitations, pitfalls, sample preparation 537(1991)514
- Hafez, A., see Goyal, S. S. 537(1991)269
- Hagenmaier, H., see Haen, E. 537(1991)514
- Hamid, H. A., see Al-Amman, A. S. 537(1991)287
- Hasunuma, R., Ogawa, T., Ishii, J. and Kawanishi, Y.  
Determination of selenium in organic compounds on a silica gel sintered thin-layer chromatographic plate with 2,3-diaminonaphthalene after direct digestion 537(1991)397
- Hermecz, I., see Papp, O. 537(1991)365
- Hermecz, I., see Papp, O. 537(1991)371
- Hermecz, I., see Papp, O. 537(1991)377
- Hina, T., see Kuno, Y. 537(1991)489
- Huisden, R. E., Kraak, J. C. and Poppe, H.  
Method for the characterization of stationary phases for the separation of proteins by high-performance liquid chromatography 537(1991)1
- Hurtubise, R. J., see Mohseni, R. M. 537(1991)61
- Iida, T., Komatsubara, I., Chang, F. C., Goto, J. and Nambara, T.  
Capillary gas chromatographic behavior of stereoisomeric bile acids with a *vicinal* glycol structure by their "mixed" alkylboronate derivatives 537(1991)345
- Ikesaki, T., see Ngan, F. 537(1991)385
- Ishii, J., see Hasunuma, R. 537(1991)397
- Joelsson, M., see Johansson, G. 537(1991)219
- Johansson, G. and Joelsson, M.  
Protein-ligand interactions studied on bovine serum albumin with free and polymer-bound Cibacron Blue F3G-A as ligand with reference to affinity partitioning 537(1991)219
- Jones, E. A., Bezuidenhout, H. S. and Van Staden, J. F.  
Separation of lanthanides and yttrium as anionic complexes by isocratic ion-interaction chromatography 537(1991)277
- Kågedal, L., Engström, B., Ellegren, H., Lieber, A.-K., Lundström, H., Sköld, A. and Schenning, M.  
Chemical, physical and chromatographic properties of Superdex 75 prep grade and Superdex 200 prep grade gel filtration media 537(1991)17
- Kanazawa, H., Nagata, Y., Matsushima, Y., Tomoda, M. and Takai, N.  
Preparative high-performance liquid chromatography on chemically modified porous glass. Isolation of acidic saponins from ginseng 537(1991)469
- Kaphalia, B. S.  
Fatty acid conjugates of chlorinated phenols and their high-performance liquid chromatographic analysis 537(1991)85
- Kawanishi, Y., see Hasunuma, R. 537(1991)397
- Kiba, N., Shitara, K., Furusawa, M. and Takata, Y.  
Post-column oligosaccharide dehydrogenase reactor for coulometric detection of malto-oligosaccharides in a liquid chromatographic system 537(1991)443
- Kökösi, J., see Papp, O. 537(1991)365
- Kökösi, J., see Papp, O. 537(1991)377
- Komatsubara, I., see Iida, T. 537(1991)345
- Kraak, J. C., see Huisden, R. E. 537(1991)1
- Krull, I. S., see Bourque, A. J. 537(1991)123
- Kuno, Y., Hina, T., Akiyama, T. and Matsui, M.  
Simultaneous determination of tributyl phosphate and dibutyl phosphate in spent fuel reprocessing streams by gas chromatography 537(1991)489
- Kwik, W. L., see Ang, H. G. 537(1991)475
- Lanin, S. N. and Nikitin, Y. S.  
Molecular interactions in liquid chromatography 537(1991)33
- Larionov, O. G., Petrenko, V. V. and Platonova, N. P.  
Determination of contributions of different types of solute-sorbent interactions in gas-adsorption chromatography by linear regression of adsorption energies 537(1991)295
- Leong, W. K., see Ang, H. G. 537(1991)475
- Lieber, A.-K., see Kågedal, L. 537(1991)17
- Linde, S., see Welinder, B. S. 537(1991)201
- Lundström, H., see Kågedal, L. 537(1991)17
- Matsui, M., see Kuno, Y. 537(1991)489
- Matsushima, Y., see Kanazawa, H. 537(1991)469
- Mauri, P., see Pietta, P. 537(1991)449
- Mohseni, R. M. and Hurtubise, R. J.  
Changes in the enthalpy and entropy of hydroxyl aromatics in reversed-phase liquid chromatography with  $\beta$ -cyclodextrin in the mobile phase 537(1991)61
- Nagata, Y., see Kanazawa, H. 537(1991)469
- Nambara, T., see Iida, T. 537(1991)345

- Nesterova, I., Rekhter, B., Roshka, G. and Witkiewicz, Z.  
Liquid crystals for the gas chromatographic determination of the stereochemistry of insect sex pheromones 537(1991)482
- Ngan, F. and Ikesaki, T.  
Determination of nine acidic herbicides in water and soil by gas chromatography using an electron-capture detector 537(1991)385
- Nichols, A., see Ford, S. H. 537(1991)235
- Nikitin, Y. S., see Lanin, S. N. 537(1991)33
- Ogawa, T., see Hasunuma, R. 537(1991)397
- Olsson, M., Sander, L. C. and Wise, S. A.  
Comparison of the liquid chromatographic behaviour of selected steroid isomers using different reversed-phase materials and mobile phase compositions 537(1991)73
- Órfi, L., see Papp, O. 537(1991)371
- Pankow, J. F., see Rosen, M. E. 537(1991)321
- Papp, O., Szász, G., Kökösi, J. and Hermecz, I.  
Correlation between structure and gaschromatographic behaviour of nitrogen-containing heterocyclic compounds. I. Methyl substitution of pyridopyrimidine derivatives 537(1991)365
- Papp, O., Szász, G., Kökösi, J. and Hermecz, I.  
Correlation between structure and gas chromatographic behaviour of nitrogen-containing heterocyclic compounds. III. Variation of ring size 537(1991)377
- Papp, O., Szász, G., Órfi, L. and Hermecz, I.  
Correlation between structure and gas chromatographic behaviour of nitrogen-containing heterocyclic compounds. II. Alkyl substitution of quinazolone derivatives 537(1991)371
- Perkins, E. G., see Rojo, J. A. 537(1991)329
- Petrenko, V. V., see Larionov, O. G. 537(1991)295
- Pietta, P., Mauri, P., Gardana, C., Facino, R. M. and Carini, M.  
High-performance liquid chromatographic determination of flavonoid glucosides from *Helichrysum italicum* 537(1991)449
- Platonova, N. P., see Larionov, O. G. 537(1991)295
- Pontelli, L., see Cartoni, G. P. 537(1991)93
- Poppe, H., see Huisden, R. E. 537(1991)1
- Quattrucci, E., see Cartoni, G. P. 537(1991)93
- Rains, D. W., see Goyal, S. S. 537(1991)269
- Rashid, B. H., see Al-Ammar, A. S. 537(1991)287
- Rekhter, B., see Nesterova, I. 537(1991)482
- Remien, J., see Haen, E. 537(1991)514
- Rojo, J. A. and Perkins, E. G.  
Isomer identification and gas chromatographic retention studies of monomeric cyclic fatty acid methyl esters 537(1991)329
- Rosen, M. E. and Pankow, J. F.  
Adsorption/thermal desorption for the determination of volatile organic compounds in water 537(1991)321
- Roshka, G., see Nesterova, I. 537(1991)482
- Šalamoun, J. and Šlais, K.  
Elimination of peak splitting in the liquid chromatography of the proline-containing drug enalapril maleate 537(1991)249
- Sander, L. C., see Olsson, M. 537(1991)73
- Schenning, M., see Kågedal, L. 537(1991)17
- Seidel, A., see Slonina, P. 537(1991)167
- Shah, R. S., see Devani, M. B. 537(1991)494
- Shah, S. A., see Devani, M. B. 537(1991)494
- Shambee, M., see Ford, S. H. 537(1991)235
- Shishoo, C. J., see Devani, M. B. 537(1991)494
- Shitara, K., see Kiba, N. 537(1991)443
- Sigalov, A., Alexandrovich, O. and Strizevskaya, E.  
Large-scale isolation and purification of human apolipoproteins A-I and A-II 537(1991)464
- Sköld, A., see Kågedal, L. 537(1991)17
- Šlais, K., see Šalamoun, J. 537(1991)249
- Slonina, P. and Seidel, A.  
Breakthrough curves of insulin, [D-Phe<sup>6</sup>]-Gonadotropin-releasing hormone and phenylalanine methyl ester on copolymers of alkylacrylate and divinylbenzene 537(1991)167
- Smith, R. M. and Finn, N.  
Comparison of retention index scales based on alkyl aryl ketones, alkan-2-ones and 1-nitroalkanes for polar drugs on reversed-phase high-performance liquid chromatography 537(1991)51
- Snyder, L. R. and Cox, G. B.  
Pitfalls in the choice of isotherms for the calculation of band profiles in preparative chromatography. A reply 537(1991)507
- Soni, K. P., see Devani, M. B. 537(1991)494
- Sørensen, H. H., see Welinder, B. S. 537(1991)181
- Speirs, R. J. and Boyer, G. L.  
Analysis of <sup>55</sup>Fe-labeled hydroxamate siderophores by high-performance liquid chromatography 537(1991)259
- Strizevskaya, E., see Sigalov, A. 537(1991)464
- Szász, G., see Papp, O. 537(1991)365
- Szász, G., see Papp, O. 537(1991)371
- Szász, G., see Papp, O. 537(1991)377
- Takai, N., see Kanazawa, H. 537(1991)469

- Takata, Y., see Kiba, N. 537(1991)443
- Thoma, R. S. and Crimmins, D. L.  
Automated phenylthiocarbamyl amino acid  
analysis of carboxypeptidase/aminopeptidase  
digests and acid hydrolysates 537(1991)153
- Tomoda, M., see Kanazawa, H. 537(1991)469
- Van Staden, J. F., see Jones, E. A. 537(1991)277
- Vogt, T. and Gülz, P.-G.  
Isocratic column liquid chromatographic  
separation of a complex mixture of  
epicuticular flavonoid aglycones and  
intracellular flavonol glycosides from *Cistus  
laurifolius* L. 537(1991)453
- Welinder, B. S. and Linde, S.  
Reversed-phase high-performance liquid  
chromatographic characterization of acetic  
acid extracts of the normal and the diabetic  
human pancreas 537(1991)201
- Welinder, B. S. and Sørensen, H. H.  
Alternative mobile phases for the reversed-  
phase high-performance liquid  
chromatography of peptides and proteins  
537(1991)181
- Wise, S. A., see Olsson, M. 537(1991)73
- Witkiewicz, Z., see Nesterova, I. 537(1991)482





  
**journal of  
chromatography news section**  
**NEW CHAIRMAN****NEW PRESIDENT FOR THE CHROMATOGRAPHIC SOCIETY**

At its meeting of 13 June 1990 the Executive Committee of the Chromatographic Society elected Professor Michael Evans as the first President of the Society on the retirement of Dr. Ian Wilson, previously Chairman. Mike Evans has been a member of the Society for 30 years, joining the then Gas Chromatography Discussion Group in 1960.

Professor Evans left school at 16 having completed his School Certificate at the King's School, Macclesfield. His first job was a technician in the analytical laboratories of the Dunlop Rubber Company in Manchester. There he was encouraged to continue his studies as a part-time student on the ONC/HNC courses at the Royal Technical College, Salford. Following the award of a Technical State Scholarship he transferred to the full-time BSc/ARIC course at Salford and graduated in 1954. After a year with the Calico Printer's Association he joined the British (now Malaysian) Rubber Producers' Research Association in Welwyn Garden City. There he was introduced to gas-liquid chromatography by Dr. John Smith who guided him to an External London University PhD degree. In 1966 Professor Evans

joined the staff of Hatfield Polytechnic, where he had been a part-time teacher since 1957. Since that time he has worked up the ranks to become a Principal Lecturer in 1972 and Head of Department in 1982.

Professor Evans' research, apart from brief encounters with infra-red spectroscopy and polarography, has concentrated on gas and liquid chromatography, for which he has gained an international reputation. In particular he is noted for his collaborative studies with scientists in industry. In 1984 his contributions to chromatographic science was recognised when he received the prestigious Royal Society of Chemistry Award in Analytical Separations Methods.

## CALL FOR NOMINATIONS

### VERN BARRY INTERNATIONAL GRADUATE STUDENT PRIZE

The Vern Berry Memorial Foundation will award the first annual international graduate student prize at the HPLC '91 meeting in Basel. The prize will be awarded to the nominee, full time graduate student, who has demonstrated outstanding achievement in the field of separations science as determined by an independent award jury. The prize winner will receive a cash award of US\$ 1500 and travel expenses to attend the meeting. In addition, the research group will receive a cash award of US\$ 1000.

The Vern Berry Memorial Foundation was established in August of 1990. Austin N. Wentworth, is Trustee. Barry L. Karger (Barnet Institute, Northeastern University), Phyllis R. Brown (University of Rhode Island) and Brian Bidlingmeyer (Waters Associates) are the Advisory Board. Fritz Erni (Sandoz), John Kirkland (E.I. duPont) and Lloyd Snyder (LC Resources) are the Award Jury.

For further information and nomination forms please contact The Vern Berry Memorial Foundation, 326 Reservoir Road, Boston, MA 02167, U.S.A. Nominations must be post marked no later than *February 28, 1991* to be considered for the 1991 prize.

## ANNOUNCEMENTS OF MEETINGS

### 2nd INTERLAKEN CONFERENCE ON ADVANCES IN PURIFICATION OF RECOMBINANT PROTEINS, INTERLAKEN, SWITZERLAND, MARCH 19-22, 1991

The scientific program consists of plenary lectures, contributed papers and poster sessions. The following plenary lectures are planned: strategies in downstream processing; new developments in preparative separation techniques using cross-filtration, with special reference to rotative filtration systems; GMP production: the lessons from biosynthetic human insulin; large scale chromatography: GMP, hygiene and registration of chromatographic materials; GMP production and in-process control; folding of recombinant proteins; glycoconjugates and biotechnology; structural characterization of proteins and glycoproteins by mass spectrometry.

Contributed papers will be accepted for oral presentations (20 min) in any of the mentioned or related areas of the main topics. Poster sessions are organized to complement the oral presentations.

The registration and accommodation fee is: for participants SFr. 1600.00; for students (presenting a paper/poster) SFr. 800.00.

For further details contact: Scientific Secretariat, H.P. Walliser, Ph.D., c/o CIBA-GEIGY, K.693.1.23, CH-4002 Basel, Switzerland, Tel.: (61) 696 50 20; Fax: (61) 696 40 69.

### BIOPOLYMER SEPARATIONS 91, MONTELIBRETTI (ROME), MARCH 19-22, 1991

Biopolymer Separations 91 is a seminar on chromatographic and electrophoretic separation techniques for peptides, proteins, nucleic acids and complex carbohydrates. Fundamentals, applications and instrumentation concerning the various techniques are covered and both analytical and preparative process scale separations are treated. Internationally recognised scientists will be formally invited to report on trends and future developments over the above reported subjects.

The registration fee will be Lit. 400 000 (US\$ 325) plus Value Added Tax and will include the seminar folder with scientific documents, lunches, refreshments, and daily transportation Rome-Montelibretti-Rome.

A select number of scholarships covering the registration fee and lodging at the guest house of the Area della Ricerca di Roma will be available.

For further details contact: Dr. Danilo Corradini, Institute of Chromatography, C.N.R., Area della Ricerca di Roma, P.O. Box 10, 00016 Monterotondo Stazione, Italy. Tel.: (0039) 6-9005328/90020254; Fax: (0039) 6-9005849; Telex 624809 CNR ML 1.

#### 6th INTERNATIONAL SYMPOSIUM ON INSTRUMENTAL PLANAR CHROMATOGRAPHY, INTERLAKEN, SWITZERLAND, APRIL 23-26, 1991

Instrumental planar chromatography (high performance thin layer chromatography) is ever-increasingly being recognized as an important analytical technique possessing the virtues of reliability and simplicity, and these bi-ennial symposia serve to emphasize the rapid growth in understanding, application and practise.

Among the topics to be covered are: biomedical analysis, electro-planar chromatography, environmental analysis, forensic analysis, hyphenated techniques, instrumentation, quantitation, radio-chromatography, sample preparation, toxicology, and trace analysis.

The meeting is designed to bring together scientists from a broad spectrum of disciplines and backgrounds in order to take best advantage of the exchange of ideas and encourage cross-fertilization.

An associated exhibition will allow producers and suppliers of instruments, ancillary equipment and consumables to display and discuss their wares with existing and potential customers.

The anticipated registration fee of sFr. 550 will include entry to both the symposium and the exhibition, tickets for the welcome cocktail party and symposium banquet and a free copy of the conference book.

For further details contact: Dr. H. Traitler, Nestlé Research Centre, Nestec Ltd., CH-1000 Lausanne 26, Switzerland.

#### 13th INTERNATIONAL SYMPOSIUM ON CAPILLARY CHROMATOGRAPHY, RIVA DEL GARDA, ITALY, MAY 13-16, 1991

The scientific program will feature the latest developments in:

*Micro separation techniques:* capillary gas chromatography (CGC), capillary GC-MS, capillary GC-FTIR, and capillary GC-AES, micro-HPLC, supercritical fluid chromatography (SFC), capillary zone electrophoresis (CZE), and micellar electrokinetic chromatography (MEKC)

*New methods and applications* in: environmental analysis, organic chemicals, pharmaceutical analysis, drug testing, petroleum and petrochemicals, flavors and fragrances, food and beverages, proteins and peptides, biochemical separations, trace analysis, sample preparation techniques, and new columns and instrumentation.

The symposium will consist of: review papers by leading scientists in the field on the latest developments in column technology, sampling, applications, instrumentation, etc.; invited papers by young scientists; submitted papers presented in poster sessions in order to achieve intensive discussion. Plenary and parallel discussion sessions on special topics will serve to augment the formal presentation. In workshop type seminars scientists of the instrument manufacturers will present and discuss the latest developments in capillary instrumentation.

In conjunction with the Symposium there will be an exhibition of capillary chromatography instruments and accessories.

The registration fee (including the symposium proceedings and the social program) will be: prior to April 15, 1991, delegates (from outside Italy), SFr. 440, DM 525; Italian delegates, Lir. 300.000; after April 15, 1991, delegates (from outside Italy), SFr. 480, DM 580; Italian delegates, Lir. 330.000. Students: 50% reduction of above fees.

For further details contact: Prof. Dr. P. Sandra, Laboratory for Organic Chemistry, University of Ghent, Krijgslan 281, S4, B-9000 Ghent, Belgium. Tel.: (32-91) 225715, ext. 2279; Fax.: (32-91) 228321.

## NATIONAL SYMPOSIUM ON PLANAR CHROMATOGRAPHY: MODERN THIN-LAYER CHROMATOGRAPHY, SOMERSET, NJ, U.S.A., SEPTEMBER 23-25, 1991

The National Symposium on Planar Chromatography: Modern Thin-Layer Chromatography will be held September 23-25, 1991 at the Hilton in Somerset, New Jersey. The Symposium will provide a forum for the exchange of ideas on all aspects of modern thin-layer chromatography. During the last decade the most dramatic change in the practice of thin-layer chromatography has been the change from a qualitative, inexpensive separation method to a fully instrumentalized, partially automated quantitative technology. These aspects and their application to a wide range of industrial, environmental and life science problems will form the focus of the meeting.

The Symposium will be designed for the most effective communication between participants with a formal program of lectures, poster presentations, discussion sessions, practical workshop, instrumentation exhibit, and proceedings. In addition, all registrants are invited to participate in the social program.

Abstracts are invited describing original research in areas including: hyphenated techniques, instrumentation, quantitation, radio-chromatography, TLC in biomedical, environmental, forensic and toxicological analysis. Suggestions for additional topics to be covered in the symposium are welcomed. The scientific committee will be happy to informally discuss with potential contributors any aspects related to their contribution. The deadline for submission of abstracts is March 1, 1991. It is foreseen that the registration fee will be \$275. One-day and student registration fees will also be available.

For further details contact: Symposium Manager, Ms. Janet Cunningham, Barr Enterprises, P.O. Box 279, Walkersville, MD 21793 U.S.A. Tel.: (301) 898-3772; Fax (301) 898-5596.

## SHORT COURSES

### ANALYTICAL CHEMISTRY SHORT COURSES, LOUGHBOROUGH, U.K.

The following short courses will be held by the Department of Chemistry at Loughborough University of Technology, Loughborough, U.K. in the spring of 1991:

Separations for Biotechnology and Biochemistry, March 18-22, 1991, fee residential/non-residential: £630/530.

Gas-Liquid Chromatography, April 15-19, 1991, fee residential/non-residential: £630/530.

Basic Microbiological Methods for the Analytical Chemist, April 15-19, 1991, fee residential/non-residential: £650/570.

For further details contact: Mrs. S. Naddison, Department of Chemistry, Loughborough University of Technology, Loughborough, Leics. LE11 3TU, U.K. Tel.: (0509) 2225; Fax: (0509) 233163.

Announcements are included free of charge. Information on planned events should be sent well in advance (preferably 6 months or more) to: Journal of Chromatography, News Section, P.O. Box 330, 1000 AH Amsterdam, The Netherlands, Fax: (31) 20-5862845.

## CALENDAR OF FORTHCOMING EVENTS

- Feb. 2-6, 1991  
Salt Lake City,  
UT, U.S.A.
- 2nd International Symposium on Field-Flow Fractionation**  
Contact: Julie Westwood, FFF Research Center, Department of Chemistry, University of Utah, Salt Lake City, UT 84112, U.S.A. Tel.: (801) 581-5419. (Further details published in Vol. 513.)
- Feb. 3-6, 1991  
San Diego, CA  
U.S.A.
- HPCE '91, 3rd International Symposium on High Performance Capillary Electrophoresis**  
Contact: HPCE '91, Ms. Shirley E. Schlessinger, Symposium Manager, 400 East Randolph Drive, Suite 1015, Chicago, IL 60601, U.S.A. (Further details published in Vol. 504, No. 2.)
- Feb. 10-15, 1991  
Melbourne, Australia
- POLYMER '91, Polymer Materials: Preparation, Characterization and Properties**  
Contact: POLYMER '91 Secretary, P.O. Box 224, Belmont, Vic. 3216, Australia.
- March 1, 1991  
Cardiff, U.K.
- Symposium on Gas Headspace Vapour Analyzers and Monitors**  
Contact: Dr. J.D.R. Thomas, School of Chemistry and Applied Chemistry, University of Wales College of Cardiff, P.O. Box 912, Cardiff CF1 3TB, U.K. Tel.: (0222) 87400, ext. 5853; Fax: (0222) 371921.
- March 4-7, 1991  
Les Diablerets,  
Switzerland
- 4th Hans Wolfgang Nürnberg Memorial Workshop on Toxic Metal Compounds (Interrelation Between Chemistry and Biology)**  
Contact: Dr. Ernest Merian, Im Kirsgarten 22, CH-4106 Therwil, Switzerland.
- March 4-8, 1991  
Chicago, IL, U.S.A.
- 42nd Pittsburgh Conference and Exposition on Analytical Chemistry and Applied Spectroscopy**  
Contact: Mrs. Alma Johnson, Program Secretary, The Pittsburgh Conference, 300 Penn Center Blvd., Suite 332, Pittsburgh, PA 15235, U.S.A. (Further details published in Vol. 513.)
- March 11-13, 1991  
Lausanne, Switzerland
- 2nd Soil Residue Analysis Workshop**  
Contact: Professor J. Tarradellas, IGE-EPFL, 1015 Lausanne, Switzerland.
- March 18-19, 1991  
Newcastle upon  
Tyne, U.K.
- \*Short Course on Experimental Design and Optimization in Chromatography**  
Contact: Dr. John R. Dean, Department of Chemical and Life Sciences, Newcastle upon Tyne Polytechnic, Ellison Building, Newcastle upon Tyne, NE1 8ST, U.K. Tel.: (091) 232-6002, ext. 3517/3505; Fax: (091) 235 8561.

- March 19–21, 1991  
Washington, DC,  
U.S.A.
- International Electrophoresis Society Meeting**  
Contact: Mrs. Janet Cunningham, IES Symposium Manager, Barr Enterprises, P.O. Box 279, Walkersville, MD 21793, U.S.A. Tel.: (301) 898-3772; Fax: (301) 898-5596. (Further details published in Vol. 513.)
- March 19–22, 1991  
Interlaken, Switzerland
- \*2nd Interlaken Conference on Advances in Purification of Recombinant Proteins**  
Contact: H.P. Walliser, Ph.D., Scientific Secretariat, c/o CIBA-GEIGY, K. 693.1.23, CH-4002 Basel, Switzerland. Tel.: (61) 691-5111; Fax: (61) 691-8189.
- March 19–22, 1991  
Montelibretti,  
Italy
- \*Biopolymers Separations 91**  
Contact: Dr. Danilo Corradini, Institute of Chromatography, C.N.R., Area della Ricerca di Roma, P.O. Box 10, 00016 Monterotondo Stazione, Italy. Tel. (0039) 6-9005328/90020254; Fax: (0039) 6-9005849; Telex: 624809 CNR ML 1.
- March 21–22, 1991  
Newcastle upon  
Tyne, U.K.
- \*Short Course on Supercritical Fluid Chromatography**  
Contact: Dr. John R. Dean, Department of Chemical and Life Sciences, Newcastle upon Tyne Polytechnic, Ellison Building, Newcastle upon Tyne, NE1 8ST, U.K. Tel.: (091) 232-6002, Fax: (091) 235 8561.
- March 26, 1991  
Maarsse, The  
Netherlands
- 4th Symposium on Fast Protein Liquid Chromatography**  
Contact: Marianne Wobma, Pharmacia Nederland BV, Houttuinlaan 4, 3447 GM Woerden, The Netherlands. Tel.: (03480) 77631. (Further details published in Vol. 513.)
- April 23–26, 1991  
Interlaken, Switzerland
- \*6th International Symposium on Instrumental Planar Chromatography**  
Contact: Dr. H. Traitler, Nestlé Research Center, Nestec Ltd., CH-1000 Lausanne 26, Switzerland.
- April 28–May 1,  
1991  
Boston, MA, U.S.A.
- 3rd International Symposium on Pharmaceutical and Biomedical Analysis**  
Contact: Ms. Shirley E. Schlessinger, Symposium Manager PBA '91, 400 East Randolph Drive, Suite 1015, Chicago, IL 60601, U.S.A. Tel.: (312) 527-2011. (Further details published in Vol. 513.)
- May 13–15, 1991  
Arlington, VA,  
U.S.A.
- 8th International Symposium on Preparative Chromatography**  
Contact: Janet E. Cunningham, Barr Enterprises, P.O. Box 279, Walkersville, MD 21793, U.S.A. Tel.: (301) 898-3772; Fax: (301) 898-5596. (Further details published in Vol. 513.)

May 13–16, 1991  
Riva del Garda, Italy

**\*13th International Symposium on Capillary Chromatography**

Contact: Dr. Pat Sandra, Laboratory for Organic Chemistry, University of Ghent, Krijgslaan 281 (S4), B-9000 Ghent, Belgium. Tel.: (32 91) 225715, ext. 2279; Fax: (32 91) 228321.

May 19–21, 1991  
Boston, MA, U.S.A.

**2nd International Symposium on Supercritical Fluids**

Contact: Mark A. McHugh, Department of Chemical Engineering, The John Hopkins University, Baltimore, MD 21218, U.S.A. Tel.: (301) 338-8752; Fax: (301) 338-5508 or (508) 794-9580. (Further details published in Vol. 523.)

May 21, 1991  
Washington, DC,  
U.S.A.

**CHROMEXPO-91 (Chromatography Exhibition, Poster Session, Educational Seminars)**

Contact: Janet E. Cunningham, Barr Enterprises, P.O. Box 279, Walkersville, MD 21793, U.S.A. Tel.: (301) 898-3772; Fax: (301) 898-5596.

May 27–31, 1991  
Rome, Italy

**2nd International Symposium on Chiral Discrimination**

Contact: Professor D. Misiti or Professor F. Gasparri, Laboratori di Chimica Organica, Facoltà di Farmacia, Università "La Sapienza", Piazzale Aldo Moro 5, 00185 Rome, Italy. Tel.: (06) 4452900; fax: (06) 49912780. (Further details published in Vol. 477, No. 2.)

May, 27–31, 1991  
Ghent, Belgium

**IVth International Symposium on Quantitative Luminescence Spectrometry in Biomedical Sciences**

Contact: Dr. Willy R.G. Baeyens, Symposium chairman, State University of Ghent, Pharmaceutical Institute, Harelbekestraat 72, B-9000 Ghent, Belgium. (Further details published in Vol. 483.)

May 29–31, 1991  
Baltimore, MD,  
U.S.A.

**\*4th International Symposium on Polymer Analysis and Characterization**

Contact: Judith A. Watson, Professional Association Management, 750 Audubon, East Lansing, MI 48823, U.S.A. Tel.: (517) 332-3667.

June 3–7, 1991  
Basel, Switzerland

**HPLC '91, 15th International Symposium on Column Liquid Chromatography**

Contact: Secretariat HPLC '91, Convention Center Basel, Congress Department, P.O. Box, CH-4021 Basel, Switzerland. (Further details published in Vol. 477, No. 2.)

June 4–6, 1991  
Egham, U.K.

**5th International LIMS Conference**

Contact: The Conference Registrar, 5th International LIMS Conference, P.O. Box 341, High Wycombe, Buckinghamshire HP11 2QG, U.K. Tel.: (0494) 24769.

June 9–14, 1991  
Bergen, Norway

**XXVII Colloquium Spectroscopicum Internationale**

Contact: Secretariat XXVII CSI, HSD Congress-Conference, P.O. Box 1721 Nordnes, N-5024 Bergen, Norway. Tel.: (475) 318414; Telex: 42607 hsd n, Fax: (475) 324555. (Further details published in Vol. 508, No.2.)

June 10-13, 1991  
San Francisco,  
CA, U.S.A.

**5th Annual Seminar on Analytical Biotechnology**

Contact: Janet E. Cunningham, Barr Enterprises, P.O. Box 279, Walkersville, MD 21793, U.S.A. Tel.: (301) 898-3772; Fax: (301) 898-5596.

July 8-12, 1991  
Amsterdam, The  
Netherlands

**\*4th Amsterdam HPLC Summercourse**

Contact: Dr. J.C. Kraak, Laboratory of Analytical Chemistry, University of Amsterdam, Nieuwe Achtergracht 166, 1018 WV Amsterdam, The Netherlands. Tel.: (31 20) 5256515; Fax: (31 20) 5255698.

July 16-18, 1991  
London, U.K.

**Two-Dimensional Polyacrylamide Gel Electrophoresis**

Contact: Conference Secretariat 2-D PAGE 1991, Department of Cardiothoracic Surgery, National Heart & Lung Institute, Dovehouse Street, London SW3 6LY, U.K. (Further details published in Vol. 504, No. 2.)

Aug. 17-22, 1991  
Budapest, Hungary

**33rd IUPAC Congress**

Contact: 33rd IUPAC Congress, E. Pungor, c/o Hungarian Academy of Sciences, Gellért ter 4, H-1111 Budapest, Hungary.

Aug. 18-21, 1991  
York, U.K.

**\*Capillary Electrophoresis Training Course**

Contact: Dr. Carys Calvert, Short Course Coordinator, Department of Chemistry, University of York, YO1 5DD, U.K. Tel. (0904) 432576/432511; Fax: (0904) 432516/433433.

Aug. 21-24, 1991  
Kumamoto, Japan

**5th International Conference on Flow Analysis**

Contact: Professor Ishibashi, Department of Applied Analytical Chemistry, Faculty of Engineering 36, Kyushu University, Hokazaki, Higashiku, Fukuoka 812, Japan. (Further details published in Vol. 475.)

Aug. 25-31, 1991  
Makuhari, Japan

**ICAS '91, IUPAC International Congress on Analytical Sciences**

Contact: ICAS '91 Secretariat, The Japan Society for Analytical Chemistry, 1-26-2 Nishigotande, Shinagawa, Tokyo 141, Japan. Tel.: (813) 490-3351; fax: (813) 490-3572. (Further details published in Vol. 483.)

Sept. 1-6, 1991  
Heslington, U.K.

**4th European Conference on the Spectroscopy of Biological Molecules**

Contact: Prof. R.E. Hester, ECSBM '91 Chairman, Department of Chemistry, University of York, Heslington, York YO1 5DD, U.K. (Further details published in Vol. 523.)

Sept. 1-6, 1991  
Lubeck-Travemunde,  
F.R.G.

**8th International Conference on Fourier Transform Spectroscopy**

Contact: Gesellschaft Deutscher Chemiker, Abt. Tagungen, P.O. Box 900440, D-6000 Frankfurt 90, F.R.G. Tel.: 17-366/360; Fax: (79) 17475; Telex: 4170497 gdch d.



Sept. 2-6, 1991  
Warsaw, Poland

**8th Danube Symposium on Chromatography**

Contact: 8th Danube Symposium on Chromatography, Janusz Lipkowski, Institute of Physical Chemistry of the Polish Academy of Sciences, Kasprzaka 44/52, 01-224 Warsaw, Poland. (Further details published in Vol. 502, No. 2.)

Sept. 4-6, 1991  
Bilthoven, The Netherlands

**3rd Workshop on Chemistry and Fate of Modern Pesticides**

Contact: Pesticides Workshop Office, Dr. P. van Zoonen, RIVM, P.O. Box 1, 3720 Bilthoven, The Netherlands. (Further details published in Vol. 472, No. 2.)

Sept. 23-25, 1991  
Somerset, NJ,  
U.S.A.

**\*National Symposium on Planar Chromatography: Modern Thin-Layer Chromatography**

Contact: Ms. Janet Cunningham, Symposium Manager, Barr Enterprises, P.O. Box 279, Walkersville, MD 21793, U.S.A. Tel.: (301) 898-3772; Fax: (301) 898-5596.

Sept. 24-25, 1991  
Baden Baden,  
F.R.G.

**Short Course on Sample Handling in Liquid Chromatography**

Contact: Workshop Office, IAEAC, M. Frei-Häusler, Postfach 46, CH-4123 Allschwil 2, Switzerland. Tel.: (004161) 632789 and (004161) 732950.

Sept. 24-28, 1991  
Yokohama, Japan

**9th International Symposium on Affinity Chromatography and Biological Recognition**

Contact: Professor Ken-ichi Kasai, Faculty of Pharmaceutical Sciences, Teikyo University, Sagamiko, Tsukui, Kanagawa 199-01, Japan.

Sept. 26-27, 1991  
Baden Baden, F.R.G.

**5th Symposium on Handling of Environmental and Biological Samples in Chromatography**

Contact: Workshop Office, IAEAC, M. Frei-Häusler, Postfach 46, CH-4123 Allschwil 2, Switzerland. Tel.: (004161) 632789 and (004161) 732950. (Further details published in Vol. 513.)

Oct. 14-18, 1991  
Budapest, Hungary

**ECASIA 91, 4th European Conference on Applications of Surface and Interface Analysis**

Contact: ECASIA 91, MTA ATOMKI, Pf. 51, H-4001 Debrecen, Hungary. Tel.: (36) 52-16181; Telex: 72210 (atom h); Fax: (36) 52-16181.

Oct. 20-23, 1991  
Washington, DC,  
U.S.A.

**11th International Symposium on High-Performance Liquid Chromatography of Proteins, Peptides and Polynucleotides**

Contact: Janet E. Cunningham, Barr Enterprises, P.O. Box 279, Walkersville, MD 21793, U.S.A. Tel.: (301) 898-3772; Fax: (301) 898-5596. (Further details published in Vol. 513.)

Jan. 6-11, 1992  
California, U.S.A.

**1992 Winter Conference on Plasma Spectrochemistry**

Contact: 1992 Conference on Plasma Spectrochemistry, Attn.: R. Barnes, c/o ICP Information Newsletter, Department of Chemistry, GRC Towers, University of Massachusetts, Amherst, MA 01003-0035, U.S.A. Tel.: (413) 545-2294; Fax: (413) 545-4490; BITNET: RBARNES@UMASS. (Further details published in Vol. 513.)

Feb. 18-21, 1992  
Antwerp, Belgium

**2nd International Symposium on Hyphenated Techniques in Chromatography**

Contact: Dr. R. Smits, p.a. BASF Antwerpen N.V., Scheldelaan B-2040 Antwerp, Belgium. Tel.: (32) 5682831; Fax: (323) 5683355; Telex: 31047 basant b. (Further details published in Vol. 508, No. 2.)

May 17-22, 1992  
Kyoto, Japan

**4th International Conference on Fundamentals of Adsorption**

Contact: Prof. M. Suzuki, Conference Chairman, Institute of Industrial Science, University of Tokyo, 7-22-1 Roppongi, Minatoku, Tokyo 106, Japan. (Further details published in Vol. 508, No. 2.)

---

\* Indicates new or amended entry

Views and opinions expressed in this section do not necessarily reflect those of the Publisher or the Editors. No responsibility is assumed by the Publisher for any injury and/or damage to persons or property as a matter of products liability, negligence or otherwise, or from any use or operation of any methods, products, instructions or ideas contained in the material herein.

## PUBLICATION SCHEDULE FOR 1991

*Journal of Chromatography and Journal of Chromatography, Biomedical Applications*

MONTH	D 1990	J	F	M	
Journal of Chromatography	535/1 + 2	536/1 + 2 537/1 + 2 538/1	538/2 539/1 539/2		The publication schedule for further issues will be published later
Cumulative Indexes, Vols. 501-550					
Bibliography Section					
Biomedical Applications		562/1 + 2 563/1	563/2	564/1	

### INFORMATION FOR AUTHORS

(Detailed *Instructions to Authors* were published in Vol. 522, pp. 351-354. A free reprint can be obtained by application to the publisher, Elsevier Science Publishers B.V., P.O. Box 330, 1000 AH Amsterdam, The Netherlands.)

**Types of Contributions.** The following types of papers are published in the *Journal of Chromatography* and the section on *Biomedical Applications*: Regular research papers (Full-length papers), Review articles and Short Communications. Short Communications are usually descriptions of short investigations, or they can report minor technical improvements of previously published procedures; they reflect the same quality of research as Full-length papers, but should preferably not exceed six printed pages. For Review articles, see inside front cover under Submission of Papers.

**Submission.** Every paper must be accompanied by a letter from the senior author, stating that he/she is submitting the paper for publication in the *Journal of Chromatography*.

**Manuscripts.** Manuscripts should be typed in double spacing on consecutively numbered pages of uniform size. The manuscript should be preceded by a sheet of manuscript paper carrying the title of the paper and the name and full postal address of the person to whom the proofs are to be sent. As a rule, papers should be divided into sections, headed by a caption (*e.g.*, Abstract, Introduction, Experimental, Results, Discussion, etc.). All illustrations, photographs, tables, etc., should be on separate sheets.

**Introduction.** Every paper must have a concise introduction mentioning what has been done before on the topic described, and stating clearly what is new in the paper now submitted.

**Abstract.** All articles should have an abstract of 50-100 words which clearly and briefly indicates what is new, different and significant.

**Illustrations.** The figures should be submitted in a form suitable for reproduction, drawn in Indian ink on drawing or tracing paper. Each illustration should have a legend, all the *legends* being typed (with double spacing) together on a *separate sheet*. If structures are given in the text, the original drawings should be supplied. Coloured illustrations are reproduced at the author's expense, the cost being determined by the number of pages and by the number of colours needed. The written permission of the author and publisher must be obtained for the use of any figure already published. Its source must be indicated in the legend.

**References.** References should be numbered in the order in which they are cited in the text, and listed in numerical sequence on a separate sheet at the end of the article. Please check a recent issue for the layout of the reference list. Abbreviations for the titles of journals should follow the system used by *Chemical Abstracts*. Articles not yet published should be given as "in press" (journal should be specified), "submitted for publication" (journal should be specified), "in preparation" or "personal communication".

**Dispatch.** Before sending the manuscript to the Editor please check that the envelope contains four copies of the paper complete with references, legends and figures. One of the sets of figures must be the originals suitable for direct reproduction. Please also ensure that permission to publish has been obtained from your institute.

**Proofs.** One set of proofs will be sent to the author to be carefully checked for printer's errors. Corrections must be restricted to instances in which the proof is at variance with the manuscript. "Extra corrections" will be inserted at the author's expense.

**Reprints.** Fifty reprints of Full-length papers and Short Communications will be supplied free of charge. Additional reprints can be ordered by the authors. An order form containing price quotations will be sent to the authors together with the proofs of their article.

**Advertisements.** Advertisement rates are available from the publisher on request. The Editors of the journal accept no responsibility for the contents of the advertisements.

## Vapor-Liquid Equilibrium Data

by S. Ohe, Department of Applied  
Chemistry, Tokai University,  
Kanagawa, Japan

(Physical Sciences Data, 37)

Vapor-liquid equilibrium (VLE) data are necessary for the design and operation of distillation processes. It is absolutely impossible to determine a distillation process without VLE data.

The author of this book has had much experience designing and constructing distillation processes and towers and knows that VLE data must be easily retrievable, readily comprehensible, and precise. This volume contains the most important VLE data for 1,446 binary systems with Wilson parameters determined by computer processing. The data are also presented graphically.

The Wilson equation, which is known as one of the most applicable to multicomponent systems, is employed for computer-aided determination of the optimum parameters using the non-linear least squares method. The data for each system include the substance names and the chemical formulae for the binary components, literature references, the Antoine vapor pressure constants or vapor pressures of the components, optimized values of the parameters for the Wilson equation, the errors, tables with smoothed values of vapor and liquid compositions and temperatures or pressures and phase diagrams for visual comparison of the experimental data and calculated values. The systems are arranged according to the Chemical Abstracts system. An alphabetical index of systems is given at the end of the book for convenient retrieval.

Thus the VLE of binary or multicomponent systems can be computed from the Wilson parameters shown in the tables of this book. The book also presents a multicomponent VLE computer program written in BASIC and examples obtained using the program. With the program and parameters provided, VLE can be directly computed on a personal computer. Furthermore, when the Wilson parameters are used as input data for a distillation computer program, the number of theoretical plates (NTP) of distillation columns can be obtained.

**Contents: Part I. Equations for Calculation of the Vapor-Liquid Equilibrium.** 1. Fundamentals Equations for the Vapor-Liquid Equilibrium Relation. 2. Excess Free Energy of Non-Ideal Solutions. 3. Equations for Calculation. 4. Accuracy of Calculation by Wilson's Equation. 5. Examples Executed by Computer Program. References. **Part II. Data Sheets.** Guide to Graphs and Tables. Data Sheets 1-1446. Index.

1989 xxx + 742 pages ISBN 0-444-98876-9

Price: US\$ 253.75 / Dfl. 495.00

Exclusive sales rights in Japan: Kodansha Ltd., Tokyo

## Vapor-Liquid Equilibrium Data at High Pressure

by S. Ohe, Department of Applied  
Chemistry, Tokai University,  
Kanagawa, Japan

(Physical Sciences Data, 42)

High pressure vapor-liquid equilibrium data are important when very pure compounds are to be prepared, and they are also needed for high pressure liquid or supercritical chromatography.

This volume is a compilation of high pressure vapor-liquid equilibrium data for 700 binary systems, processed and plotted by computer for ready inspection of the whole spectrum. The information given for each system comprises: the components' names, chemical formulae, cited literature, and critical temperature, critical pressures, acentric factors of the components, optimized values of the parameters for the Peng-Robinson equations, the errors, and phase diagrams for visual comparison of the experimental data and calculated values.

An alphabetical index by system name is included in the book which will be a useful reference for chemical engineers, research chemists, and graduate students who are interested in the chemical process industry.

**Contents: Part I. Equations for Calculation of the Vapor-Liquid Equilibrium at High Pressure.** 1. Method for Predicting Vapor-Liquid Equilibrium at High Pressure. 2. Prediction Examples for Binary and Multicomponent Vapor-Liquid Equilibria at High Pressure. 3. Prediction Program for Multicomponent Vapor-Liquid Equilibrium at High Pressure. References. **Part II. Data Sheets.** Guide to Graphs and Tables. Data Sheets 1-700. Index.

1990 xxviii + 356 pages ISBN 0-444-98797-5

Price: US\$ 202.50 / Dfl. 395.00

Exclusive sales rights in Japan: Kodansha Ltd., Tokyo



**ELSEVIER  
SCIENCE  
PUBLISHERS**

P.O. Box 211, 1000 AE Amsterdam,  
The Netherlands

P.O. Box 882, Madison Square Station,  
New York, NY 10159, USA